AGARD-CP-560

AGARD

ADVISORY GROUP FOR AEROSPACE RESEARCH & DEVELOPMENT
7 RUE ANCELLE, 92200 NEUILLY-SUR-SEINE, FRANCE

DTIC
ELECTE
MAR 16 1995
S G D

AGARD CONFERENCE PROCEEDINGS 560

Active Control Technology: Applications and Lessons Learned

(Les technologies du système de contrôle actif : applications et enseignements)

Copies of papers presented at the Flight Mechanics Panel Symposium held in Turin, Italy, from 9-13 May 1994.

NORTH ATLANTIC TREATY ORGANIZATION

DISTRIBUTION STATEMENT A
Approved for public release;
Distribution Unlimited

19950313 004

Published January 1995

Distribution and Availability on Back Cover

AGARD

ADVISORY GROUP FOR AEROSPACE RESEARCH & DEVELOPMENT
7 RUE ANCELLE, 92200 NEUILLY-SUR-SEINE, FRANCE

DTIC
ELECTE
MAR 1 6 1995
S G

AGARD CONFERENCE PROCEEDING 560

Active Control Technology: Applications and Lessons Learned

(Les technologies du système de contrôle actif : applications et enseignements)

Copies of papers presented at the Flight Mechanics Panel Symposium held in Turin, Italy, from 9-13 May 1994.

Accesion For
NTIS CRA&I ☒
DTIC TAB ☐
Unannounced ☐
Justification
By
Distribution /
Availability Codes
Dist | Avail and / or Special
A-1

North Atlantic Treaty Organization
Organisation du traité de l'Atlantique Nord

DISTRIBUTION STATEMENT A
Approved for public release;
Distribution Unlimited

The Mission of AGARD

According to its Charter, the mission of AGARD is to bring together the leading personalities of the NATO nations in the fields of science and technology relating to aerospace for the following purposes:

- Recommending effective ways for the member nations to use their research and development capabilities for the common benefit of the NATO community;
- Providing scientific and technical advice and assistance to the Military Committee in the field of aerospace research and development (with particular regard to its military application);
- Continuously stimulating advances in the aerospace sciences relevant to strengthening the common defence posture;
- Improving the co-operation among member nations in aerospace research and development;
- Exchange of scientific and technical information;
- Providing assistance to member nations for the purpose of increasing their scientific and technical potential;
- Rendering scientific and technical assistance, as requested, to other NATO bodies and to member nations in connection with research and development problems in the aerospace field.

The highest authority within AGARD is the National Delegates Board consisting of officially appointed senior representatives from each member nation. The mission of AGARD is carried out through the Panels which are composed of experts appointed by the National Delegates, the Consultant and Exchange Programme and the Aerospace Applications Studies Programme. The results of AGARD work are reported to the member nations and the NATO Authorities through the AGARD series of publications of which this is one.

Participation in AGARD activities is by invitation only and is normally limited to citizens of the NATO nations.

The content of this publication has been reproduced
directly from material supplied by AGARD or the authors.

Published January 1995

Copyright © AGARD 1995
All Rights Reserved

ISBN 92-836-0007-X

Printed by Canada Communication Group
45 Sacré-Cœur Blvd., Hull (Québec), Canada K1A 0S7

Preface

Active Control Technology (ACT) has emerged in the last decade from the realm of theoretical and limited experimental applications to full-scale use on prototype and production aircraft. This technology has been used on military aircraft to maximize maneuverability and agility even at the edges of the flight envelope. In new civilian transports, ACT has led to reduced trim drag, lower pilot workload, and improved ride qualities. This symposium summarized the state-of-the-art in ACT and spotlighted the lessons learned in the recent flight test applications. Priority was given to papers presenting proven flight results of ACT for fixed and rotary-wing aircraft projects.

Two keynote papers were given, the first presenting a perspective on inter-disciplinary aspects of ACT by a leading expert in aircraft flight control; the second presenting a perspective from the military operator's point of view on the introduction of a new technology in service use. The symposium was organized in five sessions covering control system specifications, design and analysis methods, system integration, and implementation experience. A final round table discussion focused on the benefits of ACT and problems/solutions encountered in implementing ACT.

A one-day Workshop on Pilot-Induced Oscillations (PIO) was held immediately after the Symposium to promote discussion among researchers working in this field, and a brief summary of the main features of this Workshop is included in this Conference Proceedings.

Préface

Au cours de la dernière décennie, les Technologies des systèmes de contrôle actif (ACT) sont passées du stade d'applications théoriques et limitées, au stade de production et à la mise en œuvre sur aéronefs prototypes et en série. Ces technologies ont été employées sur des avions militaires afin d'atteindre un maximum de manœuvrabilité et de maniabilité même aux limites du domaine de vol. En ce qui concerne les nouveaux avions de transports civils, l'ACT a permis de réduire la traînée de compensation, d'alléger la charge de travail des équipages et d'améliorer les qualités de vol. Ce symposium a fait le point de l'état de l'art dans le domaine de l'ACT en mettant au premier plan les enseignements tirés des applications récentes lors des essais en vol. La priorité a été accordée aux communications qui présentaient des résultats d'essais en vol validés pour l'ACT dans le cadre des projets d'aéronefs à voilure fixe et à voilure tournante.

Une première allocution d'ouverture a présenté une perspective des aspects interdisciplinaires de l'ACT vus par un expert dans le domaine. Elle était suivie d'une deuxième présentation sur la mise en service d'une nouvelle technologie du point de vue de l'opérateur militaire. Le symposium a été organisé en cinq sessions portant sur les spécifications des systèmes de contrôle, les méthodes de conception et d'analyse, l'intégration des systèmes et l'expérience de la mise en œuvre. Les atouts de l'ACT, ainsi que les problèmes et les solutions rencontrés lors de la mise en œuvre ont été examinés lors d'une table ronde en fin de séance.

Un atelier sur le PIO, d'une durée d'un jour, a été tenu immédiatement après le symposium afin de stimuler les discussions entre chercheurs travaillant dans ce domaine. Un résumé des principaux éléments de cet atelier est inclu dans le présent compte-rendu.

Flight Mechanics Panel

Chairman: Professor L.M.B. da Costa Campos
Instituto Superior Tecnico
Pavilhao de Maquinas
1096 Lisboa Codex
Portugal

Deputy Chairman: Dipl.-Ing. H. Wünnenberg
Head of Flight Mechanics
Dornier Luftfahrt
D-88039 Friedrichshafen
Germany

TECHNICAL PROGRAMME COMMITTEE

Mr. F. Sella
ALENIA Aeronautico
Divisione Velivoli Difesa
EFA Project
Corso Marche, 41
10146 Torino
Italy

Dr. M. Tischler
Army Aeromechanics Laboratory
Ames Research Center, MS N211-2
Moffett Field, CA 94035
U.S.A.

Dr. Ir. J.A. Mulder
Professor
Delft University of Technology
Dept. of Aerospace Engineering
Kluyverweg, 1
2629 HS Delft
The Netherlands

HOST NATION COORDINATORS

Mr. F. Sella
ALENIA Aeronautica
Divisione Velivoli Difesa
EFA Project
Corso Marche, 41
10146 Torino
Italy

Prof. F. Quagliotti
Dpt. Ingegneria Aeronautica e Spaziale
Politecnico di Torino
Corso Duca Degli Abruzzi, 24
10129 Torino
Italy

PANEL EXECUTIVE

Mr. M.K. Foster

Mail from Europe:

AGARD-OTAN
Attn: FMP Executive
7, rue Ancelle
92200 Neuilly-sur-Seine
France

Mail from USA and Canada:
AGARD-NATO
Attn: FMP Executive
PSC 116
APO AE 099777

Tel: [33] (1) 4738-5770
Telex: 610176 (France)
Telefax: [33] (1) 4738-5799/4738-6720

Acknowledgements

The Flight Mechanics Panel wishes to express its thanks to the National Authorities of Italy for the invitation to hold this meeting in their country as well as to ALENIA and the Politecnico di Torino for the facilities and personnel which made the meeting possible.

The Flight Mechanics Panel also wishes to express its thanks to the Structures and Materials Panel for its assistance in proposing an author for a paper presented at this Symposium.

Contents

	Page
Preface/Préface	iii
Flight Mechanics Panel	iv
Acknowledgements	v
	Reference
Technical Evaluation Report by H.A. Mooij	T
Keynote Address 1 by D. McRuer	K1
Keynote Address 2 by BGen. V. Camporini	K2
The Role of Handling Qualities Specifications in Flight Control System Design by R.H. Hoh & D.G. Mitchell	1
The Prevention of PIO by Design by J.C. Gibson	2
The Importance of Flying Qualities Design Specifications for Active Control Systems by J. Hodgkinson & K.R. Rossitto	3
Experiences with ADS-33 Helicopter Specification Testing and Contributions to Refinement Research by C.J. Ockier & H.-J. Pausder	4
LAVI Flight Control System Design Requirements, Development and Flight Test Results by M. Shmul, E. Erenthal & M. Attar	5
Robust Control: A Structured Approach to Solve Aircraft Flight Control Problems by S. Bennani, J.A. Mulder & O.H. Bosgra	6
Dynamic Inversion: An Evolving Methodology for Flight Control Design by D. Enns, D. Bugajski, R. Hendrick & G. Stein	7
Évaluation des techniques de contrôle flou pour le pilotage d'avion by N. Imbert & A. Piquereau	8
The Control System Design Methodology of the STOL & Maneuver Technology Demonstrator by D.J. Moorhouse & K.D. Citurs	9
Control Law Design Using H_∞ and μ-Synthesis Short-Period Controller for a Tail-Airplane by L. Mangiacasale	10
Model Following Control for Tailoring Handling Qualities — ACT Experience with ATTHeS by G. Bouwer, W. von Grünhagen & H.-J. Pausder	11

X-29 Flight Control System: Lessons Learned 12
by R. Clarke, J.J. Burken, J.T. Bosworth & J.E. Bauer

Advanced Gust Management Systems — Lessons Learned and Perspectives 13
by R. König, K.-U. Hahn & J. Winter

Flight Evaluation of Forebody Vortex Control in Post-Stall Flight 14
by L.A. Walchli

Automatic Flight Control System for an Unmanned Helicopter System Design and Flight Test Results 15
by M. Weidel & W. Alles

The FCS-Structural Coupling Problem and its Solution 16
by B.D. Caldwell

IFPC Design for a SDLF STOVL Vehicle —
by P.A. Tait & R.C. Loschke
(Paper not made available for publication)

Structural Aspects of Active Control Technology 18
by H. Hönlinger, H. Zimmermann, O. Sensburg & J. Becker

Flight Test Results of the F-16 Aircraft Modified with the Axisymetric Vectoring Exhaust Nozzle 19
by D. Kidman, D. Vanhoy & Maj. Gerzanics

Catapultage du Rafale — Conception et expérimentation 20
by D. Fleygnac & L. Lequeux

Digital Autopilot Design for Combat Aircraft in ALENIA 21
by A. Tonon & P.L. Belluati

Experimental Aircraft Programme — (EAP) Flight Control System Design and Test 22
by A. McCuish

An Investigation of Pilot-Induced Oscillation Phenomena in Digital Flight Control Systems 23
by W.A. Flynn & R.E. Lee

Flight Demonstration of an Advanced Pitch Control Law in the VAAC Harrier Aircraft 24
by C. Fielding, S.L. Gale & D.V. Griffith

X-31 — A Program Overview and Flight Test Status 25
by H. Ross & U. Neuberger

Advanced Flight Control Technology Achievements at Boeing Helicopters 26
by K.H. Landis, J.M. Davis, C. Dabundo & J.F. Keller

Practical Experiences in Control Systems Design Using the NRC Bell 205 Airborne Simulator 27
by S.W. Baillie, J.M. Morgan & K.R. Goheen

Les qualités de vol des avions de transport civil à commandes de vol électriques 28
by D. Chatrenet

Pilot-Induced Oscillation — A Report on the AGARD Workshop on PIO PIO
by K. McKay

Technical Evaluation Report

by

H.A. Mooij
Mooij & Associates
9 Leidsestraatweg
2341 GR Oegstgeest, NL

1 INTRODUCTION

In the last decade, Active Control Technology (ACT) has emerged from the realm of theory and modest experimental applications to full-scale use on production aircraft, while more elaborate forms of ACT are under test for the future production of aircraft.
New technologies have been applied in military fighters to maximise manoeuvrability and agility, and in civil transports to reduce trim drag, lower pilot workload and improve riding qualities.
During the AGARD symposium "Active Control Technology: Applications and Lessons Learned", the status of ACT development was assessed in the light of the experience gained over the last decade.
As the intended scope of the symposium, held in Turin, Italy, from 9-12 May, 1994, the following four topics had been forwarded: Specifications for flight control system design, Design and analysis methods, System integration and Implementation of experience.

2 KEYNOTE SPEAKERS

The Theme and Scope of the symposium were emphasized in the introduction by two keynote speakers.

First Keynote Speaker: D.T. McRuer
The speaker, with his vast background experience in the subject area, was very well qualified to set the tone for the symposium. In an orderly fashion, Mr. McRuer demonstrated the balancing act of applying the full capabilities of ACT by presenting two examples illustrating the need for an integrated approach amongst various technical disciplines. One example showed the complexity of aircraft-specific interactions, another demonstrated unfavourable oscillatory aircraft-pilot coupling. He suggested three categories of Pilot-Induced Oscillations (PIO), based on the pilot-behaviour theory: Category I - Essentially Linear Pilot-Vehicle System Oscillations, Category II - Quasi-Linear Pilot-Vehicle System Oscillations with Surface Rate or Position-Limiting and Category III - Essentially Non-Linear Pilot-Vehicle System Oscillations with Transitions. Avoiding Category III is identified by him as one of the great challenges of Active Control Technology applications. The reason for this is, that post-transition effective aircraft dynamics are almost always unforeseen, as are the PIO "triggering" events.

Second Keynote Speaker: Gen. V. Camporine
The second keynote address, again of high quality, was presented by someone, with a vast operating experience, who represented the user community. "Interaction" between the military and scientific worlds was the expression Camporini used when answering the question: do military needs drive research or is it achievements in the technological field which dictate tactics, strategies and eventually doctrines? He highlighted some of the problems associated with this interaction. After explaining his feelings about aircraft as "man-environment interfaces", and formulating the arguments for the need for further advances, he underlined the arguments by stating that the cold war was won without any combat and only a technological edge would allow us to win the peace for future generations.

3 SYMPOSIUM ORGANISATION

The symposium was organised around four sessions comprising 28 technical papers in all. It was concluded with a round-table discussion focused on the benefits of ACT, problems encountered and solutions forwarded.

The general layout of the symposium was as follows:

Session I - "Specifications for Flight Control System Design". - Although not all elements of the scope for this session, as indicated in the original call for papers, were covered in the

contents of the set of papers presented, all papers were clearly of interest. New for the open community was the information about the requirements for, as well as the development of the Lavi flight control system.

Session II - "Flight Control Design and Analysis Methods". Actual case studies (four) and theoretical treatises (three) was the split of papers in this session. The emergence of the relatively new "H-infinity/Mu-synthesis" and "Dynamic Inver-sion" methods was clearly exemplified in the "theoretical treatises".

Session III - "System Integration". - Of the six papers presented in this session, three may be ranked under the structural aspects of active control technology, two under propulsion aspects of active control, while one paper dealt with quite a novel form of active control, i.e. the forebody vortex control for the post-stall flight regime.

Session IV -"Implementation Experience: Handling Qualities and Flight Control Performance". - The organisers' intention was in this session to highlight the discussion of actual flight and flight-test experience with ACT, emphasising the comparison of predictions with flight test results. Considering the papers presented in this session, it is observed that nine out of ten papers were flight-test oriented, although in most cases no detailed comparisons between predictions and flight-test results were given. Highly-manoeuvrable fighter aircraft and helicopters were discussed, as well as large transport aircraft.

The range of expertise of the participants in the symposium was reflected by presentations based, amongst others, on the following specialisms: Flying Qualities Specifications, Flight Control System Design and Analysis, Structural Dynamics, Propulsion Control Systems, Digital Flight Control System (FCS) Implementation, Handling Qualities Flight Testing. Participants included scientists, engineers, (test) pilots from military services, government and private laboratories, universities and industry. The symposium authors represented a wide cross section of national centres as may be seen from the balance of US and non-US papers: 9 US papers and 19 non-US papers. The total symposium participation was outstanding for AGARD, i.e. 159, of whom 38 were authors, 45 panel members and 76 observers. The single largest group was the non-presenting observers. This is a strong indicator of the level of interest in the symposium topic, despite the difficult travel budget environment in both the US and Europe.

4 TECHNICAL EVALUATION

Session I - Specifications for Flight Control System Design

The first three presentations of the first session covered background information on FCS design specifications. The fourth and fifth presentations gave accounts of two flight-test programmes with an in-flight rotor-craft simulator and a fighter-technology demonstrator, respectively.

Regarding **Paper 1**, on the role of handling qualities specifications in Flight Control System design, it is observed that the necessity to incorporate handling qualities specifications in the FCS design process is not recognised by Industry. This may be deduced from the numerous handling qualities problems, some of which are Pilot-Induced Oscillations. It is recognised that MIL-STD-1797A, for aeroplanes is not perfect and presently under revision. The importance of the incorporation of demonstration manoeuvres in future specifications is stressed, while the potential value is explained of a "flight-test guide" to provide compliance with criteria. As a first step towards this achievement, the rotor craft ADS-33C specification has been defined and found very useful.

The following presentation, **(Paper 2)**, was dedicated purely to the problem area of Pilot-Induced Oscillations. In this paper, it is stated that a number of simple criteria may be applied during control law design, in order to prevent PIO resulting from unnecessary lags or excessive gain. For more background information about these criteria, reference is made to the report on the Workshop on PIO, contained elsewhere in these Proceedings.

The evolution of flying qualities criteria for ACT fighters was discussed in **Paper 3**. The experience with ACT fighters has been a valuable contribution towards the development of ACT transports. The need for a set of flight-validated flying qualities criteria and requirements for a range of possible response types of ACT transports is emphasized. Presentations 2 and 3 both stress that handling qualities criteria specifications for any new aircraft should be required rather than merely recommended.

A solid piece of research into the applicability of ADS-33C for rotorcraft incorporating ACT was presented in **Paper 4**. The DLR contribution to the verification and expansion of the ADS-33C data base is described. It has been demonstrated that some of the ADS-33C criteria are not directly

applicable to rotor craft with ACT. The author proposes a new frequency domain criterion for an improved coverage of all types of pitch-roll coupling. Results also indicated an upper limit on phase delay boundaries in the bandwidth/phase delay criterion, while criteria needing further verification were identified.

New was the presentation in **Paper 5** of the design requirements, development and flight-test results of the Lavi, a light, multi-mission fighter technology demonstrator. The FCS design was presented vis à vis Flying Qualities and other requirements. A detailed account was given on how the moving-base flight simulator of the National Aerospace Laboratory NLR and a fixed-base flight simulator were used (total 835 simulation hours flown) following analytical work defining the flight control laws. Calspan's NT-33 was used to confirm the results obtained in the ground-based simulators for the high-gain landing approach phase. Problems uncovered and solutions applied are put forward in this interesting paper. The presentation was concluded with a video recording.

Session II - Flight Control Design and Analysis Methods

In the second session, a number of papers was presented which illustrated robust control methodologies, such as H-infinity optimisation and Mu-synthesis, as stand-alones or in combination with classical methodologies. Theory-oriented papers with results of numerical simulation of robust control methodologies were Papers 6, 8 and 10. Papers 7, 9 and 11 were more experiment-related. Paper 12 concentrated on lessons learned from flight-testing the X-29 flight control system. A possible drawback of some of the robust methodologies is that full-state feedback is required. Performance versus complexity trade-off will determine the best solution in each case. Concerning fuzzy control, a lack of proof is observed regarding the usability in flight control system applications. The method of dynamic inversion seems to have more and better potential, because it combines retainment of physical insight with avoidance of the gain-scheduling steps of the classical design methods. These steps are time-consuming and therefore costly.

Paper 6 is a tutorial on the H-infinity and Mu-synthesis theory. It explains notions used in robust control theory such as signal norms, induced norms and Linear Fractional Transformations (LFTs), and relates these, in terms of general control engineering, to classical control. After explaining the aims of H-infinity optimisation and Mu-synthesis, it was shown how an LFT model of aerodynamic and other uncertainties can be extracted from the state-space form. The paper gives details of an application to a realistic example and shows how stability and required handling qualities criteria are guaranteed to be met under uncertainties.

In **Paper 7**, non-linear dynamic inversion is suggested as an alternative design method for flight controls. The technique is illustrated with a design case for the super-manoeuvring F-18 High Angle-of-Attack Research Vehicle, HARV. On-board models and full-state feedback are assumed, while gain scheduling is avoided. Piloted flight evaluation on a simulator is already taking place, while flight tests are foreseen in 1994. The author of the paper states that the strength of the method stems from the capabilities of modern computer hardware and (aircraft) instrumentation which allow on-board model derivation and full-state feedback. Non-linear dynamic inversion has been successfully flight-tested on the NASA QSRA aircraft. The method is well-suited to aircraft which must be reconfigurable in a predictive way (VSTOL, STOL, etc.) over a known transition corridor.

The area of fuzzy control application in aircraft FCS design **(Paper 8)** is new. It remains to be seen what future applications could be. Fuzzy logic allows easy integration of saturation, control switching and multiple objectives. It remained unclear whether control laws for inner loops around highly-unstable elements could be designed on the basis of the principles outlined in this paper. Design attempts followed by simulation and ultimately by flight-testing should provide the required insight in the matter.

Paper 9 is a good example of the many aspects of the design challenge for the complex system of the STOL and Manoeuvre Technology Demonstrator (S/MTD) of the US Air Force. Through development, analysis and flight-testing, new technologies have been explored, such as STOL capability and enhanced combat mission performance. In the process, convergence was reached in a design process in which the best of "two worlds" (classical and multi-variable design techniques) was selected in the end. This is probably a wise approach, because checks of one method on proposed solutions from the other method can be performed in a number of cases.

In **Paper 10** the H-infinity and Mu-synthesis theories, as presented in Paper 6, are applied to generate low-order control law architectures.

In **Paper 11** it was explained how explicit model-following was employed for in-flight simulation with the Advanced Technology Testing Helicopter System (ATTHeS) of DLR. (Reference is also made to Paper 4.) Explicit model-following is useful when high operational flexibility is required due to the wide range of commanded models used for research or educational purposes. The capabilities of this versatile tool for training test pilots as well as for research are explained. A video recording showed the Hover-Position hold over a moving vehicle. Position information was derived from real-time video image analysis. Furthermore, an automatic navigation system was demonstrated.

Paper 12 emphasized the flight-testing techniques applied to an aircraft which was totally dependent on the proper functioning of the FCS. The X-29 incorporates a number of unique characteristics, while the level of relaxation of longitudinal static stability is unusually high. A detailed account was given on how, in near real-time, Fast Fourier Transfer (FFT) techniques were used to measure longitudinal open-loop frequency response characteristics for the purpose of analysing stability margins. As classical frequency analysis methods are inadequate for the lateral-directional degrees of freedom, multi-loop singular values were used. The insight gained from comparing flight-data derived values with predicted values was discussed. Two important lessons were learned from the flight-test: a) the importance of testability of an FCS and the high advantages of real-time capabilities, in flight-test data analysis, in particular; b) the critical nature of air data for highly-unstable airframes at high angles of attack.

Session III - System Integration

This session on system integration covered a wide range of technologies, such as open-loop gust-management systems, flight-testing a vortex flow control system, design of an automatic take-off and landing system for an unmanned helicopter and FCS-structural coupling experiences. A paper on the exploratory evaluation of an Integrated Flight and Power Control System for a STOL vehicle was introduced (Paper 17), though not accompanied by a written version.

The know-how about the system-integration aspects of gust-management systems is steadily being expanded by Dornier and DLR since 1976, as indicated in **Paper 13**. It is pointed out that loads from structural oscillations (wing bending and fuselage bending) must be counteracted using fast actuators for the DLC surfaces and elevators. It is also pointed out that specific forces in the horizontal degree of freedom associated with DLC surface deflections are important for passenger comfort and cannot be ignored. The authors believe that turboprops using Full Authority Digital Engine Control (FADEC) may be able to generate the required longitudinal compensating forces through variations in the pitch of the propeller blades. It is proposed by the authors that the potential of ACT can be used to develop, in future commuter aircraft, an integrated "wind management" system to manage relevant wind effects from gust and turbulence alleviation up to windshear and elastic mode control.

Vortex Flow Control (VFC), discussed in **Paper 14**, is a method to improve the controllability of aircraft when the fuselage is blanking the tail at large angles of attack. The X-29 was used for proof of the concept. A transparent transition had been experienced between the yawing moment obtained with the rudder and the yawing moment obtained by VFC. In order to use forebody blowing to its best advantage, i.e. roll coordination and side-slip management, it was clear that the vortex flow control must be blended with the rudder over the entire operating envelope of the aircraft . Apart from its technical contents, the paper was also of interest for its attention to the project-organisational aspects.

The control system for the unstable roll-and-pitch axis of an unmanned helicopter is another example of ACT. The outer loops incorporated in the automatic flight control system for such a helicopter were outlined in **Paper 15**. An FCS design developed along "classical" methods with gain scheduling was successfully flight-tested on a moving ship-deck simulator, as was shown in an interesting video recording. One of the interesting features was the logic applied in the activation of the various modes for automatic take-off, automatic landing and touchdown.

Paper 16 (as well as paper 18) gave tutorial accounts of a wide range of "aero-servo-elasticity" phenomena. Paper 16 concentrated on solving the problems related to "flight control system/-adverse structural coupling", resulting from interactions of sensors/computers/actuators with the aero-elastic aircraft in case ACT is applied to realize overall aircraft performance requirements such as mass, size and aerodynamic efficiency. The experience gained at BAe Warton from the early sixties (TSR 2) through the mid-eighties (EAP) is delineated. Refining the "flight control system/adverse structural coupling" design and clearance requirements form the goal of the

various developments described in the paper. It is concluded that substantial improvements are needed in the modelling of structural modes, as well as prediction of the unsteady aerodynamic forces of lifting surfaces and aerodynamic control surfaces to ensure, in an efficient manner, freedom of "flight control system/adverse structural coupling".

Only very limited information became available concerning **Paper 17**, as its author was unable to attend and one of his colleagues at Lockheed's gave a short introduction on the basis of a handout of the figures of the paper.

Paper 18 is aimed at a discussion of mechanisms to achieve structural benefits through the use of ACT in flexible aircraft. Two groups are distinguished here: a) changing the external forces acting on the structure in order to reduce the stresses in the structure, and b) changing the structural system properties, in order to improve modal damping and dynamic stability. It is observed that hardly any in-flight experience is available, with regard to flutter-suppression systems. It is stated that, from the very start, the negative influence of ACT on fatigue life of an aircraft should be considered very seriously. In order to take full advantage of electronic flight control systems, a multi-disciplinary design approach covering the structural implications of ACT is already required in the design stage. Although such an approach is still under-developed, reassessment of traditional views in aircraft design is taking place and making room for the acceptance of "aero-servo-elasticity" aspects in the initial design.

Session IV - Implementation Experience: Handling Qualities and Flight Control Performance

Surveying the papers presented in Session IV, it is concluded that handling qualities aspects, including a number of interesting cases of pilot-induced oscillations, were covered well. A large percentage of the papers presented flight-test results, some explaining in addition how a flight-test programme had evolved over a period of time. The tactical utility of novel flight control system concepts was treated in two presentations.

Paper 19 may be considered as tutorial on the topic of thrust-vectoring. It covers a description of the F-16 modified with the vectoring nozzle, FCS development, flight-test approach, flight-test results and tactical utility assessment. A video recording with high-quality 3D graphics, based on recorded flight data was very enlightening. True, post-stall manoeuvring was demonstrated with a near-production, thrust-vectoring nozzle in an operationally representative environment.

The operation-oriented **Paper 20** focused on a particular aspect of ACT: how to use the FCS design freedom for optimizing the performance of a given system under special operational circumstances. A "catapulting" mode has been developed for the Rafale, using shore-based and carrier-based catapults, as was shown on a video recording. In this interesting presentation, the importance for design purposes was stressed of accurate modelling of the aircraft itself, the aircraft-carrier deck interface, carrier dynamics, wind, gusts and the sea state.

Paper 21 presented an account of developments regarding an autopilot for the AMX. In the paper, the following aspects are dealt with: design to specifications, system development and clearance before flight and flight test. It explained the peculiar problems resulting from outer-loop (autopilot) and inner-loop (basic stabilisation) interaction in the design of a similar system for the EF 2000. The autopilot will have altitude, pitch-angle and bank-angle hold modes. Acquire modes will comprise altitude and heading, while in addition an "auto-climb" mode will be available.

The Experimental Aircraft Programme (EAP) presented in **Paper 22**, may be considered as a demonstrator, using the experience of the predecessor programme Jaguar FBW and preparing for the EF2000. This paper is a thorough treatment of the philosophy and method used to design the flight control laws and the evolution of the FCS through the life of the EAP programme. Carefree handling and complete absence of pilot-induced oscillations were impressive aspects to all of those involved in the evaluations of the system. The manipulator used for flight control, was a simple spring/damper system. The selected values for the stick travel, the force levels and damping characteristics were considered important parameters in avoiding pilot-induced oscillations. Three different phases of the evolving flight control system are described clearly, together with their associated flight tests.

As a result of the growing number of pilot-induced oscillation-related incidents/accidents in aircraft with digital flight control systems, the US Air Force Materiel Command formed a technical review team to investigate the matter, as described in **Paper 23**. The major flaws in the flight control development process, as perceived by the review team, are described in the paper. Three

noteworthy recommendations were presented: a) enhancement of flying qualities research programmes to improve the criteria and analysis methods available; b) incorporation of the "best practices" related to the subject area in the reference tool used by USAF acquisition managers, [clearly, certain lessons are never learned, as the authors had to stress the use of full-up ground simulation and in-flight simulation to assess handling qualities and PIO-tendencies]; c) establishment of an integrity approach for flight control development, similar in nature to formal programmes established for structures and propulsion. The intent of such a programme would be in each stage of development to "proceed only when resistance to the PIO problem is proven". This paper may be considered as an appetiser for the Workshop on PIO, which was held following the Symposium.

Valuable experience in the area of the pilot-aircraft interface for low-speed flight control, handling and cockpit displays is gathered in the two-seat in-flight STOL simulator (VAAC) project sponsored by the UK Ministry of Defence (**Paper 24**). An integrated flight and power-plant control system using ACT will be an essential element for future STOVL aircraft. The paper deals with the design, development and flight-testing of an advanced pitch-flight control law, for this category of aircraft in transition from wing-borne to jet-borne flight, hovering and vertical landings. Flight-testing the VAAC Harrier has shown that the two-manipulator (LH: fore/aft, RH: up/down) and one-manipulator solutions (RH: up/down plus thumb switch for fore/aft control) resulted in a large reduction in pilot workload, as compared to the basic aircraft's three manipulator arrangement. This was demonstrated in a video recording of a transition from hovering to a vertical landing.

Since **Paper 25** was presented as a substitute for a withdrawn paper, no written handout was available. In the presentation, a comprehensive overview was given of this first "international" version in the (US) X-series of projects. A low-cost solution was presented for effectuating thrust-vectoring (a tacked-on set of thrust-vectoring paddles), as well as the way the FCS takes care of velocity-vector rolls at higher angles of attack.
A video recording was used to demonstrate the impressive tactical advantage measured in 150 combat sorties of a total of 400 flights executed, so far. It was indicated that the concept of the "quasi-tailless" aircraft is under evaluation using the X-31. To this end, the rudder is used to destabilize the aircraft in yaw, while the thrust vectoring is used to re-instate stability. Through exploitation of thrust-vectoring as stabilizer in yaw, an additional operational advantage may, in principle, be obtained.

Paper 26 presents an overview of advances in flight control design made by Boeing and the way these advances are applied in the production of the V-22 Osprey tilt rotor and the RAH-66 Comanche scout/attack helicopter. The paper progresses in a systematic manner from design requirements to flight control law design, cockpit manipulator integration, pilot interface with the multi-mode control laws to integration of flight control, engine control and fire control systems. Partitioning of control laws over primary flight control systems and automatic flight control system forms the basis for explicit model-following control laws. Integration of these control law functions, along with advanced cockpit displays and controls, engine control and fire control systems have proven to be the key in providing a total vehicle management system capable of meeting future military requirements. The authors predict that in the near future, integrated design approaches will simultaneously optimize handling qualities, manoeuvre control, elastic stability and airframe and rotor structural loads limiting characteristics.

Paper 27 was presented as a substitute paper; no printed version of the presentation was available. In the presentation it was indicated that three different design methodologies were followed to develop a practical controller for the model-following NRC Bell 205 airborne simulator. It is hoped that a printed version of this interesting presentation will be included in the Conference Proceedings.

In conclusion of the symposium, **Paper 28** went into the flying qualities and flight control systems of transport aircraft equipped with electrical FCS, as seen by Aerospatiale. Before going into some of the differences between the Airbus A340 and A320, developments over the past 25 years were surveyed. Starting with the Concord, with full-time electrical FCS with analog computing, via the Airbus A310 with digitally-controlled spoilers, to the first transport with a closed-loop digital primary FCS, the A320, some interesting features of each were presented. The rationale was given for the differences in FCS mechanisation for the Airbus A320 and A340: the main points are associated with the compensation effects of the more flexible structure of the A340, its design for long-range ("minimum drag") and the inherent limitations in take-off performance (four-engine

aircraft). With this interesting paper the technical sessions of the symposium were concluded.

Round Table Discussion

During the round table discussion, held at the end of the fourth day of the symposium, a number of noteworthy observations were made concerning the symposium itself as well as suggestions for future directions. The most important observations regarding possible future directions are listed under five headings below:

1 Data base for Flying Qualities Specifications; quality/expansion - There was a general consensus that the required improvement of the Specifications and Requirements for Flying Qualities of ACT aircraft can only be obtained by expanding and refining the data base through systematic research efforts using ground-based and in-flight simulators. A range of controlled aircraft states and a (wide) range of manipulator/feel system characteristics should be incorporated. The capability of ACT aircraft to exhibit characteristic response shapes entirely different from classical aircraft, should be recognized in the specifications. Proper task selection/description should be developed in this type of research. Level 1 Handling Qualities should be a mandatory design objective, not just a recommend one.

2 Modern Control Theory - It seems an appropriate time to try and integrate the experience obtained with the modern control theory by teams designing the FCS for unstable aircraft in recent demonstrator and prototype projects. The papers forwarded in the symposium have left the impression that there are advantages in certain classes of design challenges, but it is evident that in some instances the attempts to apply the modern control theory have failed. An AGARD Working Group may be a means to improve insight in the matter.

3 System Identification - The need to improve the availability of comprehensive system-identification routines cannot be stressed enough. In consonance, the need was mentioned to select the proper manoeuvres to excite the aircraft for identification purposes. The difficulties associated with system identification in the non-linear high angle-of-attack range should be tackled.

4 Experience and Loss of Experience - A frequently expressed concern was the high probability that invaluable experience gained in the design of flight control systems for unstable aircraft could be lost. This fear is based on the reduced number of new aircraft projects expected and the increasing time which will elapse between projects within one Industry. Two ideas to fight this possible loss of experience were forwarded. The first was the production of a form of Handbook encompassing existing knowledge as well as a narrative of the evolutionary introduction of ACT over the past 25 years. Particular attention should be given to describing the proper analysis methods to be used in validating the designs. The second was the plea for "demonstrator programmes" (specification, design, analysis, system integration and implementation) to be executed to keep design teams in existence, while advancing the state of the art.

5 Oscillatory Aircraft-Pilot Coupling - As stated earlier in this report, the prediction of "essential, non-linear pilot-aircraft oscillations with transition" will not always be possible. A total system (pilot plus aircraft) "integrity qualification" as regards PIO should be mandatory. A systematic approach should be stressed towards clearing the design with all known tools (including manned simulation) before first flight. In the flight-test schedule, ample time should be reserved for the in-flight search for the "black holes" through excitation of the aircraft in various flight conditions. Pilot inputs should be applied which deviate appreciably (much more aggressive) from those in standard operational use. [More detailed observations/recommendations resulting from the Workshop on P10 held after the symposium are included elsewhere in the underlying document.]

5 CONCLUSIONS

- The intended scope of the symposium was very well covered by the twenty-eight presentations given.

- Judging by the number of participants (159), the level of interest in the symposium was high.

- Certain elements of the ACT system-development process, such as specifications, design, implementation and verification, are not yet fully matured.

- There is a lack of a set of specifications covering all handling and system stability aspects (including PIO) as well as of the tools to verify/-validate the system as designed against the specifications. It is clear that system identification forms a critical tool in this respect.

• Either the modern or classical control system design approach will work, when in the hands of competent and experienced practitioners. The material presented at the symposium indicated that a certain degree of maturity has been reached with respect to control law design methodology.

• ACT using a thrust-vectoring nozzle has clearly led to fully-controlled post-stall manoeuvring.

6 RECOMMENDATIONS

• Persons who, within their organisation, are responsible for both quality of the theoretical background and experience of FCS designers, should look for a balanced knowledge base in classical as well as modern control system theories.

• An AGARD Working Group might be the proper means to consolidate valuable insights gained during recent demonstrator and prototype projects in the areas of handling of the specifications, design methods (particularly control law design methodology used for the FCS of unstable aircraft), integration and testing.

• In five years time, the structure of this symposium could be used by the Flight Vehicle Integration Panel as a starting point for the organisation of a comparable, valuable exchange of information.

ACTIVE CONTROL TECHNOLOGY AND INTERDISCIPLINARY INTERACTIONS

Duane McRuer
Chairman
Systems Technology, Inc.
13766 S. Hawthorne Blvd.
Hawthorne, CA 90250
USA

1.0 SUMMARY

The exploitation of Active Control Technology in aircraft entails a satisfactory balance among aerodynamic, structural, propulsion, and automatic and manual control disciplines. To achieve such a balance requires broadened perspectives, greatly enhanced interdisciplinary understanding, and an appreciation for the strengths and weaknesses within the individual disciplines. This paper presents two examples to illustrate some of the more detailed aspects of interdisciplinary interactions arising in the application of active control technology. Because dynamic interactions are inherently vehicle-specific, the first example uses a very large helicopter which inherently exhibits many interdisciplinary interactions. With manned vehicles in which the pilot plays an important active role as a controller, interactions between the pilot and the effective aircraft dynamics can be central. The second example treats one such interaction, oscillatory aircraft-pilot coupling or pilot-induced oscillations, which are an all-too-common accompaniment of some advanced actively-controlled systems.

2.0 INTRODUCTION

The major promises of aircraft "Active Control Technology" are to enable novel capabilities and achieve improved "performance" (in the broadest sense) levels. The traditional objective of the systems integration process is to make individually designed subsystems work together on an aircraft; that is, to ensure compatibility and minimize adverse interactions. Active Control Technology permits, even demands, a changed perspective. As a systems integration enterprise Active Control Technology is intrinsically concerned with establishing a dynamic synergism among the technical disciplines of aerodynamics, structures, propulsion, controls and, in manned aircraft, pilot dynamic behavior. This is accomplished in principle by co-operative consolidation and interaction of functions and subsystems; it is effected by concurrent multi-disciplinary designs in which the technical disciplines are deliberately made highly interactive dynamically. Thus in practice Active Control Technology must deal with the ubiquitous presence of dynamic interactions between the technical disciplines at their cutting edges.

While the creation and exploitation of favorable interactions are the desired ends, there is no guarantee that they will not be accompanied by other interactions that may be less than favorable. To achieve a satisfactory balance requires broadened perspectives, greatly enhanced interdisciplinary understanding, and an appreciation for the strengths and weaknesses within the individual disciplines. The purpose of this paper is to discuss two examples that illustrate some of the more detailed aspects of interdisciplinary interactions arising in the application of active control technology in aeronautics. Because dynamic interactions are inherently vehicle-specific, the first example will consider a very large helicopter to provide a concrete illustration of some of the details that must be appreciated. With manned vehicles in which the pilot plays an important active role as a controller, interactions between the pilot and the effective aircraft dynamics can be central. Favorable aircraft-pilot couplings are the goal; unfavorable ones the scourge. A notable unfavorable aircraft-pilot coupling results in an oscillation, which has generally been referred to as a pilot-induced oscillation (PIO). Because PIO is an all-too-common accompaniment of some advanced actively-controlled systems the second example will introduce enough of the subject to permit some connections with ACT.

3.0 HELICOPTER DYNAMIC INTERACTIONS

Figure 1, adapted from Ref. 1, shows the rolling-velocity-to-cyclic transfer function of a very large modern helicopter. The dynamics shown are those of the effective vehicle as presented to the pilot. They thus include the rigid body and lower-frequency flexible modes and other characteristics of the helicopter, the control system, etc. The values of the inverse time constants and undamped natural frequencies are defined by the break points in the asymptotic Bode plot. The amplitude ratio Bode plot shows several resonances and anti-resonant conditions directly connected with quadratic poles and zeros.

Also shown in Figure 1 are data points from which the model transfer function was derived. These were obtained from an extraordinary and extensive series of

Paper presented at the Flight Mechanics Panel Symposium held in Turin, Italy, from 9-13 May 1994.

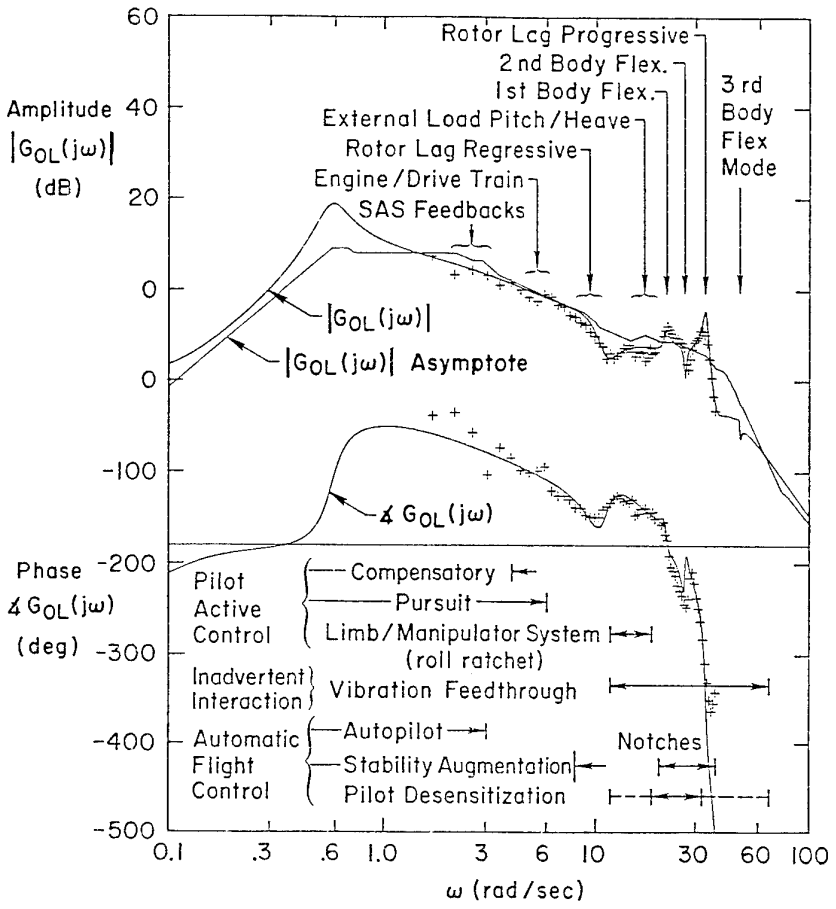

Figure 1. Roll Rate to Cyclic Transfer Function of a Large Modern Helicopter

flight and ground tests using a variety of forcing functions including transient inputs, single and sums of sinusoids, and frequency sweeps (Refs. 2-3). The model transfer function determined for rolling-velocity/cyclic is not simply a best fit of the particular data shown. Instead it was developed based on compatible identifications for all axes and measured state variables of the helicopter (Ref. 2).

The Figure 1 data exemplify the sort of information needed to define the effective controlled element. It exhibits the many dynamic modes involved. To get to this level of thorough, yet still preliminary, understanding of system interactions relies, for openers, on modelling, identification, and physical system measurement disciplines which themselves constitute major players in interactive disciplinary systems technology.

Let us now disclose just what kinds of interactions underlie this dynamic model. The domain of conventional aerodynamic stability and control is reflected in the rigid body modes of the helicopter, shown in Figure 1 as the lateral hovering cubic, modified at mid-frequencies by the stability augmentation system (SAS). The rotor dynamics are present in the rotor lags, regressive and progressive. Structural dynamics contribute to the action by way of the first, second, and third body flexible modes. The propulsion system makes a minor contribution by introducing a dipole pair due to the engine drive. In fact, several of the modes are represented by dipole pairs that nearly cancel in this particular transfer function, although they remain important elements in other degrees of freedom, and can be sources of surprises when the dipoles shift or separate. Even the external load dynamics enter the picture: first by adding an additional pitch/heave oscillation due to the load bouncing on cables and, second, by the general raising or lowering of the aircraft gain by virtue of the need to balance the load with collective.

The major conclusion to be drawn from Figure 1 is that there are extensive interactions between a large number of phenomena that have diverse origins and that untangling this big mess demands further interactions among many cooperative disciplines.

So far, nothing has been said about placing this messy set of dynamics under control. In this respect, there are

two kinds of control: manual control by the pilot and automatic control with stability augmentation and autopilot.

From the pilot's perspective, there are many different modes of concern, some active and others inadvertent. The frequency ranges of these pilot-centered phenomena are indicated in Figure 1. The lowest frequency activity corresponds to closed-loop manual control, which can be characterized in terms of compensatory and pursuit control models (Ref. 4). At somewhat higher frequencies (above 10 $rads^{-1}$), biodynamic coupling can occur (Ref. 5). This is dominated by the dynamics of the combination of the pilot's neuromuscular system and the manipulator (stick) and feel system. The pilot-aircraft coupling phenomenon can take the form of high-frequency (2Hz to 3Hz) limit behavior (Ref. 6).

Finally, the pilot may participate as part of a 'vibration feed-through' phenomenon that extend to even higher frequencies. Typically, this results when structural mode or other vibration at the pilot's station is transmitted through the pilot to the stick. Depending on a variety of seating, constraints, and manipulator design factors, this biomechanical feedback can amplify structural mode response (Ref. 7). Control system elements that are intended to deal with structural modes, typically notch and/or lag filters, may simply replace one part of the manual control problem with another. In this case, filtering to attenuate the structural mode response may result in effective time delays that are unacceptably large for manual closed-loop control (Ref. 8). Putting all these factors together, a very wide range of frequencies are involved: from near zero up to 10Hz.

The frequency domain interactions for the stability augmenter and autopilot are simpler to define. Even here the stability augmenter, as a high bandwidth controller, can be interfered with by higher frequency modes which it is not intended to modify. The notch and/or low-pass filtering, which is essential to stability and viability of the SAS/autopilot/manual control system, represent yet other interactions as well as a need for dynamic systems integration.

An automatic system role on some helicopters is the process of pilot desensitization; that is, processing the pilot's inputs so that high frequency pilot output, either of a limb/manipulator active nature or of an inadvertent vibration feedthrough, does not excite the malevolent tendencies of the nasty high-frequency modes.

Superimposing the regimes of control action over that of the vehicle dynamics reveals the coincidence of the two. It is easy to conclude that there are two great challenges: (1) quantitatively understanding the extensive composite dynamic entities and their interactions and, based on this understanding, (2) integrating and balancing the dynamic design of the several systems involved incorporating both inanimate and animate elements.

4.0 OSCILLATORY AIRPLANE-PILOT COUPLINGS

4.1 Introductory Remarks

A particularly unwanted interaction between animate and inanimate elements in aeronautics is the phenomenon of pilot-induced oscillation (PIO), which is one form of unfavorable airplane-pilot coupling. These fascinating and complex pilot-vehicle interactions have, in one form or another, been around since the Wright Brothers. On an ad hoc basis both minor and severe PIO incidents have been studied, suspects and causes ascribed, and corrective actions taken; and aperiodic generalized experimental and analytical efforts have led to increases in understanding. A lore has developed from these steps, and considerable attention is devoted in new designs to avoiding or alleviating those aircraft dynamics and control system characteristics which have been charged in the past as sources or accomplices. As a consequence, many of the "old" factors associated with PIO occurrance no longer exist in modern aircraft. Yet PIOs continue to persist and, in fact, grow in variety and complexity as aircraft systems otherwise advance. Recently, for example, the confluence of some highly visible accidents (e.g. the YF-22 and JAS 39 PIOs) has captured a great deal of attention.

Because of this current and continuing interest in what is surely THE senior flying qualities problem, this conference week will end with a day-long discussion of PIOs, and some of the conference papers also address this subject. Accordingly, I will attempt here only to focus on some aspects of Active Control Technology which, if not handled effectively, can potentially contribute to severe PIOs.

The provision of "good" flying qualities in precision, high urgency tasks requiring very high gain closed-loop piloted control is an important and primary factor in minimizing the probability of PIOs. But this alone is not enough. Detailed investigations of the causes of specific severe PIOs (e.g., Refs. 9 - 14, and many other references cited in Ref. 9) reveal that many factors are needed to explain the phenomena, especially for the severe PIOs of most interest here. These include: triggering events, pilot adaptation, and the impact on closed-loop piloted control of such nonlinear effects as actuator rate and position limiting, hysteresis, transitions in effective vehicle dynamics as a function of pilot input amplitude, etc.

4.2 Pilot-Aircraft System Oscillations — Minor Wiggles and Severe PIOs

There are several varieties of pilot-vehicle system oscillations, with consequences ranging from annoying aircraft motions leading to poor task performance to dramatic, unforgetable, traumatic, and even catastrophic

oscillations. In all cases, pilot-induced oscillations involve the pilot's active participation in a feedback system. That is, the pilot's dynamic behavior is conditioned by the dynamic behavior of the "effective airplane" with which he interacts. The "effective airplane" dynamics comprise aircraft rigid body and lower frequency flexible modes, manipulator(s) and manipulator restraints, actuation, stability and control augmentation, and "effective display" characteristics. When this combination is consolidated into a single dynamic entity, the "controlled element", characterized by a describing function $Y_c(j\omega)$, the presence of an oscillation demands that

$$Y_p(j\omega)Y_c(j\omega) = -1 \qquad (1)$$

where $Y_p(j\omega)$ is the describing function of the pilot. While this is a necessary and sufficient condition for an oscillation, it is not the only condition for the oscillation to be a severe PIO. Instead, the oscillation may be a very temporary, easily-corrected, low-amplitude bobble often encountered by pilots when getting the feel of and used to a new configuration — basically a learning experience. It can happen on every airplane, and has undoubtedly been experienced by every pilot at one time or another. On the other hand, a fully-developed, large amplitude oscillation with near or actual catastrophic consequences is a chilling and terrifying event, even though it obeys the same general law (Eq. 1). This kind of oscillation is not, and cannot be permitted to be, a common occurrence. It must be avoided for reasons of safety as well as operational performance. Accordingly, primary concern here is with the large amplitude, potentially catastrophic version, and this is what we mean by a severe PIO.

Both pilot and controlled element properties are prime elements in Eq. 1. In the simplest cases where the pilot-aircraft coupling acts like a predominantly single-loop system, Eq. 1 creates a useful duality in that either pilot or effective vehicle dynamics can be used to quantify matters. It is generally easier to quantify the effective airplane dynamics than the pilot behavior. Further, these dynamics are subject to adjustment by control engineering means, aircraft configuration modifications, etc. Consequently it is convenient when appropriate to emphasize the concretely known effective airplane dynamics in considering criteria and procedures (although the fundamental closed-loop nature of the phenomena must never be forgotten). But there are problems even at this very basic level — just what particular Y_c is the important entity in a given PIO? For example, in a longitudinal PIO — is Y_c the transfer characteristic relating pilot output to attitude, to normal acceleration at the pilot's location, to some variable on a display, or ...what? And, what is the pilot's output (input to Y_c) — is it force, position, or a composite? Just how much of the limb-neuromuscular-manipulator subsystem is involved?

Further, while PIO's often start with fairly low amplitudes, which can adequately be treated with small perturbation linear theory, the severe ones can become very large. In fact, almost all the PIO time history records available (see e.g. Refs. 9 - 14) show surface rate limiting (and sometimes stick or surface position limiting as well) in the fully developed oscillation. Rate limiting in these instances has had two major effects — adding to the effective lag in series with the pilot, making the effective aircraft dynamics worse; and limiting the ultimate amplitude of pilot-vehicle system oscillation, perhaps as a lifesaver!

Particularly insidious nonlinearities lead to a sudden change in effective aircraft dynamics in the midst of a high-gain urgent task. Such sudden "transitions" include changes in effective vehicle dynamics due to sudden configuration modifications (such as afterburner light-off, engine unstart, stability augmenter failure, asymmetric stores release, etc.) and changes driven by pilot output-amplitude shifts from small (e.g. stick motions around trim which are largely contained within a control system hysteresis band) to large (e.g. pilot attempts to counter perceived major upsets). Effects of such pilot-amplitude-sensitive effective controlled element "transitional changes" range from ancient PIOs in which the primary manual control system appeared in several guises (e.g. bobweight-in/bobweight out in the T-38 PIO described in Ref. 10) to many of the most modern PIOs in which actuator rate limiting, surface and/or SAS position limits, nonlinear stick shaping of pilot commands, various fader combinations, etc. interact to create a confounding variety of input-amplitude-sensitive effective vehicle dynamics. These are an almost unavoidable consequence when Active Control Technology is fully applied.

4.3 Historical Perspective

A study of aeronautical history reveals a remarkably diverse set of severe PIOs. Although we will subsequently propose a different classification scheme for PIOs, it is useful here to form groups based on two primary features: the number of aircraft control axes which are fundamentally involved; and the frequency of the closed-loop aircraft-pilot couplings, which can range from about 1/2 to 3 hz. These distinguishing features serve to divide PIO's into four different groups. Each group can be exemplified by well-known incidents of aircraft-pilot couplings, all notable or even celebrated, and some catastrophic.

4.31 *Essentially Single Axis, Extended Rigid Body Effective Vehicle Dynamics*

Most of the PIO research to date (and nearly all the attempts at criteria development) has been directed to effective aircraft dynamics characteristic of rigid body longitudinal or lateral-directional properties. Higher frequency dynamics representing the control actuators, effects of SAS dynamics, digital system time delays, etc.

have been incorporated, usually approximated as parts of an effective time delay or some equivalent. For many PIOs such approximations are both appropriate and adequate. Some specific examples of severe PIOs where the key effective vehicle dynamics are of this "extended rigid-body" variety include:

Longitudinal PIOs — Extended Rigid-Body

XS-1 PIO during gliding approach and landing
XF-89A PIO during level off from dive recovery
F-86D PIO during formation flying when pulling G's
F-100 tight maneuvering
F-101 aft CG
F-4 low altitude record run second pass
X-15 approach and landing
Sea Dart post-takeoff destructive PIO
Shuttle ALT-5 during landing approach glide
Dryden FBW F-8 during touch and goes
YF-22 PIO after touchdown and wave off

Lateral-Directional PIOs — Extended Rigid Body

B-52 Roll PIO while refueling
B-58 Lateral-directional control-associated crash
M2-F2 Lifting Body Lateral-directional PIO
Paraglider Research Vehicle (Parasev) Lateral rocking PIO during ground tow

4.32 *Essentially Single Axis, Extended Rigid Body with Significant Manipulator Mechanical Control Elements*
PIO's in this group are similar to those described above, with the addition that the primary mechanical control system plays a major role. The aircraft included are of more traditional design, and may incorporate such elements as single or dual bobweights, various artificial feel devices, etc. Some older aircraft or modern aircraft with simpler primary controls have tab or servo-tab controls, power boost rather than fully powered surface actuators, etc. System friction and hysteresis effects can be very important, since they tend to create two different sets of effective airplane dynamics (e.g. corresponding to stick free and stick fixed, or small-amplitude and large-amplitude pilot inputs). In these systems the aircraft dynamics are still extended rigid body, but the dynamics of the primary control and artificial feel system also enter as important contributors. In the simplest situations, the effective airplane dynamics differ primarily as a function of the pilot's output amplitude and the pilot's inability to adapt to large changes from pre- to post-transition effective airplane dynamics is central to the PIO. In some cases the limb-neuromuscular-manipulator system dynamics are major factors, either as a simple limb-bobweight effect, or as a much more elaborate dynamic entity. Past examples of severe PIOs in this group involved the A4D-2, T-38, and F-4.

4.33 *Multiple Axis PIO's, Extended Rigid Body*
Of all the essentially rigid body PIOs these are by far the most interesting, dramatic, and least well understood. Perhaps best known and surely the most widely viewed PIO in this category was the remarkable unintended "first flight" of the YF-16. Descriptions of the participating events are given in Refs. 9 and 13. As remarked by Einar Enevoldson, a noted retired NASA Dryden test pilot, "3-D PIOs are extreme, and are present in many aircraft under asymmetric conditions. Besides the AD-1, another example was a PIO in a F-14 at large sideslip, which resulted in a departure which was very difficult to recover." Thrust-vectoring aircraft, damaged aircraft, and aircraft with asymmetrically-hung stores, are also subject to unusual asymmetries. For aircraft with elevon or ailevator controls, which can create conflicts between axes, the multi-axis PIO phenomenon can be further complicated by differential position and/or rate limiting.

Known examples of severe PIOs in this group include the X-5, YF-16, Shuttle ALT-5, F-14 at high angle of attack with some sideslip, and the AD-1 (Oblique Wing).

4.34 *PIOs Involving Higher Frequency Modes*
A downside of the trend for more highly integrated aircraft using active control technology, and especially aircraft that are flown unstable, is the insurgence of the lower frequency flexible modes into the frequency range of stability augmentation and pilot control. For these vehicles the extended rigid body characteristics are not sufficient or, sometimes, even relevant. Instead, the lower frequency flexible modes enter and the pilot's neuromuscular dynamics play key roles.

Cases in which the limb-neuromuscular dynamics are central to pilot-vehicle oscillations are fairly common even with extended rigid body or extended rigid body plus mechanical controls. The roll ratchet phenomenon is a notable example (e.g. Refs 6, 15). Here the characteristic frequency is set primarily by the limb-manipulator combination, tending to range from 2 - 3 hz. This type of oscillation is probably not catastrophic in the safety sense, although it can severely limit the airplane's maneuvering performance.

Pilot interaction with lower frequency flexible modes can be severe. Their possibility has been of concern in some circles in connection with the NASP (Ref. 8), and may be prominent in the High Speed Civil Transport (Ref. 16). Of the documented cases to date, the flexible mode coupling present on the YF-12 (Ref. 12) was relatively mild while the couplings observed with a very large helicopter were quite the opposite. These severe interactions, in fact, are extremely important harbingers of things to come as flexible modes become significant elements in aircraft-pilot coupling.

5.0 PIO CATEGORIES

5.1 Factors to be Considered

Several source elements enter into any severe PIO. These are discussed at some length in Ref. 9, listed under the headings: "Effective Aircraft Dynamic Characteristics"

(Fig 10, Ref 9); "Pilot Aberrant-Behavior Characteristics" (Fig. 9, Ref 9); and "Precursor/Trigger Mechanisms/Pilot Mode Shifters" (Fig. 18, Ref. 9).

Pilot aberrant behavior is the source factor which distinguishes the severe PIO problem from most aircraft design problems. The differences reside in those uniquely human properties related to the enormously adaptive characteristics of the human pilot for which there are no parallels in an automatic flight control system. First, different pilot behavior patterns are associated with different PIO properties. For example: compensatory behavior and low-frequency neuromuscular dynamics with PIOs in the 2-4 rad/sec range; synchronous pilot (pure gain) dynamics with PIOs in the 1-2 hz range and with flexible mode interactions; more complete limb/neuromuscular/manipulator dynamics with PIOs in the 1-3 hz range, etc. Second, pilots exhibit peculiar transitions in the organizational structure of the pilot-vehicle system. These transitions can involve both the pilot's compensation (e.g. when a pilot adapted to high-gain compensatory tracking/regulation suddenly shifts to a "synchronous" pure gain mode) and the effective architecture of the pilot's control strategy (i.e. what variables the pilot senses and processes).

The last source element, "Triggers" et al is described below:

5.2 Triggers as Central Features in Severe PIOs

An attribute which is a central and complicating feature of severe PIOs is an initiating event, upset, or trigger which starts the sequence. These come in many varieties (see Ref. 9) which are difficult to generalize. A few typical examples for PIOs already cited are:

T-38 — Failed stability augmenter; disconnect sequence created a major upset (Ref. 10)

B-58 — Failed stability augmenter, creating sideslip and subsequent rolling and, simultaneously, unfavorable roll-control dynamics;

YF-16 — Several undesired inputs coupled with limiting effects (see Ref. 9)

ALT-5 — 30 mph over-speed on very first runway approach; speed brake actuated, nosed down to make desired impact point; pilot plus transient upset basic approach.

DFBW
F-8 — Major unexpected change in effective controlled element dynamics (see Ref. 9)

YF-22 — Afterburner start, pilot input, plus mode transition circuitry, faders, etc. interacted to create a major upset (see Ref. 14)

Note that these examples are themselves uncommon events, which probably goes a long way towards explaining the rarity of severe PIOs.

Upsets can also arise from shifts in the pilot's organization of behavior (see Ref. 9 for a detailed discussion), or from the surrounding environment. The latter category includes gusts, wind shears, etc. as well as control system shifts acting on the airplane. It also includes changes which enter the pilot-vehicle system via the pilot, such as drastic evasive maneuvers, as well as changes in the pilot's goals, attention levels, and tension which reflect into higher pilot gains or control reversals.

5.3 Suggested Pilot-Behavior-Theory-based Categories for PIO

Because of the diverse considerations entering into oscillatory aircraft-pilot couplings several kinds of classification schemes could be proposed. One such was used above in the "Historical Perspective" general discussion of mild and severe PIOs. The detailed studies (e.g. see Ref. 9 - 13) of some "Famous PIOs" relied on pilot behavioral models (Refs. 4, 17) and closed-loop analysis procedures (e.g. Ref. 10, 18) to elicit understanding and rationalization of the phenomena and their associations. Then, in some cases, pilot-vehicle behavioral models were used as a basis for designing and assessing changes to the effective vehicle to allieviate the PIO potential.

The classification scheme suggested here follows from the successes of this past experience. It divides the world of potentially severe PIOs into three categories based on utilization of existing pilot behavior models and analysis techniques. These are described below:

Category I — Essentially Linear Pilot-Vehicle System Oscillations — The effective controlled element characteristics are essentially linear, and the pilot behavior is also quasi-linear and time-stationary. The oscillations are associated with high open-loop system gain. The pilot dynamic behavior mode may be pursuit, compensatory, precognitive, or synchronous (Ref. 4).

In this category no significant nonlinearities are involved in the controlled element dynamics (hence there is just one effective Y_c/K_c) and no behavioral mode shifts occur in the pilot (so Y_p/K_p is fixed). There may be changes in either the pilot or the controlled element gain, so such things as nonlinear stick sensitivity or pilot attention shifts may be admissable as features consistent with Category I. The pilot-vehicle oscillations in this category may be casual, easily repeatable, readily eliminated by loosening control (lowering pilot gain), and generally non-threatening. On the other hand, with a major triggering input the oscillations may be quite severe even though nonlinearities are not involved.

For a given pilot cue structure, analyses of Category I oscillation possibilities can reveal the oscillatory frequencies consistent with a presumed type of pilot behavior (e.g. compensatory or synchronous), pilot gain levels, nominal high-gain pilot-vehicle system bandwidths, various sensitivities to effective vehicle characteristics, etc.

Much of the flying qualities generic data base that can be associated with the reduction of PIO potential has dealt with the situations covered by Category I. Consequently, the occasional presence of mild PIO tendencies in tight tracking tasks can be minimized by simply providing "good" flying qualities as defined in MIL-STD-1797. Thus, appropriate criteria for Category I PIOs are generally tantamount to those for Level 1 flying qualities, with emphasis on those criteria of most importance in high-gain closed-loop piloting tasks and demonstration maneuvers.

Category II — Quasi-Linear Pilot-Vehicle System Oscillations with Surface Rate or Position Limiting — These are severe PIOs, with oscillation amplitudes well into the range where actuator rate and/or position limiting in series with the pilot are present as the primary nonlinearities. The rate-limited actuator modifies the Category I situation by adding an amplitude-dependent lag and by setting the limit cycle magnitude. Other simple nonlinearities (e.g. stick command shaping, some aerodynamic characteristics) may also be present. These are the most common true limit-cycle severe PIO's.

Category II PIOs are very similar to those of Category I except for the dominance of key series nonlinearities. They are invariably severe PIOs, whereas Category I covers both small and large amplitude levels.

The oscillatory conditions remain those of Eq. 1, although it is usually modified to the form,

$$Y_p Y_c = -1/N \qquad (2)$$

where the left hand side represents the linear parts of the open-loop pilot-vehicle dynamics and the right hand side is a composite describing function of the series nonlinearities. The describing function N typically depends on the nature of the nonlinearity and the input amplitude. Many examples of "N" may be found in Ref. 18, and a rate-limited actuator describing function plus a typical illustrative analysis is given in Ref. 10 for the X-15 PIO.

Category III — Essentially Non-Linear Pilot-Vehicle System Oscillations with Transitions — These PIOs fundamentally depend on nonlinear transitions in either the effective controlled element dynamics, or in the pilot's behavioral dynamics. The shifts in controlled element dynamics may be associated with the size of the pilot's output, or may be due to internal changes in either control system or aerodynamic/propulsion configurations, mode changes, etc. Pilot transitions may be shifts in dynamic behavioral properties (e.g. from compensatory to synchronous), from modifications in cues (e.g. from attitude to load factor), or from behavioral adjustments to accomodate task modifications.

The Category III PIOs can be much more complicated to analyze than the other two in that they intrinsically involve transitions in either the pilot or the effective controlled element dynamics. Thus there are a minimum of two sets of effective pilot-vehicle characteristics involved: pre- and post-transition. When these differ greatly, as in the T-38, YF-12, and YF-22 circumstances, very severe PIOs can occur.

The categories suggested above do not differentiate as to PIO severity, and have little if anything to say about the emotional aspects of a severe PIO. The pilot involved cares not at all whether his encounter was a Category I, II, or III! For the analyst, on the other hand, such details are essential to permit the use of available tools and analysis techniques with which to develop understanding of the event and determine corrective action.

5.4 Relevance to Active Control Technology Applications

The full application of active control technology in flight control systems for modern high performance aircraft invariably results in multiple-redundant, multi-mode, task-tailored, fly-by-wire (or light) systems. These are technological marvels! Great efforts are taken in design to put limits in the right places, to seamlessly transition from one set of effective aircraft characteristics to another, to foresee all possible contingencies. Unfortunately, with even the most modern and elaborate systems (e.g. YF-22) some upsetting condition within the FCS itself or pilot behavior transitions within the pilot-vehicle system seem to creep through. In this event, a Category III PIO is a likely consequence when appropriate triggers also arise. Avoidance of Category III PIOs is one of the great challenges of Active Control Technology applications.

Past history indicates that the Category III PIOs are highly unusual but also very severe events. The post-transition effective vehicle dynamics are almost always unforeseen, as are the triggering possibilities. This type of PIO is particularly insideous because, in the best modern fly-by-wire designs the pre-transition (normal) effective aircraft dynamics are designed to have excellent flying qualities. Most of the system nonlinearities (e.g. limiters, faders, mode-switches, etc.) are deliberately introduced to counter anticipated problems. In all these systems the lure of software "solutions" to all sorts of imagined problems has become easy to espouse; but

unimagined events can remain submerged only to surface in an untimely way. Indeed, it is only when the known-problem fixes act in peculiar, unanticipated, ways in the presence of large pilot inputs that the "bad" post-transition vehicle dynamics are created. Yet modern systems are so complex and elaborate that more rather than fewer Category III PIOs are likely to occur in the future unless matters change.

In trying to minimize the potential for Category III PIOs at the design stage the initial conceptual problem is the systemmatic imagination and enumeration of all the sets of effective controlled element dynamics that could conceivably be exposed to the pilot. The effective dynamics for the design set is easy — they define the nominal effective dynamics. Then, in one axis of control, there are the sets defined by all possible pilot input amplitudes. These sets include the impact of various limits hither and yon either in or out, multiple effectors (e.g. canards, elevators, flaps, thrust vectoring), with their different limiting conditions, etc. Follow this with the combined axes case, especially with shared effectors (e.g. elevons, ailevators) which allocate the limited capabilities among the pilot demands. Then, there are all the asymmetrical conditions, legal and illegal (but conceivable) configuration and propulsion shifts, etc.

After enumeration and definition, all the sets of effective vehicle dynamics discovered are potential entries in Category III PIO considerations. Normally, the design or nominal effective dynamics are pre-transition, while all the non-nominal sets of effective controlled element dynamics are conceivable candidates for the post-transition conditions. Further, there are likely to be hidden triggers implicit in the possible transitions, in the fading schemes, etc. Attempts to discover all these are needed as part of the design assessment process if highly undesirable downstream surprises are to be avoided or at least anticipated.

The transition sets which suggest the more extreme differences between pre- and post-transition characteristics are subjected to further examination. Comparison of the two conditions suggests PIO potential in that it gives a direct indication of the amount of adaptation needed on the part of the pilot to tolerate the shift. In some cases these assessments will lead to detailed changes in relative limits (e.g. SAS actuator rate limits should be greater than the surface actuator rate limits), adjustments in fader circuits, modifications in switching sequences, changes in assignments of rate and/or position limiting priorities for dual-purpose surfaces, etc.

All of this smacks of failure mode and effects analysis and sneak circuit analysis, with ramifications of software verification and validation. Indeed, parallels with these procedures may be central to the means ultimately developed to treat the Category III PIO probability assessments.

We come, finally, to the question of just what levels of differences in pre- and post-transition dynamics can be tolerated if the pilot is knowledgable and/or appropriately trained. This issue is currently critical in attempting to lay out potential criteria. Some guidance can be developed from past systems and occurrences, although the data base is quite sparse. Therefore, the question is fundamentally one for future experimental research to examine.

REFERENCES

1. McRuer, Duane T., "Interdisciplinary Interactions and Dynamic Systems Integration," *International Journal of Control*, Vol 59, No 1, January 1994, pp 3-12.

2. Aponso, Bimal L., Donald E. Johnston, Walter A. Johnson, and Raymond E. Magdaleno, "Identification of Higher-Order Helicopter Dynamics Using Linear Modeling Methods," *American Helicopter Society, 47th Annual Forum Proceedings*, May 1991, pp 137-153.

3. Kaplita, Thaddeus T., Joseph T. Driscoll, Myron A. Diftler, and Steven W. Hong, "Helicopter Simulation Development by Correlation with Frequency Sweep Flight Data," *American Helicopter Society 45th National Forum Proceedings*, Boston, MA, May 1989.

4. McRuer, D.T. and E.S. Krendel, *Mathematical Models of Human Pilot Behavior*, AGARDograph AG-188, 1974.

5. Jex, H.R. and R.E. Magdaleno, "Biomechanical Models for Vibration Feedthrough to Hands and Head for a Semisupine Pilot," *Aviation, Space, and Environmental Medicine*, Vol 49, No 1, pp 304-316, 1978.

6. Johnston, D.E., and D.T. McRuer, "Investigation of Limb-Side Stick Dynamic Interaction with Roll Control," *J. Guidance, Control and Dynamics*, Vol 10, No 2, March-April 1987, pp 178-186.

7. Jex, H.R., G.L. Teper, D.T. McRuer, and W.A. Johnson, *A Study of Fully-Manual and Augmented-Manual Control Systems for the Saturn V Booster Using Analytical Pilot Models*, NASA CR-1079, 1968.

8. Cheng, P., S. Chan, T. Myers, D. Klyde, and D. McRuer, "Aeroservoelastic Stabilization Techniques for Hypersonic Flight Vehicles," AIAA-91-5056, *AIAA Third International Aerospace Planes Conference*, 3-5 December 1991.

9. McRuer, Duane, "Human Dynamics and Pilot-Induced Oscillations," *22nd Minta Martin Lecture*, MA Institute of Technology, 2 December 1992.

10. Ashkenas, I.L., H.R. Jex, and D.T. McRuer, *Pilot-Induced Oscillations: Their Cause and Analysis*, STI TR- 239-2, Norair Report NOR 64-143, June 1964.

11. Ashkenas, I.L., R.H. Hoh, and G.L. Teper, "Analyses of Shuttle Orbiter Approach and Landing," *J. Guidance, Control and Dynamics*, Vol 7, No 1, pp 106-112, January-February 1984.

12. Smith, John W. and Donald T. Berry, *Analysis of Longitudinal Pilot-Induced Oscillation Tendencies of YF-12 Aircraft*, NASA TN D-7900, February 1975.

13. Smith, John W., *Analysis of a Lateral Pilot-Induced Oscillation Experienced on the First Flight of the YF-16 Aircraft*, NASA TM 772867, September 1979.

14. Dornheim, Michael A., "Report Pinpoints Factors Leading to YF-22 Crash," *Aviation Week and Space Technology*, May 4, 1993, pp 52-54.

15. Johnston, D.E., and B.L. Aponso, *Design Considerations of Manipulator and Feel System Characteristics in Roll Tracking*, NASA CR-4111, February 1988.

16. Ashkenas, I.L., R.E. Magdaleno, and D.T. McRuer, *Flight Control and Analysis Methods for Studying Flying and Ride Qualities of Flexible Transport Aircraft*, NASA CR-172201, Aug. 1983. (A shorter summary appears as "Flexible Aircraft Flying and Ride Qualities," in *NASA Aircraft Controls Research 1983*, NASA Conference Publication 2296, October 25-27, 1983, Gary P. Beasley, Compiler)

17. McRuer, D.T., W.F. Clement, P.M. Thompson, et al, "Pilot Modeling for Flying Qualities Applications," *Minimum Flying Qualities Vol. II*, WRDC-TR-89-3125, January 1990.

18. Graham, D. and D. McRuer, *Analysis of Nonlinear Control Systems*, John Wiley and Son, New York, 1961 (Dover, 1971).

ACTIVE CONTROL TECHNOLOGY: APPLICATIONS AND LESSONS LEARNED

Brigadier General Vincenzo CAMPORINI
Chief, OPS Branch IT Air Staff
Stato Maggiore
Aeronautica - Capo 3^ Reparto
Viale Universita', 4
Rome, Italy

Let me express my deep satisfaction for having been invited to speak in such a significant occasion. Indeed I feel honored and my appreciation is also justified by my long association with AGARD in the framework of the Aerospace Application Studies Committee: having been a member of this body for many years I have had precious opportunities to enjoy the benefit of the works performed by the various Panels, with an in depth knowledge of the trends of research in the forefront of technology. And here I would like to pay a tribute to those who founded the AGARD, for the wise structure they devised, a structure in which an institutional link between the military planners and the scientists has a fundamental place, allowing the former a better insight of the feasible developments in technology and letting the latter have a first hand knowledge of the real needs emerging from doctrine, strategy and in general geopolitical situations.

I firmly believe this to be a crucial point, and an argument worth of the greatest consideration by anyone who has responsbilities not only in the scientific or in the military world.

A very simplistic question is whether it is true that military needs drive research in the scientific fora or, on the contrary, the achievements in the technological fields dictate the developments of tactics, strategies and eventually doctrines.

Like all simplistic questions, the answer is neither simple nor unilateral: looking back on history good and solid examples can be found to support both thesis: at Crecy the technology of longbows had the upper hand of the knights' cavalry that till then had been the decisive factor in battles and hence in wars. Can we derive from this episode that technology has changed the course of history by itself and that strategists were forced to change their attitude?

On the other hand, later on, the achievements in fortifications and strongholds were such that apparently conficts were at a stalemate: no one could win, and only the death for natural causes of one of the contenders could eventually put an end to strifes. It was quite natural then to see the rulers of those times urging the scientists to devise new means to increase the probability of success of a siege: Leonardo da Vinci was a very welcome guest of many European courts not only for his artistic skills but also for his far sighted ingenuity in inventing new war machines. Can we then deduct that the advancement of technology is due to the demand for new devices and weapons made by strategists to scientists?

I am firmly convinced that the answer is much more complex than the questions and that the magic word is "interaction": instead of discussing fruitlessly whether the push for advancement is given by the military or by the science world, I believe it is more convenient, and it bears more concrete results, to study the continuing interrelationship between the two in an effort to improve the means of dialogue, opening doors and establishing institutional tables, around which aerodynamicists and pilots, chemists and gunners, technicians and colonels can sit together, to inspire and to be inspired in both directions, reciprocally.

I am fully aware that this is not a new idea: indeed the establishment of AGARD some decades ago responded to this concept, giving birth to a body, or better a set of bodies, that have proven a very reliable and effective means of dialogue and thence progress. In a very humble and realistic attitude, we must continue along the lines which have been indicated by our predecessors, rendering this dialogue more and more open, establishing new fora, opening new opportunities for cooperation at all levels, not only at the level of the planners of the grand strategy but also during the day-to-day activity in the laboratories and in the test sites and fields.

The papers that are about to be presented show many good examples of such an attitude and similar procedures: we shall hear how the military staff and their technical bodies are heavily involved during development programmes. Military personnel daily cooperates with contractors to ensure that the results of the work by defence industry, both hardware and software, are fully in line with the expectations and the needs of the men and women who will be the final users in the field, putting them in the position to win the battles that they will be asked to fight, with the minimum risk for their lives.

Although this cooperation is performed at various levels, with procedures tailored to the contractual environment of the specific programme and with the legal constraints peculiar to each single nation, my experience shows that sometimes the initiative is taken

Paper presented at the Flight Mechanics Panel Symposium held in Turin, Italy, from 9-13 May 1994.

informally by the operators on both sides, officials and industry, at working level, but when the matters are raised to the managerial teams, then some difficulties arise: the industrialists being reluctant to accept what they consider unduly interference by the officials and on the other side with the military keen to sponsor technical solutions they are in love with.

If this is the situation, and sometimes it is so, I think it is of the greatest importance that institutional ways be found and agreed so that an open discussion can be held at all times, thus enhancing the final result of development programmes. I am aware that some difficulties exist: the first one that comes to my mind is the cost of this cooperation, which can be identified as direct and indirect: direct costs would be related to the organization of meetings, preparation of documentation and presentations, but what planners seem to be much more worried about are the indirect costs related to the modifications to hardware and software caused by the interference of the military, all resulting on the one side to what is commonly referred to as "goldplating" and on the other giving grounds to claims by the contractor either for delays and disruptions, allegedly originated by changes to specifications, or for major costs due to evergrowing requests by the officials. Nevertheless I believe that it would be very wise and beneficial if a code of rules could be established, giving terms of reference as clear and detailed as possible, so that the greatest benefit for future developments can be gained in a deep and thorough understanding by the contractor of the real concrete needs if the operator.

Leaving now this issue, which is for sure, in a way, philosophical but has far reaching practical consequences, I would like to address now something more specifically relevant for the activities of this distinguished audience.

The first consideration I want to underline is the obvious one that man was not intended in the beginning as a dweller of the third dimension: we were not given wings, nor we possess an instinct of orientation like the one of the migratory birds. Nevertheless we want to fly higher and faster and more than that, we want to be able to operate in such an unfriendly environment. This is the ultimate scope: to have the capabilities to exploit the air and, being military, to deny its use by the opponent.

During the last decades the expresion "man-machine interface" has become very common, to indicate the facilities (controls, gauges, screens, warnings and what else) that allow an operator to use a complex system, be it mechanical, hydraulic, electronic etc.

Well, I consider an aircraft a similar interface: an interface between the man and the environment above the ground. In this sense I call it a "man-environment interface" and then I apply to this system the same criteria and the same logic used in ergonomy. In particular, one of the most important parameter is the degree of "user-friendliness", which for an aircraft translates into ease of conduct, harmonized controls, carefree handling and not only for the flight controls, but also for the engine and for the systems, for the weapons and for the utilities. I belong to the generation of the F-104 and if you ask any pilot with a Starfighter experience in his career, I have no doubt that his preference goes to it, for the unsurpassed sense of power, but more so for the awareness of having broken in a wild horse, ready at any moment to unsaddle his rider. Very romantic, but also very impractical. What is asked today of you is an interface between the man and the air to which the pilot has to devote almost no attention, so that he may dedicate nearly all his capabilities and his resources to execute his mission, be it a dogfight or a logistic airlift.

But one can easily object that this aim has already been achieved. The aircraft of this generation, and even those of the former one, are already easy to fly: a "first tourist" is no longer the exception, but the rule, on a first line fighter. More than that, the active control technology has already attained such levels of sophistication that the performances of flying machines have reached and surpassed the limits of human beings: you can easily design a system capable of a 15 Gs turn but nowhere can be found a pilot able to sustain it. So the question is whether there is any room left for further advances which still are possible are worth the effort and the money they are going to cost. Has the ultimate aircraft been designed? Is the F22 the maximum usable technological development? Of course the answer is no. Otherwise we would not be here to discuss and to share our ideas on how to open new domains.

The point is that the environment for which you are designing the interface is not static, it is not only a physical concept; its challenges are modified and increased almost on a daily basis by the various actors in the geostrategic scene. Hence the need for continual reasearch so as to be always in a position to counter the threat or, to use a more fashionable word, the risk. The likely opponents have better sensors? More accurate and reliable radars with better electronic counter counter measures? No problem: we will open the door to the stealth technology; but how compatible are the stealth requirements with the basic laws of physics? I suspect there is no compatibility at all and a close look at the F117 is the best proof of that. I also suspect that only the joint efforts of a bunch of scientists, ranging from aerodynamics, through computer sciences, could succeed in making such a thing fly, and fly effectively, with valid operational results. I recall that once Sir Geoffrey De Havilland expressed the concept that only beautiful aircraft can fly beautifully. This is no longer the case: also ugly aircraft can fly, albeit with the help of a complete suite of computers and today the ugliness is dictated by operational considerations. I can well imagine, therefore, that future developments in flight mechanics will be devoted to the severance of the links of conventional physics in an effort to release flying qualities from the observance of the laws we have been living with up to now.

It is not an easy road: after the initial enthusiasm, which is typical wherever a new door is opened, a more cautious approahc has become necessary. What has happened during the development programmes of

the Gripen and the F22 has undoubtedly introduced a degree of uncertainty into the minds of engineers and programme managers with and everincreasing need for validataion procedures with an absolute degree of reliability.
This is certainly a field worth of further analysis: the validation tools require daily refinements and room exists for increased and more reliable capabilities which will yield safer developments while allowing shorter times for achieving fully tested operational envelopes.
Finally I would like to draw your attention to a spin-off offered by the active control technology, which in the present and foreseeable circumstances is becoming increasingly important. I am talking of the influence of this technology on life cycle costs in general and on structural life in particular.
Too often in the last decades we have witnessed cases of flight lines being grounded for sudden failures of vital components of airframes. These occurences have thus given birth to heavy and costly fixes with very unpleasant consequneces on the operational as well as on the financial side. I do believe that the tools you are developing will prove extremely beneficial to smooth and reduce the fatigue spectrum of all types of aircraft. The consequence will be ligther structures, longer maintenance cycles and therefore and overall reduction of ownership costs.
The same beneficial effects will be experienced by the systems and the equipments on board that in their operating life will stand stresses of a reduced magnitude, thus increasing the in-field reliability of weapon systems.

Let me conclude now, underlining that we, the military, as final users of your efforts and your studies, do expect further advances. The world scenario which has emerged after the fall of the Soviet empire may induce a dangerous trend of reducing the momentum of research in the field of military technology. I firmly believe it is important to stress that this would represent an error which would not be forgiven by our successors.
The message I want to leave you with is that NATO countries must maintain their technological edge: by this edge the cold war has been won without any combat and only such an edge will allow us to win the peace for the future generations.

THE ROLE OF HANDLING QUALITIES SPECIFICATIONS IN FLIGHT CONTROL SYSTEM DESIGN

Roger H. Hoh
David G. Mitchell
Hoh Aeronautics, Inc.
Vista Verde Center, Suite 217
2075 Palos Verdes Drive North
Lomita, CA 90717
USA

ABSTRACT

The handling qualities specification should be an essential element of the flight control system design and testing for an active control technology (ACT) aircraft. This is a significant departure from previous conventional aircraft where handling qualities depended more on the configuration (tail size, control surface sizing, etc.). The necessity for incorporating the handling qualities specification into the flight control system design process has not been recognized by the industry, as evidenced by the fact that most of the ACT aircraft do not meet the requirements of the current handling qualities specification. This has resulted in excessive phase lag in the flight controls, and numerous cases of pilot induced oscillation. This paper reviews key handling qualities criteria for ACT aircraft as well as lessons that should be incorporated into specification upgrades and flight control design efforts.

BACKGROUND

Active control technology (ACT) has become the basis for the flight control system design on essentially all new commercial and military aircraft. Ideally ACT technology eliminates the compromise between good handling (e.g., large tail, forward cg) and good performance (e.g., small tail, aft cg). Such an ideal case allows the use of very high gains to make the aircraft respond "naturally" regardless of the configuration, for example consider some of the recent stealth designs. Experience has shown that there are three factors that prevent this ideal situation: 1) the knowledge of what constitutes a "natural" response is not well understood; 2) filtering necessitated by flexible modes, noise, controller characteristics, and digital processing limits the use of very high gains; and 3) high gains can only be achieved with adequate control power (e.g., large tail). Recent work on the handling qualities specification for rotary wing aircraft has been heavily oriented towards developing requirements that take these factors into account. Such upgrades are planned for the fixed-wing specification (MIL-STD-1797A)[1] at the next major revision, planned in approximately three years.

Early handling qualities specifications[2,3] were met primarily through design of the aircraft configuration. Final refinements were made through the use of aeromechanical flight control devices such as bobweights, downsprings, q-bellows, servo-tabs, and spring tabs. Properly designed, none of these devices significantly affected the dynamic stability metrics such as short period frequency and damping. The shapes of the Bode plots of these aircraft were essentially constant, and hence simply specifying values of a few parameters was sufficient. Generally speaking, this held true even for aircraft with limited authority stability augmentation systems. With ACT, however, the shape of the response to a control input can be drastically modified from that of the conventional aircraft. To cope with this, the specification criteria can no longer be based on a few parameters that define the Bode plot of a classical airplane (e.g., phugoid mode, short period mode).

In the United States, the current MIL-STD-1797A[1] represents a first cut at making the transition from the specification of handling qualities of classical airplanes to those designed around the ACT concept. For example, the Lower Order Equivalent System (LOES) criteria are based on the concept of using equivalent values of the classical parameters,[4] with the addition of a time delay factor to account for the filtering noted above. Because the lower-order model used in the specification is the short period approximation, this criterion is restricted to ACT designs that result in an airplane that responds "like a classical airplane."

This gives rise to a need to define, in precise terms, what is meant by a classical response. Further, it raises the question, Is a classical response the best response? It is important to recognize that, historically, the response of airplanes was not something that could be drastically altered. A great deal of effort was expended to extend the cg range, or to decrease the required tail size just a few percent. In the end, the flying qualities resulted from a compromise with performance, and by today's standards were not good. At forward cg the stick forces tended to be very heavy and the gust response excessive. At aft cg, the stability was often near neutral. Hence, the answer to the question of what is the best response is not simply to make it fly "naturally." To address this problem, the concept of Response-Type was incorporated in the U.S. Army's rotorcraft flying qualities standard, ADS-33C.[5] This was done after the MIL-STD-1797 development[6] was completed in November of 1982, so it does not occur in that document at this time.

Early fixed-wing handling qualities specifications (e.g., Reference 2) recognized that the required response should be a function of the task. For example, MIL-F-8785B[7] incorporated three Categories of task. Category A covered non-terminal precision tasks, Category B was established for non-precision, non-terminal tasks, and Category C covered all terminal flight phases such as approach and landing. During the development of the new rotorcraft specification,[5] this concept was extended so that each requirement was applicable to a set of maneuvers called Mission-Task-Elements (MTEs). These maneuvers represent the basic elements of a mission in terms of handling qualities tasks. Each criterion boundary in the specification is associated with one or more MTEs. As expected, the more stringent

Paper presented at the Flight Mechanics Panel Symposium held in Turin, Italy, from 9-13 May 1994.

boundaries are associated with the more demanding MTEs, such as target acquisition and tracking.

Response-Types can also be defined in terms of the Mission-Task-Elements. For example, for divided attention tasks ADS-33C requires an attitude command/attitude hold Response-Type. The Response-Type/MTE methodology allows the handling quality specification to be tailored to the needs of the user.

Few, if any, commercial or military aircraft flying today meet the flying qualities specification. This is true even for aircraft that were designed and built in recent years, when the requirements were either included in the specification or published in the open literature. The consequence of not meeting the handling qualities specifications is typically not catastrophic. In practice, it means that the required tasks can be accomplished, but with increased workload. Implicit in increased workload is reduced safety and mission effectiveness, but the exact nature of this relationship is not known. Of greater concern is that a result of not meeting the specification criteria is potentially a seriously PIO-prone aircraft. This is discussed in more detail later in the paper.

The U.S. Army has been in the process of developing a handling qualities specification that accounts for active control technology in rotorcraft for over 10 years. In its current form, the specification is an Army Aeronautical Design Standard (ADS-33C). It is currently in the tri-service review process to replace MIL-H-8501A. ADS-33C was specified as the handling qualities requirement for the RAH-66 Comanche, an ACT rotorcraft being designed and built by Boeing and Sikorsky. While the aircraft has not yet flown, U.S. Army pilots have indicated that the flying qualities are Level 1 on the simulator. Those evaluations included very demanding maneuvers, and flight in a degraded visual environment.

This experience suggests that an up-to-date handling qualities specification, combined with a willingness on the part of the government to insist on compliance, results in good handling qualities for complex ACT aircraft. This conclusion is, of course, tentative until the aircraft has actually flown and gained test and operational experience. A primary ingredient to the success of ADS-33C is the close cooperation that existed between the Army elements -- the specification developers (Aeroflightdynamics Directorate), the testing activity (Airworthiness Qualification Test Directorate), and the procurement activity (Aviation Systems Command) -- and the rotorcraft manufacturers. All these activities agreed on one set of criteria. Such agreement does not exist in the fixed-wing community, and each activity tends to use different criteria, or in some cases no criteria at all. As will be discussed below, some criteria are equivalent and in such cases the use of a "favorite metric" does not represent a problem. Some criteria, however, are in serious conflict, and can actually encourage ACT designs that are PIO-prone.

ACT HANDLING QUALITIES: THE RECORD

The promise of the ACT aircraft is to eliminate handling qualities as an issue in the design of the configuration, allowing a focus on mission critical factors such as performance and radar signature. In that sense, we have been successful, witness the F117, F-16, Shuttle, etc. These aircraft have been notably successful in the performance of their designated missions. Handling qualities problems have been common, however, and in some cases with catastrophic results. ACT flying qualities problems usually take the form of pilot induced oscillations (PIO). Some examples are:

- The YF-16 "flight zero" lateral PIO. This flight was intended to be a taxi test, but the occurrence of a rapidly diverging PIO caused the pilot to lift off to avoid leaving the side of the runway.
- The infamous Shuttle ALT PIO. This divergent PIO resulted in stop-to-stop control activity in the landing flare. Fortunately the aircraft touched down before control was lost.
- The recent YF-22 PIO that resulted in a crash on the runway.
- The Gripen PIO that also resulted in a crash on the runway.
- The F-18 lateral PIO during aerial refueling. This PIO resulted in a major redesign of the lateral flight control system.
- Reports of PIO tendencies in the C-17 with the initial versions of the flight control software installed.

Numerous articles have been written indicating a need for a better criterion to prevent such PIOs in ACT aircraft. The simple fact, however, is that every one of the handling qualities problems and PIOs encountered would very likely have been prevented if the aircraft met the primary short term pitch and roll control criteria in the current MIL-STD-1797A (i.e., the Bandwidth or Lower Order Equivalent Systems criteria). These criteria are discussed later in this paper. Before proceeding with that level of detail, we shall consider lessons that have been learned that, if heeded, may improve the record of ACT handling qualities.

LESSONS (LEARNED?)

During the past 15 years of flying qualities specification development and use (or lack thereof) on ACT flight control system designs, certain lessons have been offered. Whether they have been learned will only become known with the passage of time. These lessons are summarized below.

Current specification criteria represent necessary but not sufficient conditions for good handling qualities. The currently available handling qualities specifications, MIL-STD-1797A for airplanes and ADS-33C for rotorcraft, are not perfect. If they are not met, however, significant flying qualities problem are likely to occur. If they are met, there may still be problems because there are not good requirements for some areas of flying qualities, e.g., stick sensitivity and sidestick controller requirements. It is not likely that a "perfect" collection of flying qualities criteria will be developed in the near future. Therefore, demonstration maneuvers should be included in the specification as an overall check on the quantitative criteria. This was successfully accomplished for ADS-33C as discussed in more detail later in the paper.

Specification Criteria are often in conflict with prototype flight test results. It is common to obtain acceptable pilot opinion during flight testing or simulation of a new aircraft

that does not meet the specification criteria. There are a number of possible explanations for this result.

- Aggressive maneuvering and flight in poor visibility, high winds, and turbulence is not consistent with the restrictions required for safety of flight with a new aircraft.

- There are no uniform standards for flight test maneuvers. (For this reason the demonstration maneuvers in ADS-33C are precisely defined).

- It is impossible to avoid vested interest among evaluation pilots assigned to a new aircraft (discussed in more detail in Reference 8).

The quantitative criteria in the specifications effectively result in predicted Cooper-Harper Handling Qualities Ratings, or HQRs[9] (i.e., Level 1 implies an HQR of 3 or better, Level 2 implies $4 \leq HQR \leq 6$, and Level 3 implies $7 \leq HQR \leq 9$). These predictions are based on pilot ratings taken from flying qualities experiments where the subject pilots had no vested interest in the outcome. Therefore, they are extremely important and should not be ignored in favor of results obtained from pilots with a vested interest in the outcome. For example, excessive phase lag (time delay) does not show up as a deficiency unless very demanding tasks and a discriminating pilot attitude are present. It is very common for prototype aircraft with excessive phase lag to be rated as acceptable during flight testing. Essentially all of the problems noted above occurred with aircraft that did not meet the specification criteria, and that were rated as acceptable by evaluation pilots.

Quantitative criteria should be supported by data. While not perfect or complete, there is a substantial handling qualities database. Any criterion proposed for use in a specification should be able to predict the Level of flying qualities in that database with at least 75% accuracy. There has been a tendency to ignore criteria in the specification that have undergone such scrutiny in favor of criteria that are advertised as successful without being subjected to such an analysis. It is important that any proposed criterion be subjected to all of the available data. It is common for an experimenter to develop a new set of criteria as soon as a new set of data is generated. As a result there are numerous criteria in the literature that work for only a single data set.

Level 1 handling qualities are rarely necessary. Aircraft that do not meet Level 1 handling qualities are often judged to be completely acceptable by their pilots. Experience has shown that in benign conditions, aircraft that are predicted to have Level 2 handling qualities by the specification are often rated as Level 1. When the task and environment are more harsh, however, these aircraft become very difficult to control. For example, most transport aircraft do not meet Level 1 in terms of short period frequency. They are completely acceptable for landing on long runways in calm air or even moderate turbulence. When subjected to a requirement to land on short runways and in moderate or severe turbulence, however, these aircraft become a handful, requiring significant pilot skill. The impact on safety is elusive to quantify, but it seems intuitively obvious. Because the need for Level 1 handling qualities is rare, it is easy for the uninformed to assume they are unnecessary. The PIOs noted above serve as evidence for the need for good handling qualities.

The relationship between Levels and mission must be scrutinized. In current specifications, Level 1 is defined as the ability to accomplish the mission with an acceptable pilot workload. Level 2 is defined as the ability to accomplish the mission, but with increased pilot workload. Finally, Level 3 implies that the mission cannot be accomplished, but that the aircraft can successfully landed. The actual specification boundaries are based on HQRs, which have phrases that are only loosely related to the Level definitions. The Level definitions should be changed to simply state what they really are, separations between Cooper-Harper ratings as shown in Figure 1. The user should then be in a position to decide how the phrases in Figure 1 relate to the ability to accomplish the mission.

Level 1 is seen in Figure 1 to be "satisfactory without improvement." This is a very stringent requirement. Few military or civil aircraft meet it. These aircraft, however, consistently do the job, i.e, successfully accomplish their mission. As a result we accept Level 2 as the norm. The danger of this is the lumping of an aircraft with HQR = 4 with one with HQR = 6: Level 2. From Figure 1, it is easily seen that successful mission accomplishment is far less likely with the latter than with the former. The most significant danger is that Level 2 handling qualities do not make a distinction between aircraft that are PIO prone and those that are not.

Recommended criteria are usually ignored. There is significant pressure in all aircraft development programs to make the specification criteria recommended rather than required. This pressure is related to the cost of meeting the criteria. Experience has shown that recommended criteria will be ignored in favor of meeting budget and schedule constraints.

A flight test guide is essential. Ideally, the specification writers could be present for every flight test. This is not possible. Experience with ADS-33C compliance has shown that, without guidance, the possibilities for misinterpretation of the requirements is enormous. The specification should be accompanied by a flight test guide that provides the user with the proper methods for compliance with the criteria. Important criteria (i.e., those that would have prevented PIOs) have been ignored because of confusion as to proper methods of compliance. This guide could also provide guidance that belongs in the recommended category such as the best Response-Type for a given task.

Active communication between the specification developers and the user community is essential. This was successfully accomplished during the development of the U.S. Army ADS-33C through numerous in-process reviews that included attendees from several governments as well as all cognizant industry. As a result the manufacturers, government testing activity, government procurement activity, and specification developers all use the ADS-33C criteria for the design and testing of the Boeing-Sikorsky RAH-66 Comanche. This is unprecedented in the industry, where it is more common to ignore the flying qualities specification.

The size of the aircraft is irrelevant. It is the mission task that should drive the handling qualities. For example, air

refueling an F-16 or a C-5 is the same task -- get the probe into the basket. The same analogy holds for landing, where the required precision depends on the mission requirements, not the size of the aircraft. If it is not practical to provide the necessary handling qualities (i.e., to make a big aircraft meet precision landing criteria), the mission requirements should be revised. A well-developed mission-oriented specification makes this tradeoff more obvious. Some do not like the answer and blame the specification (the shoot-the-messenger syndrome).

PROPOSED ELEMENTS OF MISSION-ORIENTED SPECIFICATION

The above lessons provided the basis for many elements of the new rotorcraft specification ADS-33C.[5] Because the old specification MIL-H-8501A[3] was hopelessly outdated, it was possible to start with a clean sheet of paper. The development of ADS-33C by the U.S. Army resulted in the following concepts for a mission-oriented flying qualities specification.

- Mission-Task-Elements (MTEs): These are elements of missions that can be broken down into specific flying qualities tasks. This includes the definition of desired and adequate performance necessary to obtain pilot opinion ratings. An obvious example of an MTE would be flare and landing. This might be further broken down into normal and precision landings, with the desired and adequate performance boundaries reflecting the difference between the two MTEs.

- Response-Type: Current specifications (except ADS-33C) do not recognize the capability of ACT aircraft to exhibit characteristic response shapes that are entirely different from classical aircraft. Examples are rate command and attitude command systems. For some MTEs, it may be necessary to provide a specific Response-Type to achieve characteristics that are "satisfactory without improvement" or Level 1. Examples of Response-Types for fixed-wing aircraft are shown in Figure 2.

- Usable Cue Environment (UCE): As visibility degrades, certain cues necessary to stabilize the aircraft may become unavailable. It has become necessary to employ vision aids such as forward looking infrared (FLIR), night vision goggles (NVGs), or even millimeter wave radar. These vision aids have been highly successful as a means to continue operations at night and in poor weather. They are not able, however, to produce the high values of spatial frequency (fine-grained texture) necessary for the human operator to perceive translational rates as required for tasks such as landing or low-speed and hover tasks in rotorcraft. The UCE scale was developed for ADS-33C to provide a minimum Response-Type requirement for conditions of degraded visual cuing.[10] The specification includes a method to quantify the visual environment in terms of the ability of the pilot to stabilize the rotorcraft. It has not been determined whether such a requirement is necessary for fixed wing aircraft.

- Demonstration maneuvers - The quantitative criteria found in all specifications are subject to some shortcomings. Demonstration maneuvers were added to ADS-33C as an overall check on the quantitative criteria. They consist of selected MTEs that test the most critical criteria. The demonstration maneuvers are discussed further later in this paper.

EXISTING SPECIFICATION CRITERIA FOR ACT AIRCRAFT

The handling qualities problems with ACT aircraft are nearly always manifested as pilot induced oscillations -- sometimes severe and other times more of a nuisance. An example of this is a full PIO vs. bobbling of pitch attitude. The culprit is nearly always excessive phase lag in the region of pilot crossover. Once the PIO has started, the large amplitude control inputs often result in rate limiting, which magnifies the problem. Control surface rate limiting can result in a PIO even without excessive phase lag.

MIL-STD-1797A addresses excessive phase lag via the Bandwidth phase delay criterion (τ_p) and the LOES equivalent time delay criterion (τ_e). There are no criteria that directly address rate limiting in MIL-STD-1797A. ADS-33C addresses the phase lag issue using the Bandwidth criterion and rate limiting with moderate-amplitude Attitude Quickness criteria. These criteria are central to ACT flight control system design and are discussed below.

The Bandwidth criteria were specifically developed for ACT aircraft as a part of the development of MIL-STD-1797A.[6] They are the result of the cooperative effort and ideas from many organizations within the U.S., as well as the U.K. For example, an upper limit on Bandwidth applied in MIL-STD-1797A has been found to be characterized by the pitch attitude dropback parameter developed in the U.K.[11] A key aspect of the Bandwidth criteria is that they do not assume a characteristic response shape (such as a short period mode), and therefore are applicable to all Response-Types.

Bandwidth, in the classical sense, is a measure of the ability of the output of a system to follow the input. At frequencies below the bandwidth frequency, the output is equal to the input, and at frequencies above the bandwidth frequency, the system is essentially open loop. This concept applies to aircraft in the sense that good flying qualities exist when the aircraft's motions follow the pilot's commands, without an excessive amount of compensation on the part of the pilot.

The Bandwidth criterion for attitude is based on the well-developed closed-loop pilot-vehicle analysis theory,[12] and is illustrated in Figure 3. The bandwidth frequency is the highest frequency where a pure-gain (unequalized) pilot can close the loop without threatening stability. This is quantified as 45 degrees of phase margin or 6 dB of gain margin, whichever is less. The criterion addresses the important phase lag issue directly with the parameter τ_p. Unfortunately, this metric has the units of time, and is often referred to as time delay. It has been shown, however, that the sensitivity of pilot rating to small variations in τ (one rating per 0.05 sec) is a result of phase rolloff in the region of piloted control. This is shown in Figure 4 where it can be seen that increasing τ_p from 0.02 to0 .17 sec results in a large change in phase and in pilot rating (data from Neal-Smith experiment). This result is well explained in terms of closed-loop pilot-vehicle analysis in that a small change in pilot gain results in a large loss of phase margin. This is

further aggravated by a shelf in the magnitude plot. Note that a small change in pilot gain results in a large change in phase, a perfect setup for a PIO. Hence, a gain-margin-limited aircraft would be highly suspect as being PIO-prone. This is a very subtle deficiency in that the phase margin could be quite large so that the aircraft seems very stable for benign maneuvering. It is only in the presence of a tight closed loop tracking task that the gain margin deficiency becomes apparent. An excellent example is the Space Shuttle PIO where the pilot intended to make a precise touchdown resulting in a divergent PIO. Previous flights and many hours of simulation did not even hint of a problem. The value of τ_p for the Shuttle was 0.188 seconds compared to the Level 1 requirement of no greater than about 0.07 seconds.

It is important to recognize that the parameters used in the Bandwidth criteria must be directly related to the task. For example, it is recognized that both pitch attitude and flight path are primary parameters in the landing flare. Therefore, the latest version of the Bandwidth criteria includes both pitch attitude and flight path bandwidth. A complete description of the current Bandwidth criteria includes limits on phase delay (τ_p), dropback, and attitude and flight path Bandwidth as shown on Figure 5. It is notable that the allowable flight path bandwidth increases directly with increasing pitch attitude bandwidth (upper boundary in Figure 5c). This is directly analogous to the requirement for increasing short period frequency with increasing n/α in the lower order equivalent system CAP criteria for classical Response-Types. Unfortunately, the version of the Bandwidth criteria shown in Figure 5 will not be included in the flying qualities standard for fixed wing aircraft until the next major upgrade scheduled to occur in three years.

The Lower Order Equivalent Systems (LOES) criteria also address the issue of time delay. It is important to understand, however, that the MIL-STD-1797A LOES criteria use a special case of equivalent system that uses the classical airplane Response-Type as a lower-order model (see Figure 2). Hence it implicitly assumes that the shape of the response is that of a classical airplane. The fitting routine adjusts the equivalent short period and phugoid frequency and damping to fit this model. Any phase lag that is left over is accounted for by the equivalent time delay τ_e. If the ACT control laws do not result in a classical Response-Type, (i.e., if the Bode plot does not look like the "Conventional" airplane in Figure 2), it is simply not correct to fit the higher order system to this model. The use of angle-of-attack feedback to augment the short period typically results in a classical Response-Type. Inertial feedbacks, such as pitch rate and pitch attitude, result in non-classical response shapes such as the rate command/attitude hold (RCAH) and attitude command/attitude hold Response-Types in Figure 2. Comparison of the Response-Type shapes in Figure 2 clearly shows that it is not appropriate to attempt to fit the RCAH and ACAH shapes to the Conventional airplane shape. Unfortunately, this mistake continues to be made. It is a good example of why a users guide for compliance is needed.

As an aside, note that the general concept of lower order equivalent systems is valid for all Response-Types. Incorporating this type of criteria would require the development of a database for each lower order type (i.e., RCAH, ACAH, etc.) to develop generalized criteria for ACT aircraft. The RCAH and ACAH Bode asymptotes shown in Figure 2 would be the obvious choices for the LOES models for these Response-Types. In the context that the Bandwidth criteria apply to the short term response of all Response-Types, however, it does not seem necessary to accomplish the considerable work and experimentation required to develop lower-order models for every conceivable ACT Response-Type.

Having stated the groundrules for application of Bandwidth and LOES criteria, it is notable that the phase lag parameters for all of the earlier noted PIOs exceeded the Bandwidth and LOES criteria by a considerable margin. That is, the Bandwidth criteria would have predicted serious Level 2, or even Level 3, as would the LOES criteria, even if applied incorrectly (the ACT aircraft that currently exist usually have a RCAH Response-Type, not classical).

Flying qualities specifications in the U.K. employ a phase slope criterion. It can be shown that if the slope of the phase curve is taken at ω_{180} and $2x\omega_{180}$ the phase slope criterion is numerically equal to the phase delay parameter (τ_p) used in the Bandwidth criterion. As it now stands it is up to the user as to the specific points used to take the slope of the phase curve.

MIL-STD-1797A includes many criteria for longitudinal short-term flying qualities with no guidance as to which criteria are appropriate. ADS-33C takes a different approach and specifies only the Bandwidth criteria. It is suggested that an updated specification contain only one requirement for any particular area of flying qualities.

The attitude quickness criterion was developed as a measure of rotorcraft agility for ADS-33C. This criterion is exceptionally useful for exposing actuator rate limiting during aggressive maneuvering. It provides the basis for a criterion for fixed-wing agility -- a subject of great attention during recent years. Work is currently under way to expand the criterion to fixed-wing aircraft.

ROLE OF PIO CRITERION -- DO WE NEED ONE?

Early in this paper it was noted that the PIOs that have occurred in ACT aircraft would have been prevented if the aircraft met the existing specification. Further, it seems clear that PIOs are one sign of degraded handling qualities, and hence are not, in a handling qualities sense, unique phenomena. So why do we need a separate PIO specification?

Experience has shown that schedule and cost constraints nearly always result in compromises during the development of the flight control system of ACT aircraft. These compromises typically result in degradations in aircraft handling qualities, and therefore failure to meet the stringent Level 1 limits (i.e., limits that specify "satisfactory without improvement"). Most (if not all) current ACT aircraft would not be classified as Level 1. Typical problems are slow actuators, stick filters necessitated by the use of force transducers, bending mode filters, anti-aliasing filters, computational time delay, excessive parallel integrator gains, and improper flight control system design.

The problem is amplified by the fact that the use of active control technology often results in a significant modification of bare airframe response characteristics. For example, the

unaugmented X-29A doubles amplitude in well under one second, and is completely uncontrollable by the pilot. The augmented aircraft is well damped with a crisp response characteristic. This requires control power. Control power has classically been achieved with increased control surface sizing. This is, however, in direct conflict with the primary performance objectives that led to the ACT design in the first place. The result is smaller surfaces that must move very rapidly. This stresses the actuators, resulting in lags and rate limiting as an inherent problem in the design. Hence, it is not surprising that we have seen many PIOs in ACT aircraft. Strict adherence to the flying qualities specification could result in excessively large control surfaces. Clearly, we need a criterion that allows the tradeoff between performance and handling qualities to be made with a firm understanding of the inviolable PIO limits.

If we accept the basic premise that Level 2 HQRs are good enough to accomplish the mission, albeit with increased pilot workload, then it is inevitable that in the context of the above tradeoffs between performance and handling, plus the usual budget and schedule crises, Level 2 can be acceptable. This, in fact, has been a fact of life for all modern aircraft development programs. Given the adaptability of the human pilot, and the proper "can do" attitude of professional and military pilots, the Level 2 aircraft is an acceptable compromise and gets the job done. When the deficiency that causes the aircraft to fall in a Level 2 region has a potential for a catastrophic PIO, however, it takes on a far more important role than simply a requirement for increased pilot workload. Therefore, it is important to make a distinction between deficiencies that cause a flying qualities parameter to predict Level 2, and one which can result in a divergent PIO.

The role of a successful PIO criterion is to make this important distinction. Work is currently under way to develop a unified PIO criterion that may be separate and independent of the handling qualities specification, or included as a "not to be violated" criterion in the flying qualities specification.

DEMONSTRATION MANEUVERS

As noted above, the quantitative criteria are necessary but not sufficient to insure good handling qualities. Until the perfect set of handling qualities criteria are available, the specification should contain a selection of flight test maneuvers to provide an overall assessment of the aircraft's ability to perform certain critical tasks. The maneuvers should:

- Correspond to the Mission-Task-Elements used to define the quantitative criterion boundaries.
- Be defined in the same rigorous manner as tasks in a handling qualities experiment with desired and adequate performance limits
- Be performed by at least three pilots who are required to assign Cooper-Harper Handling Qualities Ratings (HQRs). The average of the assigned ratings should be consistent with the requirement for the predicted ratings from the quantitative criteria; e.g., HQR $\leq$ 3.5 for Level 1.

Such maneuvers were successfully developed in ADS-33C through a cooperative effort between the specification writers (U.S. Army Aeroflightdynamics Directorate), a flight test research facility (the National Research Council of Canada), the U.S. Army flight test activity (Airworthiness Qualification Test Directorate), and the manufacturers. It is important to emphasize that the maneuvers are required -- not recommended -- and the assigned HQRs are an essential part of the specification compliance. The results of the demonstration maneuvers carry a weighting comparable to the results from the quantitative requirements.

The Boeing-Sikorsky RAH-66 Comanche design has been successfully subjected to the ADS-33C maneuvers in simulation. The subject pilots have been representatives of the U.S. Army and the manufacturers.

It is notable that the U.S. Air Force flight test facility at Edwards currently does not do closed-loop handling qualities testing because it is not required by MIL-STD-1797A. As a result there is a potential for identifying problems very late in the program during operational tests.

The one test that is performed by the U.S. Air Force is the "Handling Qualities During Tracking" (HQDT)[13] maneuver. This is a very loosely-defined test; typically the pilot is instructed to "track as tightly as possible." There is no requirement to provide formal handling qualities ratings. Experience has shown that this type of testing results in widely varying results, a fact that has led to generally-accepted guidelines for flight testing.[8] While these guidelines are aimed at handling qualities tests, they are equally applicable to tests to be conducted for specification compliance.

While there are plans to add demonstration maneuvers to the next version of MIL-STD-1797A, the current concept is to make them recommended, not required.

SUMMARY COMMENTS

- ACT aircraft have encountered catastrophic cases of pilot induced oscillations that could have been avoided by meeting the appropriate criteria in the current handling qualities specification.
- Most handling qualities tasks can be satisfactorily accomplished with a Level 2 aircraft. The requirement for Level 1 is to provide good handling when the task requires operating near aircraft performance limits and in moderate or greater turbulence (i.e., when the pilot needs it the most). Since these conditions are rarely encountered, there tends to be a misconception that the specification requirements are too stringent.
- Cost and schedule constraints often dictate that a Level 2 aircraft is good enough because the mission can be accomplished (albeit with increased pilot workload). An independent PIO criterion is needed to make a distinction between Level 2 (and Level 3) aircraft that are PIO prone and those that are not.
- The Bandwidth criteria were developed using inputs from numerous organizations worldwide. They were specifically developed for ACT aircraft, and they emphasize the important issues of phase lag in the region of piloted crossover, and attitude dropback.

Bandwidth applies to small amplitude precision maneuvering tasks.

- The Attitude Quickness criterion was developed to extend the Bandwidth criteria to moderate-amplitude maneuvering. It is particularly effective for exposing actuator rate limiting problems that tend to be endemic to ACT flight control systems.

- The specification criterion boundaries should be a function of the required Mission-Task-Elements, and sometimes the usable cue environment. The size of the aircraft is irrelevant.

- Criteria that are provided as recommended (not required) are "nice to have." Nice to have items are the first to go when the inevitable budget and schedule crises arise.

- Specifications for ACT aircraft handling qualities should incorporate the mission-oriented methodology developed for the rotorcraft ADS-33C (Mission-Task-Elements, Response-Types, Usable Cue Environment, and Demonstration Maneuvers).

REFERENCES

[1]*Military Standard, Flying Qualities of Piloted Vehicles*, MIL-STD-1797A, Jan. 1990.

[2]*Military Specification, Flying Qualities of Piloted Airplanes*, MIL-F-8785(ASG), April 1959.

[3]*Military Specification -- Helicopter Flying and Ground Handling Qualities; General Requirements for*, MIL-H-8501A, Sept. 1961.

[4]Hodgkinson, J., LaManna, W. J., and Heyde, J. L., "Handling Qualities of Aircraft with Stability and Control Augmentations Systems – A Fundamental Approach," *Aeronautical Journal*, Feb. 1976, pp. 75-81.

[5]*Handling Qualities Requirements for Military Rotorcraft*, U.S. Army Aviation Systems Command, St. Louis, MO, ADS-33C, Aug. 1989.

[6]Hoh, Roger H., Mitchell, David G., et al., *Proposed MIL Standard and Handbook -- Flying Qualities of Air Vehicles. Volume II: Proposed MIL Handbook*, AFWAL-TR-82-3081, Vol. II, Nov. 1982.

[7]*Military Specification, Flying Qualities of Piloted Airplanes*, MIL-F-8785B(ASG), Aug. 1969.

[8]Hoh, Roger H., "Lessons Learned Concerning the Interpretation of Subjective Handling Qualities Pilot Rating Data," AIAA 90-2824, presented at the AIAA Atmospheric Flight Mechanics Conference, Portland, OR, Aug. 1990.

[9]Cooper, George E., and Harper, Jr., Robert P., *The Use of Pilot Rating in the Evaluation of Aircraft Handling Qualities*, NASA TN D-5153, Apr. 1969.

[10]Hoh, Roger H., "Handling Qualities Criterion for Very Low Visibility Rotorcraft NOE Operations," *Rotorcraft Design for Operations*, AGARD CP-423, June 1987, pp. 6-1 through 6-15.

[11]Gibson, John C., "Piloted Handling Qualities Design Criteria for High Order Flight Control Systems," *Criteria for Handling Qualities of Military Aircraft*, AGARD CP-333, Apr. 1982, pp. 4-1 through 4-15.

[12]McRuer, D. T., and Krendel, E. S., *Mathematical Models of Human Pilot Behavior*, AGARD AG-188, Jan. 1974.

[13]Schofield, B. Lyle, Twisdale, Thomas R., Kitto, William G., and Ashurst, Tice A., "Development of Handling Qualities Testing in the 70's -- a New Direction," *Criteria for Handling Qualities of Military Aircraft*, AGARD-CP-333, June 1982, pp. 23-1 through 23-16.

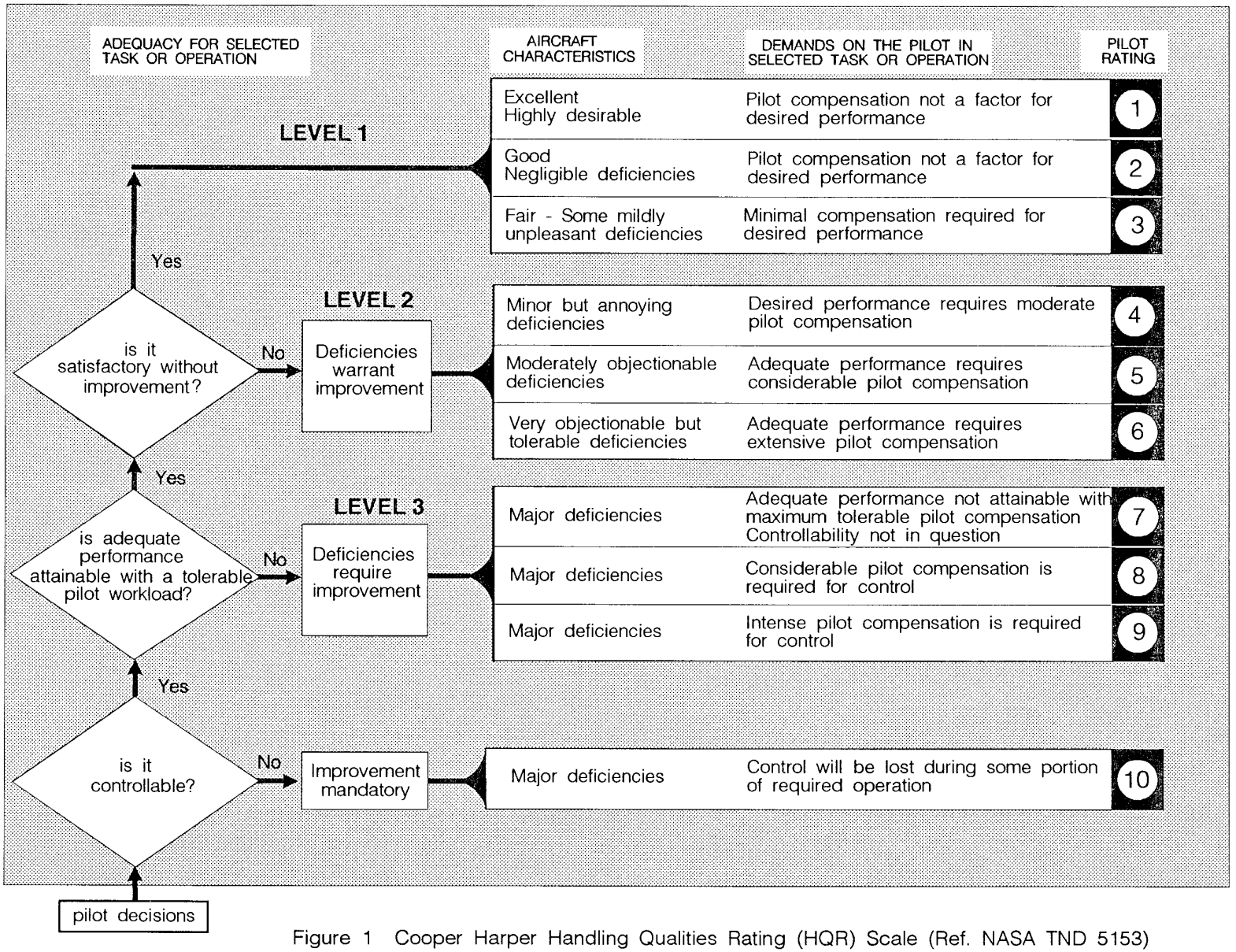

Figure 1 Cooper Harper Handling Qualities Rating (HQR) Scale (Ref. NASA TND 5153)

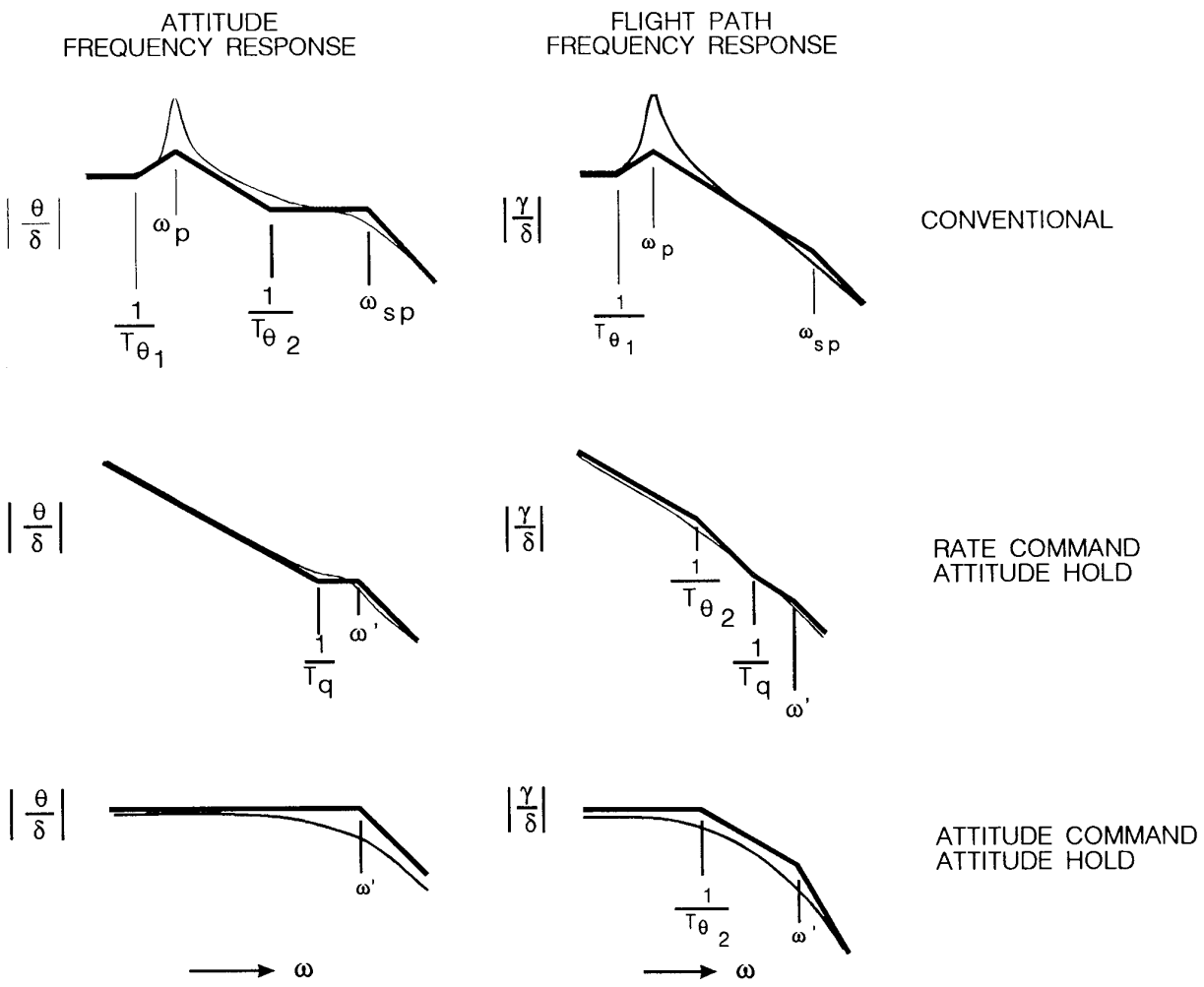

Figure 2 Generic Characteristics of Three Response-Types

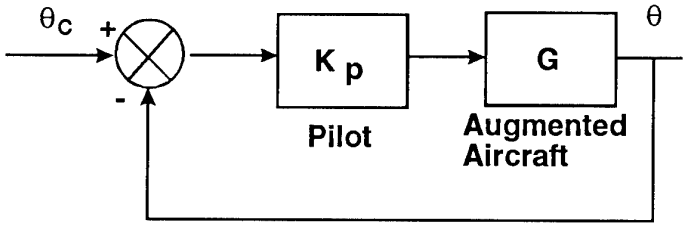

$$\Delta = 1 + K_p G = 0$$

$$G = \frac{-1}{K_p}$$

$$\tau_p = \frac{\Delta\phi_{2\omega 180}}{57.3\,(2\omega 180)}$$

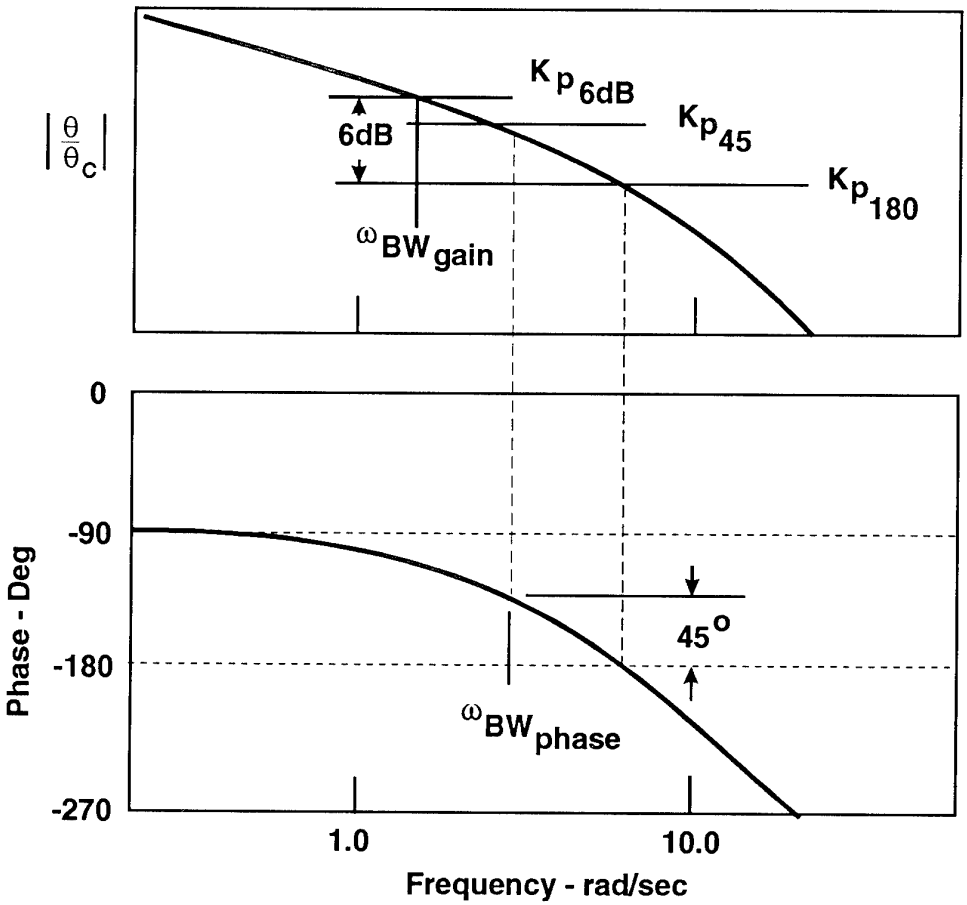

Figure 3 Definition and interpretation of Bandwidth Criterion

(DATA FROM NEAL-SMITH T-33 FLIGHT TESTING)

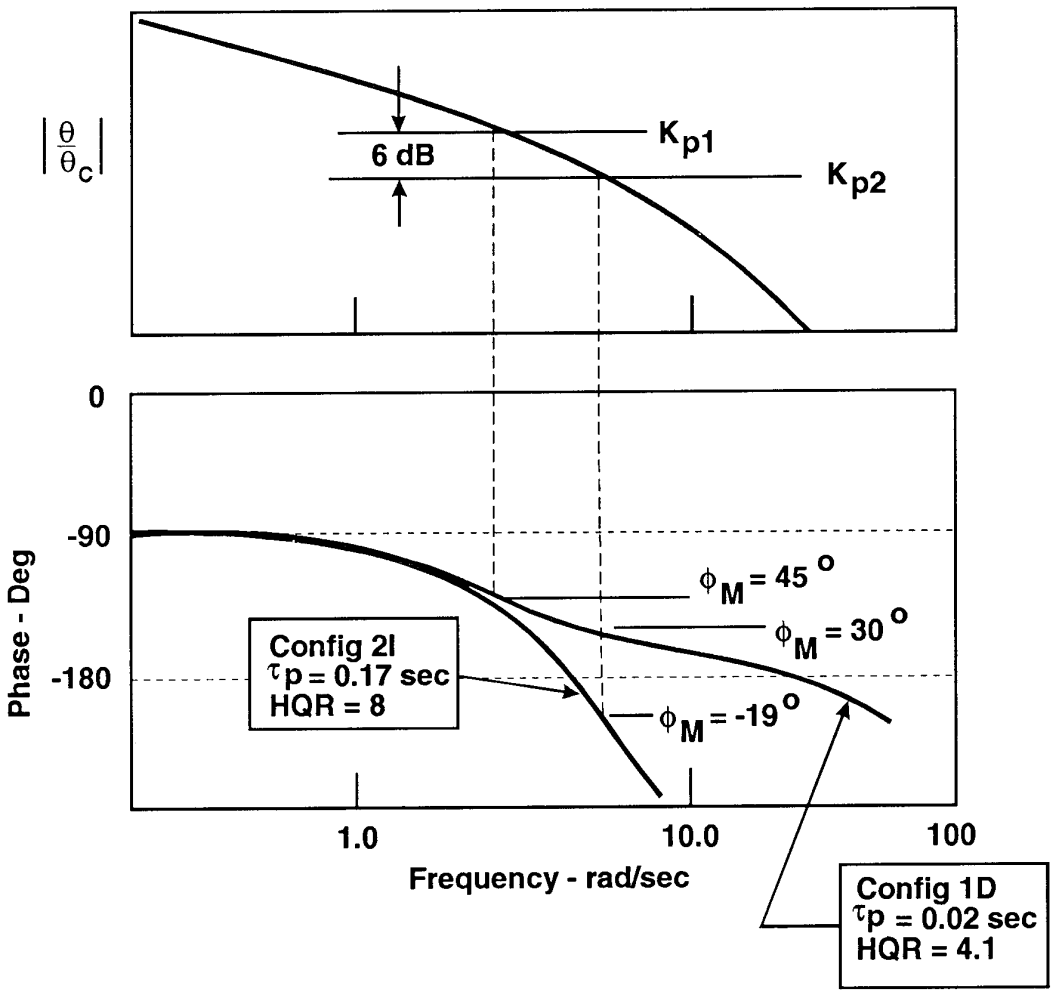

Figure 4 Anatomy of a Pilot Induced Oscillation - Effect of τ_p

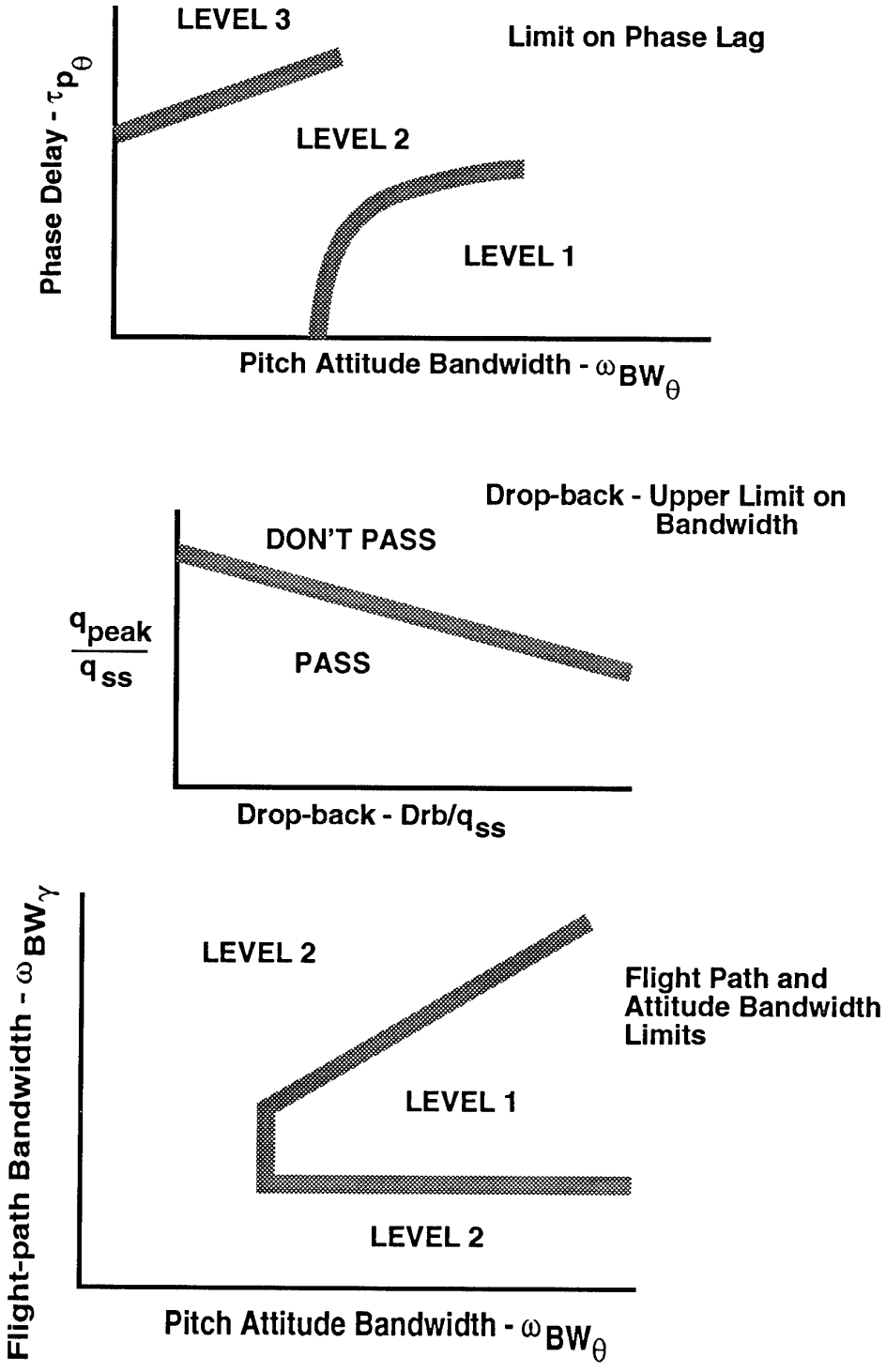

Figure 5 Unified Criterion For Small-Amplitude Short-Term Control

THE PREVENTION OF PIO BY DESIGN

J C Gibson
19 Victoria Road
St.Annes, Lancs.
FY8 1LE, U.K.

Summary

Despite the best efforts of designers, the modern problem of the "high order" pilot induced oscillation continues to provide spectacular evidence of its apparent resistance to solution. The solutions initiated 17 years ago at British Aerospace (Warton), tested and developed on two FBW demonstrator aircraft with excellent resistance to PIO, the FBW Jaguar and EAP, and being applied to the EFA with confidence, are based on simple and repeatable observations of fundamental characteristics of pilot behaviour in these events described in the literature.

Early PIO theories were based on the first high order FCS type, the spring and bobweight system, or on the dynamics of pilot-aircraft closed loop tracking performance. Examples include the low order lateral-directional parameter $(\omega_\phi/\omega_d)^2$, though studies of this have led to a surprising conclusion, and the so-called linear PIO parameter $(2\zeta_n\omega_n \leqslant 1/T_{\theta_2})$, aerodynamically impossible but pointing to the future high order problems. Currently Mil Std 1797 specifies a method which assumes a switch from an attitude tracking closed loop to an unstable normal acceleration loop. The solutions to a wide range of pilot-aircraft closed loop problems are reviewed to show that there is a common thread through most of them. The "high order" PIO contains the additional factor of substantial pitch acceleration lag which leads to a loss of "connection" between the pilot and the aircraft response. It is uniquely confined to a specific open loop pitch response characteristic differing from all the earlier PIO examples, but its solution is essentially similar.

The "synchronous pilot" was proposed over 30 years ago, able when in a PIO to drop all tracking equalisation and time delay because of the regularity of the oscillation and applying control inputs in anti-phase with the attitude response. This is not feasible with a quasi-classical pitch mode because the necessary 180 degrees of lag is not present at a sufficient amplitude, but the latter has been readily supplied by designers in a number of cases. Examination of PIO responses published over many years has shown that the dominant feature is a pilot reaction to the reversal of angular rate, leading to three basic variations in behaviour. These are the original essentially synchronous pure attitude gain mode, a relay switching mode, and a mixture of the two, which seem to be related to the stick and feel design.

The fact that such PIO can be demonstrated in fixed base simulators is added confirmation of the attitude dominance. The attitude response characteristics which can lead to PIO are readily identified without recourse to pilot modelling, however, and it is unnecessary to assume any pre-PIO tracking. Adverse features include excessive phase roll-off beyond 180 degrees lag (ie phase delay), excessive gain at this frequency, and low values of this frequency. Proper attention to these in the FCS design eliminates high order PIO.

Introduction

Film of the Wright Brothers provides the earliest record of pilot induced oscillations. The continuous overcontrolling inputs were the result of the large pitch instability of the "Flier", estimated to diverge to double amplitude in 0·6 seconds. A later less unstable version was still characterised "as stable as a bucking bronco". From that time to the present, man and machine have sometimes coupled in an unsatisfactory or unstable manner, but for a wide variety of reasons.

Pitch instability remained a problem for a while in a number of World War I fighters. It was not totally banished even by WWII, where it caused a range of difficulties from requiring constant attention in cruising flight to occasional fatalities due to severe pitch overcontrol. Other than this, the heavy short period damping typical of conventionally stable aircraft of the time was coupled with generally benign dynamics, and although good handling was not guaranteed there was no unavoidable mechanism for unstable man-machine coupling. Overcontrol might occur due to inexperienced pilot gain adaptation to light controls, or to faulty technique, e.g. attempts at unstable loop closures around parameters such as height, rather than to pilot or airframe dynamic deficiencies.

The handling qualities of post-WWII aircraft, more especially combat types, deteriorated with increasing performance and flight envelope boundaries. Reduced damping in pitch did not create a PIO mechanism per se, though it could undoubtedly lead to poor handling. If the classical response form was retained sufficiently closely, e.g. with only small additional lag dynamics from power control actuators, aircraft with good artificial feel systems could remain free of pitch PIO through more than 30 years of Service life, for example the 1950's English Electric Lightning.

Early use of the simple spring and bobweight introduced serious PIO, sometimes with loss of aircraft. Even before the power control era, a related problem was found in attempts to replace the aerodynamic control hinge moments by close balancing and use of a bobweight to provide the stick force, creating confusing and unpleasant stick force/displacement phasing and low dynamic feel forces. Their use with power controls introduced additional non-classical response characteristics from coupling of the airframe short period and pitch control system oscillation modes, typically with low damping and large resonance at a moderately low frequency.

During this period, theoretical pilot modelling allowed the analysis of many problems of the pilot-airframe closed loop, particularly in pitch attitude tracking. A possible "linear PIO" was proposed for combinations of low frequency and damping of the classical pitch response form, ie without additional unconventional lag dynamics. Experiments in variable stability aircraft did indeed reveal such tendencies, somewhat resembling the high order mechanism actually seen later in fly by wire aircraft. In the lateral-directional axes, the possibility of PIO in closed loop bank angle control was shown to arise when low Dutch roll damping and proverse aileron yaw were combined.

Solutions to such problems were found by application of common sense engineering judgement allied later to theoretical analysis. When fly by wire technology came into use, however, the new "high order" PIO problem arrived with it. Like the earlier bobweight PIO, it has often appeared suddenly and without apparent warning, giving rise to handling ranging from the unacceptable to the catastrophic. It continues to provide spectacular evidence of resistance to a general solution. In all of these events there appears to have been no failure in the functioning of software or hardware. While it has long been obvious that a major element is excessive phase lag which is not present in conventional aircraft, formal requirements intended to prevent this form of PIO have not been sufficient.

Nevertheless, enough evidence exists from the past three decades to provide a consistent picture of high order PIO and of the handling behaviour associated with it. Its prevention by design has proved to be achievable through close attention to critical aspects of the flight control laws. A fundamental axiom has emerged, which is that if a large or divergent oscillation of a specified form can be deliberately excited, no matter how unlikely the necessary control inputs may be judged, then such an oscillation will eventually occur inadvertently.

A Survey of Some PIO Characteristics

The pilot may be an active or a passive element requiring different approaches to the solution. In most cases it will be found

Paper presented at the Flight Mechanics Panel Symposium held in Turin, Italy, from 9-13 May 1994.

that the problem can be stated generally as the existence of an excessive response amplitude at inappropriate values of frequency and/or phase lag. It is worth while to examine the basis of some "conventional" PIO mechanisms and the lessons to be learned from them, before turning to the specific high order problem. A summary of several PIO phenomena was published 30 years ago in Ref 1.

- Bobweight Problems

A comprehensive analysis of the effects of bobweights in powered and unpowered control systems is given in Refs 2 and 3. The twin problems of the control displacement confusingly leading the force and the usually large and poorly damped stick-free response resonance caused by coupling of the control system and short period modes are discussed. Practical solutions include careful choice of the bobweight/spring gain ratio, use of a viscous damper, and the double bobweight system.

Ref 1 applied pilot-airframe closed loop analysis to the T-38 case. The assumption is that essentially stick-fixed attitude dynamics exist in small amplitude pre-PIO conditions, the bobweight being masked by friction. When the bobweight is fully active, with larger forces and accelerations breaking through the friction, the stick free response amplitude resonance is so large that the pilot cannot adapt quickly enough, and an overcontrol PIO ensues. The two modes are shown in Figure 1 at a constant value of pilot gain. (The substantial attitude dropback visible in the basic pitch dynamics - the right hand "knee" - require the use of pilot equalisation to eliminate the closed loop droop at low frequency and resonance at high frequency. With the pilot time delay included, the total open loop stick fixed dynamics would then follow the closed loop 0 dB line quite closely. To emphasise the controlled element dynamics, the pilot model shown here is restricted to a pure gain.)

The solution was to increase the feel spring stiffness and reduce the bobweight mass, increasing the static force per g slightly and decreasing the bobweight gain by a factor of four, greatly reducing the dynamic resonance. The bobweight-active response was reshaped by depressing the response amplitude at the higher frequencies where pilot control is ineffective, relative to the low frequency region in which pilot control is exercised. At the same time the confusion caused by a low initial feel force in advance of motion-generated feel forces through the bobweight was alleviated by a more nearly conventional phasing.

The event was actually a very early example of a "high order system" handling problem, although the damage was done more by amplitude effects rather than by the additional phase lags seen in the more recent examples. The analysis used the concept of the "synchronous pilot", able when in a PIO to abandon both equalisation and time delay because of the predictability of the motion. This has been a powerful tool in the derivation of simple and successful criteria to prevent PIO.

In normal control conditions the predominant pilot inputs must have been stick displacements. Pure force inputs would continuously excite the stick free mode to give intolerable handling. Once in the PIO, there is no reason to suppose that the pilot would abandon displacement inputs altogether in favour of pure force inputs, but something certainly changed. It is extremely likely that biodynamic coupling, with very large g excursions of up to $\pm$ 8g, strongly influenced the actual control inputs through the stick free response. Records show that deliberate attempts to freeze the stick in a large amplitude PIO are not always entirely successful, with continued but reduced activity.

In a modern fly by wire aircraft, a significant difference between the stick fixed and free dynamics is unlikely. The added pilot's arm mass would not bring the feel system mode frequency too close to the short period or its equivalent. Biodynamic coupling will then be improbable as a cause of pitch PIO. It has proved sufficient in the author's experience to assume that the feel system dynamics play no important part in prevention of PIO for such aircraft. The level of stick forces, ie heavy or light, is of course a factor accounted for in the static gain of the response.

- The "Linear PIO"

It is shown in [1] that given the synchronous pilot assumption and negligible control system dynamics, PIO involving only attitude control should be essentially impossible. This results from the fact that the maximum phase lag of the classical attitude frequency response does not exceed 180 degrees. Greater lags, and therefore PIO, are theoretically possible if

$$2\zeta_n\omega_n \leqslant 1/T_{\theta_2}$$

Figure 2 shows a typical attitude response plot of such a "linear PIO" example. The attitude closed loop gain and phase margins are small even with the moderately heavy stick force of 6·0 lbs/g for which the response was calculated. The damage is done by the resonance and rapid phase shift due to the low damping at very low frequency where the basic K/S gain is still high. In essence the response switches rapidly from K/S-like to K/S^2-like, with 180 degrees lag and an attenuation of more than 40 dB/decade.

This is virtually impossible to achieve by aerodynamic means, as it typically requires the pitch and angle of attack rate damping to be of opposite sign. It has been regularly tested in in-flight and ground based simulation by forcing unnatural combinations of low frequency and damping. PIO tendencies have indeed been found in such cases. The pilot adaptation associated with compensatory tracking in this region was identified by Hall [4] as less than 50% linear with a very large lead component, the non-linear remnant resulting in "a rather frantic switching technique", Figure 3. The stick pulsing is commonly associated with acceleration control. The boundary found between linear and non-linear pilot behaviour lies closely along the "linear PIO" line.

- Closed Loop Tracking

Figure 4 represents pitch attitude closed loop tracking in a low altitude strike aircraft with high wing loading and low lift slope. The pilot model includes only gain and time delay. The pronounced "shelf" in the upper response is the result of the wide spacing between the $1/T_{\theta_2}$ numerator and short period break frequencies. This is associated in particular with large attitude dropback and "bobble PIO". The very substantial equalisation necessary to achieve good tracking performance, which must normally be generated by the pilot, is provided here by command path filtering in the lower response. This achieves excellent tracking and gives considerable freedom to the pilot for some limited equalisation and gain adjustment to increase the closed loop bandwidth if desired.

An intermediate development half way to the final version shown gave good general handling, but was subject to small tracking PIO when tight loop closure was attempted. Detailed "Neal and Smith" analysis would undoubtedly reveal such a trend, but it is preferable to apply their lessons to the control law design given the freedom to do so in a fly by wire system. This enables the "no tracking" hypothesis [5] to be satisfied. It states that "Optimum handling qualities demand minimum closed loop control by the pilot", and that it ought to be possible to identify the open loop aircraft responses which promote this state. This principle was independently adopted in the work discussed in [6 - 10]. Just as in the bobweight example, but by very different means, the closed loop control problem here was eliminated by reshaping the response in a way which reduces both the droop and closed loop resonance.

The generic process is illustrated in Figure 5, resulting in a modified open loop response following the general form of the shape template suggested in [7] (referred to sometimes as the "Gibson Criterion"). This entails reducing the excessive phase advance at low frequencies with negligible gain alteration, and reducing the excessive gain at high frequencies with negligible phase alteration. For best results, this is performed in conjunction with analysis of the transient response where the attitude dropback and pitch rate overshoot can be directly controlled. It is purely an open loop design process, from which the closed loop dynamics can be readily inferred from the background Nichols plot. Further adjustment may then be required to achieve satisfactory response gain levels.

- Sensitivity

It is well known that a response with satisfactory dynamics may be found oversensitive and PIO-prone if its gain is too high, or sluggish and unresponsive if the gain is too low, perhaps leading

to the "overdriving" PIO. There is considerable evidence to suggest that the traditional measure, the stick force per g, plays only a minor part.

CAP has been a candidate, but it does not involve the element of stick force gain necessary to define sensitivity. The upper ranges of allowable CAP, associated with excellent manoeuvrability, give poor attitude precision. It seems a common design practice to limit CAP to middle to low values for optimum attitude handling. Excellent results were obtained on the EAP demonstrator with CAP less than 0·5. Originating as a measure of precision flight path control in landing approaches [11], CAP provides a rationale for the choice of the short period natural frequency. With the damping, the latter determines the rapidity with which a flight path angle rate change is initiated. CAP itself defines only the initial angle of attack acceleration, but not the subsequent transient attitude and rate behaviour which often dominates the pilot's behaviour and opinion [7 - 10].

It has been shown [7,12] that the pilot-selected stick forces in the LAHOS experiment [13] can be much more closely correlated with the attitude gain at the open loop bandwidth frequency than with the stick force per g. This frequency is defined as that at which the phase angle is -120 degrees [7] or the better known 135 degrees [12]. The upper gain limit marks the boundary of oversensitivity, and the lower limit that of sluggishness, but the actual values decrease with increasing bandwidth. Although this parameter has been useful in design, the absence of a reasonable explanation of its dependency on bandwidth in human pilot terms is unsatisfactory.

This may be resolved by the "Pitch Rate Sensitivity Criterion" [14], modified slightly in [15]. This proposes upper and lower pitch rate frequency response gain boundaries against the pitch rate response phase angles. Over a range of frequencies close to the pitch attitude bandwidth definition point, these limits are nearly constant. They are therefore independent of the bandwidth itself. The design process can be simplified by using only the unique limit values at the bandwidth phase angle. Plotted against bandwidth in Figure 6, the corresponding attitude and acceleration boundaries can be derived. These have the same form as the attitude criterion in [7] and a pitch acceleration criterion suggested in [9], which should be expected as they are all derived from the same data [12].

It seems logical to accept that the well known pilot preference for rate-like control for many purposes, expressed by the nearly universal K/S optimum for closed loop control, makes sense of a constant range of satisfactory rate gains in the crossover region. The simple design criterion obtained from this is a check on the rate gain at the bandwidth frequency to ensure that it lies within the proposed limits. The method is shown in Figure 5. It has produced good agreement with pilot assessment of sensitivity in simulations, though it has yet to be tested seriously in flight. The shaping process discussed in the previous section is extended by gain adjustments, either static or dynamic, to bring the rate gain within the limits.

- Neuromuscular "Dither"

It has been observed that some pilots may generate a high frequency stick dither, presumably due to neuromuscular tension effects, when performing very tight closed loop tracking. If the aircraft response gain is high enough, the oscillation may visibly intrude into the tracking task. The attitude phase lag at the typical frequency of around 2·5 Hz or 15 radians per second will certainly exceed 180 degrees, even with the best design practices and a generally low order-like response. Despite this, it is unlikely to be a PIO in the commonly accepted sense, as significant closed loop control at such a high frequency is improbable.

No systematic study of dither amplitudes has been made, but a typical stick force input of ±1 lb is assumed. To prevent this nuisance effect, an arbitrary choice of maximum attitude gain at 2·5 Hz can be made, say ± 0·5 mil/lb. This is readily added to the shaping process in Figure 5, applicable at least to small control amplitudes for flight cases appropriate to precision tracking.

- Bandwidth

Upper and lower limits have been a feature of several proposals, e.g. Figure 6, the early Northrop Criterion, and the Bandwidth Criterion. A fixed range of bandwidth is not a natural feature of conventional aircraft, in which it varies with speed approximately in proportion to the short period natural frequency [9]. Considerable variation in bandwidth is therefore natural in a wide speed range. Excessive bandwidth at a particular flight condition results from high short period frequency and the corresponding attitude "shelf". This creates the attitude dropback and pitch rate overshoot effects which lead to "bobble PIO". This is typical of examples in the upper range of allowable CAP. No conclusion can be drawn about bandwidth limits at other flight conditions.

In a comprehensive tracking experiment [15], all the cases lay well into the Level 2 region of the Bandwidth criterion, despite many ratings of 2 to 3. Bandwidth "islands" seem to resemble the early short period frequency and damping thumbprints, inconsistent between different experiments but actually characterised by consistent internal measures of attitude, pitch rate and flight path behaviour. It was shown in [10] that such elements had much more influence on tracking efficiency than the bandwidth *per se*. However, when these elements can be optimised by command path filters, it may be that the higher the bandwidth is the better the tracking performance will be - i.e. the response will remain K/S-like to higher frequencies, unlike the purely classical response form.

At the other end, low bandwidth may or may not be a sign of sluggish handling, which can be identified more clearly by those internal elements mentioned above. This is particularly true for cases prone to high order PIO. As will be shown later, this problem is marked by a completely different set of parameters, and can be resolved without reference to the "handling" bandwidth.

Universal bandwidth requirements do not appear to be available to assist in the shaping process of Figure 5, therefore. Nevertheless, it is useful to note the values during an overall handling qualities assessment design exercise, if only to help to curb the enthusiasm of designers to push up the bandwidth at inappropriate conditions simply because it can be done.

- Flight Path

In conventional aircraft, difficulties can be experienced in the explicit control of flight path as opposed to its general management in association with attitude and thrust control. Flight path angle lags pitch attitude by the T_{θ_2} time constant, and reaches 180 degree phase lag relative to the stick at the short period frequency. Flight path vertical displacement lags by a further integration, with a phase lag always greater than 180 degrees relative to the stick. In practice, the strategies for path control are not particularly difficult when the path cue is obtained from a distant visual aid. Pilots readily adapt to using thrust or attitude as the effective rate command input for long or short term path adjustments as appropriate, in what is principally pursuit tracking. Analysis becomes more difficult for the multiple loop landing flare task, and for height tracking tasks in general which become more compensatory in nature. Some of this is studied for example in [16].

The lesson for control designers is that the flight path angle response should be K/S-like at least over the appropriate bandwidth of interest. This is usually ensured by satisfying the allowable minimum short period frequency for conventional aircraft, so that the delay until the new flight path angle rate is established is acceptably short. It is readily quantified by the "flight path time delay" measure [7-10] which accounts for both frequency and damping. Figure 7 [10,17] shows that large parts of the Cat.C Level 1 area give long and unsatisfactory delays. The corner point "X" was shown [10] to produce a K/S^2-like path angle response in the bandwidth of interest, with an accelerating time response prolonged far beyond a pilot's predictive limits. Values of 1·5 and 1·0 seconds have been proposed [10] as limits for normal and precision landings. There is close agreement with proposed bandwidth limits of 0·6 [18] and 0·8 [19] radians per second for these tasks. Some in-house Cat.C design criteria feature an increase above the specified minimum frequency to ensure good path control.

In superaugmented aircraft, a similar K/S^2 effect results from a different cause [16] which is outlined in Figure 8. Here a tight proportional plus integral attitude rate control introduces addi-

tional flight path phase lag from below $1/T_{\theta_2}$ radians per second, which unfortunately is usually within the bandwidth of interest for landings. The physical result is to suppress the normal pitch rate overshoot, possibly but mistakenly seen as a desirable end in itself, which prevents rapid acquisition of the large angles of attack required for low airspeed manoeuvres. The attitude and more importantly here the flight path become sluggish. Reintroduction of the overshoot by command path lead-lag filters to cancel the added lag-lead dynamics can restore short term flight path precision, though not the benefits of longer term speed and angle of attack stability for which other remedies are needed.

Such problems demonstrate in a greatly exaggerated form the dynamics added to improve attitude precision by lag-lead tracking filters. These eliminate only the unwanted excess pitch rate overshoot to obtain K/S-like attitude response. Because the bandwidth in up-and-away flight is generally much higher, the lag added to the flight path response, termed "g creep" [20], can be acceptable. At the least, a trade-off can be made between attitude and path effects in a logical design process. PIO associated with flight path control at higher speeds has not been widely reported, but one example has been given from the Shuttle Orbiter [21]. This occurred while attempting to zero a flight path error on a cockpit display, made more difficult by the usual flight path lag. This problem can be avoided by quickening of the HUD velocity vector or climb/dive symbol, adding a deflection proportional to pitch rate. The symbol response to control input then more nearly resembles K/S. Although the flight path response is not altered in any way, its control is much easier in demanding situations such as very high speeds at extremely low heights, or where it is used to assist performance of a landing flare.

- Lateral-Directional PIO

The possibility of pilot/aircraft closed loop bank angle PIO in a conventional aircraft with low Dutch roll damping and proverse yaw roll control was identified very many years ago, associated in principle with $(\omega_\phi/\omega_D)^2 > 1$. In flight testing of the unaugmented handling of aircraft types with low natural Dutch roll damping and with differential tail roll control giving strong proverse yaw, many small lateral PIO's have been recorded. Typically these were induced at the point of switching from augmented to unaugmented mode and were not a flight safety issue. In the overwhelming majority of examples, the PIO was in heading angle, the bank angle version being seen only briefly if at all. When the latter did occur it would evolve rapidly into a heading PIO.

Figure 9 shows such a PIO recorded in the "spin recovery" mode of the FBW Jaguar (in its early aerodynamically stable test phase). In this there were only purely direct stick to control surface links to enable the pilot to apply the specific inputs required for recovery from a spin. Simulation showed that lateral overcontrol was easily excited at high speeds, but was manageable. When the mode was tested in normal level flight, a very persistent PIO resulted. This could be kept small by a delicate touch on the stick, but the amplitude ratios were such that full stick would have produced more than ±20 degrees of bank and this was considered unacceptable. However, the stick oscillations were not out of phase by 180 degrees to the bank angle, as expected, but to the roll rate. No sensible justification could be found to support such a closure, and theoretical analysis of this closed loop did not match the flight results.

The stick was also out of phase with the heading angle as indicated by the yaw rate zero crossings. Analysis of this loop closure showed excellent agreement with flight, Figure 10. It also made sense, as a pilot's primary use of the roll control is to steer to a desired heading. (Indeed, a similar PIO is often seen in aircraft with high Dutch roll damping and pronounced adverse yaw, when pupils attempt to steer to a precise heading before they have learned the necessary rudder coordination.) A lateral stick to rudder interconnect was added, producing a close match of both the frequency and damping in the transfer function numerator and denominator. Analysis showed a 9 dB increase in closed loop gain margin and a 90% reduction in the open loop response amplitudes at the Dutch roll frequency. Flight tests showed very much improved and acceptable handling.

This is another example of PIO caused by a large amplitude at the wrong phase angle combination, resolved by adjusting them to values which cause no problem. The heading loop should always be considered in the design process if the possible aircraft states include low damping and large control induced yaw.

- Roll Ratchet

Roll ratchet is typified by a roll oscillation at relatively high frequency, between 2 to 3 Hz. This puts it outside the possibility of a conscious tracking action. Two mechanisms have been suggested, a biomechanical coupling involving roll acceleration forces on the stick and arm mass, or a neuromuscular phenomenon.

It has been shown that with a rigid side stick, resonance of the neuromuscular system, or neuromuscular peaking, can produce such an oscillation [22]. Another study [23] incorporating a neuromuscular model showed that the assumption of a lateral acceleration bobweight loop could produce roll ratchet with both rigid and moving sticks. The high frequency behaviour of the aircraft was found to be of much greater significance than the neuromuscular effects. There was however a difference in the stick height above the roll axis necessary to produce ratchet. The bobweight loop analysis has been entirely successful in the case of aircraft with conventional centre-mounted sticks.

Actuation loops quite typically have a moderate damping with a natural frequency in the 2 to 3 Hz region, and this can also typify lateral feel systems with the arm mass included. There can be ample scope for roll ratchet in such cases. Figure 11 shows oscillatory roll behaviour in early test flying of a spoiler-equipped aircraft. The principal cause was a local increase in spoiler control power at small deflection angles, with a loss of stability in the roll damper loop at low roll rates. A significant part was also shown to be played by the lateral acceleration bobweight loop. This enabled adjustments to be made to remove its influence while linearising the control moments by aerodynamic and spoiler command modifications to restore the stability margins. The overall solution was thus able to account for all the factors involved in a logical manner.

A mild roll ratchet was found in the FBW Jaguar at high speeds [9]. It occurred only when the stick was held lightly, but was prevented completely by a firm grip. Lateral bobweight analysis identified the necessary control law change, and with the addition of a stick damper the ratchet was eliminated. This analysis was performed in control law design of the EAP, showing ratchet gain margins of some 30 to 40 dB. In flight, despite "spectacular" roll acceleration considered to be on the upper limit (more strictly this was a head level lateral g limit), no ratchet occurred and the well-damped stick was completely inert to motion effects.

- Nosewheel Steering

While the tricycle landing gear revolutionised ground handling, its stability under heavy braking relies upon the free castoring of the nosewheel. If nosewheel steering is engaged, as it is permanently on some aircraft, this condition produces a marked divergence tendency which commonly leads to a mild steering PIO. Flight records show that the pilot applies pedal inputs which are 180 degrees out of phase with the heading angle. Thrust reversing for short landing runs is also very likely to produce unpredictable yaw moments. The combination may produce serious difficulties, as was found on the SAAB Viggen for example. These were solved by thrust reverser and steering system modifications.

With FBW systems coming into use, it became a simple matter to add yaw rate feedback to the nosewheel steering system. Analysis shows that not only is the damping improved, but that there is a marked degree of directional stiffness. This greatly simplifies the task of tracking along the runway centre line even in the presence of thrust reverser disturbances. Figure 12 shows the generic heading response characteristics of the basic and damped systems. The pilot gain is derived from flight records, expressed as the ratio of nosewheel angle to heading error. Unaugmented, instability is indicated at a frequency very close to typical flight experience. With augmentation, very large stability margins are present which are fully supported in practice.

Here again, a closed loop problem created by a poor amplitude/phase angle combination is eliminated by modifying the response to a K/S-like form.

The High Order PIO

This class of PIO has many similarities to the early bobweight PIO which destroyed several aircraft and frightened a number of other pilots. Both have been distinguished by their ability to lie dormant and unseen, suddenly making an appearance after many trouble free flights. They differ in two important respects. The bobweight PIO was primarily a high speed phenomenon where sufficient energy could be supplied to the normal acceleration feedback loop, and was marked by a sudden or non-linear transfer from stick-fixed to stick-free dynamics. The high order PIO has been primarily associated with low speeds, mainly in the landing task, and with linear flight control laws which contain elements absent from the conventional or "classic" type. It may however occur at other flight conditions and can appear at the beginning of test flying. The results can range from the spectacular or catastrophic to the serious nuisance.

The studies reported in [6-10] suggest that the problem can be empirically understood sufficiently well to derive FCS design methods and criteria which ensure its prevention. These have been based on analysis of the open loop characteristics of aircraft prone to PIO, coupled with assumptions about the pilot behaviour and loop closure consistently apparent in PIO flight records. Like the solutions discussed above for the conventional PIO problems, the high order PIO solution requires the adjustment of inappropriate gain and phase characteristics, but unlike the former it is focussed on a different and readily predictable "PIO frequency" region. It has not been found necessary to consider the transition from normal control to the PIO situation.

- Pilot models

The problem of experimentally determining the actual pilot model involved in PIO was discussed in [1]. This notes that the pure gain pilot assumption had distinct success in early PIO investigations, though this could not be certain for all cases. Experience showed that most of them could be understood by considering attitude and/or normal acceleration as the dominant sensed quantities. Nevertheless, it emphasised "that in spite of the accompanying vertical accelerations, attitude cues will be those the pilot consciously uses in attempting to get out of a PIO situation".

A PIO theory was developed [24] which postulated that concern over flight path or path-related acceleration components was an essential part of genuine PIO. It was assumed to start with highly resonant closed loop dynamics resulting from pitch attitude tracking. The pilot loop closure was assumed to switch from attitude to normal acceleration, given certain conditions. A simplified version of this appears in the current requirements [25]. However, this work was based on conventional aircraft. A later study of roll PIO [26] was extended to the pitch axis. It concluded that attitude-only pitch PIO was possible in the presence of high order phase lags, in which the normal acceleration dynamics were irrelevant.

Ample justification exists to support the notion that only the pitch attitude dynamics need to be considered in these PIO cases. It has been conclusively demonstrated that fixed base simulation can excite identical PIO characteristics to those found in flight, e.g. [27]. Figure 13 shows one example (with a control law intentionally constructed to prove the principle) with an initial half-cycle input followed by an attempt to suppress the response. Its violence is not artificial and it is identical to a real event with a quite recent fighter prototype. There is little difference between the attitude and angle of attack response, showing that the flight path changes are negligible. PIO has on occasion grown out of small oscillations with control inputs out of all proportion to any possible pilot concern about the normal acceleration amplitudes. When close to the ground, undemanded attitude changes are an infinitely more pressing cue that the aircraft is out of control than the initially moderate oscillations in g.

In every example of a PIO flight record available for study, the pilot's control action is related to the attitude response. Three types of control input can be found. Many PIO's show the synchronous sinusoidal behaviour in Figure 13, e.g. the landing PIO example in [10]. Sometimes there is a relay-like behaviour as shown in Figure 14, a roll PIO example from the M2-F2 lifting body vehicle [26]. Here the bang-bang control reversals are precisely triggered by the zero crossings of the roll rate, i.e. at each bank angle peak. The same behaviour is found in some pitch PIO cases, the trigger being the pitch rate zero crossings. This is clearly seen in the published flight record of the YF-22 PIO [27]. A third form combines the first two. The control is applied in a half-cycle quasi-sinusoid and is then held until the rate crossing occurs as in the example of Figure 15, or there may be a momentary hesitation just prior to this point.

Which type of behaviour will occur seems to depend on the stick characteristics. The smoother sinusoidal type can be expected from a conventional stick with traditional displacements, and with more modern sticks with smaller but still significant travels of two or three inches. However, lateral inputs are by custom more likely to be abrupt and can often show the combined "too-fast-then wait" type. Sticks with very small travel will readily provoke the relay type of behaviour.

Because pilots are not machines, a certain amount of output noise is usually evident. There is often some higher frequency oscillation which may be neuromuscular in origin, or a short break in the rhythm as the pilot tries to make sense of the event. A mathematically pure model of their behaviour is unlikely, but it is unnecessary provided that the essentials are captured. This permits attention to be devoted solely to evaluating only those open loop aircraft dynamics which promote the PIO coupling.

- The PIO Elements

The elements of the PIO evaluation methods presented here [8,9] are shown in Figure 16. No feel system dynamics are included but the pilot gain is referenced to stick force. The pilot/aircraft closed loop instability occurs at the usual unity gain and 180 degrees of phase lag. As the assumed pilot has no lag, and possibly a little lead, the PIO occurs at the frequency where the aircraft phase angle is in the region of -180 degrees or a little more.

The significance of this region was noted as a consequence of the Bihrle theory of stick pumping [6,11]. This excites a threshold level of pitch acceleration at a frequency in phase with the stick input. It is thought to provide assurance of good pitch control as the stall is approached near the ground, though pilots are usually unaware of it. It occurs only in the final landing flare. Bihrle's pumping was found on and is appropriate to many land based aircraft where a landing flare is performed. It was accurately predicted before flight for the Tornado, FBW Jaguar and EAP. (A different carrier approach pumping is described in [24]. A voluntary, monitored excitation of normal acceleration oscillation was found with the apparent purpose of providing an adaptive cue for the rapid detection of aircraft settle in the carrier ramp downwash.)

Stick pumping naturally produces an attitude oscillation with a phase angle of -180 degrees. When the PIO discussed in [6] occurred, it grew straight out of the stick pumping oscillation, which led to a study of the pitch dynamics in this region. The pitch angle response while generating the nominal ±6·5 degrees per second^2 acceleration depends on the pumping frequency, Figure 17. In conventional aircraft, where the normal pumping frequencies are typically 1·0 to 1·5 Hz, its amplitude is very small and remains unnoticed. As the 180 degree lag frequency decreases, a natural consequence of increasingly high order phase lags, the pitch amplitude increases to levels which will inevitably become obvious to the pilot. When this happens, a ready-made PIO activity is presented, particularly as the pilot's gain will probably increase at this point.

Another consequence of low PIO frequency is a low pitch acceleration gain, discussed in [10]. In a low frequency landing PIO example rated 10, a stick input of some ±6 lbs was needed to generate the nominal pitching acceleration threshold. This PIO was unstoppable. It is a common experience that pilots in similar cases believe that the aircraft is not responding to their inputs in any way. This seems to be because the conventional connection between input and response appears to be absent. In a much higher frequency tracking PIO, only ±1 lb was needed to produce the nominal acceleration. Although oscillations of over

±2 degrees could not be prevented while tracking, the PIO could be stopped at will by abandoning the task. With an ample acceleration response to the stick, the input-response connection would be obvious. There would be no doubt that the aircraft was responding to the input, even though the task could not be performed adequately.

The feeling of a connection between the stick and the response is conventionally provided by an essentially instantaneous pitch acceleration when the stick is moved. Higher order effects produce a lag (not a delay!) in this response with a reduced amplitude. It is suggested in [10] that this response should peak in not more than 0·25 seconds, or ideally in much less, to avoid noticeable problems. The worst rated cases in [13] have transient peaks lagged by as much as 0·6 seconds, a parameter far more effective as an indicator of problems than the "effective time delay" extracted from the pitch rate response. The culprit is almost invariably a lag deliberately placed in the direct path between the stick and control surface, for example in the mistaken belief that it will attenuate the response. As seen in Figure 16, it amplifies the PIO response.

A close though not exact connection between higher order frequency and time response effects is represented by the phase delay [25] or phase rate [8-10] parameters. These quantify the rate per unit frequency at which the pitch attitude phase lag increases beyond the 180 degree lag point, which of course is zero for a truly low order classical pitch response. Phase rate can be adversely influenced in some cases by localised variations near the PIO point, and an extended version accounted for this to some extent. A simplified average phase rate which captures more accurately the high order effects is shown in Figure 18 together with previously published "PIO frequency" minima. Identical to phase delay in principle, when expressed as such its value seems typically to be some 33% to 50% of the time of the peak in pitch acceleration after a step input.

The attitude response gain in a PIO is obviously of importance, as if it is small enough then no serious problem can arise - which is in effect part of the principles used in solving many of the closed loop control difficulties discussed above. While a nominal maximum gain design aim is given in [7-10], this makes no allowance for the inevitable occasions when it cannot be - or has not been - satisfied and whose handling cannot therefore be fully quantified. A new trawl through LAHOS [13] has revealed a remarkably consistent set of upper gain boundaries for the pitch attitude response, shown in Figure 19. A retrospective check of some other PIO data showed good agreement with them. In marginal cases with respect to any of these limits, a response with a slope steeper than the boundary can be considered more leniently than one with a shallower slope.

Although Level values are ascribed to the amplitude boundaries, they are strictly to be interpreted as design aids only. This applies equally to the phase rate/frequency boundaries in Figure 18. They represent a long evolution, from initiation to solve a PIO [6], through perhaps the first control laws ever intended to prevent PIO in the FBW Jaguar, to the EAP control laws guaranteed to prevent PIO. No example of a significant high order PIO has been found which did not violate one or more of the criteria. It is reasonable to demand higher standards for the design process, such as a smaller amplitude limit and a higher minimum frequency more in accord with the natural conventional response.

- Non-linearities

The high order PIO is generally a problem of linear control law design. However, it is obvious that non-linearities have played a major role in some. Rate limits in older conventional aircraft existed at the actuator and did not necessarily influence any stability augmentation feedbacks to a serious extent. If they did then the aircraft often had enough reserve of stability to stay out of trouble. This was not always the case, e.g. the X-15 landing PIO [1] where extremely low tail actuator rates, a non-functioning pitch damper and a small travel stick combined into a problem.

Fly by wire aircraft may depend completely on a functioning feedback system, and if this stops working because its signals pass through a rate saturation point, then trouble can certainly be expected. Actuator acceleration limits may be even more important. The supposedly sharp saw-tooth shape of a rate limited response may actually be rather round cornered, adding even more positional error to the control surface, Figure 20. The jump resonance phenomenon can also be introduced, where the phase lag can very suddenly increase to a large value especially when large inputs are applied. Such problems are entirely predictable and can be dealt with accordingly.

A rate limit on the stick signal itself, outside the closed loop feedbacks, may have a less serious effect and can be on occasion a useful device. Although it will probably reduce the PIO frequency, it may have little effect on the gain there because its extra phase lag is countered by its reduced gain. If the frequency is reduced too much in an overcontrol situation, however, that vital connection between stick and response will begin to be lost.

- Testing for PIO

Since a PIO problem may remain hidden for some time, despite the best efforts of designers, it is essential to hunt it down before the first flight. A number of well established handling tasks have been evolved to ensure that pilots operate at the highest possible closed loop gain, notably the offset landing manoeuvre. These seem to be quite effective in fixed based simulators, although as is well known the real flight environment provides an ultimate stimulus not to crash the aircraft as well as the motion cues which affect the pilot's perceptions and control.

If in-flight simulation is not available or feasible, and certainly during the design stages, it is possible to unearth a PIO problem by the simple expedient of exciting the PIO frequency oscillation. All three types of input noted above depend on the attitude response for their timing and are readily learned. A fast and small oscillation remains very obviously forced. If it diverges as in Figure 13, a serious problem exists. In between, there will be a point at which the oscillation is not very large and does not diverge, but nevertheless gives the impression that the aircraft is not fully under control. It is hard to quantify this but pilots seem to agree quite well. Performing this test while flying very low along a runway provides an excellent reference.

A preliminary comparison of PIO assessment in the simulator at the Technical University of Delft showed that the feeling of connection between stick and response for a non-PIO prone aircraft was obvious with motion on. This feeling was so reduced for a seriously PIO prone case that motion could barely be detected, and there was no real difference without motion. Also, provision of strong peripheral vision cues, now available in many simulation visual displays, can be an effective substitute for motion [28], and this is especially true if the motion is inaccurately represented.

It is unlikely that the landing flare stick pumping will be found in a ground based simulation. This is not an important consideration for discovery of a PIO, which can be deliberately excited in this artificial manner. A PIO can also begin at a large amplitude if its trigger is a sudden control input, for example when recovering from the last stage of an offset approach. The tests must include stick amplitudes from small to the maximum nominally sinusoidal limits possible between the stick stops. It is of course necessary to model any control law, aerodynamic and actuation non-linearities very closely in all forms of simulation. It hardly needs to be said that all possible flight configurations must be assessed, including wheels up near the ground and degraded failure modes.

The most dangerous assessment result of all is the one which says "The pilot will never do that!".

- Roll PIO

High order roll PIO is seldom discussed and there is a shortage of flight data from which to derive criteria for its prevention. It can be said with certainty that it is identical in its essentials to the high order pitch PIO, and involves the bank attitude closed loop where the open loop response has 180 degrees of phase lag.

Application of the frequency/phase delay criterion in Figure 18 to the roll axis has been found to work well. Obviously, a different amplitude criterion must apply, and this can only be a matter of judgement. Some research in this area is planned in the Delft simulator. Clearly a smaller limit should apply to the landing case, since only here is the pilot seriously concerned about bank

angle control from a safety viewpoint. Once again, it should be assumed that the pilot may use full lateral control inputs and the question answered - "How much bank angle would be acceptable?".

Using such criteria, a slight deficiency was predicted in the initial lateral flight control laws of the EAP, but judged to be acceptable until the following update. This did indeed lead to the slight roll oversensitivity noted in [29], which amounted to a tendency for one or two cycles of small wing rock just before touchdown. The amplitude was typically ±0·5 degrees of bank angle and ±5 mm of stick input. With the updated laws fully satisfying the criteria, the deficiency was eliminated.

The criteria were also used to set up a limited familiarisation exercise in the Calspan Learjet. A number of theoretically PIO-prone roll handling cases produced pilot ratings satisfyingly close to the predicted values. In the case intended to produce a 10 rating, the extremely skilled pilot at first resisted but then fell victim to an unstoppable PIO at touchdown.

Conclusions

Control problems caused by poor pilot-aircraft closed loop characteristics have existed for as long as aircraft have been flown. The majority of them have been the result of excessive response amplitudes and phase lags conflicting with simple stability margin requirements. Their solutions have been rather straightforward and often amount to the provision of K/S-like responses, or sufficiently similar, within the bandwidths of interest.

Most high order PIO problems have been introduced, not by more complex fly by wire control laws, but by unnecessary lags or sometimes by excessive gain placed between the pilot and the response. The pilot is forced to operate in a region of excessive phase lag and response gain, typically with the impression that the aircraft is not actually responding to the commands. The solutions address the provision of adequate stability margins in much the same way as in earlier problems.

The high order PIO problem is identified in the open loop attitude behaviour in the uniquely defined PIO frequency region, in which the response lags the stick by 180 degrees or more. It is not necessary to model the pilot, who is found to operate in a synchronous manner with the attitude oscillation. The dominant feature in this is the rate zero crossing which acts to trigger the reversals of the control input. The input itself may take the form of a sinusoid, a relay switching action, or a mixture of the two.

A number of simple criteria can be applied to control law design which have been found to ensure the prevention of high order PIO. The existence of a PIO problem can be identified with great certainty before flight by specific test methods, which should be applied with rigour no matter how much confidence exists in the design methods.

Finally, it is crucial for all concerned to understand that if the underlying problem is there, no matter how extreme the pilot inputs may have to be to excite it, then it can be expected to happen in flight. It will be impossible to prevent it by pilot briefings.

References

1 Ashkenas, I.L. *et al*, "Pilot Induced Oscillations: Their Cause and Analysis", STI TR-239-2, 1964

2 Chalk, C.R. *et al*, "Background Information and User Guide for Mil-F-8785B(ASG), 'Military Specification - Flying Qualities of Piloted Airplanes' ", AFFDL-TR-74-9, 1969

3 Neal, T. Peter, "Influence of Bobweights on Pilot-Induced Oscillations", J.Aircraft Vol.8, No.9, September 1971

4 Hall, I.A.M. "Study of the Human Pilot as a Servo-Element", Jnl. of the R.Ae.S., Vol.67, No.630, June 1963, pp 351-360.

5 Smith, Ralph H. *et al*, "Handling Quality Requirements for Advanced Aircraft Design: Longitudinal Mode", AFFDL-TR-78-154, 1979

6 Gibson, J.C., "Flying Qualities and the Fly-by-Wire Aeroplane", AGARD-CP-260, 1978

7 Gibson, J.C., "Piloted Handling Qualities Design Criteria for High Order Flight Control Systems", AGARD-CP-333, 1982

8 Gibson, J.C., "Handling Qualities for Unstable Combat Aircraft", ICAS-86-5.3.4, 1986

9 Gibson, J.C., "Evaluation of Alternate Handling Qualities Criteria in Highly Augmented Unstable Aircraft", AIAA 90-2844-CP, 1990

10 Gibson, J.C., "The Development of Alternate Criteria for FBW Handling Qualities", AGARD-CP-508, 1991

11 Bihrle, William, "A Handling Qualities Theory for Precise Flight Path Control", AFFDL-TR-65-198, 1966

12 Hoh, Roger H. *et al*, "Proposed Mil. Standard and Handbook - Flying Qualities of Air Vehicles", AFWAL-TR-82-3081, 1982

13 Smith, R.E., "Effects of Control System Dynamics on Fighter Approach and Landing Longitudinal Flying Qualities", AFFDL-TR-78-122, 1978

14 Sturmer, S.R., "Pitch Rate Sensitivity Criterion for Category C Flight Phases - Class IV Aircraft", AIAA 86-2201, 1986

15 Wilson, D.J. *et al*, "Unified Flying Qualities Criteria for Longitudinal Tracking", AIAA 90-2806-CP

16 Myers, T.T. *et al*, "Space Shuttle Flying Qualities and Criteria Assessment", NASA CR-4049, 1987

17 AGARD WG.17, "Handling Qualities of Unstable Highly Augmented Aircraft", AGARD-AR-279, 1991

18 Hoh, Roger H., "Recommendations for Approach and Landing Flying Qualities", STI Working Paper 2361-1, 1988

19 Hoh, Roger H., "Concepts and Criteria for a Mission-Oriented Flying Qualites Specification", AGARD-LS-157, 1988

20 Moorhouse, D.J. *et al*, "The Control System Design Methodology of the STOL and Manoeuvre Technology Demonstrator", International Journal of Control, Vol.59, No.1, Jan.1994

21 Twisdale, Thomas R. *et al*, "Prediction and Occurrence of Pilot-Induced Oscillations in a Flight Test Aircraft", J. Guidance and Control, Vol.7, No.4, July-August 1984

22 Johnston, Donald E. *et al*, "Investigation of Limb-Side Stick Dynamic Interaction with Roll Control", J. Guidance and Control, Vol.10, No.2, March-April 1987

23 Paassen, MM van, (Delft T.U.) "Modelling the Neuromuscular System for Manual Control", 9th European Annual Conference on Human Decision Making and Manual Control", Ispra, September 1990

24 Smith, Ralph H., "A Theory for Longitudinal Short-Period Pilot-Induced Oscillations", AFFDL-TR-77-57, 1977

25 Military Standard, "Flying Qualities of Piloted Airplanes", MIL-STD-1797 (USAF), 1987

26 Smith, Ralph H., "Notes on Lateral-Directional Pilot Induced Oscillations", AFWAL-TR-81-3090, 1981

27 Dornheim, Michael A., "Report Pinpoints Factors Leading to YF-22 Crash", Aviation Week and Space Technology, November 9, 1992

28 J.C.v.d.Vaart, "Modelling of Perception and Action in Compensatory Manual Control Tasks", Thesis, Delft University Press, 1992

29 McCuish, A., "Development and Flight Experience of the Control Laws in the Experimental Aircraft Programme", International Journal of Control, Vol.59, No.1, January 1994

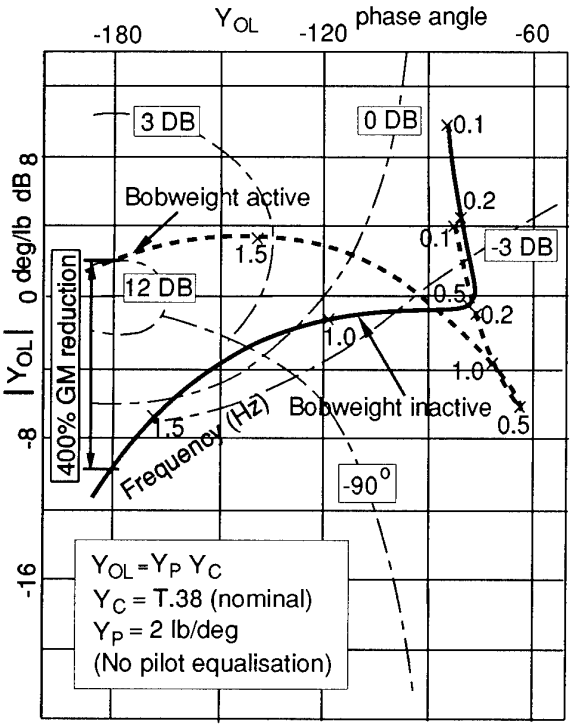

Figure 1 T-38 Bobweight Dynamics

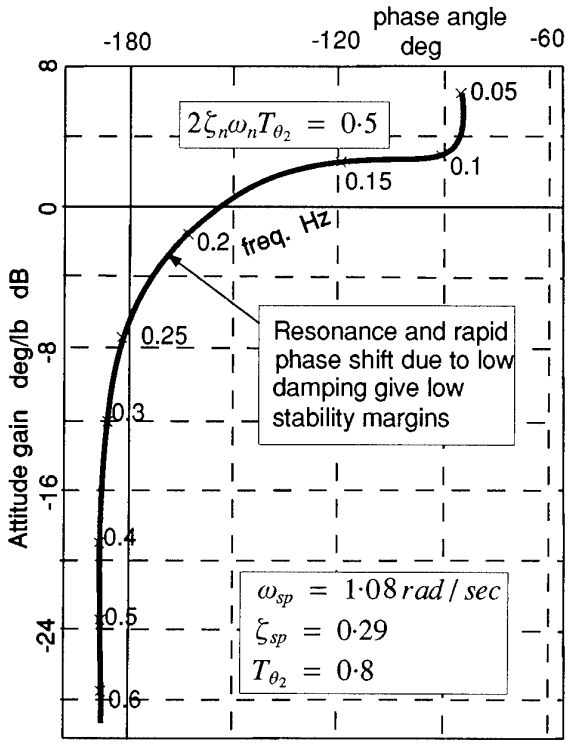

Figure 2 "Linear PIO" Characteristics

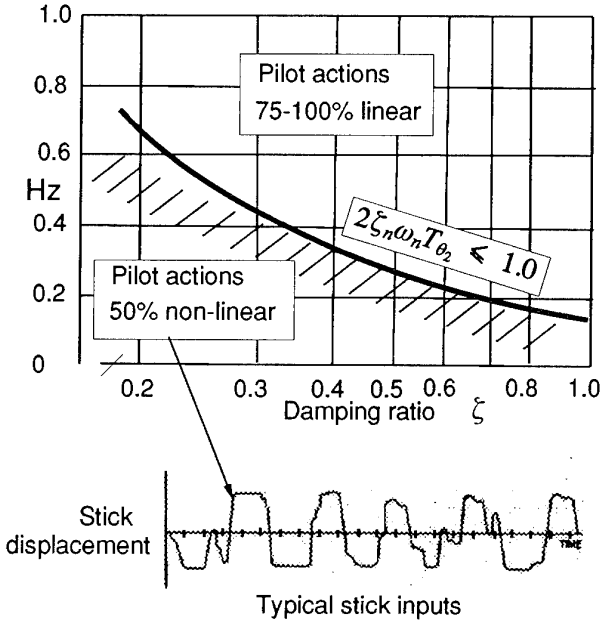

Figure 3 Effect of "Linear PIO" on Pilot

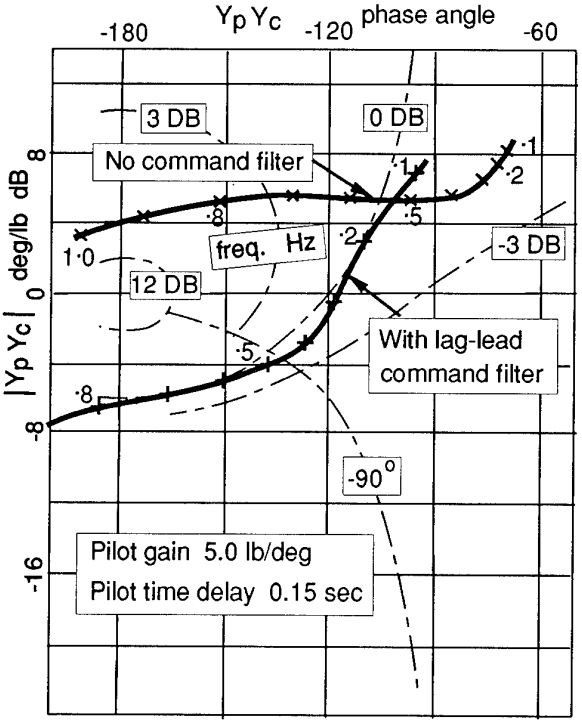

Figure 4 Elimination of Tracking PIO

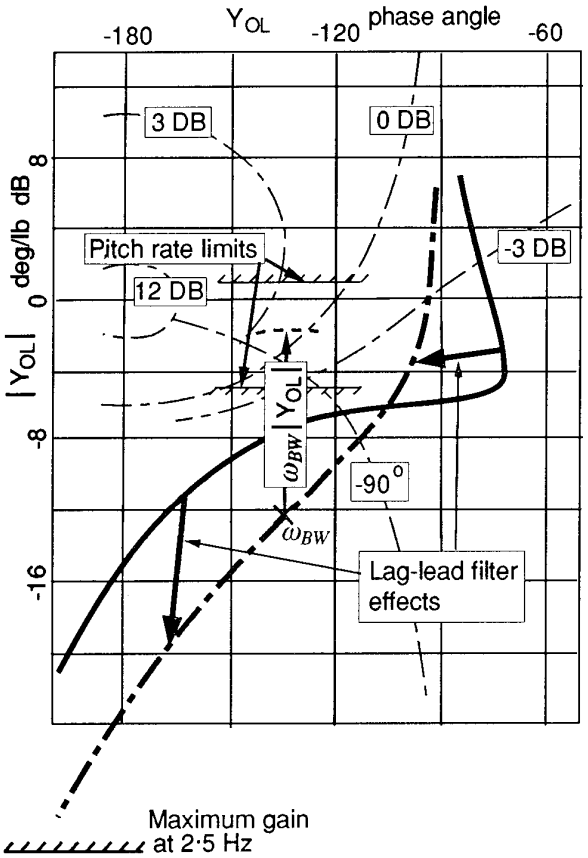

Figure 5 Pitch Attitude Shaping

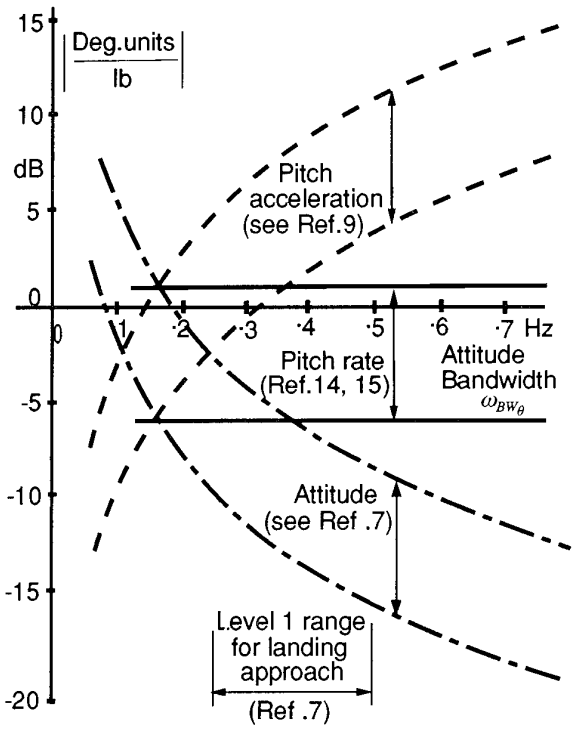

Figure 6 Measures of Sensitivity

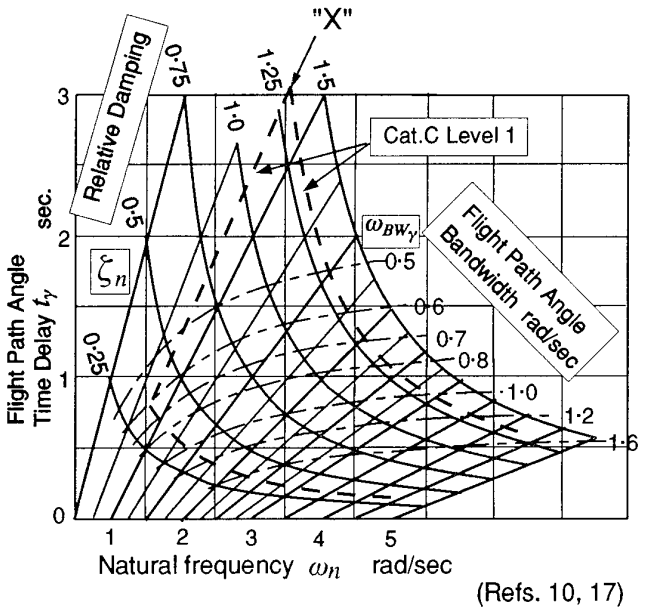

Figure 7 Flight Path Bandwidth

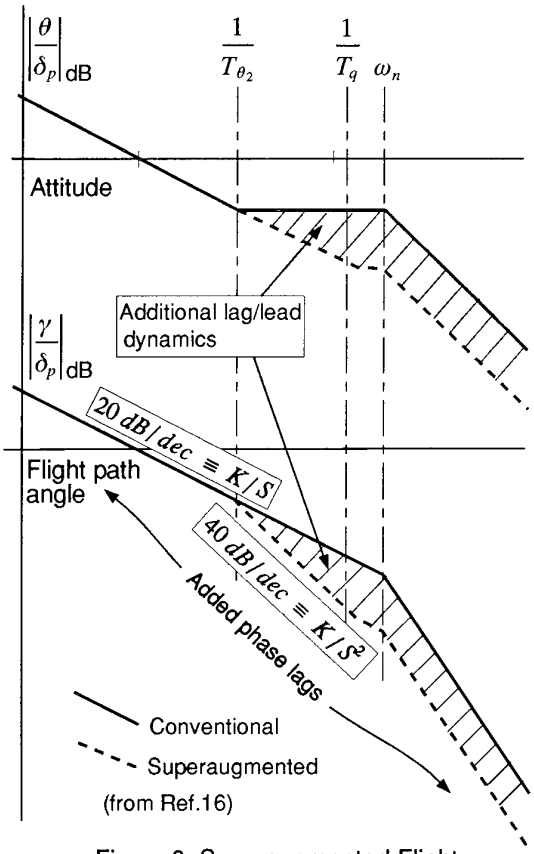

Figure 8 Superaugmented Flight Path Effects

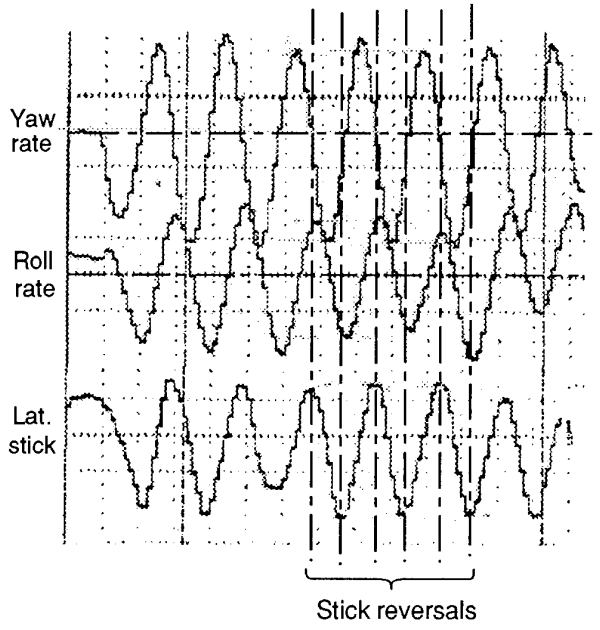

Figure 9 Heading Angle PIO

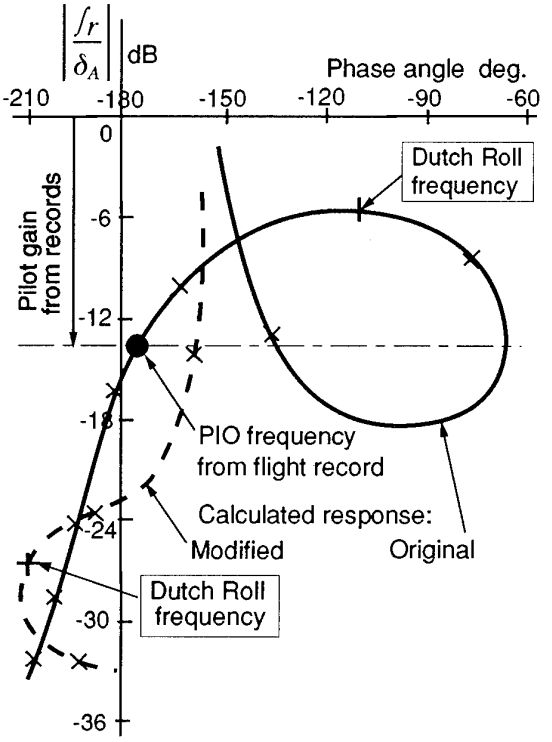

Figure 10 Heading Response to Roll Stick

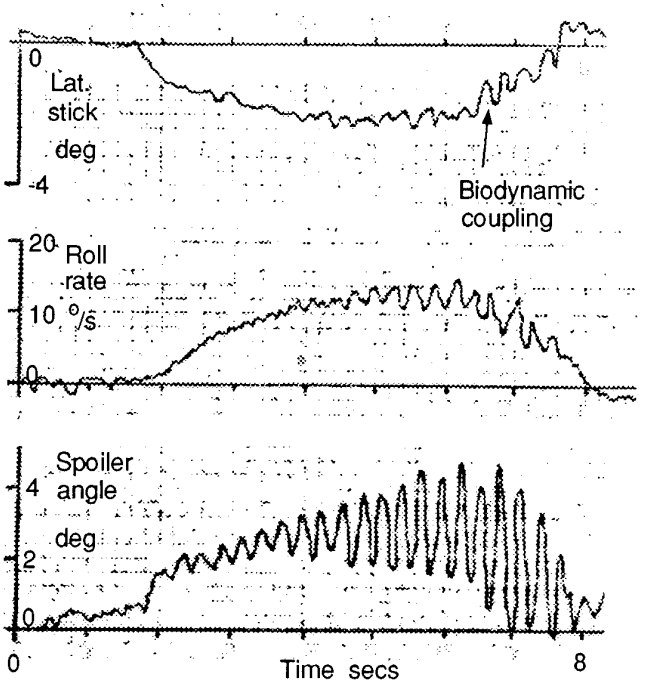

Figure 11 Lateral Acceleration Coupling

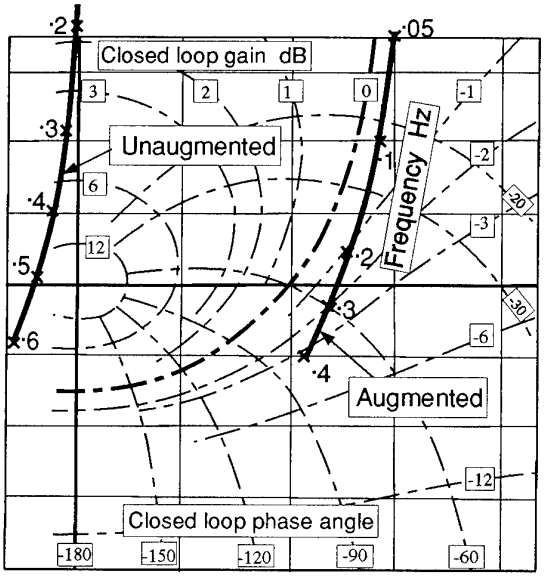

Figure 12 Nosewheel Steering Dynamics

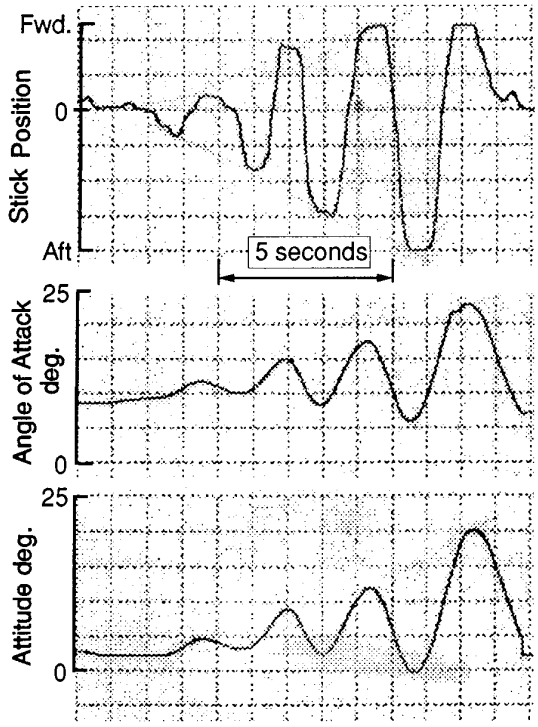

Figure 13 PIO in Fixed Base Simulator

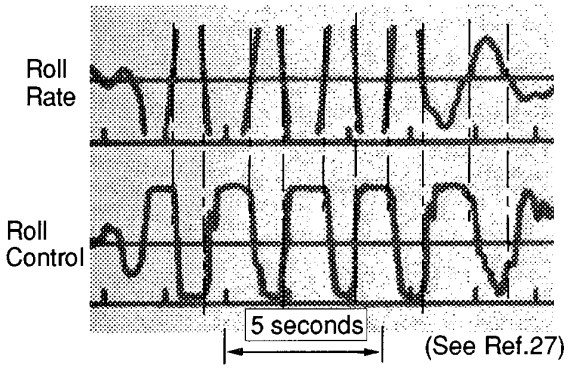

Figure 14 Relay Type Control Action

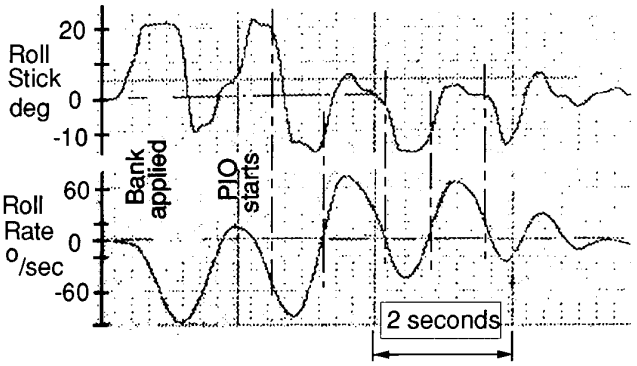

Figure 15 Mixed Sinusoid/Relay Control

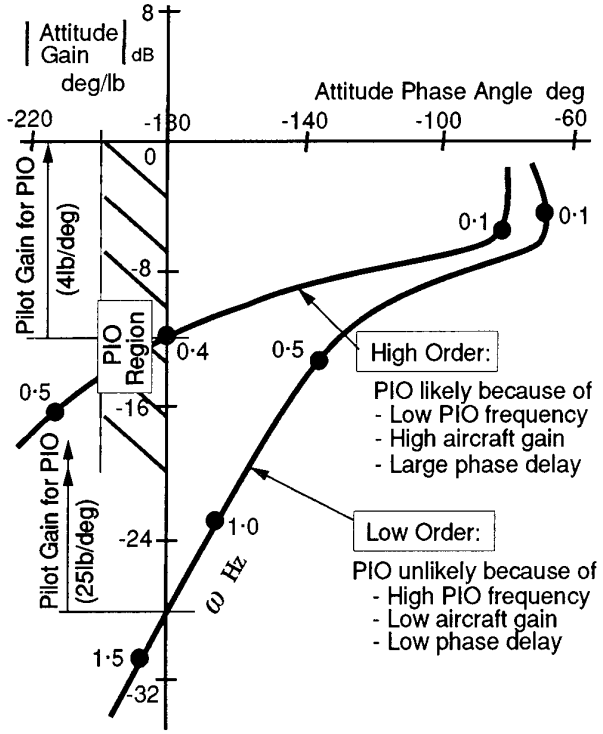

Figure 16 High Order Attitude PIO Conditions

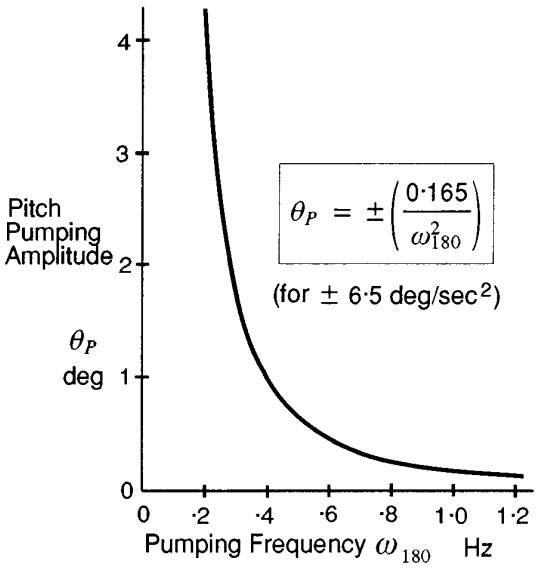

Figure 17 Nominal Stick Pumping Angle

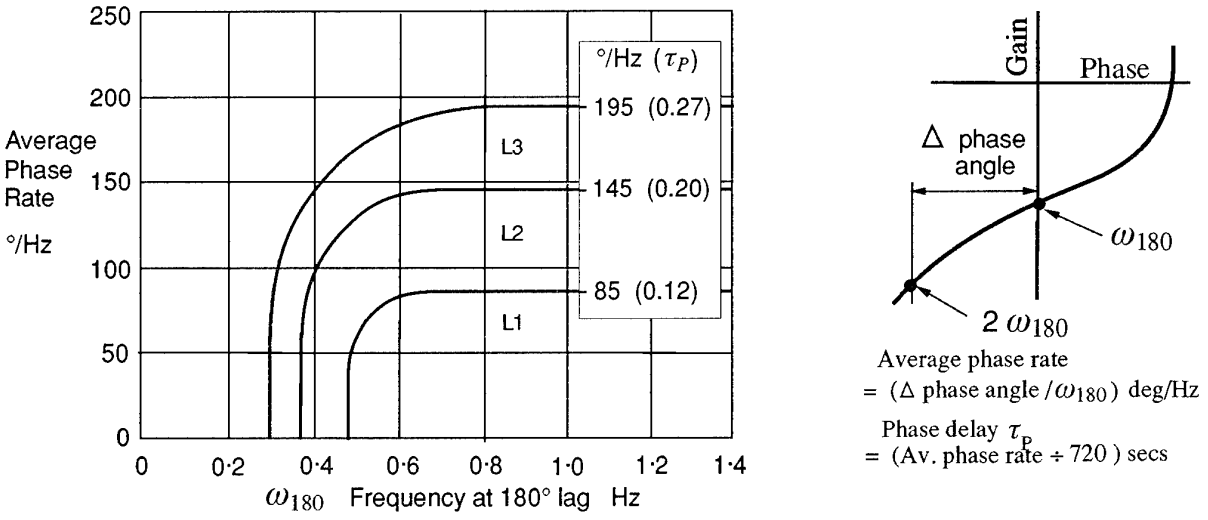

Figure 18 High Order PIO Boundaries

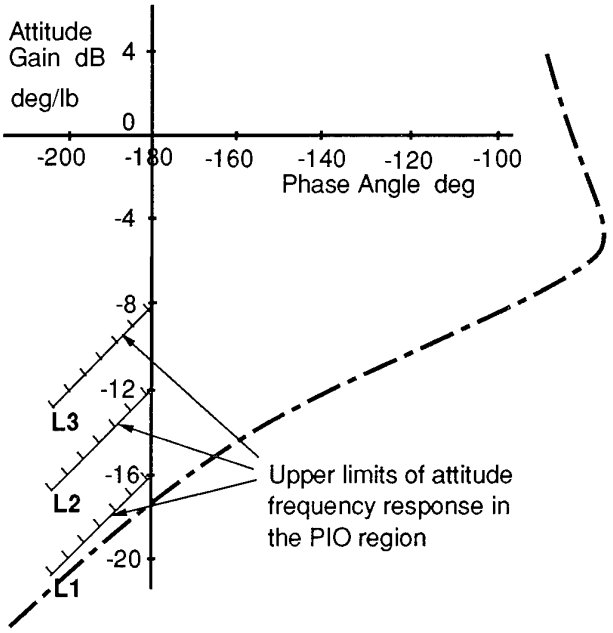

Figure 19 Maximum PIO Frequency Gain

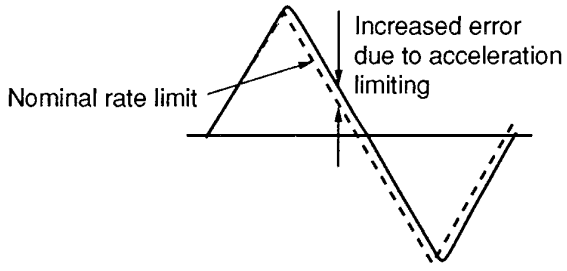

Figure 20 Actuator Acceleration Limit Effect

The Importance of Flying Qualities Design Specifications For Active Control Systems

J Hodgkinson
K F Rossitto

McDonnell Douglas Aerospace
3855 Lakewood Blvd
Long Beach, CA 90846, USA

ABSTRACT

The first part of this paper consists of recollections of how some of the flying qualities specifications for active control fighters emerged. These recollections include some lessons learned. The second part, with these recollections and lessons as motivation, introduces new data on the much more recent developments in active control transports.

INTRODUCTION

Fighters with active digital flight control systems are mature today. For example, in the United States, analog systems were in service in the early 1970's and digital systems in the late 1970's. Active control transports, however, are comparatively in their infancy. Significant Airbus experience has been accumulated in the commercial world, however in the more demanding military arena we are just beginning to gather experience. Fortunately, we have been able to incorporate some of the lessons learned in fighter development into the new generation of transports.

Active Control for Fighters-the Promise

The transition from analog to digital active control for fighters was occurring in the early 1970's. There is an important distinction between the two mechanizations because implementation of the control laws in software (in the digital systems) provided the opportunity for hitherto unheard-of complexity in the control laws. This held the promise of tailoring the responses for different piloting tasks, of maintaining constant, predictable flying qualities in the face of store drops, fuel burn, configuration changes etc, and of coping with changes in the basic configuration or mission as the airplane matured. There was also the promise of direct lift and side force control as a 'new way to fly'.

Presented at the AGARD Flight Mechanics Panel Symposium on Active Control Technology: Applications and Lessons Learned, Politecnico di Torino, Italy, May 9-12, 1994

At that time, however, the digital implementation was seen in the short term as a more reliable way to implement control laws conceived in the analog domain and, most important of all, to implement changes in the control laws very rapidly. In the longer term, however, we anticipated performing direct digital design without reference to the continuous design methods appropriate for analog systems. Meanwhile, we implemented control law criteria by closing the key stabilizing loops with adequate gain and phase margin. The resulting well-damped responses, we thought, would then produce excellent flying qualities. And the force-command control inceptors would ease the pilot's task as well as freeing up valuable cockpit space and eliminating stick jams.

Finally, the flying qualities specifications of the day were not expected to be of much use because they referred to earlier configurations with the poor damping and cross-axis coupling that the high gain control laws could easily obviate. It seemed that specification methods involving mathematical models of the pilot offered the most promise, since the aircraft responses were characterized by large numbers of parameters, rather than the few modal parameters seen in traditional specifications.

Active Control Fighters-the Realization

Active digital flight control systems more than fulfilled the promises of providing excellent platform stabilization and of tailoring responses. They have also allowed us to solve, for example, apparent aerodynamic problems by changing software. And production digital systems are indeed very reliable. Active control has emerged as a key enabling technology in, for example, stealth, agility/post-stall maneuvering, self-healing systems, wing load alleviation, gust suppression, airframe/engine performance optimization, flexible mode control, emergency propulsion-alone control, and integration with avionics. So the benefits of active control

Paper presented at the Flight Mechanics Panel Symposium held in Turin, Italy, from 9-13 May 1994.

exceeded most predictions. But in many of our original predictions, we were more wrong than right. And in our failed predictions lie some of our most valuable lessons.

Briefly revisiting some of the other expectations, first, the process for changing a digital system is not simple. One price of the complexity of our systems is the lengthy and expensive change process that is necessary for safety.

Today we are not generally designing systems using radically new methods but are using tried-and-true techniques originating from the continuous analog era. These techniques are still valuable not only because the digital processor now runs so fast that we can treat it as essentially analog. Their value survives because those earlier design methods emphasize insight rather than mathematical elegance. So today industry generally uses variations of classical/eigenstructure methods that keep in sight the basic airplane response, the closed loop response and the effect of the different paths and components in the system.

As for the force-command inceptors, though pilots have accommodated fixed spring rates (doing away with one function of the dreaded 'q' bellows) we have come to realize that some position cues are beneficial, and that the dynamic response requirements generally favor use of position command sticks.

Finally, and this certainly came as a surprise to the writer, we came to realize that the existing specifications for flying qualities were indeed adaptable to the active systems. This was recognized officially with the publication of Mil-F-8785C.

Thus the fighter experience differed in many areas from our expectations. In no area is this more true than in flying qualities criteria. We would like to build on this experience to aid development of active control transports. It therefore seems worthwhile to review specifically the fighter experience with handling qualities criteria closely as a sort of introduction to criteria for active control transports.

THE EVOLUTION OF FLYING QUALITIES CRITERIA FOR ACTIVE CONTROL FIGHTERS

The Paper Pilot (References 1 and 2) was originally conceived as a way of specifying flying qualities for high order active control aircraft, since the existing criteria were based on low order classical modal characteristics. This research originated with the guardians of the flying qualities specification, the US Air Force, and produced excellent pilot rating predictions (Figure 1). Therefore it sparked interest among researchers and fighter manufacturers. At McDonnell Aircraft, a multi-phase project was conceived. The concept was first to examine existing criteria to confirm, as we thought, that they had little or no applicability to active control aircraft. Then we planned to evaluate progressively more complex criteria as necessary to explain flying qualities phenomena of active control fighters.

Equivalent Systems

The first step, then, was to apply existing criteria to the high order responses. It had been remarked by many that choosing a subset of the many roots of the high order response to compare with the few modal parameters of the specification did not make much sense. The neglected poles and zeroes clearly contributed to the response. One approach appeared to be to match the responses with appropriate low order forms. In this concept, the short term pitch rate response to longitudinal control would be matched with a first over second order lag, the roll rate response to lateral control input with a first order lag, etc.

In reviewing the literature on this approach, we found a longitudinal study by Stapleford et al of Systems Technology and Cornell Aeronautical Laboratory studies by DiFranco and by Neal and Smith (Reference 3). DiFranco's study added lags to longitudinal low order systems in such a way that they resembled low order aircraft with added time delays, and so seemed too specialized to deal with the mid-frequency response shaping expected in active control fighters. Neal and Smith, however, examined shaped responses. They also included an evaluation of the low order approach to high order systems using analog matching. They included a delay term in the match, following DiFranco's approach, and concluded that though the delay was needed to get a good match, the matches were not unique and that the evaluator had no guidelines to deal with mismatch.

Though Neal and Smith's results on equivalent systems were not encouraging, we decided that manual analog matching was not perhaps as precise as needed, so we decided to revisit their data by

mechanizing a frequency response match process in a computer program. This program used a search algorithm to minimize the squared differences between gain and phase. Using frequency responses rather than time responses appeared to be a better approach because small differences in step time histories, for example, became relatively large differences in gain or phase.

We were surprised that the equivalent system matches to Neal and Smith's data were quite good provided we too included the delay term in the match. Some experimentation showed that with the computer frequency response technique the matches were unique and that factors like gain/phase weighting did not strongly affect the results (Reference 4). Cases with poor matches tended to have poor parameter values and poor ratings. We reexamined Neal and Smith's configurations to see if, as in the DiFranco data, there was an explanation for our results in the experimental design- perhaps that certain types of configuration had been chosen that would be inherently low-order-appearing. However considering the number of configurations evaluated, Neal and Smith had clearly spanned a broad range of likely high order responses.

Equivalent Delay

The delays involved ranged from about 50 to about 250 milliseconds. A cursory examination of the data showed that the larger time delays were always associated with poor pilot ratings. These delays seemed small. At that time, we were considering dynamic characteristics in the frequency range of piloted crossover (say 1 to 3 radians/second) to govern flying qualities, and these delays cause little phase shift at these low frequencies. For example, 100ms delay produces only 5.73 degrees of phase lag at 1 radian /second. And yet, according to the in-flight simulation data, this is enough lag to preclude pilot ratings better than Level 2.

At this point, therefore, we did not know if we had a viable method on our hands or merely a scientific coincidence. But we decided to invest more time in further examination of this equivalent systems approach, and to postpone the other more complex approaches, even though at that time those other approaches still appeared more promising. Calspan had already remarked that ground-based simulation did not reproduce the piloting difficulties seen in in-flight simulation of the lagged, active control configurations, and so Neal and Smith's data, which were in-flight, seemed to present the best data set for analysis.

Rating Prediction Using Equivalent Parameters

Using multiple linear regression, we attempted to find the parameters that strongly affected pilot ratings in the Neal-Smith data base, with a view to building criteria around them. Our regression-based rating prediction equation also allowed us to plot predicted vs actual pilot rating to compare with the Paper Pilot method. (For example, see Figure 2). The prediction accuracy appeared to be at least comparable to that using the Paper Pilot parameters. We did not see our prediction equation as a particularly useful way of predicting rating, but more as a way of pointing out that accurate rating predictors did not require a pilot-in-the-loop method.

The regression invariably told us that time delay was by far the most deleterious factor in the data. The next factor proved to be excessive low-order lag or lead, which produced poor matches and poor pilot ratings. We tried matching those by freeing the numerator term in the pitch response and obtained excellent matches. However the sometimes extreme values of the numerator term were artificial, having no relationship to the aircraft's flight path time constant. We christened this extreme shift 'galloping Lalpha' after the approximate term in the pitch numerator. (In later work we essentially fixed this numerator term. This approach was physically more correct but left the equivalent system without a good way of flagging configurations with excessive lead, or dropback). We compared the data with the current Military Specification, and the data were consistent with the requirements. Adding a requirement to restrict delay resulted in excellent correlation.

At this point a separate group at McDonnell decided to test the method against the high order responses of the Survivable Flight Control System F-4, a fly-by-wire system that had not been designed using concepts from low order systems, but using time response envelopes. This group was surprised by the good matches also. Matches to demanding square wave inputs were demonstrated and even for the 'poor' matches, the data were usable. This study (Reference 5) lent us more confidence and pointed to the possibility that we could specify active control flying qualities using equivalent systems.

The sensitivity of the Neal-Smith ratings to small delays however was still at odds with the ideas of piloted crossover. The crossover theory was fundamental to the optimal pilot concept. There seemed therefore little point in extending our research into optimal pilot methods until we understood better how the ratings of these augmented, active control systems were so dramatically affected by delays.

A variable stability NT-33 simulation (Reference 6) provided an opportunity to determine directly whether the delay was truly responsible for the flying qualities problems. A configuration with substantial longitudinal delay (.19 seconds) was evaluated in landing. Then a filter was added that cancelled the phase contribution of the delay at the short period frequency. The rating worsened. Because part of the deterioration was due to the increased steady state gain of the lead-lag filter, we then lowered the command steady state gain so that the local gain at the short period frequency was the same as that of the original configuration. The rating returned to the original value. For completeness, we designed a lead-lag filter that cancelled the phase lag at a higher frequency. This filter did not improve the rating either. So all these configurations had poor flying qualities and Figure 3 shows that they all have similar high frequency phase slope, ie, similar equivalent delays.

Crossover-Based Methods

In a similar time frame, several researchers were pursuing pilot-in-the-loop methods. One approach was particularly simple, using measurements from the attitude frequency responses to infer whether the pilot could close a satisfactory control loop. Hoh (Reference 7) and Smith and Geddes (Reference 8) both used this approach.

Hoh's method estimated the bandwidth of the pilot-in-the-loop system, wherein a gain-only pilot would close the attitude loop with a specified gain and phase margin. The Smith-Geddes method estimated a crossover frequency and then measured the phase lag at that frequency. The theory behind these methods should have enabled them to show degradation due to delays, but again the small phase lags produced by the delays at the comparatively low crossover frequencies made their parameters insensitive to delay. Smith defined pilot rating boundaries based on the Neal-Smith data, but these boundaries show large rating degradations with quite small lag additions. (Figure 4).

Hoh found that adding delay as a second dimension to the bandwidth criterion put more distance between good and bad configurations. To justify this, Hoh hypothesized that while bandwidth covered the normal control capability of the aircraft, delay was a measure of resistance to control loss as the pilot attempted to increase crossover frequency. Increased crossover frequency implies increasingly demanding tasks. This hypothesis matches the observation that delays do not cause problems when the piloting task is benign, but cause control loss when the task is difficult. (This hypothesis has been supported in ground-based simulations of transport aircraft in Reference 9). At about this time, Wood at McAir (Reference 10) suggested a simple way of estimating time delay from a Bode plot of the pitch response, so that an equivalent system determination was not required to complete the bandwidth analysis. At this point, the bandwidth method was a particularly simple 'pencil and paper' method using the aircraft frequency response (Figure 5). It used ideas from the pilot-in-the-loop modeling concepts that underlie the paper pilot method, plus the delay concept that originated from equivalent systems.

LESSONS LEARNED

There were a number of lessons learned in this period of time. These lessons became part of a specification that was enormously useful in development of digital flight control systems.

1. Active control aircraft, at least insofar as they have high order characteristics, need not be treated as entirely different entities, but represent a subset of the aircraft on which we already have experience.

2. The piloted crossover concept can be used as the basis of a very simple pilot-in-the-loop criterion.

3. High frequency phase lag (delay) is bad. This becomes more true for demanding tasks. High command gains, typical of some control system designs, could exacerbate tendencies for aircraft-pilot coupling caused by delays by involving the pilot in the loop and by causing rate limiting of the actuators.

4. Ground-based simulators typically did not predict the problems seen in flight. Command gains optimized on the ground-based simulator were

typically too high in flight, and the effects of time delay often do not appear in the ground-based simulator.

The most important lesson learned, however, was that a validated specification was a very important part of designing digital systems. High frequency phase lag in particular would probably not have been identified as the cause of flying qualities difficulties in some early designs unless in-flight-validated criteria had been available. To develop criteria, a wide range of response characteristics must be examined so that different levels of flying qualities can be defined.

FLYING QUALITIES ISSUES FOR ACTIVE CONTROL TRANSPORTS

Response-Types

Unfortunately the flying qualities specifications for large transports are not as well-developed as for fighters. This situation has been evident for a number of years (see Reference 11, from 1981, for example). As an additional complication for transports, we are also now considering unusual response-types. These response-types include such concepts as pitch rate command/attitude hold, attitude command, flight path command, etc. Table I summarizes some of the features of these response-types, which can have exceptionally simple piloting characteristics but can also introduce some problems.

Some of the problems are as follows. One is the question of pilot training. Pilots are trained with conventional dynamics, and new response-types, however straightforward, mean learning some new piloting techniques. Another concern is that of graceful degradation during failures. An unconventional mode failing to a set of degraded conventional dynamics may require unnatural piloting adaptation at a time when the pilot is already busy. An unconventional response-type may require changes in command strategy in various flight condition regions- for example in the flare maneuver or at large attitudes. These characteristics are well-known, however.

What is not often considered is the need to define flying qualities requirements for each candidate response-type. A range of characteristics is required, not just an optimum, because flight envelope extremes and failure conditions require building a data base that spans the whole range of pilot ratings. Because of this large quantity of needed data, there is great economy in determining the optimum response-type and then gathering the data base only for that.

Recently we embarked on studies to define what would be the best response-type for a transport. Among many sometimes confusing results, we are beginning to conclude that with sufficient work, any of the new response-types could be made acceptable to pilots. The remaining work is in details of the mechanization- for example, trim logic, and actuator useage, and in deciding to what extent training should influence the decision to choose a particular response-type. These 'details' are of course not trivial.

In building the data base of specifications for active control transports, our fighter experience dictated that we first determine allowable levels of time delay. We accomplished this work in the Total In-Flight Simulator (TIFS) and in the NASA Ames Vertical Motion Simulator in a cooperative MDC/USAF/NASA study. For most of our work, we used the classical-appearing angle-of-attack command response-type.

Time Delays in Transports

The question of how much delay is allowable for transport operations has been a controversy for many years. Figure 6, reproduced from a recent AGARD presentation (Reference 9), shows inconsistent results between different aircraft types.

We have been gathering data to help us with this problem in both TIFS and VMS. This paper briefly describes the TIFS data. Reference 12 will contain more detailed results.

TIFS Data

Our experiment to determine delay values for transports used a demanding task as illustrated in Figure 7. We were simulating a very large transport (close to a million pounds) and TIFS is a smaller airplane. Therefore we could not continue our landings to touchdown and at the same time replicate the pilot's eye height above the runway for a very large aircraft. Therefore we employed a 'simulated eye-height' touchdown in which the altitudes were called off during the flare maneuver and the sound of gear contacting the ground was simulated at the appropriate time. This technique

produced quite consistent results in the parts of the experiment dealing with mid-frequency characteristics, which will be described here before discussing the delay data..

Control Anticipation Parameter

The configurations without significant added delays were compared with the Control Anticipation Parameter (CAP) of the specification. These data are for an angle-of-attack command response-type, which is essentially a conventional aircraft. We did not implement an autothrottle. The data are remarkably consistent among themselves and with CAP.

As Figure 8 shows, our data would support moving the lower Level 1 CAP boundary upwards, ie making it more stringent, and relaxing somewhat the lower Level 2 boundary. We were surprised by the apparent need to raise the Level 1 boundary. We had previously thought that very large transports could be less rapid in their short period response than the requirements suggested.

Time delay

The results on time delays appear in Figure 9. The ratings are consistently better for the faster short period frequency. Compared with the fighter data, the transport is less sensitive to delay. The simulated touchdown is possibly a contributor to this difference (we plan to compare actual touchdowns in a later experiment) but there is a fundamental difference in the requirements for transports compared with smaller fighter aircraft.

Our piloting task was considered about as demanding as an operator of a commercial aircraft would experience. There is still however a question regarding allowable delays for military transports that perform precision STOL operations and such precision maneuvers as those in Low Altitude Parachute Extraction (LAPES). Unfortunately there is no in-flight experiment, comparable to these TIFS data, which includes LAPES or STOL operations. Therefore the current military specifications do not contain validated requirements for this class of transport in this type of task.

Finally, Figure 10 shows ratings for different natural frequencies of a pitch attitude command response-type. Unfortunately there is large spread in the ratings. The pilot comments suggest that unfamiliarity with this response-type is a contributing factor in the poorer ratings. Also, we did not mechanize an autothrottle, so the ratings reflect a failure case. To confuse the picture further, we have other experience suggesting that attitude command is easy to fly when an autothrottle controls speed or when the pilot uses the backside technique. These data are only a beginning in developing criteria for advanced response-types.

COMPARING DELAY DATA FOR FIGHTERS AND TRANSPORTS

The generic plot that describes trends of rating sensitivity to delay for various tasks appears in Figure 8. The transport data show different trends. It is at first tempting to say that the allowable delay is an inverse function of response rapidity, so that for example larger delays would be tolerable for slower short period frequencies. This turns out not to be true, however, either within the fighter data or within the transport data, but does hold across the aircraft types. That is to say only that transports do have slower short period frequencies and are more tolerant of delays. This has always been somewhat of a mystery since both aircraft types approach runways of similar dimensions at similar speeds. One discussion of the contrast between small and large aircraft in the landing approach is to be found in an AGARD paper by A'Harrah and Woodcock (Reference 12) which invokes the pilot's distance ahead of the center of rotation of the aircraft as a correction factor for the Control Anticipation Parameter. Center of rotation may also underlie the relative insensitivity of transports to delays.

CONCLUSIONS

One of the main risk reducers in development of all classes of aircraft is a well-understood, in-flight-based, set of flying qualities criteria and requirements. This has been demonstrated to improve program safety and to reduce cost and development time. The experience with active control fighters has been a valuable introduction to the development of active control transports, for which more criteria are needed.

REFERENCES

1. Anderson, R. O., "A New Approach to the Specification and Evaluation of Flying Wualities" AFFDL-TR-69-120, Nov 1969

2. Dillow, J. D., "The 'Paper Pilot'- a Digital Computer Program to Predict Pilot Rating for the Hover Task" AFFDL-TR-70-40, 1970

3. R. E. Smith in Wunnenberg, H., "Handling Qualities of Unstable, Highly Augmented Aircraft" AGARD Advisory Report 279, May 1991

4. Hodgkinson, J., LaManna, W. J. and Heyde, J. L., " Handling Qualities of Aircraft With Stability and Control Augmentation Systems- a Fundamental Approach", J R Ae S, February 1976

5. Hodgkinson, J., et al, " Analysis of High Order Aircraft/Flight Control System Dynamics Using an Equivalent System Approach" 7th Annual Pittsburgh Conference on Modeling and Simulation, April 1976

6. Smith, R.E., et al, "Equivalent System Verification and Evaluation of Augmentation Effects on FIghter Approach and Landing Flying Qualities" AFWAL-TR-81-3116, Vol 2.

7. Hoh, R.H. et al, "Development of Handling Qualities Criteria for Aircraft with Independent Control of Six Degrees of Freedom" AFWAL-TR-81-3027

8. Smith, R.H. and Geddes, N.D., "Handling Qualities Requirements for Advanced Aircraft Design: Longitudinal Mode" AFFDL-TR-78-154, August 1979

9. Hodgkinson, J., Rossitto, K.F., and Kendall, E.R., "The Use and Effectiveness of Piloted Simulation in Transport Aircraft Research and Development" AGARD Symposium on Simulation, Brussels, Belgium, October 1991

10. Hodgkinson, J., Wood, J. R., and Hoh, R.H., "An Alternate Method of Specifying Bandwidth for Flying Qualities" AIAA Paper

11. A'Harrah, R.C. and Woodcock, R.J., "The Military Flying Qualities Specification, a Help or a Hindrance to Good Fighter Design?" AGARD Flight Mechanics Panel Symposium, Florence, Italy, October 1981

12. Rossitto, et al, "Comparison of Results from an In-Flight and Ground-Based Simulation of Longitudinal Flying Qualities for Augmented, Large Transports in Approach and Landing" to be published in the Proceedings, AIAA Conference on Atmospheric Flight Mechanics, Scottsdale, Arizona, August 1994

TABLE 1. *COMPARISON OF VARIOUS RESPONSE-TYPES*

RESPONSE-TYPE		ADVANTAGES	DISADVANTAGES	IN-FLIGHT EXPERIENCE	INSTRUMENTATION
COMMAND	HOLD				
α	α^{1}_{Trim}	• Natural aircraft response	• Trimming required • Preserves phugoid • Vertical gust causes pitch variation • Dives in negative wind shear	• MIL-F-8785C database • Calspan data	• Alpha vanes prone to damage, recommend using static pressure alpha measurement
θ	θ^{1}_{Trim}	• Simple to design • Suppresses pitch phugoid • Holds pitch in gust • Natural pitch response • Attitude and flight path very stable • With auto-throttle is like γ - command	• Trimming required (large trim change two segment approach) • Hard ride in turbulence if gains are too high • α increases in negative wind shear without auto-throttle • May require non-linear gearing for agility	• Very limited experience, need data	• θ and $\dot{\theta}$ measurements are easily obtained
γ	γ^{1}_{Trim}	• Same as θ - command but much better wind shear regulation • Holds γ in wind shear	• Trimming required • Vertical gust causes pitch variation • Auto-throttle is a minimum equipment list item • Design is not simple	• Essentially untested; need data	• Sensing requires an inertial navigation system
$\dot{\theta}$	θ^{2}_{New}	• Simple to design • No trimming required • Suppresses pitch phugoid • Holds pitch in gust	• Agile hippo favorite • α increases in negative wind shear without auto-throttle • Tendency for airspeed control problems • Must place $1/\tau_q \approx 1/\tau_{\theta_2}$ • Flare logic tuning to prevent floating • Requires higher bandwidth than θ - command	• MIL-F-8785C database • Calspan data • DAC data but limited	• θ and $\dot{\theta}$ measurements are easily obtained
$\dot{\gamma}$	γ^{2}_{New}	• Same as $\dot{\theta}$ - command but much better wind shear regulation • No trimming required • Suppresses phugoid • Holds γ in wind shear	• Design is not simple	• Same as γ - command	• Same as γ - command

KEY:
1. Returns to trim attitude when column is released.
2. Stays at new attitude when column is released.

Table 1
DEG 4/28/94

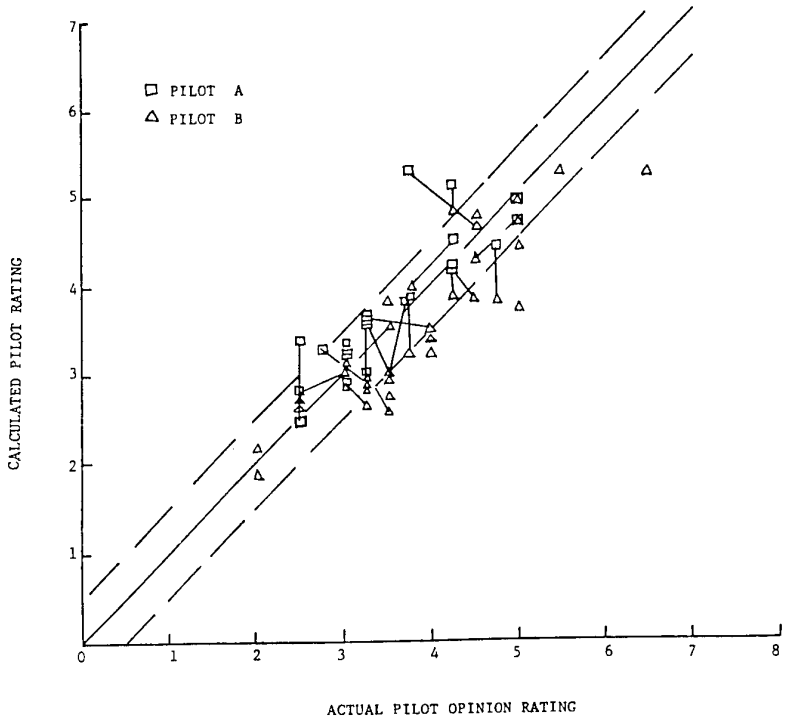

Figure 1 Calculated vs Actual Pilot Rating : Paper Pilot Method

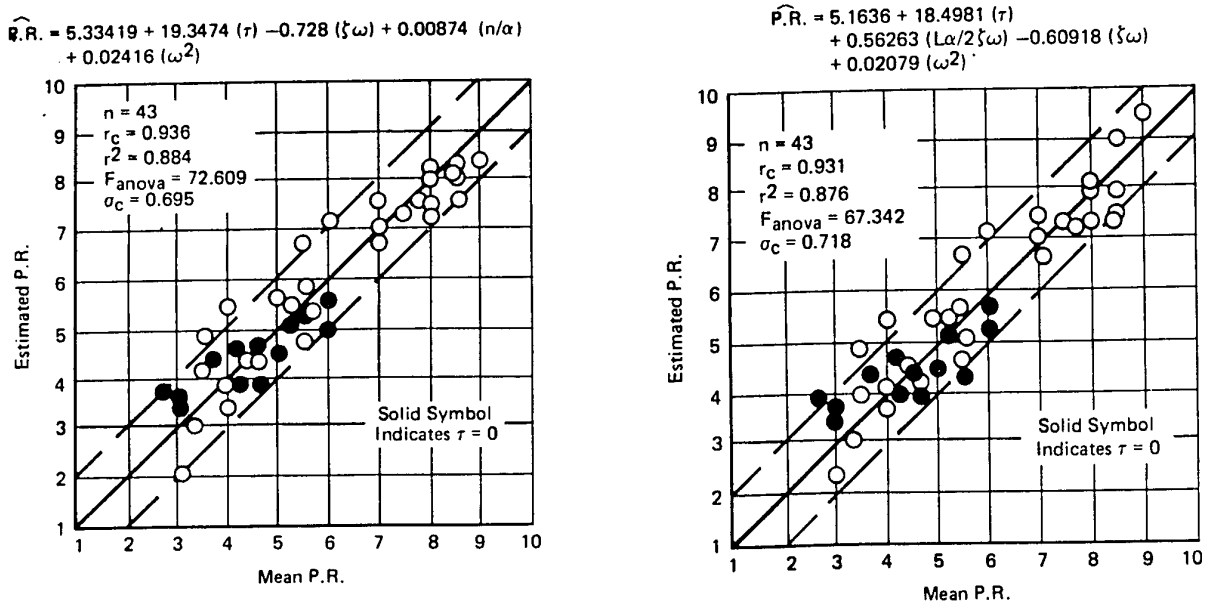

Figure 2 Calculated vs Actual Pilot Rating :Equivalent Systems Method

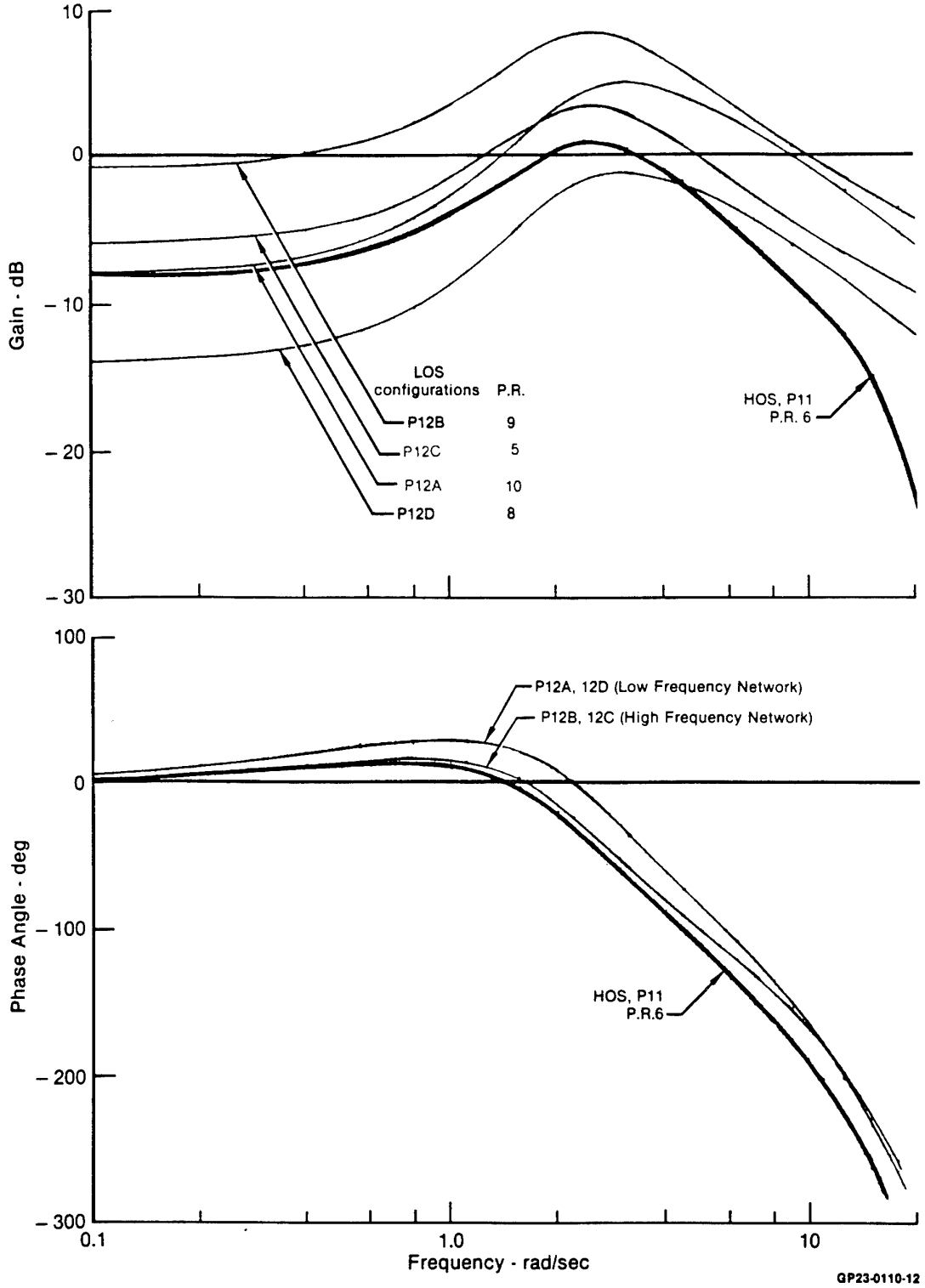

Figure 3 Configuration with Delay and Lead-Lag Compensation Networks

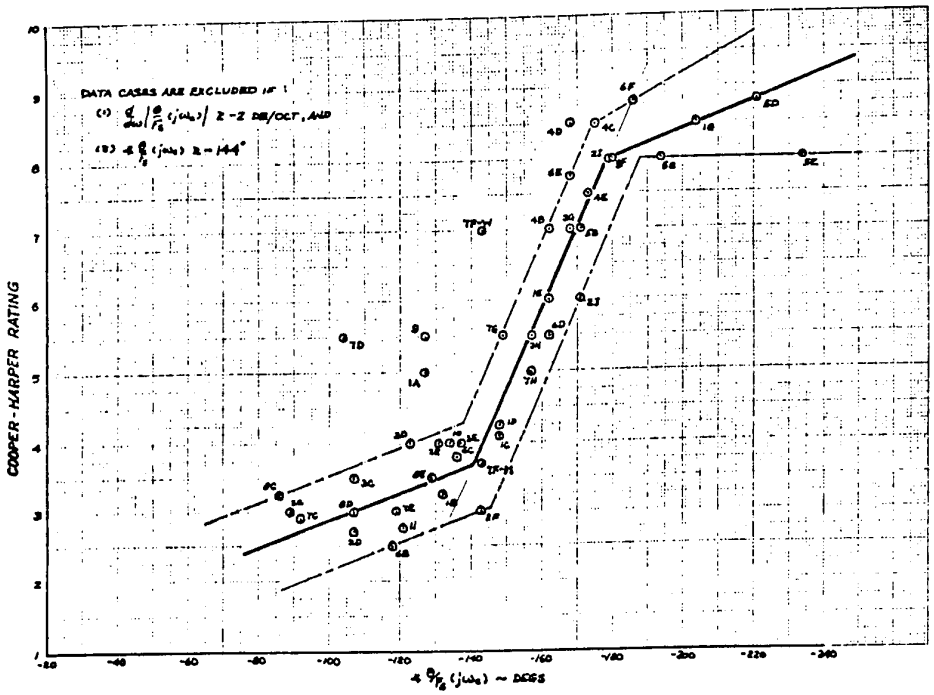

Figure 4 Smith-Geddes Criterion for Effect of Phase Angle on Pitch Attitude Flying Qualities-Shows Rapid Rating Degradation for Small Lag Additions.

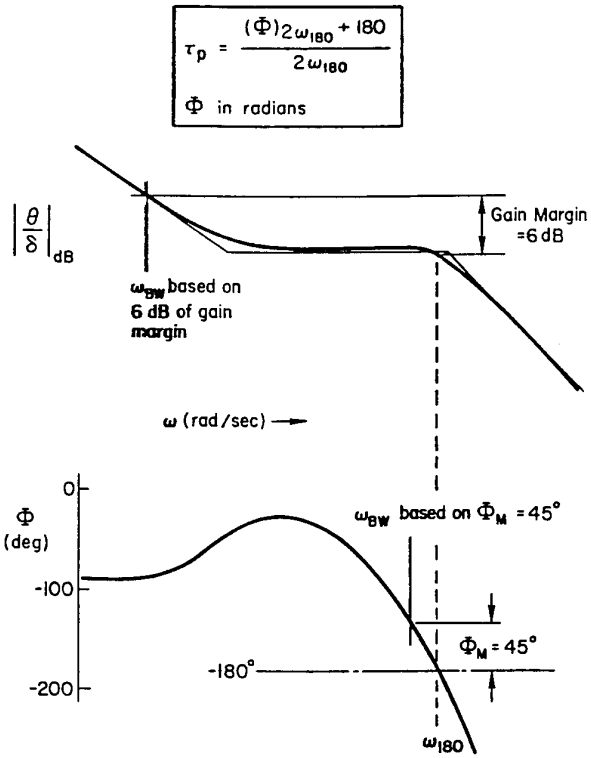

To Obtain Bandwidth:

1. Calculate ω_{BW} based on phase margin
2. Calculate ω_{BW} based on gain margin
3. Use lowest value

Figure 5 Bandwidth Criterion Addresses High Frequency Phase Lags

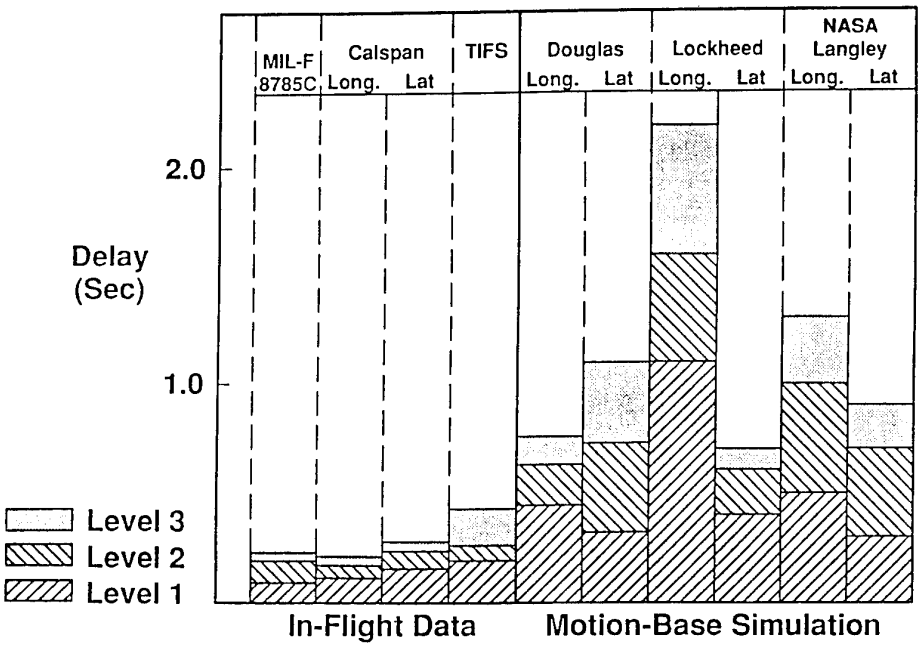

Figure 6 Delay Effects Differ in Different Data Sources (for source references, see Ref. 9)

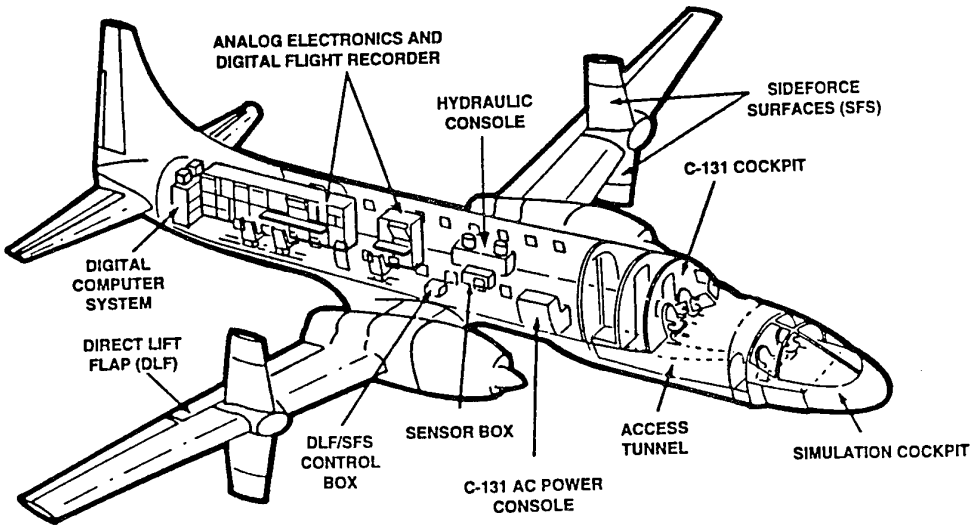

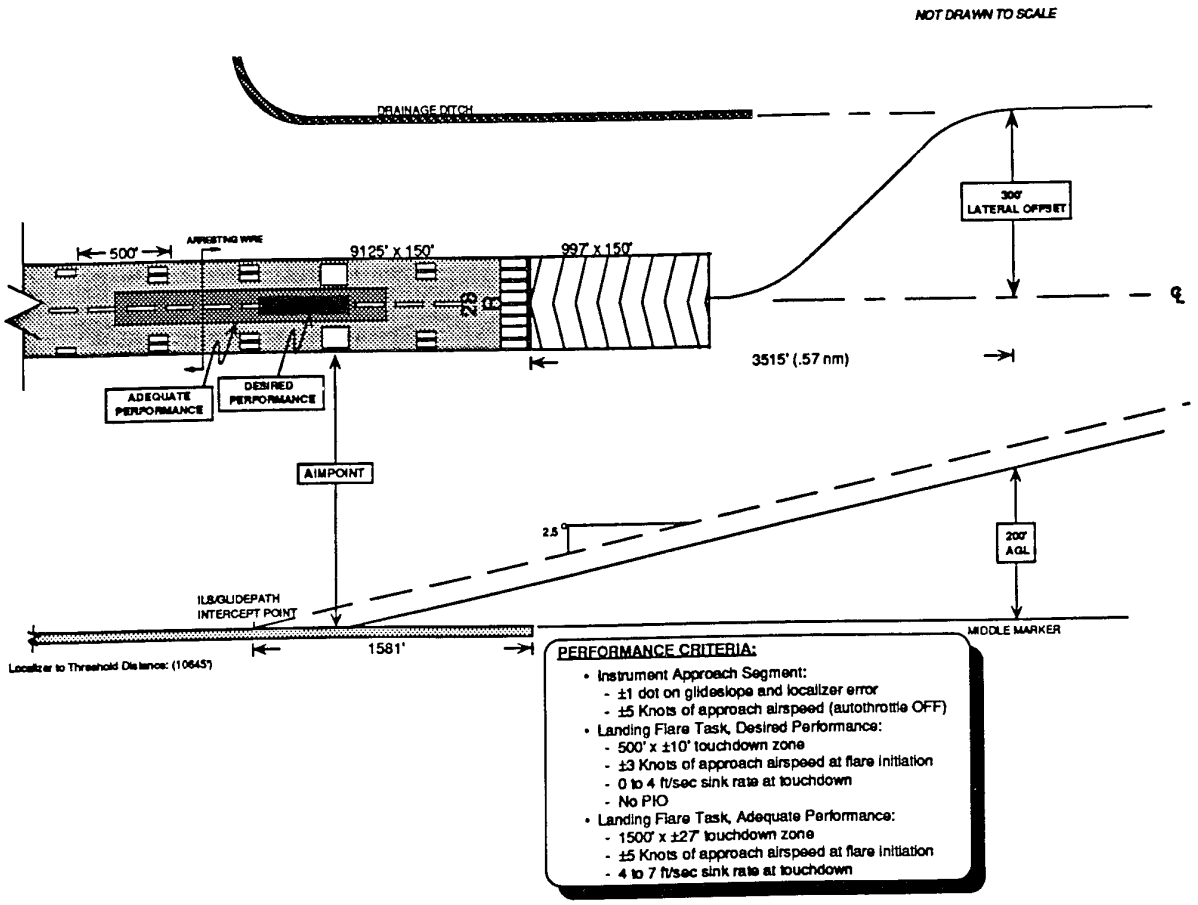

Figure 7 Total In-Flight Simulator (TIFS) and Landing Task

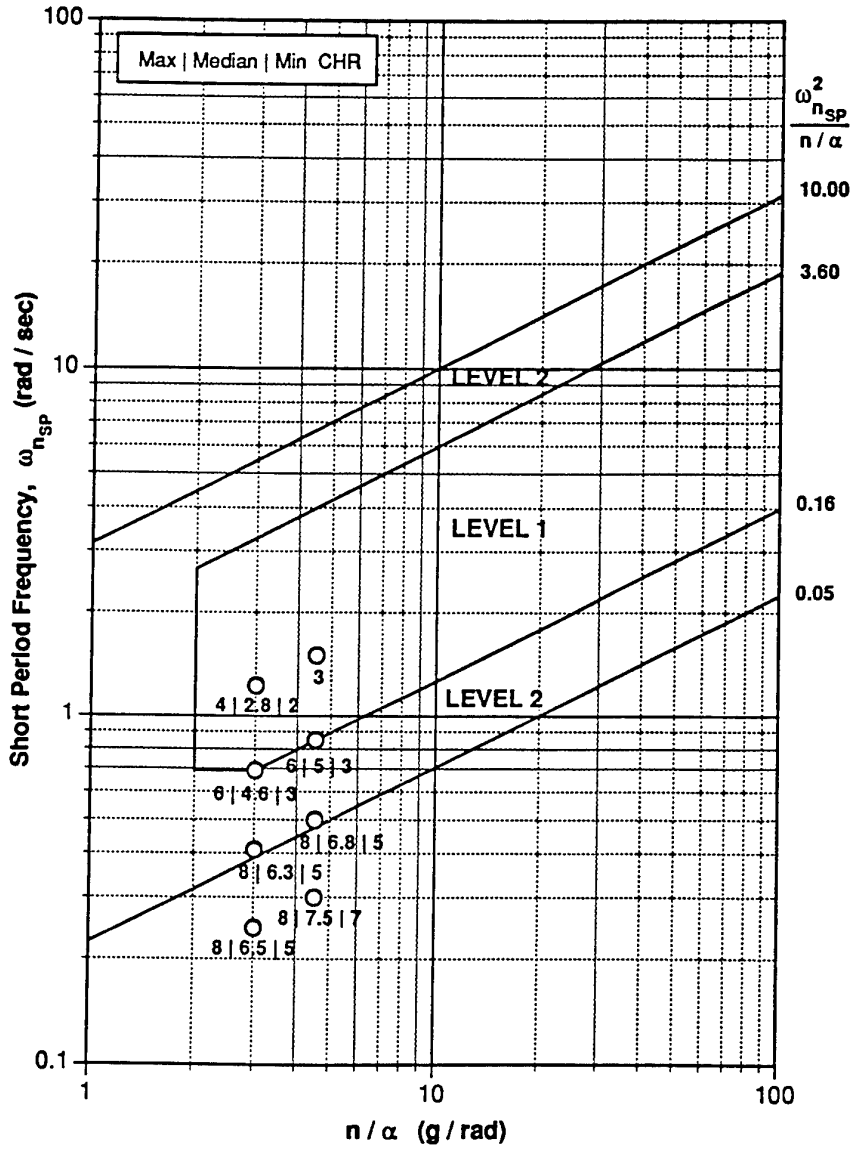

Figure 8 TIFS Angle-of-Attack Command Data Compared with Control Anticipation Parameter Requirements

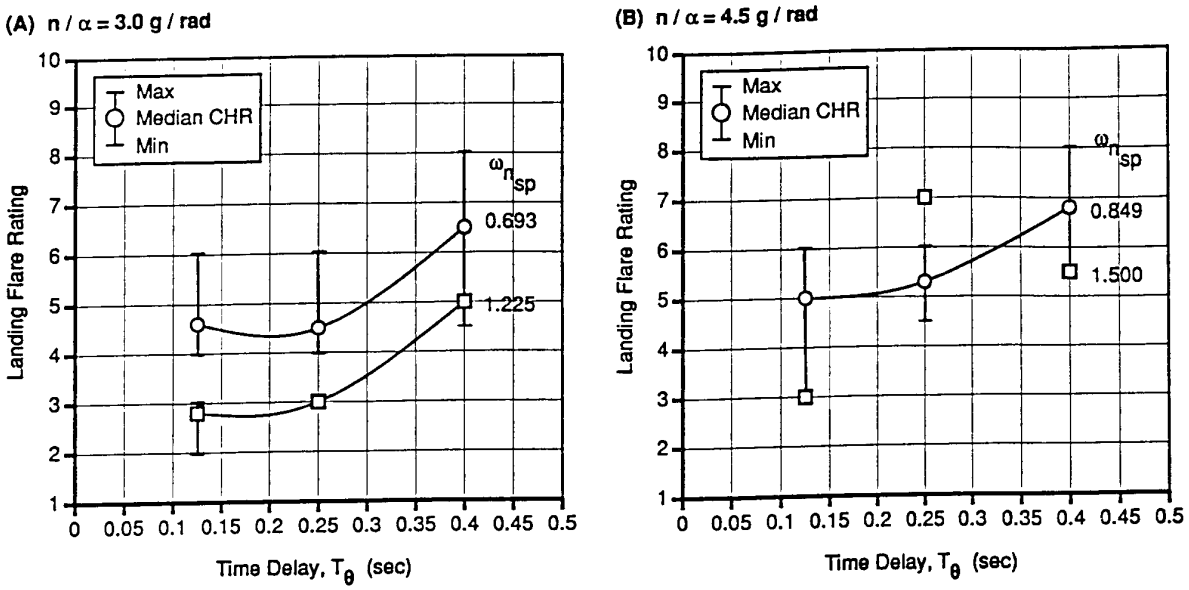

Figure 9 Pilot Ratings Degrade with Time Delay
(TIFS Angle-of-Attack Response-Type in Landing)

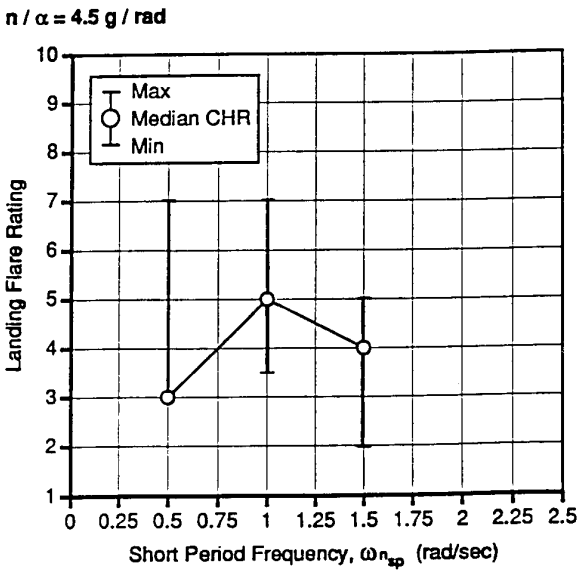

Figure 10 Pilot Ratings Show No Clear Trend with Short Period Frequency (TIFS Pitch Attitude Command Response-Type in Landing)

Experiences with ADS-33 Helicopter Specification Testing and Contributions to Refinement Research

C. J. Ockier
H.-J. Pausder
Deutsche Forschungsanstalt für
Luft- und Raumfahrt e.V. (DLR)
Institut für Flugmechanik
Lilienthalplatz 7
38108 Braunschweig
Germany

1. SUMMARY

The introduction of Active Control Technology in rotorcraft created the need for new handling qualities requirements. In response to this, a new helicopter handling qualities specification was developed under the leadership of the US Army and published as Aeronautical Design Standard 33 (ADS-33). Since its introduction, research has been conducted to expand the handling qualities database on which ADS-33 is based. This paper presents DLR contributions to this research. A standard BO 105 was used to evaluate the applicability and repeatability of the current ADS-33C criteria in forward flight. As a result of this study, some data gaps were recognized and the criteria that need further verification were identified. The in-flight simulator ATTHeS was used for an investigation of the effects of bandwidth and phase delay and pitch-roll coupling on helicopter handling qualities in a high gain slalom tracking task. Results are shown that indicate a need to more tightly constrain the phase delay for the roll axis than in the current ADS-33 requirements. For the pitch-roll coupling criterion it is shown that although the format of the current ADS-33 requirements is valid for control and rate coupling, it cannot be used for coupling types typical of actively controlled helicopters. A frequency domain criterion that offers more comprehensive coverage of all types of pitch-roll coupling is proposed.

2. INTRODUCTION

The next generation of military helicopters will have to be capable of precise and aggressive maneuvering close to the ground at night and in poor weather [1]. During each mission, the pilot will have to perform a broad spectrum of tasks that spans between high agility and high precision tasks, and that will include tasks traditionally reserved for fixed-wing aircraft. Parallel to this, the pilot will also have to operate a whole complex of mission specific equipment. To achieve this with an acceptable workload, the use of Active Control Technology (ACT) will be indispensable. Helicopters with a conventional control system are often unstable, strongly coupled, or sluggish, which results in flying qualities that are inadequate to surmount those new challenges. Design changes can make improvements, but often have significant drawbacks (e.g. the use of a stiffer rotor system can make the helicopter more agile, but increases interaxis coupling and instability).

By using Active Control Technology, the helicopter's handling qualities can be tailored to the specific demands of the individual mission phases (e.g. rate command for nap-of-the-earth (NOE) flight, attitude command for precision hover, etc.). Fig. 1 shows the integrated flight system and its design environment. Handling qualities are listed both as top and bottom level requirements. Handling qualities requirements provide guidelines for the design of the integrated flight control system. At the same time, they also form one of the bottom-line acceptance tests for the integrated flight system. The use of ACT in rotorcraft can also introduce new handling qualities problems. Fig. 1 also shows the different components that form the integrated helicopter system (controller, sensors, displays, interfaces). It is this integrated system that will ultimately be evaluated by the pilot. Each of the components in this figure introduces additional dynamics which enter into the final evaluation of handling qualities [2,3]. As an example, effective time delays are accumulated as a result of AD/DA conversion, computing times, and display latencies; filtering and shaping is part of the sensor, actuator, and pilot interface systems. Because of the dual role of handling qualities as top and bottom level requirements for the integrated flight system, it is important that handling qualities specifications are inclusive and valid for all types of helicopters, regardless of the type of control system or the level of integrated ACT.

A recent effort, under the leadership of the US Army, to

Paper presented at the Flight Mechanics Panel Symposium held in Turin, Italy, from 9-13 May 1994.

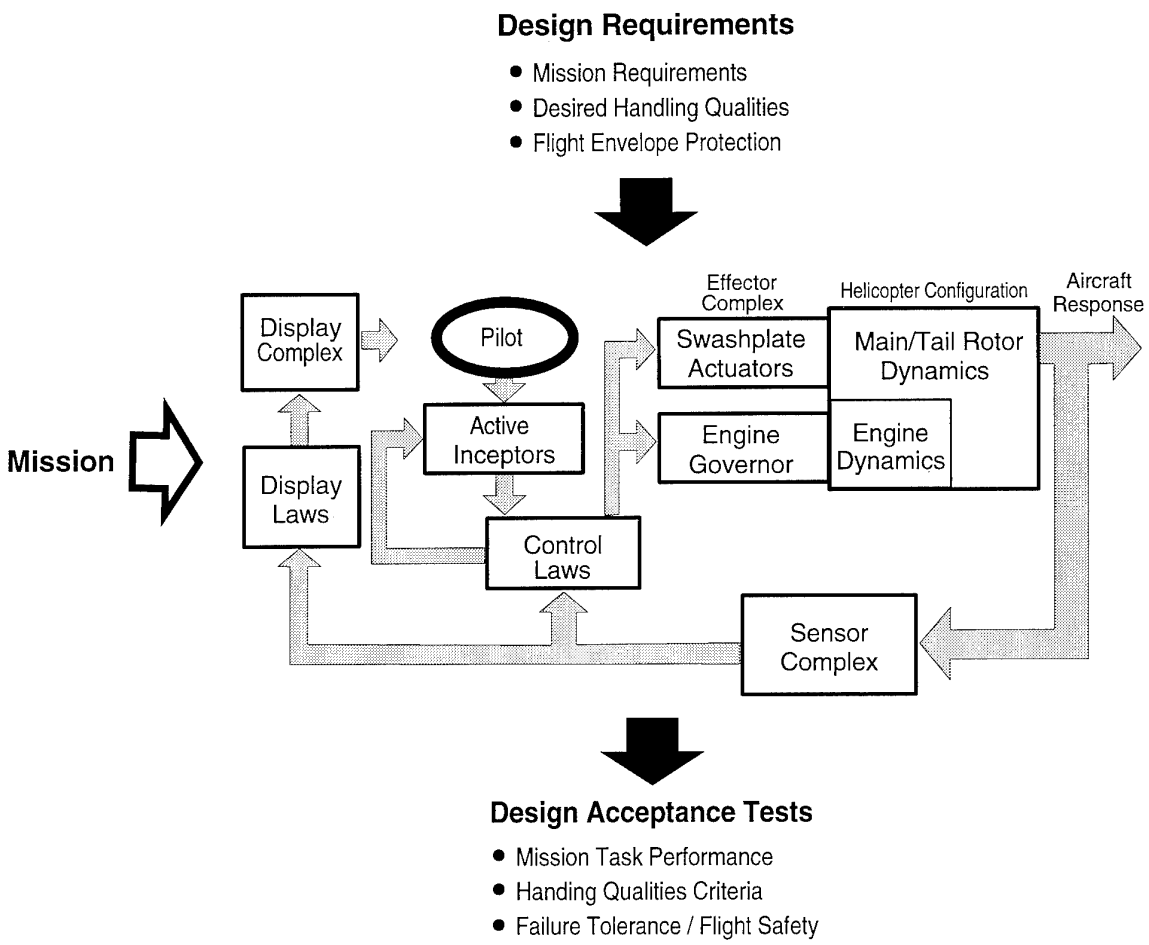

Fig. 1: The integrated pilot-vehicle system and its design environment.

establish comprehensive criteria, culminated in a new set of helicopter specifications known as Aeronautical Design Standard 33 (ADS-33). ADS-33 is essentially a mission oriented specification, with criteria depending on selected mission task elements, helicopter response types, failure probabilities, and pilot attention states. In order to accommodate night and poor weather operations, the handling qualities requirements are made dependent on the quality of the visual cues. ADS-33 comprises both quantitative and qualitative criteria. The quantitative criteria are computed directly from the aircraft response to prescribed inputs; they constitute a 'design and troubleshooting guide' which, if not satisfied, will almost certainly result in degraded flying qualities. The qualitative criteria are determined from specific flight test maneuvers, using pilot ratings on the Cooper-Harper scale; they constitute a comprehensive evaluation of the overall helicopter flying qualities.

In the US, ADS-33 has already been used for the simulator assessment of the competing designs for the LH (now *Comanche*) helicopter. In Europe, selected tailored flight test maneuvers from ADS-33 will be used for compliance testing of the *Tiger* helicopter. For NH-90, a tailored version of ADS-33 is foreseen as the design guide for the flight control system and for compliance testing. Since the first draft of the new specification in 1985, several reviews of ADS-33 have been completed, the latest of which is known as ADS-33C [4]. Since then, numerous studies [5,6,7,8] have further expanded the data base on which the criteria are based, and several problem areas have been recognized [9].

This paper discusses the contributions by DLR to the expansion of this database. First, an evaluation of the quantitative forward flight criteria of ADS-33C is discussed, some applicability and repeatability aspects of ADS-33C are critically examined, and areas for further research are identified. Then, two handling qualities aspects are studied in more detail: the bandwidth and phase delay criteria, and pitch-roll interaxis coupling. Both aspects were analyzed for a high gain slalom tracking task, and bear particular importance to the implementation of active control technology in helicopters.

3. THE DLR RESEARCH HELICOPTERS

The DLR operates two BO 105 helicopters used for hand-

Fig. 2: The Advanced Technology Testing Helicopter System (ATTHeS) in-flight simulator.

ling qualities research: the conventionally controlled BO 105 S-123 and the in-flight simulator ATTHeS.

3.1 The BO 105 S-123 Helicopter

The BO 105 S-123 is a conventionally controlled BO 105 helicopter without any flight control or stabilization systems. The BO 105 is a light, twin-engine, multi-purpose helicopter used in both civil (transport, police, ambulance) and military (liaison, scout, anti-tank) applications. The single rotor helicopter has a hingeless, soft in-plane rotor system with four composite blades, and a very high equivalent hinge offset (of about 14 %). The BO 105 has a high control sensitivity, an extremely high bandwidth, and is considered one of the most maneuverable helicopters around. For handling qualities testing, the BO 105 is equipped with a standard set of flight test instrumentation and a digital data acquisition system with a sampling rate of 200 Hz. Analog filtering is limited to a sole filter with an 80 Hz cut-off frequency to prevent phase shift errors.

3.2 The ATTHeS In-Flight Simulator

The BO 105 S-3 (Fig. 2), better known as the Advanced Technology Testing Helicopter System (ATTHeS), is the in-flight simulator version of the BO 105. The BO 105 was selected as the platform for the in-flight simulator because of its high bandwidth and excellent maneuverability. ATTHeS is equipped with a full authority, non redundant fly-by-wire (FBW) control system for the main rotor and fly-by-light (FBL) system for the tail rotor. The aircraft is operated by a crew consisting of a simulator pilot and a safety pilot. The safety pilot's position is equipped with the standard mechanical link to the rotor controls, whereas the simulator pilot's controls are linked to the rotor via a control computer and the FBW/L system. The FBW/L actuator inputs, which are commanded by the simulation pilot via the control computer, are mechanically fed back to the safety pilot's controls who can overrule the FBW/L actuator inputs at any time should the need occur. In the simulation mode, the flight envelope of ATTHeS is restricted to not lower than 50 ft above the ground in hover and 100 ft in forward flight.

The control system of ATTHeS is based on an explicit model following control system (MFCS) design [10]. It provides high quality simulation fidelity in the on-axis and allows almost complete decoupling of the axes [11]. For the experiments described in this paper, a control computer cycle time of 40 msec was realized. The equivalent time delays for the overall system – due to high order rotor effects, actuator dynamics, computational time, and pilot input shaping – were 100 to 110 msec in the roll axis and 150 to 160 msec in the pitch axis, related to a first-order rate command response.

4. EVALUATION OF THE ADS-33C CRITERIA IN FORWARD FLIGHT

A comprehensive evaluation of selected quantitative ADS-33C criteria was carried out in the summer and fall of 1992 with the conventionally controlled BO 105 S-123 helicopter [12]. The objectives of this study were: (1) to assess the suitability of the ADS-33C criteria for conventionally controlled and extremely maneuverable helicopters like the BO 105, (2) to evaluate the applicability and repeatability of the ADS-33C test procedures, (3) to develop and evaluate analysis tools for the ADS-33C criteria, and (4) to identify handling qualities areas that need further research. All flight tests were carried out in calm air at a forward flight speed of about 80 kts.

ADS-33C Criterion	Parameter		Std. Deviation (Nr. of samples)	H.Q. Level
Bandwidth / phase delay criteria				
Small amplitude pitch attitude	Bandwidth	2.7 rad/sec	0.21 rad/sec (2)	1
	Phase delay	77 msec	3 msec(2)	
Small amplitude roll attitude	Bandwidth	5.8 rad/sec	0.43 rad/sec (2)	1
	Phase delay	48 msec	2 msec (2)	
Small amplitude yaw attitude (Air Combat requirement)	Bandwidth	3.5 rad/sec	0.21 rad/sec (2)	1-2
	Phase delay	17 msec	16 msec (2)	
Attitude quickness criteria (see text)				
Control power criteria				
Large amplitude roll response	Max. roll rate	85 deg/sec right 72 deg/sec left	-	1
Large amplitude heading changes	Max. heading change	33 deg left 30 deg right	-	1
Stability criteria				
Mid-term pitch attitude response	Frequency	0.32 rad/sec	0.03 rad/sec (6)	1
	Damping ratio	-0.06	0.02 (6)	
Small amplitude roll oscillations	Frequency	2.44 rad/sec	0.15 rad/sec (15)	2-3
	Damping ratio	0.155	0.057 (15)	
Lateral-directional oscillations	Frequency	2.44 rad/sec	0.10 rad/sec (30)	2-3
	Damping ratio	0.162	0.027 (30)	
Vertical response criterion				
Flight path control	Time delay	146 msec	118 msec (15)	N/A
	Time constant	1.26 sec	0.48 sec (15)	
Interaxis coupling criteria				
Collective to attitude coupling (< 20 % full travel)	$\lvert\theta_{pk}/n_{z,pk}\rvert$	3.9 deg.sec^2/m	0.31 deg.sec^2/m (17)	2
Collective to attitude coupling (> 20 % full travel)	$\lvert\theta_{pk}/n_{z,pk}\rvert$	-	-	N/A
Pitch-due-to-roll coupling	θ_{pk}/ϕ	30 % (right rolls only)	5 % (8)	2
Roll-due-to-pitch coupling	ϕ_{pk}/θ	126 %	13 % (15)	3
Bank angle oscillations	$\lvert\phi_{OSC}/\phi_{AV}\rvert$	0.189	0.112 (6)	1-2
Turn coordination	$\lvert\Delta\beta/\phi_1\rvert$	0.43	0.13 (6)	1-2
	$\lvert\Delta\beta/\phi_1\rvert\times\lvert\phi/\beta\rvert_d$	0.31	0.09 (6)	

Table 1: Summary of the handling qualities parameters of the standard BO 105 helicopter.

Aircraft mass was maintained between 2200 and 2050 kg. All maneuvers were started from straight and level flight and inputs were performed manually by the pilot. An on-board CRT that allowed the pilot to monitor his own inputs was available.

Table 1 shows a list of the criteria that were evaluated, their corresponding handling qualities parameters and standard deviation, and the predicted handling qualities Levels for the BO 105. For the determination of the handling qualities Levels, all mission task elements except air combat were considered. As can be seen, the BO 105 scores Level 1 handling qualities for most pitch and roll axis criteria. The yaw axis criteria tend to be

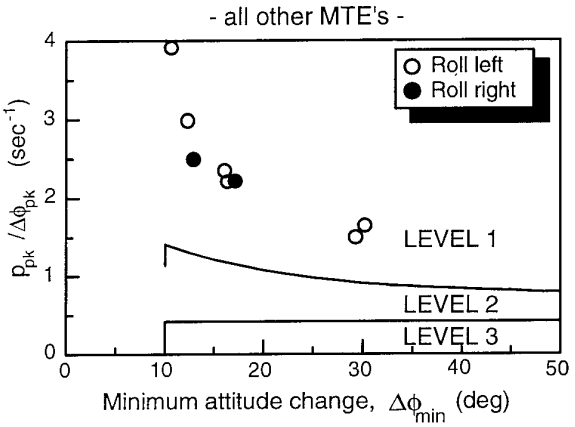

Fig. 3: Results for the moderate amplitude roll criterion in forward flight. All MTEs except air combat.

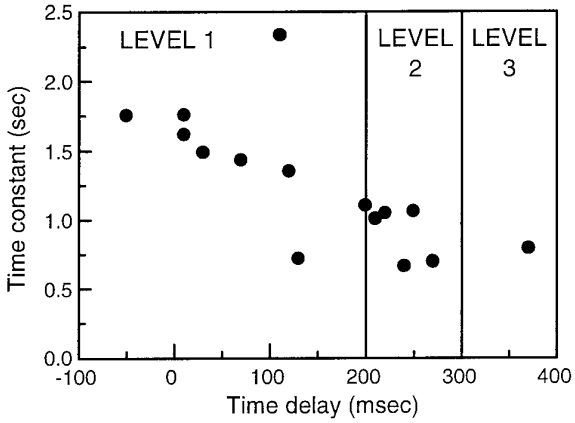

Fig. 4: Time delays and time constants as determined from 15 vertical rate responses, each of which met the ADS-33C first order 'goodness-of-fit criterion.

mostly in the Level 2-3 range, with some Level 1 and Level 3 data points. Interaxis coupling for the BO 105 was predicted at Level 2-3. This overall assessment is more or less compatible with general pilot opinion, although some assessments seem too severe. An evaluation of the BO 105 S-123 using the qualitative ADS-33 criteria should allow a more direct comparison between the predicted and the actual handling qualities Levels. Such an evaluation is currently under way at DLR.

The criteria in Table 1 are separated into several types: bandwidth/phase delay, attitude quickness, control power, stability, vertical response, and interaxis coupling. Two types of criteria can be considered 'classical': the stability criteria and the control power criteria. Their determination is straightforward and poses few repeatability or analysis problems. The other evaluated forward flight criteria are new to helicopter handling qualities testing and bear particular importance to actively controlled helicopters.

The attitude quickness (or moderate amplitude) criteria pertain to the aircraft's agility and measure the ability to achieve rapid, moderately precise attitude changes. The criteria are based on the premise that a decreasing bandwidth is allowed with increasingly large maneuvers [13]. The forward flight criterion applies to attitude changes between 10 and 60 degrees in roll, and thereby covers the range between the small amplitude bandwidth criterion and the large amplitude control power criteria. Fig. 3 shows the flight test data obtained for the BO 105. As can be seen, clear Level 1 handling qualities are predicted for all MTEs except air combat. All data in Fig. 3 lie within a relatively narrow band which indicates excellent repeatability.

The vertical response or flight path control criterion requires the vertical rate response to have a "qualitative first order appearance for at least 5 seconds following a step collective input." Parameters are determined using a parameter estimation procedure, and limits are specified in terms of a 'goodness of fit', a time delay and a time constant. Evaluations of this criterion with the standard BO 105 indicate that this criterion is difficult – if not impossible – to evaluate with a conventionally controlled helicopter. A collective step input with the other controls fixed produces a response that is not first order (because of the pitch response of the aircraft). When longitudinal cyclic is used to keep pitch attitude constant during the collective step input, an approximate first order response can be obtained. The results of the parameter identification, however, show very poor repeatability of the experiment. Fig. 4 presents the results for 15 different collective steps with pitch attitude held constant, each of which met the first order response 'goodness-of-fit' criterion. There is a very large spread in both the time constant and time delay parameters which makes it impossible to correctly determine the handling qualities level. The results seem to indicate that the current criterion has only limited relevance for conventional helicopters. More research is needed to determine exactly what handling qualities are required of the vertical response of a helicopter and how these are best measured.

The interaxis coupling criteria deal with the desired and undesired effects of interaxis coupling. Desired coupling between the roll and yaw axis (also known as turn coordination) is evaluated in the roll-sideslip coupling criteria. The roll-sideslip criteria in ADS-33C are identical to those for VSTOL aircraft [14], and consist of two requirements: (1) a limit on bank angle oscillations following bank angle changes and (2) a limit on sideslip excursions during turn entry. The flight tests with the BO 105 S-123 showed some difficulties with the application of this essentially fixed wing criterion to helicopters. Repeatability of the experiments was low and handling qualities levels were difficult to determine because of the large spread in the data. Analysis of the criterion showed that it might be possible to either simplify this very

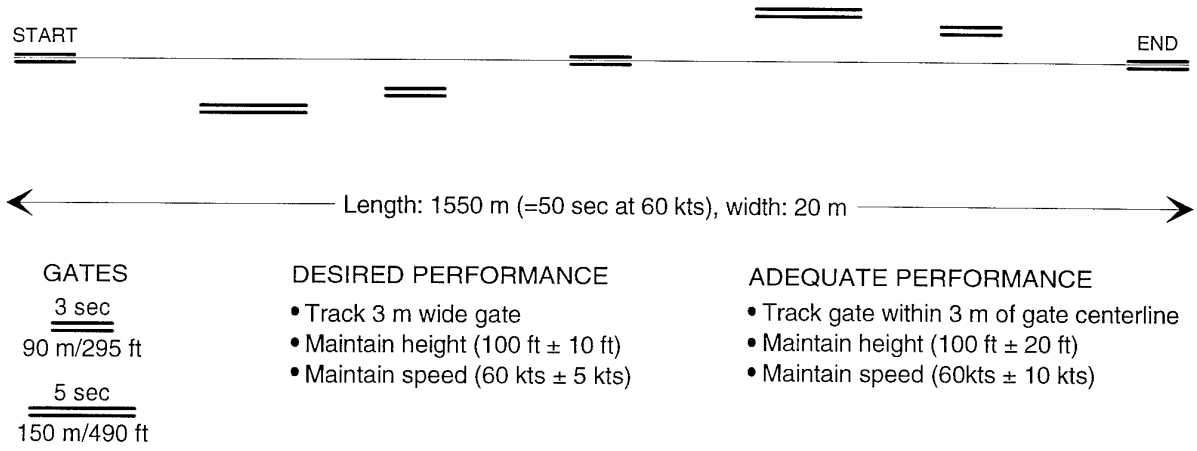

Fig. 5: The slalom tracking course for the ATTHeS flight tests.

complex criterion or to replace it by more easily determined criteria.

Undesired interaxis coupling is measured with two criteria: collective to attitude coupling and pitch-roll coupling. The collective to attitude coupling criterion places limits on the pitch attitude that can occur within the first 3 seconds following a collective step input. The criterion is expressed in terms of the peak change in pitch attitude to the peak change in normal acceleration. Repeatability of the experiment with the BO 105 was relatively good, despite the large amounts of coupling.

Two other criteria that were evaluated with the BO 105 S-123 – the bandwidth/phase delay criteria and the pitch-roll coupling criteria – were the subject of a more thorough study at DLR and will be discussed in the remainder of this paper. Both criteria bear particular importance to actively controlled helicopters.

5. THE ATTHES FLIGHT TESTS

In order to have desirable handling qualities over a large spectrum of applications, it is necessary for the helicopter to be very agile and still have an excellent precision during high gain tasks. Agility is defined by moderate to large amplitude maneuvers, such as those that occur during the positioning phases of air combat, contour flying, bob-up/bob-down, etc. Precision is defined by high gain tasks such as the lock-on phases in air combat and ground attack, slope landings, NOE flight, etc. Traditional slalom tasks (e.g. ADS-33C rapid slalom) mainly apply to the agility aspects of handling qualities. Because the precision aspects were most decisive for the ACT related bandwidth/phase delay and coupling studies of DLR, a precision high-gain roll axis task was required.

For the tests with ATTHeS, the complimentary use of ground-based and in-flight simulators was envisaged. Therefore it was vital to develop an appropriate precision

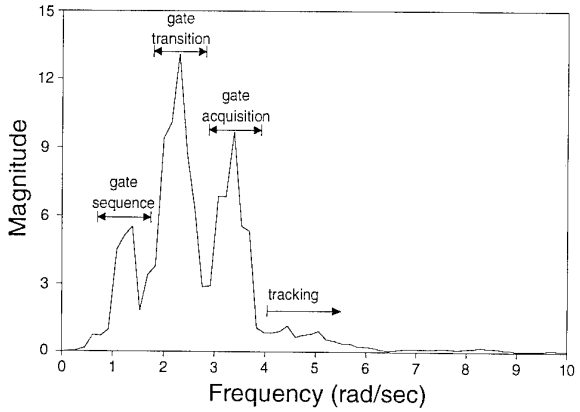

Fig. 6: Power spectrum of the lateral control input during the slalom tracking task (Level 1 rate command configuration).

task that could be easily implemented on both simulators while considering the constraints of each. For the ground-based simulator some of these constraints include a reduced field of view and visual resolution, whereas for the flight tests these include a 100 feet minimum altitude. In addition, it was desired to limit the task to a single axis roll task. This made it easier to analyze the effects of the different parameter changes and eliminated the need for exotic or expensive task cues. A modified slalom task with precise tracking phases through a set of ground marked gates was found most suitable for this purpose. The slalom course layout included transition and precision tracking phases. The transition phases were intended to be a lower frequency disturbance with the main emphasis of the task being the higher frequency acquisition and tracking phases just prior and through the gates. The gates were 3 meters wide (desired performance) and 90 or 150 meters long (Figure 5). The primary task was defined as the tracking through the ground marked gates, with the maintenance of height and speed (± 10 ft and ± 5 kts for desired performance) as secondary tasks. Target ground speed and height were 60 kts and 100 ft.

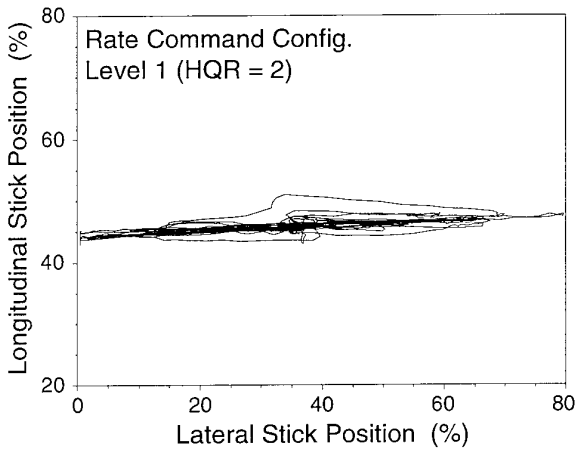

Fig. 7: Crossplot of the pilot's cyclic control inputs during the slalom tracking task (decoupled Level 1 rate command configuration).

Figure 6 shows the measured power spectrum of the lateral control input during the slalom task for a Level 1 rate command configuration. Four task elements can be clearly distinguished: (1) gate sequence or the lateral displacement of the gates, (2) gate transition or the S-shaped slalom between the gates, (3) gate acquisition, and (4) tracking within the gate. The large amplitude inputs used in the transition between the gates can be clearly discerned from the higher frequency small amplitude inputs used for final gate acquisition and tracking through the gates. From this figure it can be seen that the slalom tracking task is a high frequency task that is contained within the band from about 1 rad/sec to about 7 rad/sec. Fig. 7 shows a crossplot of the pilot's cyclic control inputs. As can be seen, there are only very few longitudinal inputs required to perform the slalom. This clearly shows that the slalom-tracking task is a pure roll axis task.

The slalom tests with ATTHeS were performed at the German Forces Flight Test Center (WTD 61) in Manching. The facilities in Manching consist of a large grass area – where the 1.5 km long slalom course could be built – and a precision position tracking system (PATS). For each configuration that was evaluated, the test pilots were given adequate time for familiarization with the configuration (typically two practice runs) before they performed two evaluation runs. This was to ensure the pilot ratings and comments were not biased by the unfamiliarity of the pilot with the configuration and the task. For each configuration, the pilot completed a questionnaire and summarized his evaluation in a handling qualities rating using the Cooper-Harper scale [15]. Questions were related to task performance, pilot workload, and system response characteristics. In general, at least two test pilots flew each configuration, but when the difference in the two ratings was higher than one rating point, an evaluation with a third pilot was conducted. This technique allows the rapid evaluation of a large number of data points while maintaining high confidence levels in the ratings. During the flight tests, the following signals were measured: (1) position of the helicopter in relation to ground course, (2) pilot control inputs, (3) angular attitudes and rates, (4) accelerations, (5) airspeed, and (6) MFCS internal signals like command to actuators. Because of the limited space in the test helicopter the tests had to be observed from the ground station. Helicopter position in relation to the ground track course and selected on-board signals were displayed on three quicklook terminals in the observation station.

6. BANDWIDTH AND PHASE DELAY STUDY

6.1 Motivation and Scope

The ADS-33 bandwidth and phase delay criteria relate to the aircraft's ability to perform small amplitude, high pilot gain tasks such as tight loop tracking, slope landing, etc. [16]. The parameters bandwidth, ω_{BW}, and phase delay, τ_p, are determined from the frequency response (Bode) plot of the rotorcraft attitude response to controller input, according to Fig. 8. The bandwidth criterion is an application of the pilot crossover model [17]. It provides a measure of the maximum closed-loop frequency a pure-gain pilot can achieve without threatening stability. Low bandwidth values indicate the need for pilot equalization during high frequency (high gain) tasks. Increasing demands on lead-equalization result in higher workload and poorer handling qualities. The helicopter's phase delay indicates how quickly the phase lag increases beyond the point of neutral stability. This is significant for piloting tasks at very high pilot gains when the pilot controls beyond the neutral stability frequency. When controlling above the neutral stability frequency, a significant amount of lead compensation is required. When the phase delay is high, excessive amounts of lead compensation will be required and pilot induced oscillations (PIOs) are likely. The phase delay can be directly related to the equivalent time delay of a system (provided the rest of the system dynamics are known). For first order rate and second order attitude command systems, the relationship between model parameters and bandwidth and phase delay is shown in Fig. 9.

Fig. 10 shows the ADS-33C roll axis forward flight requirements for bandwidth and phase delay. Different requirements exist depending on the applicable mission task elements (MTEs). The more severe requirements apply to the higher pilot gain tasks such as air combat. In each category, an increase of phase delay is allowed with increasing bandwidth.

For design of actively controlled helicopters, bandwidth and phase delay are two important design parameters. Bandwidth is one of basic parameters used for the layout of a control system. Phase delay is directly related to the effective time delay of the pilot-vehicle system, and is mostly a function of the basic helicopter and the hardware

BANDWIDTH

RATE COMMAND SYSTEMS

ω_{BW} is lesser of $\omega_{BW_{gain}}$ and $\omega_{BW_{phase}}$

ATTITUDE COMMAND SYSTEMS

$\omega_{BW} = \omega_{BW_{phase}}$

PHASE DELAY

$$\tau_p = \frac{\Delta\phi_{2\,\omega_{180}}}{57.3\,(2\,\omega_{180})}$$

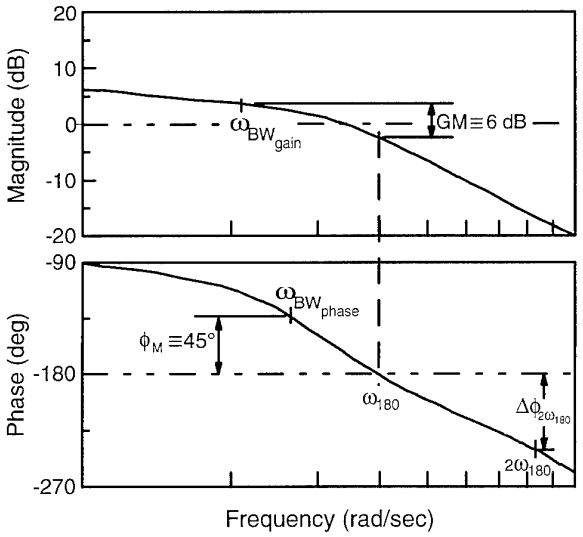

Fig. 8: Definition of bandwidth and phase delay (ADS-33C).

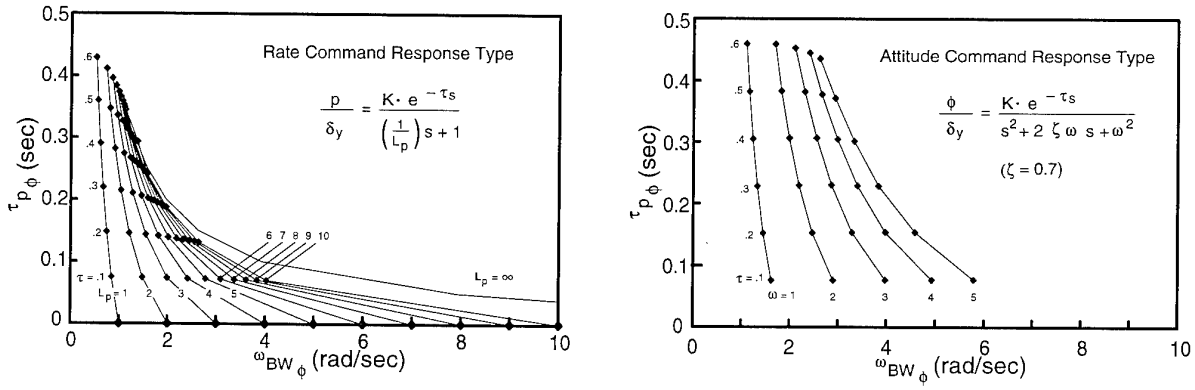

Fig. 9: Effect of model parameters on bandwidth and phase delay.

and software used. Flight tests with ADOCS and an early ATTHeS design with a time delay of more than 200 msecs [2,18] revealed poor handling qualities in high gain tasks, despite the fact that bandwidth and phase delay were within the ADS-33 Level 1 limits. Fixed wing requirements [19] allow an equivalent time delay of 150 msecs for Level 1 handling qualities. Such small time delays are difficult to obtain in helicopters because of the inherent time lag in the rotor system.

A review of the data base used for the definition of the ADS-33C requirements showed that these were primarily obtained from ground-based simulation and flight tests with low-bandwidth rotorcraft, and that the tasks used for the evaluations were mainly low-precision, moderate to large amplitude tasks. Therefore, the DLR in Braunschweig – in cooperation with the US Army – conducted a study into the effects of bandwidth and phase delay on helicopter handling qualities. The standard BO 105 S-123 was used to verify the applicability and repeatability of the ADS-33C bandwidth and phase delay criterion in forward flight and to assess the tools available for the determination of the criterion [12]. The variable stability BO 105 S-3 (ATTHeS) was used to investigate the effects of different bandwidths and phase delays on helicopter handling qualities for a high gain slalom tracking task [20].

6.2 ADS-33C Testing Experience

In order to establish test and analysis procedures and to verify the applicability and repeatability of the bandwidth/phase delay criterion, flight tests were conducted with the conventionally controlled BO 105 S-123. To obtain a Bode plot of the attitude response to control input, frequency sweep inputs were made and the response recorded. Each frequency sweep had a duration of about 30 to 50 seconds and was preceded and followed by a trim condition. The frequency sweeps were performed manually, as this is easier and safer and generally produces better results than synthetic sweeps. To investigate the repeatability of the experiment, frequency sweeps were recorded during two different flights. As with all frequency sweeps, extreme care was taken not to excite any dangerous structural modes during the experiment.

The analysis of frequency sweep data is complex and

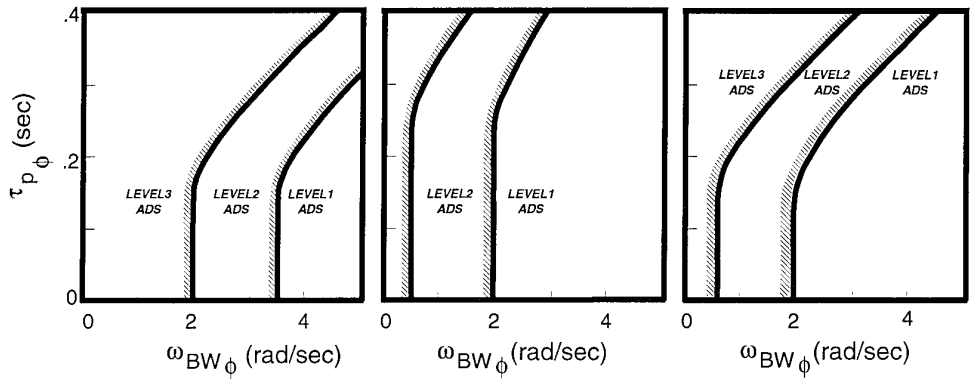

a) Air Combat *b) All Other MTEs-VMC and Full Attended Operations* *c) All Other MTEs-IMC and/or Divided Attention Operations*

Fig. 10: ADS-33C requirements for small amplitude roll attitude changes in forward flight.

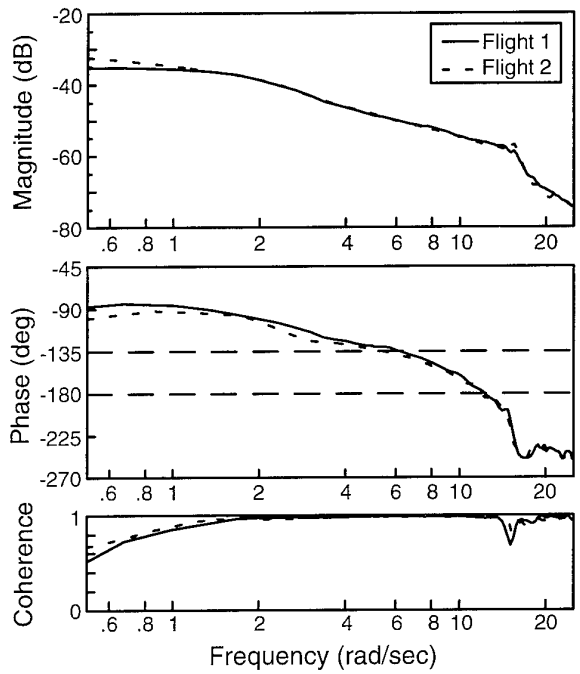

Fig. 11: Bode plot of the roll attitude response to a lateral controller input. Shown are results for two different flight tests with the BO 105 S-123.

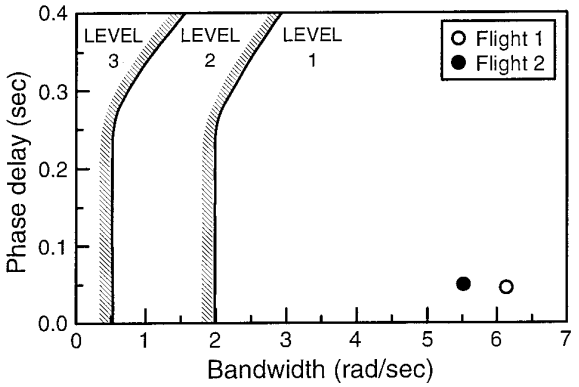

Fig. 12: Data points of bandwidth and phase delay for the BO 105 S-123. Boundaries are for all fully attended MTEs except air combat.

requires sophisticated data analysis programs such as the DLR program MIMO [21] or the US Army program CIFER [22]. From the sweep data obtained with the BO 105, conditioned frequency responses were calculated using the MIMO program. Concatenated sweeps and weighting and windowing functions were used to reduce the random error, and to prevent side-lobes and leakage effects in the Bode plots.

The Bode plot of the roll response (i.e. integrated roll rate) to lateral cyclic input is shown in Fig. 11 for two different flight tests. It can be seen that the repeatability of the experiment is outstanding. The frequency response curves are smooth and consistent and coherence is excellent (> 0.8) between 1 and 25 rad/sec. There is a noticeable coherence drop at about 16 rad/sec, which is the frequency of the air resonance mode. From this figure, the bandwidth and phase delay of the roll response can be determined. Results are summarized in Table 1 and Figure 12. For the standard BO 105, Level 1 air combat roll axis handling qualities are predicted.

6.3 Description of the variable stability tests

For the bandwidth/phase delay evaluations with the ATTHeS in-flight simulator, two response systems were used: a first order rate command (RC) and a second order attitude command (AC) system. These command systems were defined for the roll and pitch axes (Table 2). Rate of climb response and sideslip command were implemented for the vertical and directional axes. The response to control inputs were fully decoupled, except for the terms governing turn coordination and roll attitude thrust compensation (pseudo altitude hold.) For the RC response, the primary experimental variables were roll damping, L_p, and time delay, τ. For the AC response, the primary variables were natural frequency, ω_n, and time

Axis	Rate Command	Attitude Command
Pitch	$\frac{q}{\delta_x} = \frac{M_{\delta_x} e^{-\tau s}}{(s + M_q)}$	$\frac{\theta}{\delta_x} = \frac{M_{\delta_x} e^{-\tau s}}{(s^2 + 2\zeta\omega_\theta s + \omega_\theta^2)}$
Roll	$\frac{p}{\delta_y} = \frac{L_{\delta_y} e^{-\tau s}}{(s + L_p)}$	$\frac{\phi}{\delta_y} = \frac{L_{\delta_y} e^{-\tau s}}{(s^2 + 2\zeta\omega_\phi s + \omega_\phi^2)}$

Table 2: Definition of the roll and pitch axis command response.

delay, τ. For the AC response, the damping ratio, ζ, was held constant at 0.7. For all configurations, the pitch axis parameters were varied in harmony with the roll axis parameters. The control sensitivities were selected based on experiences gained in the ground-based Vertical Motion Simulator (VMS) at NASA Ames.

To verify the bandwidth and phase delay values for the test configurations, the computed values were compared to values measured during flight tests. The overall ATTHeS response had a bandwidth about 0.1 rad/sec higher than the bandwidth calculated from the command model. The phase delay was approximated with an accuracy of about 10 msec, which is within the accuracy of the phase delay measurement. This clearly indicated that ATTHeS is capable of simulating high bandwidth systems and confirms the credibility of the flight test data.

The flight tests were conducted in June 1991 at the German Forces Flight Test Center (WTD 61) in Manching. Twenty-eight flight hours were performed in 10 days. Four experienced test pilots, one each from DLR, U.S. Army, WTD 61, and DRA-Bedford were involved in the tests. The flight test configuration matrix (Table 3) was selected based on results from VMS simulator tests [23].

In Figure 13, the measured ground tracks for a Level 1 and a Level 2 rated rate command system are shown. The ground track for the Level 1 configuration shows clear tracking phases through the gates. The track of the Level 2 configuration shows some problems in the acquisition and tracking phases. The tracking accuracy is degraded especially through the second and fourth gate. This change in task performance correlates with the Cooper Harper rating scale and underscores the consistency of the ratings.

Command Response	Sensitivity	Added Delay	Damping/ Frequency	Bandwidth	Phase Delay	Average HQR
-	rad sec^{-2} %$^{-1}$	msec	L_p, sec^{-1}	rad/sec	msec	-
Rate	.085	0	2	1.45	81	6.5
	.093	0	3	1.93	80	5.25
	.093	40	3	1.74	109	5.5
	.100	0	4	2.34	80	4.25
	.100	40	4	2.06	107	5.0
	.100	80	4	1.85	134	5.5
	.115	0	6	2.97	78	3.3
	.115	40	6	2.55	105	3.75
	.115	80	6	2.25	131	5.0
	.130	0	8	3.44	77	2.5
	.130	40	8	2.91	103	3.7
	.130	80	8	2.52	127	5.0
	.130	120	8	2.23	151	5.5
	.145	0	10	3.82	76	4.0
	.145	40	10	3.18	101	4.0
-	rad sec^{-2} %$^{-1}$	msec	ω_ϕ, rad/sec	rad/sec	msec	-
Attitude (ζ = 0.7)	.060	0	1.7	2.49	83	3.5
	.060	40	1.7	2.34	114	5.0
	.060	80	1.7	2.20	145	5.0
	.060	120	1.7	2.11	175	6.5
	.060	160	1.7	2.02	206	6.5
	.100	0	2.3	3.17	84	3.0
	.100	40	2.3	2.95	114	3.7
	.100	80	2.3	2.77	145	4.75
	.180	0	3.0	3.89	84	4.25
	.180	40	3.0	3.58	115	5.25
	.180	80	3.0	3.34	145	6.5
	.180	120	3.0	3.14	176	6.75
	.180	160	3.0	2.97	207	7.0
	.300	40	4.0	4.38	115	6.0

Table 3: Commanded roll axis configurations for the bandwidth and phase delay study.

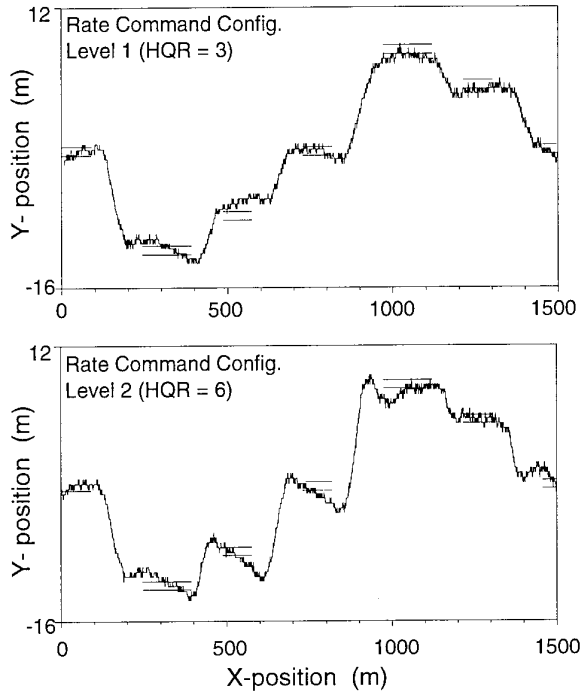

Fig. 13: Comparison of measured ground tracks for a Level 1 and a Level 2 rate command system.

6.4 Discussion of the results

Figure 14 shows the individual handling qualities ratings (HQRs) for both response systems: rate and attitude command. A high degree of consistency between the attitude and the rate command configurations can be seen. This confirms not only the independence of the bandwidth/phase delay criterion with regard to the response type, but also illustrates the appropriateness of the slalom tracking task for the investigation. By giving the pilots sufficient time to familiarize themselves with the task and the configuration, the spread in the ratings could be kept very small. For most configurations the differences in HQRs are not more than one rating point. This underscores the quality of the generated database.

In Figure 14 the averaged ratings of the flight tests are presented together with recommended Level boundaries. The shape of the recommended Level boundaries is significantly different from the current ADS-33 requirements (see Figure 10). In particular, there is a much clearer upper limit to the phase delay. In the mid bandwidth range, the maximum allowable phase delay seems to be about 100 msecs for Level 1 and about 170 msecs for Level 2 handling qualities. For first order rate command systems, this corresponds to a maximum equivalent time delay of about 145 msecs for Level 1 and about 230-300 msecs for Level 2. For a second order attitude command system, the maximum allowable time delays are about 130 msecs and 230 msecs, respectively. This result agrees, at least in concept, with the fixed wing requirement for a maximum equivalent time delay [19]. As bandwidth increases, the flight test data suggest that even less phase delay is tolerable. For these high bandwidth configurations, pilot comments suggested a relatively higher importance of the phase delay. More data would, however, be required to substantiate this trend.

Another observation from Figure 14 is that the minimum bandwidth limits from the flight data do not coincide with the ADS-33C limits. This probably has to do with the

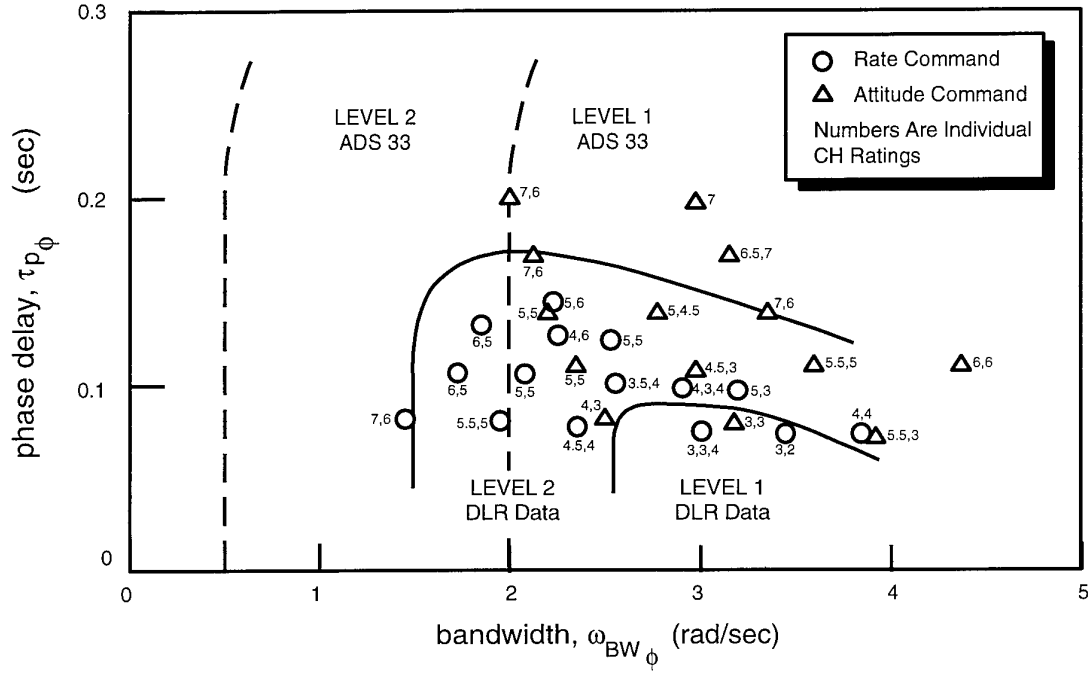

Fig. 14: Flight test data points of the bandwidth and phase delay study.

nature of the slalom tracking task used for this study. Pilots who participated in the tests placed the slalom task somewhere between air combat (air tracking) and the other MTEs used in ADS-33. VMS tests with an identical task suggested still different boundaries [20]. These variations in task bandwidth point out the need for a better understanding of the effects of task bandwidth on helicopter bandwidth requirements. Further work, which systematically addresses the dependency between task bandwidth and Level boundaries and which aims at refining the task categorization, is under way.

7. THE PITCH-ROLL COUPLING STUDY

7.1 Motivation and Scope

Typical high agility, high bandwidth helicopters, such as the BO 105, exhibit severe pitch-roll cross-coupling. This coupling is inherent to the stiff rotor system and the large hinge offset required to generate the large rotor moments needed for agility and responsiveness. Strongly coupled helicopters are difficult to fly: even the simplest single axis task requires multi-axis inputs, which increases the workload and degrades handling qualities. ACT can provide an answer to this problem by actively de-coupling the helicopter. However, whether flight control systems can and should be designed to eliminate all coupling at all times is questionable – cost and available technology may determine differently. Also, the helicopter must be controllable after a flight control system or component failure. If the basic flight control system cannot guarantee this, expensive redundant elements may be required.

Maximum allowable levels of pitch-roll cross-coupling are defined in ADS-33C. The pitch-roll cross coupling criteria in forward flight apply only to the more aggressive mission task elements, i.e. ground attack, slalom, pull-up/push-over, assault landing, and air combat. The criteria are defined in terms of the ratio of peak off-axis response to peak on-axis response to a given cyclic input, i.e. θ_{pk}/ϕ for pitch-due-to-roll and ϕ_{pk}/θ for roll-due-to-pitch. The peak off-axis response must be measured within 4 seconds following an abrupt longitudinal or lateral cyclic step input; the peak on-axis response must be measured exactly 4 seconds following the input. The coupling limits, as specified in Table 4, are the same for pitch-due-to-roll and roll-due-to-pitch. ADS-33C further specifies that this requirement "shall hold for control input magnitudes up to and including those required to perform the specified mission task elements." ADS-33C requirements in hover are identical to those in forward flight.

By defining a four second segment from which the maximum attitudes are taken, the ADS-33C pitch-roll coupling criterion only considers mid to long term cross-coupling effects. During high-gain tasks, where the pilot needs to work constantly to reduce the effects of coupling, mid to long term coupling may be secondary to the short term effects that occur as part of the initial response of the helicopter. The short term effects are particularly important for ACT. Long term coupling can easily be eliminated by a simple feedback control system; the elimination of short-term coupling requires a much larger effort on the part of the control system designer. To establish a more comprehensive cross-coupling database that can be used to define more precise handling qualities requirements, the DLR – in cooperation with the US Army – started a two-year research program. Flight test experiments with the standard BO-105 S-123 were conducted to evaluate the applicability and repeatability of the existing ADS-33 cross-coupling criteria [12]. The in-flight simulator ATTHeS was used to investigate the effects of different types and magnitudes of cross-coupling on helicopter handling qualities [24]. During the investigations, there was a strong emphasis on the investigation of coupling types typical of actively controlled helicopters. For the pitch-roll coupling study with ATTHeS, the same task and the same on-axis model were used as for the bandwidth and phase delay study.

Parameter	Level 1	Level 2
$\left\lvert \frac{\theta_{pk}}{\phi} \right\rvert_{\delta_y}$	±0.25	±0.60
$\left\lvert \frac{\phi_{pk}}{\theta} \right\rvert_{\delta_x}$	±0.25	±0.60

Table 4: Maximum values for pitch-roll coupling (ADS-33C).

7.2 Experience with ADS-33C Testing

The standard BO 105 S-123 was used to verify the applicability and repeatability of the existing pitch-roll coupling criteria. A large number of longitudinal and lateral cyclic steps with the other controls fixed were performed. Contrary to what is specified in ADS-33C, the input magnitude of the steps had to be kept relatively small because of the large amplitudes that developed within 4 seconds.

Fig. 15 shows the measured pitch-due-to-roll coupling of the BO 105 S-123. As can be seen, there is a significant difference between the coupling that results from rolling to the left and to the right. From right rolls, coupling was determined at about 30 %, which is clearly Level 2 according to ADS-33C. For left rolls, the average coupling is only about 14 % which is within the Level 1 range.

Fig. 16 shows a typical time history of a step roll input to

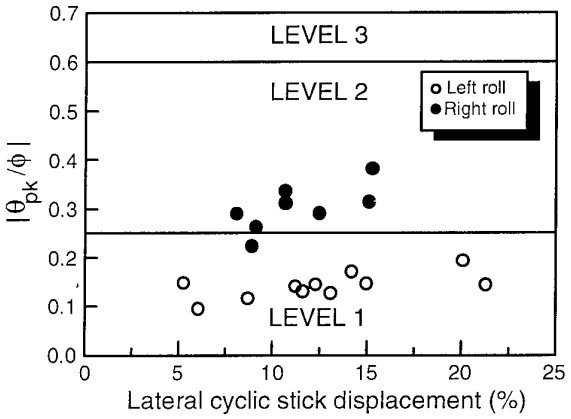

Fig. 15: Pitch-due-to-roll coupling criterion (BO 105 S-123 data points).

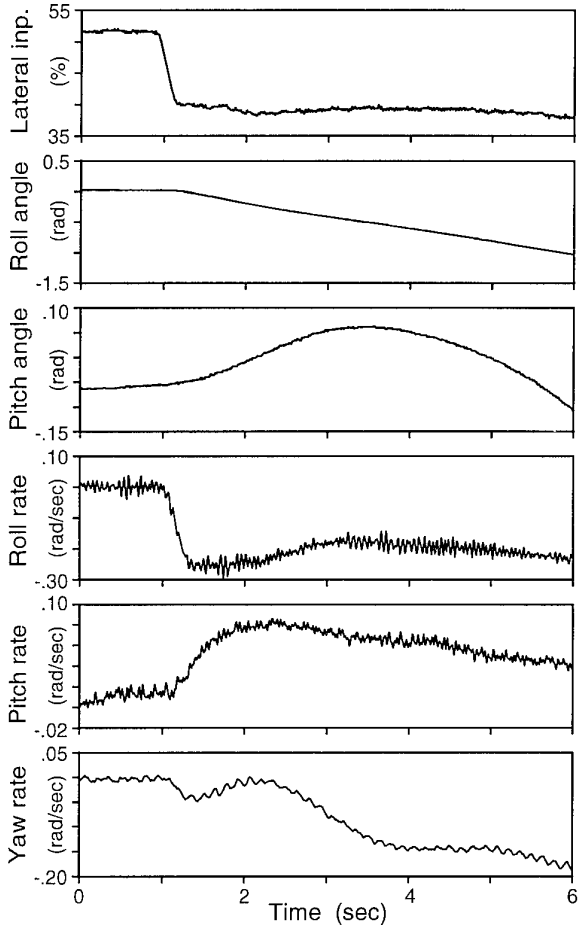

Fig. 16: Typical time history of the response to a roll step input to the left with a conventionally controlled BO 105.

the left. As can be seen, the helicopter responds with a negative roll rate (roll to the left) and a positive pitch rate (nose up). Both roll and pitch rate attain a more or less steady value. Yaw rate is oscillatory, negative, and almost double the steady pitch rate. The bank angle, ϕ, shows a constant increase as a result of the left roll input. The pitch angle, θ, initially increases, peaks after about 2.5

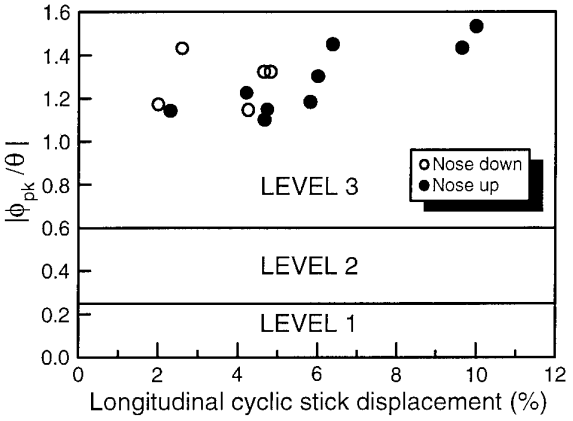

Fig. 17: Roll-due-to-pitch coupling criterion (BO 105 S-123 data points).

seconds and then decreases. With θ given by:

$$\dot{\theta} = q\cos\phi - r\sin\phi$$

it can be seen that while q remains more or less constant, the contribution of the term $(q \sin \phi)$ to θ becomes smaller as the bank angle increases. Conversely, the contribution of the term $(r \cos \phi)$ to θ increases as the yaw rate and bank angle increase. About 2.5 seconds after the step input, the contributions of pitch rate and yaw rate cancel each other and the pitch angle reaches its maximum. For a perfectly coordinated turn and in the absence of pitch-due-to-roll coupling, the effects of pitch and yaw rate cancel each other and θ remains zero (as could be expected in a coordinated turn). However, when turn coordination is not perfect (as is the case for the BO 105), there will be a change in pitch angle, even when there is no pitch-due-to-roll or roll-due-to-pitch coupling. Hence with a four second attitude requirement, it is very difficult to differentiate between the effects of cross coupling and non-perfect turn coordination, especially when large bank angles are allowed.

Fig. 17 shows the roll-due-to-pitch coupling parameters for the BO 105. Average roll-due-to-pitch coupling is about 127 % (i.e. a pitch input causes more roll than pitch). This would place the BO 105 severely into the Level 3 range ("Adequate performance not attainable with a tolerable workload"). This very severe evaluation of roll-due-to-pitch coupling is a direct result of the equality of the pitch and roll coupling limits, and did not agree with the opinion of the DLR pilots. The pitch-roll coupling criterion is based primarily on hover data where the perceptual difference between pitch and roll motions is not as strong. Discussions with pilots indicated that, in forward flight, large bank angles are more tolerable than large pitch angles, and that the equality of pitch and roll coupling limits in forward flight may place too severe requirements on the roll-due-to-pitch coupling.

7.3 Description of the variable stability tests

For the study of pitch-roll coupling with the in-flight

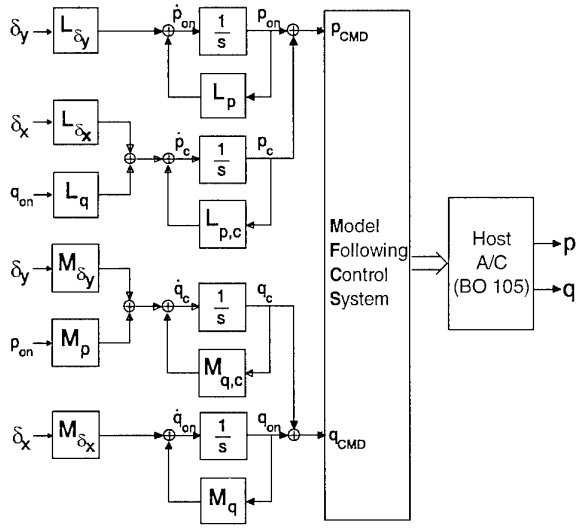

Fig. 18: Roll-pitch axis model used for the coupling study.

simulator ATTHeS, a coupled first order rate command system was used. The simulation model consisted of two parts: (1) an uncoupled baseline model with Level 1 handling qualities and (2) a pitch-roll cross-coupling model. This allowed changing the cross-coupling response without changing the remaining helicopter dynamics.

The uncoupled baseline model was a first order rate command model, identical to the rate command model used for the bandwidth and time delay study. A configuration with known Level 1 handling qualities was selected from the bandwidth/phase delay study (Table 3). This configuration had no added time delay, and a roll axis bandwidth and phase delay of 3.44 rad/sec and 77 msecs, respectively. Pitch axis bandwidth and phase delay for this configuration were 2.00 rad/sec and 114 msecs.

The coupling model was based upon the following simplified pitch and roll equations of motion of a helicopter:

$$\dot{p} = L_p p + L_q q + L_{\delta_y} \delta_y + L_{\delta_x} \delta_x$$

$$\dot{q} = M_p p + M_q q + M_{\delta_y} \delta_y + M_{\delta_x} \delta_x$$

These equations describe the dominant aircraft motions for lateral and longitudinal cyclic inputs and show the on-axis terms damping (L_p and M_q) and control sensitivity ($L_{\delta y}$ and $M_{\delta x}$), and the off-axis terms representing the rate coupling (L_q and M_p) and control coupling ($L_{\delta x}$ and $M_{\delta y}$). To be able to simulate rate and control coupling independently of each other, this model was simplified to the coupling model shown in Fig. 18. In this figure, two parameters have been added: $L_{p,c}$ and $M_{q,c}$. These parameters allow the dynamics of the coupling to be varied independently of the on-axis response (as could be the case with actively controlled helicopters).

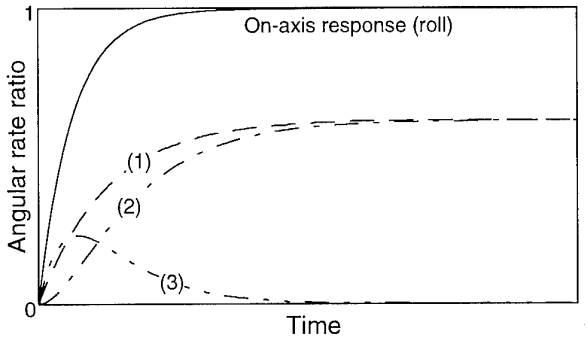

Fig. 19: Off-axis response to a step input for three different types of coupling: (1) control coupling, (2) rate coupling, and (3) washed-out coupling.

For this model, the ratio of the off-axis response to the on-axis response is given by:

$$\left.\frac{q}{p}\right|_{\delta_y} = \frac{s - L_p}{s - M_{q,c}} \cdot \frac{M_{\delta_y}}{L_{\delta_y}} + \frac{M_p}{s - M_{q,c}}$$

$$\left.\frac{p}{q}\right|_{\delta_x} = \frac{s - M_q}{s - L_{p,c}} \cdot \frac{L_{\delta_x}}{M_{\delta_x}} + \frac{L_q}{s - L_{p,c}}$$

One of the objectives of this study was to investigate the cross coupling behavior of helicopters with feedback control systems. In such an ACT helicopter, any off-axis rates that result from control or rate coupling will be reduced to zero by the feedback system. This results in a washed-out response characteristic in the off-axis. Figure 19 shows the off-axis response to a step input for three different types of cross-coupling: (1) control coupling, (2) rate coupling, and (3) washed-out coupling. In addition, the ratio of roll-due-to-pitch coupling to pitch-due-to-roll coupling was varied to investigate the effects of the coupling introduced as a result of the corrective pitch inputs.

Two pitch-roll coupling flight test campaigns were conducted with the BO 105 ATTHeS at the German Forces Flight Test Center (WTD 61) in Manching. During each campaign about 30 in-flight simulation hours were logged over a two and a half week period. The first flight test campaign took place in June 1992 and focused on basic coupling effects. Four experienced test pilots participated in the tests: one NASA-Ames, one DRA-Bedford, and two German Forces (WTD 61) pilots. The second flight test campaign took place in July 1993 and was aimed at investigating more complex coupling phenomena and filling data gaps left by the first test series. Five experienced test pilots participated: one NASA-Ames, one DRA-Bedford, one US Army, and two German Forces (WTD 61) pilots. The NASA-Ames and DRA-Bedford pilots were the same in both flight test campaigns. DLR pilots functioned as ATTHeS safety pilots.

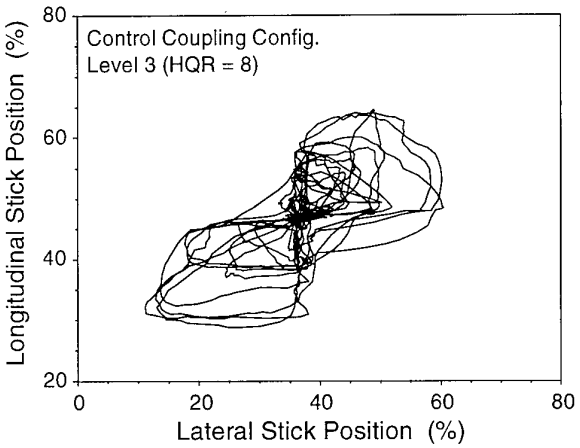

Fig. 20: Crossplot of a typical strongly coupled control coupling configuration.

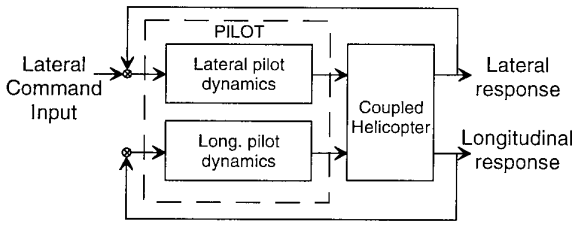

Fig. 21: Simplified block diagram of the pilot control strategy for the elimation of pitch-roll coupling.

7.4 Discussion of the results

Pilot control strategy. To gain a better understanding of how coupling affects the handling qualities, the pilot control strategy was studied in detail [25]. During the discussion of the bandwidth and phase delay study, it was already shown that the pilot tracking task is essentially a roll axis task, i.e. the task can be completed with only a minimum of longitudinal inputs. In the presence of cross-coupling, the pilot uses increasing amounts of longitudinal input to compensate for the off-axis response. The typical pilot used a 'figure-of-eight' type input (see Fig. 20) to compensate for the coupling encountered during rate and control coupling configurations. Such a "figure-of-eight" type input is indicative of a two-axis single loop feedback control strategy shown simplified in Fig. 21. While acting as a feedback system, the pilot primarily controls the roll axis and uses his spare capacity to remove the unwanted coupling. As coupling increases, more attention needs to be channelled towards the pitch axis. This is reflected by a poorer task performance, reduced lateral input power, and poorer handling qualities ratings.

Fig. 22 shows the lateral and longitudinal power spectra

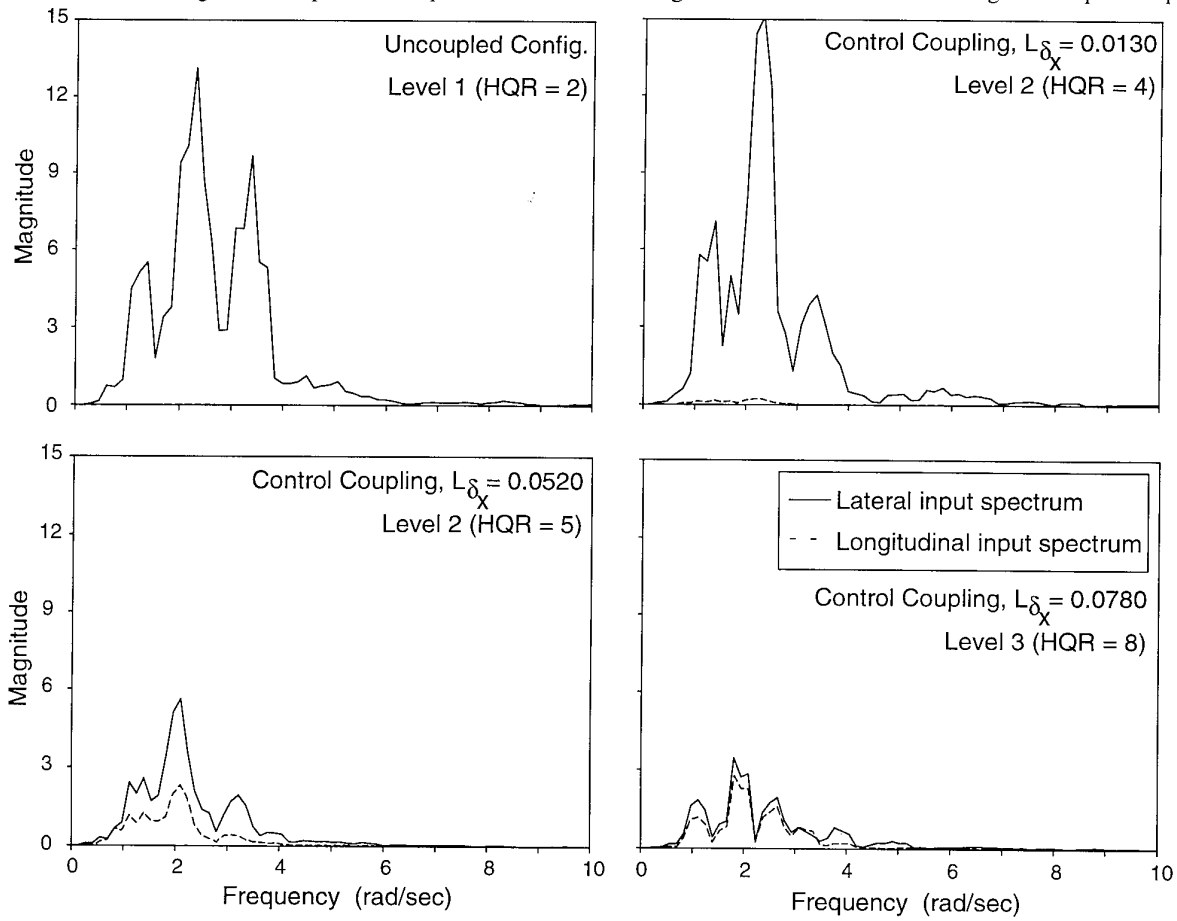

Fig. 22: Lateral and longitudinal power spectra for some selected control coupling configurations.

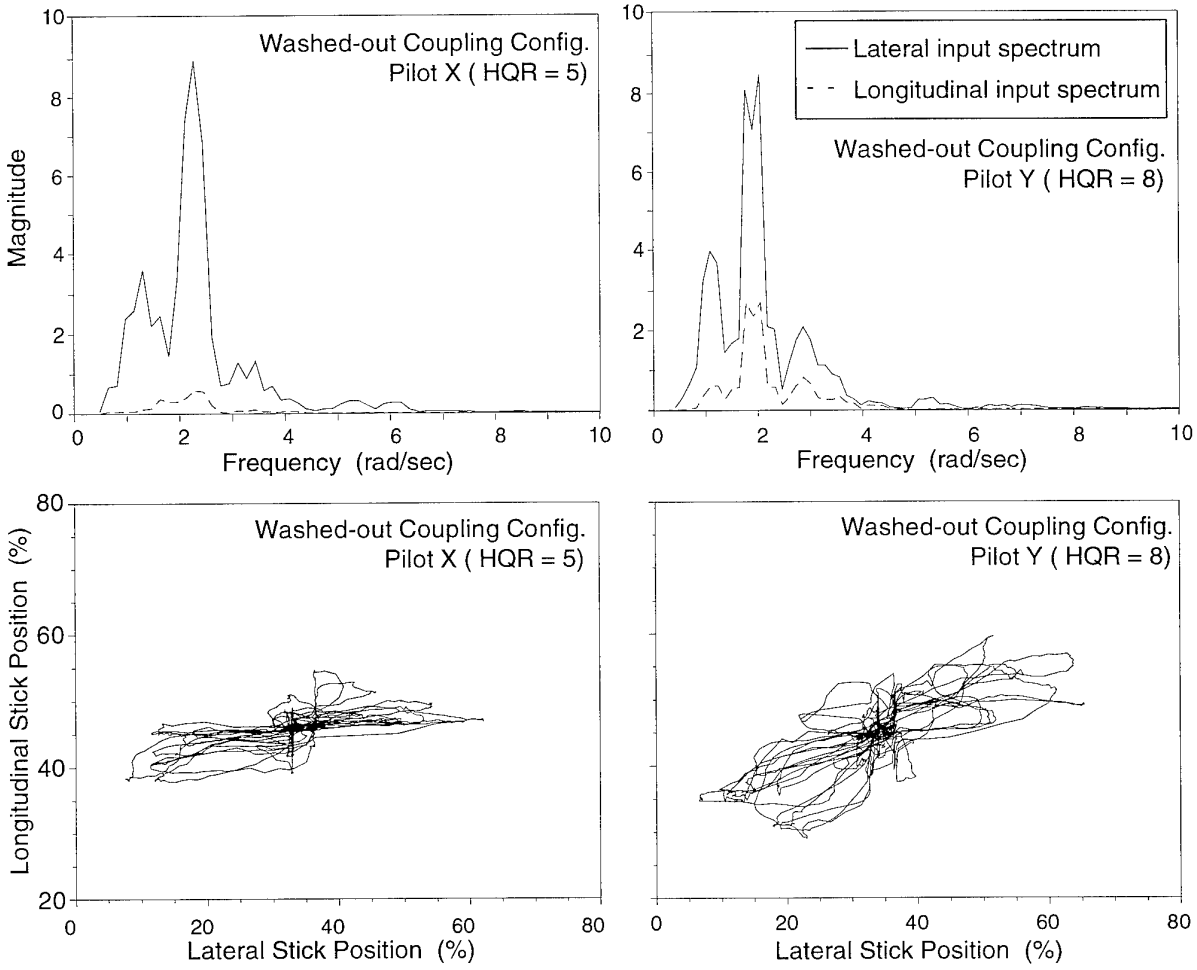

Fig. 23: Comparison of the control strategy of two pilots for a typical washed-out coupling case.

for some selected control coupling configurations. The power spectra clearly show a reduction of lateral input power for cases with an HQR of 5 and above. They also show a steady increase of longitudinal input power and frequency with increased coupling. For mild coupling cases, most longitudinal input activity is centered around the pitch bandwidth frequency of 2 rad/sec. For more severe coupling cases, longitudinal input activity shifts to about 3 to 4 rad/sec. For some of the most severe coupling cases, input activity above the pitch axis neutral stability frequency, ω_{180}, was observed. During these cases, some mild pilot induced pitch oscillations were observed.

The above assertions for the control coupling configurations were confirmed for the rate and combined control/rate coupling cases. For the washed-out configurations, similar trends were observed, but these were overshadowed by the differences between the evaluating pilots. Fig. 23 compares the control strategy of two pilots for a typical washed-out coupling case. On-axis aggressiveness of both pilots is comparable (this is evident from the lateral power spectrum and the cyclic input crossplots). There are, however, significant differences in the off-axis control strategy. Pilot X seems to just 'ride the coupling'. His inputs are aimed only at reducing the attitude changes resulting from the washed-out coupling (only the rate part of the coupling is washed-out). Pilot Y, who a slightly poorer task performance reacted to the washed-out rate component of the coupling. His longitudinal control inputs are stronger, more irregular, and contain more high frequency components. This results in an increase in workload and poorer handling qualities ratings as compared to pilot X. Nothing in the data or comments, however, warranted the elimination of the data of either pilot from the database.

Analysis in the time domain. The pitch-roll cross coupling criterion as defined in ADS-33C places a requirement on the mid to long term behavior of the aircraft attitude following a step input. For the slalom tracking task, the pilot uses compensatory longitudinal inputs up to a frequency of about 4.5 rad/sec. This seems to confirm that short term effects play a significant role in the perception of coupling.

Fig. 24 shows the individual pilot HQRs for the control,

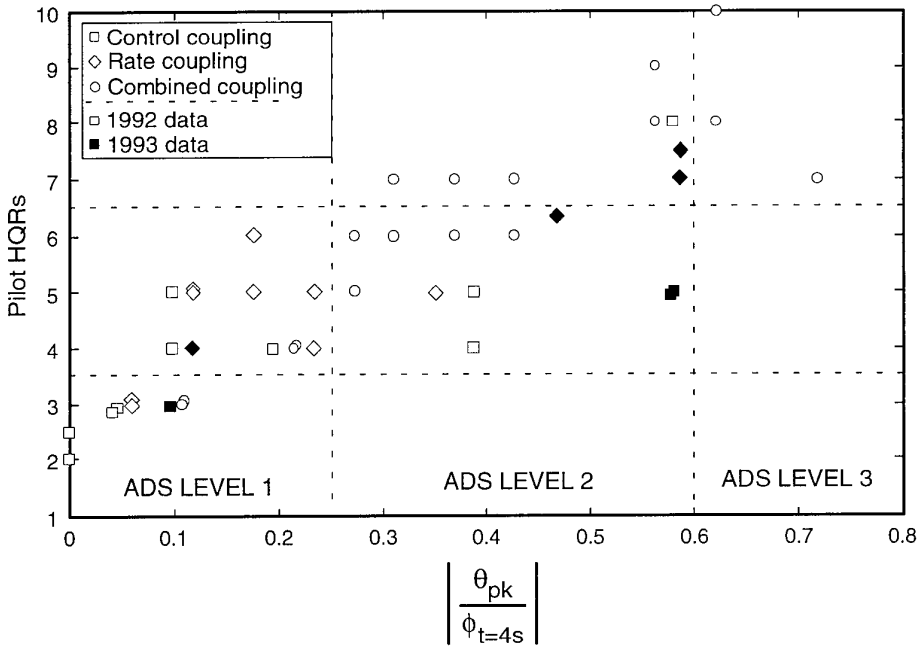

Fig. 24: Selected control and rate coupling data points in the 4 second time format.

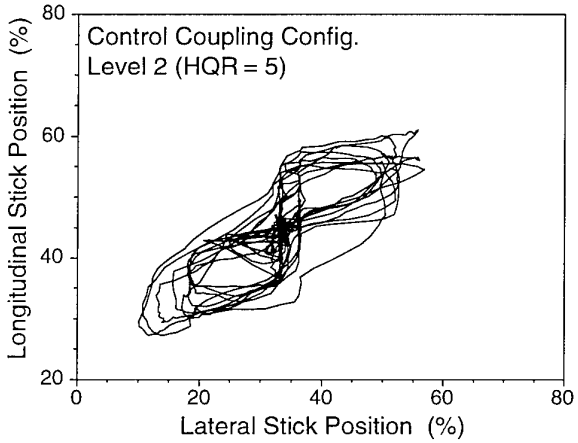

Fig. 25: Crossplot of a coupling configuration where the pilot used diagonalized inputs.

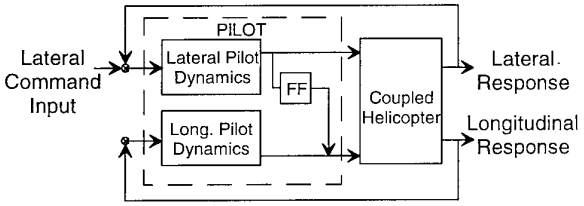

Fig. 26: Simplified block diagram of the feedforward pilot control strategy for the elimination of pitch-roll coupling.

rate and combined coupling configurations in the 4 second time domain format of ADS-33C. Although there is a relatively large spread in the data, the trend toward deteriorated handling qualities with increased coupling is obvious. In general, the coupling configurations from the 1992 flight tests received a more severe rating than those from the 1993 flight tests. Careful analysis revealed that some pilots used diagonalized inputs in 1993 (Fig. 25). Diagonalized inputs characterize a feedforward control strategy as shown in Fig. 26. The use of a feedforward control strategy seems to be the result of a rationalization of the coupling problem, rather than of normal adaptation. The pilots who used diagonalized inputs all had flown many slaloms with coupled configuration and when the direction (but not the magnitude) of the coupling was reversed, they were unable to adapt to this new configuration and reverted to the regular "figure-of-eight" pattern. It is therefore questionable whether this feedforward strategy would be usable during real operations, and therefore the use of the lower rating boundaries – rather than the higher limits that are the result of feedforward inputs – seems more appropriate for handling qualities requirements.

Fig. 27 shows the individual pilot HQRs for the washed-out configurations in the ADS-33C time domain format (notice the abscissa is different from Fig. 24). For reference, a selected number of control coupling configurations are included in the figure. The washed-out coupling, which has a predominantly short term character, is clearly misrepresented in the 4 second time domain format. Therefore, if ACT typical coupling types are to be included in the handling qualities specification, a different format will be needed.

Frequency domain analysis. It was shown how longitudinal control inputs roughly between the pitch

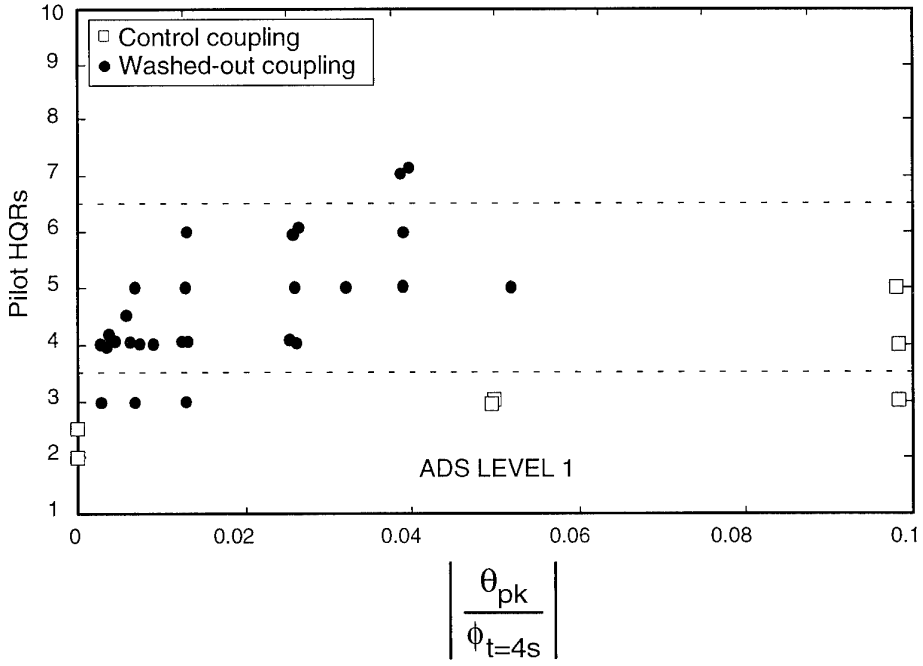

Fig. 27: Control and washed-out coupling configurations in the format of ADS-33C.

bandwidth frequency and the neutral stability frequency are used to eliminate coupling. Since the ability of the pilot to suppress coupling will depend largely on the system capabilities of the axis he uses to compensate for this coupling (i.e. the pitch axis in the case of a roll axis slalom task), it seems logical to choose coupling parameters that are a function of the frequency characteristics of the compensatory axis for the evaluation of handling qualities. In this paper, the relative coupling amplitudes determined at the bandwidth and neutral stability frequency of the compensatory axis are selected as a basis for discussion.

Fig. 28 shows the magnitude of *q/p* vs *p/q* at the respective bandwidth and neutral stability frequencies for the control, rate and washed-out coupling cases. Using a double sided analysis format allows the effects of the roll-due-to-pitch coupling on pitch-due-to-roll to be included in the diagram. Averaged handling qualities ratings are plotted with the data points. For the control and rate

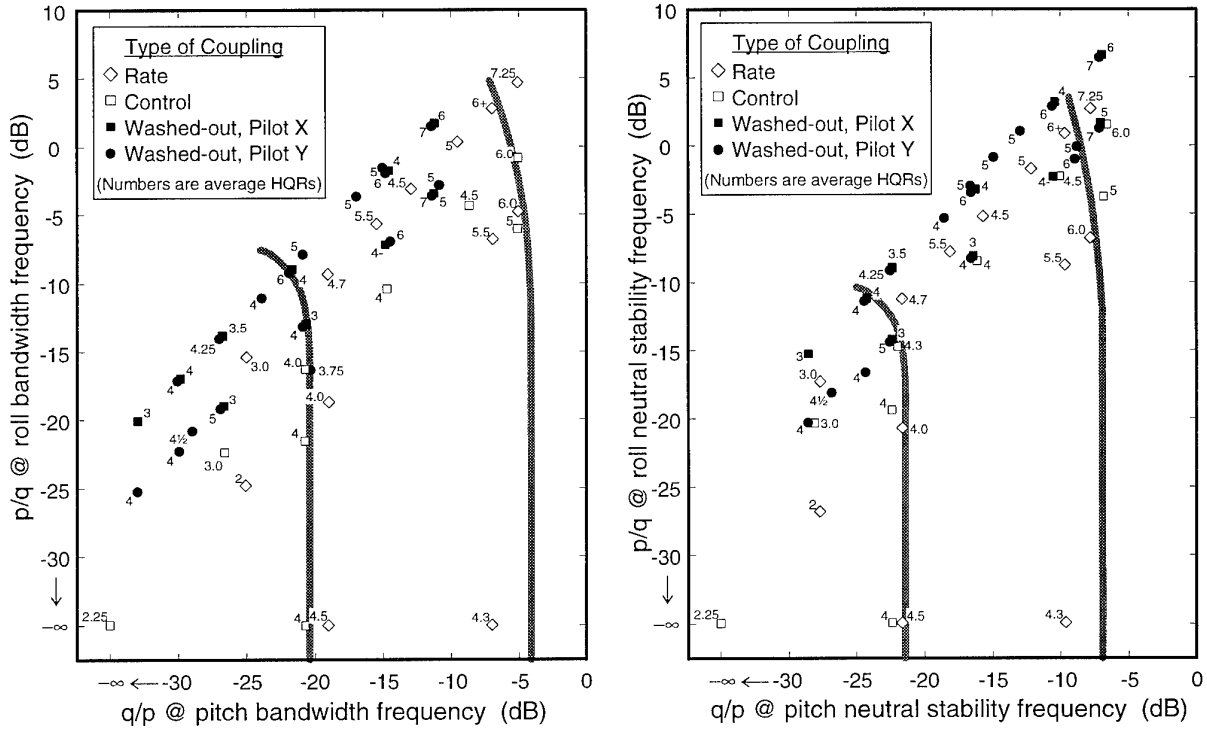

Fig. 28: Flight test data points of the coupling study in a frequency domain format.

coupling cases, correlation between the data points is good both for the bandwidth and the neutral stability frequency diagrams. The tentative level boundaries in the diagram were based on the rate and control coupling cases and correlate well with the time domain limits. For the washed-out coupling configuration, results are pilot dependent. As could be expected from the main input frequencies of the pilots, correlation of the data from pilot Y is excellent at the (higher) neutral stability frequency and correlation of the data from pilot X is excellent at the (lower) bandwidth frequency. For ACT, however, both frequencies seem relevant. The tentative level boundaries in Fig. 28 show decreasing limits for *q/p* as *p/q* increases to include the effects of roll-due-to-pitch coupling on pitch-due-to-roll coupling. It should be emphasized that only limits on *q/p* are suggested in the figure. The roll axis piloting task does not allow the imposition of limits on *p/q*.

8. CONCLUSIONS

In this paper, an overview was given of recent handling qualities research at DLR. The overall objectives of this research were to expand the database used to establish handling qualities requirements. Particular attention was given to those aspects that are crucial to actively controlled helicopters. To achieve this, complementary use was made of the two DLR research helicopters: the conventionally controlled BO 105 S-123 and the in-flight simulator ATTHeS. The results of the research led to several important conclusions:

1. The quantitative criteria of ADS-33 should provide an excellent tool for the prediction and evaluation of helicopter handling qualities, especially during the control system design and early flight testing phases. Robustness of most of the criteria was demonstrated by the excellent applicability and repeatability of the criteria.
2. Some of the ADS-33 criteria were shown to be problematic. Those criteria require further research in order to fill data gaps before new recommendations can be made.
3. A new slalom task with distinct tracking phases was developed. This task is a high gain piloting task that requires pilot inputs between 1 and 7 rad/sec. It is particularly suited for the evaluation of short term effects.
4. A bandwidth/phase delay study indicated that upper limits to the phase delay are required. These limits are about 100 msecs for Level 1 and about 170 msecs for Level 2 handling qualities in the roll axis.
5. A pitch-roll study has indicated that a long term time domain criterion format as used in ADS-33C is not capable of predicting handling qualities during high gain tasks. Especially the more complex coupling types such as those exhibited by actively controlled helicopters are poorly covered. A frequency domain format was presented that provides a more comprehensive criterion for pitch-roll coupling.

9. ACKNOWLEDGEMENTS

Thanks are due to many people at DLR who helped make the experiments possible and to the pilots and engineers from US Army, NASA, DRA and the German Forces (WTD-61) who actively participated in the tests. This research was conducted as part of the US/German MoU on Helicopter Aeromechanics.

10. REFERENCES

1. Horton, R.I., "Design for Future Combat Rotorcraft, A Pilot's Perspective," Presented at the *Royal Aeronautical Society* International Conference on Helicopter Handling Qualities and Control, London, UK, 15-17 November 1988.

2. Tischler, M.B., Fletcher, J.W, Morris, P.M, and Tucker, G.T., "Application of Flight Control System Methods to an Advanced Combat Rotorcraft," Presented at the *Royal Aeronautical Society* International Conference on Helicopter Handling Qualities and Control, London, UK, 15-17 Nov. 1988.

3. Huber, H. and Hamel, P., "Helicopter Flight Control – State of the Art and Future Directions," Presented at the 19th European Rotorcraft Forum, Paper A3, Cernobbio (Como), Italy, 14-16 Sept. 1993.

4. Anon, "Handling Qualities Requirements for Military Rotorcraft," Aeronautical Design Standard ADS-33C, Aug. 1989.

5. Whalley, M.S. and Carpenter, W.R., "A Piloted Simulation Investigation of Pitch and Roll Handling Qualities Requirements for Air-to-air Combat," American Helicopter Society 48th Annual Forum, Washington D.C., June 1992.

6. Ham, J.A., Metzger, M. and Hoh, R.H., "Handling Qualities Testing Using the Mission Oriented Requirements of ADS-33C," American Helicopter Society 48th Annual Forum, Washington D.C., June 1992.

7. Cappetta, A.N. and Johns, J.B., "An Evaluation of the Proposed Specification for Handling Qualities of Military Rotorcraft, MIL-H-8501B, Utilizing Predicted and Actual SH-60B Handling Qualities, "American Helicopter Society 46th Annual Forum, Washington D.C., May 1990.

8. Morgan, J.M. and Baillie, S.W., "ADS-33C Related Handling Qualities Research Performed Using the NRC Bell 205 Airborne Simulator," Presented at *Piloting Vertical Flight Aircraft: A Conference on Flying Qualities and Human Factors*, San Francisco, CA, Jan. 1993.

9. Key, D.L., Blanken, C.L., and Hoh, R.H., "Some

9. Key, D.L., Blanken, C.L., and Hoh, R.H., "Some Lessons Learned in Three Years with ADS-33C," Presented at *Piloting Vertical Flight Aircraft: A Conference on Flying Qualities and Human Factors*, San Francisco, CA, Jan. 1993.

10. Grünhagen, W. von, Bouwer, G., Pausder, H.-J., Henschel, H.-J., and Kaletka, J., "Helicopter In-Flight Simulator ATTHeS – A Multipurpose Testbed and Its Utilization," *International Journal of Control*, Vol. 59, No 1, pp 239-261, Jan. 1994.

11. Bouwer, G., "Model Following Control for Tailoring Handling Qualities - ACT Experience with ATTHeS," Presented before the AGARD Flight Mechanics Panel symposium on Active Control Technology: Applications and Lessons Learned, Turin, Italy, May 1994.

12. Ockier, C.J., "Flight Evaluation of the New Handling Qualities Criteria Using the BO 105," Presented at the American Helicopter Society 49th Annual Forum, St. Louis, MO, May 1993.

13. Heffley,R.K. *et al*, "Study of Helicopter Roll Control Effectiveness Criteria," NASA CR 177404 (USAAVSCOM TR-85-A-5), April 1986.

14. Chalk, C.R., Key, D.L., Kroll, J. Jr., Wasserman, R. and Radfors, R.C., "Background Information and User Guide for MIL-F-83300 Military Specification – Flying Qualities of Piloted V/STOL Aircraft," AFFDL-TR-70-88, Nov. 1971.

15. Cooper, G.E. and Harper, R.P., "The Use of Pilot Rating in the Evaluation of Aircraft Handling Qualities," NASA TN D-5153, April 1969.

16. Hoh, R.H., "Dynamic Requirements in the New Handling Qualities Specification for U.S. Military Rotorcraft," Presented at the *Royal Aeronautical Society* International Conference on Helicopter Handling Qualities and Control, London, UK, 15-17 Nov. 1988.

17. McRuer, D.T. and Krendel, E.S., "Mathematical Models of Human Pilot Behavior," AGARD-AG-188, Jan. 1974.

18. Pausder, H.-J. and Bouwer, G., "Realisation Aspects of Digital Control Systems for Helicopters," Presented at the *Royal Aeronautical Society* International Conference on Helicopter Handling Qualities and Control, London, UK, 15-17 Nov. 1988.

19. Hoh, R.H., *et al*, "Proposed MIL Standard and Handbook – Flying Qualities of Air Vehicles; Volume II: Proposed MIL Handbook," AFWAL-TR-82-3081, Nov. 1982.

20. Pausder, H.-J. and Blanken, C.L., "Investigation of the Effects of Bandwidth and Time Delay on Helicopter Roll-Axis Handling Qualities," Presented at the European Rotorcraft Forum, Avignon, France, Sept. 1992.

21. Sridhar, J.K., and Wulff, G., "Multiple Input/Multiple Output (MIMO) Analysis Procedures with Applications to Flight Data," *Zeitschrift für Flugwissenschaften und Weltraumforschung*, Vol. 16, pp. 208-216, 1992.

22. Tischler, M.B. and Cauffmann, M.G., "Frequency-Response Method for Rotorcraft System Identification: Flight Applications to BO 015 Coupled Rotor/Fuselage Dynamics," *Journal of the American Helicopter Society*, Vol. 37, Nr. 3, July 1992.

23. Pausder, H.-J. and Blanken, C.L., "Generation of Helicopter Roll Axis Bandwidth Data through Ground-Based and In-Flight Simulation," AGARD CP-519, Oct. 1992.

24. Blanken, C.L., Pausder, H.-J., Ockier, C.J., and Simmons, R.C., "Rotorcraft Pitch-Roll Decoupling Requirements from a Roll Tracking Maneuver," Presented at the American Helicopter Society 50th Annual Forum, Washington D.C., May 1994.

25. Ockier, C.J., Pausder, H.-J. and Blanken, C.L., "An Investigation of the Effects of Pitch-Roll (De)-coupling on Helicopter Handling Qualities," DLR Institute of Flight Mechanics, IB 111-94/08, May 1994.

LAVI FLIGHT CONTROL SYSTEM
DESIGN REQUIREMENTS, DEVELOPMENT AND FLIGHT TEST RESULTS

Menahem Shmul
Director Flight Operations
and
Chief Test Pilot

Eli Erenthal
Deputy Manager
Flight Sciences

Moshe Attar
Senior
Control Laws Engineer

ISRAEL AIRCRAFT INDUSTRIES
BEN GURION INT. A.P. 70100, ISRAEL

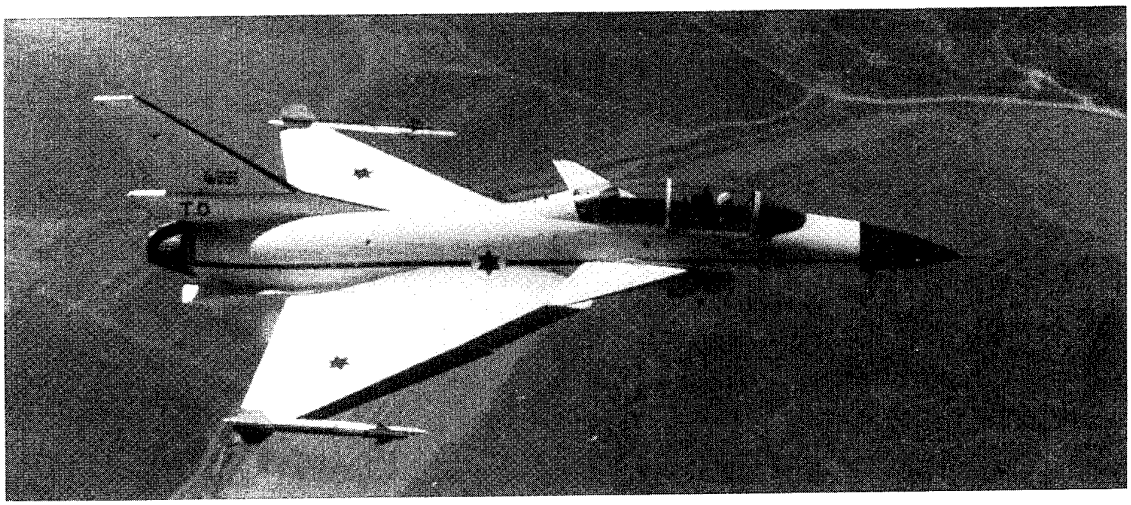

FIG. 1 LAVI TECHNOLOGY DEMONSTRATOR

SUMMARY
The flight control system of the Lavi Multimission fighter is described. The control laws design philosophy is given along with the control laws development, the flying qualities requirements and the final structure of the pitch axis (DFCS). The simulation phase is covered along with special control laws features. The question *"how does the Lavi fly?"* is adressed. Problems uncovered during flights, and solutions found, are detailed and the flying qualities data are given. Finally the program status is explained.

1. INTRODUCTION
1.1 *OPERATIONAL REQUIREMENTS & TACTICAL ROLES*
According to the operational requirements, the Lavi is a light multimission fighter capable of day and night, short and medium range operations (see Fig. 1). The primary mission of the aircraft is Battlefield Air Interdiction and Close Air Support (BAI/CAS). That operational envelope includes a high order of Air-to-Air (A/A) defense capability.

In order to fulfill these requirements, initial design and development has started from the weapon carriage capabilities alternatives. Fifteen (15) hard points were designed and built under the fuselage and wings. This part of the design, determined the aircraft geometry and size. Meeting the requirement for very high interdiction speed in Military Power resulted in low drag semi-conformal ordnance carriage. This requirement, combined with the different types of bombs, namely, two thousand and four hundred pounds (2400 LB) MK 84 with smart guiding heads or one thousand pounds (1000 LB) cluster bombs, caused a large stability margin range. Such a wide range of stability margin associated with the various configurations, introduced significantly different aircraft behavior and response, both in the longitudinal and lateral axes. Therefore, the Flight Control System (FCS) had to be task tailored, enabling the pilot to fly the aircraft with no adaptations, regardless of its configuration.
Three (3) Flight Control Laws (FCLs) configurations were developed: The "Hobo" configuration which relates to A/C

Paper presented at the Flight Mechanics Panel Symposium held in Turin, Italy, from 9-13 May 1994.

configuration with high *Ixx* and aft Center of Gravity (CG) (see Fig. 2); the "Cluster Bomb" configuration which relates to A/C configuration with high *Iyy* and very forward CG (see Fig. 3) and the A/A configuration (see Fig. 4).

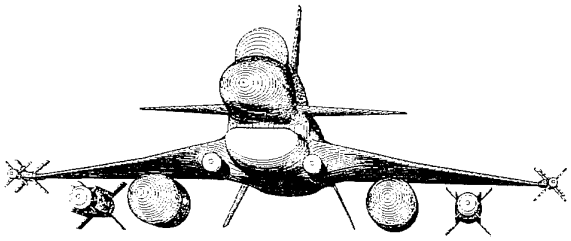

FIG. 2 LAVI "HOBO" CONFIGURATION

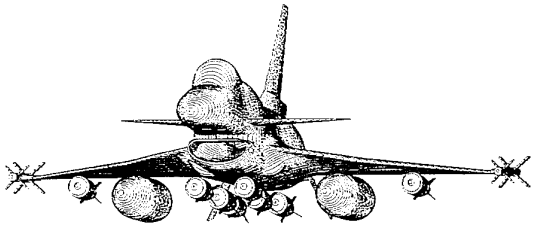

FIG. 3 LAVI "CLUSTER BOMB" CONFIGURATION

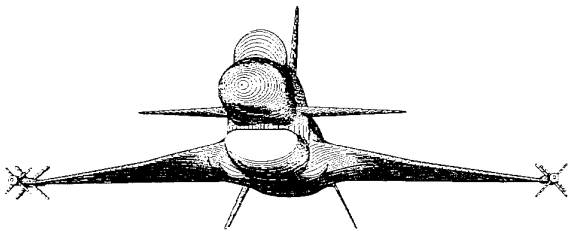

FIG. 4 LAVI "AIR TO AIR" CONFIGURATION

The FCS could cope successfully with these three wide-spread configurations using the nine (9) individually driven and controlled flight control surfaces, which are shown in Fig. 5.
The Control Law (CL) gains were reconfigured via smoothing functions, in order to keep the closed loop bandwidth near 2Hz. Other safety functions such as Angle of Attack and Roll Rate limiters were also rescheduled.
The initiation of the Lavi program was announced by the Israeli Government in February ninteen and eighty (1980) and IAI was selected as the Prime Contractor in July ninteen and eighty two (1982).

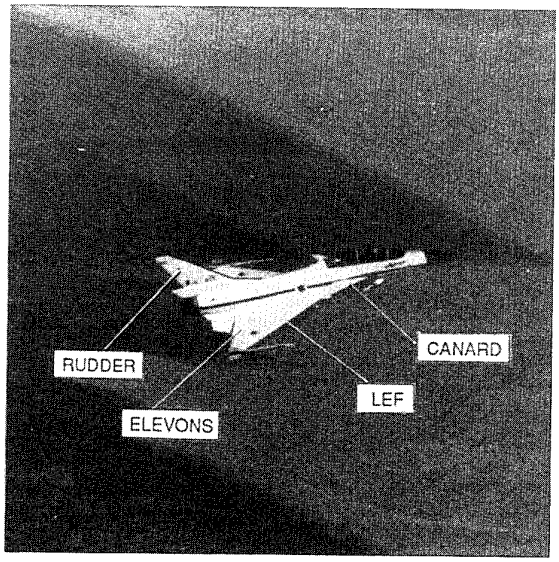

FIG. 5 LAVI FLIGHT CONTROL SURFACES

The objectives were to design, develop and manufacture a new modern multi mission fighter for the Israeli Air Force. This aircraft was intended to replace the aging A-4 Skyhawk, F-4 Phantom and Kfirs.
The Lavi's first flight took off on 31 December 1986.
The program was terminated by the Israeli Government on 30 August 1987.
Later in 1987 IAI decided, in an attempt to preserve technologies and know-how, to build one of the planned prototypes as a Technology Demonstrator (T/D), using its own (IAI) funds.

1.2 *AIRCRAFT TECHNICAL DATA*

TYPE : Light multi-mission fighter
MISSIONS : Air-to-air, air-to-ground, advanced operational training
CREW : 1 (2 in training version)
DIMENSIONS : Wing Span: 8.78m 28.97ft
Length : 14.57m 48.08ft
Height : 4.78m 15.78ft
Wing area: 33.05m^2 360ft^2
Wing sweepback (leading edge): 45°
(see Fig. 6)
BASIC TAKE-OFF WEIGHT: 9900kg 22000Lb
ALL UP WEIGHT: 18400kg 40500Lb
(Air-to-ground configuration)
ENGINE: Pratt & Whitney 1120
Thrust 9400kg 20700Lb
ARMAMENT:
Internal Gun 30MM
Air-to-air infra-red/radar missiles
"SMART" weapon capability

Integral passive & active
Electronic Counter Measure Systems.

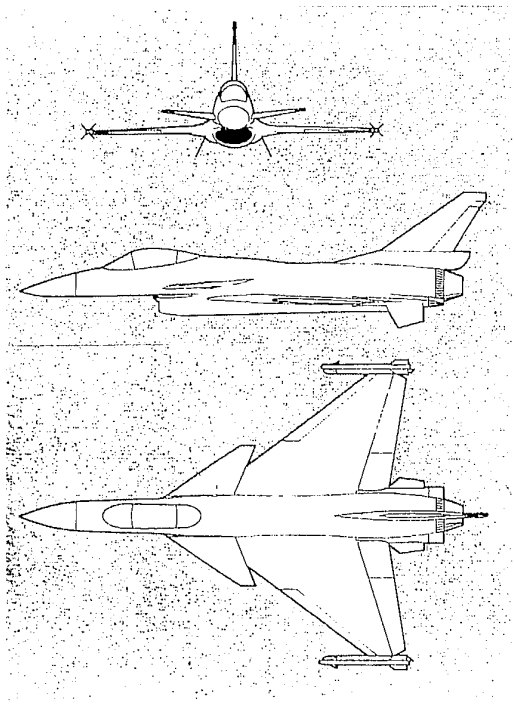

FIG. 6 LAVI THREE VIEWS

PERFORMANCE:

Combat thrust/weight :	1.07
Combat load factor :	9g
Maximum speed	: 800KCAS Mach 1.8

TURN PERFORMANCE (15KFT/ISA):

Sustained	12.5 DEG/SEC
Instantaneous	23.0 DEG/SEC

PENETRATION SPEED (SEA LEVEL/ISA):
(6 x CBU, 2x600 USG ext. fuel tanks, 2xAIM 9)
Military power 550 KCAS

COMBAT RADIUS:

Air-to-air (Combat Air Patrol)	1850km	1000_{NM}
Air-to-ground		
HIGH-LO-HIGH	2130km	1150_{NM}
LO-LO-LO	1110km	600_{NM}

1.3 FULL-SCALE DEVELOPMENT PROGRAM

The full scale development program of the Lavi called for five (5) flying prototypes. The first two aircraft were basically identical. The Lavi "configuration freeze" was accomplished in October, 1982.
As a result of the full-scale development effort that followed, specific aerodynamic and systems lessons were learned. Among these, prototype assembly and systems testing in particular, were implemented in the fabrication of the second prototype aircraft. The third planned prototype, which was under fabrication when the program was terminated was supposed to be the first production configured airframe, incorporated all known modifications through October 1984. It was not, however, planned to incorporate final avionics.
Both first two (2) prototypes, designated B-1 and B-2, where the "B" stands for a two-seater airframe configuration, flew eighty one (81) flights, accumulating seventy-eight (78) hours. The number four (4) prototype was planned to be the first real two-seater aircraft (where the aft cockpit was not occupied with instrumentation and telemetry equipment) and to incorporate the full suite of the Lavi avionics. The number five (5) aircraft planned to be the first single-seat configuration also incorporating a production airframe and avionics configuration. As stated above after the project was terminated, IAI decided to build the Technology Demonstrator. Discussions resulted in the decision to build the number four (4) prototype, to configure it with a full two-seater capability as well as installing the Lavi avionics, as originally planned.
When this aircraft first flew on 25 September 1989, it already had the modified wings with the enlarged elevon surfaces.
This aerodynamic configuration change was evidently discoverd and required during the simulation phase, as will be discussed later. This change caused a significant FCL updating and, therefore, when it first flew, it had to prove that the new CL and aerodynamic configurations were airworthy.
Some twenty five (25) flights were devoted to envelope opening. As off 31 December 1993 the T/D has flown one hundred and twenty five (125) flights, amounting to one hundred and forty three (143) hours. All of the flights (after finishing envelope opening) were devoted to the avionics development and to demonstration flights.
From the FCS and CL standpoint both configurations, B-1/B-2 and the T/D proved to be very successful. Qualitative and quantitative results are shown later. On a comparative basis the T/D with the enlarged elevons and the updated CL shows better pilot control in each of the critical phases (like crosswind landing) than the B-1/B-2 demonstrated.

2. FLIGHT CONTROL SYSTEM (FCS)

2.1 *DESCRIPTION*

The FCS is a quadro redundant digital system (DFCS) with a dual redundant

emergency analog system (E-FCS). In the prototypes, Direct Link (DL) capability both in the DFCS and EFCS is installed. The Lavi is truly a Controlled Configured Vehicle (CCV). In the A/A configuration, the aircraft is flown with a five (5) percent negative static margin. In the Air-to-Ground (A/G) configuration, the aircraft is up to fifteen (15) percent unstable.

The pilot controls the Lavi with a traditional center stick. Control is achieved via a limited motion position command which uses Linear Variable Differential Transformers (LVDT) (see Fig. 7).

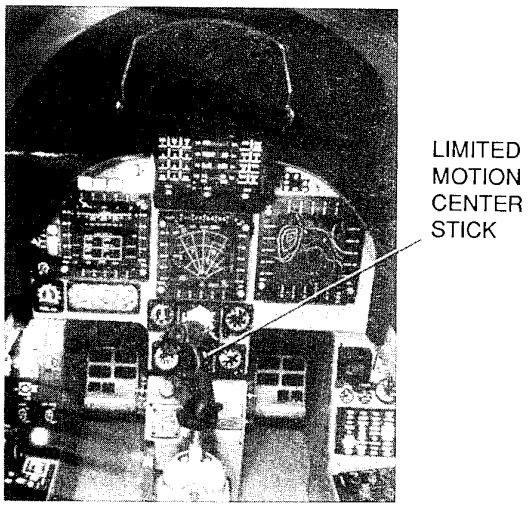

FIG. 7 LAVI LIMITED MOTION CENTER STICK

Rudder pedals are of a ± 1/2 inch limited motion type and also utilize LVDTs. Pitch trim is carried out by a mechanical motor with ailerons and the rudder being electrically trimmed. The question of how much motion should be given to the stick and therefore the corresponding forces, was a major discussion item during the development. Each pilot had his own opinion. Three point three (3.3) inches for aft travel and two (2) inches for forward and lateral stick travel were chosen. A single spring in each plane gives the desired level of artificial feeling.

The main components of this system include the following:

(a) Two (2) Flight Control Computers (FLCCs), each having two (2) DFCS channels and one (1) (plus one (1) monitor) EFCS channel.

(b) Three (3) Angle of Atack (AOA) sensors. Two (2) of them on the left side of the aircraft.

(c) Four (4) Rate Gyro's for each of the three (3) axes - pitch, roll and yaw (total 12 RGs).

(d) Four (4) Accelerometers for longitudinal and for lateral axes (total 8 ACCs).

(e) Three (3) Anemometric (static & impact pressure) sensors.

(f) Seven (7) quadro redundant Fly-By-Wire (FBW) Servo Actuators (SA) for primary control: Four (4) Elevons (Elevator + Aileron),two (2) Canards and one (1)Rudder.

(g) Two (2) Leading Edge Flaps drive systems for secondary control.

(h) Mechanical Stick/Artificial feel system with quadro redundant LVDTs (travel measurement), both in Pitch and Roll.

(i) Mechanical Pedal system with quadro redundant LVDTs.

Fig. 8 shows the FCS main elements.

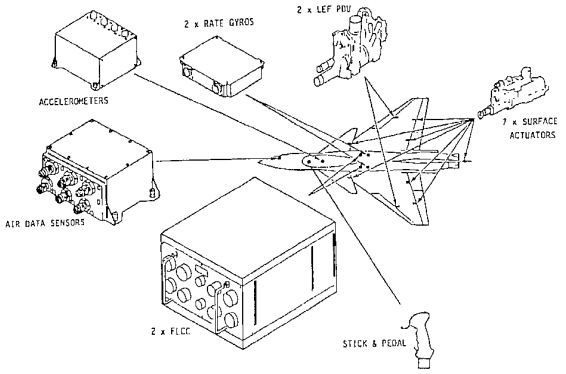

FIG. 8 LAVI FCS MAIN ELEMENTS

The digital system is based on a Zilog Z8000 cpu. Thw programing languages were 'C' and Assembler.

A Cross-Channel Data Link (CCDL) enabled voting and monitoring (mainly in S/W) of the system's inputs. Special treatments were given to the AOA and Anemometric systems, as these were triple mechanically redundant. The system was incorporated with Output Command Monitoring logics, Channel Fail logics, Pre-flight and In-flight Built-In-Tests (BIT) and with Channel Synchronization Algorithms.

The EFCS was basically simple, with only rate feedbacks *(P, Q, R)*, and few gain scheduling.

The system enabled flying with one (1) EFCS channel (EFCS-1 or EFCS-2), as available. In this paper we shall limit our discussion to the main DFCS Control Laws.

2.2 *CONTROL LAWS DESIGN PHILOSOPHY*

The control laws were designed by classical design methods. These methods provided better insight into the system dynamics and were found to be better than other design methods to handle the different, and sometimes contradicting, design requirements. Optimal design methods were used during the preliminary design phase. Elements like Back-Up gains for anemonetric system failure and Elevons Separation gains were designed by these methods.

MIL-F-8785C and other published papers on Flying Qualities served as guidelines and criteria for CL design. The "Equivalent-System" method was used to represent the actual High Order System (HOS) dynamics.

The main tool for Flight Control Laws (FCL) evaluation was the Flying Qualities Simulator. Major changes had been made in the CL during these simulator sessions. Many gains were reduced and some changes were made in the CL architecture.

The Flying Qualities Simulator sessions have proved that CL should be designed to achieve good pilot-plus-vehicle dynamics. Minor changes to CL (in roll sensitivity) were made during the NT-33 in-flight simulations for the approach and landing tests.

Our main conclusions regarding the CL design are that:

(a) The classical method is intuitive and time consuming but it is preferable for manned air vehicles' control system design.

(b) Flying Qualities Simulator serves a vital role in CL design. Simulation should be started from the preliminary design phase.

(c) Interaction between structures and FCS (mainly aeroservoelasticity) should be handled very carefully, when designing high gain, Fly By Wire, Systems.

2.3 *FLIGHT CONTROL LAWS DEVELOPMENT*

The first FCL set was very simple and had a basic structure. This was done intentionally in order to be able to concentrate on *understanding* the flying qualities requirements using "Pilot In The Loop" simulations. One of the major problems in developing FCL is that it involves many engineering skills, far beyond the classical control theory. In order to achieve good results, the FCL engineer should have knowledge in the following areas:

(a) Control Theory (classical & modern).

(b) Control System Architecture (sensors, stick & pedal, LCCs..,).

(c) Aerodynamics.

(d) Aircraft Dynamics (including at high angles of attack).

(e) Aero (and Aero-Servo) Elasticity.

(f) Aircraft Loads.

(g) Weight & Balance.

(h) Simulation and Modeling Methods (SDF, landing gear, wind, gusts).

In addition the FCL engineer should understand how the aircraft flies, from the pilot's point of view. In practice, such an engineer that *really* knows all of these areas does not exist. That is why, even today, where more modern control design methods are in hand, it is advisable to avoid complexity and concentrate on the main issues of concern.

3. FLYING QUALITIES & OTHER REQUIREMENTS

Every FCL design starts with an in-depth review of the requirements. MIL-F-8785 served as a guide together with several other requirements from IAF and the open literature. It was hard to establish a very precise set of requirements, which to our opinion, do not exist, even today. An example, often discussed in many publications, is the famous requirement for the Short Period frequency (versus n/α). It had already been determined that these requirements should be met with an equivalent system.

However, several questions arose:

(a) As is known, different transfer functions(q/Fs,α/Fs)yield different values of equivalent Wnsp. Which one should be dominant? (some say both, others α/Fs and some q/Fs).

(b) Should the HOS include all dynamic elements including structural modes? If the answer is yes, matching such a system to a Second Order is quite impractical.

(c) The most important question was: Why should we try to build a modern fighter according to old conventional aircraft behavior? As is known, this requirement reflects the natural behavior of a conventional aircraft.

The answers to these questions, which were given during the Lavi program development process are as follows:

(a) The q/Fs transfer function was considered as the dominant one.

(b) All dynamic elements were included (like sensors dynamics, H/W filters etc.). The structural modes were excluded. Matching of HOS to Low Order System (LOS) was done up to 10-12 rad/sec, only.

(c) A compromise was taken: The Wnsp should increase with n/α, but with a moderate slope. An example of a matching of HOS to LOS

of pitch rate to stick input, is shown on Fig. 9.

In any case, meeting the MIL-F-8785 requirements was quite easy, not only for Wnsp, but for other requirements as well. The Israeli Air Force added some new requirements, but still we were looking for more modern or "tougher" requirements.

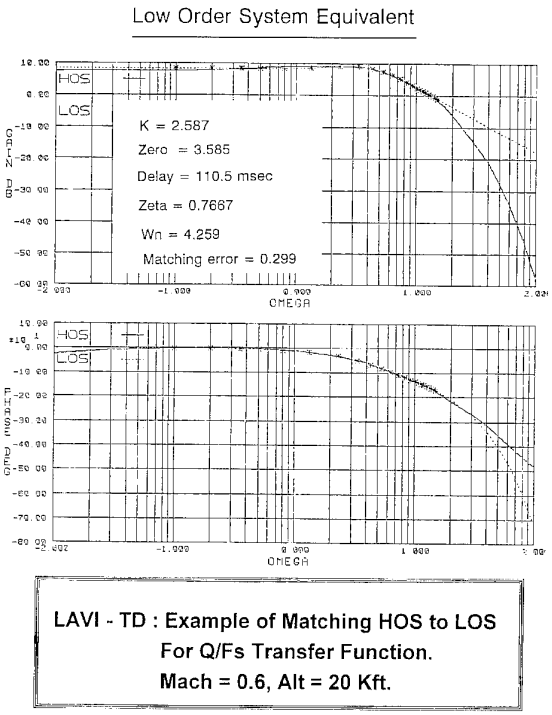

FIG. 9 LAVI T/D HOS TO LOS MATCHING

Examples of other requirements that were considered are the "Neal-Smith", the "Bandwidth" and the "YF-17" Frequency Response Criteria. The only one supported with a lot of data and reasoning was the "Neal-Smith" criterion. It was used extensively for evaluating the Category - C CL.

The "YF-17" Criterion was one which the IAF insisted on. Meeting this requirement was one of the reasons why the pilots rejected the Category-A CL, flying the simulator.

The requirement was obviously misleading, (see Fig. 10).

Up until now, there has been no real "Cook-Book" for flying qualities. The FCL engineer must therefore participate in extensive "Pilot In The Loop" simulations in order to complete the CL design before the first flight.

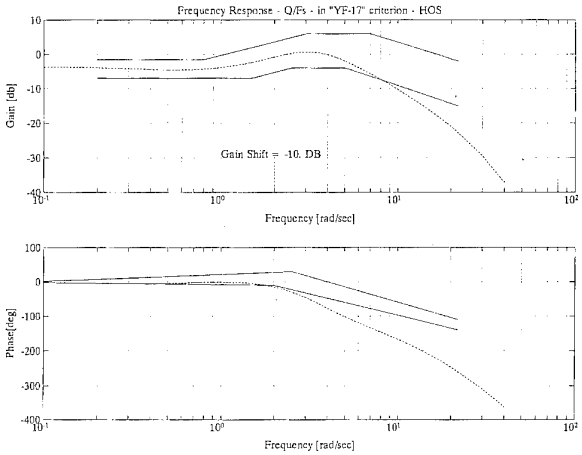

FIG. 10 "YF-17" CRITERION

During the early days of the Lavi CL development, it was decided to put relatively large stability margin requirements: at least 60 degrees Phase Margin (PM) and 10 DB Gain Margin (GM). The reason was the large amount of uncertainty in all areas, but especially in the structural modes. The wings and some parts of the fuselage & tail were made from composite materials, causing doubts about their structural modes. Later in the program, when additional models were inserted, the margins became smaller.

The first flight was conducted with expected PM of 45 and 8 DB GM in some flight conditions. At Mach 0.95 the PM measured in flight was smaller. However GM were kept as predicted for all flight conditions and configurations.

4. FINAL STRUCTURE OF THE DFCS

Fig. 11 presents the pitch loop CL structure. As can be seen, it is quite simple. In fact, the CL of the Lavi had more than 100 scheduled gains and functions. The Complexity was in those functions that were built step-by-step through extensive simulations and analyses.

The pitch control laws consisted of a basic blend of pitch rate & normal acceleration *(Nz)* in the low-speed regime, and pure *Nz* for high-speed. The Angle-of-Attack Limiter (AOA-Lim) control law feedback was compared with the low frequency control law feedbacks. When AOA-Lim became larger, it overrode the *q-Nz* blend and became dominant.

The inner loop blend of AOA and Low-Pass Pitch Rate to the elevons, provided stability augmentation in low airspeed, and destabilizing effect at high airspeed, to augment the aircraft response where it was too sluggish due to over-stability.
Special care was given to the Elevons Separation Logic (ESL). This logic was designed to maximize Control Power with minimum Control surfaces deflection. As a result, the outboard elevons were mainly deflected for roll and the inboard elevons mainly for pitch . Inboard elevons served as lift augmentation devices during take-off, approach and landing, as they were biased towards trailing edge down. This arrangement, enabled slower (15 KCAS) lift-off speeds for configurations that were heavy and had a very forward CG.

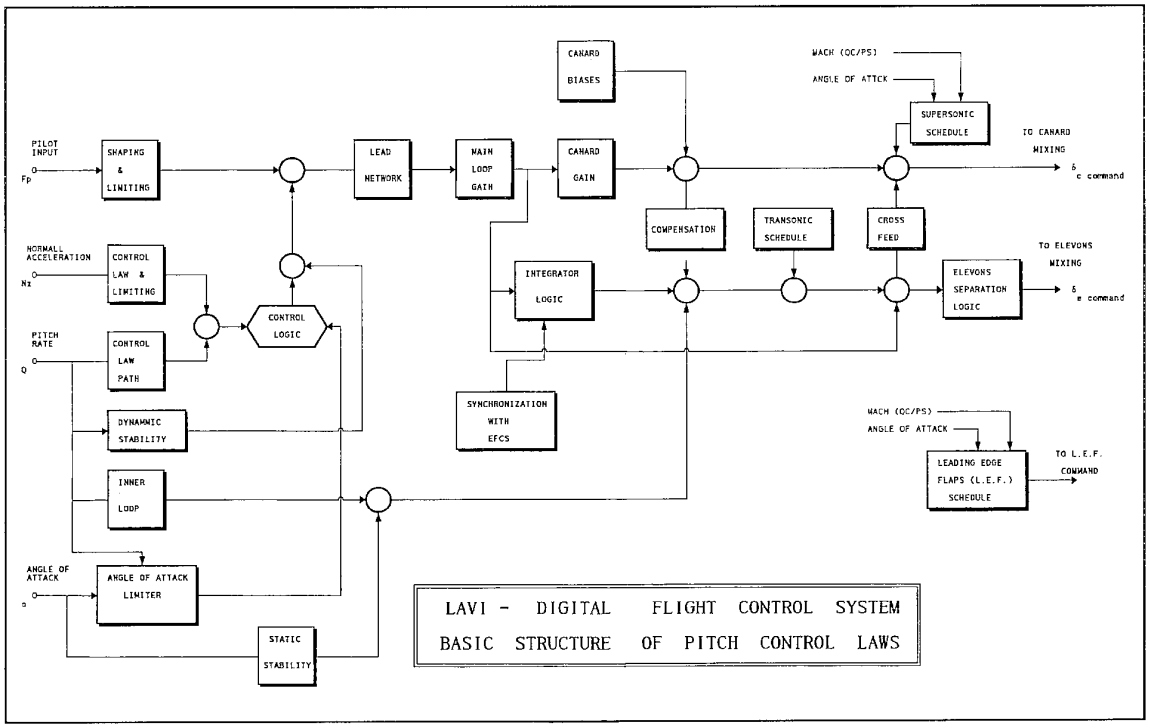

FIG. 11 LAVI DFCS-PITCH CONTROL LAWS

In addition to the elevons, the canards were biased during Category C and thus reduced even further the approach airspeed and enhanced pilot's visibility.
All transitions from one set of CL to another (e.g. upon landing gear extraction or upon weight on wheels) where properly smoothed via fading logics.
The design of the lateral directional CL mostly consentrated on two major issues: reducing sideslip during roll and on the other hand, avoiding large yaw rates in response to lateral control commands. These two requirements were contradictory in most of the flight envelope regimes, as the Lavi is of a *"proverse"* yaw nature. The need to suppress the sideslip as much as possible (highly augmented Dutch Roll), even if it produced large yaw rates, was proved to be wrong mainly for small or moderate roll commands. As a result, the control laws were built to yield different responses for different amplitudes of commands.

5. SIMULATION

The FCS development phase started in 1981. In mid 1983, this analytical work resulted in a set of classic FCLs. These FCLs were first introduced to the evaluation pilots group in a moving-base flying quality simulator. This simulator is located in the Netherlands National Aerospace Laboratory- NLR. The objectives of this simulation were to find whether the theoretical FCLs design could be accepted and flown by the pilots. The first evaluation determined that an increased level of effort would be required to rework the initial FCLs.
At that time we also built, at home, a fixed-base flying quality simulator. A definite difference was found between the fixed and the moving-base simulators. It is strongly believed that, in order to develop FCLs for a highly augmented

fighter, a moving-base simulator is a necessity. It was found that motion gives the pilot much more information than that which can be gained from a fixed simulator; the final results are far better.
A great deal of basic design can be carried out on a fixed-base simulator, but good flying qualities can best be achieved by using the motion simulator. Increased assets derived from moving-base simulation encompass all high gain tasks, especially air-to-air tracking, air-to-ground bombing, close formation flying and landing. In addition to these two ground-based simulators, the Calspan's NT-33 in-flight simulator was also used.
Owing to the somewhat limited capabilities of the NT-33 to simulate Lavi's dynamics in the entire flight envelope, the objective of this simulation was to confirm the Closed-Loop high-gain landing approach phase. This in-flight simulation confirmed the initial ground-based simulation. Most of all,it gave the assurance that the FCLs were good.
Pilot involvement in development of the flight control system began 3-1/2 years before the first flight. A total of 835 simulation hours were flown. A major lesson learned during that effort was that a complete aerodynamic, aeroelasticity and aeroservoelasticity data package should be available to the cognizant FCL engineers as soon as possible. Because this data package was not available on time, the set of FCLs had to be updated several times during the simulation phases. Further, final design and Weight and Balance changes forced us to enlarge the elevons area in order to maintain a sufficient pitch-down moment at a given Angle-Of-Attack (AOA) and aircraft configuration. This change resulted in a new wing version with enlarged elevons and caused a significant FCL redesign.

The build-up of applicable simulation methodology was a task in itself. A primary result of our simulation effort was a growing recognition that, to gain full benefit from the program, each flight had to be executed as a real test flight. Therefore, a team consisting of two flight control system engineers, a flight test engineer, a pilot and a senior FCS engineer participated in each flight. These flights began with a preflight briefing covering specific test objectives and fully detailed testing methods. Flights lasted about an hour and a half and were run on an item-by-item basis duplicating airborne testing. Flights were video recorded because this contributed significantly to the success of the FCL development. It helped the test pilots to explain and show the FCS engineers what they were talking about. A typical post flight debriefing lasted 3 hours. By having the FCS engineers actually sharing the pilot's sensations through the video, the pilots were able to explain fully what they wanted.
It is worth mentioning that the time and effort put in the different ground-based and in-flight simulation, including the engineering Six Degrees of Freedom (SDF) computer program, produced very good FCL and later on, excellent aircraft flying qualities. It is the authors' opinion that future aircraft and FCL development should use extensive ground and in-flight simulation, minimizing flight test unneccessary risks.

Four (4) IAF and six (6) IAI pilots participated in the 3-1/2 years simulation phase. As all of the involved pilots have combat experience,they brought to the program a high degree of applicable know-how. Some of the pilots have a degree in aeronautical engineering, are graduates of Test Pilot School or hold both qualifications. All of the IAI pilots are in active reserve duty. Their background experience covers most of the past and current IAF inventory, namely the A-4, F-4, Mirage, Kfir,F-15 and F-16. In addition, they have experience in transport aircraft, which was found to be very helpful especially for the development of the auto-pilot.The availability and utilization of different flying techniques associated with the different background experience produced an important advantage. The "bandwidth" of the Lavi's flying qualities is wide enough to span the various flying techniques of the Lavi aircraft's future pilots. The operational aspect of flying qualities such as A/A tracking, A/G bombing and Air Combat Maneuvering (ACM) were an important part of Lavi flight control development.
At one point of that development it was decided to stop the "fine tuning" for A/A tracking. This decision proved to be very cost effective, as actual flights showed that some aerodynamic coefficients were different from those which had been predicted with wind tunnel data. It was felt that further development would best be accomplished at a later stage, when flight test data would update simulation.

6. SPECIAL CONTROL LAW FEATURES

6.1 *PEDAL TO AILERON INTERCONNECT (PAI)*

While trying to decrab the aircraft before touchdown, pilots experienced difficulties in the roll axis when a significant crosswind factor occurred during landing approach simulation. This phenomenon was more aggravated in the A/G load configuration when the moment of inertia around the *X* axis *(Ixx)* was significantly larger. Holding a constant runway heading with rudder and ailerons inputs caused a definite lateral Pilot Induced Oscillation (PIO).

There was no apparent reason for the PIO that appeared in the simulation. In order to minimize the pilot's lateral inputs a new interconnect was implemented. A rudder pedal input automatically introduced aileron deflection; a "mirror" image of the ARI. The results were exceptionally good. Level 3 handling quality ratings rose to Level 1. Fig. 12 presents strip chart data on how lateral stick activities and aircraft responses were reduced.

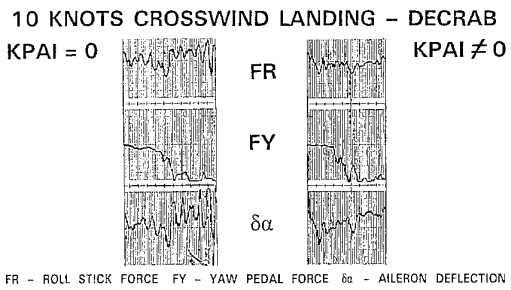

FIG. 12 LAVI KPAI

6.2 *DFCS TO EFCS AUTO TRANSFER*

The IAF specified a "Fail-Op Fail-Op Fail-Safe" concept for the FCS. This specification required a backup. That backup must, at all times, follow the DFCS. During maneuvering, the stick can be at maximum travel. In this case, *Nz* or AOA limiters override the pilot command and actually prevent the aircraft from overstress or departure. When an automatic transfer to the back-up system occurs, the aircraft could depart or overstress because no limiters exist in this system. In order to eliminate this danger, a special feature was introduced. At the instant of transfer, for one (1) second, the stick input to the FLCC is limited. The pilot feels the transfer due to the reduced maneuvering. The pilot then releases the stick and, after one second can resume command in the back-up mode knowing the system's limitation. Fig. 13 presents an example of a manual three (3) G DFCS to EFCS transfer.

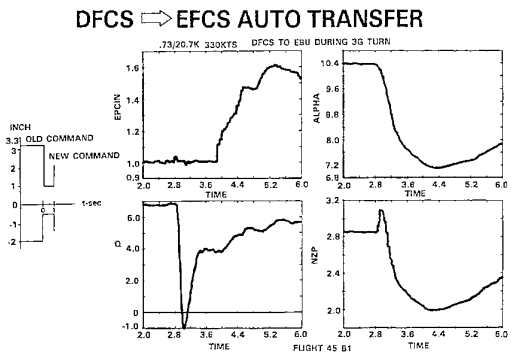

FIG. 13 LAVI DFCS TO EFCS AUTO TRANSFER

6.3 *CANARD SCHEDULE*

The "Delta-Canard" combination requires different canard positions and responses to various flight conditions. Overall it is activated dynamically to improve the initial response of the aircraft and statically to maximize L/D.

In the supersonic regime, the Canard is biased as a function of AOA, releasing hinge moments from the elevons, allowing better maneuverability.

In the subsonic regime, the canard is activated together with the elevons in high AOA and aft Center-of-Gravity (CG) to provide maximum pitch-down moment.

In the power approach (CAT-C) the canard is biased in order to decrease AOA, at a given approach speed, so improving forward visibility. On touchdown, the canard moves to pitch down the nose.

6.4 *ROLL COMMAND GRADIENT-AS A FUNCTION OF LOAD FACTOR*

The basic roll command gradient had a parabolic shape. During the piloted simulations it was found that the overall roll command is too large at a high load factor. In addition, the roll axis response was too sensitive for precise tracking at high G. For this reason, the roll gradient coefficients were scheduled as a function of load factor. This relatively simple feature, (Fig. 14) solved the above mentioned problems, and resulted in very good pilot comments. Another important benefit was the significant reduction in aircraft loads at high G. All together, this feature proved to be highly beneficial.

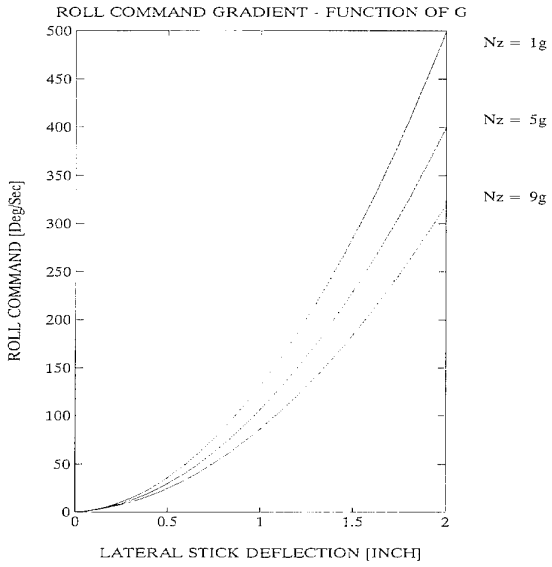

FIG.14 ROLL COMMAND GRADIENT-(*f*) OF G

6.5 *ANTI-SPIN*

The so called "Anti-Spin" mode of the FCL was designed for two purposes:
The first was to avoid, with all possible power, aircraft departure from controlled flight. The second was to activate the control surfaces during spin in an anti-spin direction.
Anti-Spin mode was designed to be engaged and disengaged automatically, as function of angle of attack. Special logics were inserted into this mode to prevent the aircraft from entering into inverted flight (or inverted spin) and, if it happened to recover from this *"unpleasant"* situation, to an erect flight.
This mode was intented to be tested during the flight test of the B4 prototype, which was supposed to be equipped with an anti-spin chute, but this prototype was never built. In the other prototypes that flew (B1, B2, T/D), the mode was never activated, as the angle-of-attack limiter function very successfully prevented the aircraft from departing.

7. HOW DOES IT FLY?

7.1 *FIRST FLIGHT*

The results of the extensive FCL development and test program promised that the Lavi would offer good handling qualities. However, many pertinent questions remained unanswered. The most critical questions concerned lift-off and touchdown transients. These transients were extremely difficult to simulate due to the uncertainties in wind tunnel data.
Utilizing the number one (1) prototype, several high-speed ground runs were performed. These tests included an idle thrust full rotation.
The first flight's take-off was accomplished with aircraft rotation and lift-off achieved at some twenty (20) knots faster than the speeds recommended in the flight manual. Take-off was both smooth and easy, with aircraft perfomance similar to simulation results.
A known problem was a pitch down one second after lift-off. Before the flights, the stabilitiy of the voted AOA value was in question. Therefore, it was decided to engage the AOA feedback only after lift-off, which caused a slight pitchdown of about one (1) degree . After collecting data from several high-speed ground runs, take-offs and landings, a solution has been found. It was incorporated in the Technology Demonstrator (FCL) which shows very smooth transition from ground-to-air and vice versa, in lift-off, and touchdown respectively.
Thanks to the enlarged elevons, Elevator Power is larger than the same coefficient in the B-1/B-2 wings. This Elevator Power enables the pilot to rotate the aircraft's nose earlier on take-off and also to hold it up, for aerobraking, until 60 knots, during landings.
Both FCL and aerodynamic configurations, namely the B-1/B-2 and the T/D, achieve, as predicted, very good handling qualities. In fact, the T/D is flown by many operational and test pilots from several countries. The aircraft is going through operational scenarios, both in A/A and A/G. It has very good responses to the pilot's inputs and demands, from *slower* than eighty (80) knots to the opend flight envelope of six hundred (600) knots at low altitude. Loading the aircraft with two (2) MK-82 bombs (240 KG/500 LB each) on the outboard wing stations, did not deteriorate the handling qualities, although the aircraft is flown with the A/A FCL configuration only, which shows that the robustness of the tasked tailord FCL is good enough to handle successfully the aircraft's Moments of Inertia changes.
The dual (2) control stick installation in the T/D, with the single-seater Artificial Feeling spring in the pitch axis, causes slightly high pitch forces. This phenomenon was mentioned by several of the pilots, after performing slow-speed Air Combat Maneuvering. These maneuvers were done in such slow-speeds that the AOA feedback and limiter is very pronounced, requiring the pilot to hold the stick in the full aft position.

7.2 *PROBLEMS UNCOVERED & SOLUTIONS*

During the first fifteen (15) test flights of the number one (1) prototype, two (2) problems were uncovered. Both of the identified problems were related to lateral-directional characteristics. In A/A tracking small aileron inputs caused too much yaw, which resulted in a snaking motion. The other problem was larger than predicted sideslips during roll reversals.

These problems became more pronounced on the T/D. This aircraft is flown with instrumentation pod installed on the Center Line fuselage station. This reduces the directional stability ($C_{n\beta}$) and causes even larger sideslip angles (β) than the B-1/B-2 appeared to have but the pilots did not really have any problem with this. However, it was suspected that the aircraft might depart from controled flight if this tendency of low $C_{n\beta}$ was aggrevated at high α. It did not happen. Even with the flight-test pod, there is still enough directional stability to maneuver freely at low airspeed/high α. Another phenomenon was discovered in the transonic regime where lower than predicted pitch damping caused pitch oscillations at Mach 0.95. This was a real problem that was caused due to a combination of unpredicted phenomena i.e.: the destabilizing effect of damping in pitch (C_{mq}), larger elevator efficiency and much higher static margin, up to 3% more stable than predicted at this Mach Number. All these resulted in a near 25 degrees PM at low altitude (0.95/10Kft). This problem was solved on the T/D version, by inserting a lead-lag network in the forward loop, and updating gains in the pitch damping path, and in the elevator power gain and the static stability path.

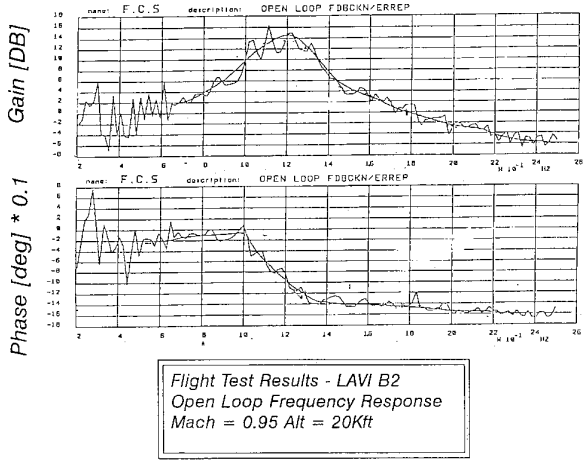

FIG.15 B-2 OPEN LOOP FREQUENCY RESPONSE

Fig. 15 is a Bode plot of the open loop transfer function, of pilot oscillations, flying the B-2 at 19KFT. The PM is near 30. A typical time response at 0.95/36,000 ft flown on the B-1 is shown on Fig. 16. The doted curve is the aircraft flight response, and the solid curve denotes the design intention. Fig. 17 shows the Lavi T/D time response.

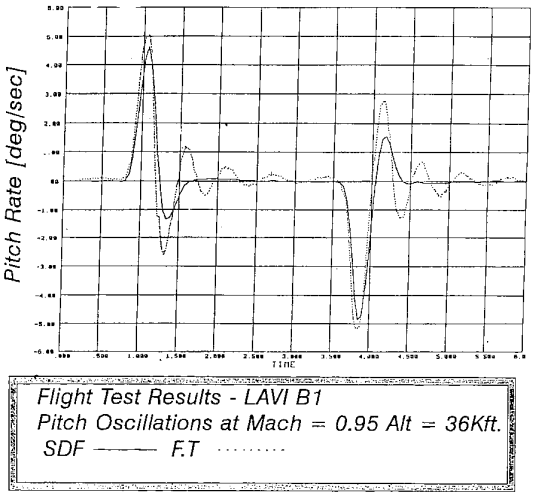

FIG. 16 LAVI B-1 TIME RESPONSE

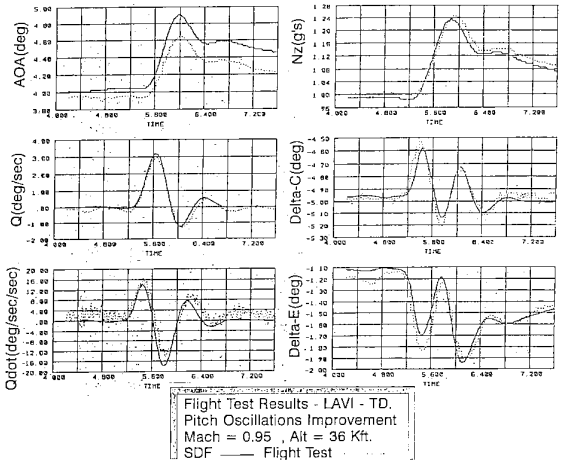

FIG. 17 LAVI T/D TIME RESPONSE

8. FLYING QUALITIES DATA

Figures 18 through 23 present the Lavi's flying qualities and characteristics as exhibited during the flight tests. The presented results reflected the aircraft's performance in relation to

MIL-F-8785C and Israel Air Force specifications. Stick force per G versus Nz/ALFA in CAT-A (Fig. 18), Wnsp versus Nz/ALFA from Q/FS (Fig. 19) and from ALFA/FS (Fig. 20) are well inside Level 1.

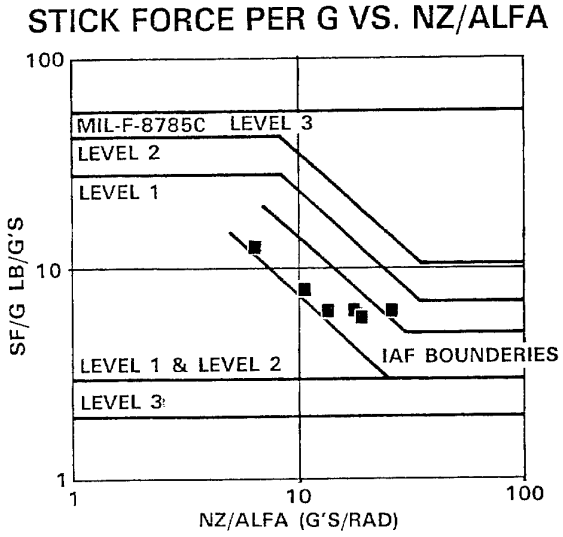

FIG. 18 STICK FORCE PER G V_S N_Z/ALFA

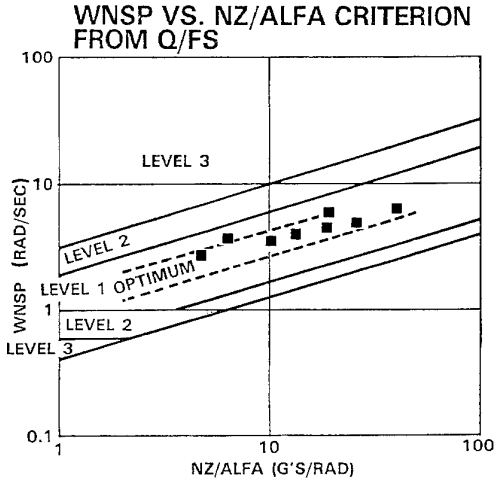

FIG. 19 W_{NSP} V_S N_Z/α FRON Q/F_S

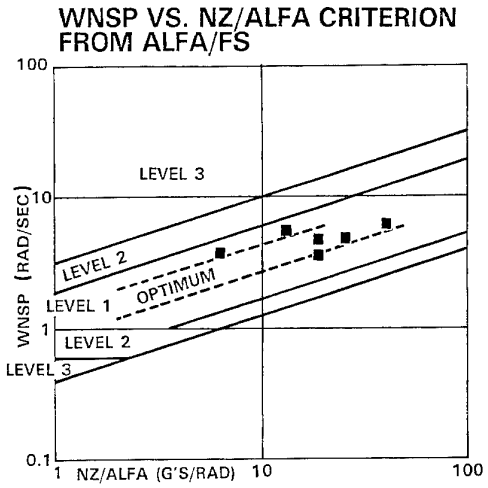

FIG. 20 W_{NSP} V_S N_Z/α FROM α/F_S

The time delay, from Q/Fs time history at the given flight condition (Fig. 21), shows a deviation of 20 msec, from Level 1. This deviation did not affect the handling qualities as far as could be judged. However this time delay was shortened on the T/D FCL by 10 msec.

The lateral directional axis results are basically the same as the longitudinal. These results can be seen in Fig. 22, where Dutch Roll frequency and Damping Ratio are again in Level 1 and generally within IAF criteria.

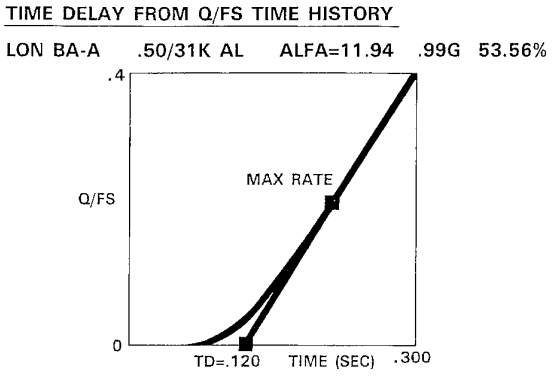

FIG. 21 TIME DELAY FROM Q/F_S TIME HISTORY

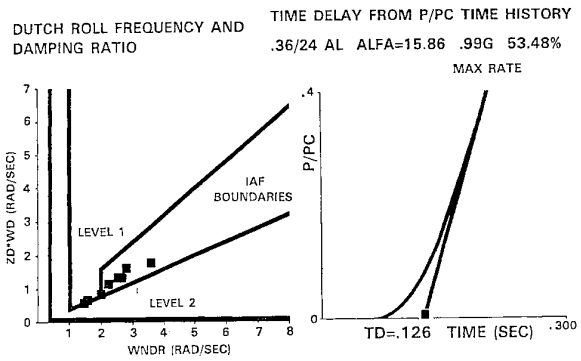

FIG. 22 LATERAL-DIRECTIONAL RESULTS

A summary of Flying Qualities Pilot Ratings is presented in Fig. 23.

FLYING QUALITIES PILOT RATINGS

TASK / PILOT #	HIGH SPEED TAXI (T.O. & LDG)	ROTATION	LIFTOFF	LANDING	FLARE & TOUCHDOWN
	HDG ±3°	INITIAL θ±2°	θ±1°	ON FINAL: θ, α ±1°	SPOT LDG ±150'
	1/8 OF RWY WIDTH	MAINTAINING θ ± 1°		1/4 RWY WIDTH	α ±1°
				Vc ± 3 KTS	Vc ± 3 KTS
1	2	2, 2	4	2, 1, 3	2, 2-3, 2-3
2	2-3	2, –	6	2, 1, 3	2, 2, –
3	2	4, 3	4	3, 2, 3	3, 3, 4
4	2-3	2-3, 2	6	4, 4, 4	2, 3, –
5	–	2, –	2	2, 2, 2	2, 2, 2
SUMMARY	2.3	2.5, 2.3 2.4	4.4	2.6, 1.5, 2.75 2.3	2.2, 2.5, 2.8 2.5

FIG. 23 FLYING QUALITIES PILOT RATINGS

9. STATUS

Since the first flight on 31 December 1986, a total of eighty-one (81) flights amounting to seventy-eight (78) hours were flown by prototypes one (1) and two (2).

Performance envelopes attained during these flights include:

(a) A maximum of one point four five (1.45) Mach from above thirty-six thousand (36,000) feet to forty-three thousand (43,000) feet.

(b) A maximum of five hundred and forty (540) knots at ten thousand (10,000) feet.

(c) A minimum speed of one hundred and ten (110) knots and twenty-three(23) degrees true angle-of-attack, as well as seven point five (7.5) G were demonstrated.

On the Technology Demonstrator one hundred and twenty five flights (125) were flown until 31 december 1993, amounting to one hundred and forty three (143) flight hours. Performance envelopes attained during these flights include:

(a) A maximum of one point two (1.2) Mach.

(b) A maximum of six hundred (600) knots at low altitude.

(c) A minimum speed of less than eighty (80) knots was flown during combat evaluation maneuvering, as well as twenty five (25) degrees AOA and eight point two (8.2) Gs.

A maximum of one point eight (1.8) Mach - eight hundred (800) knots - fifty thousand (50,000) feet - nine (9) G and twenty five (25) degrees true angle-of-attack are the designed envelope.

The T/D is continuing to fly routinely, testing, evaluating and demonstrating the Lavi's avionics and exceptional airframe capabilities.

10. FINAL WORDS

Comparing the Lavi's FCL and FCS to the KFIR's Autocommand, (which was developed and produced during the early 70s) shows significant differences. The Autocommand, an analog pitch Control Augmentation System, gives the pilot some improvements in areas where the unaugmented aircraft exhibit some handling qualities problems. Low altitude high speed flight characteristics as well as air-to-air and air-to-ground fine tracking have been improved. Very heavy takeoffs, where smooth and precise pitch control is needed is also improved.

The basic control laws of pitch rate *(Q)*, load factor *(G)* and some AOA feedback are being used in both systems.

The techology level and the precise tailoring of the advanced digital fly-by-wire FCS in the Lavi, is a "full time" three (3) axes control system, providing the pilot with an excellent handling qualities combat flying machine. The pilot is free to operate the aircraft's combat systems, with minimum pilot compensation and work load in piloting the Lavi.

Robust Control: A Structured Approach to Solve Aircraft Flight Control Problems

S. Bennani [1] J. A . Mulder [1] O.H. Bosgra [2]

[1] Sec. Stability and Control, Fac. Aerospace Eng.
Delft University of Technology, Kluyverweg 1, 2629 HS Delft, The Netherlands.
E-mail s.bennani@lr.tudelft.nl
E-mail j.mulder@lr.tudelft.nl

[2] Mechanical Engineering Systems and Control Group,
Delft University of Technology, Mekelweg 2, 2628 CD Delft,
The Netherlands.
E-mail bosgra@tudw03.tudelft.nl

Abstract

This paper discusses an application of several robust control methodolgies such as H_∞ optimal control, μ-synthesis and gain scheduling via linear fractional transformations applied to a flight control system. To illustrate the approach, a design model for the short period approximaton of the Cessna Citation 500 has been chosen, for which certain handling quality requirements have to be met over a large set of operating conditions. For all these methods the design framework remains the same, only the system "norm" changes to the object to be minimized. The paper shows how these methods work and illustrates the features of the new approach.

Keywords

Robust Control, H_∞ Control, μ-Synthesis, Linear Matrix Inequalities, Gain Scheduling, Linear Fractional Transformation.

1 Introduction

In the last decade, much effort has been devoted by control theoreticians [13, 14, 17, 21, 19, 24, 29, 43, 44, 45, 54] to develop a framework that is general enough to handle a large class of realistic control problems that are relevant to practical engineering. This framework associates a general system representation and certain classes of system "norms" to form the fundament for modern control synthesis and analysis. To be more specific, the new class of systems is shaped into in a *Linear Fractional* representation. This has the advantage that it describes a set of systems obtained through a perturbation affecting the nominal system in a feedback way, see [14, 35, 15, 40]. To achieve stability for such perturbed systems we require the system's output to remain bounded under all possible perturbations. In terms of signal norms, we have to detect the worst case input signal on the system and assure that the output is bounded in norm by a factor γ. If so, we are able to garantee robust stability of the system for the set of prescribed perturbations. This worst case amplification is the H_∞ norm of the system. The H_∞ norm minimization problem, is to find a stabilizing controller that minimizes the worst case amplification γ of the system over all frequencies. Firstly, we will introduce norms, Linear Fractional Transformations (LFT') and a basic stability result called the "Small Gain" theorem required for the exposition of the general framework as given in [11, 50]. Then we will show three design methods: H_∞ optimal control, μ-syntesis and Linear Parametric Control (LPV), all developed in this framework.

Finally, we apply these methods to a fly-by-wire control problem where the objective is to find a controller achieving a stick-to-pitch rate response specified by handling qualities. We will design a

Paper presented at the Flight Mechanics Panel Symposium held in Turin, Italy, from 9-13 May 1994.

control law for a set of systems having variations in the aerodynamic and actuator models, while the control effort has to remain within bounds such that the elevator does not hit the stops and the flight control system does not saturate. A similar problem has been studied in [3] for a high-angle-of-attack fighter.

Important to remark is that all the design specifications are required a priori, as opposed to classical methods. In this sense we speak of closed-loop design where our design parameters are not any more the controller but the closed-loop design specifications. When applying these methods, the simple single-input single-output (SISO) system can become a complex multivariable matrix structure, the design and analysis model, where stability and performance requirements are stacked together into one large matrix. To make the synthesis problem meaningful, both the stability and performance requirements are formulated as quantities that have to remain small in an ∞-norm sense. In this way the synthesis problem is transformed into a stability robustness problem called the robust performance problem. This has two subproblems, i.e. the robust stability problem to perturbations and secondly the nominal performance problem. These problems are simultaneously minimized by the robust performance objective. Unfortunatly, the H_∞-norm minimization yields quite conservative robustness levels. To resolve this problem, the structured singular value μ is used as a refinement of the ∞-norm. As a specialization to H_∞ control, μ-synthesis has been developped to find a controller solving the robust performance problem. Excellent references for a detailed discussion of the method are [11, 15, 50].

To show the conservativeness of the H_∞ control problem and the power of μ-synthesis we shall revisit the fly-by-wire control design problem with a slight modification on the uncertainty model where the aerodynamic coefficients are allowed to vary substantially. However, even if μ-synthesis provides an answer to the robust performance problem it does not allow the adaption of changes in the performance requirements to changing flight conditions.

In practice, flight control engineers know how the aerodynamic forces and moments acting on the vehicle vary with changing operating conditions. Based on this knowledge engineers make the control law dependent on the dynamic pressure, Mach or some other physical parameter. Gain scheduling is mostly adhoc, moreover due to the non-linear time-varying nature of the schedule parameter there is no more guarantee for closed-loop stability by linear time invariant methods, see [42, 47, 48, 49, 52]. To tackle the common problem in flight control system design of gain scheduling we will finally demonstrate the generality of the framework associated with "μ". For this purpose the framework will be extended to Linear Time Varying (LTV) systems. Under the condition that the schedule parameters can be measured we can formalize the gain scheduling problem such that the achieved control law has the required gain schedule while meeting prespecified stability and performance levels. The method is called LPV control (Linear Parametrically Varying) and its problem formulation was first stated in [37, 27, 29], for which solutions have been provided in [32, 33, 38, 19, 1]. The method will be illustrated by the fly-by-wire control design example where speed and altitude variations are extracted from the system in the mentioned linear fractional way to reflect the system's dependence on the schedule parameters. This system parametrization provides the schedule information for the controller. In this formulation the evolution of the time-varying parameters has not to be known in advance. For controller synthesis it is only required to know the bounds of the parameters and have them available as measurements. The controller can be synthesized via a set of Linear Matrix Inequalities (LMIs) which are solved by efficient optimization algorithms proposed in [16, 30, 31, 22, 51]. For our application we used the method of [19] and solved the problem within a Matlab environment called LMI-Lab, see [20], giving the designer a flexible and powerful tool to setup LMIs and solve a general class of control problems.

2 Preliminaries

For simplicity, suppose that we deal with SISO linear time invariant (LTI) systems. We are interested in how large certain transfer functions $H(j\omega)$ can get before instability occurs. To measure these transfer functions we need norms. There are two ways to look at the problem, one is to find the maximum amplification that can occur in the system and the other one is to look for the worst case normed input/output signal ratio. The first way characterizes operator norms which can be obtained by different normed signal ratios. Formally an operator norm is induced by the largest normed signal ratio. The H_∞-norm is such an oprator norm

and our focus in this section is to provide a short glance at some formalities within normed vector spaces called Banach spaces. Then we shall review a general system representation called *Linear Fractional Transformations* (LFTs). We will show how well known control theoretic objects as transfer functions or state-space systems can be formulated as LFTs. Finally, we shall study the stability of a simple LFT in the sense of a Nyquist like criterion which turns out to be characterized as an H_∞-norm bound.

2.1 Signal Norms and Induced Norms

The different ways in which the H_∞ norm arises will briefly be given. For completeness we shall also discuss the more classical H_2 norm to see the practical relevance of these measures. From an engineering point of view the H_∞ norm of the transfer function $H(j\omega)$ as shown in figure (1) is defined as:

$\|H\|_\infty$ = maximum, over all frequencies ω, of the transfer function, $H(j\omega)$. Notice that this quantity can be easily detected on a Bode magnitude plot and reflects the largest peak amplification over all frequencies.

On the other hand the H_2-norm is given by:

$$\|H\|_2 = \left\{ \frac{1}{2\pi} \int_{-\infty}^{+\infty} |H(j\omega)|^2 d\omega \right\}^{\frac{1}{2}} = \left\{ \int_{-\infty}^{+\infty} |h^2(t)|\, dt \right\}^{\frac{1}{2}}$$

Notice that $\|H\|_2^2$ is proportional to the total energy in the impulse response.

Consider a system with transfer function $H(j\omega)$ with impulse response $h(t)$ and the corresponding input/output signals $w(t)$ and $z(t)$ respectively, as depicted in figure (1).
Suppose $w(t)$ is unit intensity white noise. Then its spectral density $|w(j\omega)|^2$ equals 1 for all frequencies ω. The spectral density of the system output $z(t)$ is then $|H(j\omega)|^2$. Integrating the output spectral density, scaling by $\frac{1}{2\pi}$ and taking the square root gives the $\|H\|_2$ norm. All these operations can be easily carried out on the system output so that this norm is in practice easily measurable by physical devices, with final result being that the $\|H\|_2$-norm is nothing more than the *rms* value of the output signal $z(t)$, due to a unit intensity white noise input $w(t)$.
To measure the $\|H\|_\infty$-norm, consider a certain input signal $w(t)$ scaled to unit *rms* value. Take for example the input signal $w(t) = \sqrt{2\omega}\sin\omega t$ and measure the *rms* value of the output $z(t)$ simply by squaring, integrating and scaling. For the output $z(t)$ we obtain $z(t) = \sqrt{2\omega}|H(j\omega)|\sin(\omega t + \phi(H(j\omega))$. Define the period T of the input signal $T = \frac{2\pi}{\omega}$, then the amplitude of the frequency response can be deduced from the *rms* value of $z(t)$ and we get $|H(j\omega)| = \{\frac{1}{T}\int_0^T z^2(t)dt\}^2$. It remains now to search over ω to find the $\|H(j\omega)\|_\infty$ norm of the system. In summary:

> $\|H\|_\infty$ = maximum *rms* value of $z(t)$
> over **all possible inputs** $w(t)$ with *rms* ≤ 1.

The formal definition of the $\|H\|_\infty$-norm comes from vector spaces that map a class of input signals into another vector space. The map is characterized through LTI operators. There are now two choices we can make. One is to choose the vector norms and the other is to choose operator norms. When we map a normed input vector space into an output normed vector space, the map is called an operator. The largest value of the operator is defined as the H_∞ norm. On the other hand the largest input/output ratio induced by the normed signals over all normed input signals is also the H_∞-norm, but now we speak about the induced norm.

The definition we get for an operator norm as an induced norm is as follows:

$\|\Theta\|$	$= \sup_{\|x\|_i \leq 1} \|\Theta x\|_o$
where	
Θ	is any operator
x	is any input vector
$\|.\|_i$	is the norm on the input space
$\|.\|_o$	is the norm on the output space

When this definition is applied to the 2-normed input and output signal spaces we get:

$$\|H\|_\infty = \sup_{\|w\|_2 \leq 1} \|Hw\|_2 = \sup_{\|w\|_2 \leq 1} \frac{\|z\|_2}{\|w\|_2} \quad (2.1)$$

which is the mathematical statement of the previous definitions of the H_∞-norm often also called *rms* induced norm.

The next interpretation of the H_∞-norm is obtained when equation (2.1) is squared. We get

$$\|H\|_\infty^2 = \text{energy gain of the system}$$

$$= \sup \left\{ \int_{-\infty}^{+\infty} z^2(t)dt \;\middle|\; \int_{-\infty}^{+\infty} w^2(t)dt \leq 1 \right\}$$

therefore the following always holds:

$$\|H\|_\infty \geq \frac{\left\{\int_{-\infty}^{+\infty} z^2(t)dt\right\}^{\frac{1}{2}}}{\left\{\int_{-\infty}^{+\infty} w^2(t)dt\right\}^{\frac{1}{2}}} = \frac{\sqrt{\text{output energy}}}{\sqrt{\text{input energy}}}$$

From the definition of operator norms, the $\|H\|_\infty$ norm has the following nice property. Suppose that the operator H is obtained from the operators G and F as $H = FG$, then

$$\|H\|_\infty \leq \|F\|_\infty \|G\|_\infty \tag{2.2}$$

Such a relation between $\|H\|_2$ and $\|F\|_2$, $\|G\|_2$ does not exist. We have yet not made any statement about stability, but the inequality (2.2) applied to certain transfer functions provides a tool to measure stability margins for feedback systems.

2.2 Linear Fractional Transformations: LFT's

The basic concept of linear fractional transformations arises from complex function theory. The mapping F from $C \rightarrow C$ characerized by:

$$F(s) = \frac{a + bs}{c + ds}$$

where a, b, c, and $d \in C$, is called a *linear fractional transformation*. In particular if $c \neq 0$ then $F(s)$ can also be written as

$$F(s) = \alpha + \beta s(1 - \gamma)^{-1}$$

for some α, β and $\gamma \in C$. The above linear fractional transformation for scalars can be generalized to the matrix case.

Consider a complex matrix M, partitioned in the following way:

$$M = \begin{bmatrix} M_{11} & M_{12} \\ M_{21} & M_{22} \end{bmatrix} \tag{2.3}$$

Consider the block structures $\mathbf{\Delta_1}$ and $\mathbf{\Delta_2}$ compatible with M_{11} and M_{22}.

According to figure (2), we obtain the following loop equations when M and Δ_1 are disconnected. For $\Delta_1 \in \mathbf{\Delta_1}$ the loop equations are:

$$\begin{aligned} z &= M_{11}w + M_{12}d \\ e &= M_{21}w + M_{22}d \\ w &= \Delta_1 z \end{aligned} \tag{2.4}$$

The set of equations is *well posed (defined)* if and only if the inverse of $(I - M_{11}\Delta_1)$ exists. In that case the vectors e and d must satisfy:

$$e = F_u(M, \Delta_1)\, d \tag{2.5}$$

with $F_u(M, \Delta_1)$ defined as:

$$F_u(M, \Delta_1) = M_{22} + M_{21}\Delta_1 (I - M_{11}\Delta_1)^{-1} M_{12} \tag{2.6}$$

$F_u(M, \Delta_1)$ is called an LFT on M by Δ_1. The index u stands for *upper* and denotes that we have an upper linear fractional representation indicating that the top loop of M has been closed. Similarly we can close the lower loop of M with a block structure Δ_2, compatible this time with M_{22} to get a *lower* LFT defined as:

$$F_l(M, \Delta_2) = M_{11} + M_{12}\Delta_2 (I - M_{22}\Delta_2)^{-1} M_{21} \tag{2.7}$$

For an interpretation of the fractional representation, consider the example of the upper LFT in equation (2.6). Equation (2.6) represents a nominal model M_{22} which is perturbed through Δ_1 by the second term of the equation. The matrices M_{12}, M_{21}, M_{22} reflect the structural knowledge on how the pertubation Δ_1 affects M_{11}. The lower linear fractional representation is often used in the controller synthesis problems where Δ_2 is replaced by the controller K, while the upper fractional representation is commonly reserved for the analysis of robustness problems.

Example 1

Consider the system in figure (3) where the nominal system $G_0(s)$ is affected by an input multiplicative uncertainty $(1 + \Delta(s))$. Further, we suppose that $\Delta(s)$ is normed to unity. The set of systems covered by this representation is given by $G(s) = \{(1 + \Delta(s))\, G_0(s) |\ |\Delta| < 1\}$. Remark that the perturbation enters the system in a feedforward way, while the controller enters the system as usually in a feedback way. To get the matrix M, we need all loop equations. Pictorially this can be done by opening the connections at each subsystem to get:

$$\begin{aligned} z &= M_{11}u + M_{12}w \\ y &= M_{21}u + M_{22}w \\ \text{i.e.} & \\ z &= 1u + 0w \\ y &= Gu + Gw \\ \text{and} & \\ w &= \Delta_2 z \\ u &= Ky \end{aligned} \tag{2.8}$$

We apply the lower LFT and the upper LFT definitions to M to get the system in figure (4), where $T = \frac{G_0 K}{(1+G_0 K)}$ is now affected in a feedback way by

Δ permitting us to study the stability of T, which represents the closed loop system under perturbations Δ.

Example 2
To appreciate the generality of LFTs, consider the state-space system (A, B, C, D) as given in figure (5). The loop equations for this system are:

$$\begin{aligned} \dot{x}(t) &= Ax(t) + Bu(t) \\ y(t) &= Cx(t) + Du(t) \\ \text{with} & \\ x(t) &= \int \dot{x}(t)\, dt \end{aligned} \tag{2.9}$$

Applying a Laplace transform to equation (2.11) the transfer function $G(s)$ from $u(s)$ to $y(s)$ is easily obtained. Furthermore, the transfer function $G(s)$ has also an LFT characterization, simply by applying the upper LFT formula to the loop equations:

$$\begin{aligned} G(s) &= D + C\tfrac{1}{s}(I - A\tfrac{1}{s})^{-1}B \\ &= D + C(sI - A)^{-1}B \end{aligned} \tag{2.10}$$

Having noticed the LFT characterization of state-space equations, we are able to study robustness problems with respect to varying elements in the matrices (A, B, C, D). Consider as an example the state-space system

$$\dot{x} = a\alpha^2 x + b\alpha x + u$$

where $\alpha \in R$ is the varying parameter. To study the effect of α variations on the state-space system, we have to view α as a perturbation. The state-space representation is pictorially given in figure (6). Since α is the varying element, we introduce in the system extra input/output signals $(w_1, w2)$ and (z_1, z_2), and disconnect the perturbation α from the system. To get again our matrix M, write the loop equations

$$\begin{aligned} \dot{x} &= 0x + u + bw_1 + aw_2 \\ z_1 &= 1x + 0u + 0w_1 + 0w_2 \\ z_2 &= 0x + 0u + 1w_1 + 0w_2 \end{aligned} \tag{2.11}$$

and for Δ

$$\begin{aligned} w_1 &= \alpha z_1 \\ w_2 &= \alpha z_2 \end{aligned}$$

Closing the bottom loop of equation (2.11) gives the LFT represntation for the system under variations α as depicted in figure (7) and closing the remaining top loop gives the perturbed transfer function. This type of nonlinear polynomial variations is common in aircraft problems and will be used later on to model variations in the aerodynamic coefficients and variations of system parameters as airspeed and altitude over the flight envelope.

2.3 Stability Characterization

Having defined norms and LFTs, let us revisit example 1 and try to find out what H_∞ norm means for system stability with respect to uncertainties Δ. The loop equation is given by $T\Delta$, where T stands now for the closed-loop transfer function $T = \frac{G_0K}{(1+G_0K)}$, which is often referred to as the complementary sensitivity function. In terms of a Nyquist like criterion, but now applied on the closed-loop quantity T, rather than the open-loop return ratio G_0K, the closed-loop system remains stable as long as the locus of G_0K does not encircle the point $(-1, 0)$. The loop for the perturbed system is given in figure (3). In terms of norms, the perturbed system is stable as long as $||T\Delta||_\infty \leq 1$. Moreover, applying the norm inequality $||T\Delta||_\infty \leq ||T||_\infty ||\Delta||_\infty$, the perturbed closed-loop system is stable as long as $||T||_\infty \leq \frac{1}{||\Delta||_\infty}$. This condition is often referred to as the "Small Gain" condition, and insures stability even to nonlinear norm bounded perturbations Δ with $||\Delta||_\infty \leq 1$, as long as $||T||_\infty \leq \frac{1}{\gamma}$. The stability margin for T under perturbations is γ, i.e. you can increase the norm of the perturbation Δ by a factor γ without causing instability. Designing a stabilizing controller K, such that the reciprocal of the stability margin $\frac{1}{\gamma}$ is minimized is the subject of $||H||_\infty$ optimal control.

Suppose now we have an idea about the shape of the uncertainty, say $\Delta(s) = W(s)\Delta$. Here $W(s)$ is a stable transfer function reflecting the uncertainty profile along the frequency axis and Δ is a scaling factor with $|\Delta| < 1$. Weighted robust stability, i.e. robust stability with respect to the given uncertainty profile $|W(s)|$, is achieved if and only if $||W\,T||_\infty \leq 1$. This means that we can bound the closed loop transfer function T in the synthesis problem by specifiying the shape of the weighting function W. In the same way this procedure is applied to achieve certain closed loop performance characteristics as for example a prespecified reference to tracking error profile. For a deeper treatement of this very important topic see [12] for the SISO case and [10] for the small gain characterization of stability.

3 General Performance Formulation

In the following the robustness characteristics will be generalized, within the framework for synthesis

and analysis. We shall see how the structured singular value μ arises when analyzing the stability of the general system representation. A general controller synthesis and analysis problem description as proposed by [50] is shown in figure (8). Associated with this representation of the problem description is a suitable measure of magnitude for matrix transfer functions and some key analysis and synthesis results defining a framework for controller synthesis and robustness analysis. The problem description consists of a generalized system P with three pairs of input/output variables including the performance and stability requirements on the nominal to be controlled system G. The first pair consists of the measured outputs $y(t)$, and control inputs $u(t)$. The second pair consists of performance variables $e(t)$, and external input signals $d(t)$, and the third pair consists of output signals $z(t)$, and $w(t)$ through which unit-norm perturbations are fed back into the system. Any linear interconnection of inputs, outputs and commands along with the perturbations and a controller can be viewed in this context and can be rearranged to match the diagram in figure (8). In this way P can be chosen to reflect many different problem specifications.

3.1 Analysis Review

Within this framework a non-conservative, necessary and sufficient condition for robust performance can be formulated [50]. To obtain this condition the compensator feedback-loop in figure (8) has to be closed to get the loop in figure (9). The system $F_l(P,K)$ in this figure has a 2×2 block-structured transfer function $M(s)$ whose blocks are defined in terms of the original 3×3 partition of $P(s)$ as follows:

$$\begin{aligned} M_{ij}(s) \;=\; & P_{ij}(s) + \\ & P_{i3}(s)\,[I - K(s)P_{33}(s)]^{-1} \\ & K(s)P_{3j}(s) \quad i,j = 1,2 \end{aligned} \tag{3.12}$$

Recall that equation (3.12) represents a linear fractional transformation of the system P through K. When the system $M(s)$ is stable, then according to the partition, the following results apply [50] as a special case of the **MAIN LOOP THEOREM** [35]:

1. **Nominal performance is satisfied if and only if**

$$\|M_{22}(j\omega)\|_\infty < 1 \tag{3.13}$$

2. **Robust stability is satisfied if and only if**

$$\|M_{11}(j\omega)\|_\infty < 1 \tag{3.14}$$

3. **Robust performance is satisfied if and only if**

$$\mu[M(j\omega)] < 1 \;\; \forall\, \omega \tag{3.15}$$

where μ is a function to be defined shortly.

Robust performance is equivalent to robust stability in the presence of the perturbation Δ augmented with Δ_p connected around the system M. Robust performance is assured, if and only if the function $\det(I - diag(\Delta, \Delta_p)M(j\omega))$ remains nonzero along the imaginary axis. This observation gives rise to the function μ. This function was defined in [14] to test this kind of determinant conditions. Its full definition for complex matrices is the following:

$$\mu(M) \triangleq \left[\min\left\{\epsilon \;\middle|\; \begin{array}{l} \det[I - \epsilon\Delta M] = 0 \\ \text{for some } \Delta = diag(\Delta_1, \ldots, \Delta_m) \\ \text{with } \|\Delta_i\|_\infty < 1 \text{, for all } i \end{array}\right\}\right]^{-1}$$

In words, μ is the reciprocal of the smallest value of scalar ϵ which makes the matrix $I - \epsilon\Delta M$ singular for some Δ in a block-diagonal perturbation set. If no such ϵ exists, μ is taken to be zero. In terms of stability μ is a measure of the smallest structured perturbation Δ that causes instability of the matrix M. It is a tight condition for robust stability with respect to two perturbation blocks, and equivalently a tight condition for robust performance. The definition of μ is not limited to 2×2 block structures Δ, so it can be used to test stability with respect to *any number of diagonal blocks.* This permits to establish robust stability with respect to sets of systems characterized by *several unstructured perturbations* at component level, and simultaneously, to establish robust performance by structured stability test at system level M. For design, the function $\mu(M)$ is evaluated as a function of frequency, providing a Bode-like plot to analyze robust stability/performance of any given design represented by the matrix $M = F_l(P,K)$. It should be clear from the argument of the function μ which kind of test is carried out. As an example, $\mu(M_{11})$ can be used as a refinement on the conservative robust stability test $\|M_{11}\|_\infty$ when the system is affected by a structured uncertainty. For deaper treatement of the numerical aspects involved in the calculation of μ, see [2]. The only fact we present is

that $\mu(M)$ is bounded below by the spectral radius $\rho(M)$ and above by the maximum singular value $\bar{\sigma}(M)$. However, these bounds can be conservative and need therefore to be refined. For the exposition we only need the upper bound of μ. It can be effectively refined by $\inf_{D\in\mathbf{D}} \bar{\sigma}(DMD^{-1})_\infty$ to approximate μ, where D is a scaling matrix. The matrix D is partitioned consistently with the matrix M in the following way:

$$D = \begin{bmatrix} D_\Delta & 0 \\ 0 & I \end{bmatrix}$$

The scaling matrix D decreases the norm of M while leaving the transfer function M unchanged. To see this it suffices to evaluate $F_u(DMD^{-1}, \Delta)$. The scalings D set off the contributions of the off diagonal terms M_{12} and M_{21} in the matrix M to the norm of M while not affecting the transfer function from d to e. In this way the matrix M is conditioned by scaling. This property will be used to synthesize controllers for the robust performance objective.

3.2 Synthesis Review H_∞ Optimization

For the purpose of synthesis, the perturbation can be normalized properly to unity so that the normalizing factor can be absorbed into P. This results in the synthesis problem as shown in figure (10). We want to find a stabilizing controller K such that performance requirements are satisfied under prescribed uncertainties. The interconnection structure P can be partitioned so that the input-output map from $\begin{bmatrix} w \\ d \end{bmatrix}$ to $\begin{bmatrix} z \\ e \end{bmatrix}$ can also be expressed as the following lower linear fractional transformation denoted F_l:

$$\begin{bmatrix} z \\ e \end{bmatrix} = F_l(P,K) \begin{bmatrix} w \\ d \end{bmatrix} = M \begin{bmatrix} w \\ d \end{bmatrix}$$

For the H_∞ optimal problem, the objective is to find a stabilizing controller K which minimizes $\|F_l(P,K)\|_\infty$. Thus find a controller K such that

$$\|F_l(P,K)\|_\infty < \gamma \tag{3.16}$$

where $\frac{1}{\gamma}$ is the minimum norm of the perturbation that destabilizes the closed-loop system M. The optimal γ value is achieved iteratively, we call this process γ iteration. Excellent references on this matter are [17, 2], the algorithms used to obtain H_∞ controllers come from [13] and are implemented in the μ-Analysis and Synthesis Toolbox [2].

3.3 Synthesis Review μ-Synthesis

μ-Synthesis has emerged as a practical approach for the design of control systems with robust performance objectives. The method essentially integrates two powerful theories for synthesis and analysis into a systematic design technique. It involves H_∞ optimization methods for synthesis and the structured singular value μ for analysis. The problem of robust controller design becomes that of finding a stabilizing controller K and a scaling matrix D such that the quantity $\| DF_l(P,K)D^{-1} \|_\infty$ is minimized. The approach for solving this problem is that of alternatively minimizing the above expression for K or D while holding the other constant. For fixed D, it becomes an H_∞ optimal control problem which we can solve using the state-space method of [13]. For fixed K, the problem consists of calculating the structured singular value $\mu(M)$ via the upper bound $\bar{\sigma}(DMD^{-1})$. The obtained scaling matrix D is then absorbed into the synthesis model P to synthesize a μ-optimal controller. This proces is carried on until a satisfactory controller is constructed. A diagram of the system on which the minimization is carried out is given in figure (11). This section is mainly inspired by the material given in [2, 36, 50]. These references provide to the authors knowledge the best explained and motivated introductory material for the practical design of H_∞ and μ controllers.

4 Setting Up the Design Model

The control problem for our example is a pitch rate command system as depicted in figure (12). The pilot controls certain parameters, like the angle of attack, the pitch rate and the normal acceleration. The effect of atmospheric turbulence is disregarded for this example. The control system to be designed should allow error free tracking by the pilot of these parameters over a wide range of operating points, while actuator effort has to remain within certain limits. We shall first discuss how to mould the operating range variations of the airframe, the aerodynamic uncertainty and control the effectiveness uncertainty into an LFT formulation. Then it will be shown how the performance requirements such as handling qualities, actuator effort and tracking error requirements are modelled in order to obtain the required general interconnection structure P for analysis and design.

4.1 The aircraft model

For simplicity we study the short period approximation which describes the aircraft's center of gravity rotational movements about the Y-axis and the translations along the vertical Z-axis. Flightspeed V is supposed to remain constant in the equations of motion. The notations for angle of attack, pitch rate, normal acceleration and the elevator are respectively α, q, n_z and δ_e. The state-space representation for the short period mode has the form:

$$\begin{bmatrix} \dot{\alpha}(t) \\ \dot{q}(t) \end{bmatrix} = \begin{bmatrix} a_{11} & a_{12} \\ a_{21} & a_{22} \end{bmatrix} \cdot \begin{bmatrix} \alpha(t) \\ q(t) \end{bmatrix} + \begin{bmatrix} b_1 \\ b_2 \end{bmatrix} \cdot \delta_e(t) \quad (4.17)$$

and is given in terms of physical parameters as:

$$a_{11} = \frac{C_{Z_\alpha}}{2\mu_c} \cdot \frac{V}{\bar{c}}, \qquad a_{21} = \frac{C_{m_\alpha} \cdot 2\mu_c + C_{Z_\alpha} \cdot C_{m_{\dot{\alpha}}}}{4\mu_c^2 K_Y^2} \cdot \left(\frac{V}{\bar{c}}\right)^2$$

$$a_{12} = 1, \qquad a_{22} = \frac{C_{m_{\dot{\alpha}}} + C_{m_q}}{2\mu_c K_Y^2} \cdot \frac{V}{\bar{c}},$$

$$b_1 = \frac{C_{Z_\delta}}{2\mu_c} \cdot \frac{V}{\bar{c}}, \qquad b_2 = \frac{C_{m_\delta} \cdot 2\mu_c + C_{Z_\delta} \cdot C_{m_{\dot{\alpha}}}}{4\mu_c^2 K_Y^2} \cdot \left(\frac{V}{\bar{c}}\right)^2.$$

The measured outputs are α, q and n_z. In the model we distinguish 3 types of quantities:

- Nondimensional aerodynamic coefficients, given by the stability and control derivatives $C_{mZ_{\alpha q \dot{\alpha} \dot{q} \delta_e}}$.
- Flight condition dependent coefficients such as V and $\mu_c = \frac{m}{\rho S \bar{c}}$.
- Geometrical and inertial elements as m, S, $\bar{c}$ and $K_{yy}^2 = \frac{I_{yy}}{m\bar{c}^2}$

The parameter variations are addressed to the aerodynamic stability and control derivatives and the flight condition dependent parameters V and air density ρ. The aircraft mass is supposed to be constant.

- Variations in airspeed V and air density ρ, reflecting the changes over operating conditions.
  - $V \in [54,\ 184]\ m/s$
  - $\rho \in [0.45,\ 1.225]\ kg/m^3$
- Parameter relative uncertainties in aero coefficients due to changing operating conditions are modelled as $C_{..} = C_{..0}(1 + \Delta C_{..})$. For each parameter the relative variations is:

$$\Delta C_{Z_\alpha} = \pm 5.5\% \qquad \Delta C_{m_\alpha} = \pm 23\%$$
$$\Delta C_{Z_{\dot{\alpha}}} = \pm 11\% \qquad \Delta C_{m_q} = \pm 9\%$$
$$\Delta C_{Z_{\delta_e}} = \pm 5.6\% \qquad \Delta C_{m_{\dot{\alpha}}} = \pm 12\%$$
$$\Delta C_{m_{\delta_e}} = \pm 7.5\%$$

4.2 LFT Modelling of System Variations

To model the system variations to aero uncertainty we take the the state space equations of motion and we allow each stability derivative to have a multiplicative uncertainty. To extract this uncertainty from the state space form, we bring the system in upper LFT form and we proceed according to example 1, while for the parameter variations in V and ρ we apply the procedure outlined in example 2. Finally, in order to include a model of high frequency dynamics in the aerodynamic model we adopt an input multiplicative uncertainty having the form:

$$W_{del}(s) = K_{del} \frac{\alpha s + \beta}{\gamma s + \delta}$$

It dictates the shape of the uncertainty in the transfer function between the elevator input and the aircraft motion parameters α, q, n_z. The parametrized set of models finally obtained is given in figure (13). It reflects the aircraft model parameter variations and the aeordynmic and high frequency uncertainties around a nominal flight condition. The resulting system variation is absorbed in a perturbation matrix Δ, which has been scaled to unity. The contributions to the total system variation is composed of $\Delta_p = \{\Delta_V, \Delta_\rho\}$ for parameter variations in V and ρ, and $\Delta_u = \{\Delta_{aerou}, \Delta_{cxu}\}$ for aero and complex uncertainties (the subscripts p, cx and u stand respectively for parameter, complex and uncertain). To see how the parametric system modelling works out see figures (14(a), 14(b), 14(c)) which represent the open loop step responses to an elevator doublet of 2 degrees of the angle of attack, pitch rate and normal load factor. Each plot contains five responses, where the lowest and highest curves represent the effect of parametric system variation in speed and altitude plus uncertainty in the aerodynamic stability and control derivatives. In between these two responses the remaining two upper and lower curves reflect only the effect of uncertainty in the aerodynamic derivatives, while the middle curve is the nominal design model without uncertainty. Notice that no design has been performed yet but an important point has to be mentioned now. The way the aircraft dynamics have been modelled gives the designer a powerful tool to analyze systematically the system behaviour to variations in any component of the state space matrix. The variations can be addressed simultaneously or separately by changing the value of the corresponding Δ which are all between 1 and -1. Further, from this representation, system charac-

teristics as pole location, damping and natural frequency as function of any modelled variation in Δ can be obtained. For purpose of control, the power lies in the fact that we can accurately cover with one model the whole flight envelope in contrast to the set of linearized models in classical design for which successive designs have to be performed. In robust control the synthesized controller will try to achieve the required performance for the whole set of parametrized models. The stability robustness indicators will then provide the information if the set has been chosen too large or not. According to the obtained information, the designer can extend or reduce his model set.

4.3 Performance Requirements

The next step is the translation of the design requirements into suitable weighting functions which have to be incorporated into the synthesis model. Again, as opposed to classical design, the requirements have to be quantified and are needed before controller synthesis can take place. This permits the robust control synthesis to directly and simultaneously take account of all the requirements over the whole modelled set of systems. In contrast to classical control, where the controller is first designed and afterwards it is checked wether each requirement is met. However, this is the hardest part of robust control, and in fact the accent has moved to the design of requirements rather than controller synthesis which is now an automatic process.

Handling Quality Requirements

The first set of performance requirements are modelled in terms of Handling Quality transfer functions. These transfer functions reflect ideal α, q and n_z responses to pilot stick input δ. They are given by equation (4.18):

$$\begin{aligned}
\frac{\alpha}{\delta}(s) &= K_\alpha \frac{1}{\left(\frac{s}{\omega_{shp}}\right)^2 + 2\frac{\zeta_{shp}}{\omega_{shp}}s + 1} \\
\frac{q}{\delta}(s) &= K_q \frac{1+\tau_q s}{\left(\frac{s}{\omega_{shp}}\right)^2 + 2\frac{\zeta_{shp}}{\omega_{shp}}s + 1} \qquad (4.18) \\
\frac{n_z}{\delta}(s) &= K_{n_z} \frac{1}{\left(\frac{s}{\omega_{shp}}\right)^2 + 2\frac{\zeta_{shp}}{\omega_{shp}}s + 1}
\end{aligned}$$

where K_α,K_q, K_{n_z} are the static gains, ω_{shp} and ζ_{shp} are the short period frequency and damping and τ_q the numerator time constant of the pitch rate transfer function to pilot stick displacements $\frac{q}{\delta}(s)$. The transfer functions in equation (4.18) reflect the shape of the responses of the to be designed control system. When we choose a certain value of the control anticipation parameter (CAP), defined in MIL-SPEC-8785C as $CAP = \frac{\omega_{shp}^2}{(n_z/\alpha)_{ss}}$, we can obtain lively, nominal or sluggish stick to pitch rate responses. The CAP is bounded within [0.16, 3.6] $rad.s^{-2}/g$. From the short period equation, the steady state relation $(n_z/\alpha)_{ss} = \frac{V}{\tau_q g}$, permits us to make a choice for ω_{shp}. The damping ζ_{shp} is chosen constant. The gains $K_q = K_{n_z}\frac{g}{V}$ and $K_\alpha = K_q\,\tau_q$ are determined for a particular choice of K_{n_z}.

Actutor effort

The actuator itself is modelled as a second order system with undamped frequency $\omega_{act} = 15\ rad/sec$ and damping $\zeta_{act} = 1$. The actuator limitations are posed on the elevator deflection, rate and acceleration. The bounds are given in the following:

$$\begin{aligned}
|\delta_e| &< 12\,\text{deg} \\
|\dot{\delta}_e| &< 30\,\text{deg}/sec \\
|\ddot{\delta}_e| &< 60\,\text{deg}/sec^2
\end{aligned}$$

The way to incorporate these bounds in the H_∞ context, consists of normalizing $\delta_e, \dot{\delta}_e, \ddot{\delta}_e$ with respect to the maximum values of $\delta_{e_{max}}, \dot{\delta}_{e_{max}}, \ddot{\delta}_{e_{max}}$. In the case that the weigthed (normalized) actuator activity is greater than unity, means that the bounds which are given by the performance requirement are violated. Further, to incorporate high frequency dynamics in the actuator an input multiplicative uncertainty $W_{act}(s)$ has incorporated in the actuator model.

Tracking Errors

The tracking error in q between the ideal model given by the handling qualities and the aircraft response are required to be less than 1 deg/sec for the pitch rate command system. This error level should be sustained up to 1.5 rad/sec. Above this frequency the error is allowed to increase up to 25 deg/sec. The shape of the error is modelled as first order high pass filter $W_q(s)$ having the shape of a classical sensitivity function. To keep errors to stick commands below the required level nothing more has to be done than normalizing the stick to error transfer function with $W_q(s)$. The normalization results in an inversion of the error filter, therefore we use $W_{q_{err}}(s) = \frac{1}{W_q(s)}$ as a weighting factor. As pointed out in [3], this dynamic weight is sufficient to fulfil requirements, therefore

the angle of attack and normal accleration errors are weighted with a constant factor of $W_\alpha = 0.01$ and $W_{n_z} = 0.01$. The total weighting filter for α, q and n_z is given by $W_{err}(s)$.

Sensor noise
In order to account for measurement imperfections in the air data system, sensor noise has been added to the measurements. These noises have high-pass band characterics. The noise shaping filters are chosen as:

$$W_{\alpha_{noise}}(s) = \frac{a_1 s + b_1}{c_1 s + d_1}$$

$$W_{q_{noise}}(s) = \frac{a_2 s + b_2}{c_2 s + d_2}$$

$$W_{n_{z_{noise}}}(s) = \frac{a_3 s + b_3}{c_3 s + d_3}$$

The total sensor noise weighting is given by $W_{noise}(s)$. Uncertainty and performance can now be stacked together into the general interconnection structure for synthesis and analysis.

4.4 General Synthesis Model

The resulting control configuration for design and analysis is shown in figure (15). The configuration contains all the requirements on the closed loop set of systems as previously given. However, we need to reformulate the problem in the general interconnection structure P as discussed before in order to make synthesis and analysis possible. Therefore we break the loops at the perturbations and the controller. Rearranging the problem accordingly to the three pairs of input/output signals (perturbations, performance variables and measurements/controls) we obtain the general synthesis structure as shown in figure (16). The first pair of input/output signals is related to the perturbation block $\Delta = \text{diag}\ \{\Delta_V,\ \Delta_\rho,\ \Delta_{aerou}\ \Delta_{cxu}\}$. It consists of Δ_V; a 8×8 diagonal repeated block for speed variations; Δ_ρ, a 5×5 repeated block for altitude variations, Δ_{aerou}; a 9×9 block for the uncertainty in the stability and control derivatives; and Δ_{cxu}, which is a 2×2 complex block for the unmodelled actuator and airframe dynamics.

The second pair is related to the performance variables from sensor noise and stick command to actuator effort and tracking errors. The remaining signal pair is from the elevator command to stick command and noisy measurements.

The complete structure has 29 inputs and 34 outputs. For design we shall use this model in increasing complexity level. By this we mean that we shall first carry out an H_∞ design (**Design # 1**) on a nominal model where the first 13 contributions to the Δ block are removed in order to get insight in the solution of the problem. For this same structure we shall apply μ-synthesis to improve the achieved performance level (**Design #2**). Then μ-synthesis is applied with respect to the whole perturbation structure (**Design # 3**). Finally, we shall shortly present the setup for the gain scheduled controller synthesis (**Design # 4**).

5 Limits of H_∞ Control

The open loop interconnection structure for design # 1 will be denoted as $P1$. We disregard the contribution of the parametric variations in speed and altitude and take into account only the uncertainties Δ_{aerou} and Δ_{cxu}. The reason for doing this is to reduce complexity of the design such that performance and stability requirements defined by the weights can be tuned appropriatly to satisfy the general robustness theorem. Initial design on $P1$ leads to a controller $K1$. The analysis structure $M1 = F_l(P1,\ K1)$ has a block partitioned structure where $M1_{11}$ reflects the robust stability contribution to $M1$. The matrix $M1_{11}$ is of dimension 11×11 and reflects how the closed loop system is affected by the perturbation. The nominal performance block is given by the matrix $M1_{22}$ having the dimension according to the performance variables 6×4. The performance block $M1_{22}$ reflects wether actuator effort and the tracking errors requirements to noises and stick commands are met by the achieved controller $K1$.

Performing a γ-iteration on the system $P1$ yields a controller $K1$ for design # 1. This controller achieves a final vaule of $\gamma = 47$. This means in the small gain contex that there exists a perturbation Δ with norm $1/47$ that destabilizes the closed loop system $M1$. Figure (17) shows the achieved ∞-norm of the closed loop system given by $\|M1\|_\infty$. In the same figure the lower curve gives the achieved structured singular value of the closed loop system, $\mu(M1) = 1.6$. Notice the gap between the achieved ∞-norm and the actual robust performance level given by the μ-plot. From the H_∞ point of view different choices of the weights are the only freedom we have to reduce the H_∞ norm of the system $M1$. However, if we look closely at the robust stability $\|M1_{11}\|_\infty$ and nominal performance $\|M1_{22}\|$ levels in figure (17) it can be deduced that the trade-off between stability and performance is

well balanced (0.42 and 0.58) and that the choice of the weights is reasonable. These facts together, bring us to proceed with a refinement step (design # 2) with μ-synthesis in order to reduce the robust performance level of the closed loop system. After one $D-K$-iteration the robust performance level has been brought down to 0.52, meaning that we have a robust performance level allowing a perturbation twice as large as the one used for this design. The reason for allowing such a large robust performance level comes from the fact that the later designs will include variations in speed and altitude which will greatly affect the performance level. The performance plots for $M2$ achieved by the second controller $K2$ are not given here. However, figure (18) shows the time histories to stick inputs of the closed loop system with the μ-controller $K2$. In each of the first three plots, both the required handling quality response and the achieved response by the control system have been plotted. The full line represents the handling quality requirements, while the dotted is the actual response of the controlled system. The error in the angle of attack is negligible while tracking on the pitch rate and normal acceleration is ideal. In the fourth plot, we see that actuator activity remains within the required bounds implying that this performance requirement has also been met by the μ controller. Since ideal stick to pitch rate response was the objective for our design we may conclude that μ-synthesis has been succesful in achieving robust handling quality requirements.

6 Performance Improvement via μ-Synthesis

For design # 3 the complete perturbation block is used, meaning that speed and altitude variations are now taken into account. The interconnection structure is $P3$. Starting in the same fashion as in the previous design, namely with an H_∞ design, we obtain after the first γ iteration a robust performance level in terms of the H_∞ norm bound on $M3$ of $\gamma = 329$. This is a drastic increase with respect to the last example. However, taking account of the structure of the perturbation and calculating $\mu(M3)$ we get a robust performance level of 2.8 wich is the upper curve in figure (19(a)). The remaing curves represent successively, from the largest to the smallest, the nominal performance level $\|M3_{22}\|_\infty$, the robust stability level $\mu_\Delta(M3_{11})$ which is built up by the real parametric uncertainty $\Delta_V, \Delta_\rho, \Delta_{aerou}$ and the complex uncertainty Δ_{cxu}. Each of these contributions to the robust stablity block are denoted as $\mu_{(\Delta_V, \Delta_{rho}, \Delta_{aerou})}(M3_{11})$ and $\mu_{\Delta_{cxu}}(M3_{11})$. As can be seen from this figure, the extra introduced uncertainty dramatically affects the robust performance level at frequencies beyond 1 rad/sec, while the nominal performance level is also heavily affected at low frequencies (compare with last design). Both nominal performance and robust stability have not been achieved in the first iteration.

To improve the performance of $M3$ we proceed by doing a $D-K$ iteration on this design. After 2 iterations we have achieved $\gamma = 1.6415$. In figure (19(b)), in the same order as in the previous figure, we have plotted the achieved robust performance level $\mu_\Delta(M3)$ which is about 1.37, and the individual contributions to it. Notice that the nominal performance level has been greatly reduced from 2.35 to 0.18 and now meets the requirements. The robust stability contribution has been reduced to about half of its original value (1.8 to 0.8) at the problem frequency, meeting now also the requirements. However the robust performance level is not yet achieved since $\mu(M3) = 1.37$. Further decrease of the robust performance level was not possible. We want to remark that we have made for this example complex μ calculations which are meant for complex valued uncertainties. On the other hand the largest part of the uncertainty in our problem is real valued meaning that these μ calculations can be viewed as conservative.

The time histories for design # 3 are given in the figures (20(a), 20(b), 20(c)). The the angle of attack, pitch rate and normal load factor responses again meet the hanling quality requirements. But from our μ analysis the handling quality requirement is not met robustly. Reducing slightly the operating range variations would improve the robust performance level. This can be done by scaling accordingly the required perturbation inputs on the matrix $P3$. The conclusion that the robust performance level is not met cannot be drawn from time analysis directly, it would require a Monte-Carlo simulation which is rather time consuming and expensive in contrast to the μ indicator which provides within minutes quite reliable robustness indications.

If we take into account the conservatism of the complex μ calculations we might say that this design was succesful in meeting the requirements.

Practically, this design is not realistic. This lies in the fact that the handling quality requirements

are chosen in our design to be independent of the flight condition. The aircraft handling should in fact be adapted to the flight condition as always has been done in industry. With μ-synthesis there is no formal way to design gain scheduled controllers that meet flight condition dependent robust performance requirements. A potential solution to this problem proposed by Packard [32] is "Gain Scheduling via Linear Fractional Transformations" which will be described briefly in the next section.

7 Guaranteed Performance for Gain Scheduled Controller

7.1 Gain Scheduled Controller Synthesis Formulation

The main fact to be recognized for the system $F_u(P, \mathcal{L}_\mathcal{N}[\delta])$ as shown in figure (21) is that a time varying parametric variations $\mathcal{L}_\mathcal{N}[\delta]$ can be formulated in linear fractional way. As long as the loop of the system P is closed with parametric variations, the system can be viewed as a linear parametrically time varying system. The second fact is that when we disconnect the parameter variations from the system P, we obtain a frozen parameter structure, representing a linear time-invariant system since time dependency has been disconnected. For our problem it is only required that the parametric variation is measurable and that it bounds are known. The resulting system can be viewed now as a classical interconnection structure where the disconnected inputs/and outputs reflect a perturbation on the system.

On the other hand for the controller to be synthesized as shown in figure (22), we require it to have a similar time varying structure in order to keep track of the parameter dependency of the system $F_u(P, \mathcal{L}_\mathcal{N}[\delta])$. In this formulation, we call both the plant and the controller LPV systems.

Combining the LPV plant with the LPV controller we obtain the closed loop LPV structure as shown in figure (23). This LPV structure is what we call the gain scheduled plant. The trick now is to wrap up the parameter dependency of the controller into the main system as shown in figure (24). This operation is legitimate since in our formulation the parameter dependency is linear. Drawn in this manner the parameter dependency becomes a perturbation for the original system and can be seen as a measurement for the controller. The new system structure is called $P_\mathcal{R}$. It remains now to disconnect the top loops in figure (24) to obtain the classical robust control problem where we want to find a stabilizing controller K such that $\|F_l(P_\mathcal{R}, K)\|_\infty < 1$. This small gain condition on the closed loop objective can be refined to a scaled small gain condition to take account of the perturbation structure. This problem is similar to the μ-synthesis problem where scalings have to be found such that "$\mu(F_l(P_\mathcal{R}, K))$" is minimized. This last condition is equivalent to find a scaling J and a controller K such that $\|JF_l(P_\mathcal{R}, K)J^{-1}\|_\infty$ is minimized. This condition is what we call scaled small gain condition and is pictorially shown in figure (26). The μ-synthesis method differs in two ways from our problem. First, the allowed scalings J are restricted to be real since the perturbation is now time varying and secondly the scales and controller are not anymore achieved via a $D-K$ iteration. In this problem both controller and scales are obtained in one time through the solution of a set of Linear Matrix Inequalities (LMIs) which are a generalization to Riccati equations. These LMIs can be efficiently programmed and solved in a Matlab Toolbox called "LMI-Lab", see [20].

7.2 Application Gain Scheduling to Flight Control Problem

When applying this method to our flight control design problem we obtain the closed loop structure as shown in figure (26) where the systems parameter dependency is reflected in the controller. The choice of the weighting functions remains unchanged and all the preparatory work has been done in the previous μ-synthesis step. We have written a program which for a certain specified γ level solves a feasibility optimization problem which returns the required scaling matrices and the parameter independent controller. The obtained controller has to be connected back through its perturbation inputs and outputs with the perturbation to form the required parameter dependent controller for gain scheduling. Results for design example # 4 are still under current investigation and will be presented in a future publication.

8 Conclusion

We have briefly shown some aspects of a general framework for modern robust control. In this framework we have seen how design methods such as H_∞ control, μ-synthesis and LPV control are formulated. Since it is not possible to cover all

the details we have included many other references than cited in the text discussing the technical aspects behind these methods. To illustrate the methods we have chosen a flight control design example and addressed to it some realistic requirements. An important advantage of the methods is that they need in advance the performance and robustness requirements that have to be achieved by the control law. By using LFT modelling on the system the designer handles a large set of models at once and can analyze systematically the system sensitivity to changing parameters. In this respect the new design methods brought a powerful modelling tool, the LFTs which can be used for many other purposes than control system design. Having specified the set of models we want to design for, we have translated the design requirements into suitable weighting functions and built up the general interconnection structure for control design and analysis. The advantage of this structure lies in that all requirements are optimized simultaneously by the methods in contrast to the classical design where we do not have such formalism. Having shown how to obtain the general interconnection structure for our flight control example, we have succesfully applied it to design methods such as H_∞ control and μ-synthesis. To appreciate the generality and flexibility we have shown that the general framework provides the possibility to formulate the synthesis problem for the design of gain scheduled controllers which has been always a serious problem in aircraft flight control design. We have not discussed all the methods that can be applied within this framework but we want to mention that a serious candidate for flight control problems which is also under investigation is nonlinear dynamic inversion recoverd by μ-synthesis, see [41]. This method does not require gain scheduling since it is directly applied on the non linear system equations. Finally, it can be resumed that the robust control community has brought with it a new fundament allowing the evolution of system modelling, identification and control within an unified framework, and that we are heading an exciting and rich future in this area.

The authors would like to thank: John Doyle (CalTech), Andy Packard (Berkeley), Gary Balas (Univ. Minnesota), Pascal Gahinet (INRIA), Carsten Scherer, Ton van der Weiden, Hans van der Vaart (Delft Univ.), Lieven Vanden Berghe (Stanford), John Gibson (UK, for fruitful discussions) and the National Aerospace Laboratory (NLR) for the financial support of this research.

9 References

1. P. Apkarian, Gahinet, P., Becker, G., "H_∞ control of Linear-Parametrically Varying Systems: A Design Example", *To appear.*
2. G.J. Balas, Doyle, J.C., Glover, K., Packard, A.K., Smith, R., (1990). $\mu-$Analysis and Synthesis Toolbox, (Musyn Toolbox).Matlab Functions for the Analysis and Design of Robust Control Systems. Sept, 1990.
3. G.J. Balas, Reiner, J., Garrad, W.L, "Design of a Flight Control System for a Highly Maneuvrable Aircraft Using μ Synthesis", *AIAA Guidance, Navigation and Control Conf.*, Monterey, Aug., 1993.
4. B.R. Barmish, Necessary and sufficient conditions for quadratic stabilizability of an uncertain system, *J. Optim. Theory Appl.* vol. 46, 1985, pp. 399-408.
5. G. Becker, A. Packard, D. Philbrick, G. Balas, Control of parametrically-dependent linear systems: A single quadratic Lyapunov approach, *Proceeding American Control Conf.*, June 1993, San Francisco.
6. S. Boyd and C. Barratt, "Linear controller design: Limits of performance," *Prentice Hall*, 1991.
7. S. Boyd and L. El Ghaoui, Method of centers for minimizing generalized eigenvalues, *Linear Algebra and its Applications*, Special Issue on Numerical Linear Algebra Methods in Control, 188 (1993) pp. 63-111.
8. R. Brockett, *Finite Dimensional Linear Systems* (Wiley, New York, 1970).
9. C. Davis, W. Kahan, and H. Weinberger, Norm preserving dilations and their applications to optimal error bounds, *SIAM Journal on Numerical Analysis*, vol. 19, no. 3, June 1982, pp. 445-469.
10. C. Desoer, M. Vidyasagar, *Feedback Systems:Input-Output Properties* (Academic Press, New York, 1975).
11. J.C. Doyle, Chu, C.C, Francis, B., Khargonekar, P., Stein, G., "Advances in Multivariable Control", Lecture Notes *ONR Honeywell Workshop*, Sept, 1984.
12. J.C. Doyle, B.A. Francis, A. R. Tannenbaum, (1992).*Feedback Control Theory.* Macmillan.
13. J.C. Doyle, K. Glover, P.P. Khargonekar, and B.A. Francis, State-space solutions to standard $\mathcal{H}_2$ and $\mathcal{H}_\infty$ control problems, *IEEE Trans. Auto. Control*, August, 1989.
14. J.C. Doyle, Analysis of feedback systems with structured uncertainties, *IEE Proceedings*, vol. 129, Part D, No. 6, Nov. 1982, pp. 242-250.
15. J.C. Doyle and A. Packard, K. Zhou "Review of LFT's, LMIs, and μ", *Proceedings Decision and Control Conf.*, pp. 1227-1232, Dec 1991, Brighton, England.
16. M. Fan, A quadratically convergent algorithm on minimizing the largest eigenvalue of a symmetric matrix, *Linear Algebra and its applications*, 188 pp. 231-253 (1993).

17. B.A. Francis, (1987). *A Course in H_∞ Control Theory.* Lecture Notes Control and information Sciences, vol.88, Springer-Verlag Berlin, Heidelberg.
18. P. Gahinet, A convex parametrization of $\mathcal{H}_\infty$ suboptimal controllers, *31st IEEE Conference on Decision and Control*, Tucson, 1992, pp. 937-942.
19. P. Gahinet, P. Apkarian, State-space $\mathcal{H}_\infty$ control: A complete solution via convex Riccati inequalities, submitted to Special Issue on $\mathcal{H}_\infty$ Control of *Int. Jour. of Robust, Nonlinear Control, To appear 1994.*
20. P. Gahinet, A. Nemirovskii, LMI-Lab. A package for Manipulating and Solving LMIs. August 1993.
21. K. Glover and J.C. Doyle, "State-space formulae for all stabilizing controllers that satisfy an $\mathcal{H}_\infty$ norm bound and relations to risk sensitivity," *Systems and Control Letters*, vol. 11, pp. 167-172.
22. F. Jarre, An interior-point method for minimizing the maximum eigenvalue of a linear combination of matrices, *SIAM Journal on Control and Optimization*, 31 pp. 1360-1377 (1993).
23. E. Kamen, P. Khargonekar, On the control of linear systems whose coefficients are functions of parameters, *IEEE Trans. Auto. Control,* AC-29, no. 1, January 1984.
24. P. Khargonekar, I. Peterson, and M. Rotea, $\mathcal{H}_\infty$-optimal control with state-feedback, *IEEE Trans. Auto. Control,* vol. 33, 1988, pp. 786-788.
25. P. Khargonekar, I. Peterson, K. Zhou, Robust stabilization of uncertain linear systems: Quadratic stability and $\mathcal{H}_\infty$ control theory, *IEEE Trans. Auto. Control,* vol. 35, March, 1990, pp. 356-361.
26. P. Khargonekar, E. Sontag, On the relation between stable matrix fraction factorizations and regulable realizations of linear systems over rings, *IEEE Trans. Auto. Control,* AC-27, 1982, pp. 627-638.
27. W. Lu and J. Doyle, "$\mathcal{H}_\infty$ control of LFT systems: An LMI approach," *31st IEEE Conference on Decision and Control*, Tucson, pp. 1997-2001, 1992.
28. G. Leitmann, Guaranteed asymptotic stability for some linear systems with bounded uncertainties, *ASME Journal of Dynamic Systems, Measurement and Control*, vol. 101, no. 3, 1979.
29. W. Lu, K. Zhou, and J. Doyle, "Stabilization of LFT systems," *30th IEEE Conference on Decisionand Control*, Brighton, pp. 1239-1244, 1991.
30. Yu. Nesterov and A. Nemirovsky, Interior point polynomial methods in convex programming: Theory and applications, Lecture notes in mathematics. (Springer Verlag, 1992).
31. M. Overton, Large-Scale Optimization of Eigenvalues, SIAM Journal on Optimization, vol. 2, no. 1, Feb. 1992, pp. 88-120.
32. A. Packard, "Gain scheduling via linear fractional transformations", *Systems and Control Letters*, 22, pp. 79-92 1994.
33. A. Packard and G. Becker, "Quadratic stabilization of parametrically dependent linear systems using parametrically dependent linear, dynamic feedback," *1992 WAM-ASME,* DSC-Vol. 43, submitted to the *ASME Journal of Dynamic Systems, Measurement, and Control*, June 1992.
34. A. Packard, G. Becker, D. Philbrick, and G. Balas, "Control of parameter-dependent systems: applications to $\mathcal{H}_\infty$ gain-scheduling," *First IEEE Conference on Aerospace Control Systems*, May 1993.
35. A. Packard and J. Doyle, "The Complex Structured Singular Value," *Automatica,* Vol. 29, No. 1, pp. 71-109, 1993.
36. A. Packard, J. Doyle and G. Balas, "Linear, Multivariable Robust Control With a μ Perspective," *Transaction of the ASME,* Vol. 115, pp. 426-437, June 1993.
37. A. Packard, K. Zhou, P. Pandey, and G. Becker, "A collection of robust control problems leading to LMI's," *Proc. of the 30th Conf. on Decision and Control,* December, 1991.
38. A. Packard, K. Zhou, P. Pandey, J. Leonhardson, and G. Balas, Optimal, constant I/O similarity scaling for full-information and state-feedback control problems, *Systems and Control Letters*, vol. 19, 1992, pp. 271-280.
39. I. Petersen, Disturbance attenuation and $\mathcal{H}_\infty$ optimization: a design method based on the algebraic Riccati equation, *IEEE Trans. Auto. Control,* vol. 32, 1987, pp. 427-429.
40. R. Redheffer, On a certain linear fractional transformation, J. Math. Phys., vol. 39, 1960, pp. 269-286.
41. J. Reiner, G.J. Balas, W.L. Garrard, Design of a Flight Control System for a Highly Maneuvrable Aircraft Using Robust Dynamic Inversion. *Submitted to the AIAA Journal of Guidance, Dynamics and Control.*
42. W. Rugh, Analytical framework for gain scheduling, *IEEE Control Systems Magazine,* vol. 11, no. 1, 1991, pp. 74-84.
43. M. Safonov, D. Limbeer, and R. Chiang, Simplifying the $\mathcal{H}_\infty$ theory via loop shifting, matrix pencil, and descriptor concepts, *Internat. Jour. Control,* vol. 50, 1989, 2467-2488.
44. M. Sampei, T. Mita and M. Nakamichi, An algebraic approach to $\mathcal{H}_\infty$ output feedback control problems, *Systems and Control Letters*, vol. 14, 1990, pp. 13-24.
45. C. Scherer, $\mathcal{H}_\infty$ optimization without assumptions on finite or infinite zeros, *SIAM Journal on Control and Optimization*, vol. 30, no. 1, 1992, pp. 143-166.
46. S. Shahruz, S. Behtash, Design of controllers for linear parameter varying systems by the gain scheduling technique, *Journal of Mathematical Analysis and Applications*, vol. 168, no. 1, 1992, pp. 195-217.
47. J. Shamma, M. Athans, Gain scheduling: Potential hazards and possible remedies, *IEEE Control Systems Magazine,* vol. 12, no. 3, 1992, pp. 101-107.

48. J. Shamma, M. Athans, Analysis of nonlinear gain scheduled control systems, *IEEE Trans. Auto. Control,* vol. AC-35, No. 8, 1990, pp. 898-907.
49. J. Shamma, M. Athans, Guaranteed properties of gain scheduled control of linear parameter-varying plants, *Automatica,* vol. 27, no. 3, May 1991, pp. 559-564.
50. G. Stein, Doyle, J.C., " Beyond Singular Values and Loop Shapes, "*A.I.A.A. Journal of Guidance and Control.*, Vol. 14, pp.5-16, 1991.
51. L. Vandenberghe, S. Boyd, Primal-dual potential reduction method for problems involving matrix inequalities, Technical Report, Informations Systems Laboratory, Electrical Engineering Dept., Stanford University, Stanford, CA.
52. J. Wang and W. Rugh, Parametrized linear systems and linearization families for nonlinear systems, *IEEE Trans. on Circuits and Systems*, CAS-34, no. 6, June 1987, pp. 650-657.
53. J. Willems, Least squares stationary optimal control and the algebraic Riccati equation, *IEEE Trans. Auto. Control*, vol. AC-16, no. 6, Dec. 1971.
54. K. Zhou, P. Khargonekar, An algebraic Riccati equation approach to $\mathcal{H}_\infty$ optimization, *Systems and Control Lett.*, vol. 11, 1988, pp. 85-91.

Figures

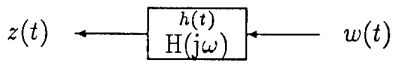

Figure 1: Input/output configuration

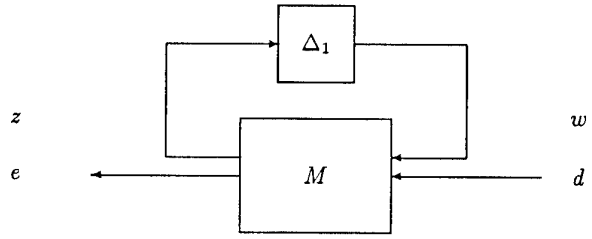

Figure 2: Linear Fractional Transformation

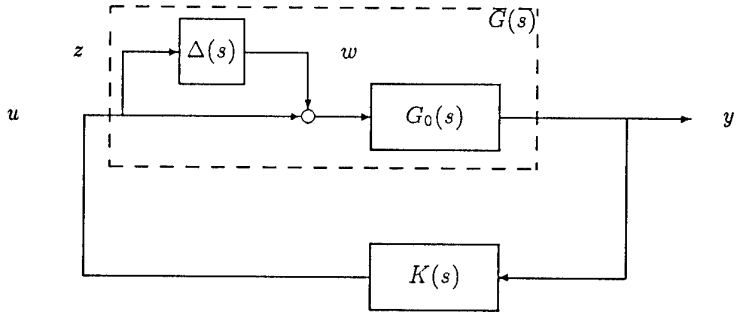

Figure 3: Closed loop system with input multiplicative uncertainty on $G_0(s)$

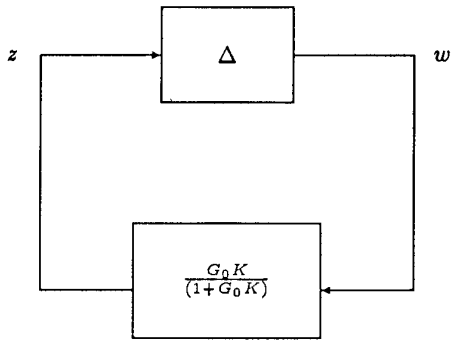

Figure 4: Analysis Configuration

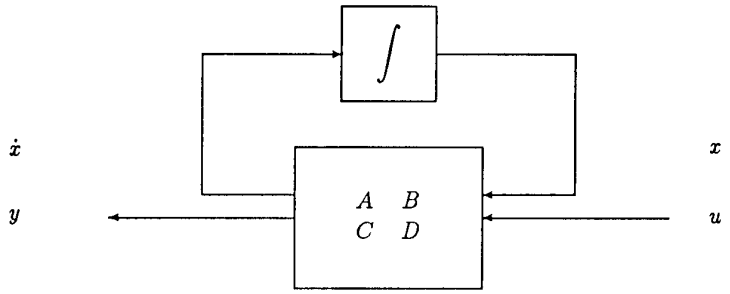

Figure 5: State-space LFT

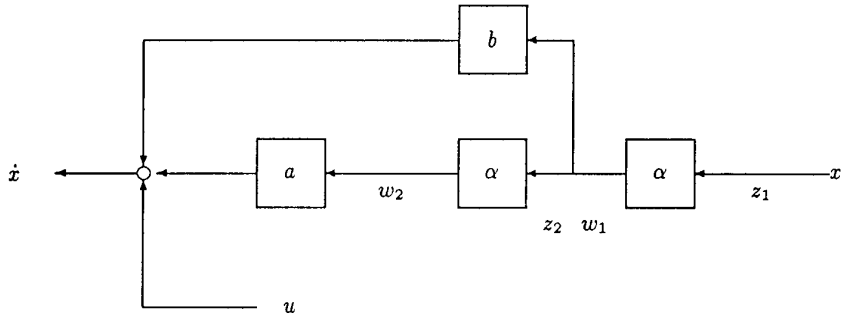

Figure 6: Perturbed state-space system

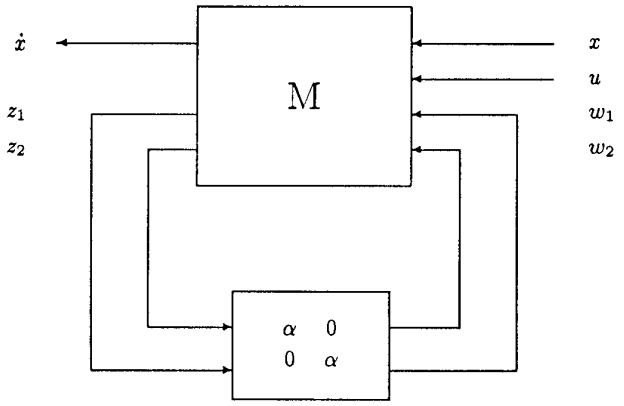

Figure 7: LFT representation varying system

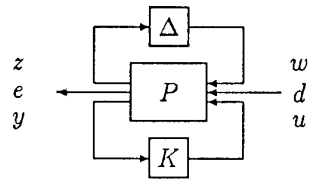

Figure 8: General Analysis and Synthesis framework.

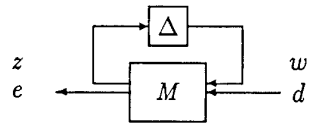

Figure 9: Analysis part General interconnection structure

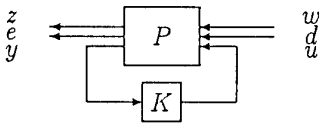

Figure 10: Synthesis part General interconnection structure

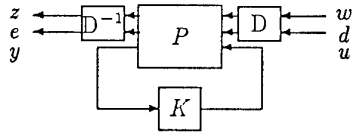

Figure 11: D-Scaled synthesis structure

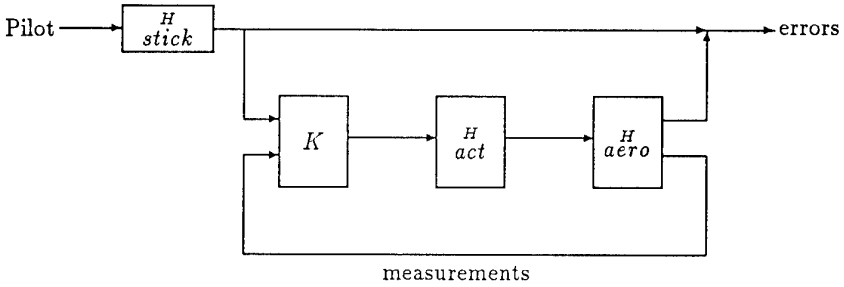

Figure 12: Fly-by-wire Control configuration

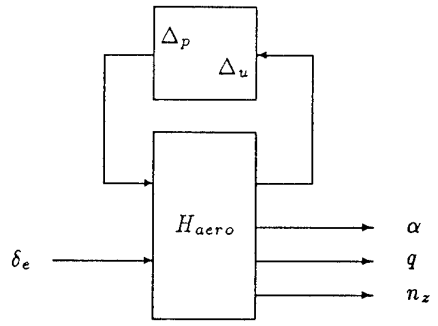

Figure 13: Aero model with Parametric variations and Uncertainties

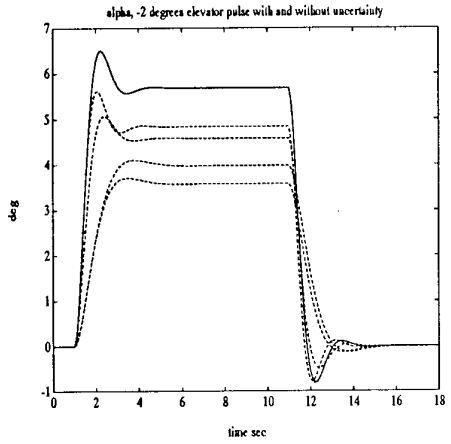

(a) α response

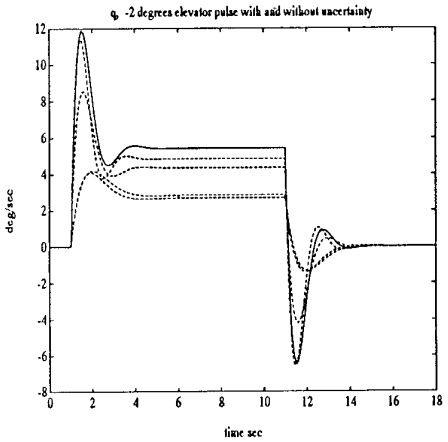

(b) q response

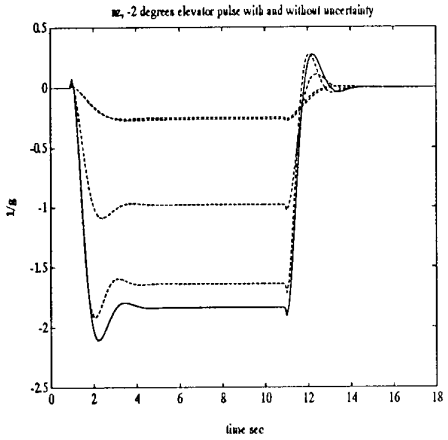

(c) n_z response

Figure 14: Step responsse LPV modelled system

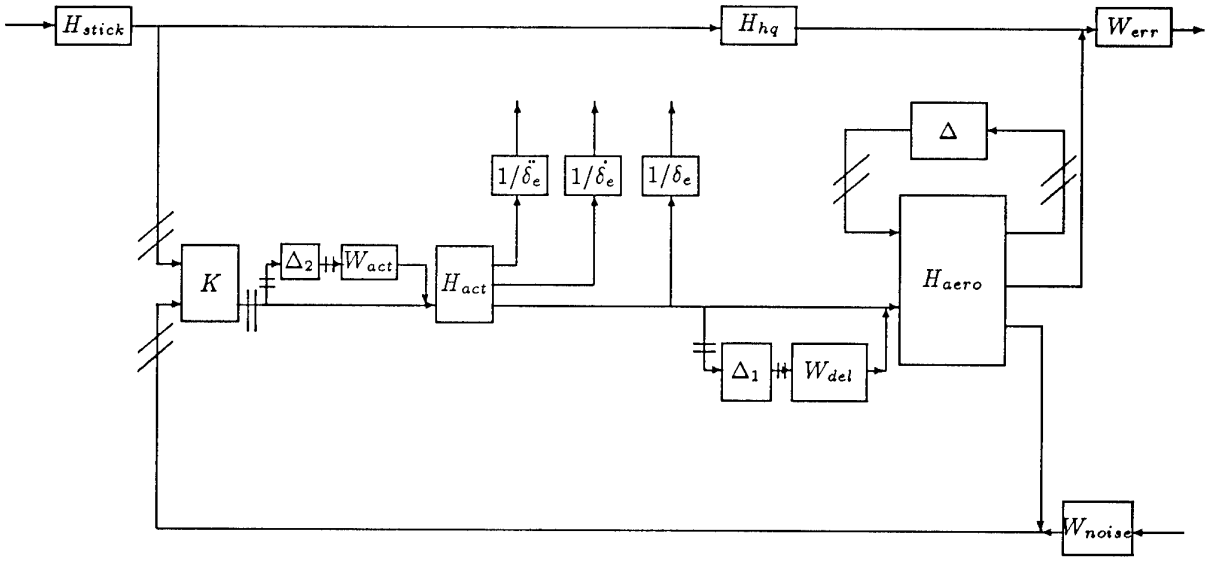

Figure 15: Control Configuration Including Requirements

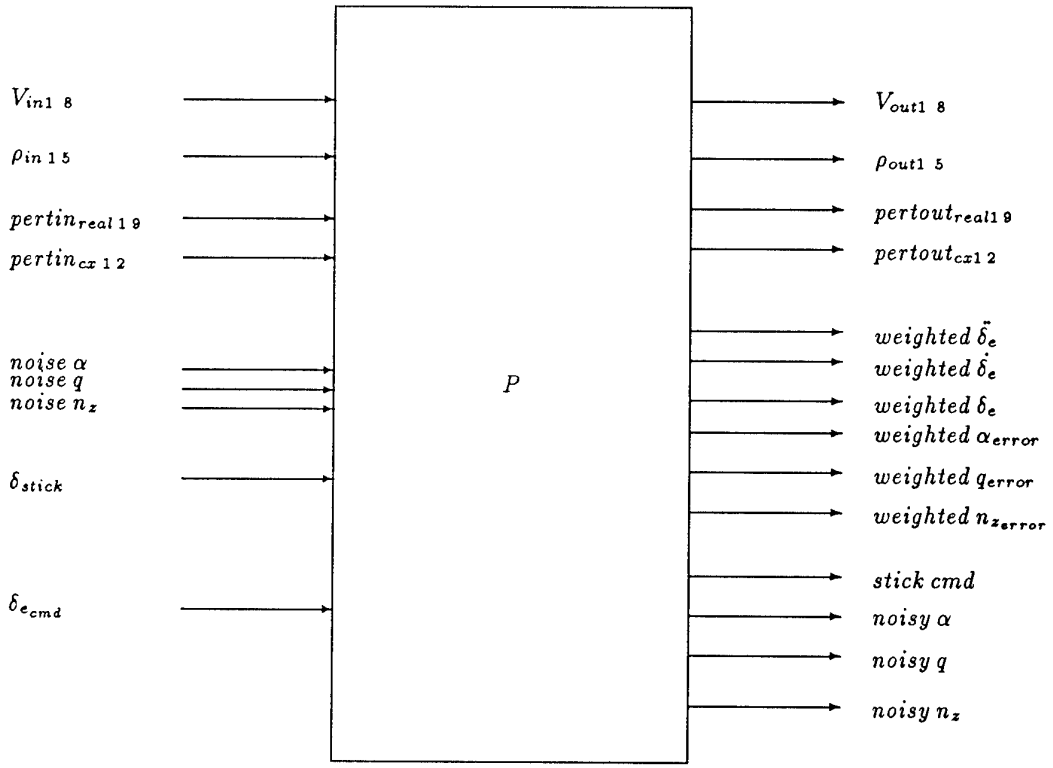

Figure 16: General Synthesis Structure

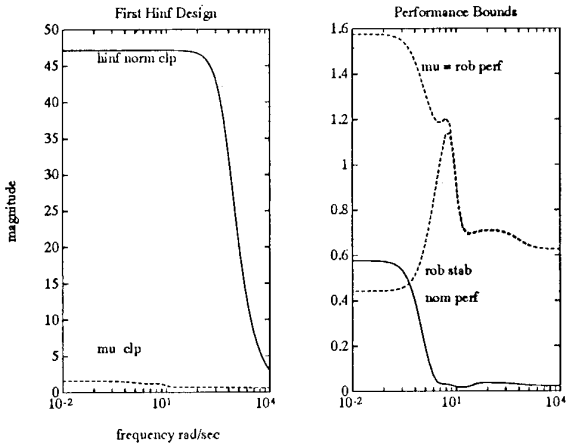

Figure 17: Initial H_∞ Design

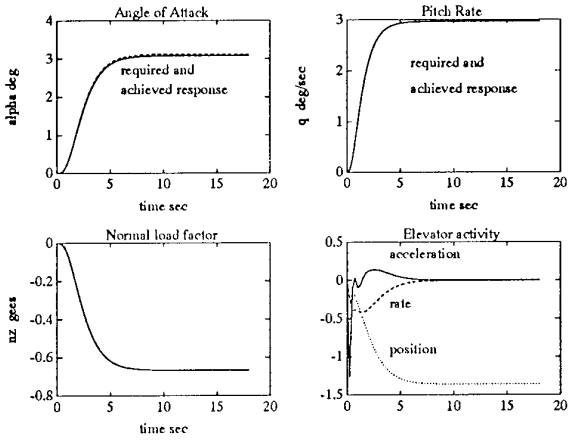

Figure 18: Achieved step responses design # 2

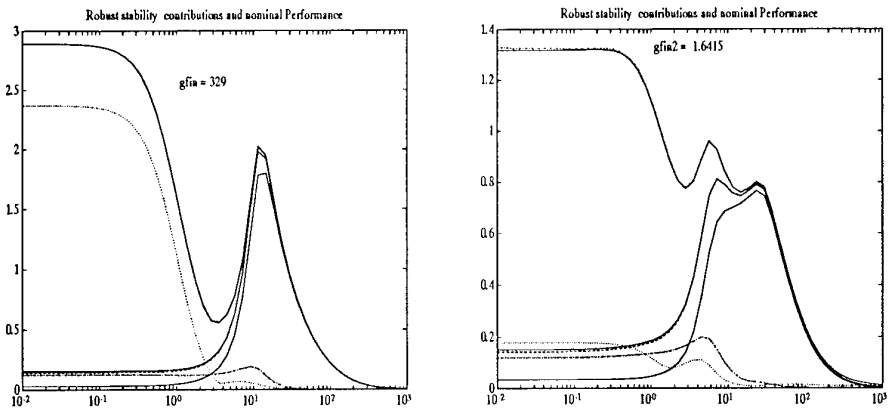

(a) Design with parametric uncertainty

(b) Performance after second $D-K$ iteration

Figure 19: Performance plots μ-design

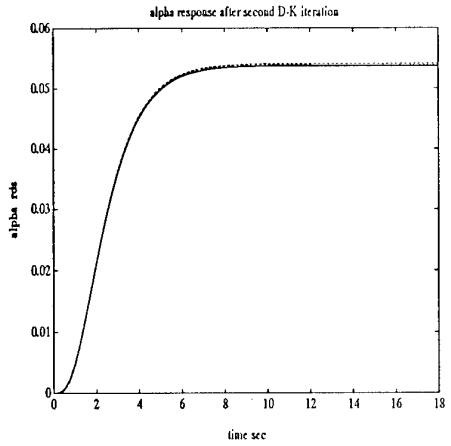

(a) Alpha responses

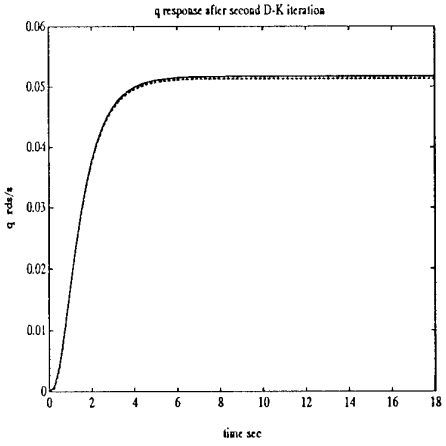

(b) Pitch rate responses

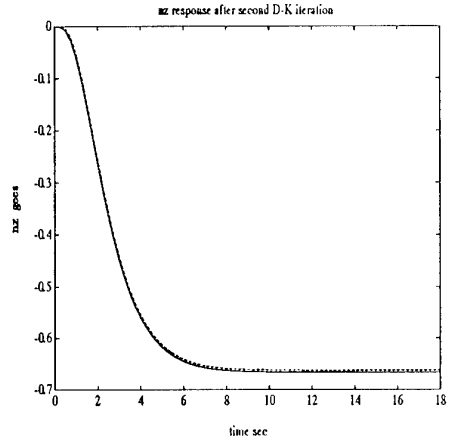

(c) Normal load factor responses

Figure 20: Responses to stick input, ideal and achieved

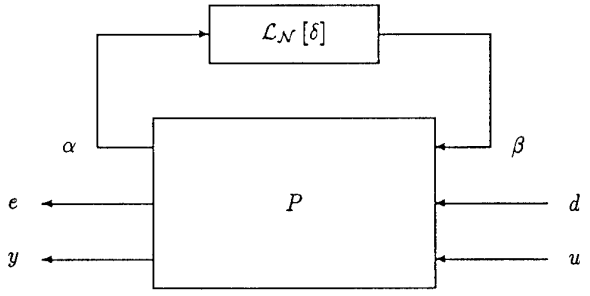

Figure 21: Parameter-dependent Plant

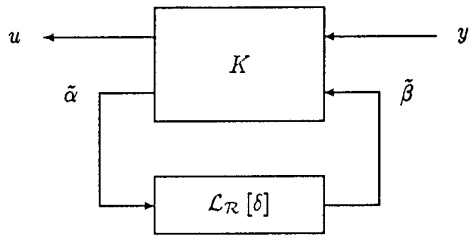

Figure 22: Parameter-dependent Controller

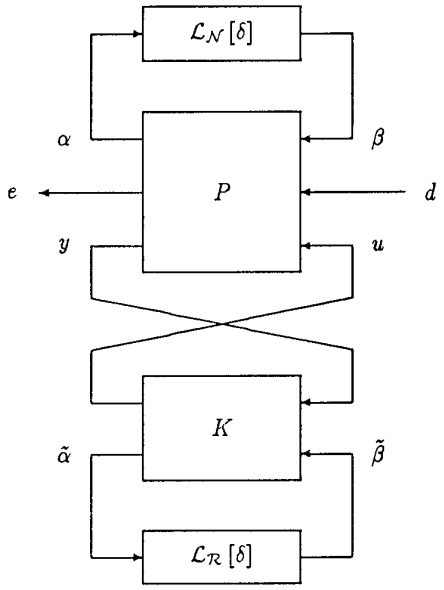

Figure 23: Closed-loop System

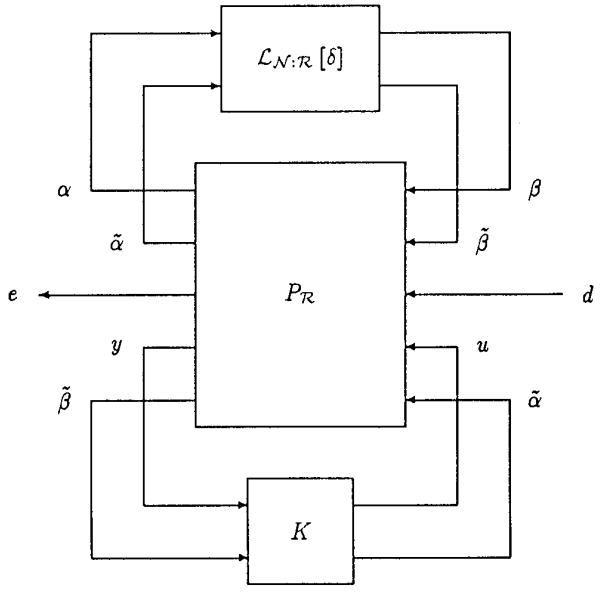

Figure 24: Parameter-dependent closed-loop system, redrawn

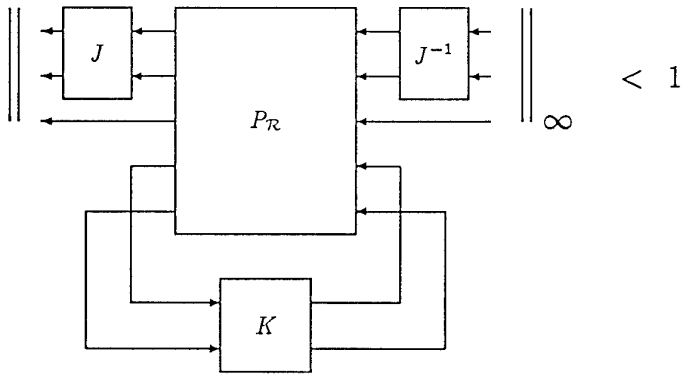

Figure 25: Scaled Small-Gain Condition

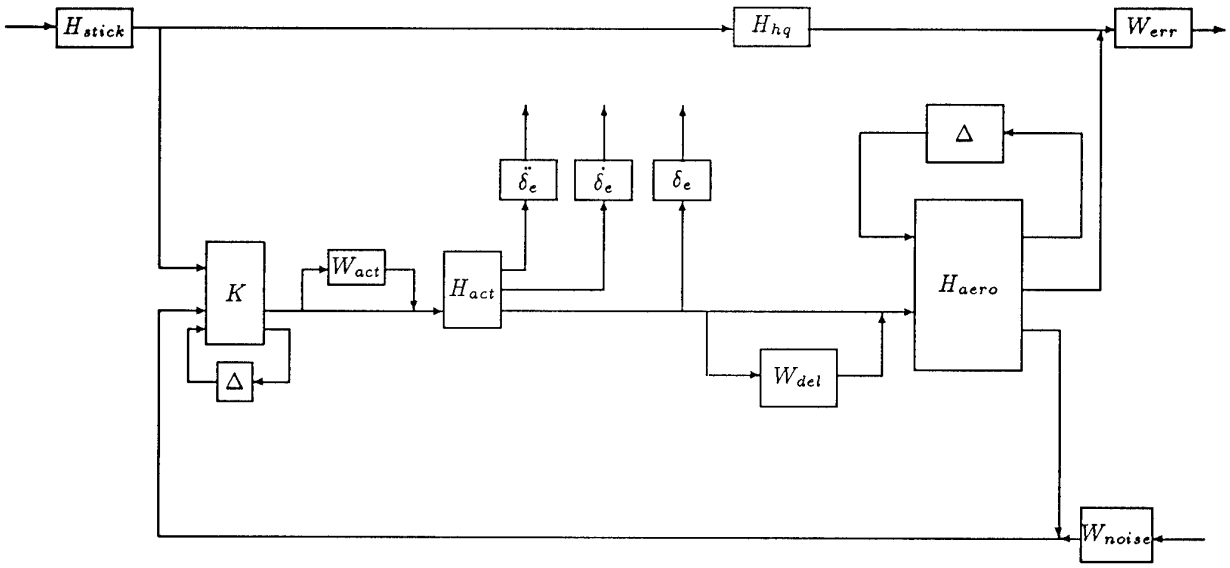

Figure 26: General Interconnection Structure for LPV control

Dynamic Inversion: An Evolving Methodology for Flight Control Design

Dale Enns[1] Dan Bugajski[2] Russ Hendrick[2] Gunter Stein[2]

[1]MN-65-2700, Honeywell, Inc., 3660 Technology Drive, Minn, MN 55418, U.S.A.

[2]MN-65-2500, Honeywell, Inc., 3660 Technology Drive, Minn, MN 55418, U.S.A.

Abstract

This paper describes nonlinear dynamic inversion as an alternative design method for flight controls. The method is illustrated with super-maneuvering control laws for the F-18 High Angle-of-Attack Research Vehicle (HARV).

1. Introduction

Flight control systems have evolved dramatically over the past few decades. They started as limited authority analog systems, intended to provide a bit of stability augmentation for otherwise well-behaved airframes. They have evolved to full-authority digital systems, critical to stability and full envelope performance for otherwise unflyable airframes.

Control laws and design methods for these systems have evolved dramatically as well. They have progressed from very simple fixed-form feedback structures (e.g., pitch rate to elevator), with gains tuned by control engineers in flight, to complex multivariable feedback laws, designed with modern multivariable tools that optimally trade off command responses, disturbance responses, and robustness characteristics of the final closed-loop airframe/controller combination.

Today's prevailing paradigm for flight control design is based on the divide-and-conquer approach common to many complicated engineering tasks. An airframe is first partitioned into many separate operating regimes (flight conditions). For each of these regimes, a linearized dynamic model approximates the airframe well, and the tools of linear control theory can be used to design individual compensators to satisfy closed-loop specs. Next, the individual compensators are 'stitched together' with gain schedules to cover the full flight envelope. The resulting scheduled control law is then verified with extensive nonlinear simulations and with carefully executed flight tests before the design is finalized. While this overall design process is intended to avoid costly surprises at the last moment, recent experiences with the YF-22, the JAS-39 and other new airplanes demonstrate that we are not always successful.

Over the last decade or so, control researchers have begun to apply an alternate methodology to flight control design [Meyer, 1984; Lane, 1988; Bugajski, 1992]. This alternative is variously called *dynamic inversion* [Morton, 1987; Elgersma, 1988] or *feedback linearization* [Brockett, 1978; Hunt, 1981; Isidori, 1985]. We believe that this methodology will eventually replace the divide-and-conquer approach as the prevailing paradigm. With dynamic inversion, the initial step of dividing the design problem into separate operating regimes is bypassed. Instead, a nonlinear control law is fashioned which globally reduces the dynamics of selected controlled variables (CVs) to integrators. A closed loop system is then designed to make the CVs exhibit specified command responses while satisfying the usual disturbance response and robustness requirements for the overall system and the various physical limitations of the aircraft's control effectors.

The chief advantage of this emerging alternative is that it avoids the gain-scheduling step of the current method. This step is time consuming, costly to iterate, and still relies substantially on engineering art. The new alternative also offers greater for generality for re-use across different airframes, greater flexibility handling changing models as an airframe evolves during its design cycle, and greater power to address non-standard flight regimes such as supermaneuvers. These advantages, and some of their costs, will become evident in our discussion of the methodology below. We begin in Section 2 with a review of the basic principles behind dynamic inversion. We then discuss its central step for flight control, namely the choice of specific controlled variables, in Section 3. Some implementation issues are described in Section 4, a serious design example for the F-18 HARV follows in Section 5, and concluding comments are made in Section 6.

2. Basic Principles of Dynamic Inversion

Aircraft Equations of Motion

Rigid body dynamics of aircraft are described globally (over the full flight envelope) by a set of twelve nonlinear differential equations, two each for six degrees of freedom. We will summarize these equations as follows;

$$\frac{dx}{dt} = \mathbf{F}(x, u) \qquad (1)$$

$$y = \mathbf{H}(x) \qquad (2)$$

where the symbols, $\mathbf{F}(.,.)$ and $\mathbf{H}(.)$, denote nonlinear functions known to us reasonably accurately as a mix of analytic expressions and tabular data [see for example, Etkin, 1972; McRuer, 1973].

The symbol, x, denotes the usual state vector comprised of the following components:

- three rotation rates about body axes (p,q,r),
- three attitudes, measured with respect to the airstream, (α,β,μ),
- three velocity components, described by total velocity , flight path angle,

  and heading angle, (V,γ,χ), and
- three inertial position coordinates, (X,Y,H).

The symbol, u, denotes the positions of all control effectors. This includes the usual elevator, aileron, and rudder surface deflections, but it also includes any additional surfaces, such as canards or leading edge devices, forebody controls, and any thrust modulation and vectoring capabilities available on the airframe.

Finally, the symbol, y, denotes selected CVs, variables to be controlled. These variables are discussed at length in Section 3.

Alternate Forms

By means of appropriate changes of variables, it is often possible to rewrite equations (1)-(2) in the following alternate form:

Paper presented at the Flight Mechanics Panel Symposium held in Turin, Italy, from 9-13 May 1994.

$$\begin{aligned} dy/dt &= y_1 \\ dy_1/dt &= y_2 \\ &\vdots \\ dy_m/dt &= f_y(x, u) \\ dz/dt &= f_z(x, u) \end{aligned} \qquad (3)$$

where $(y, y_1, y_2, \ldots, y_m, z)^T = \mathbf{T}(x)$ is a transformed version of the original state vector.

To obtain this alternate form formally, we can time-differentiate $y(x(t))$ in equation (2) and define its derivative expression to be a new function, $y_1(x)$. Next, we time-differentiate $y_1(x(t))$ and define its derivative expression to be $y_2(x)$, then we time-differentiate $y_2(x(t))$ and define $y_3(x)$, etc. We stop when the control variables, u, appear explicitly in the next time-derivative. Then, as a final step, we must complete the state transformation by selecting a function, $z(x)$, which fills out $(y_1(x), y_2(x), \ldots, y_m(x), z(x))^T = \mathbf{T}(x)$ and makes it invertible for all x.

This formal process does not always work for arbitrary nonlinear systems. However, sufficient conditions under which the process is rigorous are known, as are conditions under which the last derivative expression, $f_y(x, u)$, turns out to be invertible in u [Hunt, 1981; Isidori, 1985]. Fortunately, for rigid body aircraft dynamics, the process always succeeds, and indeed, it does so with m=0. This happens because equations (1)-(2) have CVs for the three pitch, roll, and yaw axes, each including a body rate, and the control effectors primarily produce torques in these same three axes. As a result, we get a single three-element equation,

$$\frac{dy}{dt} = \left[\frac{\partial \mathbf{H}}{\partial x^T}\right] \mathbf{F}(x, u) \qquad (4)$$

Furthermore, the right hand side of this equation turns out in most cases to be linear in u, thus yielding the form,

$$\frac{dy}{dt} = f(x) + g(x)\, u \qquad (5)$$

with $g(x)$ invertible for all values of x.

Globally Linearizing Controllers

Given equation (5), it is easy to fashion control laws which reduce the controlled variables' dynamics to linear ones. For example, the control law,

$$u = g(x)^{-1} [-f(x) + v] \qquad (6)$$

yields simple integrations for y,

$$\frac{dy}{dt} = v \qquad (7)$$

and it also provides new control variables, v, which will be used later to make y(t) behave as desired. Of course, while these new controls are 3-dimensional, they are in general produced by more than three physical control effectors. For such cases, $g(x)^{-1}$ in (6) should be interpreted as a (non-unique) right inverse. Potential versions of this inverse are discussed further in Section 4.

Zero Dynamics

At this point, astute readers will have raised at least two major concerns about the concept:

1) How good must airframe models be to realize equation (6) adequately ?

2) What happens to the remaining variables, z, in the new state vector when y is controlled but not z ?

The first question deals with robustness of the control law and is addressed in detail in Section 3. The second question deals with so-called *zero dynamics* [Isidori, 1985] or *complementary dynamics* [Elgersma, 1986] of equations (1)-(2) and must be addressed by insuring that these dynamics are stable and well-behaved.

Conceptually, zero dynamics are nothing more than the remaining motions permitted by equation (1) when the CVs in equation (2) are constrained to be constant or prescribed. That is, they are the solutions of

$$\frac{dx}{dt} = \mathbf{F}(x, u) \text{ with constraints } \mathbf{H}(x) = c \qquad (8)$$

If $\mathbf{F}(.,.)$ and $\mathbf{H}(.)$ were linear functions, i.e.. $\mathbf{F}(x,u) = Fx+Gu$ and $\mathbf{H}(x) = Hx$, then these constrained solutions would be determined by the zeros of system (1)-(2). Specifically, with v=0 they would satisfy

$$x(t) = \sum_i a_i x_i \exp(z_i t) \qquad (9)$$

where a_i, i=1,2,..,m, are arbitrary constants, and (z_i, x_i), i=1,2,..,m, are zero/zero-direction pairs, defined by a generalized eigenvalue problem [Rosenbrock, 1970].

$$0 = \begin{bmatrix} z_i \mathbf{I} - \mathbf{F} & \mathbf{G} \\ \mathbf{H} & 0 \end{bmatrix} \begin{bmatrix} x_i \\ u_i \end{bmatrix} \qquad (10)$$

Note that these constrained solutions are not observable in the outputs, i.e. Hx=0, and they are stable and well-behaved whenever all zeros of the CVs are located in the left half plane and have reasonable damping ratios.

Zero dynamics are simply nonlinear generalization of these same ideas, and CVs must likewise be chosen to make them stable and well-behaved. We will use the linear interpretation in Section 3 to verify that our selected CVs do indeed have such properties.

3. Controlled Variable Selections

It is already evident that CVs play a central role in the dynamic inversion concept. We must actually be concerned with two aspects of CVs. The first is the choice of the variables themselves, and the second is the closed-loop dynamic characteristic we elect to impress upon them by means of an (as yet undetermined) control law for v. Both aspects influence the quality of final designs. They determine how we satisfy handling quality specs, how we attenuate disturbance responses, how we get good zero dynamics, and how we get favorable performance/robustness trade-offs for the overall closed loop system. We treat each of these considerations in turn.

Handling Quality Specifications

One of the main jobs of a flight control system is to produce good responses for pilot commands. The characteristics of 'good responses' are well known from years of studies, piloted experiments, and flight experience, and are documented in existing military specifications [MIL-STD-1797A, 1987]. They usually take the form of equivalent linear system models for the primary commanded variables, with model parameters constrained to fall into specified ranges. The following table

summarizes CV selections and associated closed-loop dynamic characteristics which provide effective ways to satisfy these specifications:

Table 3.1: Recommended Controlled Variables

Axis	Variable (y_i)	Closed-Loop Response
Pitch	$q + n_Z/V_{CO}$	first order with ω=5r/s, τ=0.2s
Roll	$p + \alpha r$	same as pitch
Yaw	$r - \alpha p$ $-g\sin(\phi)\cos(\theta)/V + k\beta$	same as pitch

These recommendations work well for most conventional flight regimes and piloting tasks. They may need modifications, however, for other situations, such as high-α and very low speed flight, and for other command modes, such as direct lift and side-force.

For example, the pitch axis variable, $q+n_Z/V_{CO}$, is motivated by the historical C*-criterion for conventional flight. It has one free parameter, the crossover velocity V_{CO}, which must be adjusted to match the separate equivalent system requirements for q- and n_Z-responses in current military specs. Moreover, its closed-loop response time constant must be selected to satisfy specific Level 1 flying quality numbers identified in the specs for the appropriate vehicle class. (The numbers in Table 3.1 are for fighters.) In order to make this variable work properly in high-α flight, it is desirable to replace n_Z with $K\alpha$ (this avoid the destabilizing effect of lift-curve slope reversal) and to add pitch/lateral-directional decoupling terms, $(g\cos(\phi)\cos(\theta)-Vp)/U$. We will also add an airspeed term later, in order to fine-tune the zero dynamics.

Similarly, the roll axis variable, $p+\alpha r$, which represents stability axis roll rate (roll about the velocity vector), would be replaced by a full nonlinear version, $p_S=\cos(\alpha)p+\sin(\alpha)r$, and the lateral-directional variable, $r-\alpha p-g\sin(\phi)\cos(\theta)/V+k\beta$, which enforces conventional coordinated turns with zero sideslip, would include the full nonlinear version of stability axis yaw rate.

Disturbance Attenuation

In addition to providing good command responses, flight controllers must, of course, also attenuate undesirable external disturbances. These are caused primarily by atmospheric turbulence and gusts, and their responses must be suppressed to the point where ride-quality is acceptable for the crew, residual motions are acceptable for the payload, and in some cases, loads are acceptable for the structure.

Fortunately, the CV selections in Table 3.1, when controlled to their recommended bandwidth (ω), do a generally good gust-suppression job. Issues usually arise only in the pitch axis and can be easily addressed by changing V_{CO} (to place more emphasis on acceleration) and/or by increasing the bandwidth beyond the handling-quality-derived number.

Of course, when these changes are made, the command responses of the closed-loop system also change. This effect must then be corrected with command pre-filters to restore the original responses. We will see shortly that there are other reasons as well to change the properties of the CV feedback loops. These reasons also call for pre-filters to restore nominal command responses, so the presence of pre-filters is inevitable.

Fine-Tuned Zero Dynamics

As discussed above, one aspect of the dynamic inversion concept is the presence of hidden zero dynamics. These dynamics are implicitly defined by our selected CVs, and we must examine them separately to make certain that they are stable and well-behaved.

While it is far from trivial to establish properties of zero dynamics globally [for an example, see Morton, 1991]), local properties obtained from linearizations are often enough to identify potential problems. To illustrate this, Table 3.2 examines the pitch axis CV from Table 3.1, using a linearized pitch axis model. The model has typical short period and phugoid modes, with the phugoid stable but lightly damped. The CV has one stable zero in the short period frequency range and two more zeros in the phugoid range. Unfortunately, one of the latter is slightly unstable. As a result, dynamic inversion controllers based on this CV would destabilize the phugoid motions.

Although the instability would not be severe (time to double ≈ 150s), it can be alleviated entirely by adding a small airspeed term to the CV. This option is illustrated as CV' in Table 3.2. Of course, this modification also requires that we include an airspeed trim term (in addition to the usual g/V_{CO} trim term) in order to command equilibrium flight. This additional trim term can consist of low-passed actual airspeed, or it can be avoided entirely by high-passing airspeed in CV'.

Similar analyses for the roll and lateral-directional CVs in Table 3.1 show no local zero dynamics problems, and simulations studies described later in Section 5 provide high confidence that none exist globally.

Table 3.2: Local Properties of Pitch Zero Dynamics
F-18 HARV, Mach=0.65, H=16000ft

State Space Model	V	α	q	γ	δ
dV/dt	-8.2900E-03	-2.9680E+01	9.8570E-02	-3.2170E+01	-3.5080E-02
dα/dt	-1.6300E-04	-1.1300E+00	9.8840E-01	3.6380E-06	-1.3650E-03
dq/dt	-7.5080E-05	-4.9820E+00	-5.0880E-01	-9.6620E-07	-8.6590E-02
dγ/dt	1.6300E-04	1.1300E+00	1.1580E-02	-3.6380E-06	1.3650E-03

Poles	Real	Imaginary	Magnitude	Damping
	-3.3222E-03	±6.5146E-02	6.5231E-02	5.0930E-02
	-8.2022E-01	±2.1966E+00	2.3448E+00	3.4981E-01

CV					
	2.7160E-04	1.7384E+00	1.0036E+00	0.0000E-00	0.0000E-00
Zeros of CV	Real	Imaginary	Magnitude	Damping	
	4.6836E-03	0.0000E-01	4.6836E-03	-1.0000E+00	
	-1.0525E-02	0.0000E-01	1.0525E-02	1.0000E+00	
	-2.7058E+00	0.0000E-01	2.7058E+00	1.0000E+00	

CV'					
	0.0000E-00	1.7384E+00	1.0036E+00	0.0000E-00	0.0000E-00
Zeros of CV'	Real	Imaginary	Magnitude	Damping	
	-3.6455E-03	5.6852E-02	5.6969E-02	6.3991E-02	
	-3.6455E-03	-5.6852E-02	5.6969E-02	6.3991E-02	
	-2.7045E+00	0.0000E-01	2.7045E+00	1.0000E+00	

Robustness Properties

Of course, good nominal responses and well-behaved zero dynamics are not enough. These qualities must also be robust with respect to various modelling errors inherent in aircraft systems. Unfortunately, robustness properties of dynamic inversion have received too little attention in the literature so far [some references are Spong, 1987; Kravaris, 1987; Akhrif, 1988]. We summarize some of the known results below. Much

stronger results will be needed to encourage broader use and acceptance of the methodology.

The major dynamic inversion robustness issues are exhibited by replacing the nominal aircraft model in equation (5) with a perturbed model, i.e.

$$\frac{dy}{dt} = (f + \delta f) + (g + \delta g)\, u, \qquad (11)$$

and also replacing the ideal control effector position in equation (6) with a perturbed value obtained by passing the ideal position through actuator dynamics, flexible structural elements, and other high-frequency uncertainties, i.e.

$$u = (\mathbf{I} + \Delta) g(x)^{-1}(-f(x) + v) \qquad (12)$$

where D(s) is an arbitrary stable dynamic perturbation, small for low frequency signals, but increasing in size to unity and beyond as frequency increases. A short derivation shows that the resulting dynamic model for y is then given by

$$\frac{dy}{dt} = (\delta f - \mathbf{D} f) + (\mathbf{I} + \mathbf{D})\, v, \qquad (13)$$

with

$$\mathbf{D} = g \Delta g^{-1} + \delta g\, g^{-1} + \delta g\, \Delta\, g^{-1} \qquad (14)$$

These equations replace the integrators in equation (7) as a new dynamic model for our CVs. Note that there are two major uncertainty terms. The first term, (δf-**D**f), is a direct disturbance input to the integrators, while the second term, (**I**+**D**)v, is a multiplicative perturbation on the control inputs of the integrators. Both terms are correlated through their common perturbation operator **D**, and all functions in this operator, f, g, df and dg, remain dependent on the state vector, $x = \mathbf{T}^{-1}(y,z)$.

The Linear Case: Note that the new model is still almost linear. Only the perturbation terms are not linear. If we ignore this fact for the moment, there are well-established design methods available to construct robust controllers. Perhaps the simplest of these are loop-shaping methods which satisfy norm-based robustness constraints on the CV-feedback loops [Doyle,1981]. We have two basic constraints:

1) Sufficient condition for robust stability with respect to the multiplicative term alone:

$$\sigma_{max}[(\mathbf{I} + \mathbf{K}(s)\mathbf{P}(s))^{-1}\mathbf{K}(s)\mathbf{P}(s)] < \frac{1}{\sigma_{max}\left[\mathbf{D}_m(s)\right]}$$

for all $s = j\omega$ (15)

2) Sufficient condition for robust stability with respect to the direct disturbance term alone:

$$\sigma_{min}[(\mathbf{I} + \mathbf{K}(s)\mathbf{P}(s))] > \sigma_{max}[\mathbf{D}_a(s)\mathbf{P}(s)]$$

for all $s = j\omega$ (16)

In these expressions, P(s)=I/s is the nominal plant, K(s) is the feedback compensator for the CV-loop, and $s_{max}[.]$ and $s_{min}[.]$ denote the largest and smallest singular value, respectively, of their matrix arguments.

The symbols $\mathbf{D}_m(s)$ and $\mathbf{D}_a(s)$ in (15)-(16) are slightly modified versions of the multiplicative and direct disturbance terms. These modifications arise when we re-write the direct disturbances as follows:

$$\begin{aligned}(\delta f - \mathbf{D} f) &= (\Delta_f - \mathbf{D})\, f(x) \\ &= (\Delta_f - \mathbf{D})\, (\mathbf{F}_{yy} y + \mathbf{F}_{yz} z) \\ &= (\Delta_f - \mathbf{D})\, (\mathbf{M}(s) y + \mathbf{N}(s) v)\end{aligned} \qquad (17)$$

Here $\delta f(x)$ is represented by a multiplicative dynamic error on f(x) (i.e. $\delta f = \Delta_f * f$), and M(s) and N(s) are transfer matrices obtained from the zero dynamics. The latter can be derived by substituting the linear version of (6) into the linear version of (1)-(2), expressed in (y,z) coordinates. This gives a state space representation for z, with transfer matrices, M(s)=f/y and N(s)=f/v :

$$\begin{aligned}\frac{dz}{dt} &= (\mathbf{F}_{zz} - \mathbf{G}_z \mathbf{G}_y^{-1} \mathbf{F}_{yz}) z + (\mathbf{F}_{zy} - \mathbf{G}_z \mathbf{G}_y^{-1} \mathbf{F}_{yy}) y + \mathbf{G}_z \mathbf{G}_y^{-1} v \\ f &= \mathbf{F}_{yz} z + \mathbf{F}_{yy} y\end{aligned} \qquad (18)$$

The y-dependent part of expression (17) is now defined as $\mathbf{D}_a y$ and the v-dependent part is lumped together with **D** to form $\mathbf{D}_m$, i.e.

$$\begin{aligned}\mathbf{D}_a &= (\Delta_f - \mathbf{D})\mathbf{M}(s) \text{ and} \\ \mathbf{D}_m &= \mathbf{D}(\mathbf{I} - \mathbf{N}(s)) + \Delta_f \mathbf{N}(s)\end{aligned} \qquad (19)$$

Note that conditions (15)-(16) constrain two frequency extremes of the CV feedback loop. High-frequency constraints are imposed by the multiplicative term, which requires that the loop be rolled off before the magnitude of $\mathbf{D}_m(s)$ exceeds unity. Low-frequency constraints are imposed by the direct disturbance term, which calls for sufficient low-frequency gain to overpower any destabilizing effects of $\mathbf{D}_a(s)$. Combining these two extremes gives us a familiar loop-shaping requirements plot illustrated in Figure 3.1.

Whenever the above loop-shape constraints are widely separated, simple CV compensators suffice. A typical example is the 5rad/sec proportional-plus-integral design in Figure 3.2, which readily satisfies Figure 3.1. It also includes feedforwards around the integrator (pre-filters) to restore first order command responses.

In more challenging situations, when the frequency-domain constraints are tight, we can no longer ignore the fact that the direct disturbance and multiplicative perturbations occur together and in a correlated way. Any of the sophisticated modern multivariable design tools could then be brought to bear to execute the design. Arguably the most powerful of these is the m-synthesis method [Stein, 1991; Packard, 1993].

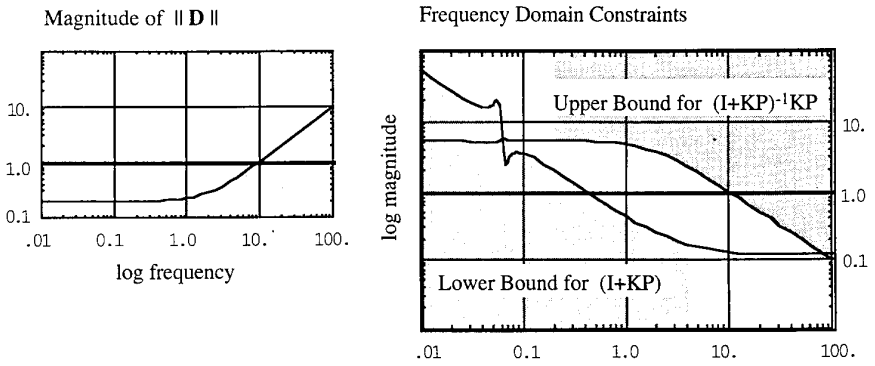

Figure 3.1: Loop-Shape Requirements for F-18 HARV Model in Table 3.2

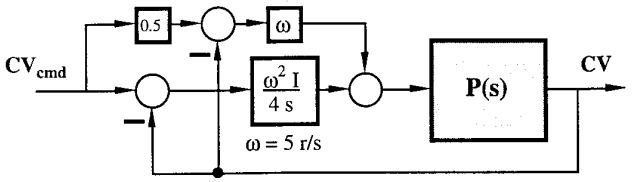

Figure 3.2: A Simple CV Control Law

An informative special correlated case arises if we set df=0 and keep only the perturbation, **D**, in (13). A short derivation shows that the following single condition then assures stability robustness:

$$\sigma_{max}[(\mathbf{I}+\mathbf{KP})^{-1}\mathbf{KP}] < \frac{1}{\sigma_{max}\left[\mathbf{D}(\mathbf{I}-\mathbf{N}+\mathbf{K}^{-1}\mathbf{M})\right]}$$

for all $s = j\omega$ (20)

Now compare (15) and (20, using (19) for $\mathbf{D}_m$ and Δ_f=0. The right hand side is modified by the term $K^{-1}M$. This term makes the effective multiplicative perturbation larger or smaller, depending upon details of the plant. Its effect is easy to see for scalar plants. For stable scalar plants, $K^{-1}M$ will be negative, reducing the effective perturbation and permitting larger bandwidth in the CV-loop. On the other hand, for unstable scalar plants, $K^{-1}M$ will be positive, increasing the effective perturbation and reducing the allowed bandwidth. This happens because the total 'inner loop' bandwidth (the bandwidth used for both feedback linearization (6) and CV control) has a maximum imposed by **D**. In the unstable case, a part of this maximum is already used by (6) to reduce the plant to an integrator, and only the remaining part is available to control the CV. (Indeed, for sufficiently large open-loop instabilities, the remaining part may not exist, indicating that (6) itself is unstable in the presence of **D**.)

The Nonlinear Case: Of course, no matter which design tools or conditions we choose, a critical assumption is still linearity. When this assumption is removed, the formal design options are much less powerful. This happens because formal norm-based robustness conditions for general nonlinear perturbations are blunt instruments. Consider the following generalizations of (15) and (16), derived from the Small Gain Theorem [Desoer, 1975]:

1) Sufficient condition for robust stability with respect to the nonlinear multiplicative term alone:

$$\left\|(\mathbf{I}+\mathbf{KP})^{-1}\mathbf{KP}\right\| < \frac{1}{\|\mathbf{D}_m\|} \qquad (21)$$

2) Sufficient condition for robust stability with respect to the nonlinear direct disturbance term alone:

$$\left\|(\mathbf{I}+\mathbf{KP})^{-1}\mathbf{P}\right\| < \frac{1}{\|\mathbf{D}_a\|} \qquad (22)$$

Here the symbol ‖.‖ denotes an induced operator norm. This norm corresponds to the largest input/output gain of the operator taken over all signals. If the operator is linear, the norm is equal to the largest magnitude of its frequency response taken over all frequencies. Thus, the left hand side of (21) is nothing more than the M-peak of the CV-loop's closed loop transfer function.

On the other hand, the right hand side of (21) is more complicated. To examine this term, consider an 'optimistic' version of $\mathbf{D}_m$, obtained by setting dg to zero and ignoring the 'Nv' term in the nonlinear analog of (17). From (14), the perturbation is then given by

$$\mathbf{D}_m = g(x)\Delta g(x)^{-1} \qquad (23)$$

and it is not difficult to show that the norm of this operator satisfies the following inequalities:

$$\sup_x\left\{\frac{\sigma_{max}[g(x)]}{\sigma_{min}[g(x)]}\right\}\|\Delta\| \le \|\mathbf{D}_m\| \le \left\{\frac{\sup_x \sigma_{max}[g(x)]}{\inf_x \sigma_{min}[g(x)]}\right\}\|\Delta\| \qquad (24)$$

The left side follows from the linear robustness literature: simply treat g(x) as a constant matrix with x fixed to produce the worst case condition number, $\kappa(x)=\sigma_{max}/\sigma_{min}$. The right side follows by letting x vary strategically in relation to the dynamics of D: first pass signals through $g(x)^{-1}$ with x chosen to maximize the gain, then pass the resulting signals through a D which delays them and rotates them into the worst direction of g(x), and finally pass those delayed signals through g(x) with x chosen (after the delay) to maximize the gain of g(x). (These arguments show that the inequalities are, in fact, tight for the two extremes.) The norm ||D|| on both sides of (24) is equal to the M-peak of the (linear) actuator/flex perturbation in the control channels of the aircraft. This norm is typically much greater than unity.

The bottom line of all this is that Condition (19) can be satisfied only if we make the M-peak of the CV-loop much smaller than unity. This requires very small loop gains, i.e. $|K(s)P(s)| << 1$ for all $s=j\omega$. Unfortunately, such gains cannot satisfy Condition (20) which requires large loop gains to make the M-peak of $(I+KP)^{-1}P$ small enough. Thus, the formal robustness guarantees of the nonlinear theory currently do not help us in design.

There are several avenues of research which promise to alleviate the current limitations of the nonlinear theory. One approach is to reduce conservatism in (19)-(20) with weighting functions [Safonov, 1980]. For example, (19) can be replaced by

$$\left\|(\mathbf{I}+\mathbf{KP})^{-1}\mathbf{KPW}\right\| < \frac{1}{\left\|\mathbf{W}^{-1}\mathbf{D}_m\right\|} \qquad (25)$$

where W(s) is any stable and stably invertible linear operator. This condition is still sufficient for robust stability with respect to $\mathbf{D}_m$. Now let W(s) be chosen cleverly, such that the input/output gain of $\mathbf{W}^{-1}\mathbf{D}_m$ is nearly unity for all signals, not large for some signals and small for others. Then (25) would reduce to a much less conservative condition similar to (15), e.g.

$$\left\|(\mathbf{I}+\mathbf{KP})^{-1}\mathbf{KPW}\right\| < 1$$

$$\Leftrightarrow \sigma_{max}[(\mathbf{I}+\mathbf{K}(s)\mathbf{P}(s))^{-1}\mathbf{K}(s)\mathbf{P}(s))] < \frac{1}{\sigma_{max}[\mathbf{W}(s)]}$$

for all $s = j\omega$ (26)

Similar weighted versions are also possible for (20).

In the absence of such improved tests, we are left for now with the linear design methods described earlier, and we are obliged to verify robustness properties after the fact via overall system linearizations and analyses and via nonlinear simulations. Some results using these interim methods are discussed in Section 5.

4. Implementation Issues

The final control laws obtained from dynamic inversion are summarized in Figure 4.1. They consist of a nonlinear block which performs the feedback linearization and a CV controller block which implements the CV-compensator. Some key aspects of this implementation include on-board models, full state feedback, and aircraft-unique surface allocation and limiting logic. We deal with these three topics briefly below.

On-Board Models

As shown in Figure 4.1, dynamic inversion controllers require aircraft models stored on-board to implement the functions $g(x)^{-1}$ and f(x). In the past, the memory needed for these functions and the computing time needed to evaluate them at inner loop update rates have been prohibitive. Modern flight computer technology has all but eliminated these prohibitions. For the F-18 HARV control design used in Section 5, for example, the complete control law requires approximately 1200 floating point memory locations, of which 900 are dedicated to the aircraft model. This covers a limited flight envelope (Mach < 0.7, 15000 < H < 45000 feet). Supersonic flight regimes will require additional memory.

The current control law software for the HARV is still in developmental form, so timing estimates are somewhat premature. However, the code runs in real-time on a SPARC processor in NASA's fixed-base piloted simulator. It has execution times consistent with the HARV's 80 Hz inner loop update rate. Of the 12.5 ms available, approximately 9.5 are due to the CV-compensator, Feedback Linearizer, formation of the CV, and pre-filter. This equates approximately to 2500 indexed floating point multiply-add operations.

Full-State Measurements

Another obstacle from the past is the availability of measurements for the complete state vector. Most modern aircraft now carry a full complement of sensors, from inner loop rate gyros to complete navigators providing inertial orientation, velocity and position. Moreover, with multi-channel redundancy and other fault-tolerant configurations, these measurements are increasingly available in flight-critical form. The only persisting sensing issues revolve around airstream-relative measurements, i.e. true airspeed, angle-of-attack, and angle-of-sideslip. Currently, observer-based blends of inertial measurements and airdata provide the preferred solution for these signals.

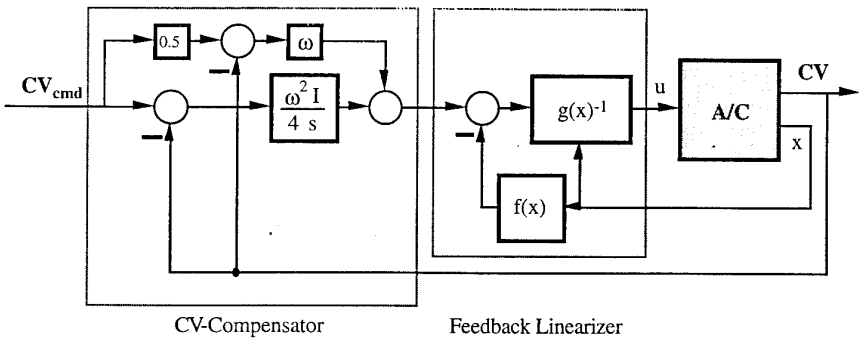

Figure 4.1: Full Dynamic Inversion Control Laws

Surface Allocation and Limiting

As noted earlier, many aircraft have more than three surfaces available to produce the desired dy/dt in equation (5). There are many ways to build $g(x)^{-1}$ to utilize this redundancy, and no one way is necessarily best for every aircraft and every mission. The approach we describe here and utilize in Section 5 is one historical option. It is the so-called *daisy chain* [Bugajski, 1992]. This approach is illustrated in Figure 4.2. It designates *primary effectors* for each of the three aircraft axes, and treats other controls as *auxiliary effectors* to be used only when the primaries saturate. Generally, the primaries will be the standard elevator, aileron and rudder aero-surfaces, or combinations of other surfaces slaved together to provide equivalent moments. The auxiliaries are whatever else is available on the aircraft, such as thrust vectoring vanes on the F-18 HARV.

The logic for switching from primaries to auxiliaries is illustrated in Figure 4.2. Basically, the primaries are always asked to produce the commanded moments. However, their predicted output, subject to rate limits and saturations, is subtracted from the command and the difference is passed on to the auxiliaries whenever the primaries are not powerful enough. In this way, primary effectors are active full-time, while auxiliaries are only active when they are needed.

Of course, it can also happen that even the primaries and auxiliaries together are too weak to generate the desired moments. In this case, there is no alternative but to lower the commanded dy/dt in the affected axes. It is then also necessary to include anti-windup logic on the corresponding integrators in the CV-control law. As another difficulty, the inverse, $g_p(x)^{-1}$, in the primary channel of Figure 4.1 can become poorly conditioned for some x. It is then necessary to use a modified inverse, such as $(g_p(x)+\varepsilon I)^{-1}$. These 'fixes' are incorporated in the super-maneuvering simulations shown in the next section.

5. An F-18 HARV Design Example

The F-18 High Angle-of-Attack Research Vehicle

The National Aeronautics and Space Administration (NASA) is conducting an ongoing high angle-of-attack flight research program. This program uses an F-18 testbed aircraft, selected in part because the production version of this aircraft has exceptional angle-of-attack capability (up to 55 deg), recovers well from spins, has excellent engine performance at high angle-of-attack, and has digital flight controls. An aircraft was obtained by NASA from the US Navy and modified in the following ways to become the HARV:

First, the testbed was instrumented: 2 telemetry systems, five video cameras, two still cameras, and various other data-taking devices.

Second, the two engine nozzles were replaced with an asymmetric arrangement of six thrust vectoring vanes; 3 per engine. Thrust vectoring is provided by deflecting the vanes into the engine exhaust plume.

Third, the Research Flight Control System (RFCS) was installed. This control system architecture retains the production F-18's flight control system, but adds another processor (Ada programmable) to store and execute the research flight control laws. The two systems communicate through dual port RAM, and any failure in the research control laws causes a reversion to the production control laws. This architecture facilitates the development and flight testing of various flight control laws.

A photograph of the final modified vehicle is shown in Figure 5.1.

For our purposes, the aircraft has 13 control effectors: 10 aerodynamic surfaces and three axes of thrust vectoring. These effectors are slaved together in various ways to provide the following effective control inputs:

Pitch Axis: two horizontal stabilators slaved together for primary (aerodynamic) control. Thrust vectoring for auxiliary control.

Lateral/Directional Axes: two slaved aileron surfaces, twin slaved vertical tails, and two differentially deflected stabilators for primary control. Roll and yaw thrust vectoring for auxiliary control.

Note that since the F-18 is a twin engine aircraft, some roll vectoring can also be obtained. Pairs of leading and trailing edge flaps follow the production F-18 control law.

A complete set of sensors is available, with airmass measurements provided by a blend of inertial and airdata sensors, as discussed previously.

The dynamic inversion design methodology described in Sections 2-4 has been used to design control laws for this research vehicle. These control laws are currently being evaluated on piloted simulators at NASA's Dryden Flight Research Facility. They are scheduled for flight evaluation in 1994. Some linear analyses conducted to support these designs and a typical supermaneuver simulation to demonstrate their global performance are described below.

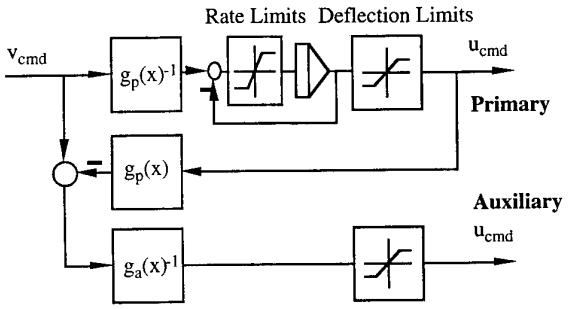

Figure 4.2: "Daisy Chain" Logic for Redundant Control Effectors

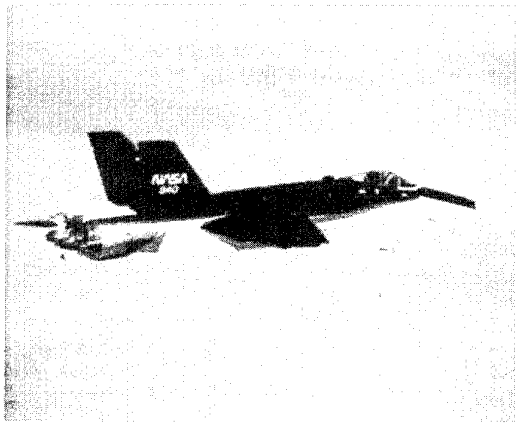

Figure 5. The F-18 HARV.

Linear Analyses

As discussed earlier, the mathematics supporting dynamic inversion do not yet provide effective tools to assure stability and performance robustness for nonlinear perturbations. In the absence of such tools, we rely upon linear analyses of the overall system, plant and controller in closed loop, linearized about various operating points. This subsection summarizes some of these analyses.

Analyses were performed at a variety of flight conditions whose angles-of-attack ranged from 2 to 80 degrees and whose dynamic pressures ranged from 34 to 390 psf. Lateral/directional and longitudinal axes were analyzed separately despite some known aerodynamic asymmetries above α=40. The daisy-chain method of allocating control effectiveness (Section 4) was not employed for the linear analyses. Instead, multiple control effectors (aero surfaces and thrust vectoring) were employed in a manner which minimizes control deflections [Snell, 1991]. This change does not affect the stability and robustness results which follow. The closed loop systems for each axis included the control laws, rigid body aircraft dynamics, 30 rad/sec first-order actuators, and 50 msec time delays that approximate the delays observed in the HARV's real-time simulator.

Results of the linear analyses are summarized in Table 5.1. This table includes four parameters for both the pitch and lateral/directional axes. The parameters are

1) minimum single loop-at-a-time phase margins across flight condition for loops broken at inputs and outputs of the controller

2) typical crossover frequencies at loopbreaking points in 1)

3) robust stability margins for unstructured uncertainty at the aircraft's actuator inputs, and

4) robust stability margins for diagonally structured uncertainty at the aircraft's sensor outputs.

The first two parameters are obtained from classical frequency response analyses. The third is obtained from the peak magnitude of the maximum singular value, $\sigma_{max}[\ (I+KP)^{-1}\ KP\ ]$, across frequency (analogous to Condition (15)), and the fourth is obtained from the peak magnitude of the structured singular value $\mu[\ PK\ (I+PK)^{-1}\ ]$ across frequency [Doyle, 1982]. Peak magnitudes of 2 for σ_{max} or m indicate that normalized modeling errors of size 1/2, or 50%, can be tolerated without instability, while peak magnitudes of 3 indicate that 33% modeling errors can be tolerated without instability.

Table 5.1: Linear Analysis Results

Axes	Minimum Phase Margin	Typical Crossover Frequency	Peak σ_{max} at actuator inputs	Peak μ at sensor outputs
Pitch	$\approx$ 55 deg	$\approx$ 5 r/s	< 2.0	< 2.0 in short period range < 15. in phugoid range
Lateral / Directional	$\approx$ 48 deg	$\approx$ 6.5 r/s	< 3.0	< 3.0

In addition to these parameters, we also examined nominal closed loop poles over the flight envelope. For pitch, the short period poles are well damped, but many of the high-a flight conditions have unstable phugoids (resulting from unstable zero dynamics in need of fine-tuning [Section 3]) These phugoid sensitivities are also evident in Table 5.1. For lateral/directional, all dutch roll and other complex poles are stable and well damped (ζ>0.4).

The results in Table 5.1 and the analyses of closed loop poles verify that the control laws have generally good small signal feedback properties.

A Simulated Supermaneuver

A high angle-of-attack, high angular rate, Herbst maneuver [Well, 1982; Herbst, 1980] was simulated to demonstrate the performance of the dynamic inversion control laws over wider operating regimes. Since the control laws are based on CVs for piloted operation (as described in Section 3) the maneuver was executed with an additional outer loop commanding the normal pilot inputs (i.e. longitudinal stick, lateral stick, rudder pedals, and power lever). Detailed descriptions of the maneuver and the various aircraft responses are given below. They demonstrate that the control laws handle the aircraft well, even when it is pushed to very high angles-of-attack and angular rates and to the limits of available control authority.

The Maneuver: The intent of a Herbst maneuver is to reverse aircraft velocity in minimum time. The maneuver begins in straight-and-level flight and proceeds into a full-afterburner climb with longitudinal stick full aft. During the climb, the aircraft develops very large angles of attack and reduces airspeed dramatically. The climb eventually stops and is followed by a rapid descent back to the aircraft's initial altitude and speed. However, near the top of the climb at very low airspeed, lateral stick and rudder pedal inputs are applied to reverse heading and body attitude by 180 degrees, so the descent occurs back along nearly the same path as the climb. This returns the aircraft approximately to the same point in space where the maneuver started but heading 'the other way'.

Detailed Aircraft Responses: Selected response variables of the F-18 HARV executing such a supermaneuver are summarized in Figure 5.2. The basic trajectory is shown in Figure 5.2e, where altitude and East position are plotted versus North position. At the beginning of the maneuver, the aircraft is flying north, and at the end of the maneuver it is flying south. The entire trajectory stays within 1300 ft of the north-south vertical plane. Note how the downward and upward portions of the trajectory are nearly coincident. The flight path angle reaches a maximum of 86 degrees near the top of the maneuver and a minimum of -57 degrees during the dive as shown in Figure 5.2d. Heading is reversed by 180 degrees as shown in Figure 5.2l, near the top of the maneuver when the velocity is less than 100 ft/sec.

Angle-of-attack, shown in Figure 5.2b, reaches 92 degrees about 8 seconds after the maneuver is initiated. The fuselage has pitched nose up through 150 degrees during the initial 8 seconds. At 6.1 sec, the nose is straight up. After this, the vertical tail points down and the aircraft rolls to wings-level and simultaneously pitches to near nose-level attitude. This can be seen in Figure 5.2m, where the aircraft's Euler angles for pitch, roll and yaw are shown (by convention, the pitch Euler angle is between -90 degrees and 90 degrees). During the lateral transient to reverse the body attitude and velocity direction, the angle-of-attack decreases to a minimum of.7 degrees and then increases to the value for maximum lift coefficient for the pullout from the dive. The corresponding pitch rate, shown in Figure 5.2c, is between -30 deg/sec and 30 deg/sec throughout the maneuver.

Normal acceleration, shown in Figure 5.2g, is less than 4.7g for the initial pullup, is zero at the top of the maneuver when velocity in Figure 5.2a, and dynamic pressure, in Figure 5.2f, are less than 20 ft/sec and 0.3 psf respectively. Acceleration then increases to 1.5g during the final pullout from the steep dive. Throughout the maneuver the lateral acceleration, shown in Figure 5.2g, is less than 0.11g despite the large sideslip, shown in Figure 5.2i, which occurs when the airspeed is negligible. The 0.11g lateral acceleration is a direct result of yaw thrust vectoring, shown in Figure 5.2p. Sideslip angle is less than 2 degrees when dynamic pressure is larger than 50 psf.

Lateral stick and rudder pedal inputs are first issued 11 seconds after the maneuver is initiated. These inputs lead to the transients in roll rate and yaw rate, shown in Figure 5.2j. These rates have magnitudes of about 10 deg/sec when angle-of-attack is between 60 to 70 degrees and increase in magnitude to 65 deg/sec for roll rate and 28 deg/sec for yaw rate during the rapid decrease in angle-of-attack from 60 degrees to 7 degrees. These are considered to be high angular rates for this low speed, high angle-of-attack condition.

The lateral-directional inputs roll the aircraft 140 degrees about the velocity vector during the period when velocity is less than 100 ft/sec. This roll angle (about the velocity vector) is shown in Figure 5.2k. The heading overshoots 180 degrees and it is necessary to roll to -30 degrees to return to the north-south plane in which the maneuver originated. The aircraft Euler angles for roll and yaw are shown in Figure 5.2m, where it can be seen that the body attitude has been reversed by 180 degrees in yaw and is close to a normal wings level attitude at the end to the maneuver.

Horizontal tail and pitch thrust vectoring are shown in Figure 5.2h. The horizontal tail and pitch vectoring reach position limits during the initial pullup and stay on the limits for about 2 seconds. A demand for nose down moment then occurs which puts both effectors on the positive rate limit. Nose up is then required and the controls are rate limited in the opposite direction. For the remainder of the maneuver these controls are neither rate or position limited. Note that the daisy chain does not call for pitch thrust vectoring until the horizontal tail limits in the initial pullup. Likewise, when dynamic pressure has increased to 50 psf and a is about 42 deg during the pullout from the dive, the horizontal tail is sufficiently effective and no pitch thrust vectoring is employed.

The rudder control surface and the yaw thrust vectoring are shown in Figure 5.2p. They are zero until 11 seconds after the maneuver is initiated, when the reversal is commanded. At this time, the angle-of-attack is 60 degrees and the rudder is not very effective. Thus, the daisy chain calls for yaw thrust vectoring. Since the daisy chain gives priority to pitch vectoring, the yaw thrust vectoring limits briefly for about 1 second, in the nose right direction and then for about 2 seconds in the nose left direction. Subsequently, the yaw thrust vectoring limits on both sides once more before dynamic pressure increases and angle-of-attack decreases enough for the rudder to become sufficiently effective again. During the low velocity period, the rudder changes from positive to negative position limits, but at the end of the maneuver the rudder is well behaved while completing the turn and yaw thrust vectoring is not employed.

There are two aerodynamic controls for roll, namely the aileron and the rolling (or differential) tail. Since there are two engines, there is also a thrust vectoring roll control based on differential pitch thrust vectoring. The aileron and differential tail control surfaces are shown in Figure 5.2n, and the roll thrust vectoring angle is shown in Figure 5.2o. The rolling tail is only used to the extent that it does not interfere with tail deflections needed for pitch control. When the reversal is commanded near the top of the maneuver, the aerodynamic surfaces are not sufficiently effective and the daisy chain calls for roll thrust vectoring. Since roll is last in priority (with pitch first and yaw second), the desired dynamics for roll can not be satisfied for most of the 10 seconds following the reversal command. At the end of the maneuver, the thrust vectoring is no longer employed because aerodynamic controls for roll are sufficiently effective.

The various traces in Figure 5.2 demonstrate that the control laws handle the aircraft well throughout the maneuver. This is true even at very high angles-of-attack and high angular rates, and also when commands exceed the total control authority available on the aircraft.

6. Conclusions

We have tried to demonstrate in this paper that dynamic inversion offers a potentially powerful alternate design methodology for flight control. Dynamic inversion avoids gain schedules. Instead, it uses on-board dynamic models and full-state feedback to globally linearize dynamics of selected controlled variables. Simple controllers can then be designed to regulate these variables with desirable closed loop dynamics. The variables themselves and their closed loop dynamics must be selected to meet handling quality specifications, to satisfy gust response requirements, to exhibit well-behaved zero dynamics, and to achieve good robustness properties for the overall system. Each of these aspects were discussed in the paper and illustrated with a design for the F-18 HARV. While these discussions show that the method's current status is already adequate for serious designs, the method will benefit substantially from additional research developments, particularly in areas of nonlinear zero dynamics and nonlinear robustness.

Because of its general control law structure, dynamic inversion is well suited for control law re-use across different airframes, for easy control law updates as airframe models change, and for non-standard flight applications such as supermaneuvering. This power is possible because modern flight computer hardware and instrumentation make on-board models and full-state feedback no longer prohibitive.

Figure 6a Herbst Maneuver

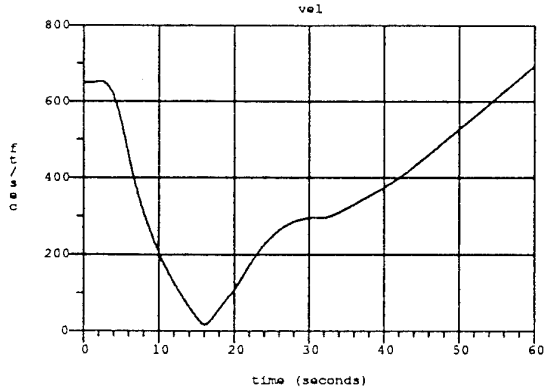

Figure 6e Herbst Maneuver

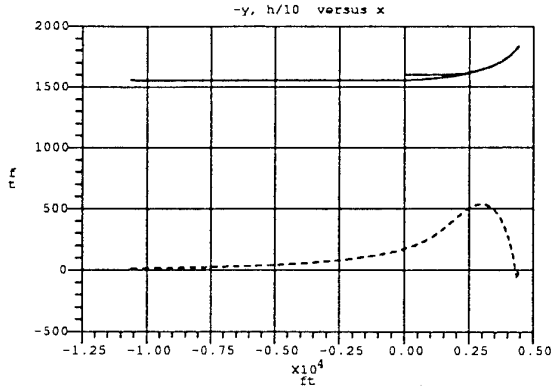

Figure 6b Herbst Maneuver

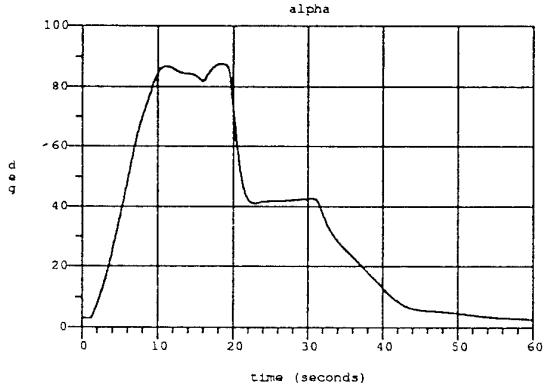

Figure 6f Herbst Maneuver

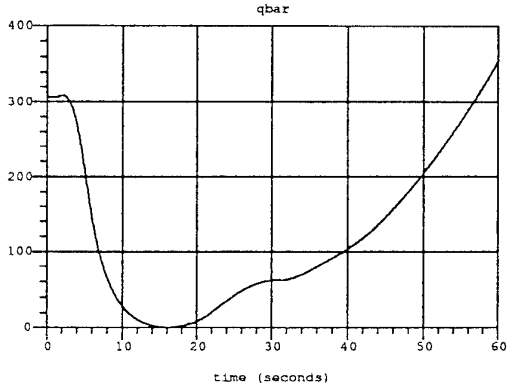

Figure 6c Herbst Maneuver

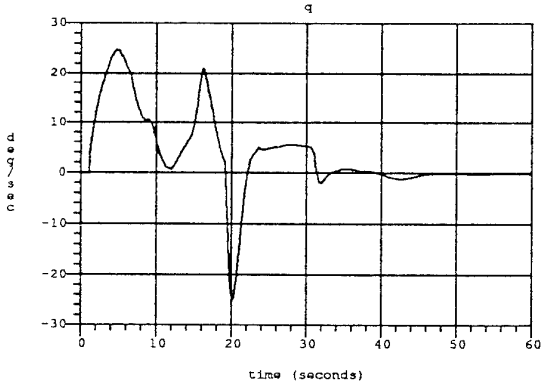

Figure 6g Herbst Maneuver

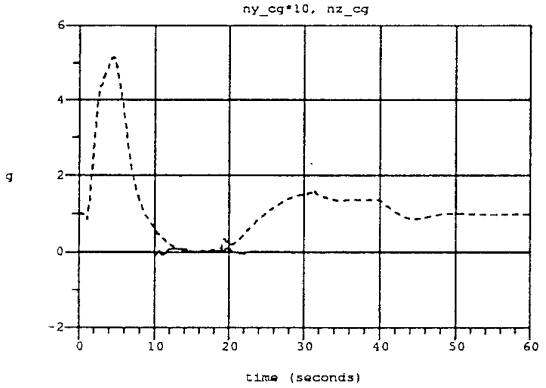

Figure 6d Herbst Maneuver

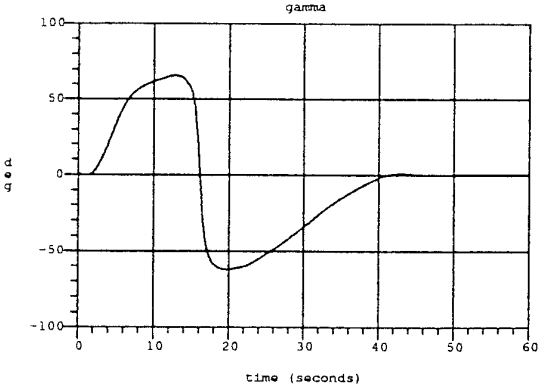

Figure 6h Herbst Maneuver

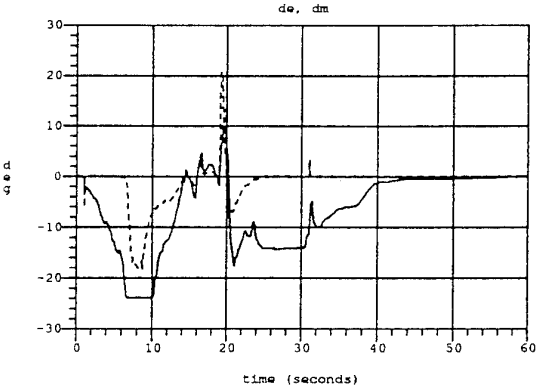

Figure 6i Herbst Maneuver
beta

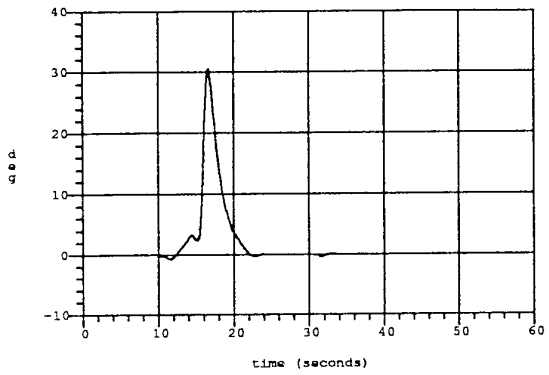

Figure 6j Herbst Maneuver
p, r

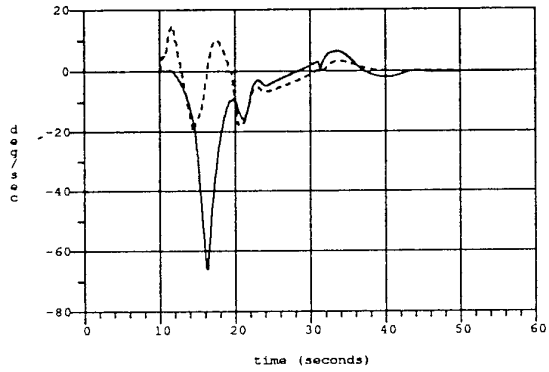

Figure 6k Herbst Maneuver
mu

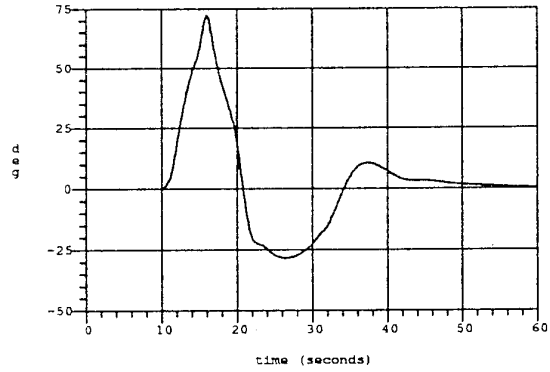

Figure 6l Herbst Maneuver
chi

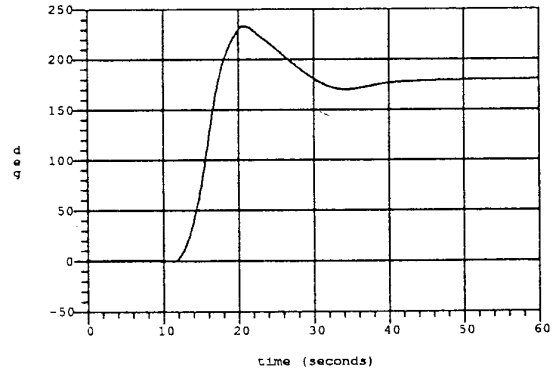

Figure 6m Herbst Maneuver
phi, theta, psi

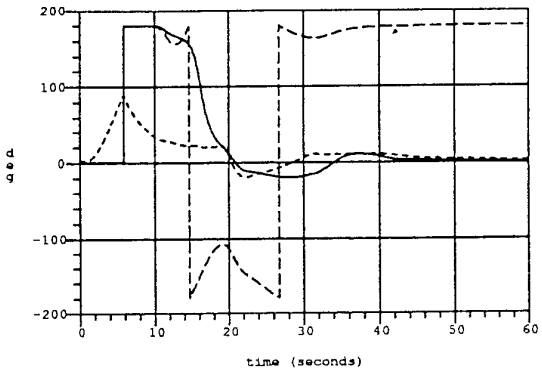

Figure 6n Herbst Maneuver
dlad, dep

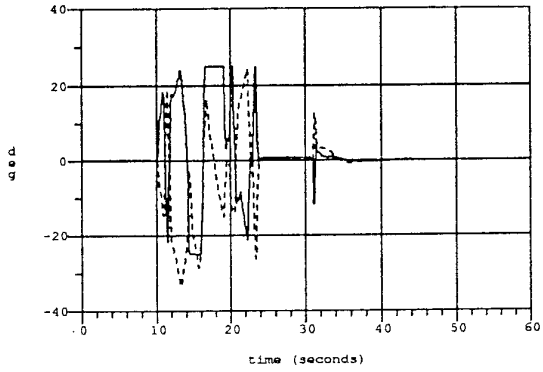

Figure 6o Herbst Maneuver
dl

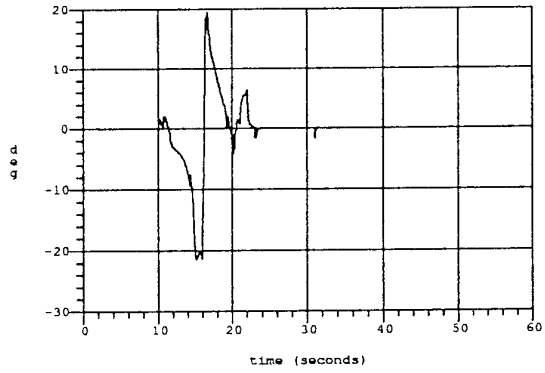

Figure 6p Herbst Maneuver
drudl, dn

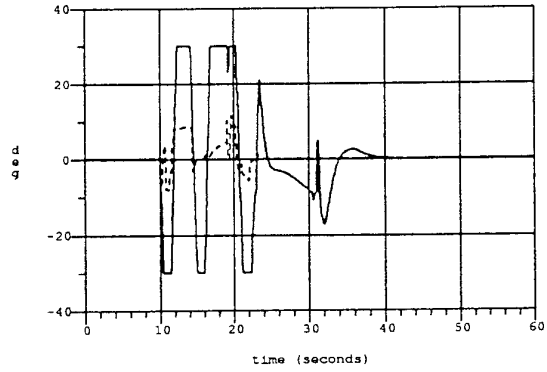

References

Akhrif, O. and G.L. Blankenship, "Robust Stabilization of Feedback Linearizable Systems," Proc. IEEE Cont. Dec. Conf, 1988.

Brockett, R.W., "Feedback Invariants for Nonlinear Systems", IFAC Congress, Helsinki, 1978.

Bugajski, D.,and D. Enns, "Nonlinear Control Law with Application to High Angle-of-Attack Flight," J Guidance, Control and Dynamics, April, May-June, 1992.

Bugajski, D., Enns, D. and R. Hendrick, "Nonlinear Control Law Design for High Angle-of-Attack, " NASA High Angle-of-Attack Projects and Technology Conference, April, 1992.

Desoer, C.A. and M. Vidyasagar, *Feedback Systems: Input/Output Properties*, Academic Press, 1975.

Doyle, J.C. and G. Stein, "Multivariable Feedback Design: Concepts for a Classical / Modern Synthesis," IEEE TAC-26(1), February 1981.

Doyle, J.C., "Analysis of Feedback Systems with Unstructured Uncertainties," IEE Proceedings, 129-D(6), November 1982.

Elgersma, M. R., "Nonlinear Control, With Application to High Angle of Attack and VSTOL Flight," Plan B Project, M.S. Department of Electrical Engineering, Univ. of Minn., January 1986.

Elgersma, M. R., Control of Nonlinear Systems Using Partial Dynamic Inversion," Ph. D. Dissertation, Univ. of Minn., April, 1988.

Etkin, B., *Dynamics of Atmospheric Flight*, John Wiley & Sons, 1972

Herbst, W. B., "Future Fighter Technologies,"Journal of Aircraft, Vol. 17, No. 8, August 1980.

Hunt, L.R. and R. Su, "Control of Nonlinear Time-Varying Systems," Proceedings of the IEEE Conference on Decision and Control, December, 1981.

Rosenbrock, H.H., *State Space and Mulitvariable Theory*, Nelson, 1970.

Isidori, A. *Nonlinear Control Systems: An Introduction*, Springer-Verlag, 1985.

Kravaris, C., "On the Internal Stability and Robust Design of Globally Linearizing Control Systems," Proc. American Control Conference, 1987.

Lane, S.H. and R.F. Stengel, "Flight Control Using Nonlinear Inverse Dynamics," Automatica, (24),1988.

McRuer, D, Ashkenas, I, and D. Graham, *Aircraft Dynamics and Automatic Control,* Princeton University Press, 1973

Meyer, G., R. Su, and L.R. Hunt, "Application of Nonlinear Transformations to Automatic Flight Control," Automatica, 1(20), 1984.

"Military Specifications - Flying Qualities of Piloted Vehicles", MIL-STD-1797A, March, 1987.

Morton, B.G., and D. Enns, "Stability of Nonlinear Inversion Control Laws Applied to Nonlinear Aircraft Pitch-Axis Models," AFOSR Final Report, Honeywell, October 1991.

Morton, B.G., Elgersma, M.R., Harvey, C.A., and G. Hines, "Nonlinear Flying Quality Parameters Based on Dynamic Inversion," AFWAL-TR-87-3079, 1987.

Packard, A., Doyle, J., and Balas, G., "Linear Multivariable Robust Control With a m- Perspective", ASME Journal of Dynamics, Measurements, and Control, June 1993.

Safonov, M.G., *Stability and Robustness of Multivariable Feedback Systems*, MIT Press, 1980.

Snell, S.A., "Nonlinear Dynamic-Inversion Flight Control of Supermaneuverable Aircraft," PhD Thesis, Aerospace Engineering & Mechanics Department, University of Minnesota, October, 1991.

Spong, M.W. and M. Vidyasagar, "Robust Linear Compensator Design for Nonlinear Robotic Control," IEEE J. Robotics Auto., 3(4), 1987.

Stein, G. and J.C. Doyle, "Beyond Singular Values and Loop Shapes," J. Guidance, Control and Dynamics, January-February 1991.

Well, K.H., Faber, B. and E. Berger, "Optimization of Tactical Aircraft Maneuvers Utilizing High Angles-of-Attack," J. Guidance, Control and Dynamics, March-April 1982.

Evaluation des techniques de contrôle flou pour le pilotage d'avion

N. Imbert

A. Piquereau

Office national d'études et de recherches aérospatiales
Centre d'études et de recherches de Toulouse
Département d'études et de recherches en automatique
2, Avenue E. Belin
31055 Toulouse Cedex
France

RESUME

La particularité d'un contrôleur flou est d'utiliser un savoir-faire exprimé en langage naturel sous formes de règles expertes, pour calculer à partir des informations numériques issues des capteurs la valeur de la commande. La mise en oeuvre d'un tel pilote nécessite l'interprétation du domaine numérique en symbolique et réciproquement. Ceci est réalisé par l'utilisation des ensembles flous. La théorie associée permet à partir d'une valeur précise de la mesure, de l'ensemble des règles expertes énoncées et du choix d'opérateurs appropriés de déduire une valeur de commande. Il en résulte un structure particulière des contrôleurs flous, dont les principales caractéristiques font l'objet de la première partie de la présentation.

La mise en oeuvre sur l'exemple du pilotage longitudinal d'un avion est ensuite présentée. Deux approches ont été retenues : la première utilise les règles de pilotage manuel formulées en langage naturel par les "experts" que sont les pilotes. La seconde utilise les lois issues d'un pilote automatique classique pour construire des règles de pilotage. Les résultats sont présentés dans l'optique d'une comparaison entre les deux types de contrôleurs, classique ou flou.

Dans une dernière partie, la technique de la commande floue est plus particulièrement appliquée au problème de l'atterrissage automatique, en utilisant les règles de pilotage de cette phase de vol énoncées par des pilotes. Trois procédures types d'atterrissage sont considérées : l'appontage, l'atterrissage de précision et l'atterrissage standard. Ce problème nous permet de mettre en évidence les spécificités de la commande floue et ses avantages au stade de la synthèse : facilité de prise en compte de contraintes de natures diverses, souplesses de changement de phase de vol et de mode de pilotage, facilité d'introduction des non linéarités, souplesse de modification des paramètres de réglage. Un autre atout de ce type de commande est la facilité de compréhension des lois utilisées, puisqu'elles sont exprimées en langage commun. Ces avantages sont appréciables et démontrent l'intérêt que peut susciter la commande floue dans le cas des systèmes pour lesquels on dispose d'une expertise ; toutefois, il est à remarquer que ce type de commande ne procure pas d'amélioration significative des performances ou de la robustesse par rapport à une loi de commande classique.

I- INTRODUCTION

L'application de la logique floue à la commande des systèmes offre une nouvelle approche au problème de la synthèse des correcteurs. Cet article se propose de développer l'application d'une telle technique pour le pilotage d'avion. Après avoir exposé les principes de la commande floue et décrit la structure particulière des correcteurs, ce papier présente l'exemple du pilotage en logique floue d'un avion sur l'axe longitudinal. Les avantages de cette approche sont alors mis en évidence sur le problème plus particulier de l'atterrissage automatique

Ces études ont pu être conduites grâce au soutien de la Direction des Recherches et Etudes Techniques (D.R.E.T) pour la partie théorique et de la Division Avions de l'Aérospatiale pour les problèmes spécifiques avion.

II - PRINCIPE DE LA COMMANDE FLOUE

L'objectif recherché dans la synthèse d'un contrôleur flou était à l'origine de reproduire le savoir faire d'un opérateur humain, qualifié "d'expert". La connaissance du fonctionnement du système et la manière de le piloter sont exprimées en langage naturel, avec un contenu souvent imprécis.

L'expertise est constituée d'un ensemble de règles de conduite de l'opérateur de la forme : *si l'erreur est trop forte et que sa variation est faible, alors la commande doit être grande.*

Les lois de commande étant exprimées sous cette forme il faut d'une part les traduire et les représenter dans le contrôleur, et d'autre part il faut effectivement résoudre le problème de commande : en effet si la manière d'exprimer l'action est imprécise, l'action elle même devra être précise : à une mesure donnée correspond une valeur précise de la commande. La mesure est une valeur numérique de la vitesse par exemple, la commande délivrée a elle aussi une valeur précise.

II.1 - Représentation de la connaissance sous forme de règles floues.

La théorie des ensembles flous permet une représentation dans le domaine numérique d'informations exprimées dans le langage naturel.

Les ensembles flous sont des ensembles dont les éléments n'ont pas une appartenance en tout ou rien, mais une appartenance graduelle. C'est-à-dire qu'un élément a un "degré d'appartenance" à l'ensemble compris entre 0 et 1. Certains éléments n'appartiennent pas à l'ensemble (degré 0) d'autres y appartiennent vraiment (degré 1), et pour d'autres l'appartenance est partielle (degré compris entre 0 et 1). Et on conçoit que cette notion permet de traduire sous forme numérique les notions exprimées dans le langage qui sont souvent vagues ou imprécises.

Ainsi si on considère pour une personne l'adjectif "grand", il est clair qu'il est difficile et même sûrement réducteur de mettre un seuil absolu entre les personnes grandes et celles qui ne le sont pas. On peut considérer la fonction d'appartenance μ_G à l'ensemble "grand" de la forme :

Paper presented at the Flight Mechanics Panel Symposium held in Turin, Italy, from 9-13 May 1994.

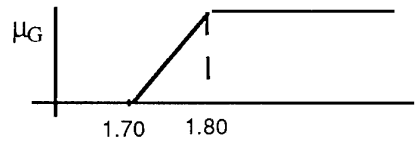

L'ensemble des règles énoncées par l'expert fait référence à des caractéristiques des variables du problème ; ces caractéristiques sont énoncées sous forme de qualificatifs imprécis, traduits numériquement par des fonctions d'appartenance.

On définit ainsi pour chaque variable le "vocabulaire" , c'est-à-dire l'ensemble des qualificatifs auquel les règles font référence.

En pratique, comme les variables du contrôle sont des nombres réels, le vocabulaire fait référence à la valeur de ces nombres, et on trouve en général les termes de grand, moyen, petit associés au signe de la variable.

Les règles peuvent avoir plusieurs entrées, et notamment pour une variable, la règle peut mettre en jeu la valeur de sa variable et de sa dérivée.

Si x est A et que Δ x est B alors y est C.

L'ensemble des règles se présente alors comme un tableau dont les entrées sont les attributs linguistiques des deux variables, et la sortie, l'attribut de la "sortie".

Par exemple

Δx / x	*negb*	*negm*	*zero*	*posm*	*posb*
negb	posb	posb	posb	posm	zero
negm	posb	posb	posm	zero	negm
zéro	posb	posm	zero	negm	negb
posm	posm	zero	negm	negb	negb
posb	zero	negm	negb	negb	negb

negb : negative big
negm : negative medium
posm : positive medium
posb : positive big

La définition du contrôleur flou passe alors par :

- la définition du nombre et du support des intervalles flous associés à chaque mot du vocabulaire correspondant à la variable x, Δx et la sortie, par exemple :

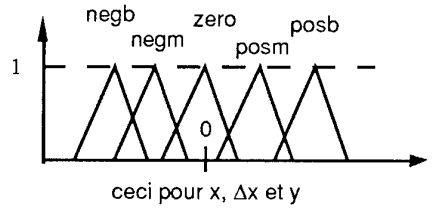

- l'ensemble des règles, par exemple le tableau ci-dessus.

II.2 - Traitement des mesures

Si le concept de règle floue paraît assez intuitif et naturel, il faut voir que la détermination en pratique d'une valeur de commande pour une valeur de la mesure passe par la résolution d'un certain nombre de problèmes.

1) la règle dit :
"Si x est A alors y est B", où A et B sont des qualificatifs linguistiques auxquels on a associé une représentation numérique sous forme de fonction d'appartenance.
L'information dont on dispose n'est pas x est A, par exemple x est "grande", mais x vaut 0,58.
Que peut-on alors conclure sur y ?

2) La valeur numérique de la mesure peut faire partie de deux intervalles représentant deux qualificatifs A et A'.
Deux règles sont alors en jeu. Comment combiner ces règles?

3) La quantité y qui résulte des opérations précédentes est "floue" , mais le contrôleur doit délivrer une seule valeur de commande. C'est le processus de défuzzification.

a - Evaluation de la conclusion pour une entrée donnée

Si en logique classique l'implication A--> B est équivalente à (nonA) ou B, en logique floue cette implication est une application F de [0,1]* [0,1] image des fonctions d'appartenance à A et B sur l'intervalle [0,1] représentatif de la validité de cette relation. On notera

$$r(x,y) = F(\mu_A(x),\mu_B(y))$$

En logique classique, l'évaluation de la conclusion est effectuée par le modus ponens ;

Si A
et si $A \rightarrow B$ alors B

Dans le cas flou, il est fréquent que les informations dont on dispose ne soient pas A mais une information A', différente de A. En particulier dans le cas du contrôle flou la règle est de la forme *"Si la vitesse est grande alors B"* et l'information dont on dispose est : *"la vitesse vaut 10.5"*.

Le modus ponens généralisé permet dans ce cas d'évaluer une conclusion :

Si $A \rightarrow B$
et A' alors B'

On évalue en fait l'appartenance de A' à A et on en déduit un degré d'appartenance de la conclusion à B.

$\mu_{B'}$ est donnée par la formule, qui combine les deux informations $A \rightarrow B$ et A'

$$\mu_{B'}(y) = \sup_m G[\mu_{A'}(m), r(m,y)]$$

où G est une norme triangulaire (généralisation du "et" logique), par exemple :

$G(a,b) = \max(a+b-1, 0)$ (1)
$G(a,b) = \min(a,b)$ (2)
$G(a,b) = a.b.$ (3)

En pratique seule l'opération min permet de ne pas faire d'hypothèse sur la dépendance entre la règle et le fait (voire les autres règles entrant en jeu également).

b - Agrégation des règles

Chaque règle appliquée à la valeur de la mesure fournit une valeur de la sortie caractérisée par sa fonction d'appartenance.
Pour agréger le résultat des différentes règles plusieurs méthodes sont proposées :

- la méthode d'intersection où l'on considère que la combinaison des différentes règles correspond à une notion de "et" .

On définit alors la sortie de plusieurs règles par :

$$\mu(y) = T[\mu_B(y), \mu_{B'}(y)...]$$

où $\mu_B(y)$, $\mu_{B'}(y)$ sont les fonctions d'appartenance résultant de l'application des différentes règles, et où T est une norme triangulaire, par exemple le min, le produit ou la norme triangulaire de Lukasiewicz. Une fois encore, c'est le min qui se justifie le plus facilement par le fait qu'il ne suppose rien sur les dépendances entre les conclusions partielles.

- la méthode d'union, où on considère que la combinaison des règles correspond à une notion de "ou".

On applique alors :

$$\mu(y) = \perp[\mu_B(y), \mu_{B'}(y)...]$$

où $\perp$ est une conorme triangulaire, par exemple le maximum ou la conorme triangulaire de Lukasiewicz $\min(1, \mu_B + \mu_{B'})$.

Il faut toutefois noter que la méthode d'agrégation doit être cohérente avec la méthode d'implication choisie pour que le résultat global contienne de l'information.

Prenons par exemple le cas d'une implication, pour laquelle une mesure $\mu_A(m) = 0$ fournit comme sortie $\mu_B(y) = 1$. Si on agrège les règles par la notion de max, la réponse sera alors "1" partout. De même dans le cas d'une conjonction, cette même mesure fournit une sortie $\mu_B(y) = 0$ partout ; si on agrège les règles par le min, la réponse est alors "0" partout.

II.3 - Méthode de défuzzification

Le résultat du traitement des règles et de leur agrégation est une quantité floue mais le résultat final doit être précis, puisque c'est la valeur de la commande qui sera appliquée. La "défuzzification" est l'opération qui permet de choisir une valeur précise y_0 représentative de l'intervalle flou de fonction d'appartenance $\mu(y)$.

Plusieurs méthodes sont possibles :

- la méthode du centre de gravité

$$y_{0G} = \frac{\int \mu(y)\, y\, dy}{\int \mu(y)\, dy}$$

- la méthode du maximum

y_{0M} est choisi parmi les valeurs de y qui ont une valeur $\mu(y)$ maximale.

- la méthode de la hauteur

$$y_{0H} = \frac{\Sigma y_i h_i}{\Sigma h_i}$$

où y_i est un élément représentatif de la sortie pour μ_i et h_i la hauteur.

- la méthode de la surface

$$y_{0S} = \frac{\Sigma y_i S_i}{\Sigma S_i}$$

où S_i représente la surface.

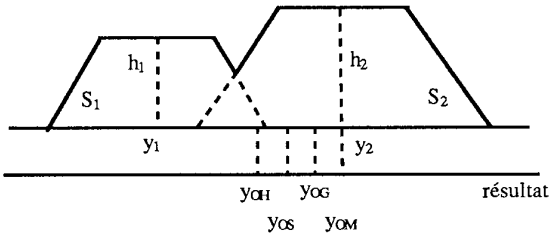

En définitive le contrôleur flou peut être considéré comme une "boite noire", composée de trois sous ensembles, dont l'entrée est constituée des mesures et la sortie de la ou des commandes, ces valeurs étant numériques.

II.4 - Méthode de Sugeno

Cette méthode diffère des méthodes énoncées plus haut car elle permet de calculer une sortie du contrôleur en s'affranchissant des étapes d'inférence et de défuzzification. Elle est donc beaucoup plus simple à mettre en oeuvre. L'idée simplificatrice de Sugeno est de supposer que les règles expertes admettent pour conclusion une valeur précise.

Par exemple :

si x *est* A *alors* $y = \alpha$

où α est une valeur numérique et A un qualificatif linguistique que l'on peut représenter par sa fonction d'appartenance $\mu(A)$. Pour une mesure donnée m, le résultat de l'application de toutes les règles est la somme de toutes les valeurs α, pondérées par les degrés d'appartenance de la mesure à la premisse.

$$y = \frac{\sum_i \alpha_i \mu_{A_i}(m)}{\sum_i \mu_{A_i}(m)}$$

où la règle i est

si x *est* A_i *alors* $y = \alpha_i$

Notons que la méthode de Sugeno permet aussi de traiter des règles où la conclusion n'est plus une valeur numérique fixée mais une fonction de l'entrée.

si x *est* A *alors* $y = f(x,...)$

Le calcul de la sortie s'effectue de la même façon par pondération des résultats des différentes règles.

Des comparaisons sur les résultats obtenus en utilisant ces différentes méthodes nous ont conduits à conclure à leur équivalence, ce qui laisse une préférence à la technique préconisée par Sugeno, pour sa simplicité de mise en oeuvre.

III - PILOTE LONGITUDINAL D'AVION

Pour illustrer les capacités d'un contrôleur flou et en préciser la technique de mise en oeuvre, une application au contrôle sur l'axe longitudinal d'un avion en phase de descente est présentée.

III.1-Modélisation du système

Le modèle d'évolution d'un avion sur son axe longitudinal est obtenu par l'écriture des équations de la mécanique du vol avec les notations précisées par la figure :

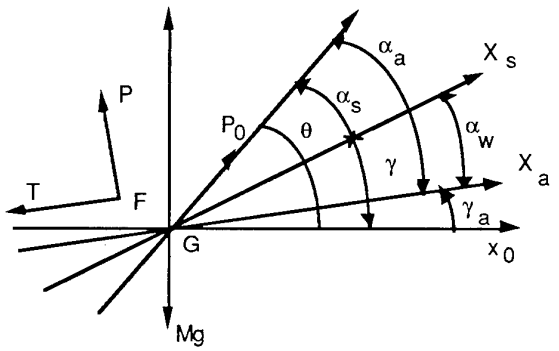

où G ext le centre de gravité, F le foyer aérodynamique, P0 la poussée des réacteurs, P et T les forces aérodynamiques de portance et de traînée.

$$\theta = \gamma_a + \alpha_a = \gamma + \gamma_s$$
$$\alpha_w = \alpha_a - \alpha_s = \frac{V_z}{Va}$$

Equation de propulsion :

$$\dot{V} = \frac{Po}{M}\cos\alpha_s - g\frac{C_{xs}}{C_{z_1}} - g\sin\gamma$$

avec :

$$C_{z_1} = \frac{Mg}{\frac{1}{2}\rho S V^2}$$

Equation de sustentation :

$$\dot{\gamma} = \left(\frac{Po}{Mg}\sin\alpha_s + \frac{C_{zs}}{C_{z_1}} - \cos\gamma\right)\frac{g}{V}$$

Equations des moments :

$$\ddot{\theta} = \frac{gl}{\rho_z^2}\left[\frac{Po}{Mg}\frac{h}{l} + \frac{C_m}{C_{z_1}} - 0.24\,(f_V\sin\alpha_s + f_{nv}\cos\alpha_s\right]$$

avec $M\rho_z^2$ inertie autour y

$$f_V = \frac{Po}{Mg}\cos\alpha_s - \frac{C_{xs}}{C_{z_1}}$$
$$f_{nV} = \frac{Po}{Mg}\sin\alpha_s - \frac{C_{zs}}{C_{z_1}}$$

Ces équations du mouvement sont complétées par la modélisation des phénomènes aérodynamiques, en tenant compte des effets des commandes de profondeur. Enfin les commandes de poussée et de braquage de profondeur sont supposées présenter un délai d'exécution modélisé par une constante de temps :

$$\dot{P}_0 = (P_c - P_0)/T_p$$
$$\dot{dm} = (dm_c - dm)/T_d$$

III.2-Commande de référence

La commande idéale d'un tel système est obtenue en supposant tous les états mesurables et tous les termes non linéaires connus de façon à les inclure dans les lois de contrôle. La détermination de cette commande, préconisée par l'Aérospatiale, s'appuie sur la technique de Naslin appliquée aux dérivées des variables d'entrée.
La commande choisie comme référence détermine les variations de poussée et de braquage à réaliser pour satisfaire les objectifs.
Ainsi:

$$\boxed{\dot{P}_c = (\dot{\gamma} - \omega_1 V_{obj})\,Mg}$$

avec :

$$\begin{cases} \dot{\gamma} = \left[\frac{Po}{mg}\sin\alpha_s + \frac{C_{zs}}{C_{z_1}} - \cos\gamma\right]\frac{g}{V} \\ V_{obj} = \frac{\dot{V}}{g} + \frac{\omega_1}{2.5}(V - V_c)/g \\ \dot{V} = \frac{Po}{M}\cos\alpha_s - g\frac{C_{xs}}{C_{z_1}} - g\sin\gamma \end{cases}$$

ω_1 est un paramètre de réglage fixant la dynamique de réponse du système piloté.
De manière identique la commande de braquage est définie par:

$$\boxed{\dot{dm}_c = -2\left(\frac{\dot{C}_m}{C_{z_{ah}}} + 1{,}3\,\dot{q}\frac{l_h}{V}\right)}$$

avec :

$$\dot{C}_m = -C_{z_1}(Q_N + 2{,}5\,\omega\,q_{obj})$$
$$q_{obj} = \left[2\frac{C_{z_1}}{C_{z_a}}\frac{g}{V}\frac{\dot{P}}{Mg} + \dot{q} + \omega(q - q_c)\right]\frac{\rho_z^2}{gl}$$
$$q_c = \dot{\gamma}_c\frac{C_{z_1}}{C_{z_{av}}}\left(\frac{2\dot{V}}{V} + \omega_1\gamma_{obj}\right)$$
$$\gamma_{obj} = +0.5\frac{C_{z_a}}{C_{z_1}}(\gamma - \gamma_c) - \frac{V}{g}\dot{\gamma}_c + \frac{V}{g}\dot{\gamma}$$

Les variables suivantes étant issues des équations de la mécanique du vol.

$$Q_N = \frac{\dot{P}_c h}{Mg\,l} + \left[\left(0{,}24 - \frac{l_h}{l}\frac{S_h}{S}\frac{C_{z_{ah}}}{C_{z_a}}(1-\varepsilon_a)\right)\right]\left(\dot{dm} - 2\frac{\dot{V}}{V}\right) - 2\frac{Po}{Mg}\frac{h}{l}\frac{\dot{V}}{V}$$
$$\dot{dm} = 2\frac{\dot{V}}{V} + \frac{C_{z_a}}{C_{z_1}}\dot{\alpha}$$
$$\dot{\alpha} = q - \dot{\gamma}$$
$$\dot{q} = \left[\frac{Poh}{Mgl} + \frac{C_m}{C_{z_1}} - 0.24\,(f_V\sin\alpha_s + f_{nv}\cos\alpha_s)\right]\frac{gl}{\rho_z^2}$$
$$\gamma_c = -\frac{\omega_1}{2.5}(\gamma - \gamma_c)$$

Ce pilote permet le suivi de consigne en pente γ_c et en vitesse V_c en calculant à partir de l'état du système les variations de poussée et de braquage de profondeur.

III.3- Commande floue

a - Commande à partir de règles de pilotage

Les règles de pilotage d'avion en vol longitudinal peuvent s'exprimer par les deux propositions suivantes :

Relation 1

- *La poussée est modulée en fonction de l'écart de vitesse (V_c-V) et de pente (γ_c-γ).*

Relation 2

- *La pente γ est contrôlée au "manche" en fonction de l'écart (γ_c-γ) enregistré et de la vitesse de tangage* q.

Ces deux règles s'interprètent en langage flou comme deux relations à deux entrées et une sortie reliées par un jeu de règle de type proportionnel dérivé. En normalisant toutes les variables utilisées entre -1 , +1, on définit sur chacun d'elles le vocabulaire à cinq termes suivant

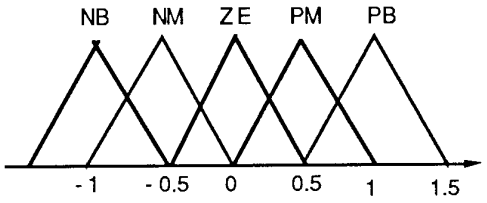

Ce choix "arbitraire" de fonctions d'appartenance triangulaire sur un domaine de définition borné est justifié par les deux constatations suivantes :

- la forme géométrique de la fonction caractéristique influe peu sur le comportement global du correcteur flou. La forme triangulaire est alors adoptée par souci de simplicité.
- le domaine d'évolution d'une variable physique est rarement infini. L'adoption d'un domaine de définition bornée et normalisé à [-1, +1] permet de prendre systématiquement en compte les saturations physiques des variables considérées.

Les tableaux de règles s'écrivent alors :

Relation 1 :

Ecart en vitesse

Ecart en pente	*NB*	*NM*	*ZE*	*PM*	*PB*
NB	NB	NB	NB	NM	ZE
NM	NB	NB	NM	ZE	PM
ZE	NB	NM	ZE	PM	PB
PM	NM	ZE	PM	PB	PB
PB	ZE	PM	PB	PB	PB

Variation de poussée

Relation 2 :

Ecart en pente

Vitesse de tangage	*NB*	*NM*	*ZE*	*PM*	*PB*
NB	ZE	NM	NB	NB	NB
NM	PM	ZE	NM	NB	NB
ZE	PB	PM	ZE	NM	NB
PM	PB	PB	PM	ZE	NM
PB	PB	PB	PB	PM	ZE

Variation de braquage

Ces deux règles peuvent se traduire sous forme linéaire par:

$$\dot{P}_c = k_1 (V_c - V) + k_2 (\gamma_c - \gamma)$$

$$d\dot{m}_c = k_3 (\gamma_c - \gamma) + k_4 q$$

correspondant au schéma bloc suivant :

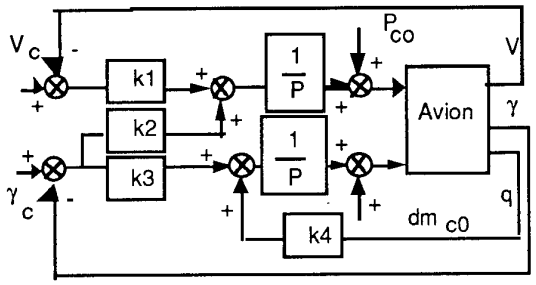

b - Commande déduite de la commande de référence

A partir de la commande de référence déterminée sur les équations de l'avion, il est possible de définir des règles de pilotage utilisées en tant que règles expertes par le contrôle flou.

Contrôle en vitesse :

Considérons les variables normalisées suivantes :

$$\varepsilon_v = (V_c - V) / \varepsilon_{vmax}$$

$$\gamma_d = \frac{\dot{\gamma}}{\dot{\gamma}_{max}}$$

$$A_{cc} = \frac{V}{\dot{V}_{max}}$$

avec :

$$\varepsilon_{Vmax} = \frac{\Delta P_{0max}}{T} \frac{2.5}{M\omega_1^2}$$

$$\dot{\gamma}_{max} = \frac{\Delta P_{0max}}{T} \frac{1}{Mg}$$

$$\dot{V}_{max} = \frac{\Delta P_{0max}}{T} \frac{1}{M\omega_1}$$

ΔP_{0max} : variation max de poussée

T : période de pilotage

La variation de poussée ΔP_0 est alors déterminée par l'application des relations floues illustrées par les tableaux suivants déduits de la relation :

$$\Delta P = \gamma_d - A_{CC} + \varepsilon_v$$

A_{CC} \ ε_v	*NB*	*NM*	*ZE*	*PM*	*PB*
NB	ZE	PM	PB	PB	PB
NM	NM	ZE	PM	PB	PB
ZE	NB	NM	ZE	PM	PB
PM	NB	NB	NM	ZE	PM
PB	NB	NB	NB	NM	ZE

et

γ_d	*NB*	*NM*	*ZE*	*PM*	*PB*
	NB	NM	ZE	PM	PB

Ce contrôle à trois entrées et une sortie est schématisé par :

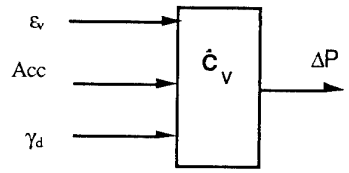

Contrôle en pente :

Les règles de contrôle en pente, tirées de l'expression de la commande en braquage du pilote de référence, peuvent être exprimées à partir de relations floues à deux entrées, une sortie mises en cascade, en considérant les variables intermédiaires

$$\gamma_{obj},\ q_c,\ q_{obj},\ c_m^{\circ}$$

Détermination de γ_{obj} :

$$\gamma_{obj} = -\left(0.5\ \frac{C_{za}}{C_{zl}} + \frac{\omega_1}{2.5}\frac{V}{g}\right)(\gamma - \gamma_c) + \frac{V}{g}\dot{\gamma}$$

Soit schématiquement une relation floue : F_1

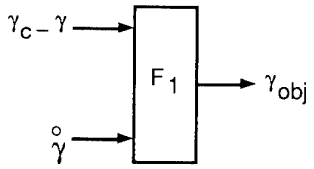

Détermination de q_C :

$$q_c = -\frac{C_{zl}}{C_{zav}}\left(2\frac{\dot{V}}{V} + \omega_1\,\gamma_{obj}\right) - \frac{\omega_1}{2.5}(\gamma - \gamma_c)$$

Soit la relation F_2 entre les variables :

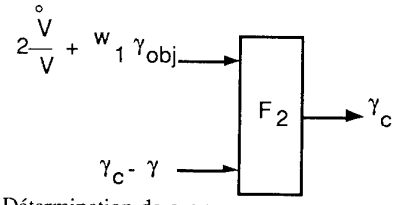

- Détermination de q_{obj} :

$$q_{obj} = \frac{\rho_z^2}{g\,l}\left[\omega(q - q_c) + \left(\dot{q} + 2\frac{C_{zl}}{C_{za}}\frac{g}{V}\frac{\dot{p}}{Mg}\right)\right]$$

D'où la relation F_3 :

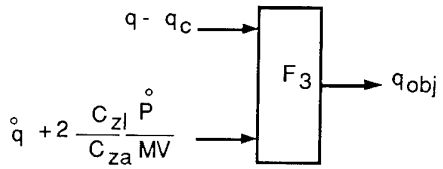

- Détermination de $C_{\dot{m}}$:

$$C_{\dot{m}} = -C_{zl}\left(Q_N + 2.5\ \omega\ q_{obj}\right)$$

D'où la relation F_4 :

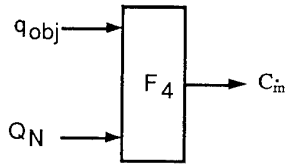

Enfin la commande du braquage d'aileron sur une période T :

$$\Delta(dm_c) = -2T\left(\frac{C_{\dot{m}}}{C_{zah}} + 1{,}3\,\frac{lh}{V}\dot{q}\right)$$

qui peut être traduite sous une relation floue F_5 :

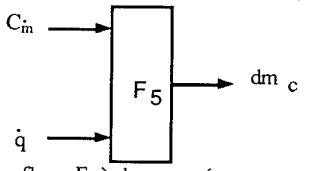

Chaque relation floue F_i à deux entrées, une sortie met en jeu le tableau de règles expertes dans lequel cinq termes de vocabulaire sont définis sur chaque variable normalisée entre -1 et +1 :

$$S = -k_1 E_1 - k_2 E_2$$

Soit S_M la saturation sur la sortie :

$$\frac{S}{S_M} = -\frac{E_1}{E_{1M}} - \frac{E_2}{E_{2M}}$$

avec

$$E_{1M} = -\frac{S_M}{k_1}$$

et

$$E_{2M} = -\frac{S_M}{k_2}$$

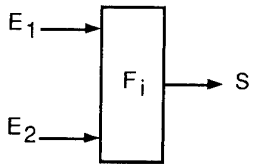

E_2/E_{2M} \ E_1/E_{1M}

	NB	*NM*	*ZE*	*PM*	*PB*
NB	PB	PB	PB	PM	ZE
NM	PB	PB	PM	ZE	NM
ZE	PB	PM	ZE	NM	NB
PM	PM	ZE	NM	NB	NB
PB	ZE	NM	NB	NB	NB

III.4-Test en simulation numérique

Les tests en simulation des différentes lois de pilotage ont été effectués avec des valeurs numériques représentatives d'un avion en phase d'atterrissage.

Pour la loi de référence, le réglage du pilote consiste à fixer les valeurs des paramètres ω_1 et ω.

Pour la première loi de commande floue composée de deux tableaux de règles pour calculer les variations de poussée et de braquage, il est nécessaire de définir le vocabulaire sur les

différentes variables utilisées en choisissant pour chacune d'elles une valeur de normalisation.

Ecart de vitesse	10 m/s
Ecart de pente	0.1 rd
Vitesse de tangage	0.03 rd/s
Variation de poussée	400 N
Variation de braquage	0.005 rd

La deuxième loi de contrôle floue utilise, pour la régulation en pente, une série de contrôles élémentaires, assimilable à une relation linéaire de type proportionnel dérivée. En utilisant une représentation normalisée des variables, la définition des normes sur les variables de sortie de chaque contrôle élémentaire suffit à la détermination de la loi de contrôle, les gains de commande étant définis par les paramètres de l'avion piloté.

Pilotage en vitesse :

$$\Delta P_0 = - k_0 (V_c - V) - k_1 \dot{\gamma} - k_2 \dot{\gamma}$$

avec

$$k_0 = - M T \frac{\omega_1^2}{2.5}$$

$$k_1 = + M T g$$

$$k_2 = - M T \omega_1$$

Pilotage en pente :

- Correcteur F1

$$\gamma_{obj} = - \quad k_3 (\gamma_c - \gamma) - k_4 \dot{\gamma}$$

$$k_3 = + \frac{\omega_1}{2.5} \frac{V}{g} + 0.5 \frac{Cz_a}{Cz_e}$$

$$k_4 = - \frac{V}{g}$$

et

$$\gamma obj_{max} = 0.1 \text{ rd}$$

- Correcteur F2

$$q_c = - \left(k_5 \gamma_{obj} + k_6 \dot{V} \right) - k_7 (\gamma_c - \gamma)$$

$$k_5 = + \omega_1 \frac{Cz_e}{Cz_{av}}$$

$$k_6 = + \frac{2}{V} \frac{Cz_e}{Cz_{av}}$$

$$k_7 = - \frac{\omega_1}{2,5}$$

et

$$q_{Cmax} = 0.1 \text{ rd/s}$$

- Correcteur F3

$$q_{obj} = - \quad k_8 \left(\dot{q} + kg \Delta P_0 \right) - k_{10} (q - q_c)$$

$$k_8 = - \frac{\rho_3^2}{g l}$$

$$k_9 = - \frac{2}{TMV} \frac{Cz_e}{Cz_a}$$

$$k_{10} = - \frac{\rho_3^2}{g l} \omega$$

et

$$q_{obj_{max}} = 0.1 \text{ rd/s}$$

Correcteur F4 :

$$C_{\dot{m}} = - \quad k_{11} q_{obj} - \left(k_{12} (q - \dot{\gamma}) + k_{13} \dot{V} + k_{14} \Delta P_0 \right)$$

$$k_{11} = + 2.5 \omega \; Cz_l$$

$$k_{12} = + Cz_a \left(0.24 - \frac{l_n}{l} \frac{Cz_a - Cz_{ah}}{Cz_a} \right)$$

$$k_{13} = - \frac{2}{V} \frac{\rho_0^h}{Mgl} Cz_l$$

$$k_{14} = + \frac{h}{l} \frac{Cz_l}{MTg}$$

et

$$C_{\dot{m}max} = 0.4 \text{ rd/s}$$

Correcteur F5 :

$$\Delta dm = - \quad k_{15} C_{\dot{m}} - k_{16} \dot{q}$$

$$k_{15} = + \frac{2T}{Cz_{ah}}$$

$$k_{16} = + 2.6 \frac{Tl_n}{V}$$

Pour les simulations tests, nous considérons l'avion en phase d'approche à basse altitude avec comme valeur de consigne une vitesse de 62 m/s et une pente de descente de 3°. A l'instant initial, l'avion présente une assiette nulle, un braquage gouverne de 2° pour une vitesse de 62 m/s sur une pente de - 3°. Pour chaque simulation, une perturbation est introduite à 10 s en considérant un échelon de vent vertical de 5 m/s. Par comparaison avec la commande idéale, les deux types de contrôleur flou présentent des performances acceptables dans ces conditions de vol. Il peut paraître surprenant que la simplicité des règles de pilotage du premier contrôle flou face à la complexité des règles de pilotage des deux autres pilotes n'entraîne pas de plus amples différences. Ceci s'explique par le fait que pour cette simulation, seule la chaîne de contrôle en pente est sollicitée minimisant ainsi les effets de couplage.

D'autres simulations, pour lesquelles les écarts de consigne sont importants à la fois en vitesse et en pente, mettent en évidence les moins bonnes performances du contrôleur flou à deux tableaux de règles par rapport aux deux autres. La complexité des lois de pilotage a essentiellement pour but d'éliminer les interactions entre les deux chaînes de pilotage. Ce découplage est réalisé par le deuxième contrôleur flou grâce aux règles déduites du pilote de référence. Vu la complexité des variables mises en jeu dans ces règles, il parait peu vraisemblable qu'un expert humain ait pu émettre en langage naturel des règles équivalentes d'un point de vue découplage. Ce problème lié à l'aspect multi-entrées du système, est un problème général des systèmes multivariables pour lesquels la commande globale non interactive reste difficile à déterminer. Pour ce type de système l'expert humain se contentera souvent d'un contrôle chaîne par chaîne à échelles de temps différentes.

La traduction en logique floue du pilote de référence montre cependant qu'il est possible d'interpréter des règles de contrôle relativement complexes en terme de logique floue. Ceci prouve la quasi équivalence entre les techniques de commande classique et l'approche floue, les différences provenant des saturations introduites au niveau des variables intermédiaires dans la mise en oeuvre floue.

IV - ATTERRISSAGE AUTOMATIQUE

IV.1 - Atterrissage manuel

La qualité d'un atterrissage s'évalue en fonction de la position du point d'impact et de la vitesse verticale au moment du toucher de piste. Suivant l'objectif à satisfaire en priorité trois sortes d'atterrissage sont effectués par les pilotes, à savoir l'appontage, l'atterrissage de précision, l'atterrissage standard.

- L'appontage

Pour ce type d'atterrissage le critère essentiel est la position du point d'impact, la vitesse verticale devant rester inférieure à 10 ft/s. Ceci est réalisé en assurant une pente de descente constante (3°) sans réduction de poussée.

La trajectoire théorique réalisée est la trajectoire d'approche (glide) jusqu'au sol.

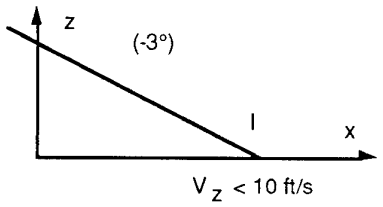

- L'atterrissage de précision

Dans ce cas l'objectif est, en plus de la précision du point d'impact au sol, d'atterrir avec une vitesse V_z inférieure à 6ft/s. Cet atterrissage est effectué en procédant comme suit :

- *Extinction des moteurs à l'entrée de piste (a) à l'altitude h_0*
- *Maintien de la vitesse "au manche" jusqu'à l'altitude h_1*
- *Réalisation de l'arrondi à partir de h_1.*

Cette procédure conduit à une trajectoire théorique qui passe sous la trajectoire d'approche pour maintenir la vitesse malgré l'extinction des moteurs, ce qui permet de rejoindre le point d'impact I, avec une vitesse V_Z plus faible.

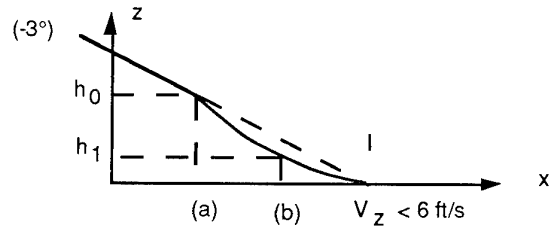

- L'atterrissage standard

Dans ce cas, la contrainte sur la vitesse verticale au toucher de piste est prépondérante. La procédure utilisée consiste à effectuer simultanément dès l'entrée de piste (a) une réduction des moteurs et un arrondi pour avoir une vitesse V_Z inférieur à 2 ft/s. L'arrondi est obtenu par variation lente et continue du braquage de profondeur. La valeur de cette variation est fonction de l'avion et est acquise par expérience.

La trajectoire théorique réalisée reste toujours au-dessus du "glide" conduisant à un impact plus éloigné que lors des deux précédentes procédures d'atterrissage.

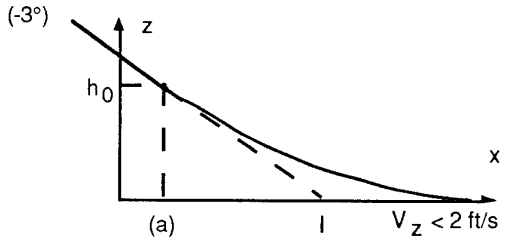

Lors de ces trois procédures d'atterrissage une règle impérative est appliquée par les pilotes : *"Ne jamais pousser sur le manche en phase finale d'atterrissage".*

IV.2 - Règles d'atterrissage

Des procédures d'atterrissage précédentes, il est possible de déduire des règles de contrôle pour une implantation en logique floue.

- Appontage

Les règles d'atterrissage sont les règles d'asservissement en pente auxquelles on peut adjoindre une règle de sécurité interdisant de pousser sur le manche en phase finale. Cette règle peut s'exprimer ainsi, avec la consigne signifiant l'ordre de commande aileron :

"Si l'altitude est basse et si la consigne est positive alors la consigne est nulle".

Le contrôleur flou assurant l'atterrissage selon une procédure d'appontage consiste alors en la mise en oeuvre des règles expertes suivantes :

- *Si l'altitude est haute, alors la consigne est inchangée.*
- *Si l'altitude est basse et si la consigne est négative ou nulle alors la consigne est inchangée.*
- *Si l'altitude est basse et si la consigne est positive alors la consigne est nulle.*

avec la variable floue altitude définie comme suit :

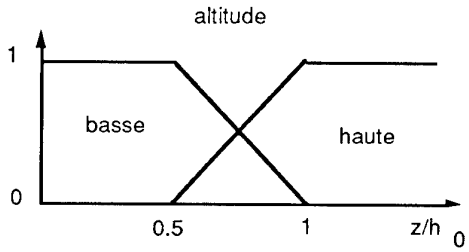

- Atterrissage de précision

Les règles de contrôle d'atterrissage portent uniquement sur la commande de profondeur, la puissance moteur étant coupée à l'entrée de piste. L'atterrissage s'effectue alors en deux phases en fonction de l'altitude, une phase de maintien de la vitesse et une phase d'arrondi. D'où les règles expertes suivantes :

- *Si l'altitude est haute alors la consigne est inchangée.*
- *Si l'altitude est moyenne alors la consigne est proportionnelle à l'écart de vitesse.*
- *Si l'altitude est basse alors la consigne est proportionnelle à l'écart en pente, si négatif sinon nulle.*

avec la définition de la variable altitude

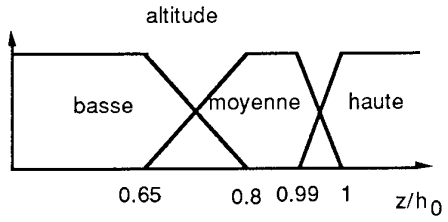

-Atterrissage standard

La réduction des moteurs est effectuée en boucle ouverte suivant un taux de variation donné. La commande de profondeur est déterminée en assurant l'asservissement sur la pente de descente auquel vient s'ajouter une valeur constante U_0 réalisant l'arrondi. Les règles mises en jeu s'expriment alors :

- *Si l'altitude est haute, la consigne est inchangée*
- *Si l'altitude est basse, et si la consigne est négative ou nulle alors la consigne est inchangée*
- *Si l'altitude est basse et si la consigne est positive alors la consigne est nulle*
- *Si l'altitude est basse et si la pente est négative alors la consigne est égale à U_0*
- *Si l'altitude est basse et si la pente est positive alors la consigne est nulle.*

IV.3 - Tests en simulation numérique

Pour permettre une simulation significative de l'atterrissage, le modèle de l'avion doit être complété par une modélisation des effets de sol. Pour cela nous utilisons le modèle proposé par l'Aérospatiale qui introduit des modifications fonctions de l'altitude au niveau de l'incidence locale des ailerons et du coefficient de portance C_Z.

Pour la profondeur, le terme ε dans le calcul de l'incidence α_h est remplacé par ε_h défini par :

$$\varepsilon_h = \varepsilon(1 - \delta) + \delta\, \varepsilon_g$$

avec

$$\varepsilon_g = 1°$$

$$\delta = 1.53 \left(e^{-\frac{h}{10}} - 0.02 \right) \quad \text{si} \quad h < 40\ m$$

$$= 0 \quad \text{si} \quad h \geq 40\ m$$

Pour la portance, l'ancien coefficient de portance, noté C^*_z, est remplacé par :

$$C_z = C_z^* + \mu\, C_{z_g}$$

avec

$$C_{z_g} = 0.15$$

$$\mu = 0.1\, \frac{40 - h}{h + 4} \quad \text{si} \quad h < 40\ m$$

$$= 0 \quad \text{si} \quad h \geq 40\ m$$

Pour toutes les simulations effectuées, les conditions initiales sont telles que l'avion est quasiment stabilisé sur la trajectoire de descente. De plus pour assurer le guidage de l'appareil sur cette trajectoire d'approche, la consigne de pente est calculée par la formule :

$$\gamma_c = \gamma + kg\ (\gamma - \gamma_g)$$

avec

$$kg = 1.5$$

et γ, γ_g définis par la figure :

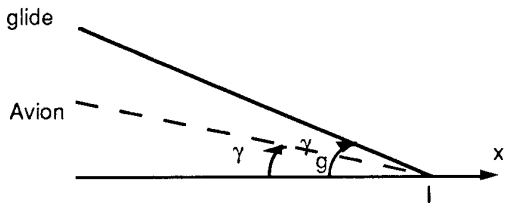

La prise en compte des règles d'atterrissage est effectuée après le calcul d'asservissement sur la pente de consigne. C'est-à-dire que schématiquement le contrôleur flou d'atterrissage est mis en série du contrôleur de pente :

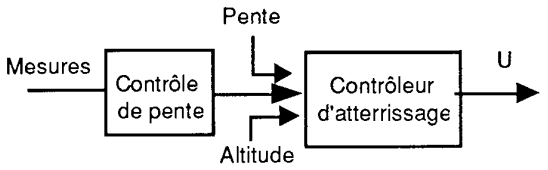

-Test de l'appontage :

A basse altitude, en l'absence de lois spécifiques à l'atterrissage, l'effet de sol provoque un contre braquage des ailerons. Ce phénomène, à éviter en pilotage manuel, peut être éliminé en refusant une commande positive à basse altitude. Le contrôleur de pente étant programmé en logique floue, l'adjonction de cette règle de sécurité s'effectue par modification des fichiers de règles et non par modification du programme de commande. Ce dernier point illustre un des points intéressants de l'approche floue dans la phase de synthèse de la commande. Elle permet une grande souplesse dans la modification des règles de contrôle par opposition à la rigidité des structures des correcteurs linéaires.

-Test de l'atterrissage de précision

La procédure décrite par le pilote pour cet atterrissage conduit à un changement de mode de contrôle sur la chaîne de commande des ailerons. A haute altitude, le manche contrôle la pente, à moyenne altitude c'est la vitesse qui est pilotée et enfin à basse altitude de nouveau la pente est assurée par la commande de profondeur.

Ce type de lois d'atterrissage permet de mettre en évidence une autre qualité du contrôle flou qui est la facilité de résolution du problème de changement de mode de pilotage sur une chaîne de commande. Le problème de discontinuité souvent rencontré lors de ces changements de mode est résolu par le chevauchement plus ou moins important des fonctions caractéristiques du vocabulaire sur la variable de changement de mode (l'altitude pour l'atterrissage).

-Test de l'atterrissage standard

Pour fixer la valeur numérique du biais sur la commande réalisant l'arrondi en phase finale, la référence choisie est la trajectoire obtenue en atterrissage automatique classique avec variation de la consigne de pente. Cet atterrissage est assuré en utilisant le contrôle en pente décrit précédemment avec une variation de consigne γ_C à partir de l'altitude h_0 atteinte à l'instant t_0 :

$$\gamma_c = \gamma_0\left(1 - \frac{2}{3}\left(1 - e^{-(t-t_0)\omega}\right)\right)$$

Les quelques tests effectués en simulation montrent que la logique floue permet une mise en oeuvre relativement aisée de règle de pilotage exprimée par les pilotes, mais qu'il ne faut pas associer contrôle flou et robustesse comme c'est souvent le cas dans la littérature. La robustesse reste une propriété liée à la boucle fermée (qu'elle soit en logique classique ou floue) et non au traitement de données floues. Ces simulations d'atterrissage standard montrent bien que la valeur U_0 assurant l'arrondi, déterminée par apprentissage et représentative en fait du savoir faire du pilote, est valable pour un type d'avion et doit être réapprise pour d'autres configurations (induisant par exemple de grandes modifications d'effet de sol). Ce sont des problèmes de ce genre qui ont entraîné le développement des techniques de contrôle avec apprentissage du type neuro-flou.
Ces techniques permettent une adaptation du contrôleur aux variations de comportement sous réserve qu'elles restent lentes mais elles ne peuvent pas améliorer la robustesse des lois face aux perturbations.

V-CONCLUSION

L'utilisation de la logique floue pour la commande des systèmes offre des caractéristiques intéressantes qui font de cette approche une technique de synthèse possible.

Le principe et la mise en oeuvre d'une commande floue sont d'une relative simplicité, et l'utilisation de logiciels permettant la lecture de variables floues et l'interprétation des règles ou relations expertes offre vite une grande souplesse de programmation.

La traduction en logique floue de correcteurs linéaires, même multivariables, d'un côté, et de l'autre l'interprétation d'un pilote flou comme loi linéaire au voisinage de l'équilibre montrent l'équivalence des performances atteignables par l'une ou l'autre approche. En particulier, le choix d'une commande floue n'induit pas une meilleure robustesse de la chaîne pilotée comme le laisse entendre la rumeur sur le contrôle flou.

Pour le problème spécifique du pilotage d'un avion, la connaissance et l'utilisation des équations de la mécanique du vol donne à l'approche classique une sécurité d'utilisation (temps de réponse, marges de stabilité) qu'il est difficile de retrouver dans l'approche floue et il serait très maladroit de prétendre réinventer l'automatique à partir de règles floues. Cependant, comme l'ont montré les quelques tests en simulation, l'utilisation de la logique floue permet un traitement élégant des non linéarités et des changements de mode de pilotage. De plus la facilité d'introduction de règles supplémentaires (règles de sécurité par exemple) donne au contrôleur flou des qualités de mise en oeuvre intéressantes au niveau de la synthèse de lois de commande. Cette approche peut contribuer alors à préciser la structure d'un pilote pour faire face à des situations particulières faisant appel à un savoir faire (phénomènes non linéaires, modification de condition de fonctionnement, ...) quitte à traduire, pour l'implantation sur le calculateur de bord, les règles floues en terme de variations de gain ou d'interpolation linéaire entre différentes lois.

BIBLIOGRAPHIE

E.H. MAMDANI "Applications of fuzzy algorithms for control of simple dynamic plant", Proc. Institution of Electrical Engineers, Control and Science, 121, 1585-1588, 1974 .

M.SUGENO "Industrials applications of fuzzy control", . North Holland, 1985.

D.DUBOIS, H. PRADE "Théorie des possibilités", Masson, 1987.

W. PEDRYCZ "Fuzzy control and fuzzy systems", J. Wiley & Sons, 1989.

B. BOUCHON-MEUNIER "La logique floue", Que sais-je ? - n°2702 PUF, 1993.

N.IMBERT,A.PIQUEREAU "Pertinence des approches non conventionnelles pour la commande des systèmes ", Rapport d'étude n° 2/7817.00 DERA, Mars 1993.

N.IMBERT,A.PIQUEREAU,D.DUBOIS "Evaluation des techniques de contrôle flou pour le pilotage d'avions", Rapport d'étude n° 1/7836.00 DERA, Avril 1993.

O.F.T.A. "Logique Floue", Arago 14 , Masson 1994.

The Control System Design Methodology of the STOL & Maneuver Technology Demonstrator

David J. MOORHOUSE
S/MTD Chief Engineer, Wright Laboratory, WL/FIMS
Building 450, 2645 5th St., Ste 16, Wright Patterson AFB,
OHIO 45433-7922 U.S.A.

Kevin D. CITURS
McDonnell Douglas Corp.
Mail Code 0341280, P.O. Box 516
St Louis, MO 63166-0516 U.S.A.

INTRODUCTION

Control theory and system design methodologies are becoming more sophisticated each year; but at the same time the aircraft systems are becoming increasingly complex. This progress is not without steps backward, as recent crashes of the Grippen in Sweden and the YF-22 in America indicate that sometimes "the dragon eats the Knight". The STOL & Maneuver Technology Demonstrator (S/MTD) program was a Wright Laboratory development of comparable flight control complexity. This program was structured to develop and validate through analysis, experiment and flight test, specific technologies intended to provide current and future high-performance fighters with both STOL capability and enhanced combat mission performance. Figure 1 shows the major modifications that were made to an existing F-15B. The subject of this paper is the integration of two-dimensional thrust vectoring and reversing exhaust nozzles into an all-new digital Integrated Flight/ Propulsion Control (IFPC) system.

The overriding requirement of the IFPC system was to be "capable of functionally integrating all aspects of flight, engine, and nozzle control including aerodynamic control surfaces, engine thrust, thrust vectoring, thrust reversing and differential efflux modulation, control and stability augmentation, high lift system, steering and braking". The intent was that integration be an objective of the demonstration program, not just a means to achieve requirements as necessary.

All the bidders on the S/MTD contract were strongly encouraged to use multivariable control theory, although it was not an absolute requirement. With integration as a program objective, there was some uncertainty that a classical approach would optimize use of all the available effectors (Figure 2). At the same time, there was no desire to commit to a totally multivariable design approach. The initial design effort compared results of classical techniques performed by McDonnell Douglas Aerospace (MDA) and multivariable techniques performed by Honeywell Systems Research Center. This early comparison provided a rational basis to choose which design method to continue for implementation into the aircraft. The purpose of this paper is to document the S/MTD experience. It is not intended as a theoretical exposition however, but as a more practical example and guide to the design of a successful control system. Results are presented in the form of pilot ratings and comments.

DESIGN REQUIREMENTS

System Requirements

The IFPC system was required to provide "good inner-loop stability and positive manual control in all axes of the air vehicle throughout its intended operating envelope both in flight and on the ground (satisfying the intent of specification MIL-F-8785C)". This requirement was intended to achieve good flying qualities over the whole envelope guided more by the intent than the letter of the specification. This recognizes that meeting the letter of the specification is no guarantee of adequate flying qualities. The "intent" was met by using additional, second-tier design guidelines. In addition, the requirement for 'positive manual control' was intended to preclude consideration of automatic landing systems. One flying qualities requirement that was explicitly called out in the Statement of Work was a maximum equivalent system time delay of 100 msec; this should be an explicit, hard requirement in any control system to be designed for any precise task, regardless of the method of design or implementation.

The system was also required to meet the intent of MIL-F-9490D with the stability margins as design goals, clarified by: "Such single-input/single-output parameters may be too restrictive or too lenient for different aspects of the IFPC system in achieving the desired compromise between stability and performance. The contractor shall analyze and document deviations from the MIL-F-9490D requirements". This was interpreted as a requirement to validate or modify the 6db gain margin and 45 deg phase margin for

Paper presented at the Flight Mechanics Panel Symposium held in Turin, Italy, from 9-13 May 1994.

a complex system.

Specific flight control modes were required with the rationale: "In order to provide the ability to assess task performance and minimize pilot workload in the flight vehicle, the integrated system shall also provide the flexibility to permit inflight selection of mission task oriented control modes as determined by analysis and simulation. Mode switching transients shall not produce unsafe aircraft responses. As a minimum, the following modes are required:

A CONVENTIONAL mode shall be designed for satisfactory performance over the flight test envelope, including conventional landing, without the use of the added technologies. This mode will serve as a baseline for performance evaluation and as a backup in the event of multiple failure of the new technology components.

A STOL mode shall be designed to provide precise manual control of flight path trajectory, airspeed and aircraft attitudes. The integrated control system and other technologies shall be combined to provide short field performance in weather and poor visibility. The purpose of this mode is to minimize pilot workload during precise manual landings, high reverse thrust ground operations and maximum performance takeoffs.

A CRUISE mode shall be designed to enhance normal up-and-away and cruise task performance. The purpose of this mode is to use the integrated control system and other technologies to optimize appropriate measures of merit representing an improvement over the cruise capability of the baseline aircraft.

A COMBAT mode shall be designed to enhance up-and-away maneuverability. The purpose of this mode is to use the integrated control system and other technologies to optimize appropriate measures of merit representing an improvement over the combat maneuvering or weapon delivery performance of the baseline aircraft".

These modes were specified in this form for technology demonstration purposes, with the above general guidance as to the intent of each mode. Once the benefits of each mode were identified, they could be implemented in a production application partly or fully as necessary.

Detailed Requirements

Both the MDA and the government project offices were committed to a principle of designing to analytical flying qualities requirements. There was complete agreement that the most critical part of a design is the definition of requirements. Any discussion of design methodology is meaningless without good requirements. The starting point was lessons learned documented in Reference 1 such as making the command paths as direct as possible by placing filtering and shaping functions in feedback paths. The next step was a definition of preferred regions, i.e. design points, within the specification boundaries which was documented in Reference 2. Many refinements and additions were made during a series of piloted simulations, however no parameter was changed by "simulation tuning". When the need for a flying qualities change was identified during the early simulations, the actual change was defined analytically and validated with further simulation.

One detail requirement was defined independent of the military specification requirements - the precision landing mode. Airspeed and pitch responses were required to be decoupled, removing the pilot task to coordinate stick and throttle inputs. In this mode, throttle commands airspeed with no change in flightpath and stick commands pitch rate with no change in airspeed. When the aircraft is at the desired approach speed, glideslope angle is controlled with only stick inputs - a simpler task. It was also required that Direct Lift Control (using flaps and ailerons) would be integrated to yield a minimum-phase flightpath response to pitch stick inputs.

DESIGN METHODOLOGIES

Classical

In general terms, a classical design develops in a step by step process to satisfy textbook inner and outer loop requirements in the military flying qualities specification (illustrated conceptually in Figure 3). Second order effects such as adverse coupling are eliminated with crossfeed, but details of these requirements are frequently a fallout as the design progresses. A significant advantage is the insight into the system that is provided by the process itself of adding complexity in steps to enhance system performance. On the other hand, the result is dependent on the fidelity of the aircraft model to an unknown extent and there is not a well-defined end to the process (other than schedule).

Classical methods were used in the design of the lateral and directional axes in all control system modes and in the longitudinal axis of the Conventional mode, both flaps up and flaps down.

The lateral/directional control system was designed using root locus and Bode plot design methods. The control effectors included differential canard and rudders for directional control, ailerons and differential stabilator for roll control (plus differential flaps in the flaps down modes). Stabilator rate and position commands from lateral control system inputs were limited to ensure pitch priority.

Flaps down: The development of the flaps down lateral and directional control laws was driven by the heavy emphasis on the crosswind landing requirements. Careful blending of differential canard and rudder produced a direct sideforce

capability which offset nearly 50% of the bank angle required during a crabbed approach. The direct sideforce was blended with a sideslip command to provide a natural-appearing response to pedal input. Full authority roll rate feedback augmented the roll mode dynamics. Directional augmentation was provided by a blend of lateral acceleration and estimated sideslip rate. In addition to the proportional feedbacks, a directional integrator was implemented to provide uniform sideslip response to pedal inputs. Lateral to directional interconnects from the differential ailerons and stabilators provide roll roordination. The interconnects are washed out at a frequency determined by the bare airframe roll damping. Hence, they provided a yawing moment command based on roll acceleration. An additional roll rate feedback path commanded yawing moments necessary to coordinate sustained roll rates.

The CONVENTIONAL mode flaps down logitudinal control system used longitudinal stick and proportional plus integral feedbacks of pitch rate and angle of attack. The blend of pitch rate and angle of attack feedback to the integrator was chosen to provide a constant pitch rate per inch of stick deflection. The angle of attack feedback was chosen to provide a stable steady state variation of stick force per degree angle of attack at zero pitch rate. The ratio of proportional to integral gains was chosen to produce a classical short period second order response. The canard deflection was scheduled with angle of attack to produce the desired pitch stability characteristics. Collective stabilator deflection was the primary pitch effecter.

Development of the ground handling control laws was complicated by the adverse effects from thrust reversing. Special logic was needed to ensure the aircraft would achieve a 3-point attitude in the presence of predicted nose-up pitching moments generated by thrust reversing in ground effect (see Reference 3). If selected by the pilot, a weight on wheels indication initiated a nose down input, retracted the drooped flaps and ailerons, cancelled the lateral to directional interconnects and commanded maximum reverse thrust and automatic braking. Ground track stability was enhanced by the addition of yaw rate feedback to nose wheel steering. The lateral directional control system architecture changed with weight on wheels to provide direct sideforce commanded by the lateral stick and yaw rate commanded by the pedals. Linear design and analysis was applied wherever possible. Due to the non-linearities and constantly changing conditions which occur during ground operations, the majority of the design was accomplished using knowledge of the forces and moments to be expected and extensive six degree of freedom modeling. Problems with unexpected jet/ground effect interference are documented in Reference 4.

Flaps Up: The flaps up lateral control laws use a conventional roll rate feedback path and a limited roll rate feedback path for gust rejection. The directional control laws incorporate lateral acceleration and estimated sideslip rate feedbacks. Interconnects from the lateral control commands to the directional controls are used for roll coordination. Differential stabilator is used to provide additional directional stability augmentation at high angle of attack. Equivalent system analysis verified that the resulting control system design provided the desired response characteristics. Sideslip excursions due to lateral stick were small, with no oscillatory roll component. All of the analytical parameters were within the Level 1 MIL-F-8785C boundaries, however, manned simulation testing resulted in Level 2 pilot ratings for fine tracking. After extensive analysis and simulation testing, a solution was identified which required modification of the roll/yaw phase angle relationship as a result of turn coordination. The investigation of this problem was thorough enough to result in a tentative criterion for use in future efforts (see References 5 & 6).

A new design approach was used in the development of the flaps up longitudinal control laws in the CONVENTIONAL mode. Figure 4 illustrates the process used in the design of this mode. The design guidelines were reformulated into low order equivalent system form complete with an allowable time delay. An initial architecture representing a classical proportional plus integral form was defined. A data base of trimmed aerodynamic derivatives was computed. Using the low order models, the initial architecture and the aerodynamic derivatives, an "Inverse Equivalent System" method was used to define the control system gains whick the designer selected to be varied. The principles involved are very similar to those used in generation of equivalent system fits for identification of flying qualities parameters. The difference is that the "high order" system is adjusted to fit the frequency domain representation of the desired flying qualities characteristics. Successive applications at each flight condition result in a series of point designs from which gain schedules are developed. Equivalent systems techniques were used to verify the resulting flying qualities characteristics. Robustness was checked by calculation of gain and phase margins. Nonlinear design and analysis was conducted using off-line six degree of freedom flight simulation to produce the final control law design.

The inverse equivalent system method is easy to use. The user specifies the low order system dynamics and desired time delay, a frequency range over which the matching is calculated, and the control system gains to be optimized. Initial values and allowable limits are specified for the selected control system gains. The program then varies the selected gains to minimize the mismatch in gain and phase over the specified frequency range of matching. The user evaluates the resulting gains to determine if they are satisfactory. The next design point is

then selected. During the S/MTD design effort, gains were calculated every tenth of a Mach across the design envelope at a given altitude. Each successive design used the gain values from the previous design point as initial values. A Mach sweep was conducted at 10,000 ft altitude increments. Use of this "envelope expansion" technique usually resulted in smooth gain trends. Curve fitting of the point designs to produce the final gain schedules was simplified by the use of a system architecture in which the designer had physical insight of the impact of gain selection or aircraft parameter variations. The key to successful application of this method is a good understanding of the desired response characteristics.

Manned flight simulation testing revealed a problem with the original MIL-F-8785C Level 1 design guidelines. Details of this activity can be found in Reference 7. The design guidelines were modified as a result of this analysis. Inverse equivalent systems were used to incorporate a subtle design change into the existing architecture. This can best be illustrated by reviewing the initial and modified designs at one flight condition.

The initial control law design effort began with establishment of a set of flying qualities goals based on MIL-F-8785C guidelines and past experience. These goals were defined in the form of classic second order pitch rate and load factor responses to stick input with the values designated as original in Figure 5. These design goals were applied at airspeeds above 300 knots calibrated airspeed, approximately the "corner speed" of the aircraft.

A simplified linear block diagram of the CONVENTIONAL mode longitudinal control laws at speeds above 300 knots is shown in Figure 6. This mode was designed to produce Level 1 flying qualities for precision air-to-air tracking. A forward loop integrator and a constant gain on the n feedback to the integrator provided the desired steady state stick force per g. The proportional gains on the stick, pitch rate feedback, and normal acceleration are used to produce the desired frequency and damping characteristics. The canard is driven by an angle of attack feedback to increase the lift-to-drag ratio while also stabilizing the unstable bare airframe. The values of the gains were computed using the inverse equivalent system method.

The resulting control law design met all the design goals. Pitch rate and load factor responses were second order in the 0.1 to 10 radian per second bandwidth. To verify the design, the pitch rate response was matched with a second order equivalent system with L_α fixed at the bare airframe value. The match had a low cost function and equivalent time delay was less than 70 msecs. Unfortunately manned flight simulation results indicated the design produced Level 2 flying qualities during precision tracking. It was decided to modify the CONVENTIONAL and COMBAT modes to improve tracking characteristics, and to leave the CRUISE mode as origionally designed. The selected solution involved modification of the desired pitch rate numerator lead term.

For a classic aircraft L_α is a function of the bare airframe and true airspeed, and cannot be modified by the flight control system. However, considering L_α simply as the numerator time constant in the pitch rate response it can be tailored by proper selection of gains in the flight control system. The value of L_α in the pitch rate numerator was increased by a factor of 1.67 to achieve a higher "apparent L_α".

The Apparent L_α can be altered in the pitch rate response, but not the "true L_α" which determines the relationship betwen pitch and flight path. Therefore the flight path rate, or normal acceleration, will no longer be a classic second order response. The result is a third order g response with some "g creep". While significant g creep is normally considered undesirable, our experience has shown a small amount to be acceptable. It was certainly an acceptable compromise to provide precise tracking. The pilots unanimously preferred the improved tracking over the CRUISE mode in all flight phases. The third order g response can be seen in Figure 7 which shows a step input with the original and Apparent L_α design.

$$\frac{n_z}{\delta} = \frac{K(s+1.67L\alpha)\,e^{-\tau s}}{(s+L\alpha)\,(s^2+2\zeta\omega_{sp}s+\omega_{sp}^2)}$$

It might seem that a prefilter would be a better method of attaining the desired response. However, the additional schedule complexity, time delay and potential aerodynamic uncertainties made this an unacceptable choice. A new set of design goals was defined to incorporate the Apparent L_α design as also indicated in Figure 5. The magnitude of the gain changes required are shown in the following table:

Gain	Original	Apparent L_α
K_δ	1.668	2.237
K_I	1.0	2.255
K_ρ	0.552	0.630
K_{nz}	1.622	2.427

Flight Condition: M = 0.7, Alt = 20,000 ft

Using an Inverse Equivalent System design approach allowed the team to implement an unusual design change while retaining the original architecture. This eliminated the potential problems involved in incorporating a prefilter and simplified the incorporation of non-linear control system elements following the basic gain selection. The basic insight and understanding of the original design were

maintained.

Multivariable

In principle, multivariable approaches start with some form of full state feedback and "perfect" performance, also illustrated in Figure 3. A compensator is designed to provide a specified first-order closed loop response when cascaded with the airframe plant. A prefilter is then added to satisfy flying qualities requirements. "Perfect" performance, however, implies that all the requirements must be specified up front, which is not a simple task. Then this formulation must be simplified to a practical implementation while maintaining performance benefits.

The multivariable designs were performed by Honeywell Systems and Research Center using the well-known Linear Quadratic Gaussian (LQG) synthesis method. Free parameters were chosen in such a way that the entire formal design process could be reinterpreted not as a least-squares error minimization problem but as a "loop-shaping" problem, i.e. a problem of designing feedback compensators to achieve desirable sensitivity and complementary sensitivity transfer functions at critical loop-breaking points in the system. This interpretation depends on a "loop transfer recovery" property. The basic theory of this LQG/LTR technique is well documented, e.g. References 8 & 9 and will only be summarized here with emphasis on the more practical aspects.

The feedback design problem for integrated control reduces to one of specifying requirements in the form of loop shapes and then using the LQG/LTR method to realize the compensator. The design tradeoffs between the sensitivity matrix and the complementary sensitivity matrix are conducted by changing the specified loop shapes and computing new compensators. The method yields a compensator of order equal to the order of the open-loop plant model plus the order of the appended loop-shape dynamics. The complexity of a full-state compensator is not practical, so that the next step is to simplify to a reduced-order compensator. Modal truncation was used to remove asymptotic roots, followed by a procedure of successively balancing the compensator and truncating one state at a time. It is emphasized that compensator reduction is an art and good engineering judgement must be used to arrive at the best practical solution. Since the performance and robustness of the compensation degrade as states are removed, it is important to check stability margins and closed-loop transfer functions at each stage in the process. Robustness was analyzed by means of the upper bound on Structured Singular Value, (see References 10 &11). Lastly, the required prefilter characteristics are defined explicitly by flying qualities requirements.

For the short landing mode, various regulated variables were considered. First, flightpath rate was approximated by subtracting high-passed angle of attack from pitch rate. This was discarded because a high enough highpass break frequency caused sensor noise problems, and also the gust response was deficient. Both pitch rate alone and a blend of low-passed load factor and pitch rate met stability and robustness requirements. Piloted simulation showed that pitch rate alone, together with airspeed as the regulated variable for the thrust axis, provided superior flying qualities.

Longitudinal control laws in the short takeoff and approach mode differ primarily in the use of pitch vectoring to augment the control power of the stabilator. The regulated variable was a linear combination of angle of attack at low frequency and pitch rate at high frequency, consistent with the control effectiveness of the effectors. A command shaping prefilter was used to precisely control angle of attack. Constant stick force per angle of attack was provided at lower angles of attack, with increased stick force required at high angle of attack. A washout filter was inserted to the pitching moment commands to the nozzles and canards so that all steady state trimming would be accomplished using the stabilator. During ground operations, the washout filter to the nozzle was set to behave like a fixed gain. This allowed the use of thrust vectoring to improve short/rough field operations.

Pitch rate was chosen as the regulated variable for the CRUISE and COMBAT modes, with a blend of low-passed load factor at subsonic speeds. The stabilator, canard and thrust vectoring were used together as a single moment effector. A 2-second washout was used on canard and nozzles so that the stabilator provided trim. This is misleading, however, because all three are on schedules to provide stability and minimum drag with trim stabilator near neutral.

Combined Approach

Specific characteristics for each mode were established from the general requirements above. In each case, MDA performed a classical design and Honeywell performed an LQG/LTR design to the same requirements. The original hope was to implement both design approaches for evaluation in flight test. As the control laws evolved, which as always means expands, it became obvious that there would be insufficient computer power to implement two complete sets. The more practical approach then was to make a choice of which design to implement in each case. The final choices, by mode and axis, are as shown in Figure 8.

The CONVENTIONAL mode was designed to have good flying qualities using only the aerodynamic control surfaces. The conventional mode used conventional controls to satisfy conventional requirements, the multivariable approach provided no practical benefits and classical techniques were used. The first consideration in either design approach, however, is controls-fixed static instability. With the addition of the canards to the F-15, controls-fixed static

stability is approximately 10-12% unstable subsonically. The first step in the classical approach was to schedule canard deflection as a function of angle of attack to provide positive stability. This change also eliminated the problem of an unstable pole from the multivariable formulation, yielding a simple plant.

For the CRUISE and COMBAT modes, additional requirements were imposed. Canard deflection and nozzle vector angle were coordinated to minimize steady-state drag at 1g in the CRUISE mode and at elevated load factors in the COMBAT mode. The canards were also used for short-term pitch control. In these cases, the benefits of the multivariable approach, guaranteeing stability and robustness, made it the best choice. The compensator order could be reduced to a practical proportional plus integral structure without significant degradation in stability margin. A more significant effect of compensator order reduction may be deviation from the ideal form of the compensated plant, which is discussed later.

Requirements for the STOL mode included decoupling airspeed from the pitch axis in order to provide the precision for minimizing touchdown dispersion. High bandwidth augmentation of airspeed stability is achieved because of the high response rates of the reverser vanes compared with changing thrust by means of engine speed. Airspeed is fed back to vane deflections with different schedules top and bottom to give zero pitching moment. Throttle deflection then commands airspeed. With this effective speed hold, pitch rate command by the stick becomes flight path angle rate command. With additional requirements to produce a minimum-phase flightpath response using Direct Lift Control, the multivariable approach was the clear choice. In this case, control system performance was measured by the amount of cross coupling. This showed a measurable increase as the order of the compensator was reduced from fifth order to second order, as shown in Figure 9. Because there are no criteria with which to judge how much degradation can be allowed, piloted simulation was required to verify that a second-order compensator was satisfactory.

For all flaps-up modes, the lateral and directional requirements are conventional so that the classical design approach was again chosen. Initially, only conventional lateral and directional requirements were considered for the STOL modes. After the choice of a classical design had been made, piloted simulations indicated that the crosswind landing imposed an additional requirement. This led to the implementation of direct sideforce (differential canard plus rudder deflection) as a function of rudder pedal input. This can now easily be formulated as a requirement to be included in the multivariable design approach, but in practice it was a fallout as the classical design progressed.

DESIGN RESULTS

The first result is not really a surprise. For modes or axes that have only conventional controls and requirements, the multivariable design technique does not offer any benefit. The modern control theoretician will cite the benefits of guaranteed robustness, however this is not an overriding concern for a "simple" system. One of the comparisons to be made when assessing two methodologies is the ease of implementing the design or, if necessary, the ease of correcting deficiencies. In this respect, the insight into the design process provided by the classical method of control law development/analysis has a distinct advantage over the multivariable techniques. For example, during the early flight testing of the CONVENTIONAL mode, it was discovered that the system damping was lower than desirable at low altitude, high speed flight conditions. While the causes and fixes for the condition were being investigated, a simple patch to the software was installed, changing the feedback gains and providing sufficient damping to continue the flight test program. If those particular control laws had been developed using the modern method, a complete analysis of the system would have been required to define the changes required to improve the flying qualities. This is further support for the conclusion that multivariable theory is not warranted for a conventional design problem. The converse is probably also true - such a problem in one of the complex modes might not be so amenable to a simple fix.

The second result follows from the previous discussion. With multiple control effectors, or complex requirements, a multivariable technique is preferred with one important qualification - the requirements must be specified a priori. The LQG/LTR technique was very effective in decoupling pitch and airspeed together with a minimum-phase flightpath response for the precision landing mode. It is these authors' contention, however, that modified or additional requirements are more likely to be extracted from the classical process than from a multivariable technique, because of the insight gained by the step-by-step development. The lateral and directional axes of the STOL mode were designed classically. Well into the development it was realized that Direct Sideforce Control was the way to meet the crosswind landing requirements. Once the requirement had been formulated, the design could have been completed using either technique.

An aspect of the development that gave totally unexpected benefits was the synergism of the parallel design process. One of the critical areas of multivariable control theory is to establish all the design requirements as the starting point. A full performance design is then synthesized to satisfy them. The classical approach addresses the requirements individually, in principle, although an experienced designer uses his past experience to approach the final solution

efficiently. Both MDA and Honeywell used experienced control system designers. Even so, the classical MDA design benefitted from knowledge of the performance attainable by the multivariable design. Simultaneously, the Honeywell design simplified the high-order compensator of the full-performance design aided by the knowledge of the performance attainable with the simpler formulations of the classical design. The result was a very effective convergence on an optimum balance of performance and complexity (depicted in Figure 10).

The program intent was to utilize multivariable control theory to the extent necessary for control integration. It was decided to do the dual development of the control laws using both the classical and modern methods, and compare the results prior to chosing the set to be programmed. As described above, the two methods essentially start from the opposite positions with respect to both performance and complexity, and evolve toward the same point, as shown in Figure 10 The use of the flight simulator to compare the flying qualities obtained with each set aided in both the evolution and in the comparison. Considering the similarity of the resulting two sets of control laws, the consensus was that both the speed and accuracy of this evolutionary process, regardless of the method being used, depended more on the capability of the individual doing the work than on the process itself. In addition, the combined approach was more efficient than either by itself for the modes or axes with more than conventional requirements.

While the contract Statement of Work called out compliance with the intent of MIL-F-8785C, it was recognized that strict compliance with those specifications was not sufficient to assure optimum flying qualities. This comment was not, and should never, be interpreted to imply that the specification boundaries can be ignored. It is critical to recognize, however, that not one flying qualities parameter violated a specification boundary during the S/MTD development. The problem was either one of defining a satisfactory point within the boundaries, or one of augmenting inadequate requirements. In order to prevent misinterpretation, it is also critical to recognize that we are talking about small differences between Levels 1 and 2. Meeting the specification boundaries and guidelines will guarantee the avoidance of truly bad characteristics, such as Pilot-Induced Oscillations. The only really inadequate requirements were judged to be for precision landing and roll/yaw phasing. Throughout the S/MTD flight test program, not one pilot rating or comment worse than Level 2 was received. At the risk of being too obvious, it is noted that problems defining or interpreting flying qualities requirements apply to both classical and multivariable design techniques equally, and are very critical to the overall design process. The results from the S/MTD program applicable to requirements definition are documented in Reference 5.

As stated earlier, one of the design goals was to meet the stability requirements of MIL-F-9490D, or to define recommended changes to the criteria. The design used the 6 db gain and 45 deg. phase limits as total loop design requirements. The flight test problem mentioned above was manifested first by the pilots complaining about the pitch axis "ringing". In other words, aircraft response to the normal flight test stick inputs did not damp out as expected. Analysis of the flight test data revealed that the gain margin had decreased to approximately 3 db. The temporary fix that restored damping also restored gain margin to 6 db and gave flying qualities satisfactory for completion of the flight test. This is not to imply that loss of margin always results in loss of damping. The physical manifestation will depend on the source of the problem. The S/MTD project has successfully used the MIL-F-9490D requirements for overall loop gain and phase margin. Although not addressed in this paper, this also applies to the 8 db requirement at structural frequencies. Although this does not constitute formal validation of the requirements, it does indicate that caution should be exercised before accepting less stabililty. In particular, the common perception that the specification allows 3db and 22.5 deg would have been unacceptable for this program.

This discussion of the practical aspects of control system design methodology must end with a reminder that we have discussed linear techniques. Starting with linear design methods is a universal approach but the steps needed to achieve a final solution can be easilu neglected. All aspects of the design need to be evaluated, but especially any non-linear behaviour must be exposed before it is encountered in flight. This is most easily accomplished in a piloted simulation using large amplitude manoeuvres or disturbance inputs. A great deal of emphasis was placed on this aspect of the S/MTD development, especially landing in winds, wind shear and turbulence. This was very successful in general, all pilot ratings were Level 1 in the flight test program. One landing did reach stabilator rate limiting, however, although not discernable in the flying qualities. This was a surprise even though the gusty conditions were more severe than the design requirements. The problem was investigated in the simulator, where it was determined that continuous turbulence could not replicate the flight results. It is recommended that a series of discrete gusts be used for flying qualities evaluation, (see Reference 12).

The most important result, of course, is how the flying qualities were rated in flight. All modes/axes were rated Level 1 where predicted by simulation. For instance, the CRUISE mode was rated Level 2 for tracking (as expected) but Level 1 for a flight path capture task. The landing mode on a very gusty day received Level 2 ratings "because of high turbulence", as allowed by the specification.

FLIGHT TEST RESULTS

The simplest and most direct form of presentation of handling qualities flight-test results would be tables or graphs of Cooper-Harper ratings, Figure 14. There is a lot more information behind the simple numbers. Here, we present the flying qualities results mostly in the form of pilot comments. These comments (with ratings) show excellent agreement with the analytical and simulation development results. They also provide an interesting diversion in comparing different likes of the different pilots, which would be masked by a simple presentation of Cooper-Harper ratings.

Handling Qualities During Tracking

Mach 0.6/10K:	Gross	Fine
CONV HQR	2	2
COMBAT HQR	3	3

- "CONV stopped when I put it there." (Pilot A)

- "COMBAT HQDT Improves with G increases." (Pilot A)

Mach 0.7/20K:	Gross	Fine
CONV HQR	3	3
CRUISE HQR	4	4
COMBAT HQR	3	3

- "Very nice pitch control in COMBAT, less pitch sensitive than CONV. This was the best mode of all for tracking." (Pilot C)

Mach 0.9/20K	Gross	Fine
CONV HQR	3	2
CRUISE HQR	4	3
COMBAT HQR	3	3

- "HQDT in all three modes was very nice. (Pilot B)

- "The biggest delineator for all tasks in the three modes was the relatively poor gross acquisition in CRUISE. The initial overshoot was large, 25+ mil, but I usual ly only had one overshoot in CRUISE. In COMBAT and CONV I generally had a much smaller overshoot, better predictability, but often more than one overshoot. One small difference was noted in that the COMBAT mode seemed to have less pitch acceleration in the gross acquisition tas k than CONV mode - to get the same performance I had to pull harder and this was evident as apparent higher stick forces." (Pilot B)

Note that all of the ratings are Level 1 for the CONVENTIONAL and COMBAT modes, and Level 1/borderline Level 2 for the CRUISE mode. Very little discrimination would be implied by the ratings alone. The comments reflect perceived differences and preferences even when the ratings are identical. Thus Pilot B says that COMBAT gross acquisition is better than CONV, but assigns a rating of 3 to both. Pilot C says that COMBAT was the best mode of all for tracking, but assigns the same rating as the CONV. Also, it can be seen that Pilot A consistently preferred the CONV mode while Pilot C chose the COMBAT mode. No explanation will be attempted to explain these results. The "engineering evaluation" of the different pilots is that both pilots A and B are high gain relative to pilot C. We can certainly rationalize their preferences on this basis, and it supports the technique of requiring multiple pilot opinions. In a development program, however, do we have to satisfy all pilots? If not, whose opinion is given precedence? In the S/MTD program we are lucky - the differences are within the Level 1 range and the distinction is academis. This aircraft is unique in having the capability to switch modes at will, and fly the modes back-to-back. Fine distinction within Level 1 characteristics is not normally a problem in a development program. What is important is that these comments do indeed repeat the comments that were noted during the piloted simulation program.

Landing Configuration

- Pitch Captures - "Nice and stable" (Pilot B)
- Flight Path Captures - "Sluggish just like normal" (Pilot B)

- "Everything was fine. I didn't see anything I didn't like." (Pilot B)

FINAL VALIDATION

The real purpose of the last flight of the program was to evaluate SLAND in conjunction with ALG in a severe environment, i.e. night. "In this, the S/MTD had its finest hour. Using SLAND made a considerable reduction in pilot workload, and was the perfect complement to ALG. The integration of the system was wonderful, and certainly the overall system is much better than the sum of its individual parts would indicate. I truly believe the testing of SLAND under day, VFR conditions is not indicative of its true worth. I felt it made my approach to a totally black airfield no more difficult than a simple video game; all I had to do was keep the velocity vector aligned with the carets".

"During most flight testing, as pilots we typically only comment on those things that don't work the way we would like them to work. As a result, you seldomly hear about those things that work well. Tonight's flight highlighted just how incredibly well the myriad of technologies incorporated in this airplane worked.

The Integrated Flight and Propulsion Control stands out in my mind as the most amazing. Integrating all the different control surfaces including the canards and the nozzles, making it all fly like a regular F-15 or better, and still only requiring normal stick and throttle inputs by the pilot is fantastic. During tonight's flight, the only obvious cue that

we weren't flying a regular airplane was that no regular airplane could do what we were doing".

CONCLUSIONS

This paper has documented the development of a full-envelope Integrated Flight/Propulsion Control system. A combination of classical and multivariable design methodologies was used, including a unique inverse procedure to produce second-order equivalent systems meeting specified flying qualities requirements. The implementation was based on a rational choice between the two methodologies. It is suggested that a parallel design approach in the beginning will produce efficient convergence on a practical optimum design.

Finally, all control law revisions should be done analytically and only evaluated by simulation. Regardless of the design technique used, the process begins by specifying detailed design guidelines selected to meet the intent of MIL-F-8785C. Once the designs were complete and analyzed based on the design guidelines, manned flight simulation was used only to validate and demonstrate the flying qualities achieved prior to flight test. Problems encountered during simulation or flight testing were addressed first by reviewing the original design guidelines and evaluating the success achieved in implementing them.

REFERENCES

1. Walker, L.A., and W.J. LaManna, "Development of the F/A-18A Handling Qualities Using Digital Flight Control Technology", Proceedings of the 26th Annual Symposium of Experimental Test Pilots, Beverly Hills, 1982

2. Moorhouse, D.J., and W.A. Moran, "Flying Qualities Design Criteria for Highly Augmented Systems", Proceedings of IEEE National Aerospace & Electronics Conference, Dayton, OH, USA, 1985

3. Moorhouse, D.J., J.A. Laughrey and R.W. Thomas, "Aerodynamic and Propulsive Control Development of the STOL and Manoeuvre Technology Demonstrator", AGARD Conference Proceedings, Madrid, Spain, CP-465, paper 1, 1989.

4. Moorhouse, D.J., J.A. Reinsberg and F.W. Shirk, "Study of Jet Effect and Ground Effect Interference Problems on a STOL Fighter", AGARD Conference on Computational and Experimental Assessment of Jets in Cross Flow, Winchester, England, April 1993.

5. Moorhouse, D.J., "Lessons Learned from the S/MTD Program for the Flying Qualities Specification", AIAA Paper no. 90-2849, Proceedings of the Atmospheric Flight Mechanics Conference, CP 898, pp 473-479; Portland, OR, USA, 1990.

6. Moorhouse, D.J., K.D. Citurs, R.W. Thomas and M.R. Crawford, "Handling Qualities of the STOL & Maneuver Technology Demonstrator from Specification to Flight Test", AGARD Conference Proceedings, Quebec City, Canada, CP 508, paper 13, 1990.

7. Bland, M.P., K.D. Citurs, F. Shirk and D.J. Moorhouse, "Alternative Design Guidelines for Pitch Tracking", AIAA Paper no. 87-2289, Proceedings of the Atmospheric Flight Mechanics Conference, CP 876, pp 40-48, Monterey, CA, USA, 1987.

8. Doyle, J.C., and G. Stein, "Multivariable Feedback Design: Concepts for Classical/Modern Synthesis", IEEE Transactions on Automatic Control, Vol AC-26, pp 4-16, 1981.

9. Stein, G., and M. Athans, "The LQG/LTR Procedure for Multivariable Feedback Control Design", IEEE Transactions on Automatic Control, Vol AC-32, no 2. pp 105-114, 1987.

10. Morton, B.G., "New Applications of Mu to Real Parameter Variation Problems", Proceedings of the 24th IEEE Conference on Decision and Control, pp 233-238, Vol. 1, Fort Lauderdale, FL. USA, 1985.

11. Morton, B.G., and R.M. McAfoos, "A Mu-Test for Real Parameter Variations", Proceedings of the American Control Conference, pp 135-138, Vol. 1, Boston, MA, USA, 1985.

12. Leggett, D.B., D.J. Moorhouse and J.M. Zeh, "Simulating Turbulence and Gusts for Flying Qualities Evaulation", AIAA Paper no. 90-2845, Proceedings of the Atmospheric Flight Mechanics Conference, CP 898, pp 445-455, Portland, OR, USA, 1990.

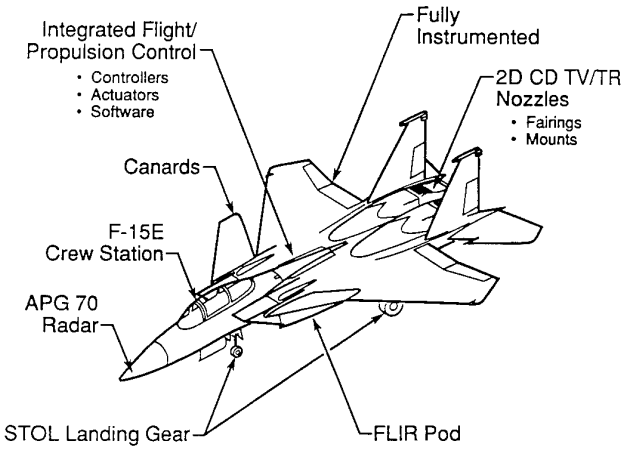

Figure 1. S/MTD Aircraft Modifications

Effector	Pitch	Roll	Yaw	X-Force	Y-Force	Z-Force
Stabilators	√	√				
Canards	√		√		√	√
Ailerons		√				√
Flaperons		√				√
Rudders			√		√	
Gross Thrust				√		
Vectoring	√	√				
Reverser Vanes	√	√	√	√		
Main Gear			√	√		
Nose Gear			√			

Figure 2. Available Control Effectors

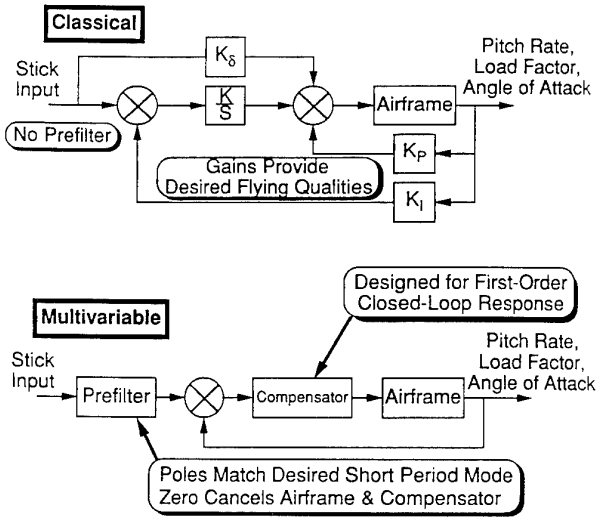

Figure 3. Design Philosophies

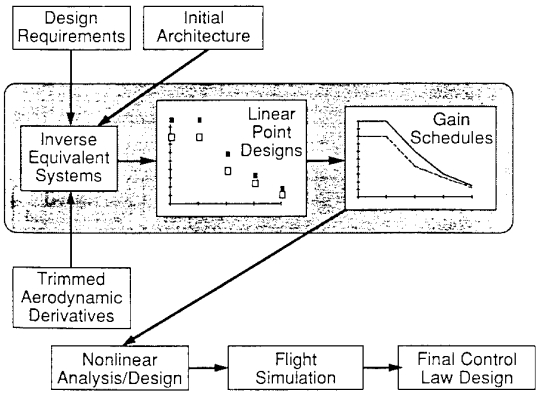

Figure 4. "Classical" Approach to Linear Design

Parameter	Original	Cruise	CONV/Combat
ω_n (rad/sec)	3.31	3.31	4.68
ζ	0.7	0.8	0.8
L_α (rad/sec)	1.2	1.2	1.2
$1/T\theta_2$ (rad/sec)	1.2	1.2	2.0
τ_e (msec)	70	65	65
CAP	0.4	0.4	0.8†
			0.47‡
† CAP Calculation Based on L_α ‡ CAP Calculation Based on $1/T\theta_2$			

Figure 5. Pitch Transfer Function Characteristics

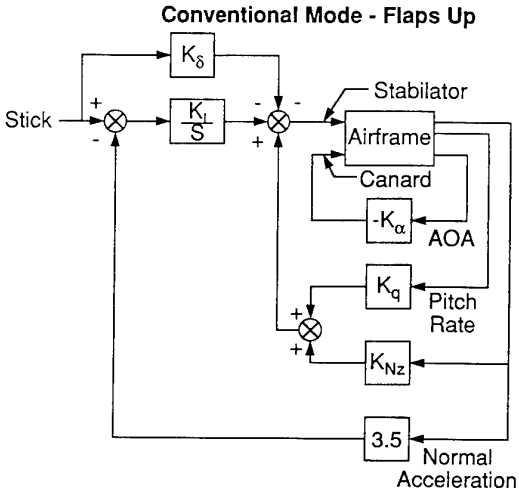

Figure 6. Simplified Linear Longitudinal Control Law

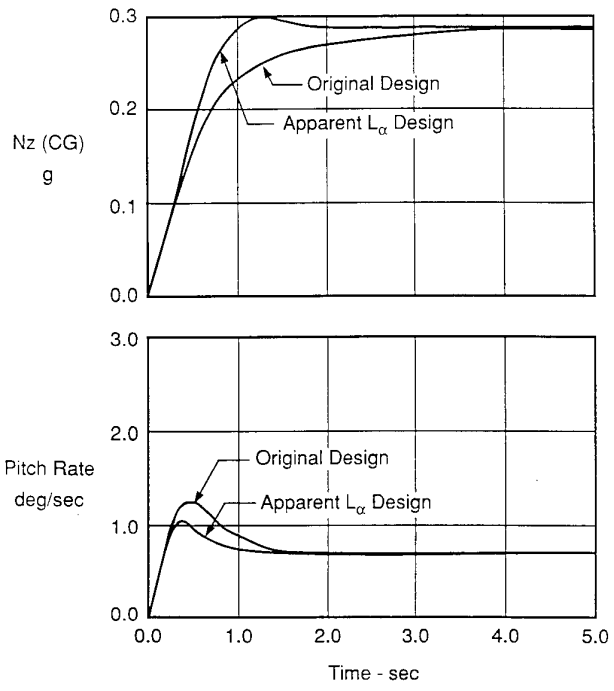

Figure 7. Apparent L_α System Time Response

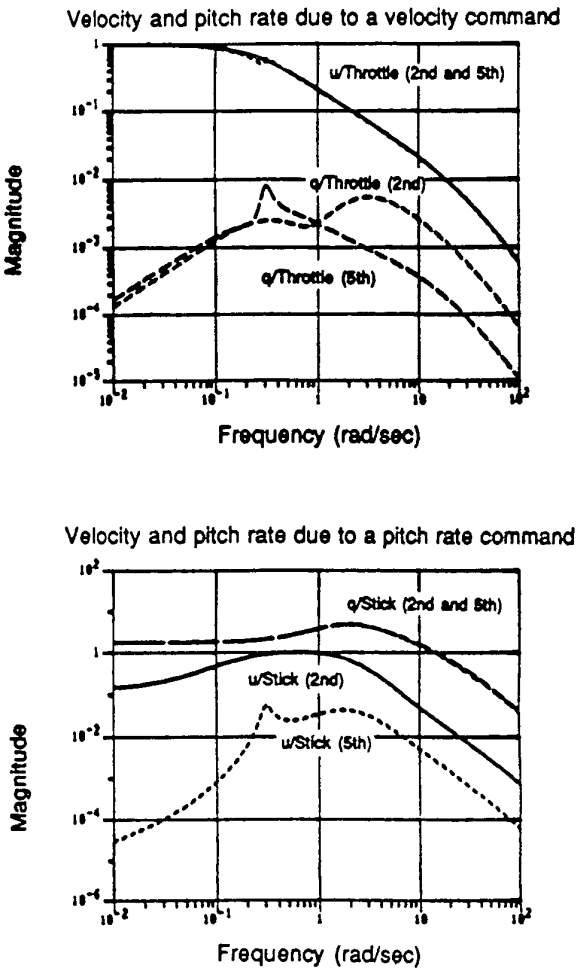

Figure 9. Decoupling with Five- and Two-State Compensators

Combination of Multivariable and Classical Analysis Methods Used to Design Control Laws

Axis/Mode	Honeywell LQG/LTR	MDA Classical
Longitudinal		
CONV		√
Cruise/Combat	√	
STOL-Land	√	
STOL-TOA	√	
STOL-GH	√	
Lateral/Directional		
CONV		√
Cruise/Combat		√
STOL-Land		√
STOL-TOA		√
STOL-GH		√
Thrust		
CONV		√
Cruise/Combat		√
STOL-Land	√	
STOL-TOA		√
STOL-GH		√

Figure 8. Choices of Design Approach

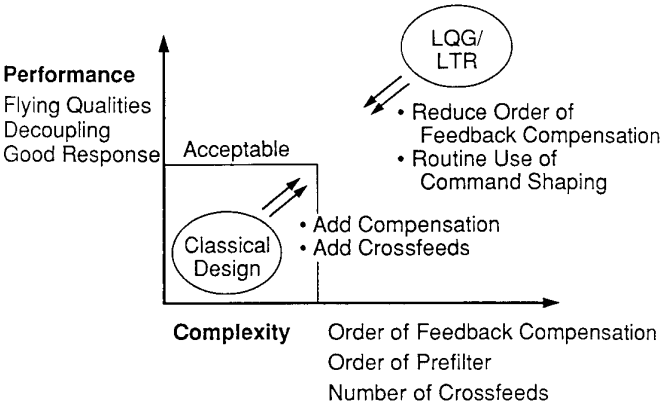

Figure 10. Convergence of Parallel Design Process

CONTROL LAW DESIGN USING H_∞ AND μ-SYNTHESIS SHORT-PERIOD CONTROLLER FOR A TAIL-AIRPLANE

L. Mangiacasale
AERMACCHI S.p.A.
Via Paolo Foresio, 1
21040 - Venegono Sup. (VA)
ITALY

Abstract.
The recently developed methods H_∞ and μ-Synthesis are used in the design of a control law for a tail controlled unstable airplane. The design procedure has been applied with success and seems to be very promising in order to solve control design problems in real applications. The $H_\infty+\mu$ controller, characterized by a very large order (namely 34th), has been successfully reduced to one having order 5th with a very low decay in the overall performance. The reduced-order controller meets all the servo technical Specifications demanded to the full-order one. At present it is under test as part of a 6-DoF simulation program in order to verify its real robustness in face of structured and unstructured perturbations.

1. Introduction.

The main aim of this work is to apply recent design techniques known as H_∞ and μ-Synthesis to an airplane control system and to draw preliminary conclusions on the physical realization of the compensator in order to assess the ability of the design procedure to generate simple (low-order) and feasible control law architectures.
The final (reduced) compensator should perform as well as the full-order one (that generated by the H_∞-μ procedure), with a minimum decay in terms of those specifications summarized in the following, but its dimensions (number of poles) shall be as low as possible in order to avoid insurmountable difficulties when trying to transform it from mathematics to the real world of the current flight control computers.
In the following paragraphs the design methodology is explained without entering the complex an difficult area of the theoretical aspects which are widely discussed in Refs. [1] and [2].

2. Plant model, Design Specifications and Performance.

The Plant to be controlled is an airplane described by the short period approximation. Measured outputs are the Normal load factor (N_{zAcc}) at the pilot position (very close to the acceleration sensor position) and the pitch-rate (q); control surfaces are the Stabilizer (S) and the Trailing-Edge-Flap (F).
In form of state variables the Plant model is given by:

$$\begin{bmatrix}\dot{\alpha}\\ \dot{q}\end{bmatrix} = \begin{bmatrix}-L_\alpha & 1\\ M_\alpha & M_q\end{bmatrix}\begin{bmatrix}\alpha\\ q\end{bmatrix} + \begin{bmatrix}-L_{\delta_S} & -L_{\delta_F}\\ M_{\delta_S} & M_{\delta_F}\end{bmatrix}\begin{bmatrix}\delta_S\\ \delta_F\end{bmatrix} \quad (1)$$

$$\begin{bmatrix}N_{z,Acc}\\ q\end{bmatrix} = \begin{bmatrix}N_\alpha & N_q\\ 0 & 1\end{bmatrix}\begin{bmatrix}\alpha\\ q\end{bmatrix} + \begin{bmatrix}N_{\delta_S} & N_{\delta_F}\\ 0 & 0\end{bmatrix}\begin{bmatrix}\delta_S\\ \delta_F\end{bmatrix} \quad (2)$$

where the terms N in the matrices (2) have a well known meaning.
The two control surfaces are driven by two electro-hydraulic actuators described by a first order transfer function:

$$\frac{\delta}{u} = \frac{\omega}{s+\omega} \quad (3)$$

Paper presented at the Flight Mechanics Panel Symposium held in Turin, Italy, from 9-13 May 1994.

where δ is the generic control surfaces deflection, u represents the electric command generated by the compensator and ω is the inverse of the actuator time lag.
A bank of two integrators ($\simeq I_2/s$) is placed at the input of the actuators in order to transform the control command from deflection to rate and to guarantee (when and if possible) a zero steady state error to input step command. Hence the order of the controlled system is n=6, but at the end of the compensator design the two integrators will become part of the controller.
The controlled (closed-loop) system should meet the following preliminary Specifications:

a) closed-loop roll-off $\leq$ -40 dB/decade
b) attenuation at 100 rad/sec < -30 dB
c) overshoot in response to step commands <10%

The closed-loop system shall demonstrate good Model-Following capabilities in terms of Variable- Stability-Variable-Performance Airplane. A good level of turbulence attenuation (Ride-Quality) is required with moderate control surface activity in terms of deflection (δ) and rate ($\dot{\delta}$); no exact figure is supplied but it is required that the Normal load at the pilot station be less than 0.08 g R.M.S. in the presence of a Dryden clean-air turbulence, at the design flight condition, value already achieved in a previous Linear-Quadratic Regulator design. Before entering the details of the H_∞ design it is convenient to spend a few words about the plant characterization.
The basic (open-loop) plant described by Eq. (1) and (2) has two real poles:

p_1 = 1.14 r/sec (unstable)
p_2 = -2.95 r/sec

and one transmission zero:

$z_1 \simeq$ 0.0(very close to the origin of the complex s-plane).

In mathematical form this fact can be expressed by the condition that the matrix:

$$\Sigma = \begin{bmatrix} A-sI & B \\ C & D \end{bmatrix} \tag{4}$$

looses rank at s=0, where A, B, C, and D are the matrices of the system composed by the airplane and the control actuators together. The consequence of this fact can be interpreted by writing the condition for the existence of a steady-state (ss) solution which is given [3] by:

$$\begin{bmatrix} 0 \\ y_{ss} \end{bmatrix} = \begin{bmatrix} A & B \\ C & D \end{bmatrix} \begin{bmatrix} x_{ss} \\ u_{ss} \end{bmatrix} \tag{5}$$

or:

$$\begin{bmatrix} x_{ss} \\ u_{ss} \end{bmatrix} = Q^{-1} \begin{bmatrix} 0 \\ y_{ss} \end{bmatrix} = \Sigma(s=0)^{-1} \begin{bmatrix} 0 \\ y_{ss} \end{bmatrix} \tag{6}$$

where Q is the quadripartitioned matrix in (5). But, by definition of transmission zero, the Σ matrix at s=0 is singular so that given a step command vector y_{ss} no steady state can be reached for the state variables (x) and for the control vector (u). This means that the Q matrix is singular too as it is easy to verify since one row of the matrix [C,D] is a linear combination of the rows of the [A,B] matrix. Looking now at Eqs. (1)-(2) one discovers that the output row N_{zAcc} is responsible of this situation with the consequence that no steady-state load factor can be commanded (with zero pitch-rate) since at $t=\infty$ this would require an infinite value of some state variable (for instance α) and of the control surface deflections (δ); the same is still valid for a pitch-rate command (with zero normal-load factor), since the transmission zeros (as well known) belong to the complete MIMO system. This preliminary observation is necessary in order to justify some result of the optimization procedure in the D-K iterations, although it is evident that in a real implementation no pilot will command a constant normal load with zero pitch-rate and vice versa.

3. Weighting functions and the H_∞ (1st step) design.

The design developed in the following paragraphs is mainly based on the formulation and procedures suggested in [4] to which the reader should refer.
The full "augmented plant" is shown in Fig.1; it is composed by:

a) the basic (short-period alone) aircraft,
b) the control actuation system (actuators)
c) the bank of input integrators (two poles at -0.001 rad/sec)
d) the weighting functions (W_u, W_i, W_s)
e) the compensator (K) to be designed
f) a Flying-Quality Model in order to verify the Model-Following performance of the closed-loop system
g) a Dryden turbulence generation model needed in order to verify the Ride-Quality performance of the controlled aircraft.

It is implicit that the first four items alone contribute to the $H_\infty+\mu$ design, while the last two are added for verification purpose at the end of the controller's design.
In the design scheme a feedback compensator is shown called "pole placement pre-stabilization" which deserves a few words. During the design process it appeared very difficult to obtain a compensator able to meet, without this pre-stabilization, the specification (c) relative to the maximum time response overshoot; many trials where performed, working on the weighting functions, with no success since the maximum overshoot (mainly in the pitch rate response) never was less than 20% with a negative impact on the Model-Following performance. The aforementioned pre-stabilization is done through a very simple pole placement procedure applied to the system in (1) employing only the feedback around the horizontal tail, then the gain matrix is transformed and applied to the output vector in (2). The closed-loop poles of the pre-stabilized aircraft are repositioned at [-1 -3] with an acceptable modification of the actuators eigenvalues. It is worth to point out that the compensator design can evenly be developed with no pre- stabilization still using the same shaping functions (W), but the overshoot will be larger and the closed-loop robustness will be in, some way, negatively affected.
The weighting functions, needed in order to drive the compensator design, have been defined after long and not-painless trials as:

- Input uncertainty

$$W_u(s) = 0.01 \text{ (constant)}$$

- Sensitivity

$$W_s(s) = 0.3125 \quad \frac{s + 40}{s + 1.25}$$

- Output uncertainty (loop)

$$W_i(s) = 12.5 \quad \frac{s + 0.25}{s + 300}$$

for both the two control and measurement channels, and are all plotted in Fig 2. The Singular Values of the 1st step design (Iter=0), with the two integrators (those at the actuator input) included, are plotted in Fig. 3. The controller performance in terms of robust stability and nominal performance of the augmented plant is shown in Fig. 4 from which it is possible to derive that the closed-loop system is "very weak" at frequencies around 30 rad/sec as can be easily verified observing the singular value plot of the closed-loop system in Fig. 5. In Bode's terminology one could say that the close loop systems possesses low phase and gain margins. The maximum Singular Value and the μ-plots of the augmented plant are shown in Fig. 6 and confirm that an important improvement of the compensator is required in order to meet Specifications and can be obtained by developing the D-K iterations of the μ-Synthesis procedure suggested in [4] and discussed in the following paragraph.

4. The D-K iterations and the final (full-order) compensator.

The D-K iterations have been performed exploiting a third-order fit for the D-scale matrices. No absolute rule can be supplied in order to optimize this choice, but the designer should develop some trade-off because a higher

order (>3) increases the computation time and the compensator order, while a lower order can produce a "bad fitting" with negative impact on the iteration success. With a third-order fit the iterations have been successful still maintaining an acceptable computation time and a moderately low order for the compensator.
The Singular Values plots of the 1st iteration's H_∞ compensator are still shown in Fig. 3 and the overall performance improvement of the augmented plant can be derived from Fig. 4 by comparison with the previous step. The improvement is remarkable in terms of robust stability and nominal performance; the maximum Singular Value and the μ-Plots have undergone a very significant modification, although the condition:

$$\mu_\Delta[F_l(P,K)(j\omega)] < 1 \qquad (7)$$

in [4] is not satisfied. The overall improvement of the controlled system can be also derived from the Singular Values plots in Fig. 5. A second iteration has been developed, in order to "fill" the small gap between the maximum S.V. and the μ-plot, still employing a third-order fit; the relevant results are plotted on the last row of Figs. 3-6 and are considered conclusive.
Before entering details about the compensator's order reduction it is useful to spend some word about the condition (7) never met in the present design. This mismatch in the "optimality condition" reported in [2] and [4] is to be ascribed (in the opinion of the author) to the transmission zero very close to the origin of the complex s-plane so that Fig. 6 (the last) contains the very interesting information that the design performance specifications in terms of sensitivity (W_s) are satisfied in the frequency range between 0.01 and 10 radians per second, but are not met in the low-very-low frequency range (ω<0.01 rad/sec); at large frequency (ω>10 rad/sec) the loop shaping is effective and the controlled system is compliant with the design specification. The large value of the μ-plot at low frequency confirms the inability of the closed-loop system to follow a vector of step-command with zero steady-state error.
The compensator derived from the D-K iterations has a very large order, namely 34th with the two integrators included, and therefore cannot be implemented in a real flight control computer of the to-day (and perhaps to-morrow) technology. Hence the order reduction is required, performed through the procedure explained in the following paragraph.

5. Compensator order reduction and performance.

The compensator order reduction has been performed in two steps as shortly explained:
1) the first step exploits balancing and truncation by making use of the routines *sysbal* and *strunc* (or *hankmr*) in [4]; the Hankel Singular Values (generated by *sysbal*) of the system matrix help the designer in the choice (by trials) of the reduced order. The compensator obtained at the end of this step has a low order, say 7th, and performs as well as the full-order one either in terms of singular values, as shown in Fig. 7, or in terms of transient response to input commands (N_{zAcc} and q) not shown here.
2) The second step has been performed in two phases; first the 7th order compensator has been diagonalized using the routine *strans* and obtaining a system like:

$$K_7 = \begin{bmatrix} A_{k7} & B_{k7} \\ C_{k7} & 0 \end{bmatrix} \qquad (8)$$

where A_{k7} is a block-diagonal matrix and C_{k7} is given by:

$$C_{k7} = \begin{bmatrix} n & L & L & n & L & L & L \\ n & L & L & n & L & L & L \end{bmatrix} \qquad (9)$$

where n means "negligible" (in the opinion of the designer) and L means "large" speaking in terms of contribution of the compensator's states to the compensator's outputs (commands to the control actuation system). Then, after zeroing the negligible elements, the previous compensator K_7 has been again reduced through balancing. The final compensator has a very low order, namely 5th, and is characterized by the following system's matrix:

K_5=

$$\begin{bmatrix} -0.001 & & & & & -0.073 & 0.194 \\ & -0.0156 & & & & -1.082 & 0.107 \\ & & 1.636 & -0.138 & & -0.065 & 0.175 \\ & & 0.138 & -1.636 & & -2.554 & 0.402 \\ & & & & -390.4 & 0.153 & 1.931 \\ -0.205 & -0.113 & -0.133 & -0.002 & -1.825 & 0.0 & 0.0 \\ -0.020 & -1.076 & -0.5871 & 0.039 & -0.629 & 0.0 & 0.0 \end{bmatrix}$$

The pole-zero map of this last compensator is shown in Fig. 8; the poles are easily derived from the A_5 matrix, the transmission zeros are:

$$\text{zeros}(K_5) = [\ -1.666 \ \pm 1.143i, \ -3.290]$$

The singular values of this compensator, together with the closed-loop, are shown in Fig. 9, and by comparison with those of the full order one it is possible to draw the conclusion that the performance degradation caused by the order reduction should be acceptable.

The performance of the system, controlled with this reduced order compensator, can be verified from the plots in Figs. 10 which refer to the airplane dynamics also containing the phugoid mode.

The closed-loop Singular Values plot indicates that the design specifications in the medium-high frequency range are met (slope=-40 dB/decade, attenuation at 100 rad/sec≅-30 dB); the Sensitivity Singular Values say that, in agreement with the previous considerations, the very-low frequency specifications are not. The transient responses to a command input vector are plotted in Fig. 10. The time histories reflect the Singular Values behavior, but the short term dynamics is correct and satisfactory; the steady state coupling is low (coupling $N_{zAcc} \Rightarrow q$ is <2%; coupling $q \Rightarrow N_{zAcc}$ <15%) and the overshoot is less than required. The control surface deflection time histories confirm the statement in Paragraph 2 relative to the steady-state behavior of a controlled system with transmission zeros close to the origin of the s-plane.

In order to assess the Model-Following capabilities of the controlled system, a linear simulation has been performed using the stick force (F_{stick}=1Kg≅2.2 lbs.) as input to the Flying-Quality Model shown in Fig. 1. The F.Q. Model is characterized by the following properties:

- short-period damping: $\zeta_{SP,MOD}$ = 1.25
- control anticipation parameter: CAP = 1.0
- load factor/AoA: N/alpha = 35 g/rad
- Stick force per g: F_{stick} = 4.5 lbs./g

The output of the simulation is show in Fig 11 and can be considered self-explanatory.

The turbulence attenuation capability of the controlled airplane has been evaluated in terms of states and outputs RMS in the presence of a clean-air turbulence with Dryden Spectrum and the results are summarized in the following table I.

TABLE I. FLIGHT IN TURBULENCE PERFORMANCE

Parameter	Value	RMS
Vertical turbulence w_g	1.76	m/sec
Longitudinal turbulence u_g	1.26	m/sec
A/C Velocity	1.14	m/sec
A/C Attitude	0.015	deg.
A/C Pitch-Rate	0.065	deg./s
A/C Normal Load	0.070	g's
Stabilizer Deflection	0.18	deg.
Stabilizer Rate	0.95	deg./s
T.E.Flap Deflection	1.72	deg.
T.E.Flap Rate	3.81	deg./s

6. Design Data.

● Aircraft matrices: short period alone, states [α q]′ expressed in radians and radians/sec, commands [δ_S δ_F]′ expressed in radians, outputs [$N_{z,Acc}$ q]′ measured in g's and degrees/second:

$$A_{AC} = \begin{bmatrix} -1.305 & 0.987 \\ 4.175 & -0.522 \end{bmatrix}$$

$$B_{AC} = \begin{bmatrix} -0.25 & -0.31 \\ -20.30 & 3.03 \end{bmatrix}$$

$$C_{AC} = \begin{bmatrix} 28.50 & 0.069 \\ 0 & 57.297 \end{bmatrix}$$

$$D_{AC} = \begin{bmatrix} -2.61 & 7.53 \\ 0 & 0 \end{bmatrix}$$

● Prestabilization control law:

$$\begin{bmatrix} \delta_S \\ \delta_F \end{bmatrix} = - \begin{bmatrix} -0.006 & -0.0019 \\ 0.000 & 0.0000 \end{bmatrix} \begin{bmatrix} N_{zAcc} \\ q \end{bmatrix}$$

● Normal Accelerometer position: 3.75m ahead of the C.G.

● Flight conditions: altitude h=1000m (≃3300ft.), Mach number M=0.6, flight velocity V_∞ =202m/sec.

● Actuator's data: first-order transfer function (as in Eq.3) with ω = 30 rad/sec, unitary static gain,

● Input integrators: two poles at s=-0.001 rad/sec.

7. Conclusions.

The design of a control law for the stabilization and the control of an unstable aircraft using the modern techniques H_∞ and μ-Synthesis has been successful and its implementation on a flight control computer seems to be possible because of the very low order of the reduced compensator.

Linear simulations, not shown here, confirm that the compensator is able to absorb plant parameters variations of more than 50% in the static stability ($C_{m\alpha}$) and of 25% in the control surface effectiveness ($C_{m\delta}$) without loss of stability and with a negligible impact on the Model-Following performance. When the compensator is applied to the complete aircraft dynamics (short period plus phugoid) the phugoid mode becomes "very lightly" unstable and should be cured by the pilot or through an autopilot. At present time this compensator is undergoing intensive tests as a part of a SIX D.O.F. off-line simulation program in order to obtain information about its robustness and conclusive answers on its use and implementation on the real airplane.

References.

[1] ------ Recent Advances in Robust Control. IEEE Press 1990, Edited by P. Dorato and R. K. Yedavalli.

[2] R. Lane Dailey: Lectures Notes for the Workshop on H_∞ and μ Methods for Robust Control. 1991 IEEE Conference on Decision and Control, Dec. 9-10,1991 Brighton,England.

[3] R. F.Stengel: Stochastic Optimal Control. J.Wiley & Sons, New York 1986.

[4] G. J. Balas, J. C. Doyle et al: μ-Analysis and Synthesis Toolbox. MuSyn Inc. The MathWorks Inc.,1991.

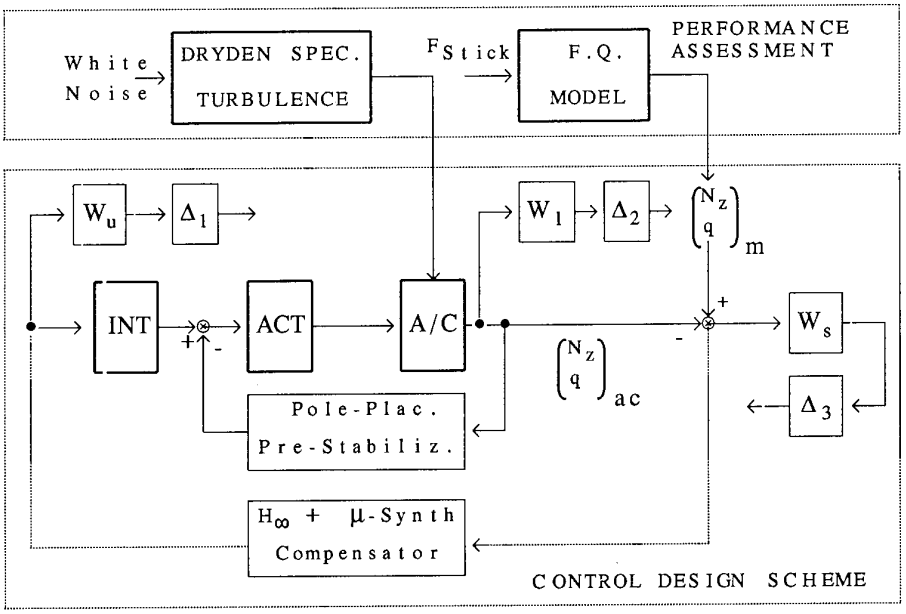

Fig. 1 General Design Scheme and Interconnection Structure

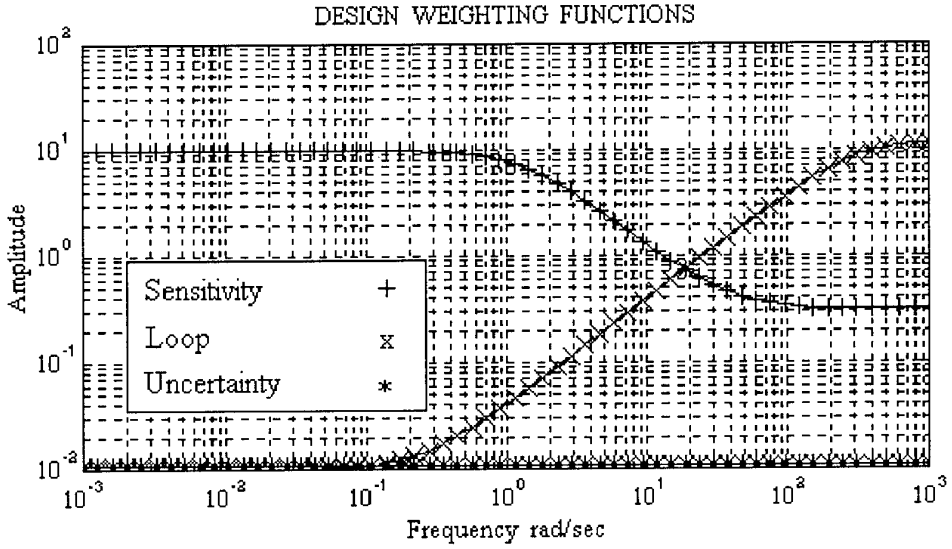

Fig. 2 Design Weighting Functions

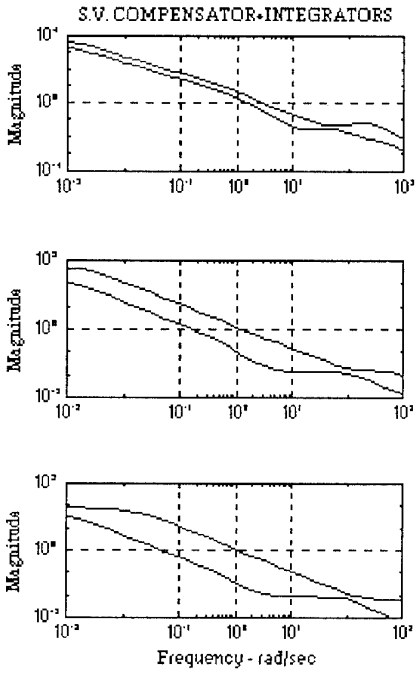

Fig.3 S.V. of the H_∞ compensator

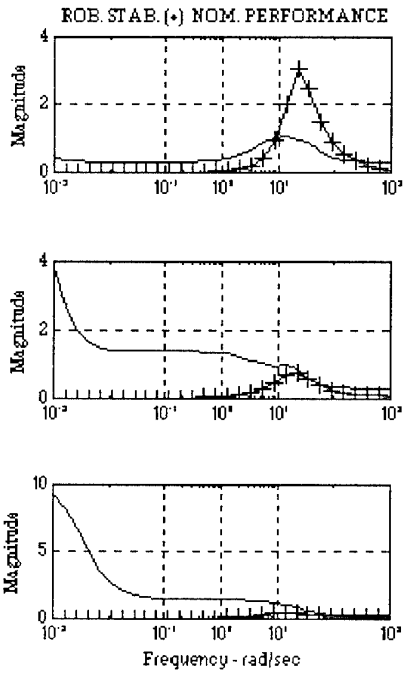

Fig. 4 Robust Stability Plots

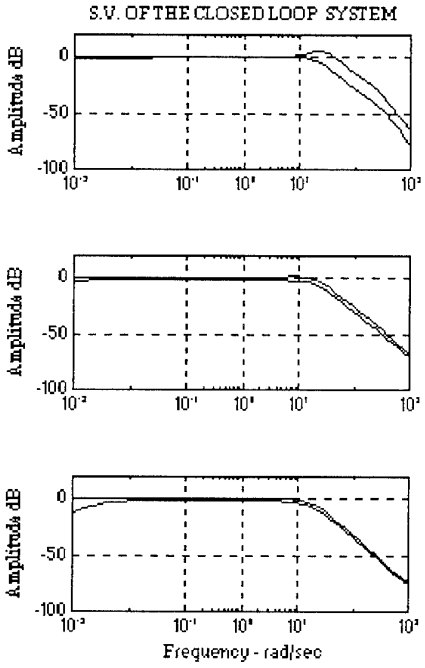

Fig. 5 S.V. of the C-L. Plant

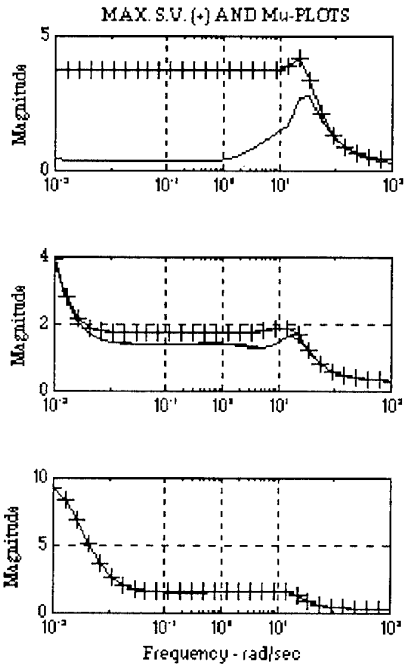

Fig. 6 Max. S.V. and μ-Plots

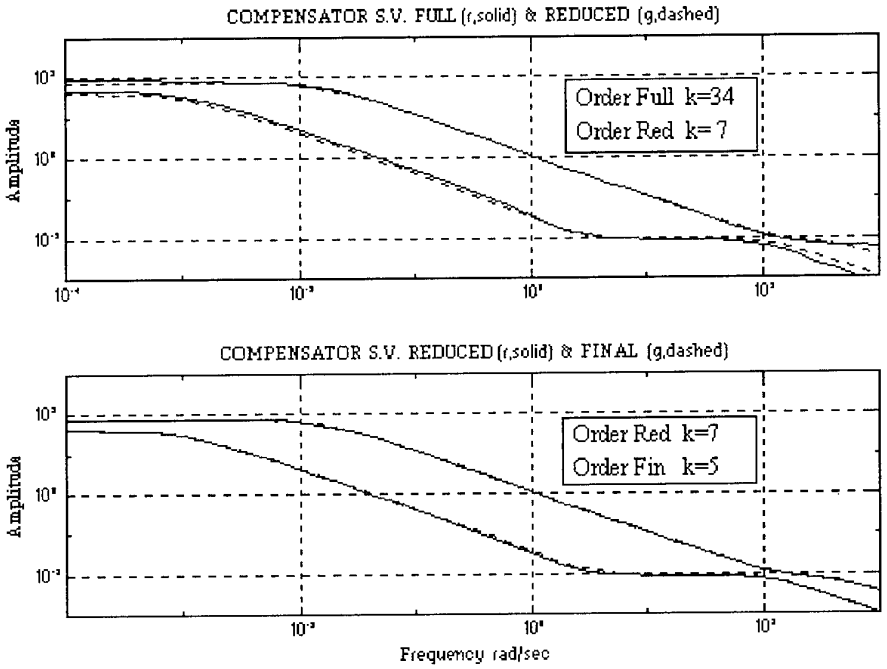

Fig. 7 S.V. of the Full, the Reduced and the Final Compensator

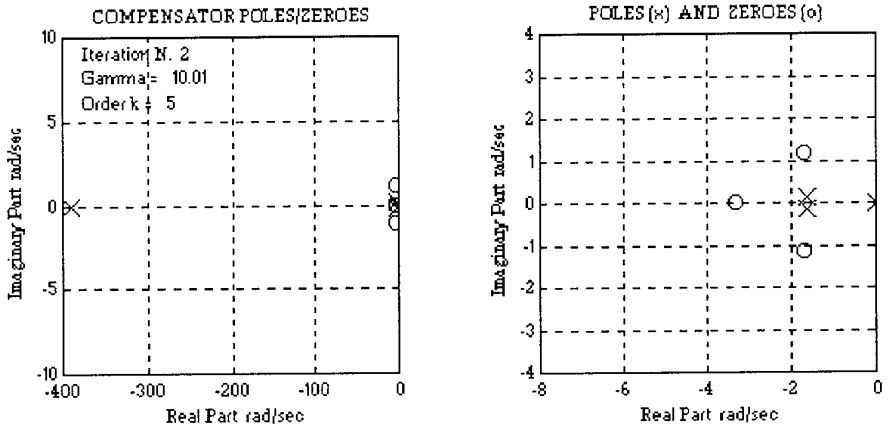

Fig. 8 Pole/Zero map of the Final Compensator

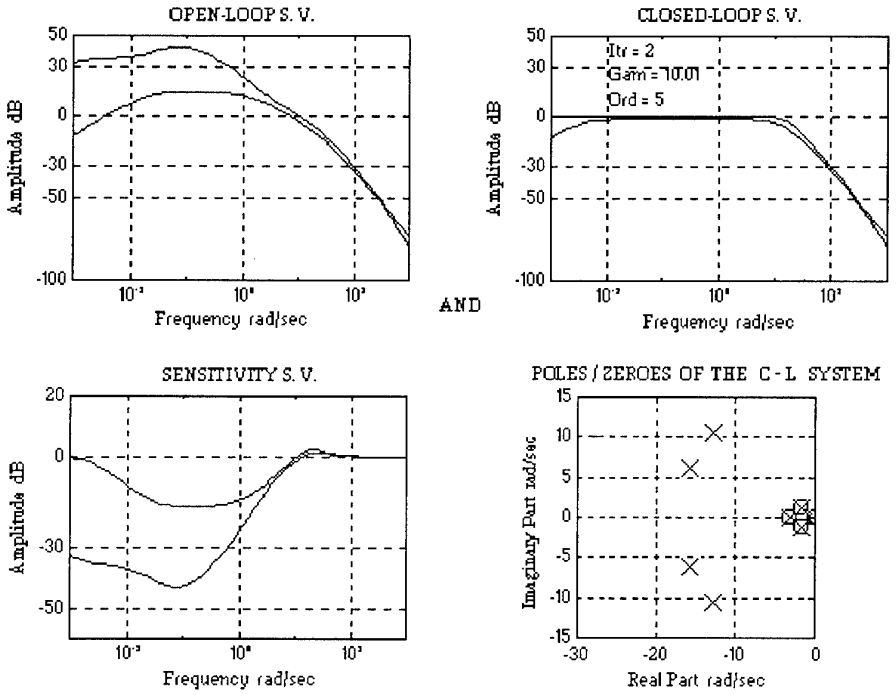

Fig. 9 Performance of the Closed-Loop system

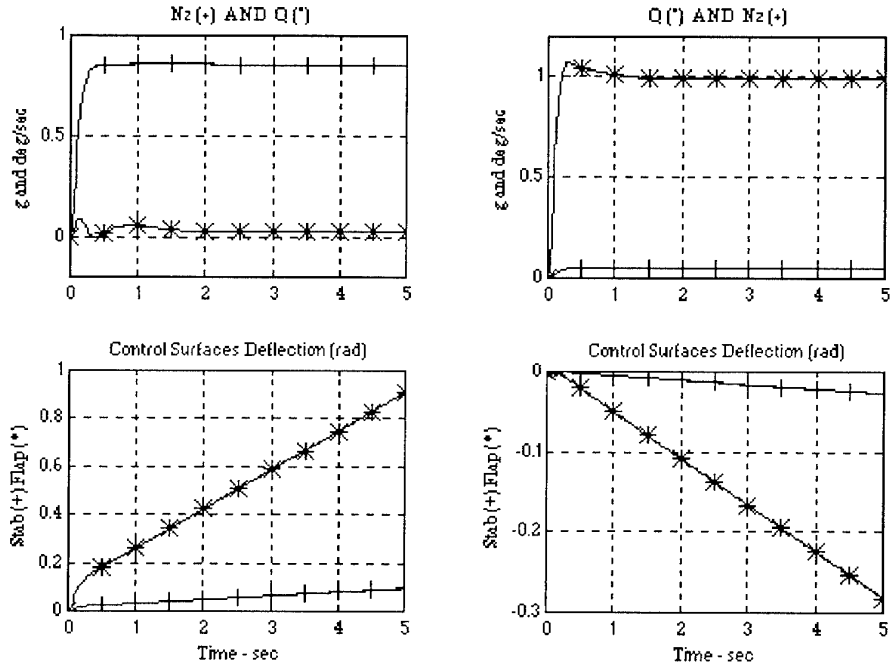

Fig. 10 Step response of the decoupled system ($N_z \neq 0$, $q=0$; $q \neq 0$, $N_z=0$)

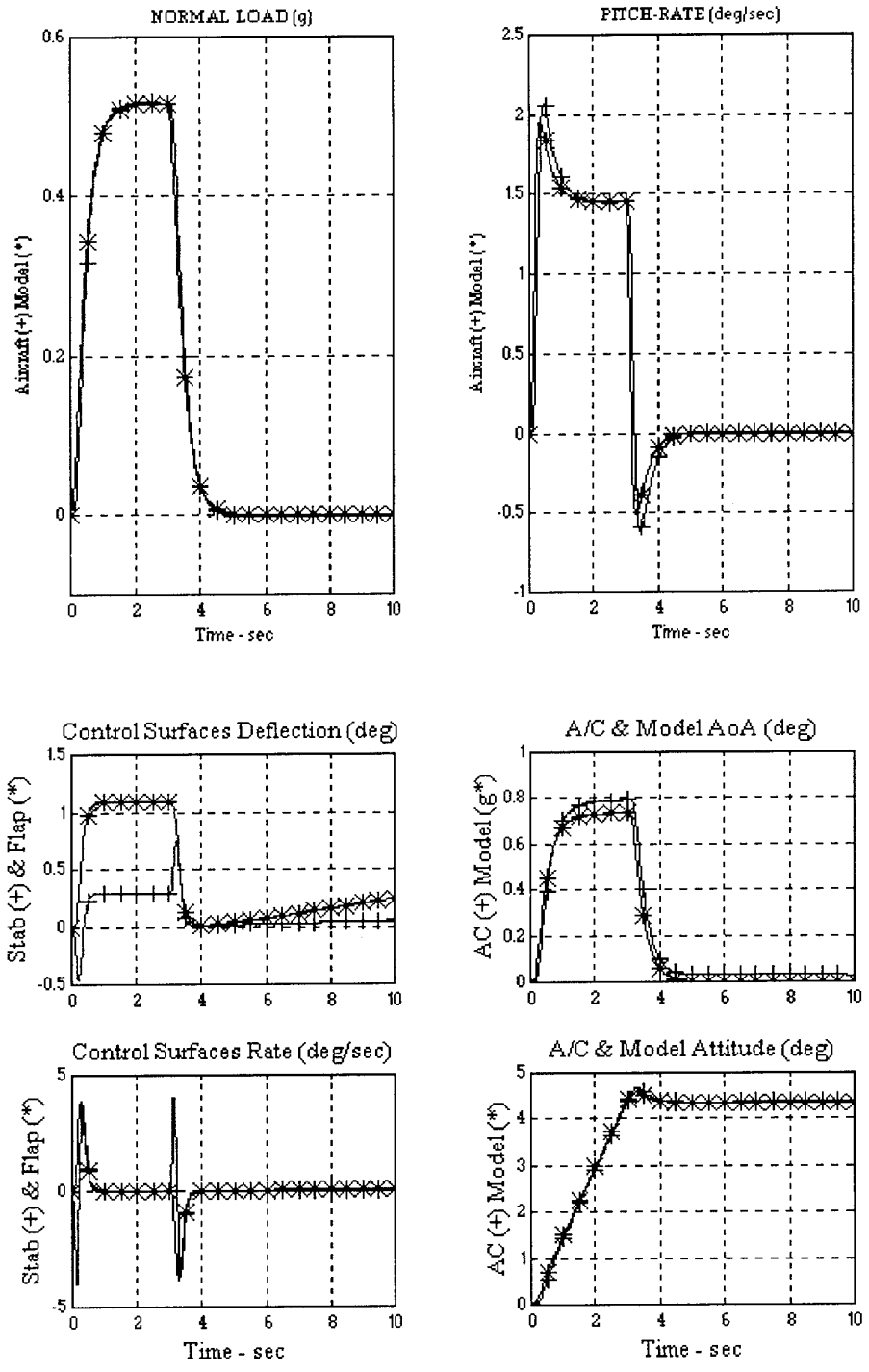

Fig. 11 Model-Following performance

Model Following Control for Tailoring Handling Qualities - ACT Experience with ATTHeS -

by
Gerd Bouwer
Wolfgang von Grünhagen
Heinz-Jürgen Pausder

Deutsche Forschungsanstalt für
Luft- und Raumfahrt e.V. (DLR)
Institut für Flugmechanik
D - 38108 Braunschweig, FRG
Germany

ABSTRACT

In-flight simulators will play an important and unique role in the development process of future helicopter systems and in generating credible handling qualities data which establish design guides for the integrated helicopter systems including sophisticated cockpit technologies and high authority control systems. The Institute for Flight Mechanics of DLR has developed the helicopter in-flight simulator ATTHeS (Advanced Technology Testing Helicopter System) which is based on a BO 105 helicopter. The testbed is equipped with a full authority nonredundant fly-by-wire control system for the main rotor and a fly-by-light system for the tail rotor. In the simulation mode the testbed requires a two-men crew, a simulation and a safety pilot.

The onboard computer system consists of two computers to which are assigned the separated tasks, data collection and digital control system. With the implemented software structure the flexibility is achieved to change the control laws without any changes in the real time process. Before undergoing any flight test with a new or modified control system, a real-time hardware/software-in-the-loop ground-based simulation has to be successfully performed. For the purposes of in-flight simulation an explicit model following control system was developed and the model following performance was evaluated in flight. This control system is composed of a dynamic feedforward, based on an extended model of the host helicopter, and an optimized feedback control system.

The capability and flexibility of ATTHeS has been demonstrated in different test programs which have been related to the use of the testbed for test pilot training, handling qualities research, helicopter simulation, and control law design and evaluation including automatic navigation and hover position hold.

INTRODUCTION

Increasing levels of mission performance are required for civil and military use of the next generation of helicopters. This aspect is pervading the application of new technologies to facilitate the pilot's task. Flying a helicopter in adverse weather with high precision close to the ground means a drastic change of the piloting task. New cockpit technologies and high authority digital control systems will be implemented with the potential to tailor the flying qualities of the integrated helicopter system [1].

Both ground based and in-flight simulation will play an important role in the development of new helicopters and helicopter systems. The results obtained from piloted ground simulations will have to be verified in flight. Especially the constraints and limits in the vision and motion systems of ground based simulators are demanding such a verification approach.

DLR IN-FLIGHT SIMULATOR ATTHeS

Recognizing the requirements for a flying testbed with a broad simulation capability, the helicopter in-flight simulator ATTHeS has been developed at the DLR Institute for Flight Mechanics [2]. The ATTHeS is based on a BO 105 helicopter (**Figure 1**). The high control power and the high bandwidth response of the BO 105 with a hingeless rotor are an excellent precondition to be used as a host for in-flight simulation. Because the next generation of helicopters are required to be flown in high pilot gain, high bandwidth, and high precision flight tasks, these demands have been especially considered in the development of ATTHeS.

The testbed is equipped with a full authority nonredundant fly-by-wire (FBW) control system for the main rotor and a fly-by-light (FBL) control system for the tail rotor. The test helicopter requires a

Paper presented at the Flight Mechanics Panel Symposium held in Turin, Italy, from 9-13 May 1994.

two-men crew, consisting of a simulation pilot and a safety pilot. The safety pilot is provided with the standard mechanical link to the rotor controls whereas the simulation pilot's controllers are linked electrically/optically to the rotor controls. The FBW/L actuator inputs,which are commanded by the simulation pilot and/or the flight control system, are mechanically fed back to the safety pilot's controllers. With this' function, the safety pilot is enabled to monitor the rotor control inputs. This is an important safety aspect, because the safety pilot can evaluate whether the inputs are adequate to the flight task. The safety pilot can disengage the FBW/L control system by switching it off or by overriding the control actuators. In addition, an automatic safety system is installed, monitoring the hub and lag bending moments of the main rotor.

The testbed can be flown in three modes:

1. the FBW/L disengaged mode, where the safety pilot has the exclusive control,
2. the 1:1 FBW/L mode, where the simulation pilot flies the basic helicopter with full authority, and
3. the simulation mode, where the simulation pilot is flying a simulated helicopter system with full authority.

In the 1:1 FBW/L and the simulation mode the flight envelope is restricted to 50ft above ground in hover and 100ft above ground in forward flight.

To incorporate the digital control system for in-flight simulation purposes, an onboard computer and a data acquisition system have been installed. In the specifications for the design the following system conditions and requirements have been considered:

- Limited space is available in the helicopter.
- Software modifications in the control system must be accomplished in a host computer on the ground.
- A system simulation facility, which is compatible to the onboard system, is needed to check any software modifications before going into flight.
- The onboard system tasks, control system and evaluation of the control system performance, have to be clearly separated.
- The flight tests have to be observed and managed from a ground station.

Figure 2 shows in a block diagram the onboard system. Two DEC PDP11 computers, ruggedized for operation in the airborne environment, are installed. The data recording task and the control system task are assigned to the computers, which allows a largely autonomous treatment of the data streams needed for the control laws and for the data recording for the control system performance evaluation.

The simulation pilot's inputs and the state variables, which are used in the control laws, are obtained directly from the preconditioned sensor signals with an installed 32 channel A/D converter. A sampling cycle of 25 Hz is realized. After the initialization, the control system is held in the trim position. The control system starts, when the simulation pilot switches on the control status. The computer generates a subcycle of 1/5 of the frame time (8 msec). The subcycle allows to refresh the highre bandwidth FBL actuator inputs in a shorter time frame than the sampling frame. The overall computation time for the commanded model and the control laws is 7 msec.

The data recording computer is equipped with a 64 channel A/D converter. All sensor signals are sampled with a frequency of 100 Hz. A sampling frequency, significantly higher than of the control computer sampling frequency, has been specified to achieve a more precise assessment of the overall system performance. Both computers are linked by a dual ported memory. The measured signals, which are used in the control computer, and the signals, which are calculated in the control computer, are transmitted via the dual port memory for recording. The data are recorded onboard on a floppy disk. In addition, the data are transmitted to the telemetry. The telemetry data are only used for quicklook purposes in the ground station. The ground station also contains a host computer, which is compatible to the control system computer. Any modifications of the software code including changes of the control laws and the command model parameters are first performed in this host computer on the ground and then transferred to the onboard computers via a floppy disk.

The control computer software is divided into two parts which are related to a system level and a user and control law level (**Figure 3**). This separation and the specific interfaces allow to incorporate different control law software without any changes in the real-time software.

The system software includes the real-time control and the input/output software. It controls via interrupts the I/O operations during the real-time process and handles the simulation pilot's keyboard and display. This software package is written in Assembly language to minimize the computation time and calls the user supplied subroutine every cycle. The cycle time can be adapted to the complexity of a control law package. The user software package includes the control laws, command model generation, and the signal conditioning specifically needed for the control laws. For the DLR internal application, this part is written in FORTRAN. For extrenal users, a software interface is available for use of control laws written in C-language.

GROUND BASED SYSTEMS

The overall computer structure and program data flow is shown in **Figure 4**. For DLR application, the control laws are developed using the DLR mainframe computer. On this IBM system, a duplicate of the real-time control software, including a linear or nonlinear simulation of ATTHeS, is installed. With this system, the proper function of the control law software can be investigated and modifications of the software modules can be undertaken easily. When this nonreal-time simulation is successfully completed, the user software is transferred to the PDP 11-23 host computer in the ground station. An external user, with its own control law design tools, has to provide his user software in a specified format, compatible with the defined interface. With the PDP 11-23 computer, the user and the real-time control software is linked together and stored on a floppy disk. This disk can be used either in the AD100/PDP 11-93 real-time simulation facility or in the ATTHeS on-board computer. If modifications of the FORTRAN or C user program are necessary, they are accomplished on the PDP 11-23 host computer.

Before undergoing any evaluation in flight, the software has to be tested under real-time conditions to examine the compatibility and to prevent hardovers in flight. Therefore, a real-time simulation of ATTHeS, including actuators and sensors, was developed (**Figure 5**). A nonlinear simulation program of ATTHeS, developed on the DLR mainframe computer in Fortran was transferred to an AD100 simulation computer and translated to it's language ADSIM [3]. The comprehensive simulation includes the models of:

- Main rotor with 10 blade elements for each blade.
- Tail rotor with tip path plane.
- Empennage and fin.
- Fuselage.
- Engine and RPM governor.
- Fly-by-wire/light actuating system as second order and 40 ms delay.
- Data acquisition module.

All the systems above are calculated on the AD100 in 2.5 ms. Via a 68030 interface computer, the states of the simulated ATTHeS are converted to the analogue output of the ATTHeS sensor equipment. A complete duplicate of the onboard control computer is connected to the simulated sensor signals and the actuator inputs. Since the ground simulation is developed only for the functional examination of the in-flight simulation software and not for pilot-in-the-loop investigations, a simple cockpit with conventional helicopter controls, a primary flight display, and a 3D display is connected to the interface computer. The in-flight simulation program is loaded from the onboard computer disk and runs in the ground simulation as it does in flight. Running the ground-based simulation, the engineers and pilots can check the handling of the flying simulator and the proper function of the software. When this ground test is successfully accomplished, the flight test can be performed.

Because only limited space is available onboard a ground-based engineers station is a part of the ATTHeS system which is necessary for conducting flight tests. The station includes:

- The host computer for the onboard system.
- One IBM-PC for continuous recording of telemetry data and display of the helicopter position in a local map. The data can be sent to the quicklook PCs or transferred to the main-frame computer.
- Two IBM-PC terminals for quicklook. On each terminal, 10 telemetried signals can be displayed. The signals and the scaling of the signals can be selected easily.
- A 3D visualization of the helicopter motion from telemetry data.
- A terminal displaying online the position of the testbed over ground if the position data are measured with a laser tracking system.
- A TV monitor showing the picture of the camera, mounted at the tracking antenna.
- A Vax computer with a hardcopy unit for post flight data analysis.

In the ground station the engineers can observe and manage the flight tests. In addition, the equipment yields the mobility to conduct flight tests undependant of the DLR research center.

MODEL FOLLOWING CONTROL SYSTEM DESIGN

The most promising and also challenging method of a control system design for in-flight simulation is to force the basic helicopter to respond on the pilot's inputs as an explicitely calculated command model. Explicit model following control is useful when a high flexibility is required to vary the commanded models. **Fig. 6** illustrates the principle structure of an explicit model following control system (MFCS) [4]. The commanded model response due to the pilot's inputs is calculated and is transmitted to the controllers. The feedforward controller, which has to compensate the dynamic of the host helicopter, is calculated from a model of the host helicopter. A vehicle state feedback is implied to minimize the influence of noise and feedforward inaccuracies and to reduce the tendency of long term drifts in the overall system response. The feedforward and feedback controller are independant on the commanded model. This modern type of control system is more and more used for

operational [5] and research [6] aircraft.

The performance and accuracy of the model following control system is highly depending on the accuracy of modeled dynamics of the host helicopter, especially for the short term behaviour, but additional components contribute to the overall performance. The design has to consider and has to be adapted to pilot's controller dynamics, pilot's input shaping, actuator dynamics, sensor dynamics, and signal conditioning [7,8].

As a consequence, an explicit model following control system has been developed for the use in the ATTHeS in-flight simulator. As mentioned before, this type of control system yields the required flexibility for the variation of the commanded model response behaviour. The presently designed MFCS is adapted for use in the forward flight between 40 to 100 kts and for the hovering flight.

For the design of the control system four main steps have to be performed :

- to define a model structure for the in-flight simulator host aircraft, including rotor states with high bandwidth capability
- to determine the parameters of the above defined model, either by system identification or simulation procedures
-to determine the feedforward structure from the model of the host aircraft by formal inversion of the defined model
-to define the feedback structure and to optimize the overall response by simulation and refinement in final flight tests.

Feedforward Design and Calculation

After having defined the host helicopter model structure and having identified the data [9] a linear state space system description is given by

$$\dot{x} = A\,x + B\,u$$

The system is assumed to have complete controllability and observability. The selected state vector y_m to be implemented in the feedforward branch of the MFCS-system leads to the special output equation (dim y = dim u , D is square matrix).

$$y_m = C\,x + D\,u$$

The transferfunction matrix representation of this system is

$$Y_m(s) = \{\, C\,[Is-A]^{-1}\,B + D \,\}\,U(s) = C^*(s)\,U(s)$$

Inversion of this system by polynomial matrix decomposition yields the feedforward system

$$U_f(s) = C^{*-1}(s)\,Y_m(s) = \{\, K(s) + \frac{H(s)}{p(s)} \,\}\,Y_m(s)$$

the first term in braces K(s) represents the *'static feedforward'*. In the time domain the relation between model states Y_m and feedforward control output U_f is given by matrix multiplication .

The second term in braces, representing the *'dynamic feedforward'*, with the polynomial p(s) as denominator can be further simplified by decomposition to partial fractions

$$\frac{H(s)}{p(s)} = \frac{H(s)}{\prod_i (s-s_i)} = \sum_i \frac{H_i^*}{s-s_i}$$

with the *'invariant zeros'* s_i and the corresponding residual matrices H_i^*. The functions

$$\frac{1}{s-s_i} Y_m$$

are in the origin of the Laplace transformations convolutions

$$\int_0^t [\, e^{s_i(t-\tau)}\, Y_m(\tau) \,]\, d\tau$$

They are solved "online" by Simpson integration. A detailed description of the method including examples is given in [10].

Feedback design

Since modelling and identification inaccuracies, changes in nominal flight conditions and mainly gusts drive the base helicopter states x apart from the desired model states x_m , feedback controllers are required to compensate these errors.

A decoupled minimum structure feedback system controls the pitch states with the longitudinal cyclic, the roll states with the lateral cyclic, the vertical velocity with the collective and the yaw states with the tail rotor control. The pitch, roll and yaw rates and the vertical velocity are controlled with proportional and integral (PI) controllers and the pitch and roll attitude and the sideslip angle with proportional feedback (**Figure 7**).

The feedback gains were optimized in a non-realtime simulation and verified in flight with the same procedure. The helicopter was disturbed in the 60 kts level flight with a control input by the safety pilot in

the collective for pitch and yaw optimization and with a longitudinal control input for roll and heave controller optimization. In the simulation, the quadratic error between the model states (trim values) and the helicopter states was minimized. In a first step, the proportional feedbacks were optimized, followed by the integral controllers, and finally the attitude feedbacks.

The influence of feedback loops to the system dynamics can be analysed with classical control theory methods. **Figure 8** shows the roll root locii of an 8 degree of freedom (DOF) linear 60 knots level flight model of the BO 105 dependant on linear and integral roll rate feedback K_P and K_I. In the first layout step, K_P is increased, which increases the roll frequency, while the roll damping decreases. With a defined proportional roll rate feedback, the integral roll rate feedback is increased. The roll damping now decreases rapidly with nearly constant roll frequency.

MODEL FOLLOWING PERFORMANCE

A good initial response and high bandwidth capability of ATTHeS was emphasized in the MFCS design. This characteristic is essentially depending on a well adapted feedforward controller. The use of the angular accelerations for pitch and roll in the BO 105 model which is used for the feedforward calculation improves the initial response behaviour of the ATTHeS simulator. The overall time delays are measured in flight tests with about 110 msec for the roll axis and 150 msec for the pitch axis. The increased value in the pitch axis results from the basic helicopter due to a higher moment of inertia [11].

The quality of long term following is demonstrated in **Figure 9**. Both, rate and attitude signals show satisfactory model matching. The ATTHeS system has been flown in roll maneuvers like slalom, constant turns, and figure eights without any long term drift tendency. Corresponding to the assessed effective time delay and the time histories of the long term behaviour, **Figure 10** shows the model following performance for the roll attitude in the frequency domain. An acceptable model following up to 8 rad/sec is achieved which allows to cover roll bandwidth configurations up to 6 rad/sec.

Figure 11 illustrates the achieved decoupling ratio of ATTHeS in comparison to the basic BO 105 in time histories and crossplots. In the upper time histories a comparison is made for disengaged and engaged MFCS modes. In both tests, the simulation pilot excited the helicopter with longitudinal control oscillations. With the disengaged MFCS, the strongly coupling response of the basic B0 105 between pitch and roll axis can be observed. With the MFCS engaged, the coupling to the roll axis is suppressed. The crossplots of the longitudinal and lateral actuator positions indicate the necessary control activity to compensate the coupling.

ATTHeS UTILIZATION

ATTHeS is mainly utilized for handling qualities research and helicopter in-flight simulation. Decoupled rate command/attitude hold and attitude command models were defined as transfer functions with selectable control sensitivities, dampings and time delays. The influence of these parameters on the handling quality level was investigated in extensive flight tests. For helicopter in-flight simulation purposes, a linear derivative simulation model with specific nonlinear extensions is developed. Specific control systems of the helicopter to be simulated can be embedded. The high fidelity of the simulation was proven in flight tests. In addition, ATTHeS is used for test pilot training in cooperation with the Empire Test Pilots' School (ETPS) since 1990 and since 1992 with the french Ecole du Personnel Navigant d'Essais et de Reception (EPNER).

Handling Qualities Research

A main objective of flight mechanics research is to generate credible data for the definition of handling qualities criteria. An updated military rotorcraft handling qualities specification (ADS-33) [12] has been published which is a mission oriented specification and considers the integration of modern cockpit and control technologies. Although the ADS-33Cc is a U.S. specification at present, it is of international interest and international studies have contributed to the data bases for the definition of requirements. In cooperation with the U.S. Army a roll axis bandwidth study was conducted using the ground-based Vertical Motion Simulator at NASA Ames and the ATTHeS in-flight simulator of DLR in complement. The objective of this study was to verify and if necessary, to refine the criteria boundaries specified in the ADS-33C. Based on previous slalom testing experience [13] a modified slalom task with precise tracking phases through a set of gates was built up. The modified slalom meets the demands of an appropriate small amplitude precision tracking task and takes into consideration the constraints of the test facilities.

For the investigations of bandwidth and phase delay influences on handling qualities, a special conceptual model was developed. This decoupled model generates pitch and roll rate command / attitude hold (RCAH) or attitude command (AC) for longitudinal and lateral cyclic, rate of climb for collective and sideslip command for the pedals. The model is

extended with a coordinated turn term defined in relation to the commanded roll attitude. Finally, the angular rates are Euler-transformed and integrated to the Euler angles.

The roll axis bandwidth has been varied between about 1.5 and 4.5 rad/sec in the flight experiment. Additional configurations were defined with added time delays between 40 and 160 msec. The overall system transfer behaviour of ATTHeS showed an excellent matching around the bandwidth frequencies, especially compared with the transfer functions of the commanded models. The summarized data of the flight tests are shown in the evaluation diagram in **Figure 12**. The results indicate the high performance of ATTHeS with respect to bandwidth capability, model fidelity, and flexibility. The results of the handling qualities tests have been published more detailed in [14, 15].

Helicopter in-flight Simulation

For the simulation of helicopters in flight, a special model to be followed was developed [16]. Either from flight test data or from runs of a generic simulation program, a linear model is defined. The model dynamic matrix A and the model control matrix B are calculated with the identification procedure described above. The necessary nonlinear terms from coordinated turn, gravity, changes of flight path, and Euler equations are programmed explicitly. In addition, the four axis Stability Control Augmentation System (SCAS) of the simulated helicopter are programmed. The SCAS can be engaged or disengaged via software switches during the flights. For the investigation of SCAS failures, several failure situations are programmed.

The in-flight simulation of the Lynx helicopter shall serve as an example. This helicopter has some couplings opposite to the corresponding couplings of ATTHeS in it's basic BO 105 mode. **Figure 13** shows an airspeed change maneuver with constant altitude and heading, which is performed by pitching up and down the helicopter. It can be observed, that the simulation pilot controls and the ATTHeS actuator positions (=MFCS output) in the left diagrams diverge, except the collective control. This is a result of the opposite pitch rate due to collective control input coupling of the Lynx helicopter, which has a mechanical linkage between collective and longitudinal cyclic controls. All ATTHeS states match very well the commanded Lynx states. In general, the in-flight simulation was deemed to be representative for the Lynx helicopter [17].

Figure 14 documents a failure situation in the simulated helicopter. In a right turn at 10 sec, the longitudinal SCAS quits. Now the Lynx helicopter is in its basic unstable mode for the pitch axis. At about 20 sec, the simulation pilots' longitudinal stick control activity increases and the Lynx is oscillating in the pitch axis. Even this situation is matched very well by ATTHeS and was rated by the simulation pilot to be representative for the real flight case.

Automatic Navigation

For autopilot research, an automatic navigation task was defined : ATTHeS had to fly in constant altitude with constant airspeed automatically via a set of defined waypoints. The existing rate command/attitude hold explicit model for forward flight was extended with controllers for altitude, airspeed and heading. A standard GPS receiver was connected to the onboard control computer and a software navigation module including wind observation was developed [18]. This module generates the heading command depending on the desired and actual position and the wind situation. Extensive use of the realtime simulation reduced the flight testing time to about one hour. **Figure 15** shows the waypoints in the area of Braunschweig (left) and the resulting flight path (right), which was automatically flown by the system in constant altitude with constant airspeed without any pilot inputs, except pressing a button to engage the system.

Hover Position Hold

The design of control systems for helicopter in hover and low speed is a basic requirement for the extension of mission profiles and new mission demands. A special task for various applications is the position hold under wind and gust conditions above a ground fixed or moving target, like a shipboard reference, or a small vessel or lifeboat in rescue missions.

ATTHeS was equipped with an innovative measurement system for the hover position above a target. A video camera in combination with a sophisticated computer for processing the optical information was used as an integrated sensor system for the measurement of the relative position of the aircraft to a target. Based on the existing model following control system of ATTHeS for the forward flight condition, this control system was modified and adopted to fulfil the special requirements of the position hold task.

For a helicopter in hover, the longitudinal and lateral accelerations can either be controlled by changing the pitch and roll attitudes, or for short term corrections directly by the sideforce capability of the rotor system with only very small attitude changes. The relative position above a target is a second order differential equation with a nonlinear function in the

attitudes. In the existing MFCS for hover special effort was layed on the stabilization of the attitude loops in pitch and roll. For the position hold task additional terms in these loops were formulated. These terms relate the commanded pitch and roll attitudes to the relative position between helicopter and target and the corresponding velocities. The coefficients of these additional control loops were preoptimized in a non-realtime simulation.

Before undergoing any flight tests, the position hold hardware and software had to be integrated in the realtime helicopter simulation(see above). To perform this integration, a special hardware configuration was built, where

- A visual system [19] simulated the view of the downward looking camera
- The camera to be used in flight was mounted in front of the visual screen of this system
- The computer system of the camera was connected to the duplicate of the on-board control computer.

With this configuration, the overall MFCS with the position hold system was extensively tested under real-time conditions. In these simulations, the defined flight task with additional maneuvers was flown, including hover position hold turn in constant winds up to 20m/sec. The handling of the position hold was found to be aqequate to start flight testing. The flight task for the evaluation pilot was defined in four steps:

1. engage the fly-by-wire system in hover about 20 m behind the target
2. engage the basic MFCS (position hold off) with rate command/Attitude hold in pitch. roll, yaw and heave
3. fly above the target
4. when the camera has found the target within the defined range, engage the position hold.

The MFCS as well as the position hold could be engaged by pressing a button on the computer-keyboard. The position hold was automatically disengaged, when the pilot moved his cyclic stick.

The target was represented by a car on top of which was mounted a black square. The car-crew was informed by radio to drive a circle with a velocity of about 15 km/h and a radius of about 40 m. In the position hold mode the control system had to fly the helicopter above the target (**Figure 16**) in constant altitude and with constant heading while the simulation pilot flies hands-off of the controls. With the constant heading , the ground track of the car results in all combinations of forward (backwards) and sidewards airspeed of the helicopter.

Figure 17 shows the time histories of the longitudinal (x-cam) and lateral (y-cam) position, longitudinal (dx) and lateral (dy) cyclic stick and the status (MFR-stat) of the control system from continously recorded telemetry data stream over 10 minutes (condition: 15 kts wind, gusts up to 30 kts). At the beginning, the pilot flies the helicopter in the regular 1:1 fly-by-wire mode (MFR-Stat=0). After engaging the basic MFCS (MFR-Stat=1) he flies the helicopter above the target until the tracking system detects it. After engaging the position hold (MFR-Stat=3), the pilot flies hands-off (dx, dy = const.). During the following 8 minutes, while three circles where completed by the car, the relative position error was about 3 m maximum, where with a non-moving target (t=2 min) is about 1 m in longitudinal and 1.5 m in lateral position. The standard deviation during this flight test was 1.2 m in the longitudinal and 1.6 m in the lateral position.

These results were achieved after about 4 hours of flight testing [20].

CONCLUDING REMARKS AND FUTURE ASPECTS

The experiences with the Advanced Technology Testing Helicopter System (ATTHeS), achieved in the design and the utilization phases of the system, can be summarized:

1. ATTHeS is an in-flight simulator with a high level of flexibility.
2. ATTHeS with the DLR developed explicit MFCS is provided with a simulation fidelity characterized by high bandwidth, high decoupling potential, and a good model following performance.
3. ATTHeS was successfully used for pilot training, handling qualities research, helicopter in-flight simulation.
4. Innovative systems such as automatic Navigation and Hover Position hold have been realized as a "proof-of-concept" on ATTHeS.
5. The system simulation of AttheS is an excellent tool for flight test preparation and reduces the necessary flying time to a minimum.

ATTHeS will be used in the described ongoing activities. To extend the operational range, the model following control and the sensor systems systems for forward and hover flight will be combined.

REFERENCES

[1] Gmelin, B., Pausder, H.J., and Hamel, P."Mission Oriented Flying Qualities Criteria for Helicopter Design via In-Flight Simulation", AGARD-CP-423, Paper No. 4, 1986.

[2] Pausder, H.J., Bouwer, G., and von Grünhagen, W. "ATTHeS In-Flight Simulator for Flying Qualities Research", International Symposium on In-Flight Simulation for the 90's, Braunschweig, FRG, July 1991.

[3] Saager, P. and von Grünhagen, W. "Real Time Helicopter Simulation", International Symposium on Simulation, INFAUTUM 89, Toulouse, France, 1989.

[4] Henschel, F. and Bouwer, G. "Design of higher Bandwidth Model Following for Flight Vehicle Stabilization and Control", 16th Congress of the International Council of the Aeronautical Sciences, Jerusalem, Israel, 1988

[5] Fogler, D.L.and Keller, J.F. "Design and Pilot Evaluation of the RAH-66 Comanche Core AFCS", NASA/AHS Conference on Piloting Vertical Flight Aircraft, San Francisco, Ca., 1993

[6] Snell, S.A., Enns, D.F. and Garrard, W.L. "Nonlinear Inversion Flight Control for a Supermaneuverable Aircraft", Journal of Guidance, Control and Dynamics, Vol. 15, No. 4, 1992

[7] Pausder, H.-J., Bouwer, G., von Grünhagen, W. "A Highly Maneuverable Helicopter In-Flight Simulator - Aspects of Realization", 14th European Rotorcraft Forum, Milano, Italy,1988

[8] Pausder, H.-J. and Bouwer, G. "Recent Results of In-Flight Simulation for Helicopter ACT Research", 15th European Rotorcraft Forum, Amsterdam, The Netherlands, 1989

[9] Kaletka, J. and von Grünhagen, W. "Identification of Mathematical Derivative Models for the Design of a Model Following Control System", 45th Annual Forum of the American Helicopter Society, Boston, MA, USA, June 1989.

[10] von Grünhagen, W., Bouwer, G., Pausder, H.-J., Henschel, F., and Kaletka, J. "A high bandwidth control system for a helicopter in-flight simulator", International Journal of Control, Vol. 59, No.1, 1994

[11] Pausder, H.-J., Bouwer, G. and von Grünhagen, W. "ATTHeS In-Flight Simulator for Flying Qualities Research", International Symposium In-Flight Simulation for the 90's, DGLR-91-05, 1991

[12] N.N., "Handling Qualities Requirements for Military Rotorcraft", Aeronautical Design Standard ADS-33C, Aug. 1989.

[13] Pausder, H.J. "A Study of Roll Response Required in a Low Altitude Slalom Task", 11th European Rotorcraft Forum, London, UK, Sept. 1985.

[14] Pausder, H.J. and Blanken, C.L. "Investigation of the Effects of Bandwidth and Time Delay on Helicopter Roll-Axis Handling Qualities", 18th European Rotorcraft Forum, Avignon, France, Sept. 1992.

[15] Ockier, C.J. and Pausder, H.-J. "Experiences with ADS-33 Helicopter Specification Testing and Contributions to Refinement Research", AGARD FMP Active Control Technology:Application and & Lessons learned, Torino, Italy, 1994

[16] Bouwer, G. and von Grünhagen, W. "LYNX Helicopter In-Flight Simulation with ATTHeS", DLR Institute Report, IB 111-92/47, 1992

[17] Howitt, J. and Lt. Cheyne, S. "Assessment of the DRA HELISIM Lynx Math Model on the DLR BO-105 ATTHeS In-Flight Simulator", Defence Research Agency (DRA) Working Paper FSB WP(92)046, Bedford, UK, 1992

[18] Hamers, M. "Programminterface zur automatischen Navigation eines fly-by-wire Hubschraubers", Diplomarbeit an der Rheinisch-Westfälischen Technischen Hochschule Aachen, April 1994

[19] Alvermann, K. "Visualization and View Simulation based on Transputers", Journal of Aircraft, Vol. 30, No 4, 1993

[20] Bouwer, G., Oertel, H. and von Grünhagen, W. "Helicopter Hover Position Hold by Optical Tracking", To be published in ZFW.

Figure 1 : In-Flight Simulator ATTHeS

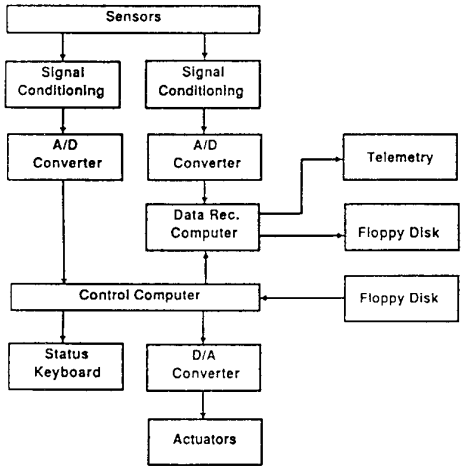

Figure 2 : Structure of ATTHeS On-Board System

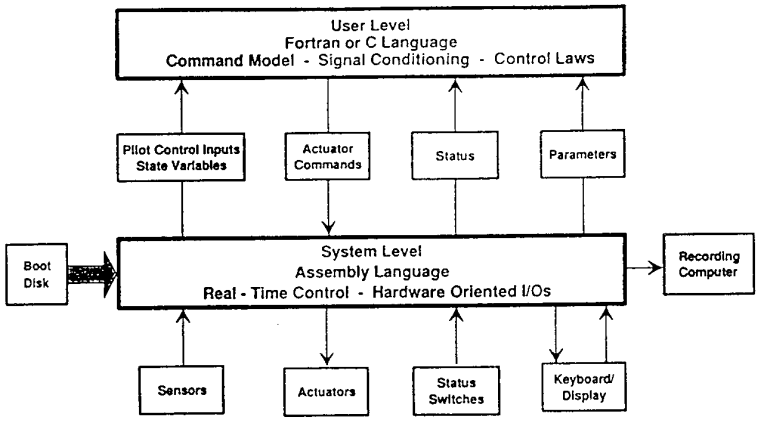

Figure 3 : Control Computer Software Structure

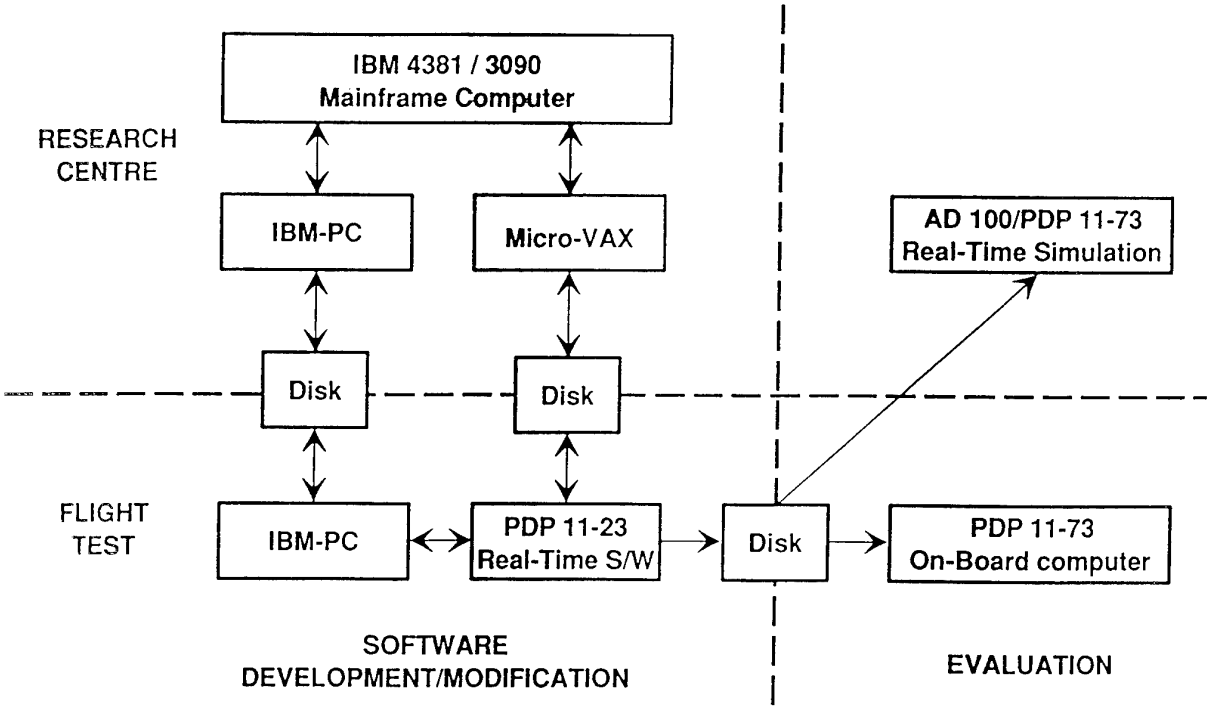

Figure 4 : Software Program Data Flow

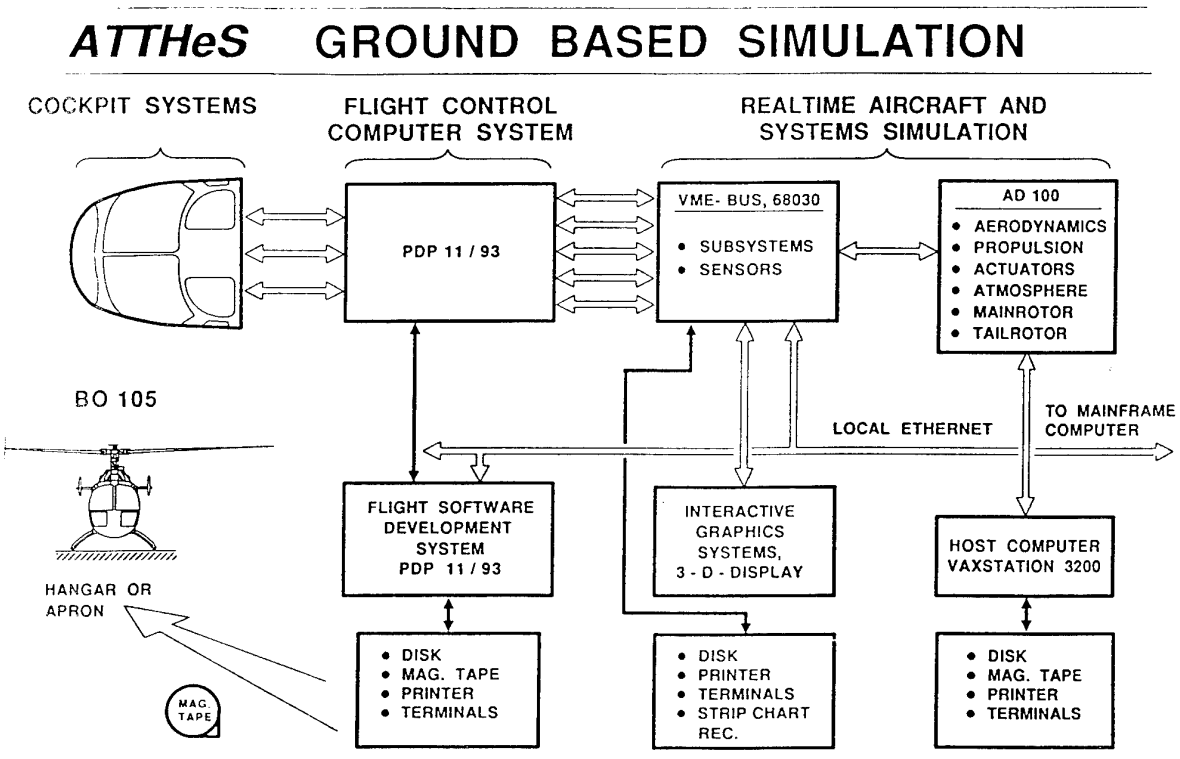

Figure 5 : Realtime System Simulation Structure

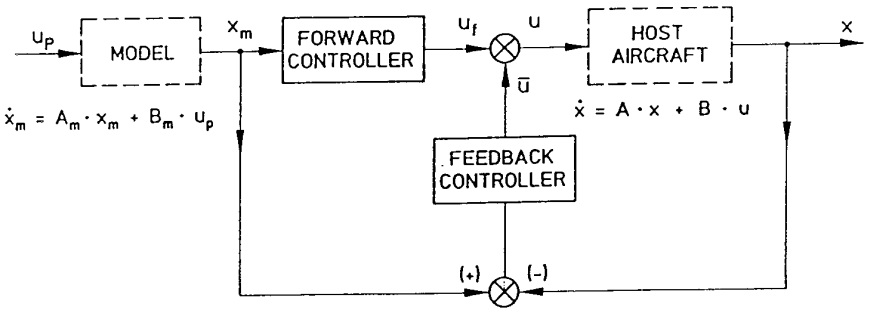

Figure 6 : Explicit Model Following Structure

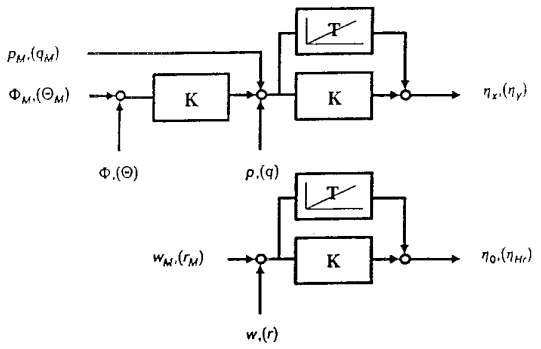

Figure 7: Structure of Feedback Control

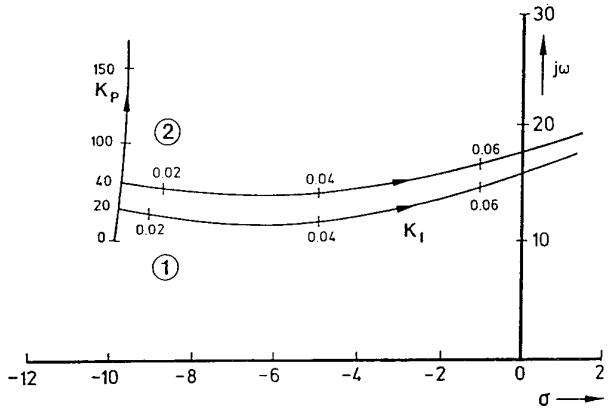

Figure 8 : Root Locii of Closed Loop System

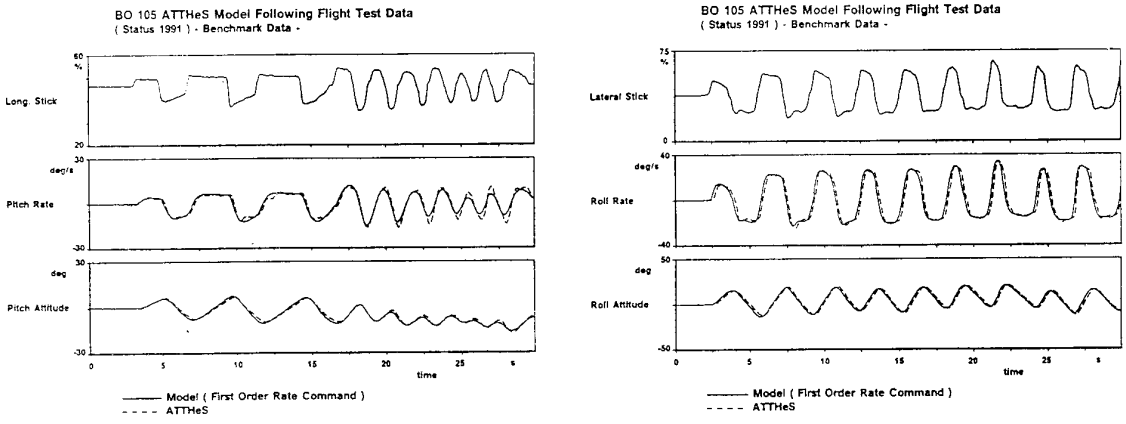

Figure 9 : ATTHeS Long Term Following

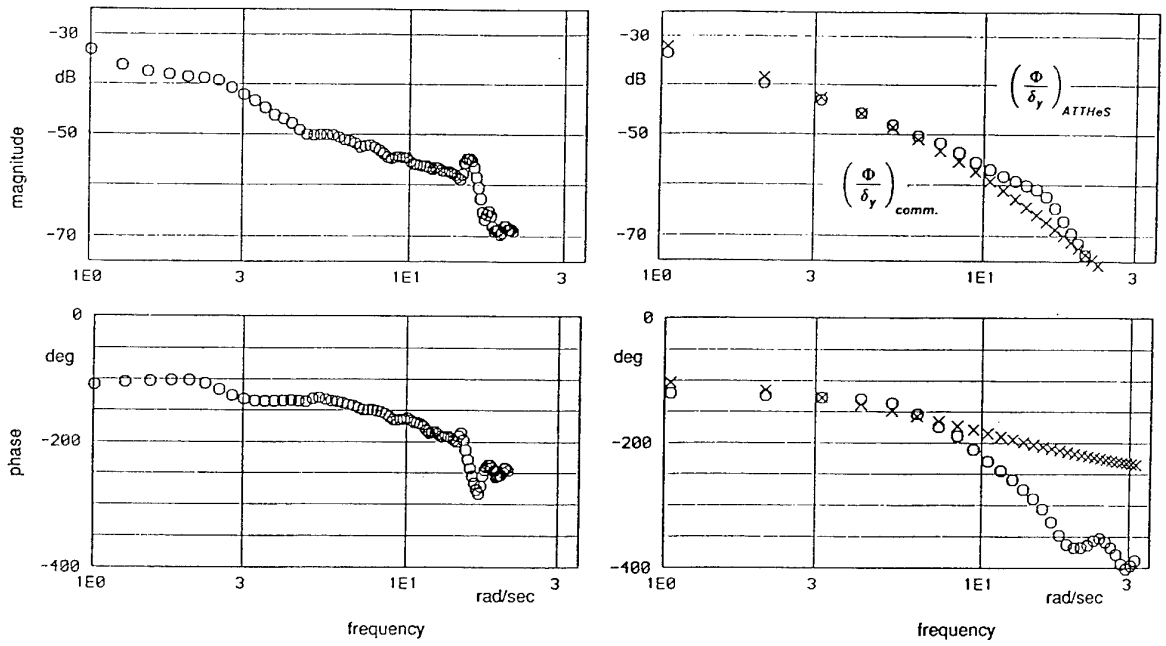

Roll attitude basic BO 105 **Roll attitude ATTHeS**

Figure 10 : Model Following Performance for Roll Attitude

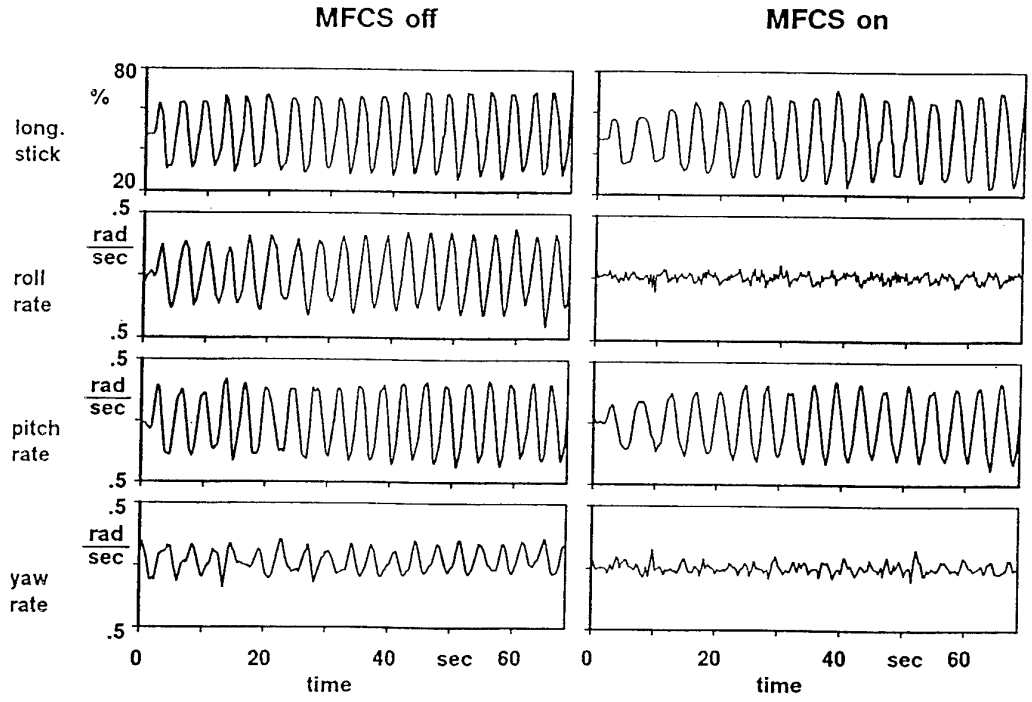

Figure 11 : Control System Decoupling Performance

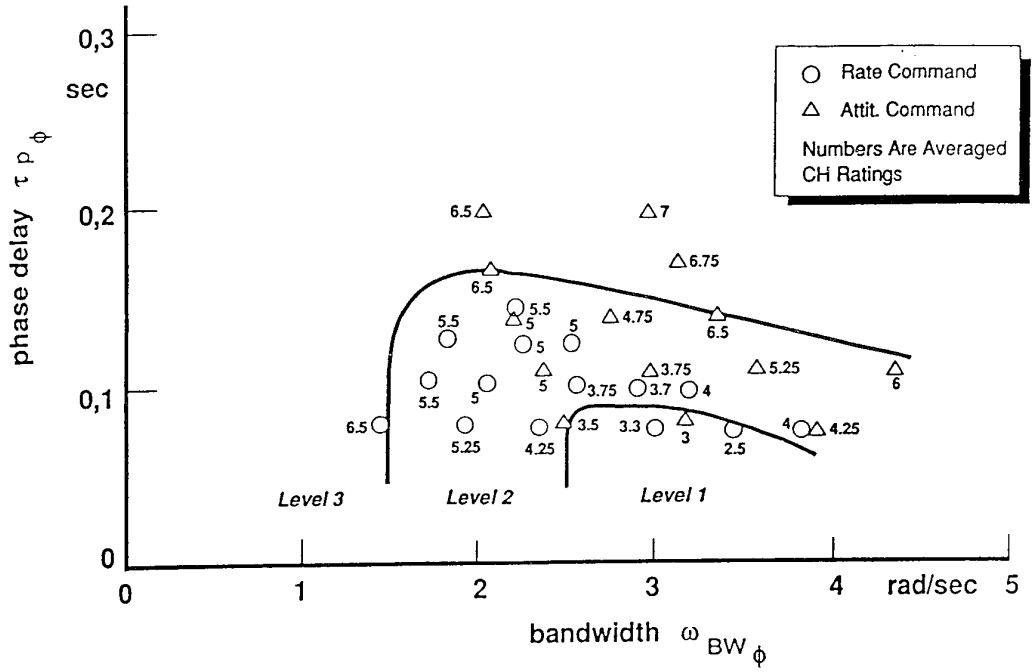

Figure 12 : Summarized Evaluations of Roll Bandwidth Tests

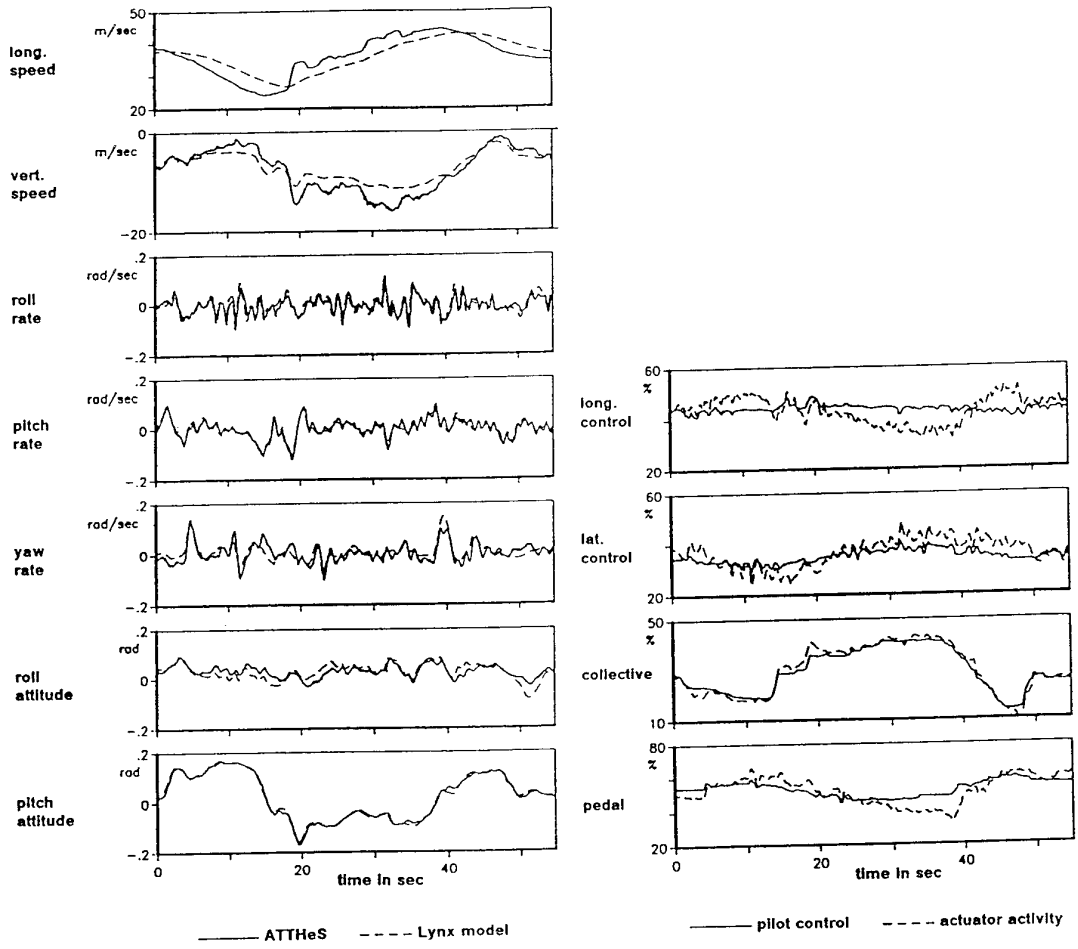

Figure 13 : Acceleration/Deceleration Maneuver with Lynx Model

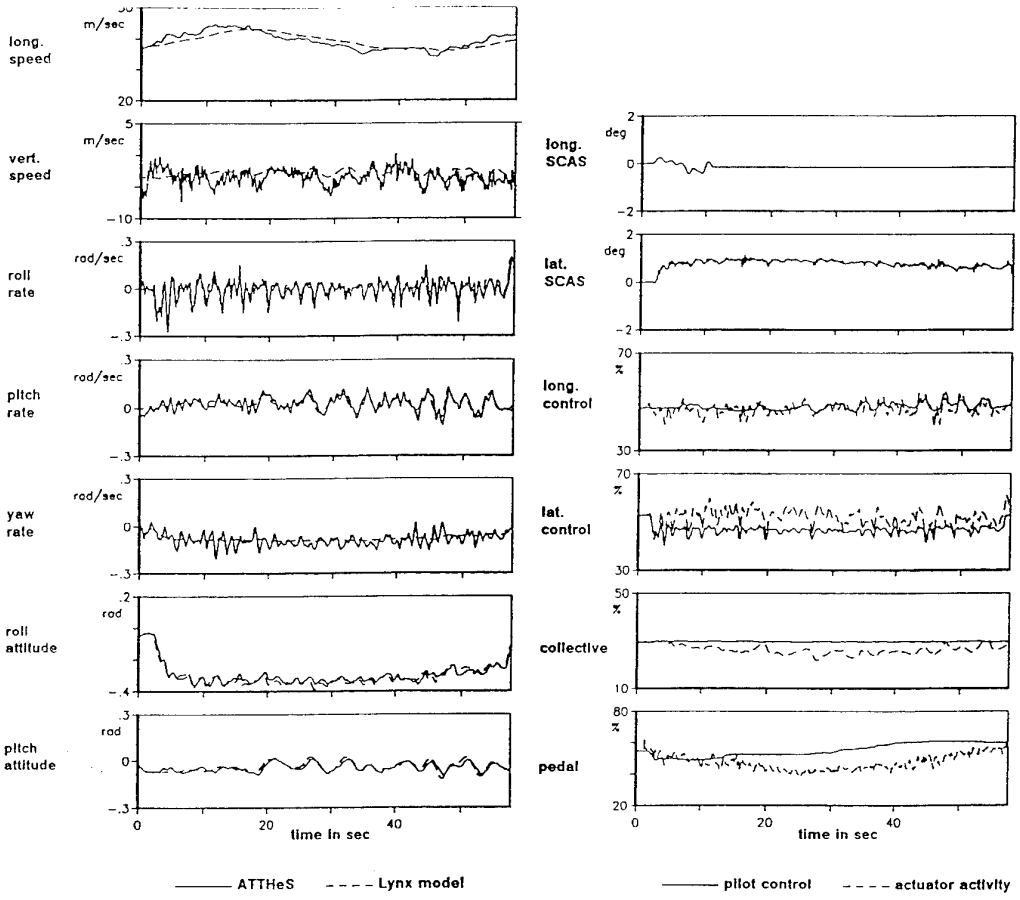

Figure 14 : Longitudinal SCAS Failure of Lynx Model

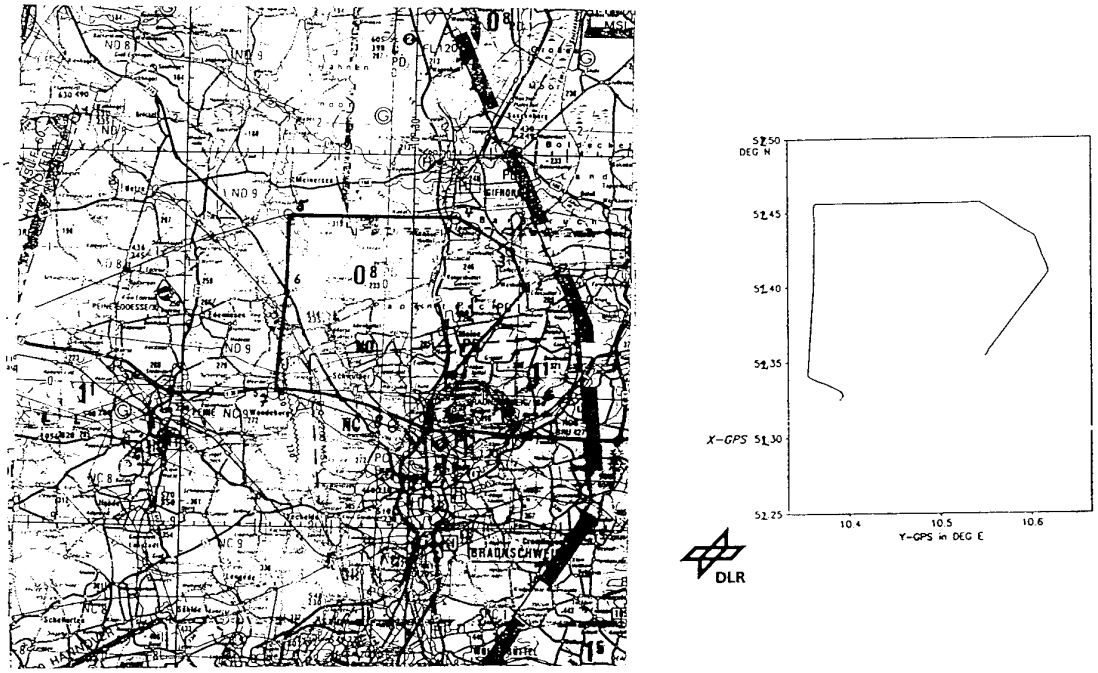

Figure 15 : Automatic Navigation via Waypoints

Figure 16 : Position Hold Flight Test Arrangement

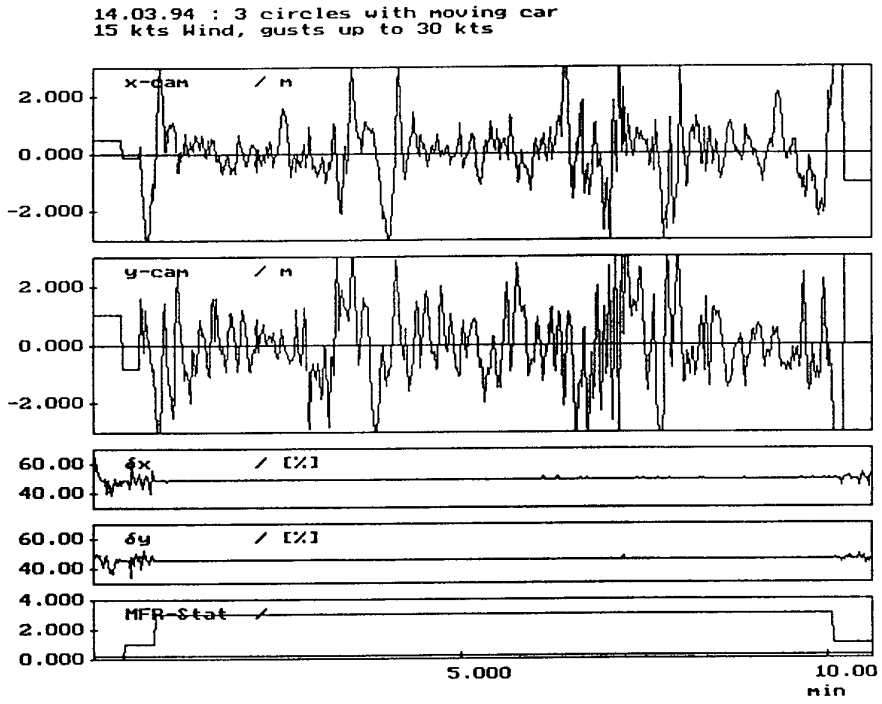

Figure 17 : Time Histories of telemetried Data during Position Hold

X-29 Flight Control System: Lessons Learned

Robert Clarke, John J. Burken, John T. Bosworth,
and Jeffrey E. Bauer
NASA Dryden Flight Research Center
P.O. Box 273, Mail Stop D484OD
Edwards, California, 93523-3311 U.S.A.

ABSTRACT

Two X-29A aircraft were flown at the NASA Dryden Flight Research Center over a period of eight years. The airplanes' unique features are the forward-swept wing, variable incidence close-coupled canard and highly relaxed longitudinal static stability (up to 35-percent negative static margin at subsonic conditions). This paper describes the primary flight control system and significant modifications made to this system, flight test techniques used during envelope expansion, and results for the low- and high-angle-of-attack programs. Throughout the paper, lessons learned will be discussed to illustrate the problems associated with the implementation of complex flight control systems.

1. NOMENCLATURE

ACC	automatic camber control (flight control system mode)
AOA	angle of attack
ARI	aileron-to-rudder interconnect
BMAX	rudder pedal command gain
$C_{L_{max}}$	maximum lift coefficient
CF	cost function
CP	constraint penalty
DP	design point
FCS	flight control system
FFT	fast Fourier transform
g	unit of acceleration, 32.2 ft/sec^2
G_{lim}	pitch stick limit gain
G_q	pitch rate feedback gain
$G_{\dot{q}}$	pitch acceleration feedback gain
G_{n_z}	normal acceleration feedback gain
GAIN1	pitch axis g-compensation gain
$GH(s)$	open-loop transfer function
GF1	symmetric flaperon gain factor
GS1	strake flap gain factor
GMAX	pitch stick command gain
GYCWSH	rudder pedal-to-aileron washout filter time constant
Hg	chemical symbol for the element mercury
HG(s)	loop gain matrix
I	identity matrix
ISA	integrated servoactuator
j	$\sqrt{-1}$
K2	roll rate-to-aileron feedback gain
K3	$\dot{\beta}$ -to-aileron feedback gain
K4	lateral acceleration-to-aileron feedback gain
K13	lateral stick-to-aileron forward-loop gain
K14	rudder pedal-to-aileron forward-loop gain
K17	$\dot{\beta}$ -to-rudder feedback gain
K18	lateral acceleration-to-rudder feedback gain
K27	lateral stick-to-rudder forward-loop gain
LOF	left outboard flaperon
LVDT	linear variable differential transducer
M	Mach number
MIMO	multi-input–multi-output
n_y	lateral acceleration, g
n_z	normal acceleration, g
NACA	National Advisory Committee for Aeronautics
p	roll rate, deg/sec
P_s	static pressure, inHg
PCE	pilot compensation error
PMAX	lateral stick command gain

Paper presented at the Flight Mechanics Panel Symposium held in Turin, Italy, from 9-13 May 1994.

q	pitch rate, deg/sec
Q_c	impact pressure, inHg
r	yaw rate, deg/sec
RDM	return difference matrix
RM	redundancy management
RPE	resonance peak error
s	Laplace transform variable
S_{aa}	generic auto spectrum of a
S_{ab}	generic cross spectrum of a to b
SF	scale factor
SISO	single-input–single-output
T_t	total temperature, °C
TE	trailing edge
V	true airspeed, knots
XKI1	pitch axis forward-loop integrator gain
XKI3	lateral axis forward-loop integrator gain
XKP1	pitch axis forward-loop proportional gain
XKP3	lateral axis forward-loop proportional gain
XKP4	yaw axis forward-loop proportional gain
XPITCH	pitch axis input sequence used in fast Fourier transform
YPITCH	pitch axis output sequence used in fast Fourier transform
α	angle of attack, deg
$\dot{\alpha}$	angle of attack rate, deg/sec
β	angle of sideslip, deg
$\dot{\beta}$	angle of sideslip rate, deg/sec
δ_a	differential flaperon deflection, deg
δ_{a_p}	lateral stick deflection, in.
δ_c	canard deflection, deg
δ_{e_p}	pitch stick deflection, in.
δ_f	symmetric flaperon deflection, deg
δ_r	rudder deflection, deg
δ_{r_p}	rudder pedal deflection, in.
δ_s	strake flap deflection, deg
θ	pitch angle, deg
σ_{SSV}	structured singular value
σ_{USV}	unscaled singular value
τ	time constant
ϕ	bank angle, deg
ω	frequency, rad/sec

2. INTRODUCTION

The Grumman Aerospace Corporation (Bethpage, NY) designed and built two X-29A airplanes under a contract sponsored by the Defense Advanced Research Projects Agency (DARPA) and funded through the United States Air Force. These airplanes were built as technology demonstrators with a forward-swept wing, lightweight fighter-type design. The use of tailored composites allowed the forward-swept wing design to be fabricated without significant weight penalties.[1] Both airplanes were flown at the NASA Dryden Flight Research Center to test the predicted aerodynamic advantages of the unique forward-swept wing configuration and unprecedented level of static instability (as much as 35-percent negative static margin; time to double amplitudes were predicted to be as short as 120 msec). Early on, the airplane designers recognized many potential advantages of this configuration. The forward-swept wing results in lower transonic drag as well as better control at high angle of attack (AOA).[2] The configuration was designed to be departure resistant and maintain significant roll control at extreme AOA. The typical stall pattern of an aft-swept wing, from wingtip to root, is reversed for a forward-swept wing, which stalls from the root to the tip.

Through the eight years of flight test, over 420 research flights were flown by the two X-29A airplanes. These flights defined an envelope which extended to Mach 1.48, just over 50,000-ft altitude, and up to 50° AOA at 1 g and 35° AOA at airspeeds up to 300 knots.

The flight experience at low AOA (below 20° AOA) with the initial flight control system (FCS) is covered in less detail since this design was done by Grumman Aerospace Corporation.[3,4] Several flight test techniques will be addressed. These techniques include in-flight time history comparison with simple linear models and stability margin estimation (gain and phase margins) as well as new capabilities (structured singular value margins) which extend these single-loop stability measures to multiloop control systems. In addition, modifications to improve the FCS will be described, in particular a technique used to improve the handling qualities of the longitudinal axis will be discussed.

The design of the high AOA FCS modifications will be presented. Techniques used to expand the high-AOA envelope will be discussed as well as the problems discovered during this effort. An FCS design feature was the incorporation of a dial-a-gain that allowed two control system gains to be independently varied during flight. This feature allowed many control system changes to be evaluated efficiently. These experiments allowed rapid incorporation of flight derived improvements to the FCS performance.

3. TEST AIRPLANE DESCRIPTIONS

The X-29A research airplane integrated several technologies, e.g., a forward-swept, aeroelastically tailored composite wing and a close-coupled, all moving canard. Furthermore, the wing, with a 29.27° leading-edge sweep and thin, supercritical airfoil, is relatively simple employing full-span, double-hinged, trailing-edge flaperons which also provide discrete variable camber. All roll control is provided by these flaperons, as the configuration does not use spoilers, rolling tail, or differential canard. The airplane has three surfaces used for longitudinal control: all moving canards, symmetric wing flaperons, and aft-fuselage strake flaps. The lateral–directional axes are controlled by differential wing flaperons (ailerons) and a conventional rudder. The left and right canards are driven symmetrically and operate at a maximum rate of approximately 100°/sec through a range of 60° trailing-edge (TE) up and 30° TE down. The wing flaperons move at a maximum rate of 68°/sec through a range of 10° TE up and 25° TE down. The rudder control surface has a range of ±30° and a maximum rate of 141°/sec. The strake flaps also act within a range of ±30°, but have a maximum rate of only 27°/sec.

The second X-29A (fig. 1) was modified for high-AOA testing by adding a spin parachute which was attached at the base of the vertical tail. The spin parachute was installed to provide for positive recovery from spins, as spin-tunnel tests had indicated that the X-29A ailerons and rudder provided poor recovery from fully developed upright spins. The addition of an inertial navigation system and the spin parachute system increased the empty weight of the airplane by almost 600 lb.

4. LOW-ANGLE-OF-ATTACK RESEARCH

Research at low AOA was the focus of all flight testing on X-29A No. 1 throughout its four years of flight test.[5–7] Initially, the focus (from a flight control designer's viewpoint) was on proving adequate stability margins and fixing problems which impacted stability or redundancy management. In the last year of flying, the focus was shifted to make improvements to the FCS to overcome the deficiencies which had been identified by the pilots. The X-29A No. 2 airplane was used primarily to examine high-AOA characteristics, but was also used to study the stability margins of the lateral–directional axes using multi-input–multi-output (MIMO) techniques at low-AOA conditions.

4.1 Description of the Flight Control System

The X-29A airplane is controlled through a triplex fly-by-wire FCS, which was designed for fail-operational, fail-safe capability. A schematic of the FCS is shown in fig. 2. Each of the three channels of the FCS incorporates a primary mode digital system using dual central processing units along with an analog reversion mode system. Both the digital and analog systems have dedicated feedback sensors. The digital computers run with an overall cycle time of 25 msec. The commands are sent to servoactuators that position the aerodynamic control surfaces of the airplane.

The initial longitudinal axis control laws were designed using an optimal model following technique.[4] A full-state feedback design was first used with a simplified aircraft and actuator model. The longitudinal system stability was significantly affected as higher order elements, such as sensor dynamics, zero-order-hold effects, actuators and time delays, were added to the analysis.[3] To recover the lost stability margins, a conventional design approach was taken to develop lead–lag filters to augment the basic control laws. Even after the redesign work, the stability margin design requirements were relaxed by the contractor to 4.5 dB and 30° (if all of the known high-order dynamics were included in the analysis). The government flight test team decided to require the use of flight measured stability margins and set minimum margins at 3 dB and 22.5°.

Figure 3 is a block diagram of the longitudinal control system. Short-period stabilization is achieved mainly through pitch rate

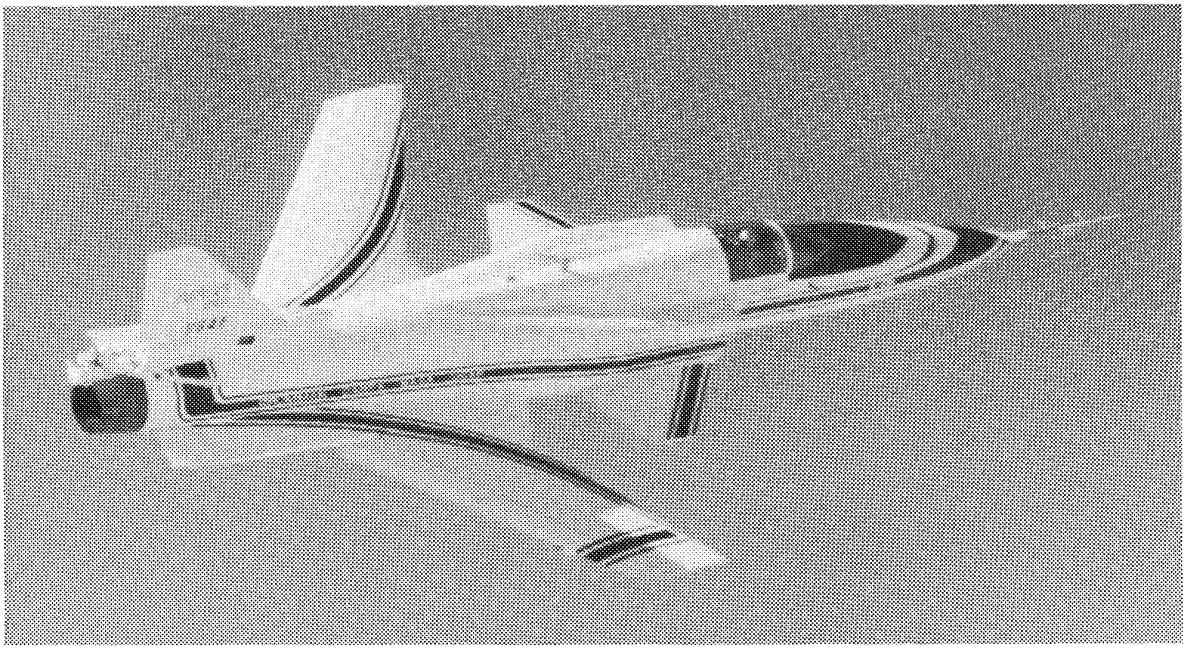

EC 89 0321-3

Figure 1. X-29A No. 2 airplane.

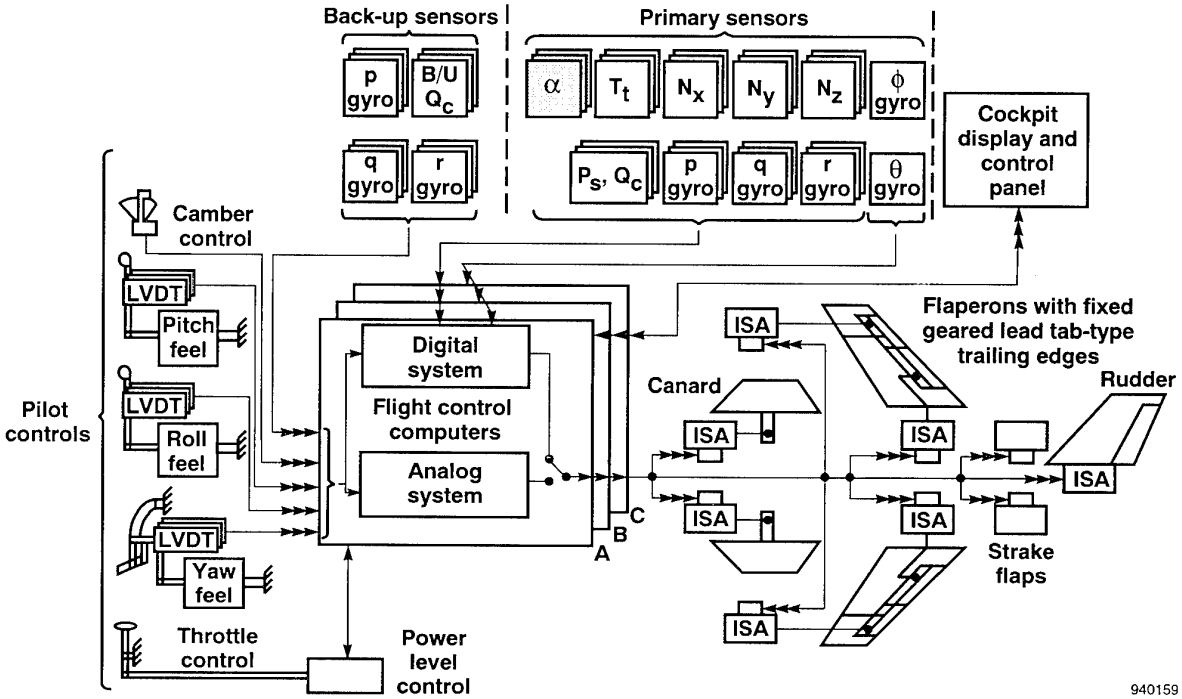

Figure 2. X-29A flight control system. (Note: Number of arrowheads designate level of redundancy and highlighted blocks represent changes made for high AOA.)

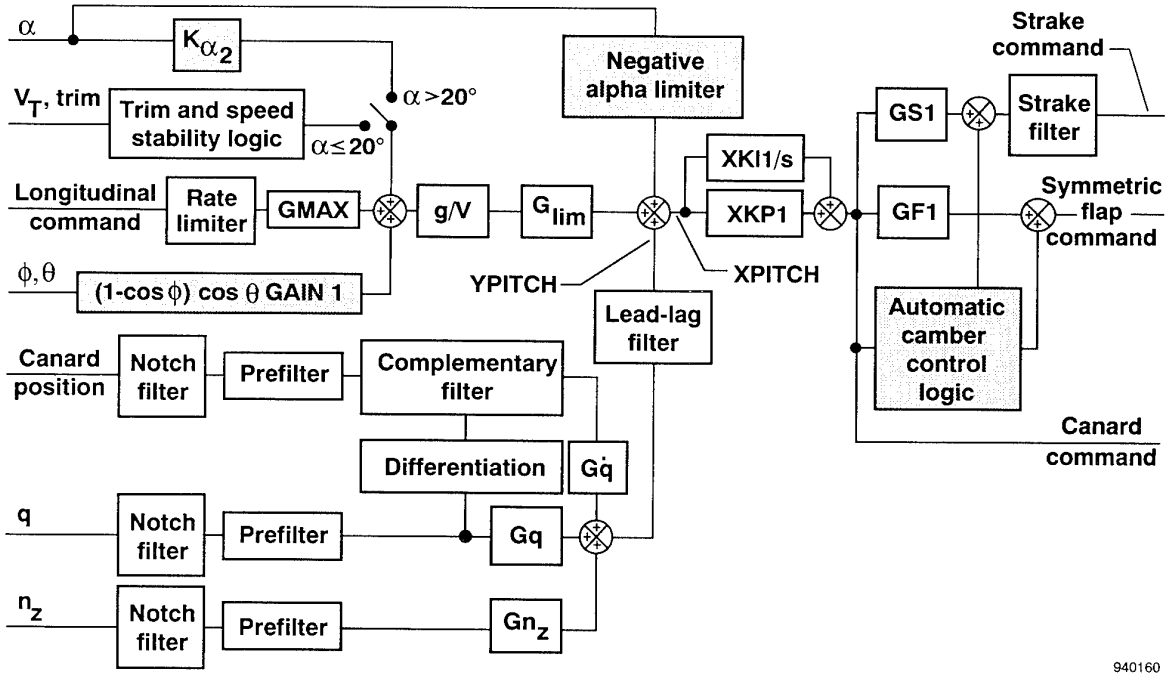

Figure 3. X-29A longitudinal control system. (Note: Highlighted blocks represent changes made for high AOA.)

and synthesized pitch acceleration feedback. Normal acceleration feedback is used to shape the stick force per g. The proportional-plus-integral compensation in the forward loop improves the short-period response and steady-state response to pilot inputs. Positive speed stability, which is important during powered approach, is provided by either automatic engagement or pilot selection of airspeed feedback.

In addition to the short-period stabilization function, the primary mode includes an automatic camber control (ACC) function which, in steady flight, generates commands to the symmetric

flaperons and strake flaps to optimize the overall lift-to-drag ratio of the airplane. The dynamic characteristics of the ACC feedback loops were designed to be significantly slower than those of the basic stability augmentation loops.

Figure 4 is the lateral–directional control law block diagram. The bare airframe lateral–directional characteristics of the X-29A are stable, and the multivariable FCS is conventional.[3] Roll rate is proportional to the lateral stick deflection through a nonlinear gearing gain that enhances the precision of small commands while still enabling the pilot to command large roll rates with larger stick deflections. A command rate limiter is implemented in the roll and yaw axis control systems to minimize the potential of control surface rate limiting, caused by large commands. Another feature is the forward-loop integrator in the roll axis which provides for an automatic trim function and helps to null steady-state roll errors. Synthetic sideslip rate feedback is used to provide dutch roll damping and to assist in turn coordination. An aileron-to-rudder interconnect (ARI) is also used to help coordinate rolls commanded with lateral stick deflections alone.

4.2 Flight Test Techniques

The following section presents some of the tools used to analyze the X-29A aircraft. The three tools used for flight data analysis were single-input–single-output (SISO) stability margins, time history comparisons, and MIMO or multivariable robustness margins. The first two tools were applied in near real-time during envelope expansion of X-29A No. 1, while the last one was only used in postflight analysis on X-29A No. 2. Both stability margin analyses, SISO and MIMO, obtained the desired frequency responses without physically opening any of the feedback loops.

4.2.1 *Single-input–single-output gain and phase margins*

Aircraft that have a high degree of static instability, like the X-29A, require close monitoring in the early envelope expansion stages of flight test. Fast Fourier transformation (FFT) techniques were used to measure the longitudinal open-loop frequency response characteristics over the entire flight envelope.

The X-29A longitudinal control system architecture lends itself to classical SISO stability margin analysis. As shown in fig. 3, the feedback paths reduce to a single path, allowing for traditional gain and phase margin analysis, such as Bode analysis. To excite the vehicle dynamics, a series of pilot pitch stick commands or computer generated frequency sweeps were used. Briefly, the technique collects the time domain variables XPITCH and YPITCH driven by the sweep, and uses an FFT to estimate the open-loop transfer function *GH(s)*. The open-loop frequency response is displayed on a monitor, and gain and phase margins are determined. The details of the near real-time SISO frequency response technique can be found in reference 8.

The frequency response of a SISO system can be estimated from the auto and cross spectra of the input and output. An estimate of the open-loop response is defined as

$$GH(j\omega) = \frac{S_{xy}}{S_{xx}} = \frac{S_{yy}}{S_{xy}} \qquad (12.1)$$

where S_{xy} is the cross spectrum of the input XPITCH with the output YPITCH, S_{xx} is the auto spectrum of the input, and S_{yy} is the auto spectrum of the output. The overall procedure is shown in fig. 5.

This test technique revealed much lower (below the established flight test minimum margins) than expected margins at a low-altitude transonic flight condition. As a result, the overall longitudinal loop gain was reduced to recover adequate stability margins. The actual amount of the reduction came directly from the comparison of predicted gain and phase margins with the analytical estimates. Once the control law change was

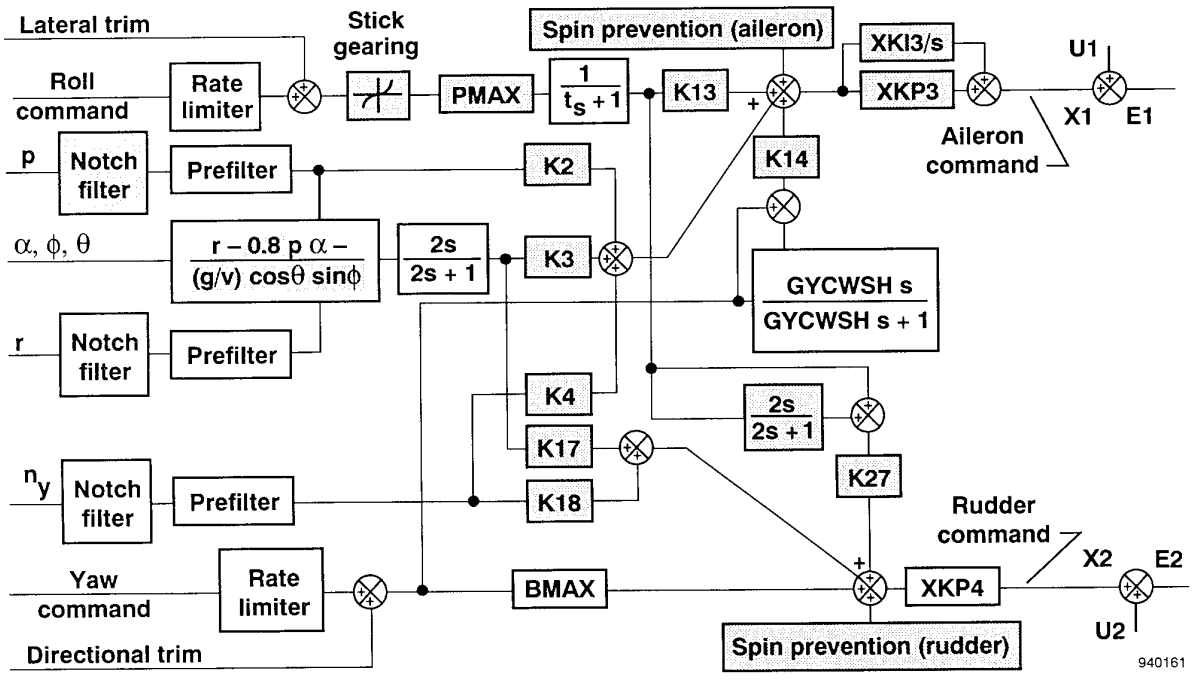

Figure 4. X-29A lateral–directional control system. (Note: Highlighted blocks represent changes made for high AOA.)

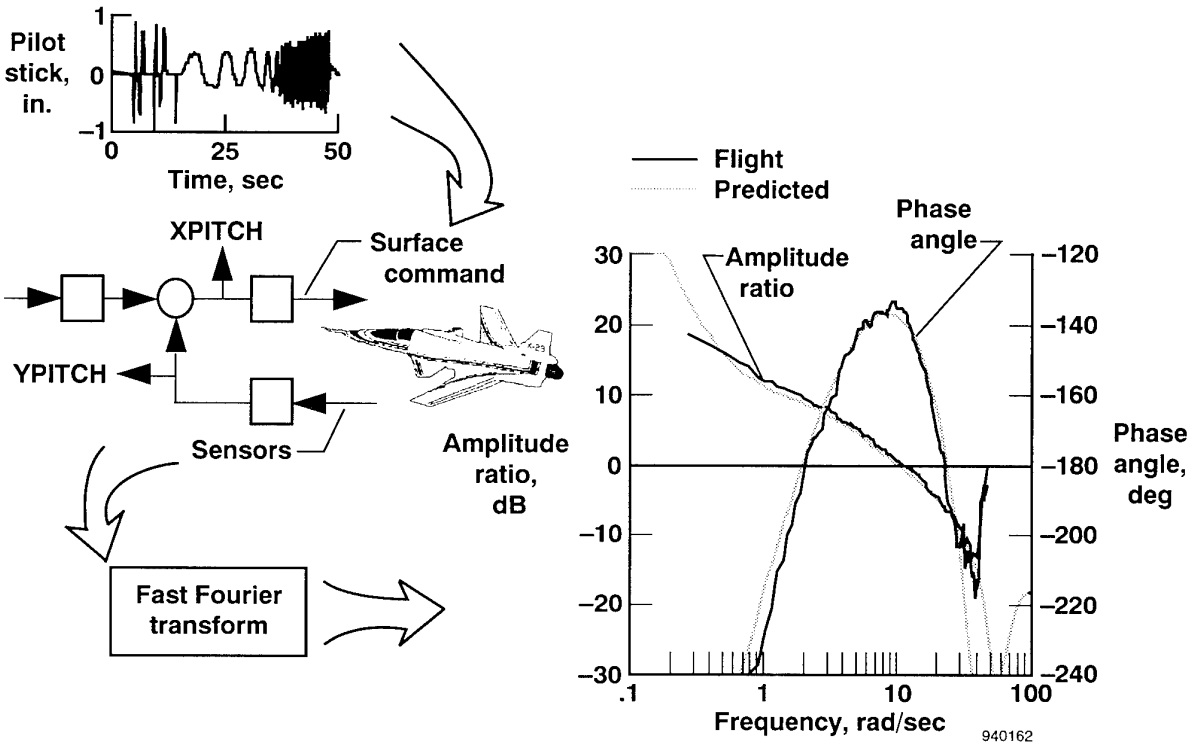

Figure 5. Near real-time determination of longitudinal axis open-loop frequency response from flight data.

made, the measured stability margins were greater than the requirement.

It was found that open-loop SISO frequency responses could be measured in-flight without physically breaking the loop. The near real-time capability enhanced the efficiency of the X-29A envelope expansion program. Gain margins greater than 3 dB and phase margins higher than 22.5° were eventually demonstrated over the entire flight envelope.

4.2.2 *Linear model time history comparisons*

The real-time comparison of the airplane response with linearized models allows the flight test personnel to verify the aircraft is performing as predicted, to determine regions of nonlinear behavior, and to increase the rate of envelope expansion.[9] Direct comparison of the measured aircraft response to those generated by a simulation, driven with identical pilot inputs, provides timely information. It is an extremely useful test tool if the comparison between the actual and simulation response can be made in real time.

Regions of nonlinear behavior of the aircraft can easily be determined. For example, surface rate limits show up dramatically when the flight data are compared to the linear simulation response. Knowledge of this nonlinear behavior can be useful in interpreting differences among results from other data analysis procedures, such as frequency response methods or parameter estimation techniques.

The success of the time history comparisons depends on a detailed and accurate math model. For the X-29A airplane the models were obtained by linearizing the nonlinear equations of motion about a trimmed flight condition. The perturbation step sizes were ±1 percent of Mach number for total velocity, ±2° for angle of attack, and ±1° or deg/sec for the remaining states and control surfaces. These step sizes provided reasonable estimates of the linear coefficients.

4.2.3 *Multi-input–multi-output stability margins*

The X-29A lateral–directional control system is a MIMO system, and the classical frequency analysis methods are inadequate for this type of control system. The classical methods, such as Bode or Nyquist analysis, do not allow for simultaneous variations of phase and gain in all of the feedback paths.[10-12] Recently, singular value norms of the return difference matrix (RDM = $I + GH(s)$ or $I + HG(s)$) have been considered a measure of the system stability margins for multivariable systems.[10,11,13] However, singular value norms of a system can be overly conservative, and a control system designer could interpret the results as unsatisfactory when, in fact, the system is robust.[12] A method for relieving the excessive conservatism is derived by structuring the uncertainties.[10,11]

To evaluate the stability robustness of a multivariable system, the Dryden Flight Research Center conducted a series of flight test maneuvers on the X-29A No 2.[14] The flight singular value technique was compared with predicted unscaled singular values (σ_{USV}), structured singular values (σ_{SSV}), and with the conventional single-loop stability margins. Although flight singular values were determined postflight, this analysis can be used for near real-time monitoring and safety testing.

As the minimum singular value ($\underline{\sigma}$) of the input or output RDM approaches zero, the system becomes increasingly less stable. The flight singular values need to be determined by using frequency response techniques. A complex frequency response of a system can be estimated from the auto spectrum and cross spectrum of the input and output time history variables by transforming these time domain responses to the frequency

domain using the FFT. The controller input-to-output transfer matrix, $\mathbf{X}_u(s)$ is defined as follows

$$\mathbf{X}_u(s)_{ij} = \sum_{k=1}^{N} \left(S_{x_j u_i}(s) \right)_k \left(S_{u_i u_i}(s) \right)_k^{-1} \qquad (12.2)$$

where $S_{xu}(s)$ is the cross spectrum of the input u and output x, $S_{uu}(s)$ is the auto spectrum of the input, and N is the number of time history arrays.

Using the relationship defined in eq. (12.2), the open-loop gain matrix is

$$\mathbf{HG}(s) = \mathbf{X}_u(s)\,(\mathbf{I}-\mathbf{X}_u(s))^{-1} \qquad (12.3)$$

Figure 6 shows the flight-determined minimum singular values, $\sigma[\mathbf{I} + \mathbf{HG}(s)]$, as well as analytical scaled structured and unscaled structured singular values. This plot shows that good agreement exists between the flight and analytical data. The analytical σ_{SSV} tend to agree slightly better with the flight data than with the analytical σ_{USV}.

For comparison purposes, the classical single-loop frequency response results (SISO) are shown in the table below along with the singular value (MIMO) analysis. These MIMO margins were obtained using the universal phase and gain relationship.[15] The MIMO analysis allows for simultaneous independent variations, while the SISO analysis allows for single-loop variation.

The minimum stability margin determined by the SISO method is 13 dB and 62°; whereas the flight singular value (MIMO) method resulted in a margin of 11.5 dB and 41°. As expected, the singular value method is conservative, but the results between the SISO and MIMO methods are similar. This is not surprising at this low-AOA condition since the X-29A lateral axis is largely uncoupled from the directional axis.

Extracting multiloop singular values from flight data and comparing the information with prediction validates the use of flight singular values as a relative measure of robustness. This comparison increases the confidence in using structured singular values for stability assessments of multiloop control systems. In addition, this technique extends the single-loop gain and phase margin concepts to multiloop systems.

4.3 Control Law Modifications

Several changes in the flight control system were required as a result of the high level of instability of the X-29A. A significant change was made to the air data selection logic. The initial control laws used three equally weighted sources (a single noseboom and two side probes) for total pressure measurements. The most accurate source, the noseboom measurement, was almost never used by the flight control system since it was usually an extreme, not the middle value. To compensate, a change was made to use the noseboom as long as it was within the failure tolerance of the middle value. This change came back to haunt the test team as the failure tolerance was very large and it was discovered that a within-tolerance failure could

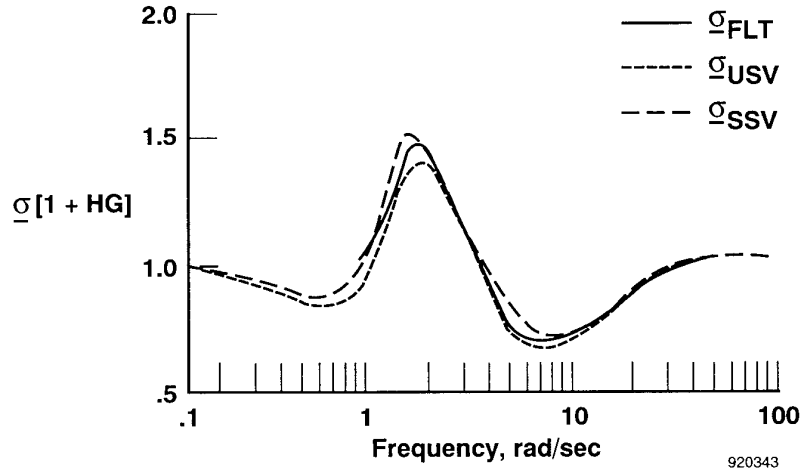

Figure 6. Flight and predicted minimum singular values of X-29A at Mach 0.7, 30,000-ft altitude, with baseline gain set.

Comparison of SISO and MIMO lateral–directional stability margins at Mach 0.7 and 30,000-ft altitude.

	Multiple-input–multiple-output			Single-input–single-output	
	σ_{USV}	σ_{SSV}	σ_{FLT}	Lateral	Directional
$\underline{\sigma}$	0.65	0.72	0.72		
Gain margin, dB	8.5	11.5	11.5	18	13
frequency, rad/sec	8	8	8	17	13
Phase margin, deg	35	41	41	77	62
frequency, rad/sec	8	8	8	2.5	4.5

result in such large changes in feedback gains that the longitudinal control system was no longer stable.

The flight data showed that reducing the tolerance to an acceptable level (going from 5.0 to 0.5 inHg) would not work as there was a narrow band in AOA from 7° to 12° where errors on the side probe measurements were as large as –1.5 inHg (airplane really faster than indicated). This large error was caused by strong forebody vortices which enveloped one or both of the air data probes located on the sides of the fuselage. The solution was a 2.0-inHg tolerance and a bias of 1.5 inHg added to the side probe measurements. This worked since the sensitivity to the high gain condition (airplane faster than indicated) was much greater than that of the low gain condition (airplane slower than indicated). The airplane had been operated for almost three years before this problem was identified and fixed.

The high level of static instability of the X-29A caused the control law designers to stress robustness over handing qualities. During flight test the aircraft models were refined, which allowed the control system to be fine tuned to improve the handling qualities.[6] To keep it simple, there was a strong desire to fine tune the control system without drastic changes in the system architecture. The process used to provide improved handing qualities involved four steps: selection of design goals, selection of design variables, translation of the design goals into a cost function, and iterative reduction of the cost function.

The Neal–Smith analysis provided a good quantitative method for assessing predictions of handling qualities. Unlike lower order equivalent system analysis, the Neal–Smith technique applies to systems that do not exhibit classical second-order behavior. In addition, there is no ambiguity introduced by the goodness of fit of the higher order system to a low-order match. The Neal–Smith method takes the longitudinal stick position to pitch rate (or attitude) transfer function, and closes the loop around it with a simple compensator, representative of a simple pilot's transfer function. The compensator consists of a lead–lag filter with a gain and a time delay (fig. 7). The application of the Neal–Smith criterion to the X-29A baseline control laws indicated a relatively large amount of lead required of the compensator to obtain the desired tracking performance. This correlated well with the pilot's comments which indicated a desire for increased pitch responsiveness in tracking tasks.

The design goals were to obtain quicker pitch response without adversely affecting the stability, control surface activity, or introducing a pilot induced oscillation problem. The point defined as the desired Neal–Smith criterion was nominally 0 dB and 10° (fig. 8). A real scalar cost function (CF) was defined as follows

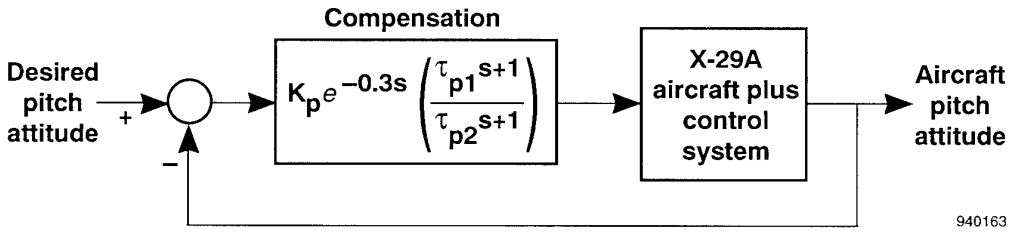

Figure 7. Closed-loop pitch attitude tracking task.

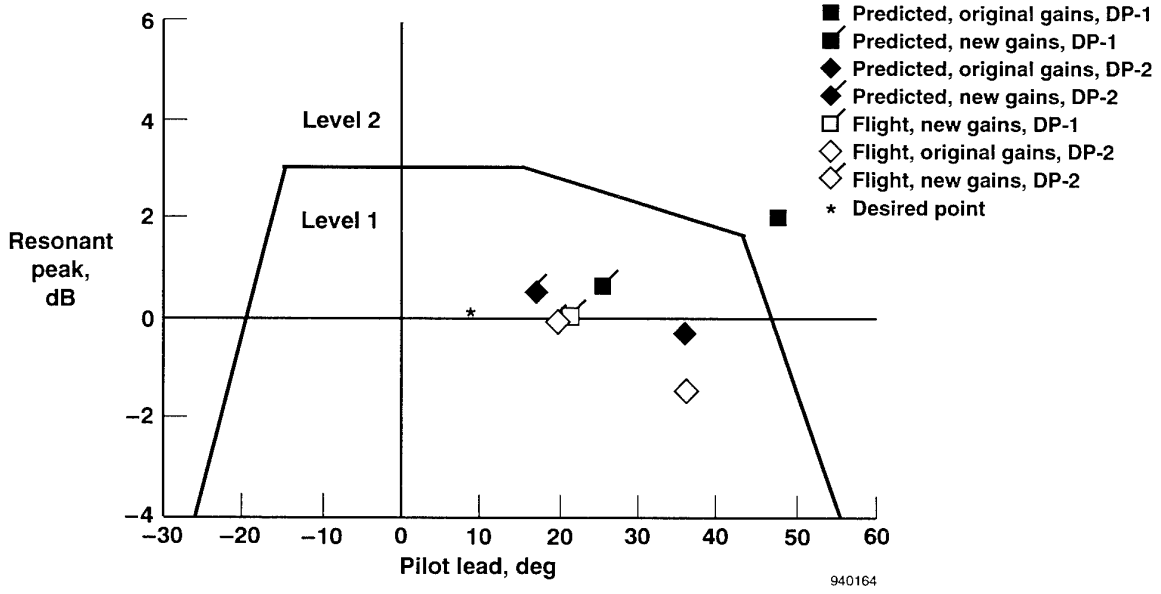

Figure 8. Neal–Smith analysis comparing the modified gains with the original gains for predicted and flight test results. (NOTE: DP represents design point.)

$$CF = RPE + PCE/SF + CP \qquad (12.4)$$

where the resonant peak error (RPE) is the distance between the achieved resonant peak and desired peak (0 dB). The pilot compensation error (PCE) is the distance between the achieved pilot compensation and the desired compensation (10°). The constraint penalty (CP) is 10,000 if either the stability margin or surface activity constraints were violated, and 0 otherwise. The scale factor (SF) is 7.0, which is commonly used to compensate for the difference in magnitude of the units of decibels and degrees.

Reference 6 covers the background and details of the improved handling qualities optimization of the X-29A airplane. The design goal of 10° of lead and 0 dB resonant peak was not achieved because of the design constraints; however, the amount of pilot lead was reduced by approximately 50 percent. The closed-loop resonant peak achieved by the modified gains was below 1.0 dB. This resulted in Neal–Smith criterion which was well within the level 1 region of the Neal–Smith plane. The design process showed a definite trade-off between the constraints and the achievable Neal–Smith criterion. The modified design gains showed a slightly reduced level of stability margin and increased surface activity. In general, the pilot comments indicated a marked improvement in the performance of the new FCS software.

This design methodology provided a practical means for improving the handling qualities of the vehicle without excessive system redesign. The method provided a 100-percent increase in the pitch acceleration (from 16°/sec^2 to 32°/sec^2) with precise control. The final design for the X-29A exhibited a problem associated with rate limiting which resulted in a lower phase margin than predicted. Fortunately the rate limiting problem occurred at frequencies higher than the range used by a pilot in handling qualities tasks.

5. HIGH-ANGLE-OF-ATTACK RESEARCH

Research at high AOA was the focus of all flight testing on X-29A No. 2. The control laws were modified for high AOA and several airplane modifications were made to assure that the program could be conducted safely. The flight tests were conducted to discover the AOA limits of maneuvering flight (which had been predicted to be up to 40° AOA) and symmetric pitch pointing flight (which was predicted to be as great as 70° AOA). The initial control laws were designed conservatively with provisions made for improvements if the flight data indicated that additional performance would not compromise stability.

5.1 Description of the Flight Control System

The control laws were designed to allow "feet-on-the-floor" maneuvering with the lateral stick commanding stability axis roll rate and the longitudinal stick commanding a blended combination of pitch rate, normal acceleration, and AOA. Rudder pedals commanded washed out stability axis yaw rate which allowed the airplane to be rolled using the strong dihedral of the airplane at up to 40° AOA.

This approach for controlling a blend of pitch rate and AOA at high AOA is different from the design philosophy of the F-18 High Alpha Research Vehicle and X-31 Enhanced Fighter Maneuverability airplanes which are primarily AOA command systems. The blended combination of feedbacks used in the X-29A FCS provided more of an $\dot{\alpha}$-type command system with weak AOA feedback. The pitch axis trim schedule provided small positive stick forces at 1-g high-AOA conditions (approximately 1-in. deflection or 8-lb force required to hold 40° AOA).

The high-AOA FCS was designed using conventional techniques combined with the X-29A nonlinear batch and real-time simulations. Linear analysis was used to examine stability margins and generate time histories which were compared with the nonlinear simulation results to validate the results. The linear analysis included conventional Bode stability margins, time history responses, and limited structured singular value analysis in the lateral–directional axes. In the pitch axis stability margins at high-AOA conditions were predicted to be higher than the stability margins at the equivalent low-AOA conditions. However, in the lateral–directional axes the unstable wing rock above 35° AOA dominated the response in linear and nonlinear analysis. Feedback gains which could stabilize the linear airplane models showed an unstable response in the nonlinear simulation driven by rate saturation of the ailerons. The control system design kept the feedback gains at a reasonable level and allowed the low-frequency unstable lateral–directional response.

5.1.1 *Design goals*

The FCS design was required to retain the low-AOA flight characteristics and control law structure which had been previously flown on X-29A No. 1. It was further required that the control system ensure that spins would not be easily entered, which required an active spin prevention system.

In the lateral axes the airplane was controlled with conventional ailerons and rudder. The ailerons had priority over symmetric flaperon deflections in the control laws. The control laws were designed in this manner since all roll control was provided by the ailerons and pitch control was provided by canards, strake flaps, and symmetric flaperons.

5.1.2 *Design of the longitudinal axis*

For the most part, the basic low-AOA X-29A normal digital longitudinal axis control laws remained unchanged at high AOA. No gains in the longitudinal axis were scheduled with AOA, but several feedback paths were switched in and out as a function of AOA. The following changes (which are highlighted in fig. 3) were made in the design of the high-AOA control laws for the X-29A longitudinal axis:

1. Modified ACC schedules which were designed to provide optimum lift-to-drag ratio canard and strake positioning at high AOA. This provides increased maximum attainable lift and reduced transonic canard loads.

2. Fade-out of velocity feedback and fade-in of AOA feedback to control a slow divergent instability. Velocity feedback was not appropriate to control the instability which developed at high AOA; AOA provided the best feedback as the divergence was almost purely AOA.

3. Active negative AOA- and g-limiters designed to prevent nose-down pitch tumble entries and potential inverted hung stall problems.

4. Fade-out of single-string attitude–heading reference system feedbacks. The attitude information only provided gravity compensation for pilot inputs and n_z feedback. The single-string nature and relatively small benefit did not warrant the risk of system failure at high AOA conditions.

5. Symmetric flaperon limit reduction from 25° to 21°. Because high-gain roll rate feedback would be required to prevent wing rock and because the wing flaperons are shared symmetrically and asymmetrically, 4° of flaperon deflection were reserved for aileron type commands. The flaperons are commanded with differential commands having priority. At high AOA the ACC schedule would otherwise command the wing flaperons on the symmetric limit and result in a coupling of the wing rock and longitudinal control loop through the symmetric flaperon.

During the accelerated entry high-AOA envelope expansion, the aft stick authority limit was reached earlier than expected (at 25° AOA full aft stick was reached for 160 and 200 knots). The original high-AOA FCS was limited, as were all previous X-29A FCS releases, to 5.4 incremental g command at high speed and 1.0 incremental g at low speed. The FCS modification increased this to 7.0 (+30 percent) incremental g command at high speed and 2.0 (+100 percent) g at low speed.

A functional check flight of the FCS change showed that although the stick sensitivity was changed it was still acceptable (since stick feel characteristics were unchanged, any change in command authority changes stick force per g). The X-29A pilots noted that during 1-g flight at 35° and 40° AOA "... the increased sensitivity of the longitudinal control was evident, but compensation by the pilot was easily accomplished."

5.1.3 *Design of the roll–yaw axes*

In the lateral–directional axes the control laws were changed significantly at high AOA from the original low-AOA control system. The lateral–directional block diagram (fig. 4) shows a full-state type feedback structure. The high-AOA changes, for the most part, were simplifications in the control law structure flown on X-29A No. 1. The new control laws required many gains to be scheduled with AOA; several were just faded to constants while four command and feedback gains used three AOA breakpoints for table lookup. These three AOA breakpoints were the maximum allowed because of computer space limitations. Computer speed limitations required that a multirate gain lookup structure be incorporated since AOA (20 Hz) was expected to change more rapidly than Mach number or altitude (2.5 Hz). The control law changes and reasons for them include the following:

1. The forward-loop integrator in the lateral axis was removed at high AOA. This eliminated a problem with the integrator saturating and causing a pro-spin flaperon command.

2. Most lateral–directional feedbacks were eliminated. This left only high-gain roll rate feedback-to-aileron and washed-out stability axis yaw rate feedback-to-rudder. The high-gain roll damper was used to suppress the wing rock which developed near $C_{L_{max}}$. The washed-out stability axis yaw rate or $\dot{\beta}$ feedback helped control sideslip during airplane maneuvers at high-AOA conditions.

3. Pilot forward-loop gains were also simplified, leaving only lateral stick-to-aileron, lateral stick-to-rudder, and rudder pedal-to-rudder. The lateral stick gearing was changed from second-order nonlinear gearing to linear gearing at high AOA and a wash-out filter was used in parallel with the ARI gain to provide an extra initial kick on rudder command.

4. Spin prevention logic was added which commanded up to full rudder and aileron deflection if yaw rate exceeded 30°/sec with AOA ≥40° for upright spins and AOA ≤–25° for inverted spins. The pilot command gain was increased to allow the pilot sufficient authority to override any of these automatic inputs.

At high AOA, vertical fin buffeting was encountered because of forebody vortex interaction. The control system was strongly affected through the excitation of several structural modes which were seen on the roll rate gyro signal. The buffet intensity was as high as 110 g at the tip of the vertical fin.

The vertical fin excited the roll rate gyro and through high-gain feedback, caused the flaperon actuators to attempt to track this high-frequency signal. Flight tests showed an unexpected hydraulic system problem resulted from this flaperon command. During a 360°-full stick aileron roll, the left outboard flaperon (LOF) hydraulic logic indicator showed a failure of the control logic for this actuator. The most probable explanation was that a flow restriction existed in the hydraulic lines driving the LOF and that this restriction showed up when large, high-frequency demands were placed on the actuator. Postflight analysis also showed that the measured LOF rates were approximately 7° to 8°/sec lower than for the right outboard flaperon.

Since the roll rate gyro signal did not originally use any structural notch filters, the vertical fin first bending (15.8 Hz), wing bending antisymmetric (13.2 Hz), and fuselage lateral bending (11.1 Hz) structural modes showed up in the commands to the ailerons. Figure 9 shows the response of the roll rate gyro. The figure shows that most of the vertical tail buffet is transferred to the roll rate gyro through the vertical fin first bending mode. Analysis of the flight data showed that the g level increased proportionately with dynamic pressure.

Notch filters and a software gain reduction on roll rate feedback were used as the long-term FCS solution to the problem. Before these changes, fifty percent of the maneuvers in the region of failures indicated LOF hydraulic logic failures. After the changes were made, these failure conditions occurred only rarely and even more severe entry conditions and higher buffet levels were encountered without incident.

5.1.4 *Other changes*

To aid in research and to allow for unknown problems in flight testing, several additional changes were made to the control system. These changes included a dial-a-gain capability to allow the roll rate-to-aileron and the ARI gains to be independently varied (K2/K27). These two gains can each have five different values.

Concerns about the severe wing rock had led to a slow build-up in AOA using the dial-a-gain variations. The airplane roll response was found to be heavily damped and the dial-a-gain system was used to examine reductions in feedback gain. The response of the airplane was significantly quicker (approximately 20 percent) with the reduced roll rate feedback-to-aileron gain. No objectionable wing rock developed because of the lower gain.

Wing rock was predicted to be a major problem with the X-29A configuration at high AOA. These predictions had been made based upon wind-tunnel[16,17] estimates and supported by drop model flight tests.[18] Early simulation predictions were that wing rock would effectively limit the useful high-AOA envelope to approximately 35° AOA. Wing rock was predicted to

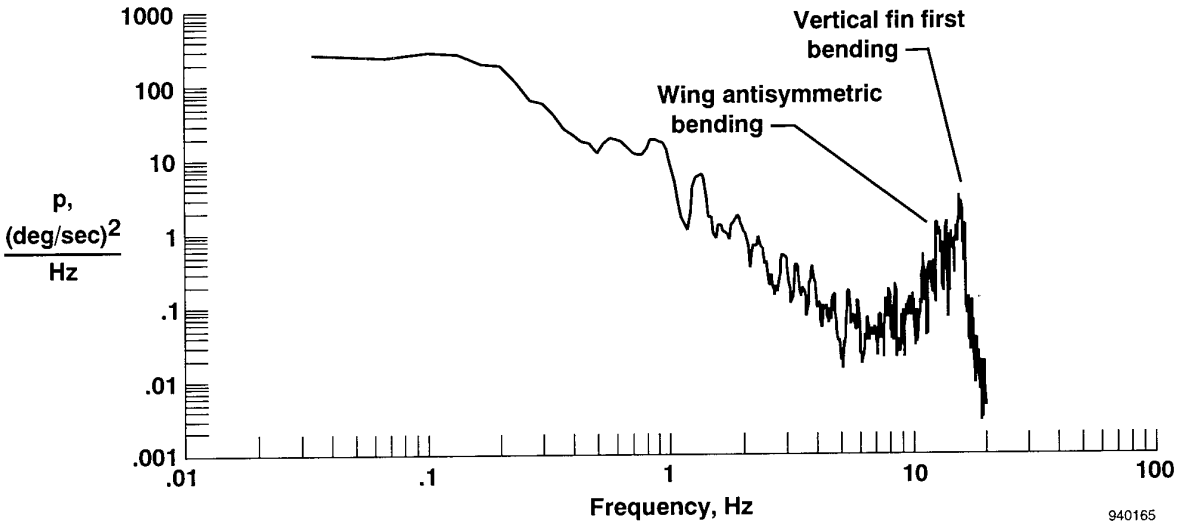

Figure 9. Roll rate gyro power spectral density.

deteriorate quickly as the roll damping became unstable and the limited aileron control power was insufficient to stop it. Roll rate-to-aileron gains as high as 2.0 deg/deg/sec were required to damp wing rock and prevent roll departures on the NASA Langley Research Center X-29A drop model. Flight tests with the dial-a-gain system showed that the K2 (roll rate-to-aileron) gain could be reduced from the initial maximum value of 0.6 to 0.48 deg/deg/sec with no significant wing rock. Decreases of this gain were required to assure that a rate limit driven instability in the ailerons at high dynamic pressures would not occur.

The second use of dial-a-gain was to increase the roll performance of the X-29A at high-AOA conditions. The stability axis roll rates were almost doubled in the AOA region from 20° to 30° at 200 knots (from 40°/sec to 70°/sec) with only small degradation in the roll coordination. Above this AOA, uncommanded reversals were seen because of control surface saturation and corresponding lack of coordination (predominantly increased sideslip). This performance improvement was accomplished with a 75-percent increase in the K13 (lateral stick-to-aileron) gain and an 80-percent increase in the K27 (lateral stick-to-rudder) gain. Increases in rates were possible throughout much of the high AOA envelope, but usually not as dramatic as this example. The dial-a-gain concept proved a valuable research tool used to test simple control law changes before the full FCS changes were made.

5.1.5 *Air data system*

Air data issues were addressed early in the development of the high AOA control laws. Measurement of accurate AOA was very important as this would be a primary gain scheduling parameter as well as a feedback to longitudinal and lateral–directional axes. Accurate air data were also important because of conditional stability of the lateral and longitudinal axes at high AOA. Stability margins would be compromised if air data errors were large.

Two of the three AOA sensors, located on each side of the airplane, had a range limited to 35°. The location and range were considered inadequate and two options were considered to solve the problem. The first option, to mount two additional AOA vanes on the noseboom, was mechanized and flown on X-29A No. 1 for evaluation and found to have excellent characteristics. The second option was to install NACA booms and AOA vanes on the wingtips. This option would have resulted in additional problems as the FCS did not rate correct its AOA measurements. With large lateral offsets, roll rate corrections would have to have been included which would have made AOA measurements sensitive to airspeed measurement errors. In the end, simplicity drove the decision to install two additional AOA vanes on the noseboom.

The second issue concerned accurate measurement of airspeed at high-AOA conditions caused by local flow effects. Several unsuccessful alternate pitot probe locations were investigated. Belly probes were tested on a wind-tunnel model and were found to change the aerodynamics, while swivel probes proved unable to be flight qualified for installation forward of engine inlets on a single-engine airplane. Since an alternate location could not be found, and the side probes were expected to have poor high-AOA characteristics, the decision was made to use a single string noseboom pitot-static probe at high AOA.

The high-AOA control system design had to be highly reliable. In general, multiple (three or more) sensors were used to provide redundancy, but for impact pressure at high AOA the FCS relied on a single noseboom probe with two independent sensors.

The air data system was carefully monitored during the high-AOA expansion. Differences between the noseboom and side probes were tracked as a function of AOA and compared with redundancy management trip levels (which were 1.5 inHg for static pressure, 2.0 inHg for total pressure, and 5.0° for AOA). Predictions about the air data system made during the FCS design were found to be pessimistic because the system worked better than expected. With the exception of the known problem with the total pressure measurements in the 7°- to 12°-AOA region, the maximum error at all other conditions was less than 0.5 inHg. In hindsight the flight data showed that the side probes performed adequately for FCS gain scheduling purposes and the system did not need to be made single string on the noseboom probe.

One in-flight incident occurred because of the air data system. Figure 10 shows the time history of a recovery maneuver. The figure shows that as sideslip exceeded 20°, the left rear AOA vane exceeded the sensor tolerance and was declared failed. This incident occurred during a recovery from 50° AOA. The airplane continued to operate on the two remaining sensors and was in no danger. Once the failure was known, the personnel in the control room were able to examine the individual AOA channels and discover that all vanes appeared to be functioning properly.

5.2 Envelope Expansion Technique

To increase the rate of envelope expansion, an incremental simulation validation technique[19] from the F-14 high-AOA ARI test program was refined and used. This analysis technique was used for postflight comparisons and model updating. It allowed the simulation aerodynamic model to be updated between flight days with local improvements, e.g., changes to lateral control power, derived from previous test points. This allowed the pilots to train with a simulation which matched the most important aerodynamic characteristics and provided engineers with a method to track the aerodynamic differences which were discovered in flight test. The magnitudes and types of changes to the aerodynamic model provided assurance that the airplane could be safely flown to the next higher AOA test point.

The updated aerodynamics were applied primarily in the lateral–directional axes as almost no changes were required in the longitudinal axis. The updates were constructed with mostly linear terms, but some local nonlinearities were also included.

The most important characteristics to match were the magnitude, frequency, and phase relationships of the airplane response. At first, attempts were made to use all six degrees-of-freedom in the simulation, but longitudinal trim differences caused the simulation to diverge from the flight measurements before the maneuver was complete. Since the lateral–directional dynamics were of primary importance, the longitudinal dynamics were separated from them. The simulation matching technique then used the measured longitudinal parameters and lateral–directional pilot stick and rudder pedal measurements as inputs to the batch simulation. This forced the airspeed, altitude, canard deflection, and AOA to track the flight measurements while allowing the lateral–directional axes complete freedom. Some work was also accomplished using an alternate technique which bypassed the control system and used the measured aileron and rudder as inputs, but the wing rock instability eventually made this too difficult. Without including the control system in the simulation the system is an unstable process, since the flight control system stabilizes the wing rock.

Several techniques were used to determine the aerodynamic model updates which would be made to the simulation model.[20] These updates were maintained in a separate aerodynamic delta math model which allowed quick and easy modification. Once the aerodynamic models were updated, sensitivity studies on the real-time simulation were used to predict the airplane response at the next flight test expansion points.

5.3 Pitch Rate Limitations

An example comparison of a full-stick pitch axis maneuver with the complete six degree-of-freedom baseline simulation is shown in figure 11. The flight maneuver required the pilot to trim the airplane in level flight at 10° AOA at 20,000-ft altitude (approximately 0.3 Mach). The simulation was matched to the initial trim condition and then driven with the pilot stick and throttle inputs. The figure shows close agreement between the flight data and simulation which allows a high confidence to be placed on simulation analysis of the X-29 pitch rate capability.

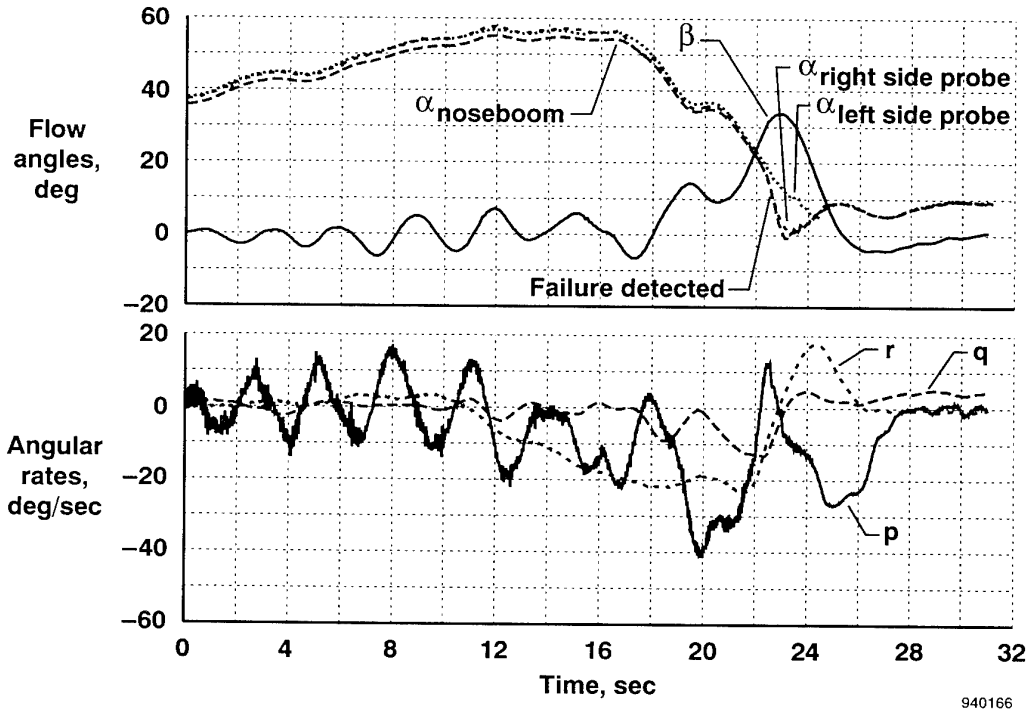

Figure 10. Angle-of-attack redundancy management failure from flight 27—time histories.

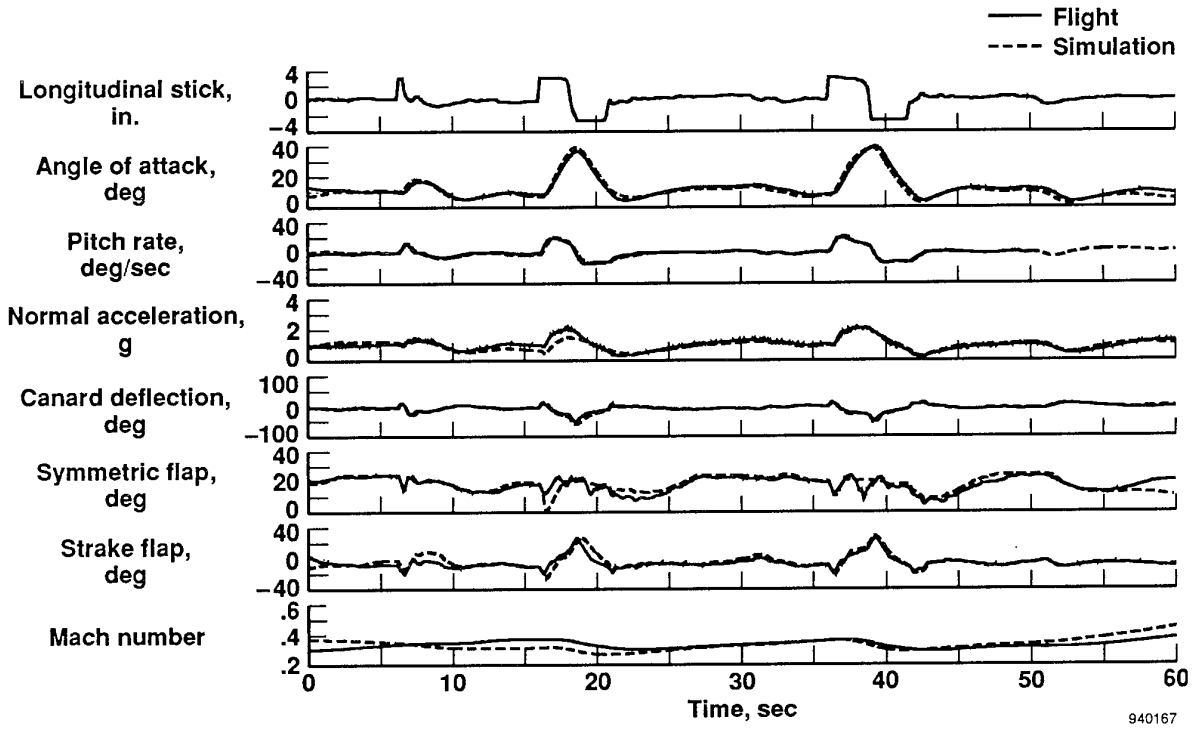

Figure 11. X-29 No. 2 flight/simulation comparison for large amplitude stick maneuver. Flight control software was the final high-AOA software.

The X-29 pilots consistently found the maximum pitch rate capability of the airplane inadequate. Figure 12 shows the predicted maximum nose up and nose down pitch rates of the X-29 as a function of Mach number (altitude varied from 10,000 to 20,000 ft). F-18 pitch rate data are included for comparison purposes. The simulation maneuvers consisted of two types of maneuvers: a full aft stick step input and a doublet type input which consisted of a full aft stick input followed by a full forward stick input timed to try to force the control surfaces to maximum rates.

It is clear from the data that the X-29 requires approximately 50 percent higher rates to be comparable with an F-18 at low-speed conditions. Examination of the peak canard actuator rates shows that the X-29 was using nearly all of the capability (104°/sec no load rate limit) with the current control system gains. Increases in the canard actuator rates commensurate with the increases in pitch rate would be required for any improvement.

The simulation showed that most of the actuator rate was used in controlling the unstable airplane response. Figure 11 shows this in detail. Close examination of the canard response shows that during the full aft stick input the initial response of the canard is trailing edge down (and trailing edge up for the flaperon and strake flap). As is typical for an unstable pitch response the surfaces then move quickly in the opposite direction to unload and control the unstable response. The second motion is typically much larger than the initial motion and in most cases is more demanding of the actuator rates especially at low dynamic pressure where large control surface motion is required. This prediction of canard rate requirements agrees very well with data presented in reference 4.

6. CONCLUSIONS

The X-29A airplanes were evaluated over the full design envelope. The flight control system successfully performed the tasks of stabilizing the short-period mode and providing automatic camber control to minimize trim drag. Compared with other highly augmented, digital fly-by-wire airplanes, the X-29A and its flight control system proved remarkably trouble free. Despite the unusually large, negative static margin, the X-29A proved safe to operate within the design envelope. Flight test showed the following lessons:

- Adequate stability to successfully test a 35-percent statically unstable airframe was demonstrated over the entire envelope in a *flight test research environment.* Extrapolations to a production–operational environment should be made carefully.
- The level of static instability and control surface rate limits did impact the nose up and nose down maximum pitch rates. At low airspeeds, to achieve rates comparable with an F-18, new actuators with at least 50-percent higher rate are required.
- Testability of a flight control system on an airplane with this level of instability is important and big payoffs can be made if provisions are made for real-time capabilities.

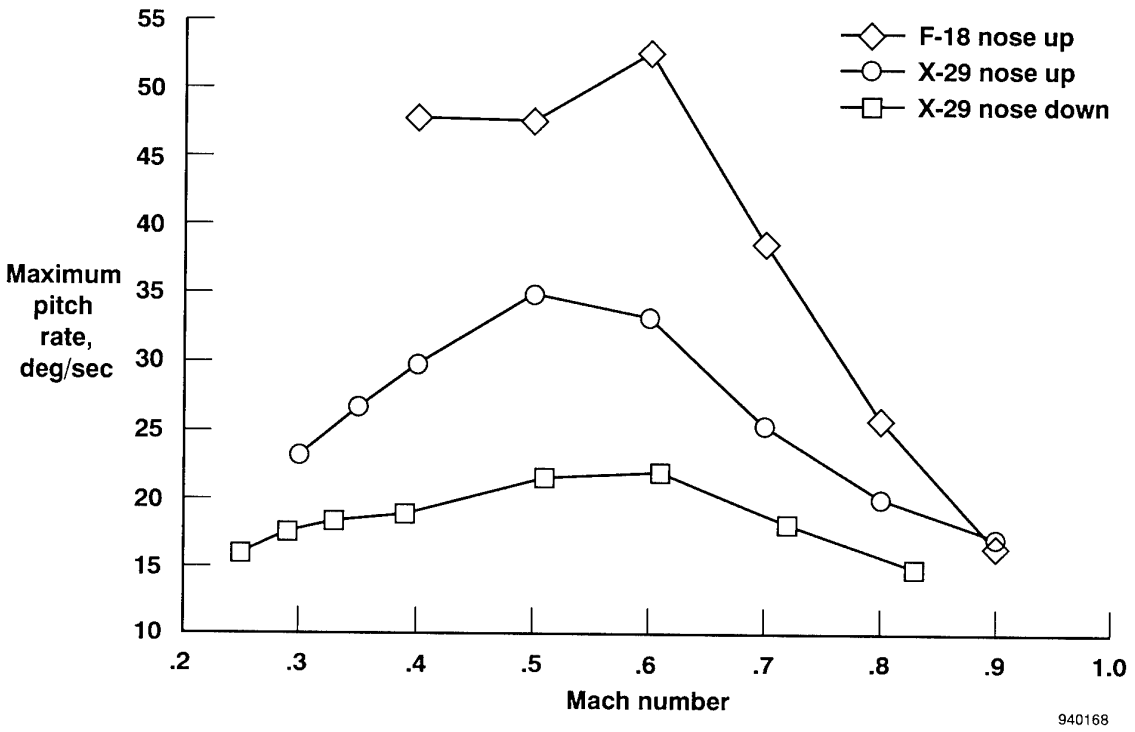

Figure 12. X-29 nose up and nose down pitch rate capability using final high-AOA flight control software.

- Air data are critical for highly unstable airframes and extra analysis is required to ensure adequate stability. Typical fighter type airplane air data redundancy management tolerances do not apply. Tight tolerances must be used even at the risk of nuisance failure detection.
- The dial-a-gain concept proved a valuable aid to evaluate subtle predicted differences in flying qualities through back-to-back tests. It was also useful to flight test proposed gain adjustments before major flight control system gain changes were made. This concept might not be easily applied to full state feedback designs, but forward-loop gains are good candidates for this use in any design.
- High angle of attack with high feedback gains will create problems with structural modes and require notch filters to eliminate flight control system response.

7. REFERENCES

1. Krone, N.J., Jr., "Forward Swept Wing Flight Demonstrator," AIAA Paper No. 80-1882, Aug. 1980.
2. Spacht, G., "The Forward Swept Wing: A Unique Design Challenge," AIAA Paper No. 80-1885, Aug. 1980.
3. Whitaker, A. and Chin, J., "X-29 Digital Flight Control System Design," AGARD CP-384: *Active Control Systems—Review, Evaluation and Projections*, Oct. 1984.
4. Chin, J., H. Berman, and J. Ellinwood, "X-29A Flight Control System Design Experiences," AIAA Paper No. 82-1538, Aug. 1982.
5. Gera, J., J.T. Bosworth, and T.H. Cox, *X-29A Flight Test Techniques and Results: Flight Controls*, NASA TP-3121, 1991.
6. Bosworth, John T. and Timothy H. Cox, *A Design Procedure for the Handling Qualities Optimization of the X-29A Aircraft*, NASA TM-4142, 1989.
7. Chacon, Vince and David McBride, *Operational Viewpoint of the X-29A Digital Flight Control System*, NASA TM-100434, 1988.
8. Bosworth, John T., *Flight-Determined Longitudinal Stability Characteristics of the X-29A Airplane Using Frequency Response Techniques*, NASA TM-4122, 1989.
9. Bauer, Jeffrey E., David B. Crawford, and Domenick Andrisani, "Real-Time Comparison of X-29A Flight Data and Simulations Data," AIAA Paper No. 87-0344, Jan. 1987; see also *J. Aircraft*, vol. 26, no. 2, Feb. 1989, pp. 117–123.
10. Doyle, John C. and Gunter Stein, "Multivariable Feedback Design: Concepts for a Classical/Modern Synthesis," *IEEE Transactions on Automatic Control*, vol. AC-26, no. 1, Feb. 1981, pp. 4–16.
11. Ly, Uy-Loi, "Robustness Analysis of a Multiloop Flight Control System," AIAA Paper No. 83-2189, Aug. 1983.
12. Paduano, James D. and David R. Downing, *Application of a Sensitivity Analysis Technique to High-Order Digital Flight Control Systems*, NASA CR-179429, 1987.
13. Newsom J.R. and V. Mukhopadhyay, "A Multiloop Robust Controller Design Study Using Singular Value

Gradients," *J. Guidance, Control, and Dynamics*, vol. 8, no. 4, July–Aug. 1985, pp. 514–519.

14. Burken, John J., *Flight-Determined Stability Analysis of Multiple-Input–Multiple-Output Control Systems*, NASA TM-4416, 1992.

15. Mukhopadhyay, V. and J.R. Newsom, "A Multiloop System Stability Margin Study Using Matrix Singular Values," *J. Guidance, Control and Dynamics*, vol. 7, no. 5, Sept.–Oct. 1984, pp. 582–587.

16. Croom, Mark A., Raymond D. Whipple, Daniel G. Murri, Sue B. Grafton, and David J. Fratello, "High-Alpha Flight Dynamics Research On The X-29 Configuration Using Dynamic Model Test Techniques," SAE Paper No. 881420, Oct. 1988.

17. Murri, Daniel G., Luat T. Nguyen, and Sue B. Grafton, *Wind-Tunnel Free-Flight Investigation of a Model of a Forward-Swept-Wing Fighter Configuration*, NASA TP-2230, 1984.

18. Fratello, David J., Mark A. Croom, Luat T. Nguyen, and Christopher S. Domack, "Use of the Updated NASA Langley Radio-Controlled Drop-Model Technique for High-Alpha Studies of the X-29A Configuration," AIAA Paper No. 87-2559, Aug. 1987.

19. Gera, J., R.J. Wilson, E.K. Enevoldson, and L.T. Nguyen, "Flight Test Experience With High-α Control System Techniques on the F-14 Airplane," AIAA Paper No. 81-2505, Nov. 1981.

20. Pellicano, Paul, Joseph Krumenacker, and David Vanhoy, "X-29 High Angle-of-Attack Flight Test Procedures, Results, and Lessons Learned," SFTE 21st Annual Symposium, Garden Grove, CA, Aug. 1990.

ADVANCED GUST MANAGEMENT SYSTEMS

– Lessons Learned and Perspectives –

R. König, K.-U. Hahn
DLR – Institute of Flight Mechanics, Braunschweig, FRG

J. Winter
Senior Flight Control Eng.
Dept. EV42, DORNIER Luftfahrt GmbH
D-88039 FRIEDRICHSHAFEN, GERMANY

SUMMARY

Aircraft operations at low altitudes often are affected by strong gusts and turbulence producing additional aerodynamic forces and moments. This results in extra aircraft accelerations and therefore in an unpleasant impact on passenger comfort and pilot workload as well as in extra structural loads. Active Control Technology is able to suppress these effects partly. The knowledge about the potential for improvement, the parameters of influence and the performance requirements for such gust alleviation systems is still quite small.

Since the mid-seventies Dornier and DLR (Institute of Flight Mechanics) have been working together on BMFT programs developing systems to improve the ride quality in gusty weather. The developed **O**pen-**L**oop **G**ust **A**lleviation System OLGA was investigated through dynamic wind tunnel experiments and flight-tested onboard the experimental aircraft Do 128 TNT. This research was continued by DLR developing the **L**oad **A**lleviation and **R**ide **S**moothing System LARS using the modified VFW 614 aircraft ATTAS (**A**dvanced **T**echnologies **T**esting **A**ircraft **S**ystem, Fig 1). The Deutsche Aerospace Dornier Luftfahrt GmbH has concentrated on simulation studies for their aircraft types Do 228 and Do 328.

The presented paper provides a brief description of the advantages of overall gust management systems considering lift, drag and pitch control. The following topics will be presented in detail:

- The basic flight mechanics of gust load alleviation.
- The design of integrated gust management systems.
- Simulation and flight test results.
- Lessons learned and general perspectives.

LIST OF SYMBOLS, INDICES AND ABBREVIATIONS

a	acceleration
$\underline{A}, \underline{B}, \underline{C}, \underline{D}$	matrices of a state space quadruple
C_D	drag coefficient
C_L	lift coefficient
$C_{L\alpha}$	lift coefficient gradient
D	drag
g	gravitational acceleration
H	height
i	counter
k	factor (Lilienthal polar)
K	gain coefficient
L	Lift
L_W	charcteristic wavelength
M	moment
Mb	wing bending moment
n_P	RPM of engine
n_x	longitudinal load factor
n_z	normal load factor
q	pitch rate
S	power density
S_f	flap area
T	thrust, time constant
u	input
u_{Wg}	horizontal wind component
V	airspeed
w_{Wg}	vertical wind component
W	weight
x	distance, state
x_H	position of horizontal stabiliser
x_N	aerodynamic centre of the wing
x_S	position of air data sensor
X	longitudinal force
y	geometric distance
y	output
z_α	dimensional dervative
Z	normal force
α	angle of attack
α_W	wind angle
β	propeller pitch angle
γ	flight path angle
Δ	difference
η	elevator deflection
η_{DLC}	DLC flap deflection
φ	alleviation factor
ν	acceleration distribution tilt angle
θ	pitch attitude
ρ	air density
σ	standard deviation
ω	oscillation frequency
$(\dot{\cdot})$	time derivative
$(\ddot{\cdot})$	2nd order time derivative
$(^*)$	denotes wing position
$(^{**})$	denotes horizontal stabilizer position
c	command
i	counter
r	reference
req	required
W	wind
ACT	Active Control Technology
BMFT	Bundesministerium für Forschung und Technologie
DF	Disturbance Feed Forward
DLC	Direct Lift Control
DLR	Deutsche Forschungsanstalt für Luft- und Raumfahrt
EDP	Electronic Data Processing
FADEC	Full Authority Digital Engine Controller
GMS	Gust Management System
IGLAS	Integrated Gust Load Alleviation System
LARS	Load Alleviation and Ride Smoothing System
OLGA	Open-Loop Gust Alleviation System
RPM	Revolution Per Minute
VFW	Vereinigte Flugtechnische Werke

1. INTRODUCTION

Wind disturbances, especially vertical gusts and turbulence, deteriorate passenger comfort, riding and flying qualities (Ref 1), and furthermore, they produce dynamic structural loads stressing the aircraft. A complete alleviation of gust effects requires aerodynamic counter forces of the same magnitude, at the same time, and the same location on the aircraft structure, as the gust induced forces. This cannot be performed by a real world system due to control surface limitations (deflection and rate), insufficient actuator dynamics, and time delays of measured signals and computing. Effective gust alleviation in the vertical direction can be obtained only if the wing has dedicated control surfaces for lift variation, such as direct lift control flaps (DLC), symmetrically operating ailerons, or flight spoilers.

Paper presented at the Flight Mechanics Panel Symposium held in Turin, Italy, from 9-13 May 1994.

Different approaches for gust/gust load alleviation systems have been realized. Structural mode damping systems have been developed for the Lockheed 1011 (Ref 2), C-5A and Boeing B-52H. The ride smoothing system OLGA (Ref 3) has been investigated and flight tested by Dornier and DLR (formerly: DFVLR) from 1976 to 1982. In recent years British Aerospace has demonstrated a system for peak load reduction to be used with the Airbus A320.

But nevertheless, the knowledge on the benefits of gust alleviation systems is very small. The same is true for the available data base concerning the parameters of influence and performance requirements. Based on the knowledge and the experience accumulated with OLGA the DLR Institute of Flight Mechanics and DASA Dornier continued their research on gust load alleviation systems.

2. FLIGHT MECHANICAL ASPECTS OF GUST LOAD ALLEVIATION

2.1 Rigid Body Aircraft

2.1.1 Aircraft Response to Gusts and DLC-Flap Deflection

The main effect of gusts on the aircraft response is caused by the vertical movement of the air (Ref 4) producing normal load factor variations. The aircraft response to such wind disturbances can be improved by Active Control Technology (ACT). Especially Direct Lift Control (DLC) surfaces enable a fast and defined lift variation for gust compensation. To illustrate the primary effects of gusts on a DLC augmented aircraft, a very simple approach will be derived using basic flight mechanics. Due to the fact that the effect of horizontal gusts is of second order, the horizontal wind component is neglected in the following considerations. But nevertheless a vertical gust affects not only the vertical degree of freedom. In Fig 2 the situation of a wing entering a vertical step gust is sketched. Starting from stationary horizontal flight the wing moves through the air with the reference airspeed V_r producing the reference lift L_r and the reference drag D_r. The DLC surface (in Fig 2 the DLC device is assumed as an extra flap) is not deflected.

Entering the step gust (negative upwind gust) an additional wind-angle-of-attack occurs which can be calculated

$$\alpha_W \approx -\frac{w_{Wg}}{V} \tag{1}$$

This is equivalent to an increased angle-of-attack which results in lift and drag variations $\Delta L(\alpha_W)$ and $\Delta D(\Delta L(\alpha_W))$ respectively. Consequently lift and drag are also affected by the deflection of the DLC device: $\Delta L(\eta_{DLC})$ and $\Delta D(\eta_{DLC})$. The sum of all effects is

$$L = L_r + \Delta L(\alpha_W) + \Delta L(\eta_{DLC}) \tag{2}$$

$$D = D_r + \Delta D[\Delta L(\alpha_W)] + \Delta D(\eta_{DLC}) \tag{3}$$

From Fig 2 it can be seen that not only the magnitude but also the direction of lift and drag is affected by the wind disturbance. Presuming a small wind-angle-of-attack ($\alpha_W \ll 1$) the normal and horizontal forces become

$$\Delta Z = \Delta L + D \cdot \alpha_W \tag{4}$$

$$\Delta X = -\Delta D + L \cdot \alpha_W \tag{5}$$

For small angles-of-attack the drag component in the normal direction can be neglected ($\Delta L \gg D\ \alpha_W$). Then from Equ (4) and (5) it can be assumed as a good approximation

$$\Delta n_z = \frac{\Delta L}{W} = \frac{\Delta C_L}{C_{Lr}} \tag{6}$$

$$\Delta n_x = \frac{-\Delta D + L \cdot \alpha_W}{W} = \frac{-\Delta C_D + (C_{Lr} + \Delta C_L)\cdot \alpha_W}{C_{Lr}} \tag{7}$$

with $W = L_r$. The effect of a DLC surface deflection on the normal forces becomes with Equ (2)

$$\Delta C_Z \approx \Delta C_L = \Delta C_L(\alpha_W) + \Delta C_L(\eta_{DLC}) \tag{8}$$

The variation of the lift coefficient due to an additional wind-angle-of-attack is

$$\Delta C_L(\alpha_W) = \frac{\partial C_L}{\partial \alpha} \cdot \alpha_W = C_{L\alpha} \cdot \alpha_W \tag{9}$$

From the ideal requirement of a constant lift for an undisturbed flight ($\Delta C_Z = 0$) the equilibrium of $\Delta C_L(\eta_{DLC}) = -\Delta C_L(\alpha_W)$ is to be satisfied. Due to DLC surface limitations, deflection restrictions and actuator dynamics, a full compensation of gusts will never be possible under real world conditions. This can be considered by a constant factor φ describing the magnitude of the gust compensation by the DLC device.

$$\Delta C_L(\eta_{DLC}) = -\varphi \cdot \Delta C_L(\alpha_W) \tag{10}$$

$\varphi = 0$ indicates the uncontrolled aircraft response (no gust load alleviation). For the ideal control of the lift with $\varphi = 1$, no n_Z variation will be produced by the wind disturbance. From Equ (8) and (10) the remaining lift variation acting on the aircraft equipped with an active gust alleviation system is

$$\Delta C_L = C_{L\alpha} \cdot (1 - \varphi) \cdot \alpha_W \tag{11}$$

or the corresponding vertical load factor

$$\frac{\partial \Delta n_z}{\partial \alpha_W} = \frac{C_{L\alpha}}{C_{Lr}} \cdot (1 - \varphi) \tag{12}$$

With Equ (3) or (5) the horizontal force becomes

$$\Delta C_X = -\Delta C_D(\Delta C_L) - \Delta C_D(\eta_{DLC}) + (C_{Lr} + \Delta C_L) \cdot \alpha_W \tag{13}$$

Presuming a drag coefficient increasing with the square of the lift coefficient

$$C_D = C_{D0} + k \cdot C_L^2 \tag{14}$$

results in

$$\Delta C_D(\Delta C_L) = \frac{\partial C_D}{\partial C_L} \cdot \Delta C_L = 2 \cdot k \cdot C_{Lr} \cdot \Delta C_L \tag{15}$$

The drag variation resulting from DLC flap activity is

$$\Delta C_D(\eta_{DLC}) = \frac{\partial C_D(\eta_{DLC})}{\partial C_L(\eta_{DLC})} \cdot \Delta C_L(\eta_{DLC})$$

$$= -\frac{\partial C_D(\eta_{DLC})}{\partial C_L(\eta_{DLC})} \cdot \varphi \cdot \Delta C_L(\alpha_W) \tag{16}$$

The horizontal load factor produced by a vertical gust under consideration of an active gust load alleviation system becomes with Equ (7), (10), (15) and (16) with a first order TAYLOR series

$$\frac{\partial \Delta n_x}{\partial \alpha_W} = 1 - 2 \cdot k \cdot C_{L\alpha}(1 - \varphi) + \varphi \cdot \frac{\partial C_D(\eta_{DLC})}{\partial C_L(\eta_{DLC})} \cdot \frac{C_{L\alpha}}{C_{Lr}} \tag{17}$$

In Equ (12) and (17) the meaning of the effectiveness of the gust load alleviation system described by the factor φ is significant. Fig 3 illustrates this influence. Especially in the flight regime of low airspeed the operation of a gust load alleviation system for the improvement of the vertical aircraft response stimulates the horizontal accelerations. The relation between horizontal and normal acceleration is derived from Equ (17) divided by Equ (12)

$$\frac{\Delta n_x}{\Delta n_z} = \frac{1}{1-\varphi}\cdot\frac{C_{Lr}}{C_{L\alpha}} - 2\cdot k\cdot C_{Lr} + \frac{\varphi}{1-\varphi}\cdot\frac{\partial C_D(\eta_{DLC})}{\partial C_L(\eta_{DLC})} \quad (18)$$

The better the n_z control ($\varphi \rightarrow 1$: $\Delta n_z \rightarrow 0$) the worse the n_x response. The relation between horizontal and normal load factor can also be understood as the orientation of the acceleration in the aircraft's symmetrical plane.

$$\nu \approx \tan\nu = \frac{\Delta n_x}{\Delta n_z} \quad (19)$$

Fig 4 shows the results of a complex numerical simulation (all real world effects like actuator dynamics and limitations (Ref 5), EDP processing time etc. are considered). The diagrams are true for a flight in light turbulence. The left hand diagram represents the load factor distribution of the uncontrolled aircraft. The right hand figure give the results with a gust load alleviation system designed for the ideal requirement $\Delta C_L(\eta_{DLC}) = -\Delta C_L(\alpha_W)$. Due to real system effects the resulting gust compensation factor is only $\varphi \approx 0.6$. From experience it can be said that a well designed real world gust alleviation system will reach gust compensation factors on the order of $\varphi \approx 0.4$ which was proved by flight test (see chapter 3.1.5).

Beside the recoupling effects from vertical to horizontal degree of freedom there is also an effect of vertical gusts on the pitch behaviour of aircraft. For the design of a complete gust management system, controlling all aircraft axes, for each degree of freedom an independent control surface is needed.

2.1.2 Frequency Range

The vertical load factor not only depends on the magnitude of the gusts but also on the frequency of the wind disturbance. Starting from stationary horizontal flight and using the linearized equation of motion (Ref 6) restricted for the vertical degree of freedom, the normal acceleration can be calculated from the linear differential equation

$$\partial\ddot{H} = -\frac{\left(w_{Wg} + \partial\dot{H}\right)}{V_{Kr}}\cdot z_\alpha \quad (20)$$

The dotted variables are the time derivatives of the height H, w_{Wg} is the vertical wind and V_{Kr} is the reference flight path speed. z_α is the dimensional derivative representing the angle-of-attack dependent forces.

$$z_\alpha = \frac{1}{2}\cdot\rho_r\cdot V_r^2\cdot C_{L\alpha}\cdot\frac{S_L}{m} \quad (21)$$

The application of the LAPLACE transformation on Equ (20) yields

$$F(s) = \frac{\ddot{H}(s)}{w_{Wg}(s)} = \frac{-s}{1+\frac{V_{Kr}}{z_\alpha}\cdot s} \quad (22)$$

which characterises the high-pass behaviour of the normal acceleration of an aircraft to vertical gusts. Neglecting the horizontal wind ($u_{Wg} = 0$) we get $V_{Kr} = V_r$. The characteristic time constant of the system described by Equ (21) then becomes

$$T_{\ddot{H}} = \frac{V_{Kr}}{z_\alpha} = \frac{\frac{m}{S_L}}{\frac{1}{2}\cdot\rho_r\cdot V_r\cdot C_{L\alpha}} \quad (23)$$

It only depends on aircraft parameters and the reference flight state. From the time constant the break frequency can be calculated by $\omega_{\ddot{H}} = 1/T_{\ddot{H}}$. Wind disturbance frequencies below $\omega_{\ddot{H}}$ are only of minor importance for the aircraft's normal acceleration response.

Another limiting factor for the normal acceleration of an aircraft is the structure of gusts and turbulence. It can be approached by a power density spectrum calculated from GAUSSian random noise shaped through a DRYDEN filter (Ref 7, 8)

$$S_W(\omega) = \frac{2\cdot T_W\cdot\sigma_W^2}{1+T_W^2\cdot\omega^2} \quad (24)$$

σ_W is the standard deviation of the wind and T_W is the time constant matching the low-pass characteristics of Equ (23) against the real world turbulence. Since the airspeed is much higher than the wind speed the time constant T_W can be calculated from the characteristic wavelength L_W of the atmospheric disturbances by applying the TAYLOR hypothesis

$$T_W = \frac{L_W}{V_r} \quad (25)$$

The break frequency of the wind field is again $\omega_W = 1/T_W$. Wind disturbances with frequencies higher than ω_W are of subordinate importance for the aircraft response.

The frequency domain of interest for the aircraft's rigid body motion affected by vertical gusts is between $\omega_{\ddot{H}} < \omega < \omega_W$. It is self-evident that these break frequencies depend on the actual weather situation and the aircraft to be investigated but some general statements can be made.

Gusts and turbulence mainly occur in the lower region of the atmospheric boundary layer (Ref 9). If only the takeoff climb and landing approach are considered, the altitude of interest can be supposed $H < 500$ m, where the density of the air is $\rho \approx 1$ kg/m^3. During the relevant flight phases the speed of conventional transport type aircraft only vary in a small range between 70 m/s < V < 80 m/s. This is also true for the wing loads which are 250 kg/m^2 < m/S_L < 350 kg/m^2. The lift slope coefficient normally is $5 < C_{L\alpha} < 6$. With these parameters the break frequency, from which the aircraft starts to intensify its response to gusts and turbulence, becomes with Equ (23) $f_{\ddot{H}} \approx 0.1$ Hz or $\omega \approx 0.63\,s^{-1}$ respectively. Gusty weather predominates for unstable atmospheric conditions. The characteristic wavelength for a very unstable atmosphere can be assumed in a range of 20 m < L_W < 25 m. From this wavelength and Equ (25) the break frequency of the wind field becomes $f_W \approx 0.5$ Hz or $\omega \approx 3.1\,s^{-1}$ respectively. In this frequency region of 0.1 Hz < f < 0.5 Hz strong aircraft response can be expected, which is confirmed by Fig. 5. The effect of the result shown in Fig 5 on the passenger comfort is illustrated by Fig 6 showing the percentage of airsick passengers versus frequency. From Fig 5 and 6 it can be learned, that for the design of a gust load alleviation system operating on conventional transport type aircraft at least the above frequency range has to be considered.

2.1.3 Effect of Control Surfaces

Due to the aircraft's inertia it is not possible to control the gust induced lift through angle-of-attack variation by means of elevator in the relevant frequency range of the wind disturbances. For a successful lift control fast control surfaces mounted at the wing are needed. The specific control surface used for the gust load alleviation affects the system design and the alleviation effectiveness as well as the resulting second order effects of the operating system.

The utilization of spoilers for lift control might be applicable for wing load reduction. Since the deflection of the spoiler always produces a lift reduction combined with a drag increase it qualitatively produces two desired effects. From Fig 2 and the consideration above we know that an upwind gust increases the

lift. The spoiler deflection can compensate this effect. The increased spoiler drag also counteracts the lift component in the horizontal direction ($A \cdot \alpha_W$) produced by the tilted lift (see Ref 10). Besides this advantage it is clear that only upwind gusts can be controlled and positive vertical load factors can be decreased ($\rightarrow$ reduction of wing root bending moment). Together with the fact that the load factors produced by downwind gusts are $n_z < 1$ ($\rightarrow$ reduction of wing root bending moment) it can be stated that for wing load reduction the lift manipulation by spoilers will work. This is not true for the improvement of the passenger comfort for which it is necessary to control up and down gusts.

Other control devices for lift variation are symmetrically operating ailerons as sketched in Fig 7 for the Do 228. The overall gust induced lift resulting from the integral of lift distribution along the wing will be compensated by the ailerons at the outer wing. The outer wing lift variation, in combination with its distance to the wing root, produces moments which can stimulate the wing bending oscillation. Another undesired effect is the drag increase for positive aileron deflections. Since a down gust already produces a force component against flight direction, the drag increase by the symmetrical aileron is contrary to the demand of an unchanged horizontal load factor.

The same unfavourable combination of a down gust and increased drag results from DLC flaps. But the effect of exciting the wing oscillation can be avoided since the DLC flaps are positioned at the inner wing close to the fuselage (see ATTAS in Fig 7).

Gust load alleviation systems reduce apart from the gust forces the gust induced wing bending moment. The magnitude of reduction depends on the location of the gust load alleviation control surfaces (see Fig 8).

$$\Delta M = \Delta L(\alpha_W) \cdot \left[y_{\Delta L(\eta_{DLC})} - y_{\Delta L(\alpha_W)} \right] \qquad (26)$$

If these control surfaces are located near the wing root, like DLC-flaps, the gust induced moment can only be reduced partly. If symmetrically operating ailerons are used a complete compensation and even an overcompensation is possible. Therefore symmetrically operating ailerons are better suited to reduce the wing bending moment.

2.2 Elastic Aircraft

Normally the aircraft modes are subdivided into a rigid and an elastic domain. The elasticity grows with the size of the aircraft, i.e. an Airbus A340 is much more flexible than a Dornier Do 228. In the case of a significantly elastic aircraft the eigenfrequencies of the elastic modes are close to the rigid modes. After an excitation a response is given by all modes since there are coupling effects. The strongest response results from modes which are close to the excitation frequency. Excitations can be produced by wind disturbances and control surface deflections. Turbulence and gusts stimulate especially the short period and the wing bending mode while wind shear excites the phugoid motion. Gust alleviation control surfaces close to the wing root effect mainly the motion of the "rigid" aircraft, that means the short period. Therefore they are suitable to alleviate vertical accelerations and to improve the passenger comfort. Control surfaces which are near the wing tip mainly effect the "elastic" aircraft, that means the wing bending mode. Consequently they can be used to damp the wing oscillations and reduce the wing bending moment.

The first elastic modes of the ATTAS aircraft are the engine mode, close to 3.5 Hz, and the wing bending mode, close to 5 Hz (Fig 9). Both modes are considered for LARS. Higher frequency modes cannot be controlled due to the limited actuator dynamics.

To investigate the elastic effects a linear differential equation system (state space system) has been used as the mathematical model

$$\begin{aligned} \dot{\underline{x}} &= \underline{\underline{A}} \cdot \underline{x} + \underline{\underline{B}} \cdot \underline{u} \\ \underline{y} &= \underline{\underline{C}} \cdot \underline{x} + \underline{\underline{D}} \cdot \underline{u} \end{aligned} \qquad (27)$$

The system Matrix $\underline{\underline{A}}$ contains four rigid states, four elastic states, three actuator states , and one state of the unsteady aerodynamic of the DLC-flaps, altogether twelve states. The coupling between the rigid and the elastic states are included.

$$\underline{\underline{A}} = \begin{bmatrix} \text{Rigid} & \text{Rigid / Elastic} & \text{Rigid / Actuator} & \text{Rigid / Unst.A.} \\ \text{Elastic / Rigid} & \text{Elastic} & \text{Elastic / Actuator} & \text{Elastic / Unst.A.} \\ - & - & \text{Actuator} & - \\ - & - & \text{Unst.A. / Actuator} & \text{Unsteady Aerody.} \end{bmatrix} \qquad (28)$$

A comparison has been made between model vertical wing tip acceleration output after DLC flap input and flight test results (see Fig 10) which differ only by a small amount.

The DLC-flaps of ATTAS are located near the fuselage. Therefore the expected excitations of the wing bending mode are only small. Nevertheless a system to perform a wing oscillation damping is taken into account.

The Dornier Do 228 aircraft is somewhat stiffer than ATTAS with elastic modes at higher frequencies. The first two elastic modes are wing bending (5.3 Hz) and the fuselage bending (12 Hz). For direct lift control functions symmetrically operating ailerons are available. As mentioned before these control surfaces are suitable to reduce the wing bending moment but excitations in the elastic frequency domain may occur. Fig 11 shows calculated frequency responses of the vertical fuselage acceleration after a Dryden turbulence input. A feed forward direct lift control system decreases the acceleration response between 0.1 and 2 Hz (short period). The corresponding aileron activity stimulates the wing and fuselage bending modes. Therefore an additional damping system seems to be necessary (Ref 16). The acceleration response using DLC-flaps (as already designed and developed for Do 228) is shown in Fig 11. An excitation of elastic modes cannot be regarded.

3. SYSTEM DESIGN, SIMULATION- AND FLIGHT TEST RESULTS

3.1 Load Alleviation and Ride Smoothing System (LARS)

The gust load alleviation system LARS has been designed by the DLR to investigate the basic effects and the potential of gust load alleviation under real world condition on board the testbed ATTAS. LARS is dedicated to the improvement of passenger comfort and to the reduction of the wing root bending. To cover the broad frequency domain of relevant wind disturbances the LARS concept consists of two subsystems (Fig 12)

a) An open-loop system to control the frequency range between 0.1 and 1 Hz which mainly affects human reactions to accelerations (see Fig. 5, 6).

b) A closed-loop controller for the damping of the elastic wing bending mode.

The choice of an open-loop system for the rigid body motion has the advantage of leaving the handling qualities (as known

from aircraft behaviour in calm air) unchanged. For the definition and design of such a system a good knowledge of all aircraft parameters, including data of relevant subsystems, and a precise gust determination from on-board measurement is required. The closed-loop controller feeds back the wing-tip normal acceleration to the DLC flaps. To avoid coupling effects to aircraft motion the signals are band-pass filtered around the frequency of the wing oscillation.

3.1.1 Lift Control

To perform the most attainable lift control for gust load alleviation the open-loop control laws for the rigid body aircraft were designed from Equ (10) by using $\varphi = 1$ (certainly the attainable factor for a real world system will be $\varphi < 1$). The wind angle-of-attack determination is done by using the air data measured at a position which normally is located away from the wing to avoid strong wing/angle-of-attack interference. To achieve a time coordinated DLC flap command the time delay between the determination of the gust at the position x_S of the air data sensor and the arrival of the gust at the wing needs to be considered (see Fig 13). The lift variation due to DLC flap deflection is

$$\Delta C_L(\eta_{DLC}) = C_{L\eta_{DLC}} \cdot \eta_{DLC} \qquad (29)$$

The consideration of a linear function for the DLC flaps efficiency is sufficient as pre-investigations with linear, square and cubic attempts showed (Ref 11). Equ (29) together with Equ (9) gives the required DLC flap command

$$\eta_{DLC} = -\frac{C_{L\alpha}}{C_{L\eta_{DLC}}} \cdot \alpha_W^* = K_1 \cdot \alpha_W^* \qquad (30)$$

where α_W^* is the delayed wind angle-of-attack (referred to the air data sensor) at the wing position. Equ (30) is true for an exclusive lift control neglecting all additional effects accompanying gusts and their alleviation.

3.1.2 Pitch Control

The DLC deflection and the gust produce pitching moments. These moments have to be compensated by the elevator. When the changed downwash of the wing and also the gust itself reaches the horizontal stabilizer (see Fig 13), additional elevator deflection is required to avoid aircraft pitching.

The resulting feed forward gains for constant lift and constant pitch moment only depend on the aerodynamic derivatives of the aircraft (Ref 12)

$$\eta_{DLC} = -\frac{C_{L\alpha}\frac{x_H + x_N}{l_\mu}}{C_{L\eta_{DLC}}\frac{x_H + x_N}{l_\mu} + C_{m\eta_{DLC}}} \alpha_W^* \qquad (31)$$

$$\eta = \frac{\partial\eta}{\partial\alpha_H}\left[\left(1 - \frac{\partial\varepsilon_H}{\partial\alpha}\right)\left(-\alpha_W^{**}\right) + \frac{\partial\varepsilon_H}{\partial\eta_{DLC}}\eta_W^{**} + \right.$$
$$\left. + \frac{C_{L\alpha}\frac{x_N}{l_\mu}}{C_{L\alpha H}\frac{S_H}{S}\frac{x_H}{l_\mu}}\alpha_W^* + \frac{C_{L\eta_{DLC}}\frac{x_N}{l_\mu} + C_{m\eta_{DLC}}}{C_{L\alpha H}\frac{S_H}{S}\frac{x_H}{l_\mu}}\eta_{DLC}^* \right] \qquad (32)$$

where α_W^* again is the wind angle of attack at the wing position. The elevator deflection is η with the wind angle of attack α_W^{**} and the DLC flaps deflections η_W^{**} accounting for the induced downwash at the position. x_H of the horizontal stabilizer η_W^* is the actual DLC flap position. For a fixed aircraft configuration the control law can be reduced to a system with constant coefficients

$$\eta_{DLC} = K_1 \cdot \alpha_W^* \qquad (33)$$

$$\eta = K_{21} \cdot \alpha_W^* + K_{21} \cdot \alpha_W^{**} + K_{23} \cdot \eta_W^* + K_{24} \cdot \eta_W^{**} \qquad (34)$$

The time shifts can be calculated from the geometrical distance divided by the airspeed. The airspeed dependent time shifts above can be used for the compensation of real world system time lags of the sensors, EDP and actuators.

3.1.3 Drag Control

The control of gust effects in the aircraft's longitudinal axis has to be performed as quickly as in the normal axis. Thrust variation of jet engines (with which ATTAS is equipped) normally are not fast enough for this task. But the DLC flaps can be used for drag control too, although the effectiveness is small.

Symmetrical Pre-Deflected DLC Flaps

In the event of an updraft the DLC flap moves upwards for lift reduction. The energy supplied by the gust accelerates the aircraft; the additional drag produced by the DLC flap leads a deceleration. Both are opposing effects which more or less cancel each other. In case of a down draft the DLC flap deflects downwards for gaining lift. The increased drag from DLC flap deflection and the gust lead to an energy loss and a deceleration of the aircraft. In order to compensate this energy deficiency induced by the gust the downward moving DLC flap has to come up with a drag reduction. This is only possible if the DLC flap is pre-deflected in the (negative) upward direction.

The magnitude of the pre-deflection can be calculated from the required drag in order to avoid gust induced acceleration or deceleration (Ref 13). This required drag has to be identical with the drag variation produced by the DLC flap deflection around a specific reference pre-deflection. This necessary reference deflection can be calculated from the equilibrium of the drag derivatives (see Fig 14).

$$\frac{d\Delta C_{req}}{d\eta_{DLC}} \stackrel{!}{=} \frac{dC_{D\eta_{DLC}}}{d\eta_{DLC}} \qquad (35)$$

This requirement can only be satisfied for large upward DLC flap deflections. However, large pre-deflections restrict DLC operation due to maximum deflection limitations. The required pre-deflection decreases if the true airspeed increases (Fig 14). So the application of this approach is only possible for the low speed flight phases. Since no complete drag control is required for the improvement of the horizontal acceleration, smaller pre-deflections as indicated by Fig 14 can be chosen, as simulations and flight tests have confirmed.

Asymmetrical Pre-Deflected DLC Flaps

ATTAS is equipped with three pairs of DLC flaps. Each pair is symmetrically mounted to the aircraft's vertical plane and can be symmetrically operated (to avoid high roll rates in a failure case). So each DLC flap of one wing has a corresponding image on the other wing (see Fig 15). Due to the fact that each pair can be controlled separately another approach for lift and drag management was investigated (Ref 14): The inner DLC flap pair (no. 3 and 4) is exclusively used for lift control. The middle and the outer pairs are used as a kind of "*split flap*". Flaps no. 1 and 6 are pre-deflected in upward direction and flaps no. 2 and 5 are pre-deflected in downward direction. Then the combination of flap no. 1 and flap no. 2 on the left wing as well as flap no. 5 and flap no. 6 on the right wing can be used for an independent drag control. If the *split* angle is expanded the drag will increase, respectively decrease for a *split* angle reduction.

The coefficients of lift and drag variation for a specific pair of flaps can be calculated from the corresponding flap area S_{fi} related to the overall flap area S_f.

$$\Delta C_{LDLCi} = \frac{S_{fi}}{S_f} \cdot \Delta C_{LDLC}\left(\eta_{DLCi} = \eta_{DLC}\right) \quad (36)$$

$$\Delta C_{DDLCi} = \frac{S_{fi}}{S_f} \cdot \Delta C_{DDLC}\left(\eta_{DLCi} = \eta_{DLC}\right) \quad (37)$$

The overall coefficients are

$$C_{LDLC} = \Delta C_{LDLC1} + \Delta C_{LDLC2} + \Delta C_{LDLC3} \quad (38)$$

$$C_{DDLC} = \Delta C_{DDLC1} + \Delta C_{DDLC2} + \Delta C_{DDLC3} \quad (39)$$

respectively

$$C_{LDLC} = L_1 \cdot \eta_{DLC} \quad (40)$$

$$C_{DDLC} = D_1 \cdot \eta_{DLC} + D_2 \cdot \eta_{DLC}^2 \quad (41)$$

Presuming the lift control is exclusively performed by the inner flaps we get with Equ (26)

$$\Delta C_{LDLC3} = -C_{L\alpha} \cdot \alpha_W \quad (42)$$

Since the middle and outer flap must produce no lift variation it is true

$$\Delta C_{LDLC1} = \Delta C_{LDLC2} = 0 \quad (43)$$

But all the horizontal force variations have to be compensated by these pairs of flaps

$$\Delta C_{LDLC1} + \Delta C_{LDLC2} = -\Delta C_{DDLC3} + C_{Lr} \cdot \alpha_W \quad (44)$$

With the Equ (40), (41) and (42) the three unknown variables for a Gust Management System (GMS) with constant lift and drag can be determined

$$\eta_{DLC3} = -\frac{S_f}{S_{f3}} \cdot \frac{C_{L\alpha}}{C_{L\eta_{DLC}}} \cdot \alpha_W^* \quad (45)$$

$$\eta_{DLC2} = \sqrt{\eta_{DLC2r}^2 + \frac{-\Delta C_{DDLC3} + C_{Lr} \cdot \alpha_W^*}{D_2 \cdot \left(1 + \frac{S_{f2}}{S_{f1}}\right) \cdot \frac{S_{f2}}{S_f}}} \quad (46)$$

$$\eta_{DLC1} = -\frac{S_{f2}}{S_{f1}} \cdot \eta_{DLC2} \quad (47)$$

This approach neglects the effect of elevator deflection on drag and the effect of the *split* flaps on the pitch moment which can be classified as third order effects.

Fig 16 shows the principal DLC flap responses to a down-draft ramp (lift and energy loss). Starting from the reference configuration in calm air ($t < t_0$) there isn't any deflection of the inner DLC flap pair but the middle and outer flaps are split. When the down draft starts at t_0 the inner DLC flap pair moves to positive deflections and the *split* flaps start falling back to the neutral position. During this phase lift, drag, and energy can be compensated completely. At $t = t_1$ the middle and outer flaps have reached the neutral position ($\eta_{DLC1} = \eta_{DLC2} = 0$) and no more drag reduction is possible. Then the system compensates lift variations exclusively. For higher required positive DLC flap deflections the inner DLC pair remains unchanged for the moment until inner and outer flaps have reached the same positive deflection at time t_2. Then all three DLC flap pairs move symmetrically to the required position until the maximum deflection is reached. Although a drag compensation is performed the lift control is able to compensate gusts up to the same magnitude as with an exclusive lift control.

With Fig 16 it is obvious that vertical gusts for which a total compensation of lift, drag, and energy can be performed are limited to small magnitudes. It becomes also clear that the maximum vertical gust $w_{Wg\,max}$ for which an exclusive lift compensation can be achieved is not restricted by the use of asymmetrical DLC flap pre-deflection.

3.1.4 Elastic Mode Damping

As mentioned before oscillations with large dynamic loads can easily be produced by turbulence or active control systems, such as the described open-loop gust alleviation system. A wing oscillation damping system may be necessary and therefore has been investigated for use with ATTAS.

The vertical accelerations of the left and right wing tip are added up, corrected with the vertical acceleration of the centre of gravity, band-pass filtered and then fed back to the DLC flaps (Fig 12). Due to the low characteristic frequency of the DLC actuator and additional system time delays, acceleration instead of velocity is fed back to increase the damping of the wing bending mode. To determine the gain value, the root-locus method was used (Fig 17). A maximum damping coefficient is obtained with K3 = - 0.02; a sufficient damping coefficient can already be reached with K3 = - 0.01. Except for the DLC actuator, the other modes do not change. The time response of the wing bending moment due to a vertical wind step is shown in Fig 18. Compared with the uncontrolled system, the damping increases distinctly and the overshoot is reduced by about 20%.

For the design of the closed-loop controller for an increased wing oscillation damping an overall system time delay of 36.3 ms was assumed. If time delayed accelerations are fed back the resulting phase shift leads to a signal similar to a velocity feedback. Therefore, time delays may increase the damping but will destabilize the oscillation rapidly if they become too large. Fig 19 shows the root locus of various time delayed accelerations fed back to the DLC flaps. The system reacts sensitively to higher time delays. For time delays of more than 43 ms the system becomes unstable.

3.1.5 Simulation and Flight Test Results

The performance of the open-loop lift and pitch compensation mode of LARS has been successfully verified by flight tests. Fig 20 illustrates the reduction of vertical loads when the system is engaged. In the relevant frequency domain the vertical acceleration can be reduced up to more than 10 dB. Tab 1 presents significant standard deviations calculated from flight test data comparing the improvement of flight sequences with and without LARS. It can be seen that besides load reduction the effort to keep the aircraft on the desired flight path (represented by the standard deviation of the pilot's elevator inputs) is also considerably reduced. This can be interpreted as an improvement of flying qualities (Ref 1).

Looking at the flight test data the improvements are evident but were not fully confirmed by the complementary pilot ratings. The pilots noticed a changed aircraft response to gusts when LARS was engaged but did not report such a great amount of improvement as analysed from the flight test data. The main reason for that is the following. The pilot is used to a specific acceleration distribution in the aircraft's vertical plane. This distribution can be approximated very well and discussed by an ellipse around the centre of gravity. Fig 21 shows the

results from a flight test in severe turbulence. The z-axis represents the normal load factor and the x-axis represents the longitudinal load factor. The bigger ellipse shows the acceleration distribution of the flight test results without lift compensation using LARS. (The ellipse covers 99% of all measured n_x and n_z data sets, every 5th data point is plotted.) It is slightly turned in clockwise direction as expected from Equ 19. The normal accelerations dominate and the crew notices only few horizontal accelerations. The LARS lift and pitch compensation mode only reduces the loads in the normal direction, but neglects longitudinal accelerations, as the smaller ellipse in Fig 21 indicates. Therefore the longitudinal aircraft response gains more importance to the crew's attention. From this point of view the quality of the gust load alleviation is less significant than suggested by Fig 20 and Tab 1. From the resulting tilt angle $\nu \approx 13°$ of the acceleration distribution in the vertical plane, the gust alleviation factor can be calculated as $\varphi \approx 0.4$ (Tab 2) which is close to the theoretical approach of Equ (19).

Already from the knowledge acquired by the first flight tests using ATTAS a tentative qualitative criterion for gust load alleviation from a passenger's subjective point of view can be formulated. To give the pilot and the passengers a subjective feeling of gust load alleviation not only normal accelerations but also longitudinal accelerations have to be suppressed (Ref 15). This must be performed in such a way that the area covered by the ellipse in Fig 21 has to be minimized. Further more its tilt angle needs to be reduced or at least remain constant to avoid the effect of an over-rating for the longitudinal accelerations. If the tilt angle can be reduced to zero then the deterministic correlation between vertical and horizontal aircraft response to gusts is artificially revoked.

A first step to improve the longitudinal response has been done by changing the characteristics of the drag over lift relation of the DLC flaps by a symmetrical pre-deflection upward. Fig 22 shows the power density spectrum of the longitudinal acceleration calculated from flight tests with a DLC flap predeflection of $\eta_{DLCr} = -10$ deg comparing LARS "on/off" sequences. The achieved improvement illustrated in this figure was qualitatively confirmed by the test crew.

For a complete gust load management the manipulation of lift and drag must be independent. As discussed above this can be accomplished by using asymmetrical pre-deflected DLC flaps. Fig 23 shows the comparison of two acceleration distributions in the aircraft's symmetrical plane. The outcome of lift, moment and drag compensation called *Gust-Management-System* is denoted by GMS. The tilt angle is significantly reduced which is synonymous with an improvement of longitudinal acceleration response. But from chapter 3.1.3 we know that the total lift and drag compensation achievable with split DLC flap pairs (due to deflection limitations) is limited to light turbulence with small gust amplitudes. (Notice: the impressive gust load alleviation of $\varphi \approx 0.4$ for the approach of chapter 3.1.2 was not reached for this flight test due to non optimized system parameters. The aim of this flight test was to demonstrate only the principle of drag variation on the aircraft's acceleration distribution in the symmetrical plane, apart from the relation described by Equ (19).)

Compared with the natural aircraft response to gusts (Fig 21 left diagramme) an overcompensation of tilt angle can be observed from Fig 23. The tilt angle of the ellipse vanishes ($\nu \approx 0$) which indicates that there is no longer a correlation between n_x and n_z as described by Equ (18). But the natural coupling between n_x and n_z can also be realised by the GMS. This can be performed by an incomplete drag compensation in such a way that the desired tilt angle $\nu \approx \nu_{uncontrolled}$ occurs. Fig 24 shows the result of a simulation with an *artificially* tilted *acceleration ellipse* compared with the complete GMS outcome. With a specific incomplete drag compensation it is possible to achieve a similar acceleration impression as performed by the uncontrolled aircraft but with a considerable reduced level of magnitudes.

The flight testing of the closed-loop wing bending mode controller has shown that the system becomes unstable since the overall time delays are too large. The DLC actuator dynamics are fast enough with a deflection rate of about 75 deg/s and the necessary deflection magnitudes are small (less than 3 deg). But since the ATTAS electronic data processing concept is more directed towards pilot in the loop investigations of flight mechanics and guidance problem areas, the over all time delay requirements correspond to such purposes. From that point of view, time delays in the order of about 100 ms are adequate; but for the objectives of the control of structural modes this is unacceptable.

3.2 Integrated Gust Load Alleviation System (IGLAS)

The design of the Open Loop Gust Load Alleviation System OLGA was based on a simplified aircraft model considering only the vertical and pitch motion of the aircraft. The flight tests confirmed the expected gust load alleviation in the frequency domain of the short period. But due to the suppression of the aircraft's vertical acceleration in this specific frequency area, the aircraft vertical response outside of these boundaries gains importance. The test pilots of the OLGA program complained about structure oscillations in the range between 4 to 8 Hz. The same is true for lateral accelerations. The Dutch roll and yaw motion can even be stimulated through the operation of asymmetric DLC surfaces (differences of lift and drag forces at each wing).

Dornier designed the **I**ntegrated **G**ust **L**oad **A**lleviation **S**ystem IGLAS for the Do 328 considering short period and phugoid motion. The objective of this approach is to improve the horizontal aircraft response as well as the vertical loads. IGLAS uses symmetrically operating ailerons with an actuator break frequency of 5 Hz.

3.2.1 Disturbance Feed Forward Control

The disturbance feed forward control is incomplete if only the short period motion is taken into account. Since the horizontal degree of freedom is uncontrolled, the phugoid motion is excited (Fig 25) and airspeed deviations occur. The shown simulation results are true for landing approach configuration of the Do 328.

If the thrust is used as a control input the horizontal aircraft response can be improved. The dynamic response of the engines is slow and only low frequency accelerations can be affected. For the Do 328 propulsion a low-pass characteristic with a time constant of $T_{propulsion} = 1s$ is identified. Fig 26 shows the reduction of vertical and horizontal accelerations below 0.1 Hz. A reduction of horizontal acceleration in the frequency range of the short period motion cannot be achieved.

3.2.2 Closed-Loop Pitch Control

To evaluate the performance of gust load alleviation systems it is common to investigate the aircraft behaviour without inner control loops. The advantageous effects of these controllers are neglected. Fig 27 shows the results of a standard pitch controller on the suppression of gusts in the frequency domain of the phugoid mode. This controller feeds back pitch attitude and rate to the elevator.

Pitch control is normally also performed by the pilot. The results above show that for simulation investigations this inner control loop has to be applied.

3.2.3 Complete System

The IGLAS disturbance feed forward controller (including thrust control) and the pitch controller are completed with an elastic mode closed-loop damping system. The wing tip vertical accelerations are fed back (according to LARS) to the symmetrically operating ailerons. The tuning of all controllers needs to be performed simultaneously, since coupling effects have to be considered.

Fig 28 illustrates the improvement of the vertical load factor of the complete system over an extended range of frequency. Only the not controlled fuselage bending mode (15 Hz) shows a smooth increase of magnitude. The horizontal load factor is reduced for frequencies below 0.1 Hz. Above this frequency thrust control is no longer applicable due to propulsion dynamics.

4. PERSPECTIVES

Gust load alleviation in the frequency domain of the short period reduces structural loads and improves the passenger comfort. To reduce loads from structure oscillations, fast actuators for DLC surfaces (wing bending mode) and elevator (fuselage bending mode) are needed. Modern fly-by-wire aircraft normally are equipped with such actuators.

The horizontal degree of freedom is important for the passenger comfort and cannot be neglected. Devices for drag control always will be accompanied by extra drag due to required initial reference deflection. Normally thrust variation is not fast enough to control the longitudinal forces. Turboprop propulsion equipped with a **F**ull **A**uthority **D**igital **E**ngine **C**ontroller FADEC (Fig 29) may be able to alter the pitch of the propeller blades while momentarily maintaining a constant RPM. This will result in a quick thrust response as required for horizontal load factor control.

Gusts not only produce additional loads but also flight path deviations. If flight path control is considered, lower gust frequencies and especially horizontal wind variations gain importance. Even a windshear can be understood as a gust with an extremely long wavelength (Ref 17). The effect of low frequency gusts on the aircraft's energy situation (Ref 18) is more serious than on its acceleration response. The boundary between both effects, load variation and flight path deviation, is fluid and so they often occur simultaneously. For the suppression of all undesired gust and wind effects an over all system has to be designed using all available aircraft control surfaces. Such an **I**ntegrated **R**ide **I**mprovement **S**ystem (IRIS) concept for wind disturbance management is illustrated in Fig 30. It can improve the passenger comfort and aircraft safety. Furthermore it will support the pilot in controlling the inner aircraft loop and give him the opportunity to concentrate on the guidance and flight management task instead of counter acting wind disturbances.

4. CONCLUSIONS

An intensified acceleration response of conventional transport type aircraft can be observed in a small bandwidth of vertical gusts and turbulence. The occurrence of airsickness coincides with this frequency range. The corresponding atmospheric conditions prevail in a very unstable boundary layer and affect generally flight phases close to the ground. Lift control leads to significant suppressions of wind induced normal accelerations, more precise flight path control, and reduced pilot workload.

The operation of gust load alleviation systems for the abatement of undesired normal loads stimulates the horizontal aircraft response. A system which is very effective against gust induced normal loads can produce horizontal accelerations with magnitudes on the same order as the remaining vertical accelerations. From flight tests it was evident that the lateral aircraft response has importance relative to pilots and passengers. The rigid body aircraft response in the vertical plane can be improved by a combination of lift and drag control devices in the area of the short period motion. The application of thrust control in this frequency domain is possible only with fast propeller blade pitch variation. Lower gust frequencies generally can be controlled by thrust command and a common inner loop pitch controller.

The distribution of the longitudinal and normal loads responses can be described by an ellipse. Reducing the area covered by this ellipse and diminishing its tilt angle will lead to an improved gust response of the aircraft.

Gusts and gust alleviation control activity can stimulate the elastic modes of the aircraft. The control of structural modes can only be performed using controllers with small overall time delays. The required control power to damp the oscillation and to reduce bending moments is marginal.

Modern transport type aircraft equipped with fly-by-wire technology provide all necessary conditions for the implementation of gust load alleviation functions. No extensive additional modifications are required. Fly-by-wire is on its way to taking a place in smaller airliners. It can be expected that even commuter aircraft, for which gust alleviation is most attractive, will be equipped with such technology. Considering the potential of **A**ctive **C**ontrol **T**echnology (ACT), it seems to be advantageous to the authors to develop an integrated "wind management" system using all available aircraft controls to manage relevant wind effects, from gust and turbulence alleviation up to windshear compensation and elastic mode control.

REFERENCES

1. Wilhelm, K. and Hahn, K.-U., "ATTAS - Recent Flying Qualities Experiments", in "In-Flight Simulation for the 90's", DGLR 91-05-12, July 1991.
2. O'Connel, R.F., "Design, Development and Implementation of an Control System for Load Alleviation for a Commercial Transport Airplane", AGARD Report 683, 1979.
3. Böhret, H., Krag, B. and Skudridakis, J., "OLGA - An Open-Loop Gust Alleviation System", AGARD CP 384, 1985.
4. Schänzer, G. "Flug in gestörter Atmosphäre", Vorlesungsmanuskript zur Vorlesung am Institut für Flugführung der TU Braunschweig, 1983.
5. Rohlf, D.; Mönnich, W., "Identification of the DLC-Flap System of the Research Aircraft ATTAS" Systemidentifikation in der Fahrzeugdynamik, DFVLR-Mitt. 87-22, Paper No. 3.1, 1987.
6. Brockhaus, R., "Flugregelung I, Das Flugzeug als Regelstrecke", O. Föllinger und H. Satorius, R. Oldenbourg Verlag, München - Wien, 1977.
7. Dryden, H.L., "A Review of Statistical Theory of Turbulence", Quarterly Journal of Applied Mathematics 1, 1943.

8. Anon., "Flying Qualities of Piloted Airplanes", MIL-F-8785C, Military Specification, November, 1980.

9. Pritchard, H. L.; Calvin, C. E.; McVehil, G. E. "Spectral and Exceedance Probability Models for Use in Aircraft Design and Operation", Air Force Flight Dynamics Laboratory, Wright Patterson Air Force Base, Ohio, 1965.

10. Schänzer, G., "Direct Lift Control for Flight Path Control and Gust Alleviation", AGARD GCP-CP-240, 1977.

11. Rommel, A., "Untersuchungen zur Stötgrößenaufschaltung als Bestandteil eines Böenlastminderungssystems", DFVLR-IB 111-88/17, Institut für Flugmechanik, DFVLR Braunschweig, 1989.

12. König, R.; Hahn, K.-U., "Load Alleviation and Ride Smoothing Investigations using ATTAS", 17th ICAS Congress, Stockholm, Sweden, 1990.

13. Hahn, K.-U.; König, R., "LARS-Auslegung und Erprobung eines fortschrittlichen Böenabminderungssystems mit ATTAS", Jahrbuch 1991 II der Deutschen Gesellschaft für Luft-und Raunfahrt e.V. (DGLR), Band II, Paper 91-201, Bonn, 1991, pp 950-963.

14. Hahn, K.-U., "Beiträge zur Realisierung eines fortschrittlichen Böenabminderungssystems", Deutscher Luft- und Raumfahrtkongress, Jahrbuch 1992 II der Deutschen Gesellschaft für Luft- und Raunfahrt e.V. (DGLR), Band II, Bonn, 1992.

15. Hahn, K.-U.; König, R., "ATTAS Flight Test and Simulation Results of the Advanced Gust Management System LARS", A Collection of Technical Papers, AIAA Atmospheric Flight Mechanics Conference, Hilton Head Island, 1992.

16. Böhret, H.; Winter, J., "Active Control System for Gust Load Alleviation and Structural Damping", AGARD FMP-CP-470, 1989.

17. Hahn, K.-U., "Effect of Wind Shear on Flight Safety", Prog. Aerospace Sciences. Vol.26, Pergamon Press, Great Britain, 1989.

18. König, R., "Monitoring and Controlling Flight in Windshear", Conference Proceedings, Aircraft Integrated Monitoring Systems Symposium AIMS, Aachen, 1989.

TABLES AND FIGURES

Standard Deviation		LARS OFF	LARS ON
Vertical Wind	σ_W	100%	103.6%
Vertical Load Factor	σ_{nz}	100%	62.0%
Pitch Attitude	σ_θ	100%	68.8%
Vertical Speed	$\sigma_{\dot{H}}$	100%	70.9%
Pilot Inputs	$\sigma_{\eta Pilot}$	100%	47.6%

Tab 1: Comparison of the Standard Deviations of Significant Parameters

φ	0.0	0.4	0.6	1.0
ν_{theory} in deg	3.5	10.0	17.0	90.0
$\nu_{simulation}$ in deg	6.5	-	18.0	-
$\nu_{flight\ test}$ in deg	6.0-7.0	13.0	-	-

Tab 2: Tilt angle of the ellipse of the acceleration distribution as a function of gust load alleviation effectiveness

Fig 1: Advanced Technology Testing Aircraft System ATTAS (DLR flying testbed)

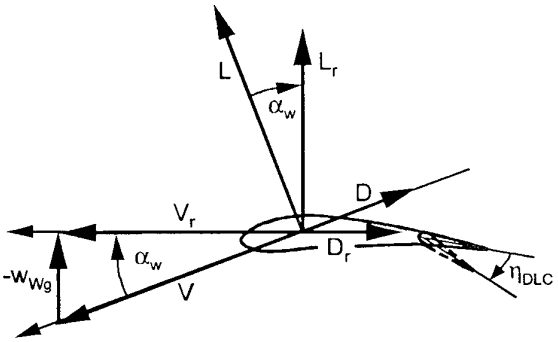

Fig 2: Flight Through a Step Gust

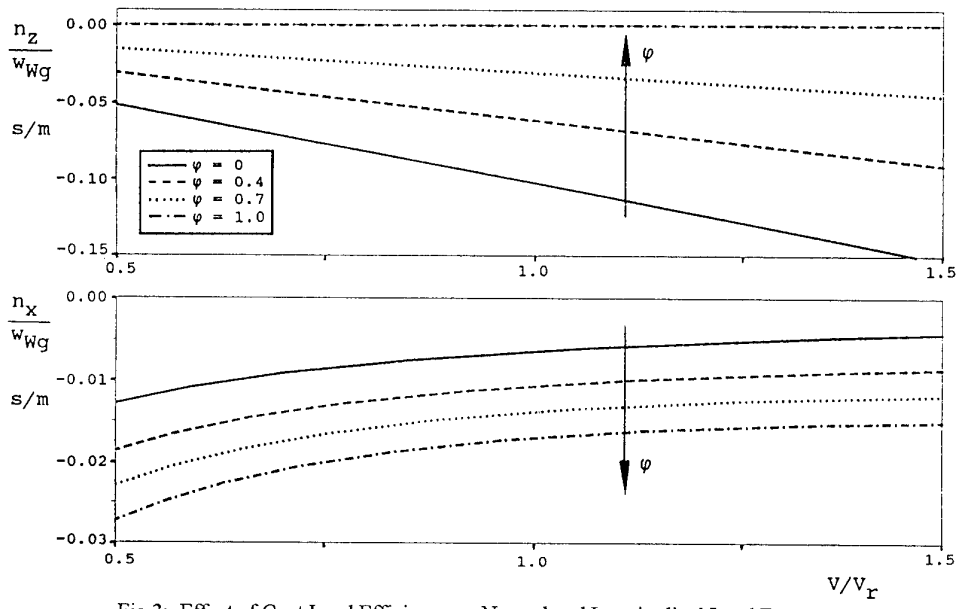

Fig 3: Effect of Gust Load Efficiency on Normal and Longitudinal Load Factor

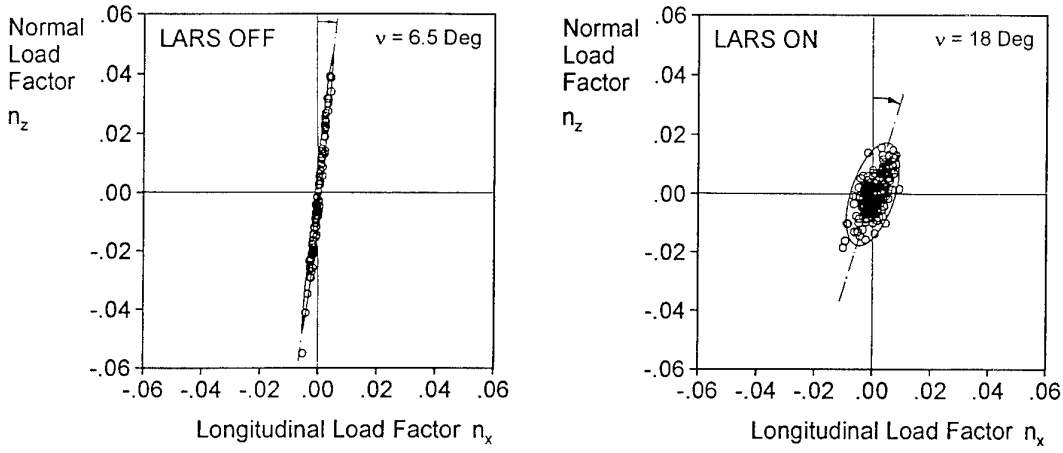

Fig 4: Load Factor Distribution in the Aircraft Symmetrical Plane
(Simulation without and with Gust Load Alleviation)

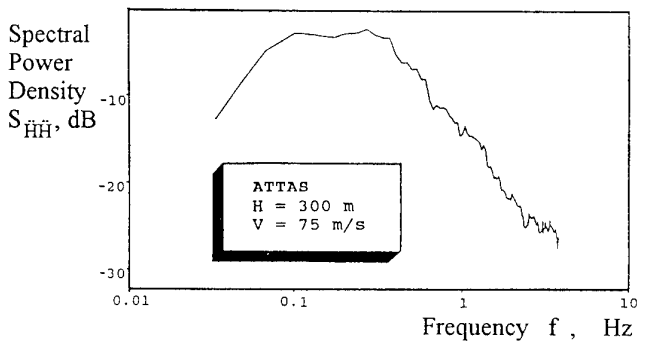

Fig 5: Spectral Power Density of the Normal Acceleration
(ATTAS Flight Test)

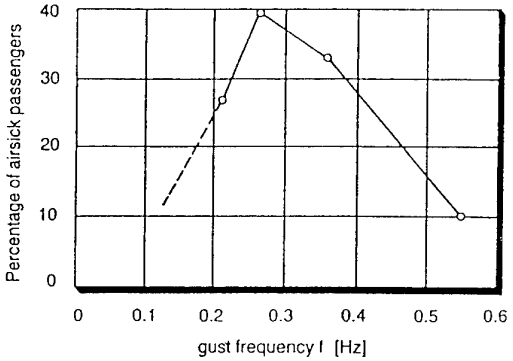

Fig 6: Percentage of Passengers to Get Airsick
as a Function of the Gust Frequency (Ref 3)

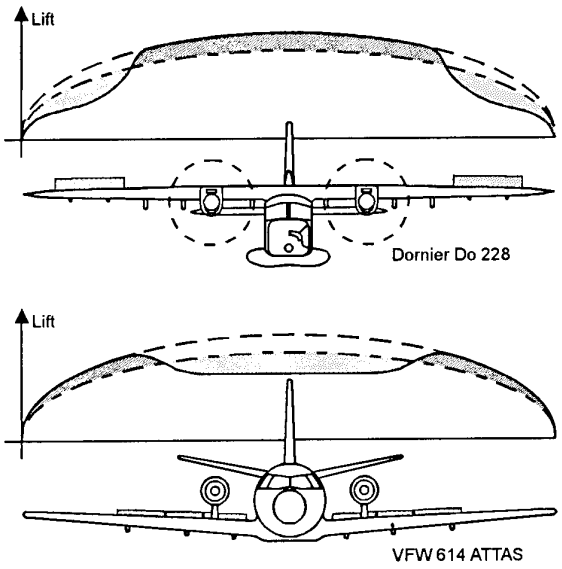

Fig 7: Lift Distribution for Gust Load Alleviation

- - - - - - Without Gusts
- - - - - - - With Gusts
——— With Gusts and DLC Surface Deflection

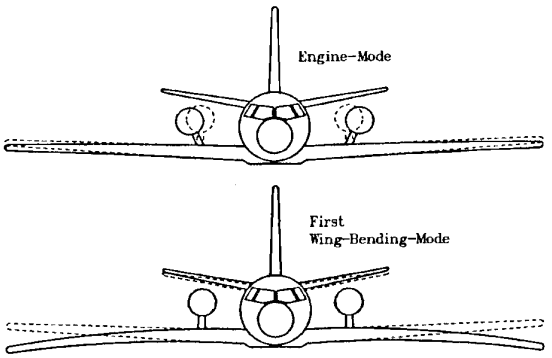

Fig 9: ATTAS First Elastic Modes

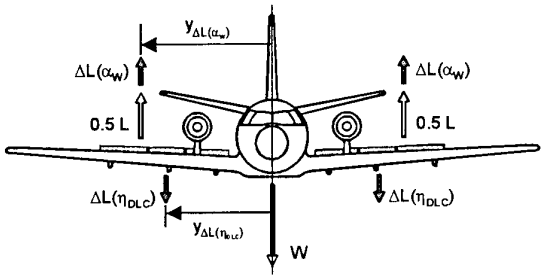

Fig 8: Wing Bending Moment due to Gusts and DLC-Surface Deflection

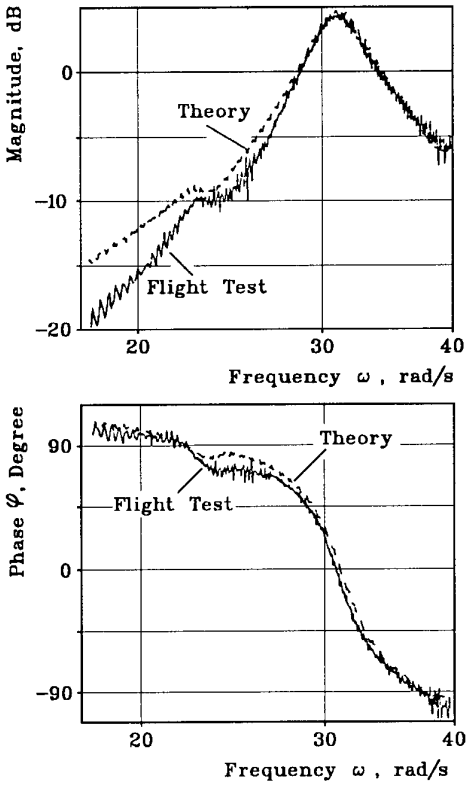

Fig 10: Comparison of Vertical Wing Tip Acceleration

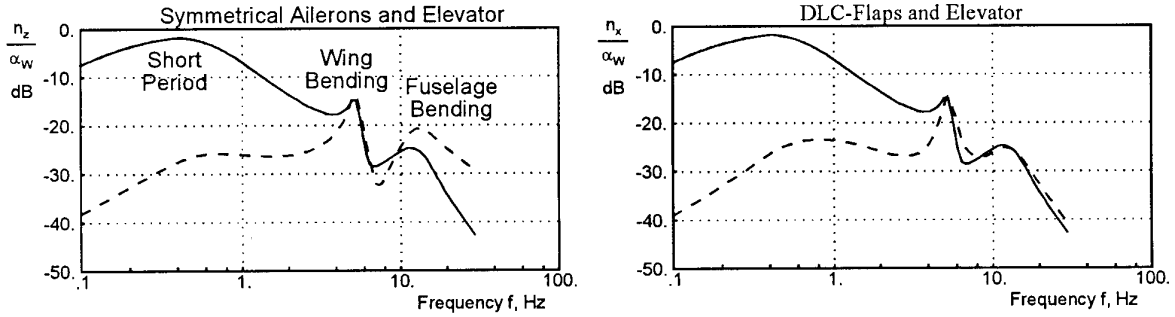

Fig 11: Frequency Response of the Vertical Acceleration due to Different Control Surface Input
——— Disturbance Feed Forward OFF - - - - - - Disturbance Feed Forward ON

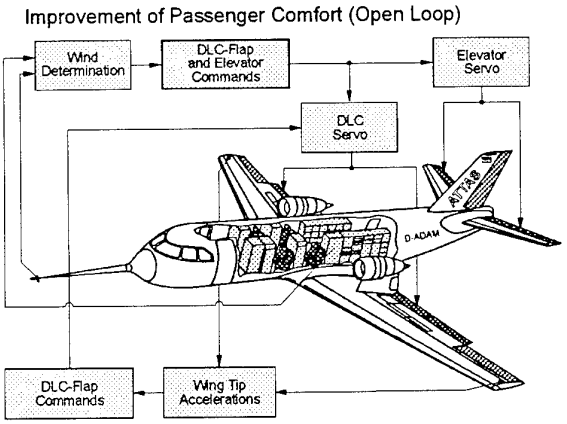

Fig 12: LARS Structure of Gust Load Alleviation

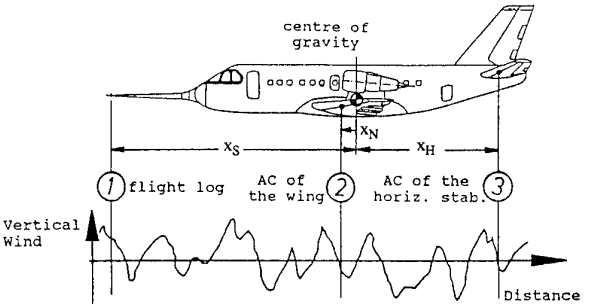

Fig 13: Effect of Aircraft Dimensions on the Time Delay of the Measured Wind Angle of Attack

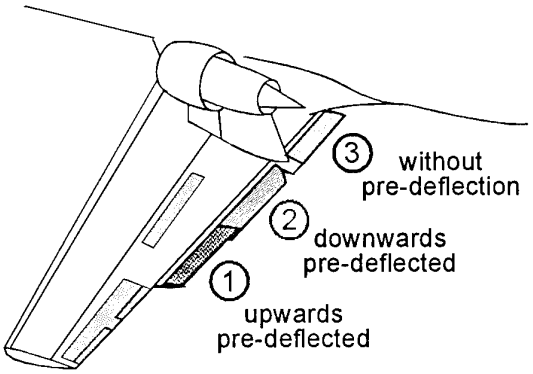

Fig 15: Split DLC Flaps

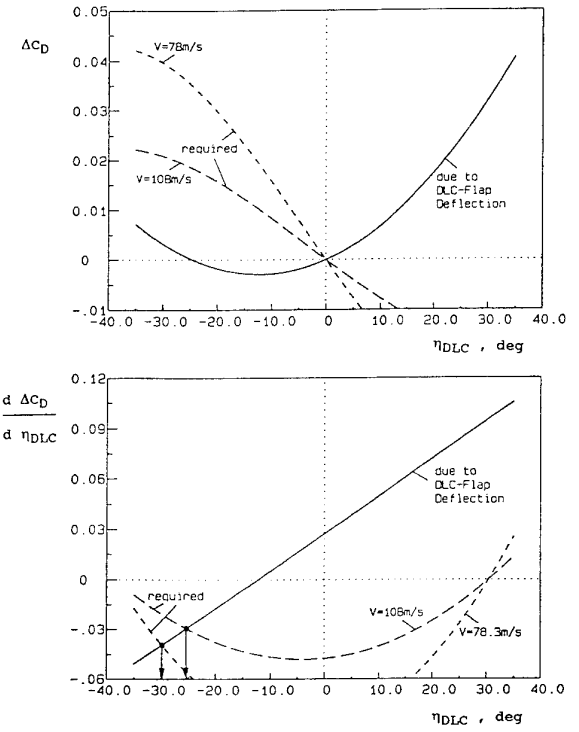

Fig 14: Determination of DLC Flap Predeflection for Drag Control

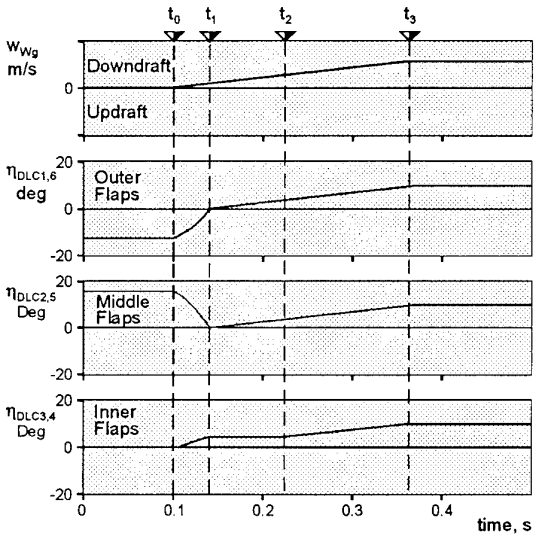

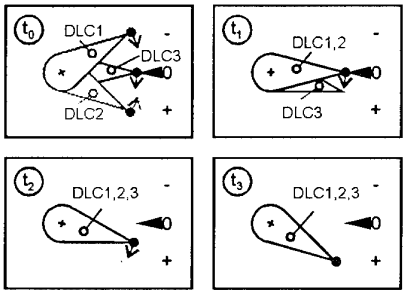

Fig 16: Principle of Asymmetrical Pre-Deflected DLC Flaps

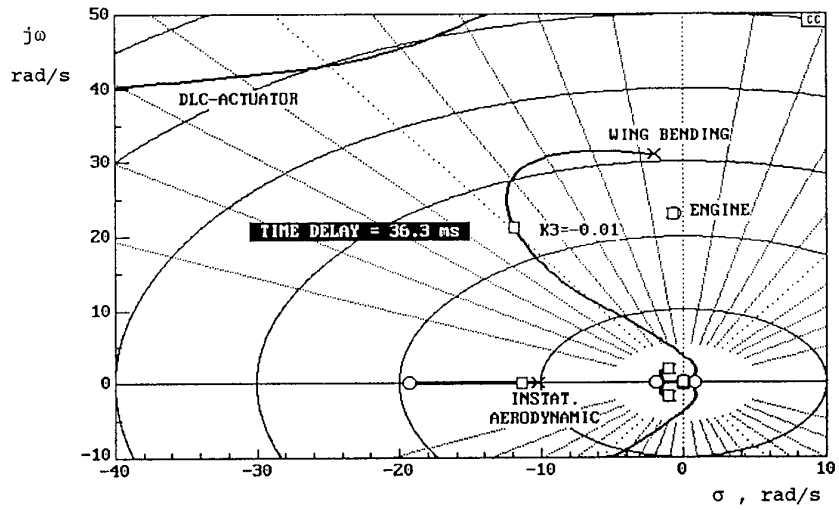

Fig 17: Root Locus for Gain Determination

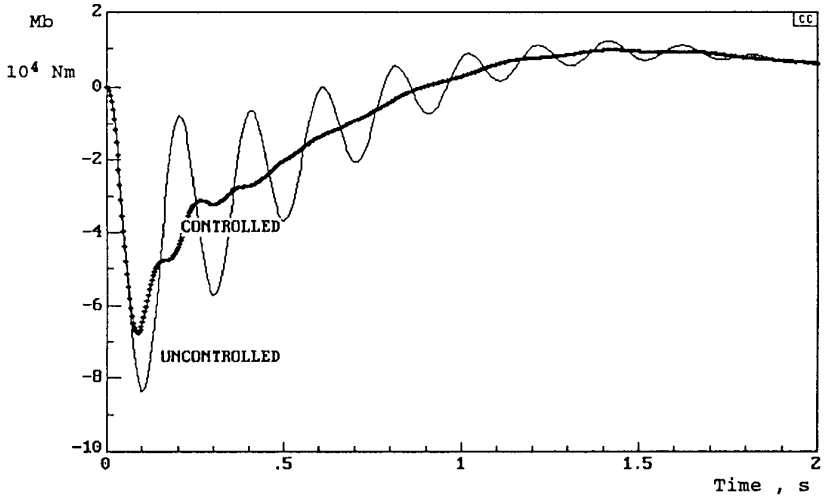

Fig 18: Time Response of the Wing Bending Moment after a Step Gust Input

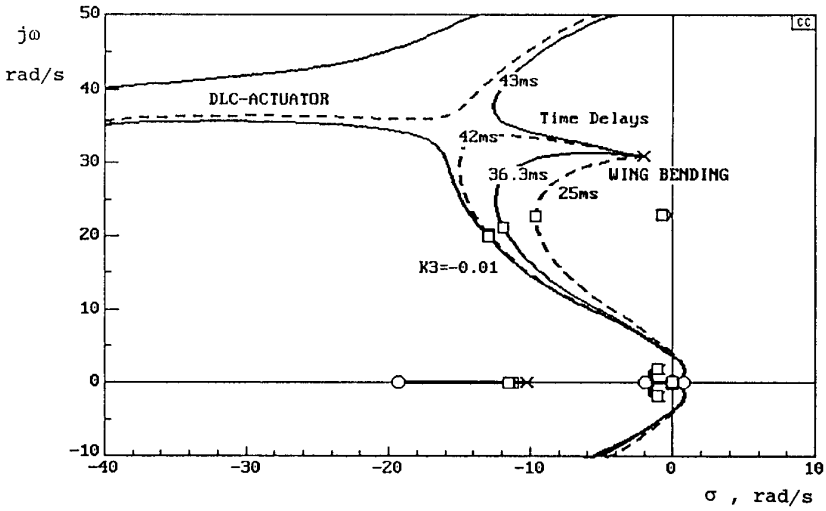

Fig 19: Effect of Time Delay on Gain Design

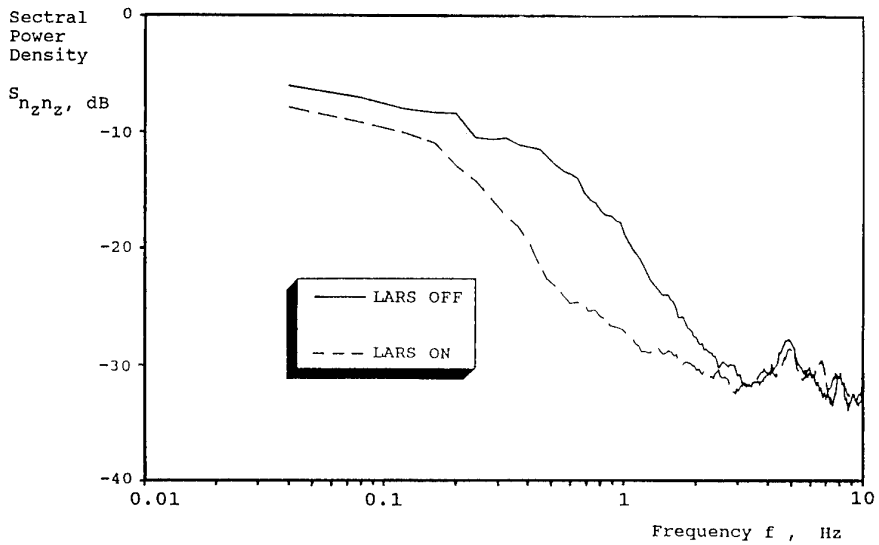

Fig 20: Spectral Power Density of the Normal Load Factor
(ATTAS Flight Test)

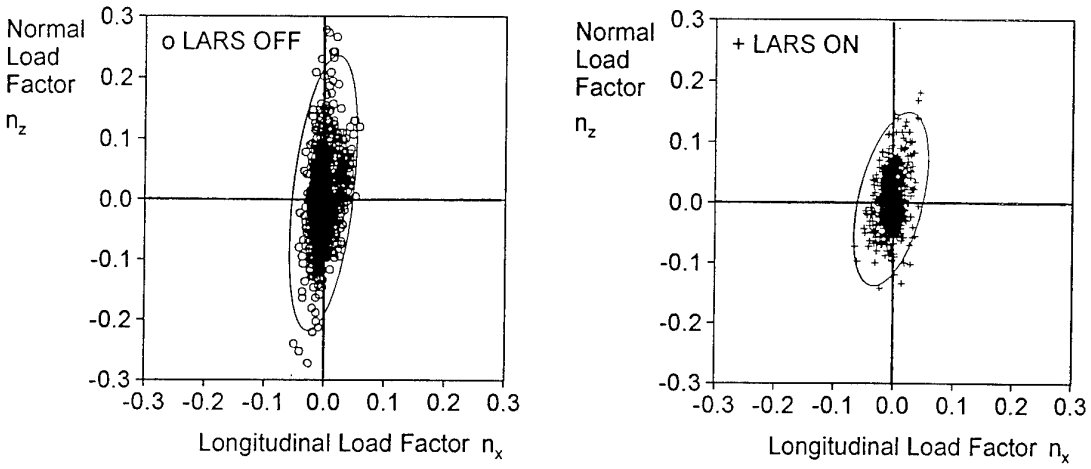

Fig 21: Load Factor Distribution in the Aircraft Symmetrical Plane
(ATTAS Flight Test)

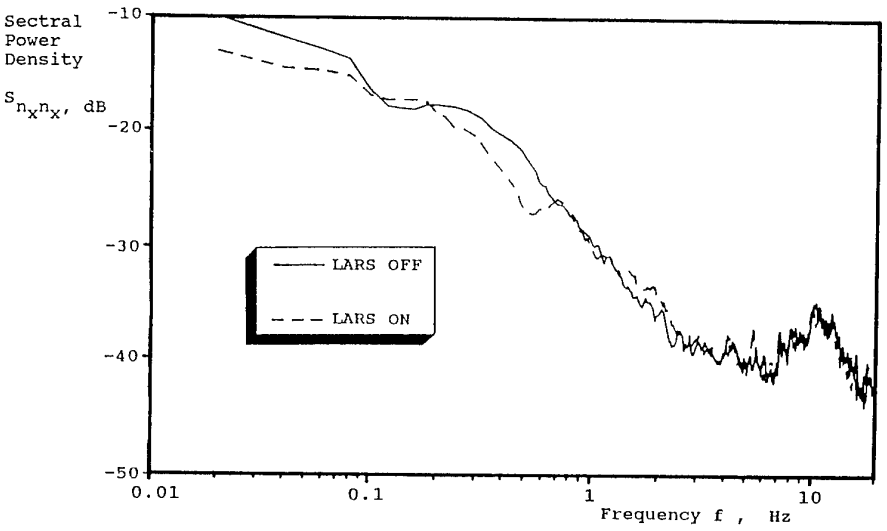

Fig 22: Spectral Power Density of the Longitudinal Load Factor
(ATTAS Flight Test with Pre-Deflected DLC Flaps)

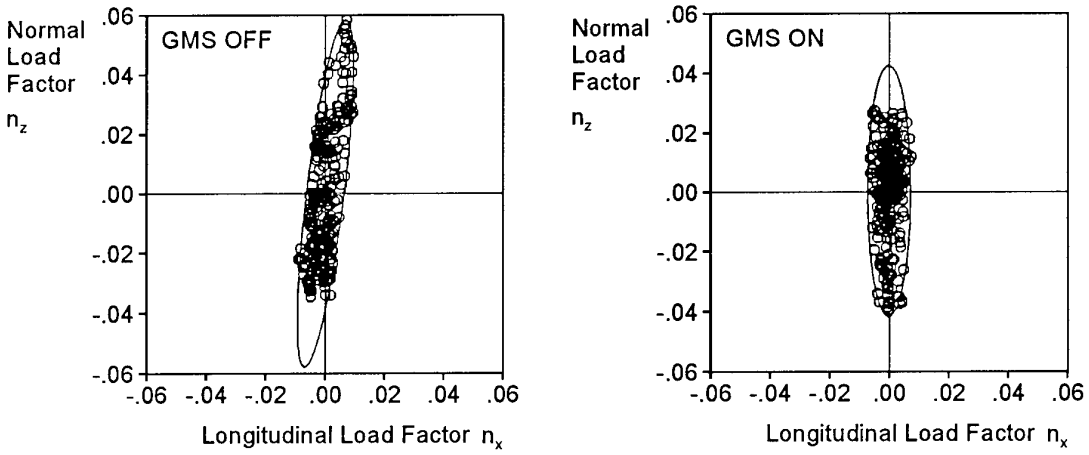

Fig 23: Load Factor Distribution in the Aircraft Symmetrical Plane (ATTAS Flight Test with Drag Control)

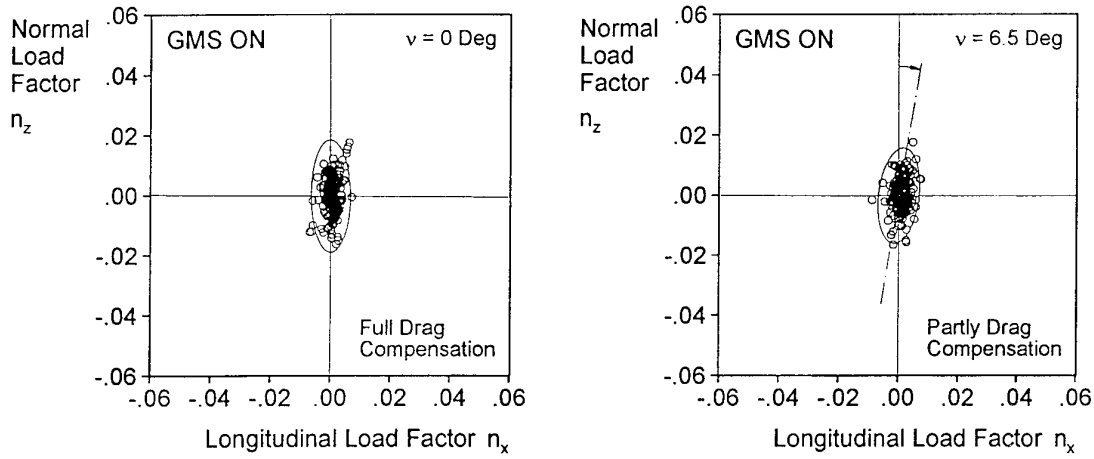

Fig 24: Load Factor Distribution in the Aircraft Symmetrical Plane (Simulation with Full and Partly Drag Compensation)

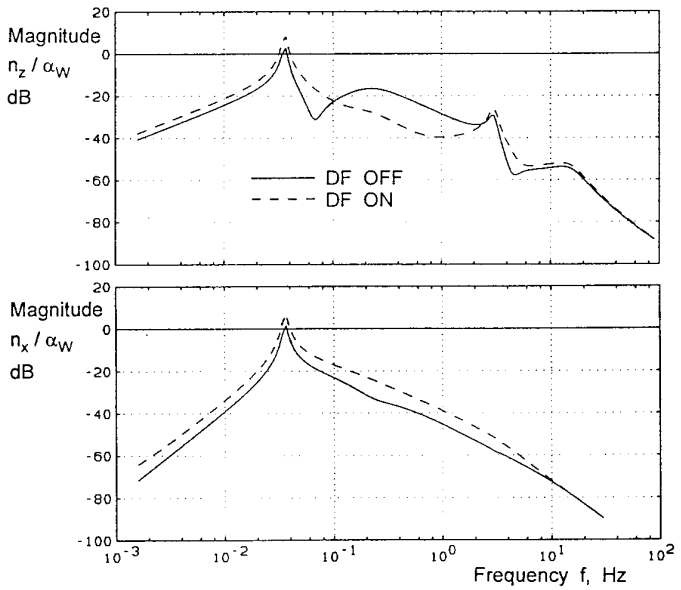

Fig 25: Frequency Response of Normal and Longitudinal Loads (Do 328)
Symmetrical Ailerons and Elevator Feed Forward Control

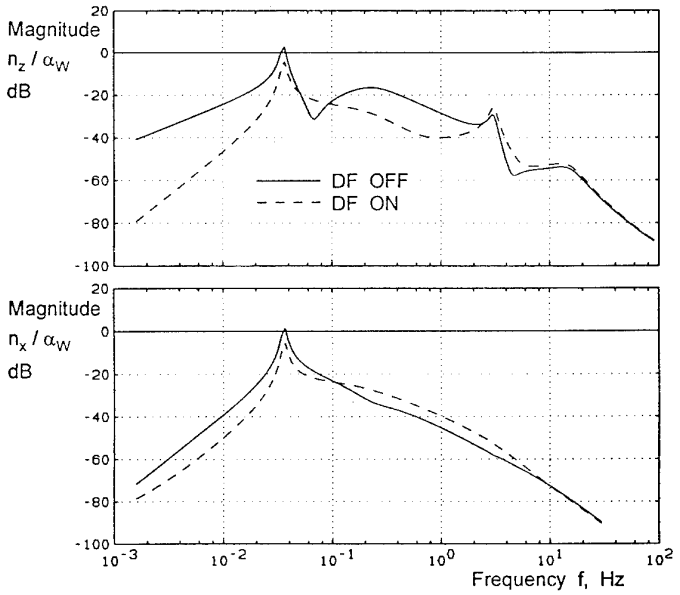

Fig 26:
Frequency Response of Normal and Longitudinal Loads (Do 328)
Symmetrical Ailerons, Elevator and Thrust Feed Forward Control

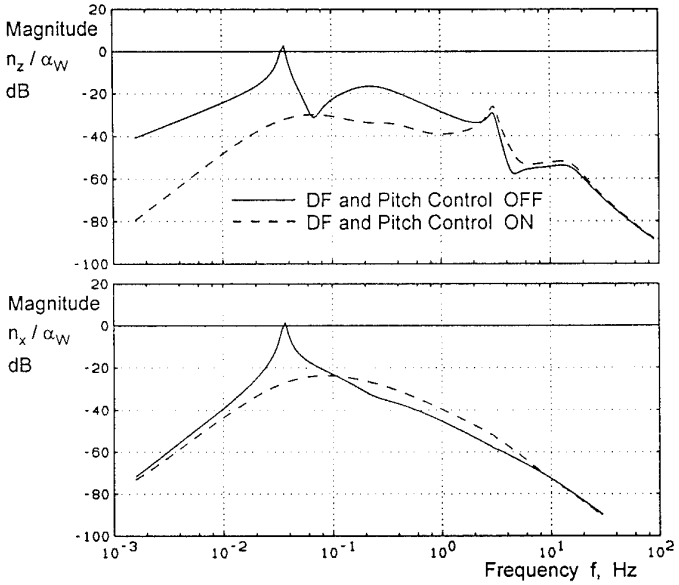

Fig 27:
Frequency Response of Normal and Longitudinal Loads (Do 328)
Complete Feed Forward Control and Closed Loop Pitch Control

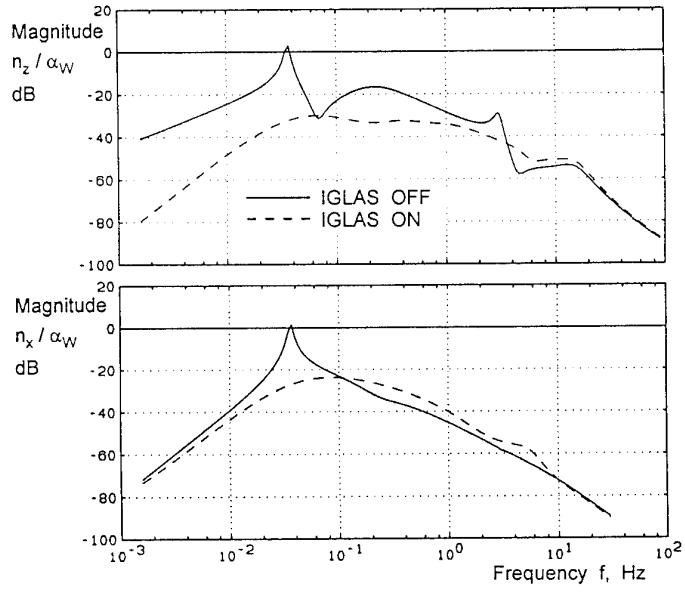

Fig 28:
Frequency Response of Normal and Longitudinal Loads (Do 328)
Complete IGLAS

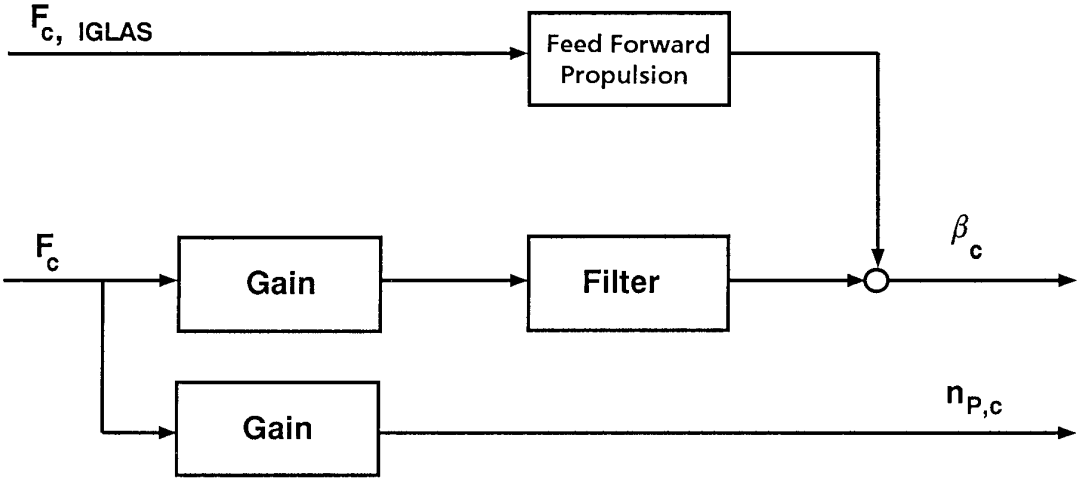

Fig 29: Set-Point Generator of the Full Authority Digital Engine Controller

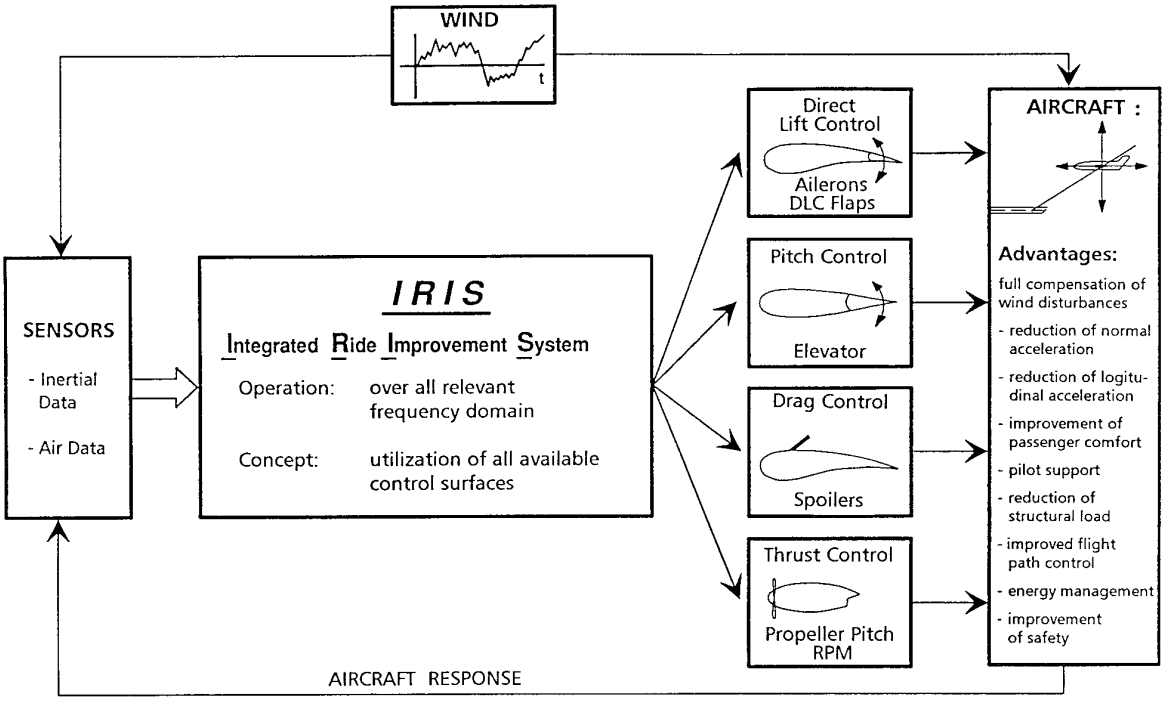

Fig 30: Concept of the Integrated Ride Improvement System with Full Wind Disturbance Compensation

Flight Evaluation of Forebody Vortex Control in Post-Stall Flight

by

Dr. Lawrence A. Walchli

Wright Laboratory
Flight Dynamics Directorate
Wright-Patterson Air Force Base, Ohio 45433
USA

ABSTRACT

Loss of directional stability in a post-stall flight environment has become a major design issue for future fighter aircraft. Numerous studies have addressed this issue, either from an aerodynamics perspective or through use of propulsive forces generated by vectoring exhaust nozzles. The X-29 aircraft, with its forward swept wing and other advanced technologies, suffers loss of directional power above 40 degrees angle of attack (AOA). An exploratory development program was undertaken on this configuration to regain the lost stability through use of a pneumatic system on the aircraft nose which influenced the external flow field, generating significant side forces useful for control. Wind tunnel test results were inserted into the X-29 flight simulator at NASA Dryden Flight Research Facility and the simulator was used to support a critical flight experiment of this technology. This experiment is the subject of this paper.

INTRODUCTION

The specific solution for enhancing directional control at high AOA which is presented herein is an aerodynamic one--specifically, forebody vortex control. The X-29, with its slender F-5A nose, produces exceptionally strong forebody vortices at angles of attack above 15 degrees. These vortices, when asymmetric, can produce yawing moments on the aircraft which are unpredictable and unwanted. This was clearly demonstrated during the X-29 High Angle-of-Attack Program (Reference 1). At 45 degrees AOA and 30K feet altitude, the aircraft exhibited a nose-right tendency which could be opposed successfully with rudder input by the pilot once he knew the tendency existed. At 50 degrees AOA, the direction reversed, and even when the pilot anticipated the motion, he could not arrest the very gradual nose-left slide without decreasing AOA. The effect was clearly a function of altitude; at 15K feet, the nose-left slide occurred at 53 degrees with a much more sudden onset. Symmetricizing the shedding vortices, thereby eliminating uncommanded yawing moments, is one potential use for forebody blowing.

The antithesis to symmetry is to stabilize the system, on demand, in an asymmetric pattern. This pattern clearly generates yawing moments on the airframe which can be useful, rather than detrimental, for control. A fighter aircraft, operating at high AOA, requires adequate directional control power to coordinate velocity vector rolls. However, under these flight conditions, rudder power is actually decreasing because of blanking by the fuselage. Vortex flow control (VFC) provides a solution to this problem. As angle of attack increases, the side forces generated by a stabilized asymmetric vortex system increase, off-setting the loss in rudder power. For a more detailed discussion of the importance of forebody vortices, see Reference 2.

Much work has already been described in Reference 2 concerning the early development work on pneumatic forebody vortex control. The program described here built on much of this early work. For example, it was a basic assumption that the individual nozzle concept we chose to pursue needed choked, underexpanded flow for best effectiveness. This criteria ensures maximum blowing momentum at the nozzle exit for a given weight flow.

The one criteria that needed to be met for a successful transition to flight had never before been achieved. A blowing system needs a working medium which is available and easily accessible on-board the aircraft without significant performance penalty. Engine bleed air is the most likely candidate. Current fighter engines can produce excess bleed flows up to about one pound per second at high altitude and low Mach number. Until now, blowing systems have required at least three times that amount to be effective. The system utilized in this experiment required only about one half of a pound per second at 0.2 Mach and 35k feet. Two important points need to be made. The experiment did <u>not</u> use engine bleed, but rather nitrogen carried on board in high pressure bottles. Further, the VFC experiment was performed <u>outside</u> the flight control system, an open-loop experiment.

AIRCRAFT, FLIGHT CONTROL SYSTEM AND VFC SYSTEM DESCRIPTION

The X-29 integrates several different technologies into one airframe as

Paper presented at the Flight Mechanics Panel Symposium held in Turin, Italy, from 9-13 May 1994.

depicted in Figure 1. The aeroelastically tailored composite wing covers cause the forward swept wing to twist as it deflects, successfully delaying wing divergence. The thin supercritical airfoil, coupled with the discrete variable camber produced by the double-hinged full span flaperons, provide optimum wing performance at all flight conditions. The aircraft was designed to be 35 percent statically unstable by adding a close-coupled, variable incidence canard, without which the wing-body combination would be near-neutrally stable. The canard, which has an area about 20 percent of the wing area, produces lift and its downwash delays flow separation at the wing root. The three-surface pitch control--the canard, flaperon, and strake flap--is used by the digital fly-by-wire flight control system to control an otherwise unflyable unstable vehicle. The success of the X-29 really rests with the integration of these technologies into a single synergistic configuration built for drag reduction in turning flight. Additional details of the aircraft can be found in Reference 3.

The X-29 flight control system (FCS) is a triplex digital fly-by-wire system with triplex analog backup (as shown in Figure 2). The fail-op/fail-safe system used MIL-F-8785C and MIL-F-9490D specifications as design guides. Flying quality design goals were Level I for the primary digital mode and Level II for the analog back-up mode.

Normal aircraft operation is accomplished through the normal digital (ND) mode with its associated functional options such as automatic camber control (ACC), manual camber control (MCC), speed stability, precision approach control, and direct electric link. ND also contains options in its gain tables for power approach, up-and-away, and degraded operation.

The normal digital mode has a pitch rate control law with gravity vector compensation, driving a discrete ACC system. This mode is gain-scheduled as a function of Mach number and altitude and incorporates a sophisticated redundancy management system allowing fail-op/fail-safe flight. MCC is a pilot-selected, fixed flaperon sub-mode of ND normally used for landing.

The analog reversion (AR) mode is the back-up flight control system, designed to bring the aircraft safely back to base. The AR mode provides a highly reliable, dissimilar control mode to protect against generic digital control failures. It incorporates functions similar to those of the ND mode. AR contains no longitudinal trim capability or pitch loop gain compensation with dynamic pressure while the aircraft is on the ground. In all other aspects, it performs like the ND control system.

In the post-stall region of flight, the aircraft has all-axis maneuvering capability to 40 degrees AOA, and pitch-only maneuvering to as high as 70 degrees AOA. A spin prevention logic is active above 50 degrees or below minus 25 degrees AOA with increasing yaw rate. The logic increases the authority of both the rudder pedals and lateral stick and disconnects all other lateral/directional feedbacks. Besides the spin prevention logic, an aileron-to-rudder interconnect provides for better roll coordination at high AOA. Also assisting in roll coordination is a rate-of-sideslip feedback to the rudder. Since substantial wing rock was predicted for the X-29 above 30 degrees angle of attack, a high gain roll rate-to-aileron feedback loop has been added to compensate for the unstable rolling moment coefficient due to roll rate. For a more detailed description of the control system, see Reference 4.

The new system, installed in the X-29 to facilitate the conduct of the control enhancement experiment, is the VFC system shown in Figure 3. Two Kevlar-wrapped, aluminum-lined storage bottles carry up to 13 pounds of 6000 psi gaseous nitrogen (GN_2) aloft. The gas pressure is reduced through two stages of regulation to a nozzle reservoir pressure of 400 psi. Flow can be directed by the pilot through the left, right, or both nozzles. Weight flow is calculated from pressure and temperature measurements at two locations -- near the storage tanks and a very precise calculation just upstream of the calibrated nozzles. Location of the system in the X-29 is shown in Figure 4. Additional system details can be found in Reference 5.

One objective of the critical experiment reported herein was to provide design details and information to future programs to allow integration of this VFC technology into both the aircraft environmental and propulsion subsystems and the aircraft flight control system. To be an active part of the FCS, the blowing jet supply must be regenerative. Engine bleed air is the only such source on-board the aircraft. The pneumatic system used in the current experiment required only about one half pound per second flow rate, a quantity well within the continuous excess bleed-air capability of current fighter engines. It is clearly feasible, then, that engine bleed can indeed power a fully integrated VFC system.

This VFC experiment was installed on the X-29 outside the flight control system, an open-loop experiment designed to provide a basis for correlating wind tunnel and flight aerodynamic data. Since the general response of the flight control system was to oppose any motion generated by the VFC jet-induced forces, direct determination of aircraft stability and

control derivatives with VFC active was not practical. But since the aircraft had been thoroughly tested at similar conditions without jet blowing, increments due to blowing could be determined quite easily. Hence, a thorough knowledge of the X-29's performance, with and without VFC, provided the information necessary for imbedding VFC in a future flight control system.

WIND TUNNEL TEST PROGRAM

Wind tunnel tests (Reference 6) were conducted in order to study the effects of forebody jet blowing on the X-29 configuration. The data from these tests were used to further the understanding of the vortex control phenomena, optimize a system for flight, and provide all necessary inputs for modeling the system in the X-29 flight simulator.

Concentrated design optimization tests were conducted on an X-29 forebody model with variations in nozzle pointing angle and nozzle exit shape (Reference 7). The goal of the tests was to provide the highest yawing moment for the least amount of weight flow. Figure 5 shows the performance of the optimum configuration over the full angle-of-attack range tested. Significant levels of yawing moment are attainable over this entire range. It is clear that at the low blowing rates (those of practical interest for flight) the control effectiveness becomes almost constant between 35 and 50 degrees AOA.

Figure 6 shows the performance of the optimum nozzle design on the full aircraft configuration in comparison with the X-29's rudder power throughout the angle-of-attack range tested. This design generates yaw power on the order of maximum available rudder anywhere above 20 degrees AOA for this blowing rate. Trend with angle of attack was well behaved and only weak dependence on AOA was observed. The sideslip trends at 35 degrees AOA shown in Figure 7 are also well behaved. These data show that the effectiveness was virtually independent of sideslip angle.

Aircraft pitch control power is a critical parameter at very high angle-of-attack conditions and pitching moment increments due to forebody vortex control can aggravate the problem. Figure 8 presents the effects on the pitching moment versus sideslip at 40 degrees angle of attack. A nose-up increment was observed at zero beta on the order of $\Delta C_M = 0.05$. The increments at sideslip depended on whether the upwind or the downwind jet was active. The downwind jet, which is the one responsible for initiating and maintaining the sideslip condition, generated a desirable nose-down pitching moment. The upwind jet, which would return the aircraft to zero beta, generated an undesirable nose-up increment. The observed increments are substantial, but fall within the nose-down authority of the X-29 aircraft up to 50 degrees AOA.

X-29 REAL TIME SIMULATIONS

Wind tunnel testing provided static aerodynamic coefficient data due to VFC through 45 degrees AOA and 9 degrees of sideslip. However, no dynamic wind tunnel aerodynamic data were obtained for the VFC program. This lack of dynamic data left several unknowns prior to flight. These included the effect of VFC on wing rock, the ability to arrest a VFC-induced yaw rate, and the effect of VFC on an existing zero-sideslip yaw asymmetry. The flight program was therefore designed to go beyond static data validation and investigate the effects of existing aircraft rates, aerodynamic delays or hysteresis, and changes to the basic aircraft dynamic stability associated with VFC, not only for data purposes but for safety of flight. To this end, the real time simulations became critical to the success of the flight test program.

The X-29 real time simulator at NASA Dryden was a fixed-base simulator with limited visuals presented on a 19-inch monitor (Reference 8). The simulation was run on a Gould SEL3297-80 computer. The VFC model was added to both the All-FORTRAN and the hardware-in-the-loop (HIL) versions of the simulation. The All-FORTRAN version was adequate for engineering analyses, while the HIL version was used for mission planning and pre-flight practice. The simulator cockpit was modified with the same VFC controls as the aircraft.

Generally, full configuration wind tunnel test data were used to incrementally update the most current flight-updated aerodynamic model residing in the simulator. Simulations were performed to assess and analyze the time history solutions to the six degree of freedom (6-DOF) equations of motion. Maneuvers evaluated corresponded to the maneuvers planned for flight.

Two categories of X-29 simulator modifications were specifically required for the VFC program -- the addition of software to simulate the fluid mechanics of providing nitrogen to the VFC nozzles, and the addition of aerodynamic data to simulate the effects of the mass flow coefficient (C_μ) on aircraft dynamics. Simulation of the fluid mechanics of the system was based on ideal gas equations and on the known characteristics of generic pressure regulators. Because little was originally known about the response of the pressure regulators to opening and closing commands, the simulation was designed to give the user the ability to quickly alter the operating characteristics of the regulators. For

example, the output pressure of each regulator, while defaulted to the design output pressure, could be altered to account for inaccurate regulation or failures. In addition, the opening and closing transients of each regulator were modeled through the use of both a simple time delay and a first order filter. The simulation user had the capability of modifying regulator performance by adjusting the delay and/or time constant for the opening and/or closing transient. This feature was not only beneficial for flight test planning, but was also required for emergency procedure development and to assure simulation-to-flight agreement. Nozzle size could also be modified by the user as a quick way to change VFC strength.

The baseline aerodynamic VFC data was added to the existing high angle-of-attack aerodynamic model through the use of incremental data tables. Tables were developed for five aerodynamic coefficients (axial force increments were insignificant) as functions of angle of attack, angle of sideslip, canard position, and C_μ. All asymmetries in the wind tunnel data, such as slight differences in the effectiveness of the left and right nozzle, were included in the simulation data tables.

In addition to the baseline VFC wind tunnel data tables, the option of adjusting the VFC aerodynamics was added in the form of additional incremental tables (called VFC delta tables). These tables were included in a file separate from the baseline VFC data tables so that the user could create a new file containing adjustments to the VFC model which were specific to each simulation task. This flexibility greatly improved the productivity of the simulation in flight planning and data analysis.

Reference 8 gives an excellent and comprehensive description of the various uses of the real time simulation. It was routinely used for maneuver design, parameter variation studies, and the establishment of flight limits.

Typical real time simulation results are presented in summarized form in Figure 9. Values shown resulted from a three second pulse of the VFC system. Figure 9a shows the maximum sideslip angle observed versus angle of attack for both left and right side blowing. Sideslip angle peaked at 25 degrees AOA and then gradually decreased to zero above 40 degrees. The region 40 and above was actually an unsteady motion due to baseline roll oscillation and the data plotted in this range were the observed mean values.

A summary of the roll rate history is shown in Figure 9b. Here the body roll rate was essentially constant up to the onset of roll oscillation. Beyond this point, as in the case of sideslip, the mean value was observed to be zero.

Figure 9c shows the yaw rate trend with angle of attack. Unlike sideslip and roll rate, the yaw rate continued to increase with angle of attack and did not exhibit oscillation. Yaw rates generated by VFC more than doubled in magnitude from low to high AOA. The high AOA cases demonstrated additional complications to the coupling problem in that the yaw rate increased more rapidly and took longer to reach maximum levels. This generated a serious flight test concern for pitch axis inertial coupling during event times greater than 5 seconds or for large variations in lateral/directional dynamic derivatives.

FLIGHT TEST RESULTS

Previous X-29 testing proved the difficulties of identifying aerodynamic coefficients at elevated angles of attack. The combination of inertial and kinematic coupling, large aerodynamic nonlinearities, and increased instrumentation inaccuracies were major contributors to these difficulties. Once identified, proper incorporation of the aerodynamic coefficients into the aerodynamic database was critical. This is a very important lesson learned in this flight experiment (Reference 9). The ability to quantify effects due to VFC would have been almost impossible without the understanding of the basic aircraft aerodynamics gathered from the high angle-of-attack expansion in the earlier flights.

Identification of aerodynamic coefficients was accomplished using three basic techniques that consisted of total coefficient matching, parameter estimation, and batch simulation. These techniques were developed and used successfully during the X-29 High AOA Program (Ref. 4). The results of these techniques were complementary and when combined formed the basis of the flight-derived aerodynamics. The results were then used to update the nonlinear 6-DOF math model for the real time simulator.

The best measure of the effectiveness of VFC is the control derivative of yawing moment due to blowing, $Cn_{C\mu}$. The selected data shown in Figure 10 represent the results obtained from one second pulses of the VFC system during stabilized 1G high angle-of-attack test points with less than one degree of sideslip. Figure 10 shows the VFC control derivative that was required to most closely match the flight-measured yawing moment coefficient using the measured mass flow coefficient. At angles of attack above 35 degrees, the wing rock and zero sideslip asymmetries of the basic aircraft complicated the analysis of the VFC flight data, resulting in the increased scatter that can be seen at 40 degrees angle of

attack. In general, the correlation between wind tunnel and flight data at zero sideslip was good, with most discrepancies being caused by the natural dynamics of the flight test vehicle during high angle-of-attack flight.

Figure 11 shows the VFC effectiveness at 35 AOA due to sideslip angle. Similar to the previous figure, all results are from one second pulses of the VFC system. The difference in these maneuvers was that the pilot attempted to use full pedal to get a maximum wings-level sideslip angle prior to the VFC pulse. Rather than being presented against the actual left or right sideslip angle, the data are presented based on whether the sideslip direction corresponded to the VFC direction. The points shown on the left side of the plot are the result of maneuvers in which VFC was used to reduce the pre-established sideslip. Points on the right side of the plot resulted from activating the VFC jet on the same side as the sideslip direction, thereby increasing the sideslip angle.

The results show that VFC strength does not decrease much when blowing on the same side as the pre-established sideslip; its strength does degrade somewhat when blowing on the opposite side. This suggests that while VFC may be very useful for extended-duration maneuvers, during which VFC causes moderate increasing sideslip, it will not be as effective in reducing a pre-existing sideslip angle.

Also shown in Figure 11 are the results of two "conventional roll" maneuvers in which a short VFC pulse was used to oppose the yaw rate generated by a full-stick roll. Results from these and other similar maneuvers were very similar to the results of the stabilized pulses, indicating that aircraft rates do not significantly influence VFC effectiveness.

Figure 12 shows the results of a "VFC-Roll" at 40 degrees AOA. The maneuver consisted of stabilizing the aircraft in 1G flight at the target angle of attack, activating the left VFC nozzle until a target yaw rate was reached, then switching to the right nozzle in order to stop the VFC-induced rate. The maneuver was flown with the lateral stick and rudder pedals neutral.

The purpose of this maneuver, beyond the demonstration of a pure-VFC roll, was to examine the aerodynamic time delay associated with switching from one nozzle to the other. This data is essential for the design of a VFC-based flight control system and can not be obtained from static wind tunnel tests. As can be seen, the time for the full reversal of the nozzle flow was about 0.1 seconds while the yawing moment reversed in less than one half second. The yaw acceleration after the reversal is as strong as the initial value. These results compare very favorably with a wings-level rudder kick. This bodes especially well for using VFC as a fully integrated control effector in a flight control system.

One of our program goals was to determine the effects of VFC on wing rock. On the X-29, as on other aircraft with slender forebodies, it has been shown that the wing rock behavior is actually a body rock caused by the oscillatory motion of the forebody vortices. With only static wind tunnel test data available prior to flight, the VFC team believed that because VFC overpowered the natural position of the vortices it would prevent the motion of the vortices with respect to the forebody and thereby eliminate wing rock.

Figure 13 shows the time-history of a 1.5 second VFC pulse at 40 degrees angle of attack. As seen in the sideslip data, this maneuver begins with typical wing rock at 0.5 Hz with a magnitude of ±2 degrees sideslip. The VFC pulse begins at a time of 1.8 seconds, and it is clear that wing rock is not eliminated. While the average sideslip angle shifts slightly nose-left, the frequency and amplitude of the wing rock remain relatively constant. It is now believed that while VFC may determine the position of the vortices over the forebody, it can not prevent the oscillatory motion over the canopy region and vertical tail as the forebody vortices propagate out of the influence of the blowing further aft on the aircraft.

VFC INTEGRATED SYSTEM DESIGN

With a solid understanding of VFC and its static and dynamic effects on an aircraft in post-stall flight, it is now necessary to integrate this new control effector into an aircraft's flight control system. In the simplest terms, this involves specifying maximum authority and response dynamic characteristics. The maximum authority required is derived from studies of maneuver rates required and provides the specified mass flow rate that must be supplied to the nozzles. Response dynamics, e.g. control bandwidth or equivalent system time delays, are derived from flying qualities requirements. These dynamic requirements can then be used to define the switching characteristics in order to meet them.

A simplified scheme was used by Adams and Buffington (Ref. 10) in a study to determine the incremental benefits of VFC on the Variable In-Flight Simulator Test Aircraft (VISTA) F-16 aircraft. Their approach was to design the blowing control laws around the existing Block 40 VISTA F-16 flight control system (Figure 14). Their blowing system model is a fast-acting

(0.10 second time delay) on-off actuation system with three possible states of actuation -- left valve open, right valve open, or both valves closed. The blowing system transitions among these three states based on a switching surface, $\sigma(x)$, and a dead band, δ. The switching surface is a function of aircraft state, e.g. sideslip, roll rate and yaw rate. The dead band represents a region about the switching surface within which the blowing system is turned off. The switching surface is used to provide acceptable stability and performance while the dead band is selected to prevent undesirable control action. The symbol F represents the switching surface gain matrix. Note from Figure 14 that the active blowing system is contained within the dashed box. If the outer loop is broken, either by design or during some system failure, the control system reverts to the baseline Block 40 F-16 control laws. Clearly, this scheme for incorporating VFC into the control system is adequate for the purpose of establishing incremental benefits from VFC.

It is not certain that the stability and controllability of the preceding study could be realized in a practical system. A very fast on-off actuation was assumed and there are also likely to be lags in moment generation that were not modeled. Another option is to use continuous control of the blowing coefficient C_μ. In control law design, it is convention to specify a requirement for a rate of movement of a control surface in terms of degrees per second. A typical rudder requirement might be 60-80 degrees per second. Obviously, what is really being specified is a rate of generation of aircraft yawing moment $\gamma C_n/\gamma t$. From the data that was acquired during the X-29 flight test of an open-loop VFC experiment, we can show that an equivalent requirement for a VFC effector could be stated as $\gamma C_\mu/\gamma t$, thereby providing the system design requirement for control valve response. This additional independent variable can then be used to tailor the characteristics to overall system requirements.

Since forebody blowing serves as a roll coordinator and sideslip regulator, functions satisfied by the rudder at low angles of attack, it behooves the designer to integrate $\gamma Cn_{c\mu}/\gamma t$ (blowing) with $\gamma Cn_{dr}/\gamma t$ (rudder) over the entire flight envelope of the aircraft. The combined system would then produce the yaw control power displayed in Figure 15. The system would be robust enough to coordinate any rolling maneuver within the confines of the aircraft's operational envelope.

An example of this integration is shown in Figure 16 (Ref. 11). This is the modified lateral control law for an F-15 aircraft. Note that forebody blowing has been blended with both the horizontal tail and rudder. A six degree of freedom (SDF) solution of the equations of motion using this blended blowing model provides the roll performance improvements depicted in Figure 17. Figure 18 from the same SDF analysis shows a substantial improvement in spin recovery of the aircraft. In this simple analysis, yaw rate is stopped in 4 seconds with VFC compared with 8 seconds for the baseline system.

CONCLUDING REMARKS

A proof-of-concept pneumatic discrete port blowing experiment was conducted using the slender-nosed X-29 as a testbed aircraft. An optimum blowing configuration was developed through extensive wind tunnel testing. Results of this testing showed conclusively that very large yawing moments could be generated through nose vortex manipulation and these moments could be used to replace the loss in directional control caused by fuselage blanking of the vertical tail at high angles of attack.

This data was then applied to the X-29 piloted simulation at NASA Dryden Flight Research Facility in the form of incremental aerodynamic coefficients. The simulator was used to expand the VFC data base over the entire X-29 high AOA envelope through parameter variation, looking for any "trouble" areas which might occur. VFC system failure modes were examined carefully to ascertain such an event would cause no vehicle departures from controlled flight. Safety limits on sideslip angle, yaw rate, and the product of yaw rate and roll rate were established. Pilots were trained in the use of the on-board system and flights were begun.

Flight test results established two very important facts. First, the discrete port blowing works, in some cases better than predicted from ground test results. Second, the effects of blowing are well-behaved and therefore quite useful for an integrated effector in a control system. Undesirable inertial coupling effects combined with natural asymmetries on the X-29 limited the usefulness of VFC to AOAs below 50 degrees. The airplane simply ran out of pitch-down authority. VFC trends were all solidly predicted by the wind tunnel tests. The magnitude of the effects, being in some cases twice as powerful as predicted, is more good news. Lower blowing coefficients, using even less engine bleed air, are apparently feasible. The flight test data also showed that VFC dynamic effects were small, and aerodynamic delays during jet activation or switching were similar to normal rudder performance.

With this information in hand, several schemes for incorporating VFC into an integrated flight control system were examined. In order to use forebody blowing to its best advantage, i.e.

roll coordination and sideslip management, it was clear that the vortex flow control derivative must be blended with the rudder over the entire aircraft operating envelope. Since VFC produced such well-behaved effects both statically and dynamically, little doubt exists in the viability of successful integration. Detailed study for a given application would be needed to define whether on-off or continuous control of blowing is required.

REFERENCES

1. Walchli, L.A. and Smith, R., "Flying Qualities of the X-29 Forward Swept Wing Aircraft", AGARD-CP-508-25, October 1990.

2. Skow, A.M. and Peake, D.J., "Control of the Forebody Vortex Orientation by Asymmetric Air Injection", AGARD-CP-262-24, May 1979.

3. Walchli, L.A., "A Look At Tomorrow Today", AGARD-CP-465-13, October 1989.

4. Pellicano, P., Krumenacker, J. and Vanhoy, D., "X-29 High Angle-of-Attack Flight Test Procedures, Results, and Lessons Learned," Society of Flight Test Engineers 21st Symposium, August, 1990.

5. Walchli, L.A., et. al., "High Angle-Of-Attack Control Enhancement On A Forward Swept Wing Aircraft", AIAA-92-4427, August 1992.

6. Maerki, G.S., "Post Test Report of a Low Speed Wind Tunnel Test on a 1/8 Scale Model of the X-29 Aircraft with Vortex Flow Control", Grumman Aircraft Systems Division No. X29-396-TR-9101, February, 1991.

7. Cornelius, K.C., Pandit, N., Osborn, R.F., and Guyton, R.W., "An Experimental Study of Pneumatic Vortex Flow Control on a High Angle-of-Attack Forebody Model", AIAA 92-0018, January, 1992.

8. Krumenacker, J. and Pellicano, P., "Flight Simulation and Data Analysis During A High Angle of Attack Vortex Flow Control Flight Test Program", AIAA 92-4108, August, 1992.

9. Moorhouse, D., Walchli, L. and Krumenacker, J., "Results and Lessons Learned from Two Wright Laboratory Flight Research Programs," AIAA-93-3661, August, 1993.

10. Adams, Richard J. and Buffington, James M., "Active Vortex Flow Control for High Angle of Attack Flight," IEEE Conference on Decision and Control, San Antonio, Texas, December 1993.

11. Doane, Paul, McDonnell Douglas Aerospace, St. Louis, Missouri, direct correspondence on 21 January 1994.

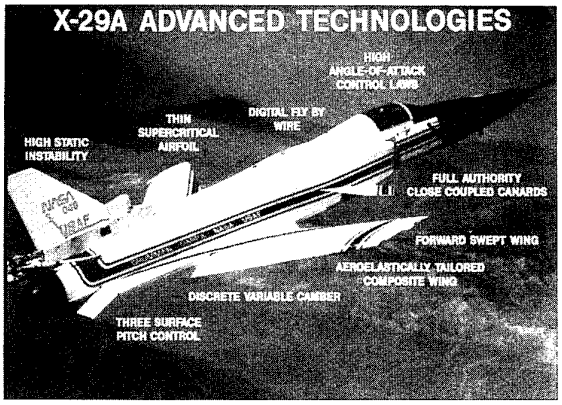

FIGURE 1. X-29 TECHNOLOGIES

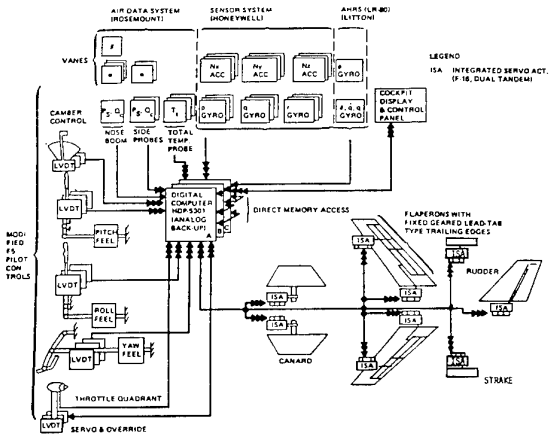

FIGURE 2. X-29 FLIGHT CONTROL SYSTEM

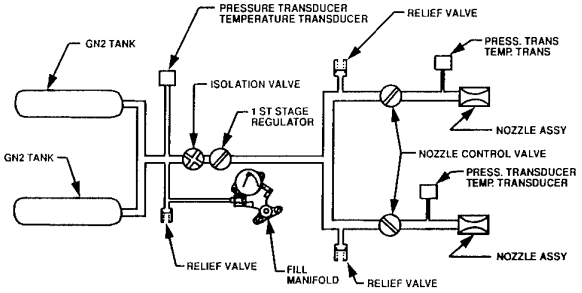

FIGURE 3. VFC SYSTEM SCHEMATIC

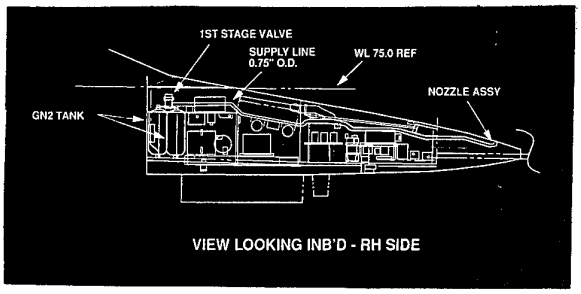

FIGURE 4. VFC SYSTEM INSTALLATION

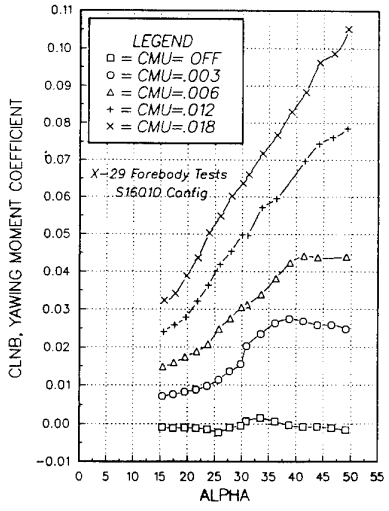

FIGURE 5. SLOTTED NOZZLE EFFECTIVENESS

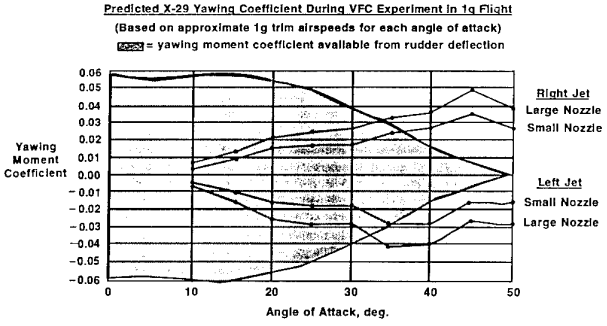

FIGURE 6. YAWING MOMENT PREDICTION

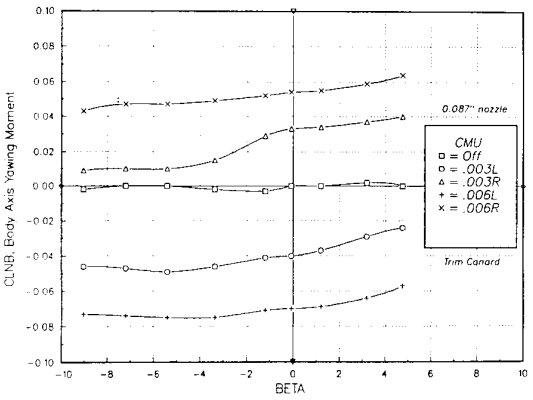

FIGURE 7. FULL MODEL SIDESLIP TRENDS

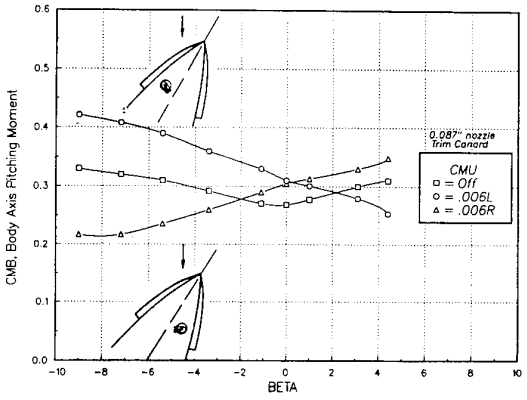

FIGURE 8. BLOWING-INDUCED PITCHING MOMENT TRENDS

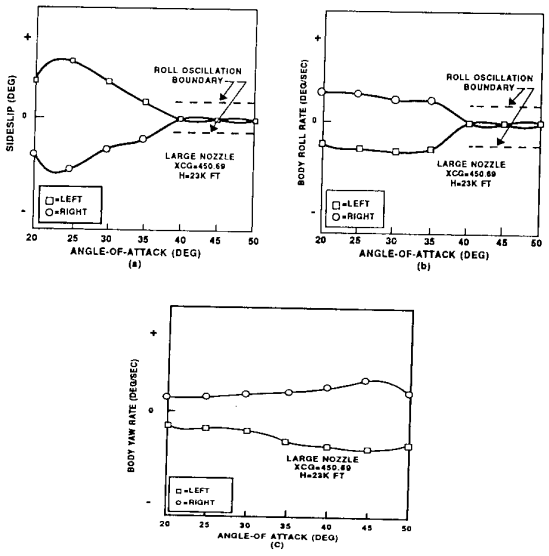

FIGURE 9. REAL TIME SIMULATION OF A THREE SECOND PULSE

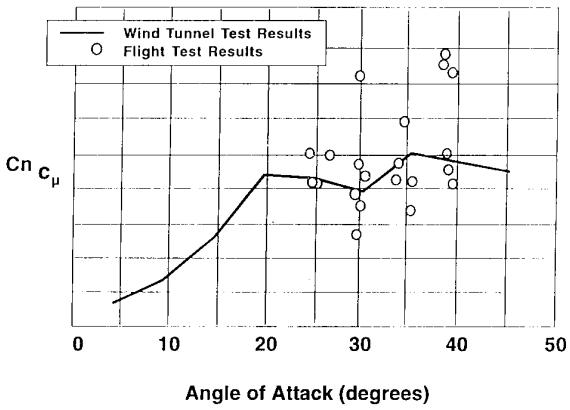

FIGURE 10. **VFC EFFECTIVENESS AT ZERO SIDESLIP**

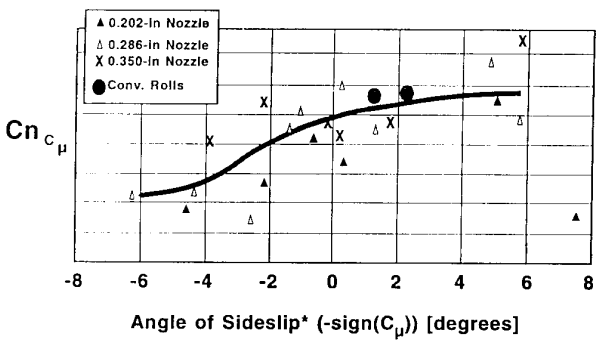

FIGURE 12. **VFC EFFECTIVENESS AT 35AOA**

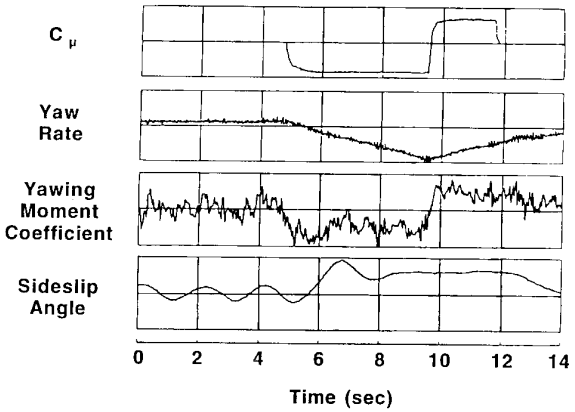

FIGURE 12. **"VFC-Roll" at 40AOA**

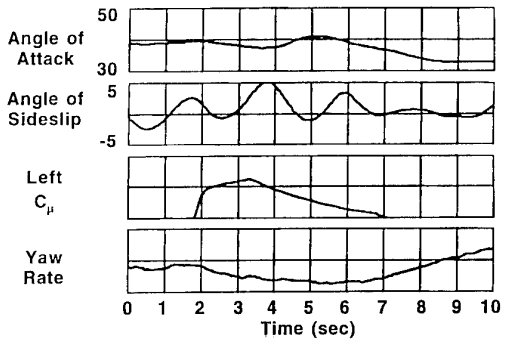

FIGURE 13. EFFECTS OF VFC ON WING ROCK

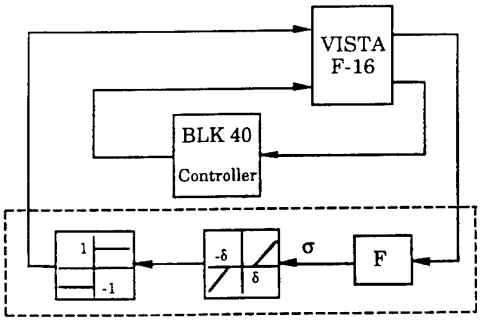

FIGURE 14. FOREBODY BLOWING CONTROL SYSTEM

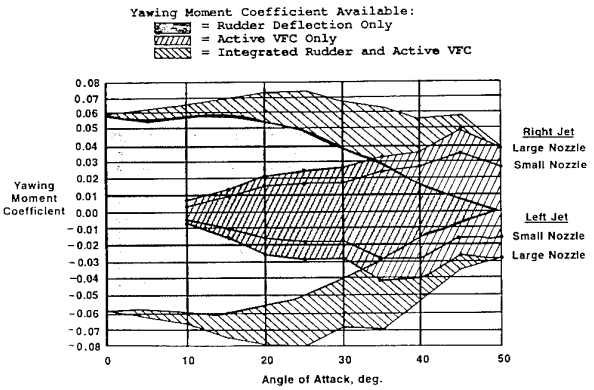

FIGURE 15. INTEGRATED YAWING MOMENT PREDICTION FOR RUDDER AND ACTIVE VFC

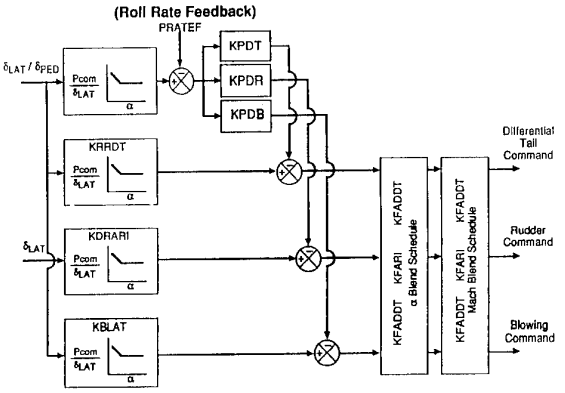

FIGURE 16. PROPOSED F-15 LATERAL CONTROL LAWS WITH ACTIVE VFC

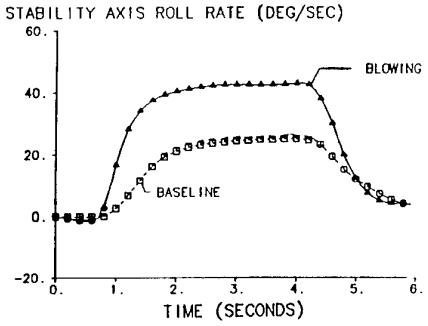

Angle of Attack = 30° Mach = 0.5 Altitude = 20kft
0.25 Second Valve Opening Time, $C_\mu \approx 0.0011$

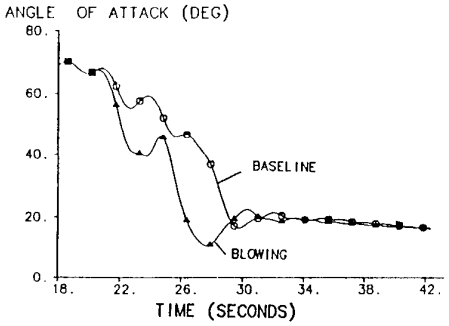

Steady Spin Mach = 0.27 $C_\mu \approx 0.0038$
0.5 Second Valve Opening Time

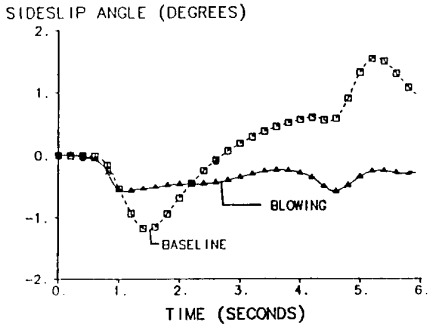

FIGURE 17. F-15 ROLL PERFORMANCE WITH ACTIVE VFC - 6-DOF ANALYSIS

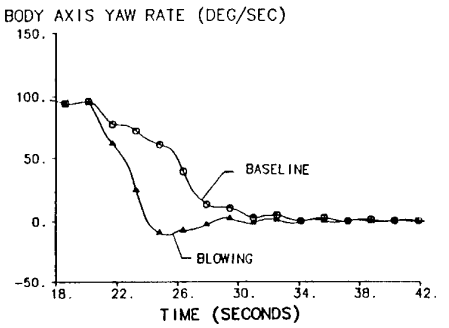

FIGURE 18. F-15 SPIN RECOVERY WITH ACTIVE VFC

Automatic Flight Control System for an Unmanned Helicopter
System Design and Flight Test Results

M. Weidel
W. Alles
Dornier Luftfahrt GmbH
88039 Friedrichshafen
Germany

1. INTRODUCTION

The use of unmanned air vehicles (UAV) in support of the Navy from small ships to fulfill tasks such as reconnaissance of large areas will succeed only, if the user gains a high amount of confidence in the reliable operation of such a system, especially during the take off and landing phase. Take off from and landing on small landing pads on aviation facility ships in all-weather conditions prefer the application of VTOL-UAV's (Vertical Take Off and Landing) with a coaxial rotor system. Manual take off and landing procedures which have to be applied during operational service both at day time and at night under all-weather conditions and ship motions overtax the service personal already at low sea-states. This fact requires automatic take off and landing procedures.

The German Ministry of Defence commissioned Dornier (DASA) in November 1990 with the development, test and demonstration of an automatic take off and landing system on the basis of the Gyrodyne QH-50 drone helicopter in order to prove the feasibilty of such a system in general. The essential ship and sea state dependent motions of the landing pad - roll, pitch and heave - were simulated with a ship deck simulator.

The customer's requirement consisted of ten automatic take offs and landings of the UAV from respectively on a 4 by 4 meters landing pad. The test and demonstration phase was performed on the airfield of Friedrichshafen in the presence of experts from several NATO-Countries by the end of 1991.

2. EXPERIMENTAL SYSTEM COMPONENTS

The experimental system consisted of several major components. Those are the coaxial UAV, the ship deck simulator, the operator control station and the telemetry/telecommand main control station.

The UAV in this experimental program was the drone helicopter Gyrodyne QH-50 (figure 1). The dynamic system consisting of coaxial rotor system, gearbox, engine, fuel system and landing gear could be taken over from Gyrodyne without modifications. The airborne flight guidance system which elements are Strap Down INS (inertial navigation system), digital computer and electro-hydraulic actuators were developed and integrated at Dornier as well as the bi-directional data transmission equipment for telemetry and telecommand, reflectors for the landing sensor and a magnetic anchoring device.

To simulate the essential ship motions a moving flight simulator was modified. The six degrees of freedom system has a diameter of about 6 meters and can carry a payload of 2 tons. For the flight tests and the demonstration the motion of a fast patrol boat at sea-state 3 was simulated in the relevant three degrees of freedom - roll, pitch and heave.

A laser tracking system, which means exactly a laser distance measurement unit combined with an electro-optical tracker, was mounted at a separate lever to the ship deck simulator. The distance between the laser tracker and the centre of the ship deck simulator amounts to 7.5 meters.

3. DEMONSTRATION PROGRAM

Figure 2 shows the different phases of the demonstration program. The operator initiates the mode "automatic take off". After the automatic take off from the moving shipdeck simulator the UAV has to hover in about 4 meters above the centre of the ship deck simulator while the horizontal position is kept constant. A manual flight by the operator to a position with a distance of about 30 meters and a height of about 10 meters relative to the centre of the ship deck simulator follows next. Having reached this point the operator initiates the mode "automatic hold of position". As a consequence of this operator action the UAV holds the position at the moment of initialization and is hovering.

The operator demand "automatic transition" guides the

Paper presented at the Flight Mechanics Panel Symposium held in Turin, Italy, from 9-13 May 1994.

air vehicle automatically back to the ship deck simulator about 4 meters above its center. The mode "automatic hold of position" is now active.

The last step of the demonstration program is the landing approach and finally the touch down on the landing pad of the moving ship motion simulator. As in the steps before the operator initiates this last phase by choosing the mode "automatic landing". The UAV then descends and touches down right at the moment when the landing pad on the ship deck simulator has the state "roll angle zero". With the exception of the manual transition after the automatic take off all the other airborne flight phases are executed "hands off".

Five different test stages were found essential in this straight forward, time limited flight test program up to the before mentioned demonstration program (figure 3).

We started with rotordrives on the moving ship deck simulator in order to gain confidence in the data link under realistic conditions. Basically, the main purpose of this test stage was to analyse interferences between the UAV and the ship deck simulator such as vibrations and possible spin forces as well as the test of the magnetic anchoring device.

Next came flights on a hovering fixture. The check of the control laws, especially the algorithms for stabilization of the UAV in all axes, the functionality of the landing switches which were used to close and open the control loops at take off respectively touch down, the check of the laser tracking system with moving UAV and vibration tests of rotor mast, landing gear and magnetic anchoring device were the main features during this test period.

Manual operator controlled flights containing take off and landing with non moving ship deck simulator could be performed next to check the tether which was required by the airworthiness authorities due to the Friedrichshafen airfield flight testing of the UAV.

Another functionality check of the laser tracking system was an aspect too.

Most of the flight test hours were taken into account for the functionality checks of the automatic modes of the flight control system. Thus we started with the automatic position hold to get informations about the gust and turbulence behaviour of the UAV.

Automatic take off as well as landing approach and touch down, which were doubtless the most challenging tasks, finished the flight test program.

Finally the already mentioned sequence of flight phases being required by the customer could be demonstrated successfully.

4. DEVELOPMENT STEPS

Figure 4 shows the development steps for the design of the automatic flight control and guidance system. Based on a mathematical model which was derived from aerodynamic, mass, geometric and performance data the flight control system was designed taking the requirements of the customers specification into account.

A system simulation containing models of all relevant subsystems such as UAV, ship, various hardware assumptions like sensors, actuators and compute delays was performed to verify the results achieved during the control law design. Functional tests as well as failure transients could be analysed in this design stage. The development of the airborne software was an iterative process within our design route. The control laws were programmed in the high order real time software language ADA.

A permanent verification of simulation results with the outputs of the airborne flight control computer on the test bench was one of the most important design steps. Before flight test started, a set of hardware tests of the subsystems needed to be done as well as the final integration process of those subcomponents into the overall helicopter drone system.

5. CONTROL LAW DESIGN

In terms of flight control system design the customer's requirements were transformed as shown in figure 5.

The most essential task was the stabilization of the UAV which originally was unstable in the roll- and pitch axis. Good handling characteristics were found necessary to fulfill the operator controlled manual flight phases. The most challenging task of course was the design of the automatic functions and in accordance with that a mode logic concept which allowed a safe hands off operation of the UAV.

Thus it needs to be mentioned here that the flight control system contained fully autonomous operating emergency functions in case of data link loss. Especially for the automatic landing approach and touch down a good suppression of atmospheric disturbances was required.

How the flight control and automatic flight guidance system is embedded in the overall system is presented in figure 6. The dot-dashed dividing line indicates the separation of the ground based components and the airborne subsystems. The components which were affected directly by the flight control law design are highlighted.

On ground it is a shipbased computer together with an INS which was mounted to the ship deck simulator. The

tasks of this computer consisted of the predicition of the time, when the bank angle of the ship deck simulator is zero, the transformation of the relative position data between the UAV and the centre of the landing pad from a polar to an earth-fixed coordinate system and the processing of the sensor data for the INS update filter.

The block automatic flight guidance on the airborne side is basically used to generate demand signals for the flight control system. Those demand signals are the output of the implemented mode logic concept which is activated by operator demand signals and therefore generated automatically and tailored to the required task. The control laws are contained in the block which is named flight control.

An overview on the flight controls is given next. According to the requirements the control laws are subdivided into the inner loops which are represented by the basic controller and the outer loops called position controller (figure 7). The basic controller was designed to give sufficient stability to the helicopter drone and good handling characteristics during manual operation. When operating in the automatic take off or landing mode flight guidance demand signals are fed to the basic controller as input signals. The position controller mainly fulfills autopilot tasks.

The control laws were executed in the airborne computer which is a Motorola 68020 with a 68881 co-processing unit. The program execution was organised according to the multi-tasking procedure. The basic controller operated at an update rate of 50 Hz and the position controller with 12.5 Hz.

Figure 8 shows the structure of the control loops of the basic controller. It consists of proportional and integral feedbacks combined with a feed forward path directly to the actuator. This structure was applied to all four axes of the UAV. Besides a turn-coordination between the roll and the yaw axis no further couplings between the different control loops where necessary. With the feed forward measure the transient response following an operator demand signal could be tailored easily according to the operators wish for control harmony in all axes. The demand signals coming from the position controller to achieve the required autopilot task is also fed into the basic controller. The differences between actual and demanded position signals are transformed into adequate demand signals for the basic controller.

The control variables of the basic controller are pitch attitude, bank angle, vertical velocity and yaw rate. Additional feedbacks of pitch rate and roll rate were used to give the desired damping characteristics. Lead-lag filters were applied in the pitch and roll axis in order to compensate the hardware effects. During the flight test program it was found out that notch filters had to be implemented into the inner loops of pitch and roll axis to avoid an excitation of the structural mode of the rotor mast.

The feedback and feed forward gains were determined analytically. The computation resulted from requirements for poles and zeroes of the different axes. Design flight condition was the hover state in sea level. The gains were scheduled with height to cover the operational flight envelope.

The control inputs are cyclic pitch, cyclic roll, collective pitch and so-called tip-brakes to generate the necessary yawing moment required by the basic controller. Besides the feed forward path, the structure of the position controller was the same. The control variables are the coordinates x, y and z respectively the height h which describe the position of the UAV and the heading. To improve the damping the horizontal translational velocity components were fed back too.

6. AUTOMATIC MODES

The demonstration program begins with the automatic take off. The UAV takes off from the moving ship deck simulator and flies to the first planned waypoint, about 4 meters above the centre of the ship deck simulator. To initiate the automatic take off procedure the operator has to manipulate a switch.

As it is required that the UAV leaves the landing pad as fast as possible, the collective pitch blade angle will be driven to about 75 percent of its maximum. This is only possible, if the UAV is chained to the ship deck simulator. In our experimental program a magnetic anchoring device was applied for this purpose. Proceeding like that causes a jump take off. The UAV takes off from the moving ship deck simulator with a high vertical velocity, right after the release of the magnetic anchoring device by the airborne computer at roll angle zero of the landing pad (figure 9).

In case of a failure, before the UAV leaves the landing pad, there is the possibility of an automatic break off guaranteed. A failure could for example be the loss of the ship based computer. The operator is also able to break off the automatic take off procedure manually.

The approach to the final standby position is an automatic transition. Its demand values are generated from the automatic flight guidance system. It leads the UAV on a given flight path from the last operational waypoint to the final position above the centre of the ship deck simulator.

Before the automatic landing approach and touch down the UAV must have a very accurate hold of position in

the final standby position above the centre of the ship deck simulator (figure 10). This requirement strongly depends on the performance of the laser tracking system. On the other hand it is very important to have the precise relative vertical motion between the UAV and the centre of the landing pad which is essential for the accuracy of the demanded touch down velocity. The requirement for roll angle zero of the ship deck simulator at touch down of the UAV requested a reliable prediction algorithm to indicate the right time for this landing pad state in advance.

The mode automatic landing approach and touch down guarantees an accurate descent and a precise touch down of the UAV on a very small 4 by 4 meters landing pad that permanently changes its attitude.

The descent begins at a height of about 4 meters above the centre of the landing pad. If this position can't be hold within predefined limits by the controller, for example caused by too strong atmospheric disturbances, the operator is unable to initiate the landing mode. A prediction algorithm is used to determine the time when the roll angle of the shipdeck simulator is zero. The vertical guidance of the UAV has been designed so that the landing procedure always takes the same time independent on the movement of the ship deck simulator. This means after successful initialisation by the operator the UAV begins the landing procedure right then when the predicted time for roll angle zero matches with the time defined for the landing procedure. The demanded relative vertical descent velocity is composed of analytically computed command signals and data of the vertical motion of the ship deck simulator.

Besides that, height, heading and position data coming from the flight guidance system were used as demand signals for the position controller. After touch down on the landing pad the magnetic anchoring system is immediately activated by landing switches which are attached to the landing gear.

In case of a failure, before the UAV touches down on the landing pad, there is the possibility of an automatic break off guaranteed. A failure could for example be to leave a 1 meter's diameter cylinder round the centre of the landing pad during descent. A manual break off by the operator is not possible in the final approach phase. After failure detection the UAV leaves the closer vicinity of the ship deck simulator automatically as fast as possible and remains in the mode position hold at a predefined position.

Figure 11 shows statistics of the vertical touch down speed coming from analytical simulation. A sine function with an amplitude of 0.5 meters and a frequency of 0.1 Hz together with a free chooseable phase shift was applied in the simulation to verify the design results. One can see the relative vertical touch down speed as a function of the phase shift which is presented as the time being proportional to the phase angle.

A random number generator for normal distributed numbers determined the 100 phase shifts which were analysed in the simulation. The design goal was to stay below 1.5 m/s and to stay as close as possible to the demanded relative vertical touch down speed, which was 0.8 m/s in our case.

A similar investigation was performed to check another main feature of the automatic landing mode. Figure 12 shows the statistics of the roll angle of the ship deck simulator, also as a function of the before mentioned phase shift. The roll motion of a fast patrol boat at sea state three was simulated with a sine function of amplitude 3.5 degrees and 0.07 Hz frequency.

7. SUMMARY

The stabilization of the UAV could be performed as the result of a very simple control law structure combined with an analytical design method of the gains. The operators of the UAV confirmed an excellent manual handling in all axes which they expressed as "control harmony". Atmospheric disturbances could always sufficiently be controlled respectively be suppressed by the automatic flight control system. Finally the functioning of the required automatic flight phases could be successfully demonstrated during the flight test program.

REFERENCES

[1] Alles, W.

Auslegung und Erprobung eines Flugregelungssystems für einen unbemannten Drehflügler

Jahrbuch 1990 der Deutschen Gesellschaft für Luft- und Raumfahrt.

[2] Weidel, M., Alles, W., Friedl, H., Engelbert, H.-P.

Entwicklung, Erprobung und Demonstration eines automatischen Landeverfahrens für einen unbemannten Hubschrauber.

Jahrbuch 1992 der Deutschen Gesellschaft für Luft- und Raumfahrt.

[3] Engelbert, H.-P., Schröder, J.

Landing of an Unmanned Helicopter on a Moving Platform - High Accuracy Navigation and Tracking.

57th AGARD Symposium on Guidance and Control, Seattle, Oct. 1993

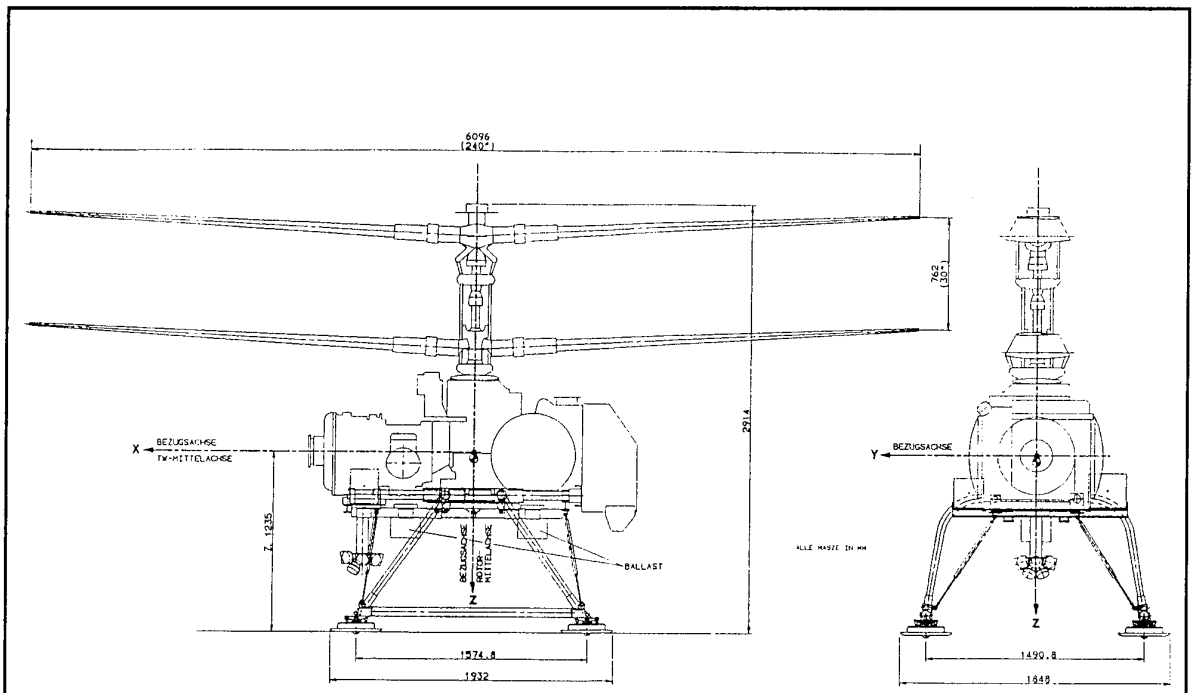

Fig. 1: Maritime Unmanned Air Vehicle

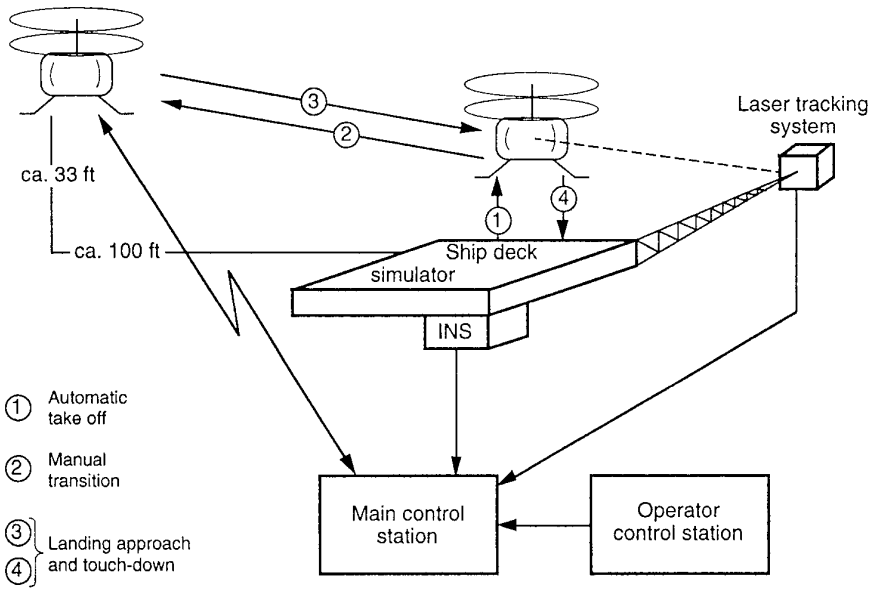

Fig. 2: Phases of Demonstration Program

1 - Rotordrive on the moving ship deck simulator

2 - Flights on the Hovering Fixture

3 - Operator controlled take off and landing (non moving ship deck simulator)

4 - Automatic hold of position

5 - Automatic take off and landing (non moving platform)

6 - Automatic take off and landing (moving platform)

Fig. 3: System and Flight Tests

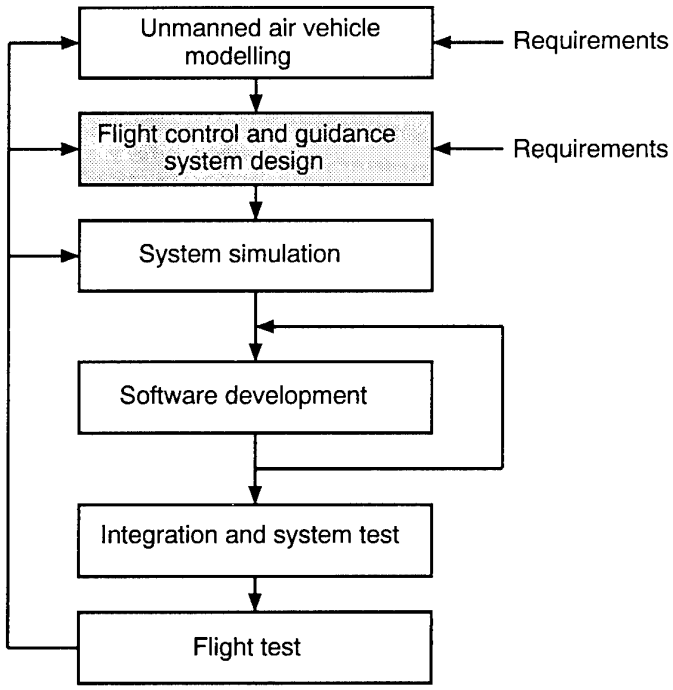

Fig. 4: Development Steps

Stabilization of the UAV dynamics

Good handling characteristics

Automatic functions

Good suppression of disturbances

Fig. 5: Flight Control System Requirements

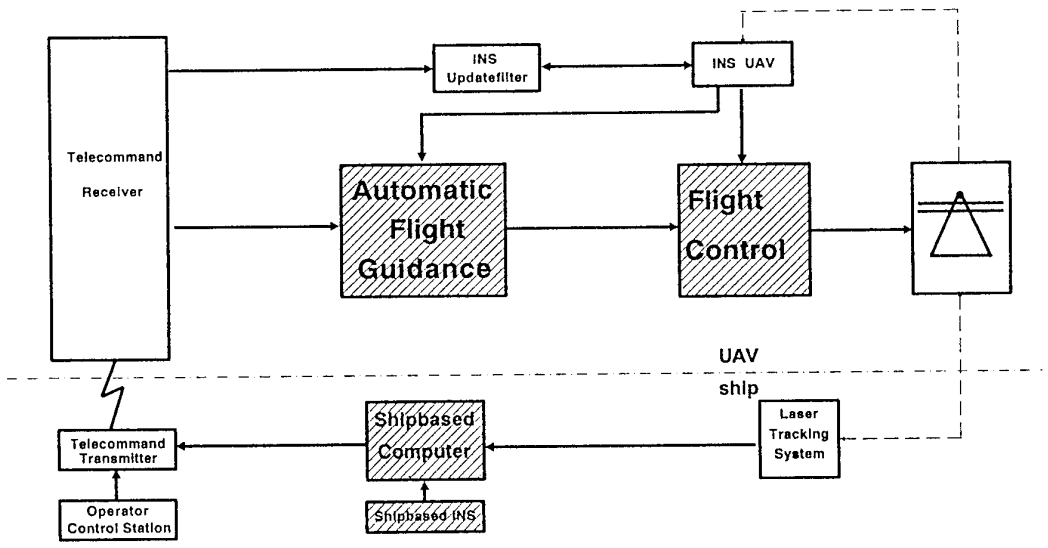

Fig. 6: Flight Control and Automatic Flight Guidance

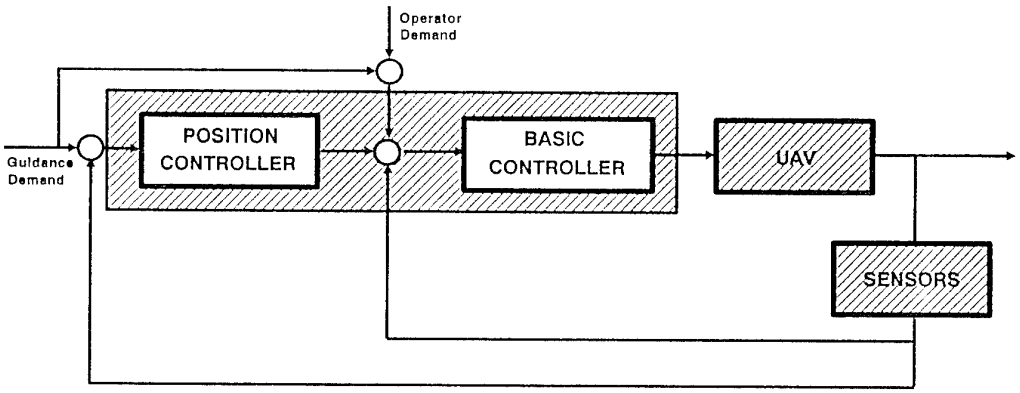

Fig. 7: Flight Control System

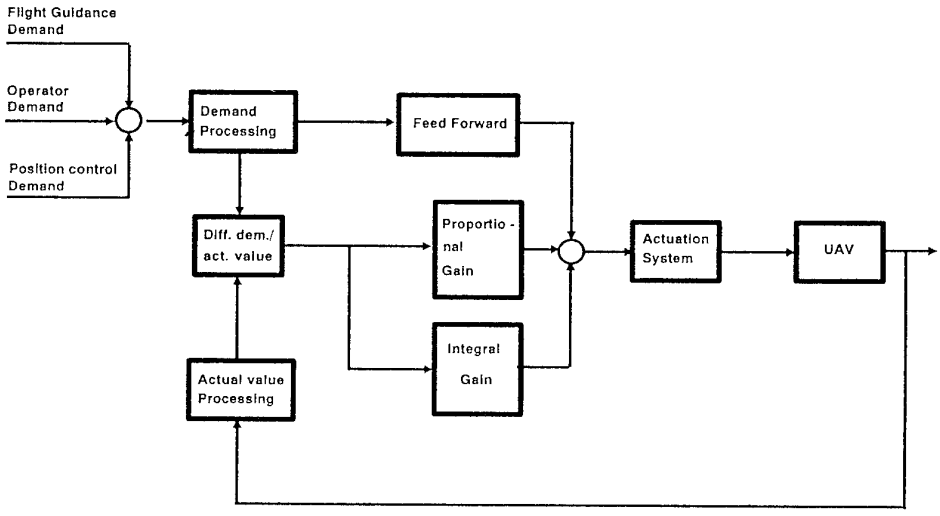

Fig. 8: Basic Controller

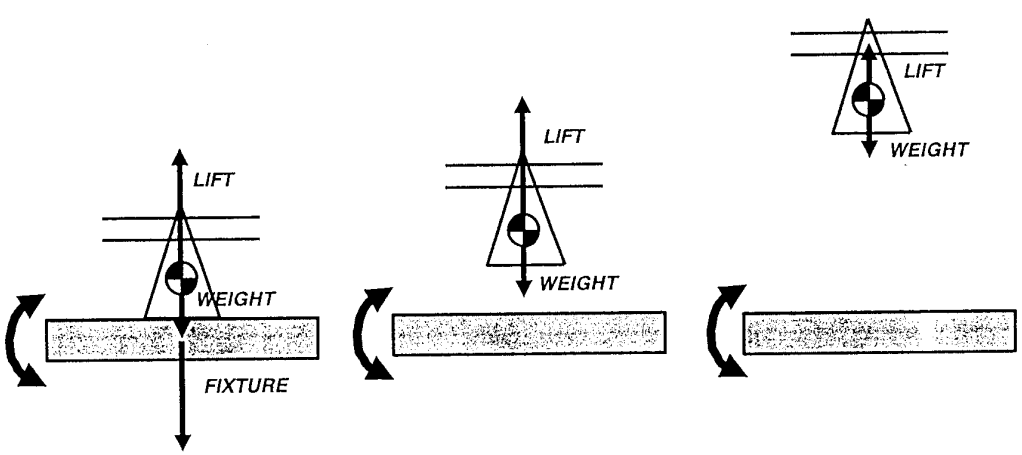

Fig. 9: Automatic Take Off

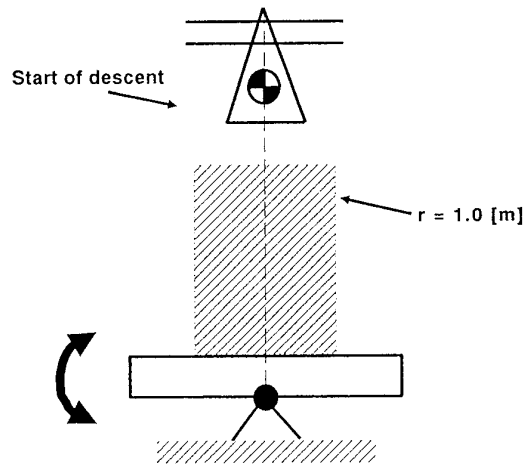

Fig. 10: Automatic Landing Approach and Touch Down

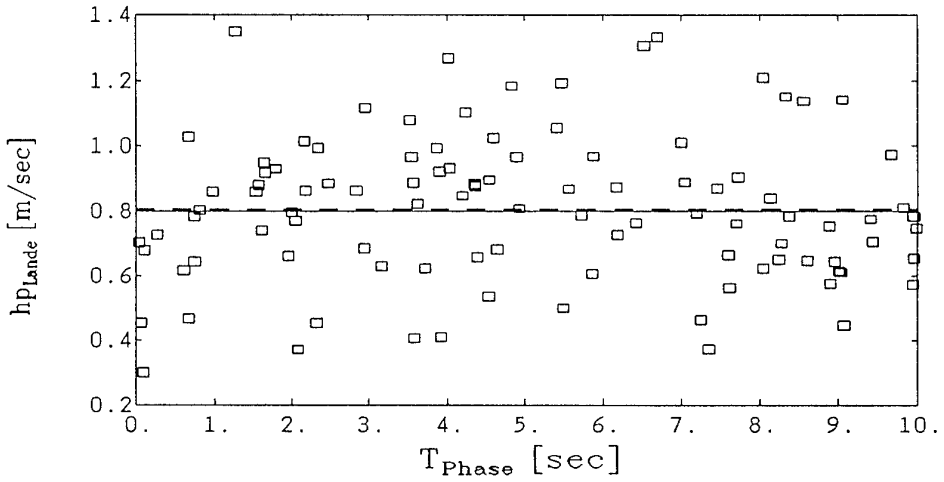

Design goal ⩽ 1.5 [m/sec]

Fig. 11: Statistics of Vertical Touch Down Speed (Simulation)

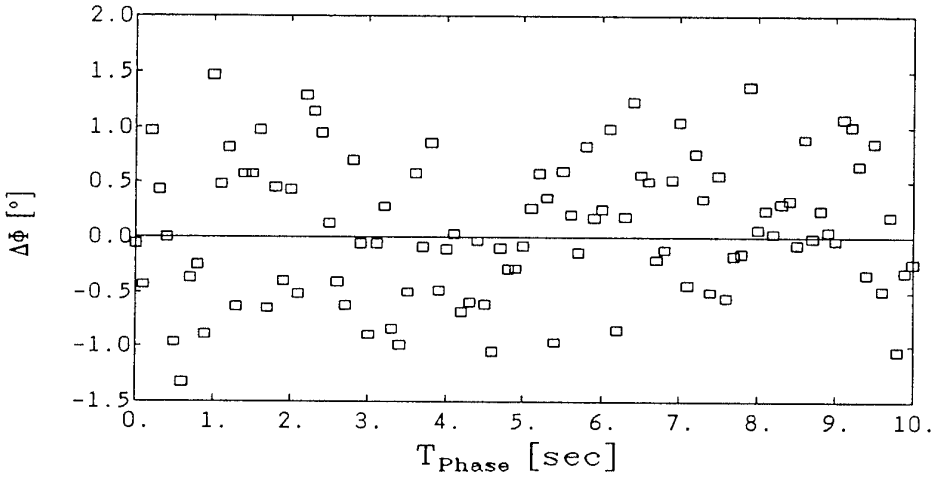

Design goal 0.0 [deg]

Fig. 12: Statistics of the Roll Angle at Touch Down (Simulation)

The FCS-Structural Coupling Problem and its Solution

B.D. Caldwell

British Aerospace Defence (Military Aircraft)
Warton Aerodrome, Preston
Lancashire, England PR4 1AX

SUMMARY

Implementation of ACT in aircraft is now almost routine, and often essential in realising performance requirements. However, unless a proactive and thorough approach is taken to ensuring that the effects of the flexibility of the airframe structure and its interaction with the FCS are analysed and accounted for, costly development delays and control system redesigns may ensue.

This paper is intended to discuss the basis of the phenomenon referred to at BAe Warton as FCS-Structural Coupling, the evolution of the methodology evolved at Warton to ensure freedom from its effects, and the development directions required to advance the state of art in this field.

NOTATION.

AAF	Anti-Aliasing Filter
AMSU	Aircraft Motion Sensor Unit
BAe	British Aerospace
CSAS	Command and Stability Augmentation System
DSP	Digital Signal Processing
EAP	Experimental Aircraft Programme
EF2000	Eurofighter 2000
FBW	Fly By Wire
FCC	Flight Control Computer
FCS	Flight Control System
FRF	Frequency Response Function
HSF	Half Sampling Frequency
NF	Notch Filter
OLTF	Open Loop Transfer Function
SC	Structural Coupling
SF	Sampling Frequency
TFA	Transfer Function Analyser
A_y	AMSU Lat. Accel. Output
N_z	AMSU Norm. Accel. Output
p	AMSU Roll Rate output
q	AMSU Pitch Rate output
r	AMSU Yaw Rate output
α	Aerodynamic incidence
δ	Trailing edge flaperon deflection (Symm.)
η	Foreplane deflection
ξ	Trailing edge flaperon deflection (Diff.)
ζ	Rudder deflection
C_{m_δ}	Pitching moment due to flap, or 'control power'.

1. INTRODUCTION

Fundamentally, FCS-Structural Coupling (SC) is a phenomenon associated with the introduction of a closed loop control system into a flexible airframe. The FCS motion sensors detect not only the rigid-body motion of the aircraft, but also the superimposed higher frequency oscillations due to the resonances, or 'flexible modes' of the structure. If the high frequency component of the sensor output is not attenuated, it will drive the aircraft's flying control surfaces, through the FCS. The controls themselves may excite the resonances, and the possibility of an unstable closed loop thus arises.

Since the performance, in the broadest sense, of the aircraft may be dependent on the FCS, it is clearly important to understand and deal with any factor which may interfere with its correct operation. Furthermore, as performance requirements become increasingly demanding, and the potential of the FCS must be exploited to the full, the commensurate effort must be made to minimise the impact of SC aspects, as their 'cost' increases.

This paper outlines the contributory elements of the SC 'problem', and, through a survey of past BAe aircraft projects, shows how the current BAe methodology for solution has developed, to the point of its application to EF2000 in collaboration with the Eurofighter Partner Companies.

The limitations of the process are described, together with the work being undertaken to continue the evolution of the method.

2. ELEMENTS OF THE STRUCTURAL COUPLING PROBLEM

2.1. Structural Flexibility.

Aircraft, like any flexible structures, exhibit many 'modes' of vibration, each mode having an associated resonant frequency and modeshape. Figure 1, for example, shows a 'snapshot' of a typical symmetric fuselage bending modeshape, which might have a resonant frequency of around 15Hz. Note the deflection in the front/mid fuselage, where the FCS sensors might be located. An aircraft will have many modes within the bandwidth of the FCS, many of which will vary significantly in frequency and amplitude of response with stores carried, fuel state or flight condition.

2.2. Excitation Via Control Surfaces.

The flexible modes may be excited, or 'forced', by oscillating the aircraft's flying controls. Figure 2 shows the results of an aircraft ground test where the amplitude of the response of the aircraft (as picked up by the FCS sensors) to control surface excitation (via the FCS actuators) was measured as a function of frequency. The peaks correspond to resonances, the peak magnitudes being dependent on the efficiency with which each control excites particular modes.

2.3. Flight Control System.

The presence of an automatic FCS links the response directly to the excitation through sensors, control laws and actuators. The resulting closed loop has the potential for instability.

2.4. Aerodynamic Effects.

The excitation force input to the structure by the oscillatory motion of a control surface has two components. The inertial component is due to the offset of the control's mass from its hingeline, and its magnitude is proportional to the control rotational acceleration. The aerodynamic component is due to the change of aerodynamic pressure distribution caused by control displacement from its datum position, and is proportional, for small perturbations, to the magnitude of the displacement, and to dynamic pressure.

The dependence of the aerodynamic input on airspeed, and the fact that the aerodynamic and inertial components are out of phase, results in the variation of the overall force with airspeed shown in Figure 3. The Figure indicates the important differences in characteristics dependent on whether the inertial forces dominate, as for a massive all moving control, for example, or whether the aerodynamics

Paper presented at the Flight Mechanics Panel Symposium held in Turin, Italy, from 9-13 May 1994.

overpower the inertial input at relatively lower speeds, as for a lightweight wing trailing edge surface.

The variation in structural response characteristics with flight condition will largely mirror the trends of Figure 3.

3. SUMMATION AND SOLUTION.

These four elements are fundamental to any SC mechanism, and the study of each, and the way in which they combine, will indicate the magnitude of the problem to be solved, and the level of detail of analysis required. Similarly, the quality of data available for each component part must be very clearly understood, and the analysis performed tailored to suit, in order to ensure safety and freedom from unexpected problems.

In any case, the elements must be assembled into a representation of the SC loop (Figure 4) to facilitate design of a solution. Commonly, solution takes the form of electronic analogue or digital noise (or anti-aliasing), or band-stop (or notch) filters incorporated into the feedback path of the FCS, to attenuate the high frequency components of the FCS sensor output. The major constraints on the filter design are the need to meet specified stability requirements for the flexible modes, and the need to minimise the additional phase lag introduced by the filters at rigid aircraft control frequencies, which is detrimental to rigid aircraft stability.

By the above reasoning, the form and content of the SC 'route to clearance' is expected to be different between different aircraft projects.

The aspects of SC problem magnitude, required detail, data quality and their influence on the analysis and solution will be illustrated by taking a SC perspective on a series of projects with which BAe Warton has been involved over the last 30 years. Throughout this period, the desire to minimise the complexity of the analysis procedure, and to maximise visibility and ease of understanding, has been a guiding principle in the approach to the problem. The continuity of development and experience has led to SC being given a high profile, with SC analysis being very closely integrated with FCS design to the point where structural dynamicists form part of the FCS team.

4. HISTORICAL PERSPECTIVE.

As already noted, the potential for SC exists in any flexible vehicle fitted with an automatic FCS. It is probable that the problem first became well known and analysed in guided missile design (References 1 & 2), although it was certainly anticipated, and even experienced, in aircraft control also (References 1, 3, 4). Total loss of guided missiles due to poorly understood or inadequately analysed SC interactions is by no means unknown, while, fortunately, none of the encounters experienced in manned aircraft has proven catastrophic (References 1, 4 to 6).

Development of analysis tools and procedures to address the problem, as experienced in aircraft flight control design at Warton, began in the early 1960s with the TSR2 aircraft, and have continued to the present with application to EF2000.

4.1 TSR 2 - First Flight 1964.

At the time of the inception of the TSR 2 project (Figure 5), previous Warton aircraft had required only low gain, low authority auto-stabilisers, which, with auto-stab. actuators of relatively limited capability, naturally avoided the occurrence of SC problems.

TSR 2, however, was unstable directionally at high speeds, and thus required high gain feedback of lateral acceleration to the spigotted all-moving fin. Although, as indicated in Figure 3, the large all-moving surface would have displayed inertially-dominated structural excitation characteristics over most of the flight envelope, the TSR 2 FCS high frequency gain was sufficiently great at high speed to lead to a significant SC problem. Exacerbated by poor actuator stability, the potential magnitude of the SC fin oscillation was such that fin spigot fatigue life under worst case conditions was estimated to be approximately 20 seconds (Reference 7).

The SC investigations were consequently detailed, and involved all of the elements which have become familiar in EAP and EF2000, including calculations based on an augmented 'flutter' mathematical model, a ground test phase leading to attenuation filter design, and a proposed in-flight verification phase.

Significant aspects of the work done included;-

- poor agreement between predicted and measured SC characteristics,
- ground test results formed a central part of the flight SC clearance,
- the importance of sensitivity studies was emphasised,
- many of the ground test techniques and procedures applied are still in use today;-
  - linearity checks,
  - use of single-sine / TFA techniques,
  - fatigue loads monitoring,
  - engine turning,
  - actuator lubrication.

The envisaged solution to the SC problem involved implementation of a total of eight notch filters (Table 1), together with the relocation of the FCS sensors. In-flight verfifcation of the predicted SC characteristics was proposed, but the project was cancelled in April 1965, before the solutions could be properly confirmed.

4.2 Jaguar - First Flight 1968.

The Jaguar (see Jaguar FBW, Figure 7) was designed to be a simple, rugged, ground attack aircraft. As for the TSR 2, Jaguar had all moving tailplanes, but here a conventional fin/rudder. The initial standard of aircraft had low gain pitch and yaw auto-stabilisers only. Anticipating minor SC effects, no SC tests were performed, but 'nominal' 10Hz/20dB notch filters were implemented, one in each axis, to attenuate potential fuselage bending mode coupling. In 1971, more than two years after first flight, a roll damper operating on the wing mounted spoilers was introduced, in order to improve roll handling in turbulence. In view of the high gain used, SC tests were performed which resulted in the relocation of the roll rate gyro to a more rigid sub-structure (a wing spar). However, following one of only two SC encounters ever experienced on a Warton aircraft (the other being during Tornado SC tests), when spoiler limit-cycling was observed during taxi trials, a 50ms low-pass filter was added to the system, to supplement the notch (Table 1). This provided a fully effective solution.

4.3 Tornado - First Flight 1974.

The Tornado multi-role combat aircraft (Figure 6) embodies a full authority CSAS, with relatively low gains owing to the positive basic vehicle stability. Analyses conducted in partnership by MBB (Reference 8), confirmed that the SC characteristics of the all-moving taileron controls, in combination with the CSAS scheduling, would result in an inertial force-dominated excitation, and hence a worst SC case at zero speed. Ground SC testing at both BAe and MBB highlighted deficiencies in the mathematical model which restricted its validity for SC use, and ground test results were used directly for notch filter design and flight clearance. Implementation of a single notch filter in each axis, together with gyro relocation to the optimum position, ensured the specified stability requirements were met throughout the flight envelope.

The range of variation in flexible mode frequencies due to the wide (and ever expanding) variety of stores carried on Tornado was potentially a severe complication of the SC problem. However, the critical modes for Tornado SC are fundamental fuselage and taileron bending, which are relatively insensitive to store configuration. Calculation identified the small number of 'critical configurations' which defined the boundaries of the SC problem, a series of ground tests then established the envelope of SC characteristics for notch filter design. Updates to the CSAS or notch filters have not been necessary during the service life of the aircraft fleet.

Expansion of the quantity of ground testing required for Tornado led to the development of automated test control equipment. The TFA-based, single sine excitation technique pioneered on TSR 2 was still preferred, but the excitation frequency was controlled by computer. This allowed fast execution of a series of test frequencies, with automatic data aquisition and processing, and near real-time plotting of results. The development promoted a very productive and efficient interactive mode of testing, under the direct control of the SC engineer.

4.4 Jaguar FBW - First Flight 1981.

This technology demonstrator programme (Figure 7) culminated in the world-first flight of an aircraft with no mechanical or analogue electrical link between the pilot and the flying controls. A quadruplex digital FCS was installed in a Jaguar airframe made unstable by the addition of ballast to move the centre of gravity aft, and the fitting of conspicuous wing leading edge strakes to move the aerodynamic centre forward. The all-moving taileron flying controls of the standard Jaguar were retained, but the gains of the control laws and the capability of the actuation system were now consistent with the provision of artifical stability and command augmentation. This resulted in a more extensive provision of attenuation filtering than for the standard Jaguar (see Table 1), but the fundamentally inertial-exciatation dominated SC characteristics, and zero speed worst case, remained. All of the information needed for filter design and flight clearance was again available from ground tests.

The digital nature of the control law implementation meant that sampling effects had to be considered in the SC assessment. However, quarter-sampling frequency anti-aliasing filters, implemented in the analogue sensors for other reasons, practically eliminated the possibility of aliasing of high frequency structural responses, and no further attention was required. The notch filters implemented in the digital part of the system had to be designed with the effects of frequency warping of digitally calculated filtering accounted for, since filter design was carried out in the continuous, Laplace, domain. This is done by 'pre-warping' the continuous filter definition prior to digitisation, in a simple transformation.

4.5 EAP - First Flight August 1986.

The Experimental Aircraft Programme was aimed at demonstrating a number of new technologies applicable to a future combat aircraft, including ACT. The airframe (Figure 8) was unstable in pitch (time to double amplitude 0.18 sec) and yaw, and incorporated all-moving foreplanes, inboard/outboard segmented, full-span trailing edge elevons, and a conventional fin/rudder in a fully integrated FCS. The FCS was designed and cleared to production aircraft standards first developed on the Jaguar FBW.

The aircraft combined, for the first time in a Warton aircraft, all of the features leading to a 'difficult' SC problem;-

- a flexible airframe, with resonant frequencies for 'significant' structural modes ranging in frequency between very close to the rigid aircraft modes and very close to the FCS sampling frequency (Figure 2),
- removable stores mounted on sensitive parts of the structure (ie wing tips), leading to stongly configuration-dependent SC characteristics,
- trailing edge flying controls, with high, aerodynamic dominated excitation forces at airspeeds where the FCS gains are high, and
- a powerful FCS (Figure 9 and Reference 9), featuring;-
  - high feedback gains at structural mode frequencies,
  - high bandwidth sensors and actuators,
  - multiple parallel paths,
  - a 'tight' phase budget for SC problem solution.

The fact that an 'in-flight' worst case was expected, away from conditions which could be examined in tests before flight, recalled TSR.2 experience. In view of this, and the overall degree of difficulty anticipated, SC was viewed as being a significant risk in the FCS programme. This was directly reflected in the analyses required in comparison with Jaguar and Tornado.

An outline of the SC Design and Clearance approach will be given in the following section.

The clearance philosophy and analysis methodology employed has led to a clear understanding of the SC problem and of the strengths and weaknesses of the approach, from which a satisfactory flight clearance was derived. The SC solution (Table 1) involved numerous notch filters compared with previous projects, indicating the magnitude of the difficulties faced. No flight envelope restrictions derived from SC considerations, and no ground or flight SC problems were experienced throughout the 259 flight, three FCS- phase history of the aircraft.

5. 'EAP METHOD' PHILOSOPHY AND REQUIREMENTS.

5.1 Motivation.

It is acknowledged that structural failure in the manner of a flutter encounter is unlikely to occur as a result of SC, since the FCS cannot, in general, input sufficient energy, and since FCS non-linearities would limit the amplitude of excitation through the control surfaces anyway. However, the TSR 2 example illustrates the profound effect SC might have on fatigue life, even subject to these constraints. This has been borne out by subsequent experience of airframe and actuator fatigue life usage during typical SC ground tests. Further concerns are that coupling with flutter modes may occur (References 1, 4), which could lead to structural damage and that the propagation of high frequency signals through the FCS could seriously degrade actuator performance for rigid aircraft control (References 10, 11).

There is ample reason therefore to seek to avoid SC. The current BAe approach has been successful in reducing the problem to such a level as to effectively eliminate potential fatigue, actuator performance, flutter destabilisation etc effects, but with attendant costs in terms of additional phase lag introduced into the system.

5.2 General Philosophy.

In seeking a SC solution, the targets will be the structural mode Design and Clearance requirements agreed with the project 'customer', and to avoid exceedence of the notch filter phase lag assumed for FCS design. BAe's philosophy has been to keep the treatment of the SC problem as simple as possible while meeting the targets, and ensuring a demonstrably safe clearance covering all considerations and fully recognising the quality of available information. This has been achieved by evolving a process with a high degree of engineer intervention and understanding, in preference to monolithic automated analysis procedures. The process involves an iterative approach, starting with broad assumptions regarding the elements of the problem, with 'patches' of detail and refinement added to enhance the assessment in areas identified as being critical to the

solution.

The objective is always to avoid any flight restrictions due to SC, and, if possible to avoid dependence on any factor which requires verification in-flight.

5.3 Design Requirements.

The structural mode Design Requirements for EAP were based on MIL-F-9490D (Reference 12). This gives a frequency domain specification (Table 2) of stability margins, consistent with the approach adopted at BAe of integrating the rigid and flexible FCS design functions; it was natural that the frequency response analysis methods and tools employed in FCS design should be extended to SC analysis.

The design information required for notch filter design is thus an open-loop transfer function (OLTF) representing the entire system of Figure 4. As noted already, there are clearly many means of assembling this OLTF, ranging from by calculation using a model representing the entire system, to a simple end-to-end test, to a combination of test and model. The means selected will be influenced by the difficulty of the SC problem, and the quality of information available from different sources, and will also determine the way in which the Design Requirements are interpreted and addressed.

In particular for EAP, the quality of the flutter model SC predictions, the in-flight worst case, and the digital nature of the FCS were expected to be strong influences.

The magnitude of the high frequency response (Figure 2) and the inadmissability of the AAF solution adopted on Jaguar FBW, meant that an understanding of the digital implementation of the FCS was required, and that a method of treating them which was consistent with the other elements of the procedure had to be devised.

Based on previous experience, the quality of the flutter model-based predictions were expected to be inadequate for confident SC clearance, where tenths of one Hertz in frequency, and one to two dBs of gain were important for optimum filter design.

The prediction of response phase at in-flight conditions not immediately accessible for verification was a further concern, particularly in the situation where response phase was changing very rapidly with response frequency, as for all but the lowest frequency structural modes.

Because of these factors, and the overall desire to maintain simplicity and visibility of the SC design and clearance process, the MIL-F-9490D stability specification was modified to set more conservative clearance requirements. For the initial phases of the EAP programme, the decision was made;-

- to specify a 9dB stability margin requirement for all structural mode frequencies, and
- to exclude phase entirely from the SC analysis.

The latter specification meant that all parallel paths in the FCS / Structure Loop were evaluated separately and added as scalars to form the OLTF, and that the alleviation in attenuation requirements for modes with apparently good phase margins was not admissable. The stability margins derived from this approach automatically satisfied the (arguably inadequate) 'multiple loop' part of the MIL specification, which would otherwise have been difficult to address in the EAP application.

This approach was adequate for the initial phases of the EAP programme, allowing completely trouble-free clearance of the entire, extensive, flight envelope, without recourse to flutter-type envelope expansion flight testing. For subsequent phases, where the structural coupling problem became yet more difficult with the requirement to cover store configuration changes, a 'relaxed' design and clearance requirement, based on additional data gained in specific flight tests was evolved.

The principal features of the EAP SC Design and Clearance methodology devised to formulate the OLTF filter design requirement are outlined in the next section.

6. PRINCIPAL FEATURES OF THE 'EAP METHOD'.

To recap, Figure 4 represents, in schematic form, the components of the SC loop; the airframe flexibility and unsteady aerodynamic effects, the control surface inertial and aerodynamic excitation, and the FCS. For SC analysis and solution, these components must be adequately represented and brought together in an appropriate manner to generate the specification for attenuation to meet the stability requirements.

EAP is seen to be a 'difficult' SC problem, and the features of the methodology described below derive principally from;-

- the inadequacy of the augmented flutter model for absolute calculation of SC characteristics,
- the need to consider in-flight conditions in detail,
- the requirement to cover potential variability in phase between the parallel paths of the FCS, and
- the need to account for digital effects on high frequency structural modes.

6.1 Structural Modelling.

The structural model is based on the standard EAP flutter model, with approximately 40 normal modes, plus control surface rotation and rigid aircraft modes. The normal modes were derived from 'branch modes' to give adequate representation with relatively few degrees of freedom. Rigid mode aerodynamics are wind tunnel-derived, unsteady aerodynamics are from kernel function based tandem surface methods at fixed Mach and frequency parameter. Actuator and sensor dynamics are included by augmenting the matrix equation, allowing interface with the FCS, or injection of simulated test inputs for frequency and time domain analyses.

It is a characteristic of notch filters that the rate of change of attenuation with frequency, near the filter centre frequency, is very high. This places a high premium on accurate knowledge of mode frequencies. However, zero speed calculations using 'matched' models adequately represented SC characteristics for only some of the sensor output / actuator input combinations, and only then up to modest frequencies. This placed constraints on the use of the model, and strongly influenced the SC procedure. For EAP, the model was used only to represent the 'flexible aircraft aerodynamics' and 'control surface aerodynamic excitation' components of the Figure 4 SC loop, to extrapolate SC characteristics measured in ground tests to in-flight conditions.

Initial calculations were conducted with relatively coarse matching of frequency parameter to modal frequency and flight condition. Where a mode was shown to be 'critical', aerodynamics for the most appropriate frequency parameter were selected to improve the prediction.

6.2 FCS Control Laws.

Preliminary frequency response analysis indicated paths which, in combination with the structure and aerodynamics, had negligible gain at structural mode frequencies. This eliminated integral paths and incidence and sideslip feedback sensor outputs. For the remaining paths (proportional pitch, roll and yaw rates, and lateral acceleration), inclusion of sensor and actuator dynamics as part of the flexible aircraft, and separate consideration of digital effects, allowed representation of the control laws as a single high frequency (above 6Hz, where the FCS phase advance filters run out) gain value at each point of

a grid of flight conditions across the flight envelope. The maximum gain at each flight condition was sought by consideration of all effects of scheduling with alpha, non-linear gearings, etc.

6.3 Combination of FCS and Structural Gains.

Addition of the FCS gain to the stuctural mode gain and frequency trends built a mode-by-mode picture of the variation of the SC loop gain with flight condition. For each significant FCS path, this indicated, in a very clear format, the critical flight conditions and the relative importance of modes and control surfaces.

6.4 Structural Coupling Testing.

Because of the inadequacy of the flutter model in this application, the remaining major part of the Figure 4 SC loop, the 'flexible aircraft dynamics' and 'control surface inertial excitation', were represented instead by data derived from ground test. Frequency response functions for each signifcant input/output combination were measured (Table 3). Preliminary assessment of the FCS digital effects had indicated a requirement for data up to the sampling frequency (SF) of the FCCs. This entailed provision of an analogue test input to the actuators and a high rate digital output from the sensor processors.

Since the test data was to form a central part in the clearance strategy, great efforts were made to maximise result quality.

- Special gains were provisioned in the FCS software just upstream of the digital to analogue (D/A) conversion, to reduce the relative amplitude of the noise picked up on the analogue test cabling and connectors, and to make the least significant bit of the 16 bit internal signals accessible through the 12 bit D/A.
- FRFs were referenced to the actuator demand, rather than actuator position. This includes actuator (and sensor) dynamics in the measurement, ie in the 'flexible aircraft dynamics' part of Figure 4.
- Great care was taken with the test set-up;- cable routing, earthing arrangements etc, to minimise analogue noise pick-up.
- Constant reference was made to the sensor response output waveforms, to ensure that adequate response amplitude relative to the digital system resolution was being achieved.
- Single-sine, TFA methods were used.

The tests also addressed factors which could not be modelled, and included;-

- Confirmation of actuator installed stability and performance.
- Assessment of the SC effect of actuator failure cases.
- Assessment of the SC effect of free-free compared with on-undercarrige SC characteristics.
- Structural linearity checks.

Significant emphasis was placed on the latter; in general the policy was to drive the structure hard enough to saturate structural non-linearities, while at the same time avoiding excessive fatigue damage and actuator rate limit. Investigation of excitation amplitude effects was an inherent part of this procedure.

Fatigue life useage was a major constraint on the tests. The aircraft was comprehensively instrumented, and all response cycles above a 'negligable damage' limit predetermined for each parameter were recorded for fatigue assessment. An absolute limit of a factor of three on 'negligable damage' was never exceeded. Other test constraints were the need to rotate the engine spools at intervals, to prevent bearing damage, and the need to avoid scoring of the actuator cylinder bores, by periodically moving the controls over large amplitudes to lubricate the actuator seals.

The test results, in the form of gain vs. frequency information for each significant FCS path (eg Figure 2), formed the absolute basis for extrapolation of modal gain trends to cover the in-flight worst cases for EAP SC. Following the extrapolation process, the parallel path contributions to the pitch (pitch rate / pitch rate through $\delta_{I/B}$, $\delta_{O/B}$, and η paths) and lateral FCS paths were summed as scalars to give the end-to-end pitch and lateral OLTFs. The resulting 'gain envelopes', covering all flight conditions, directly specified the attenuation required to meet the Design and Clearance requirements. It still remained, however, to include the effects of the digital nature of the FCS, prior to notch filter design.

6.5 Treatment of Digital Effects.

Careful consideration of sampling theory (eg Reference 13), led to a simple treatment which included all of the important effects.

First of all, design of the DSP included in the AMSU in the form of rolling average and downsampling processes provided a very effective anti-aliasing function. Together with the characteristics of the FCC sampling and zero-order hold (ZOH), this effectively eliminated signal components at frequencies above the FCC sampling rate. This defined the upper frequency of interest throughout the analysis.

Secondly, analysis showed that the effects of the FCC sampling and ZOH functions could be represented by applying the attenuating characteristics of the sample and hold to the 'overall envelope' OLTF, then folding the data about the half-sampling frequency (HSF), summing the upper and lower frequencies (as scalars), to represent the effects of aliasing. The treatment is explained more fully in Reference 14 (see also Reference 6).

For EAP this resulted in OLTFs for q/q, ζ/ζ, and p/p over the zero-to-HSF range, that is; representations of open loop gain at strategic points in the control laws, within the digital FCCs. These data are then directly used for notch filter design.

6.6 Notch Filter Design.

As previously noted, the DSP in the AMSUs provided an anti-aliasing function for frequencies higher than the FCC sampling frequency. Conventional AAFs proved, in this circumstance, to be a less efficient solution for the HSF to SF band than broad notch filters, located, of course, upstream of the FCC sampling, in the AMSU.

Advantage was taken, on EAP of the exclusive excitation of some modes by particular control surfaces, as illustrated by Figure 2. Obvious examples are the excitation of the Foreplane Bending mode (18Hz) by the foreplane, and excitation of Wing Bending (7Hz) by the outboard trailing edge flap. Positioning of notch filters in the actuator command paths, rather than on the sensor outputs, gave the required attenuation, but reduced the overall phase lag penalty associated with the particular filters. Table 1 compares the notch filter configuration for EAP with those of previous projects, illustrating the magnitude of the SC problem addressed on EAP.

7. 'EAP METHOD' DEVELOPMENT.

It was recognised that the 'EAP Method' as originally developed, while being very satisfactory for the initial phases of the EAP, would become increasingly costly as a range of stores configurations for a production aircraft

were developed. The approaching EF2000 programme drove the implementation of an 'EAP In Support Of EFA' extension to the EAP. For SC, this consisted primarily of development of flight test techniques to support a relaxation in Design and Clearance requirements, which would in turn facilitate clearance of a broad range of stores. In addition, enhancements were made to the ground test procedures, in recognition of the continued importance of the SC test in the clearance process.

7.1 Flight Test Techniques.

The Design and Clearance requirements originally defined (5.3) were considered to be entirely consistent with the information, and quality of information available at the inception of the EAP. To relax the Requirements would therefore require additional data; the most immediate means of gaining this was seen to be through flight test. Accordingly, an In-Flight Structural Mode Excitation System (IFSMES) was developed for flutter and SC flight test use, Reference 15 describes the development and flutter application of the system.

Development and use of an IFSME System was intended to demonstrate that two factors which directly constrained the EAP Method could be addressed through flight test. Demonstration of the ability to clear into flight a number of EAP store configurations with a common notch filter design was set as a tangible objective.

The limiting factors to be considered were;-

- firstly, the lack of direct validation of the predicted SC response at in-flight conditions, and
- secondly, the use of potential flow-based unsteady aerodynamics methods for all flight conditions.

The first factor led directly to the inadmissability of phase margin in the SC analysis, and the latter meant that incidence effects on the aerodynamic excitation input were not represented, so that in assembling the representation of the SC loop, worst-case, high α FCS gains were used with zero α unsteady aerodynamics. It was thought probable, however, that the unsteady aerodynamic force input, to the lower frequency modes at least, would follow similar trends with incidence to the steady flow equivalent, C_{m_δ}. The steady term represents flap 'control power', which on the EAP configuration reduces with increasing α; the increased FCS gain mentioned above is necessary to preserve rigid aircraft stability.

Thus it was proposed to demonstrate the feasibility of measuring in-flight the variation of the pitch rate : flap transfer function frequency response with;-

- speed and Mach number, to verify model predictions, and
- α, to investigate the correspondence of steady and unsteady control power.

IFSMES flight testing was conducted with all notch filters in place, under the SC clearance given to the original, 'basic' Requirements. The tests were therefore inherently safe. The attenuation of the filters also meant that the measurements were effectively 'open loop', exactly as required, without any need for further processing.

Note also that, in the EAP case, the philosophy was to measure the flexible aircraft transfer function part of the SC loop of Figure 4, in preference to attempting to verify the predicted overall closed loop gain margins. The proposed measurements would give information directly relevant to the aspects of the SC problem under examination, and would also benefit from improved signal-to-noise characteristics compared with the alternative approach, since the excitation was input downstream of the FCS notch filters, and measurements made upstream, thereby excluding the filters' high frequency signal attenuation from the analysis.

The IFSME system proved very effective for SC, as well as flutter use. Achievements included;-

- demonstration of the feasibility of the concept for EF2000,
- satisfactory data quality within the required (for SC) range of;-
  - 2-12Hz
  - M0.4, 3000ft to M1.2, 33,000ft
  - zero to 18°α

Figure 10 shows typical results.

At the conclusion of the work, the SC objectives were considered to have been met, and the confidence gained is feeding directly into the EF2000 programme.

7.2 Design and Clearance Requirements.

A refinement of the SC Design and Clearance requirements accompanied the expectation of additional data being available, from IFSMES flying. It was proposed to allow phase stabilisation of modes for which appropriate flight test data would be available, thus easing the notch filter design sufficiently for clearance of the desired store configurations.

The range of modes which were to be considered for phase stabilisation was to be limited by:-

- The capability of the flight test techniques available; in this case IFSME was limited by the excitation capability of the actuators and the system digital effects.
- The benefit to be gained from phase stabilisation; to avoid additional complication and cost in the clearance process, the relaxed Requirements were only to be applied to modes most influenced by stores configuration.
- Basic considerations of, for example, sensitivity of the resulting SC clearance to small frequency tolerances, which rules out modes with high rates of change of phase with frequency.

For EAP this led to an objective of proving phase stabilisation for the symmetric fundamental wing bending mode for all wing-tip store configurations. Since excitation of this mode was dominated by the outboard flap, the need to address multi-loop aspects was conveniently negated, and the work required reduced significantly.

The 'relaxed' Requirements evolved blended from the rigid aircraft requirements (Reference 9) into the 'basic' 9dB flexible mode margins through a region where phase stability was allowed. The stability margin requirements were expressed as prohibited regions on a conventional Nichols chart;- plotting the OLTF against these regions indicated filtering requirements directly.

7.3 Ground Test Enhancements.

Anticipating that ground SC testing would continue to be of central importance to SC clearance, the BAe approach to testing was examined, particularly concerning the preference for 'single sine' TFA- based techniques over frequency sweep / spectral analysis methods, which are potentially faster. A number of commercially available, spectral analysis based test packages were assessed against the TFA 'benchmark' in a series of tests on the EAP airframe. Not surprisingly, it was concluded that the optimum approach was to combine the single-sine and frequency sweep approaches. Since none of the commercial systems offered this combination, enhancement of the existing in-house equipment was recommended, and has since been completed, Figure 11.

The updated system now comprises;-

- a Solartron SI1250 TFA, for single sine testing where quality of data is a particular requirement, or signal to noise ratios are poor,
- a Solartron SI1220 Spectrum Analyser, for frequency sweep (chirp), random noise and impulse tesing, for use where speed and economy of data acquisition is a priority over premium quality of data,
- a custom- built sub-system for fatigue load exceedence protection and fatigue damage accumulation monitoring and recording,
- chart / tape recorders for monitoring and recording of test inputs and outputs, and
- a Hewlett Packard 9000- series computer to implement;-
  - a 'windows' based graphical user-interface for test definition and data acquisition,
  - automatic closed loop control of test signal amplitude,
  - test definition and results recording and printing, and real time results plotting,
  - integration and central control of all the test equipment.

EF2000 SC tests have proven the system 'in the field'.

8. FUTURE DEVELOPMENT DIRECTIONS.

The 'cost' of SC solution, in terms of the additional phase lag introduced into the FCS, is not insignificant when compared with the lag from other sources such as primary actuators. As lag is forced out of the system due to increased pressure to realise FCS performance potential, the SC costs must also be minimised.

The approach to SC at BAe is therefore under continual review; a number of the development directions where work is required or underway are outlined below.

8.1 Structural Modelling.

The perceived inadequacy of current modelling and model matching techniques has been shown to be a major influence on the SC analysis and solution methodology. Although published papers (eg Reference 16) indicate progress in the model matching area, a procedure able to result in a model which reproduces test-measured modal frequency response characteristics for all modes of interest, and all excitation / response combinations of interest, while maintaining physical validity, still seems not to be available.

8.2 Aerodynamic Modelling.

The EAP IFSME flight testing revealed a strong relationship between α and mode response, which conformed closely to predictions made based on imposing a rigid C_{m_δ} vs α variation on the corresponding matrix equation term. Although theoretical / wind-tunnel work has been done on the variation of the overall unsteady forces with incidence (References 17, 18), this needs to be extended to examine the 'control power' terms which are of particular interest for SC.

Experimental work at Bath University (Reference 19), sponsored by BAe, has focussed on reproducing the steady and unsteady effects observed on EAP in the wind-tunnel, and identifying the responsible flow-field features. The objective is to confirm the steady / unsteady link and to understand its basis, so that steady data, which will inevitably be available from the early stages of a project, can be interpreted for SC analysis. The eventual goal is to return to a SC clearance process which has no dependence on flight test.

8.3 Effect of SC on Actuator Performance.

Work during the IFSMES development (Reference 10), identified effects of propagation of high frequency signals in the FCS which might compromise actuator performance for rigid aircraft control. Work is in progress, (References 11, 14) to further understand and quantify these effects in BAe sponsored research at Loughborough University. The work will examine in detail the consequences of high frequency signal propagation, including the effects of FCS non-linearities, with the objective of further refining the current SC Design and Clearance requirements and procedures.

REFERENCES

1. IAS Paper No.62-47
   An Industry Survey on Aeroelastic Control System Instabilies in Aerospace Vehicles.
   W.K.Weymeyer, R.W.Sporing
   1/62

2. MIT E-1210
   Simplified Analysis of Flexible Booster FCS.
   L.G.Hofmann, A.Kezer
   6/62

3. TM IAP 649
   Notes On Some Problems of High Speed Aircraft Programmes.
   Royal Aircraft Establishment
   3/57

4. Journal of Aircraft Vol.16 No.7 Article 78-1289
   Aeroservoelastic Encounters.
   L.R.Felt, L.J.Huttsell, T.E.Noll, D.E.Cooley
   7/79

5. Flight International Magazine
   AMRAAM Block Placed On Lockheed F16s.
   G.Norris
   20/10/93

6. AIAA-90-1240-CP
   An In-Flight Interaction of the X29A Canard And FCS.
   M.W.Kehoe, E.J.Laurie, L.J.Bjarke
   1990

7. AGARD FMP S&C
   Auto Aeroelastic Mode Coupling, A Comparison of Predicted and Actual Characteristics.
   G.J.Evans, B.J.Beele
   9/68

8. UFE 1237 AGARD SMP
   Interaction Between Structure and CSAS.
   O.Sensburg
   3/76

9. IJC Vol.59, No.1
   Development and Experience of The Control Laws in the EAP.
   A.C.McCuish
   1/94

10. BAe-WFC-RP-EAP-2047
    EAP Primary Actuator Performance Tests For IFSCMES Feasibility Study.
    A.Watts
    7/11/88

11. 1994 Guidance Navigation and Control Conf., Scotisdale
    The Effect of Actuator Non-Linearities on ASE.
    R.Taylor, R.W.Pratt, B.D.Caldwell
    TBP

12. MIL-F-9490D
    FCS- Design Installation and Test of Piloted Aircraft, General Specification For.

13. ISBN 0-471-88760-9
Discrete-Time Signal Processing.
S.A.Tretter.....C 1976 John Wiley & Sons, Inc.

14. 1994 IEEE Conference on Decision and Control,Baltimore
The Effects of Sampled Signals on the FCS of An Agile Combat Aircraft With A Flexible Structure.
R.Taylor, R.W.Pratt, B.D.Caldwell
TBP

15. AGARD CP 519, Paper 15
In-Flight Structural Mode Excitation System for Flutter Testing.
R.B.Ramsey
4/92

16. AIAA Journal, Vol.29, No.11
Techniques for Implementing Structural Modes Identification Using Test Data.
J.J.Allen, D.R.Martinez
11/91

17. AGARD CP 483, Paper 7
Unsteady Aerodynamic Forces on an Oscillating Wing at High Incidences and Flow Separation.
H.W.Forsching
4/90

18. 68th AGARD Fluid Dynamics Panel Specialist Meeting.
Aeroservoelastic Stability of Aircraft at High Incidence.
J.Becker
5/91

19. ICAS 1994 Conference
Unsteady Aerodynamic Effects of Trailing Edge Controls on Delta Wings.
D.J.Pilkington & N.J.Wood
TBP

Note:- TBP = To Be Published

Table 1. Notch Filter Solutions.

Aircraft	Feedback	Solution
TSR-2	Pitch Roll Yaw N_z A_y	1 NF 2 NFs, 1 2nd O Lag, 1 Lag / Lead 2 NFs 1 NF, 1 1st O Lag 2 NFs
Jaguar	All Axes	1 1st Order lag (4Hz), 1 NF (10Hz)
Tornado	Pitch Roll Yaw	1 NF (11.5Hz) 1 NF (11Hz) 1 NF (5Hz skew notch)
Jaguar FBW	Pitch Roll Yaw N_z A_y	1 AAF (12.5Hz), 1 an.(25Hz), 2 dig.NF (11Hz,12Hz) 1 AAF (12.5Hz), 1 an.(8Hz), 1 dig.NF (12Hz) 1 AAF (12.5Hz), 1 dig.NF (12Hz) 1 AAF (12.5Hz) 1 AAF (12.5Hz)
EAP	Pitch Roll Yaw N_z A_y	0 AAF (AMSU gives AAF), 1 'analogue', 6 dig.NF 0 AAF, 2 'analogue', 1 dig.NF 0 AAF, 2 'analogue', 1 dig.NF 0 AAF, 2 'analogue', 1 dig.NF 0 AAF, 2 'analogue', 1 dig.NF

Table 2. MIL-F-9490D GAIN AND PHASE MARGIN REQTs (dB,Degrees)

Airspeed Mode Freq. Hz	Below $V_{O\,min}$	$V_{O\,min}$ to $V_{O\,max}$	At Limit Speed V_L	At 1.15 * V_L
$f_M < 0.06$	GM = 6dB No Phase Reqt. below $V_{O\,min}$	GM = ± 4.5 PM = ± 30	GM = ± 3.0 PM = ± 20	GM = 0.0 PM = 0.0 Stable at Nominal Phase and Gain
$0.06 \leq f_M < 1stASE$		GM = ± 6.0 PM = ± 45	GM = ± 4.5 PM = ± 30	
$1stASE < f_M$		GM = ± 8.0 PM = ± 60	GM = ± 6.0 PM = ± 45	

Table 3. EAP SC TEST TRANSFER FUNCTION MEASUREMENTS.

Axis	Rate	Acceleration
Pitch	q/δ_{IBDmd} q/δ_{OBDmd} q/η_{Dmd}	N_z/δ_{IBDmd} N_z/δ_{OBDmd} N_z/η_{Dmd}
Lateral	p/ξ_{IBDmd} r/ξ_{IBDmd} p/ξ_{OBDmd} r/ξ_{OBDmd} p/ζ_{Dmd} r/ζ_{Dmd}	A_y/ζ_{IBDmd} A_y/ζ_{OBDmd} A_y/ζ_{Dmd}

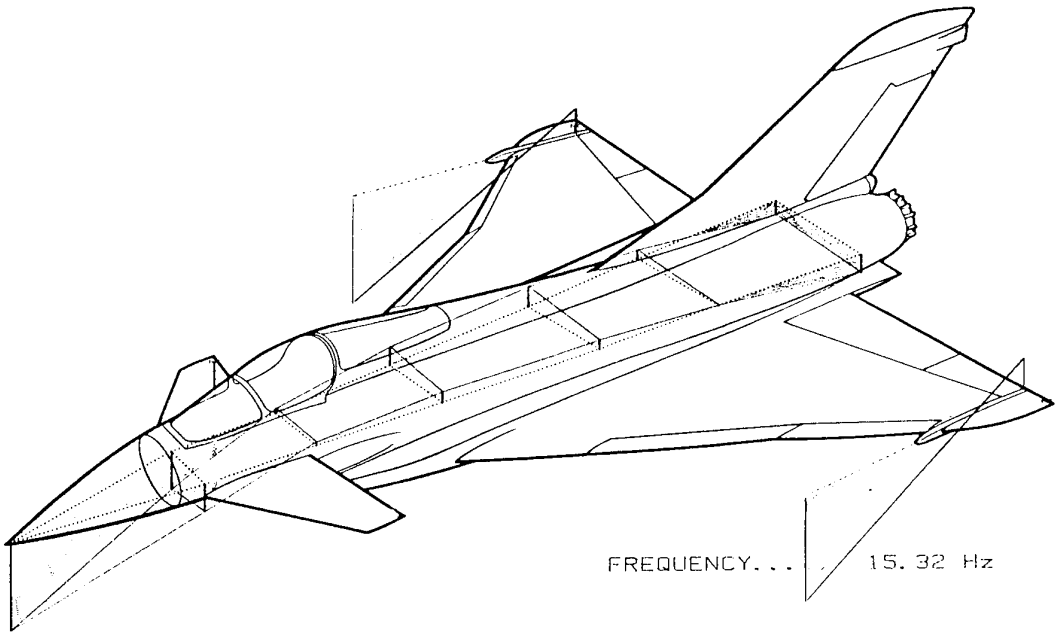

Figure 1. Typical Fuselage Bending Modeshape.

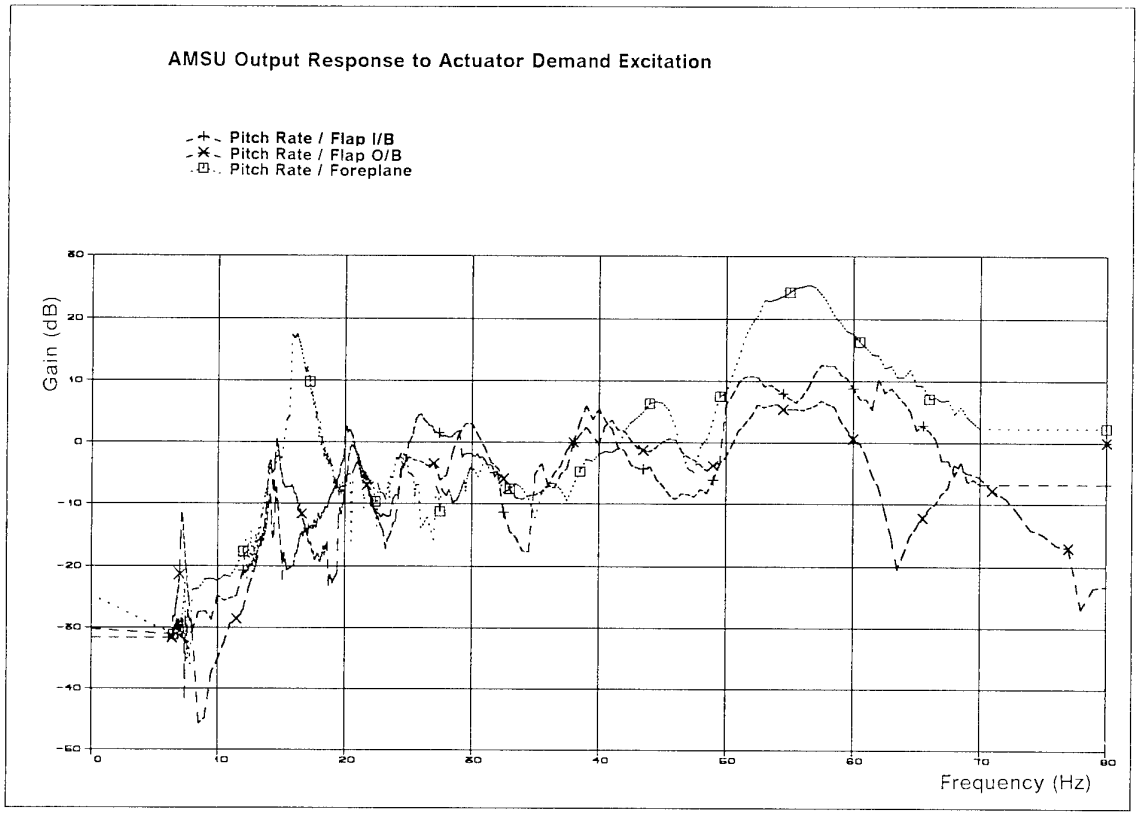

Figure 2. Ground Test Results.

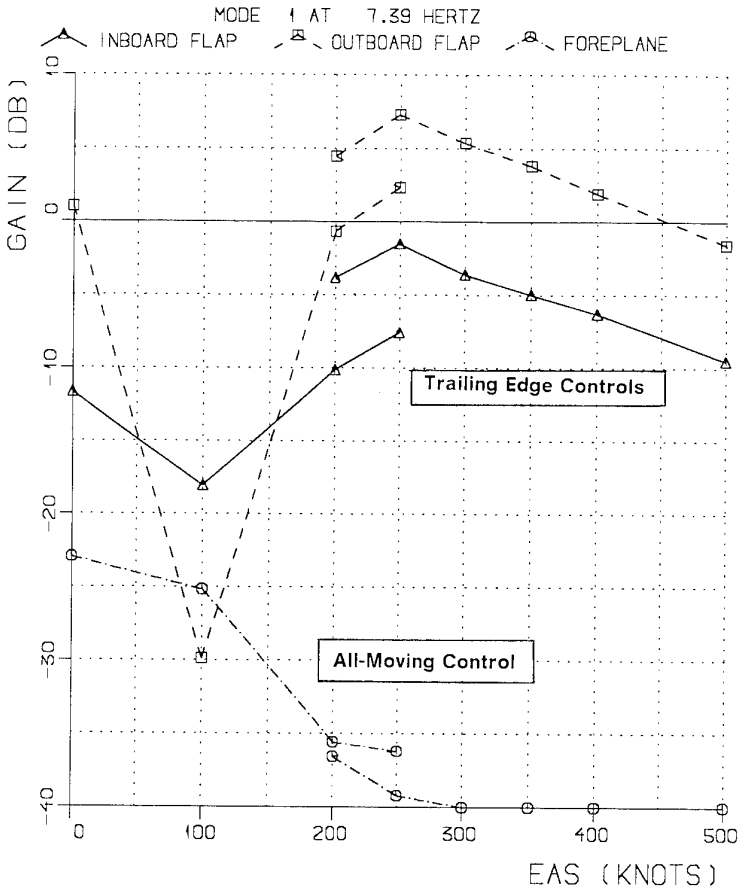

Figure 3. Variation in Control Surface Excitation Forces With Flight Condition.

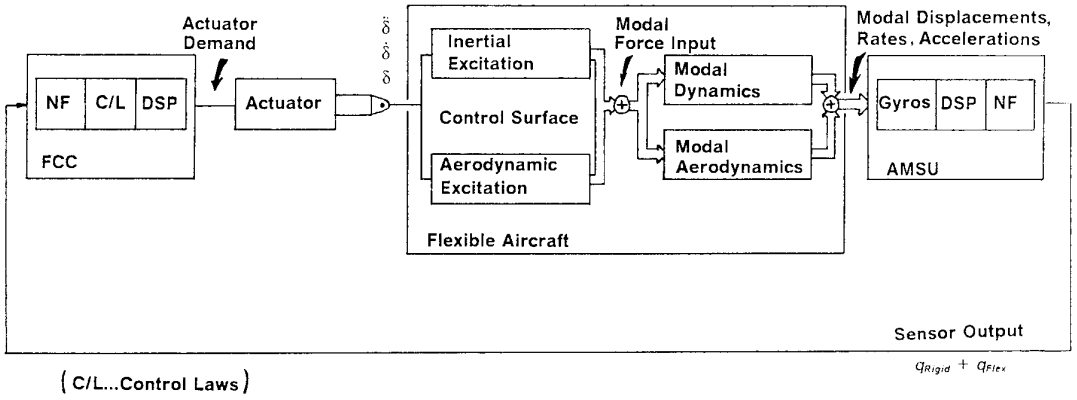

Figure 4. Schematic Representation of the SC Loop.

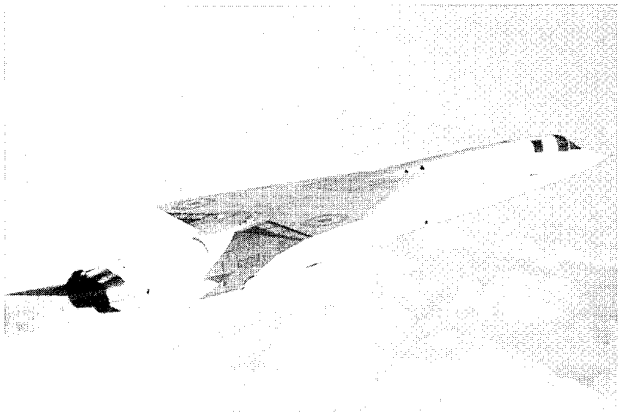

Figure 5. TSR-2

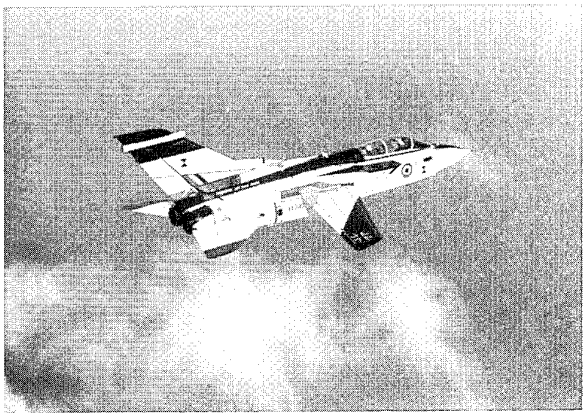

Figure 6. Tornado

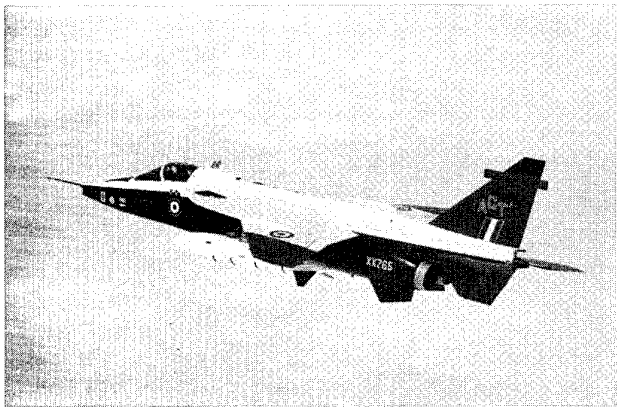

Figure 7. Jaguar FBW

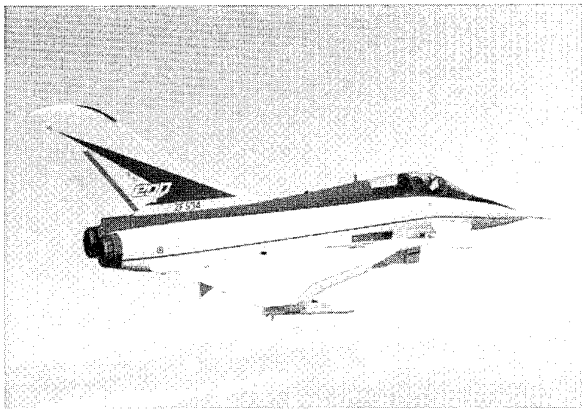

Figure 8. EAP

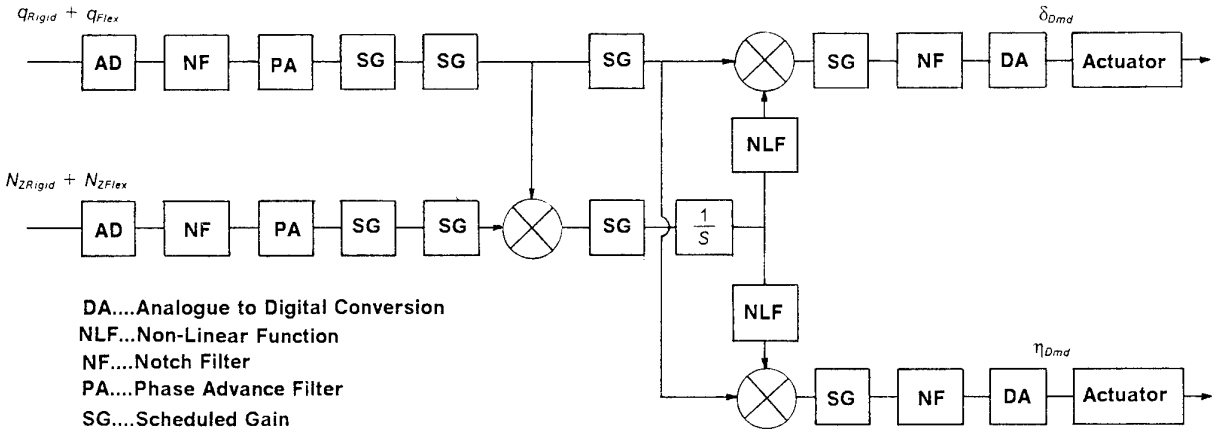

Figure 9. Schematic Diagram of EAP Pitch FCS.

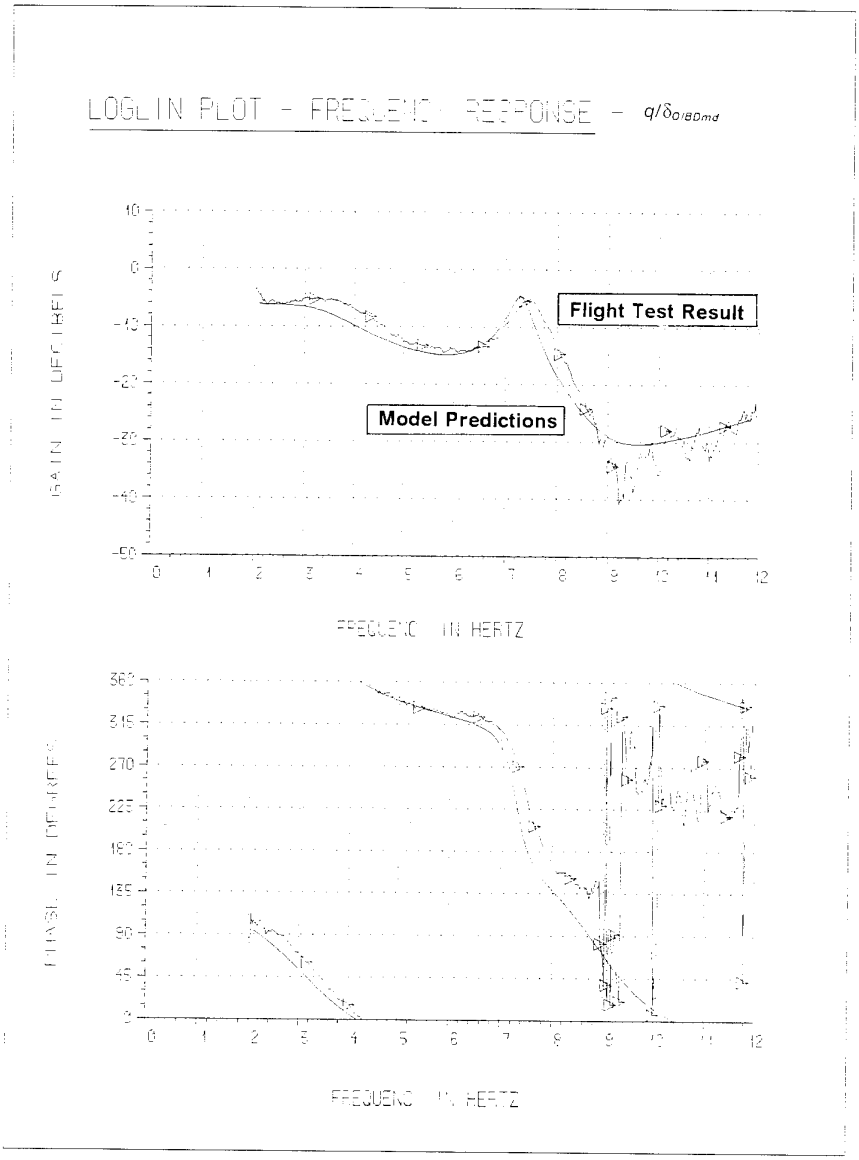

Figure 10. Typical Results from EAP IFSME Flight Test.

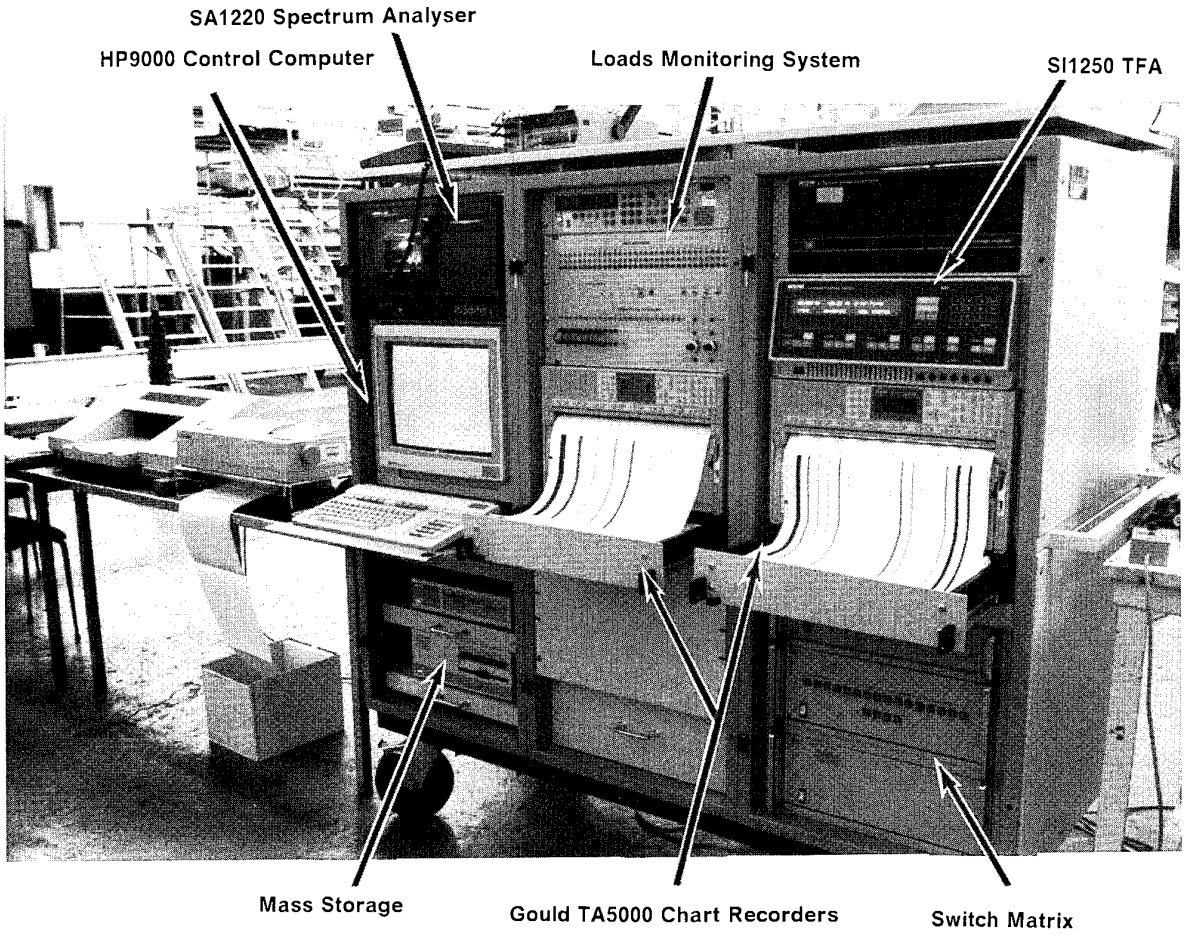

Figure 11. Structural Coupling Test Equipment.

Structural Aspects of Active Control Technology

H. Hönlinger
Deutsche Forschungsanstalt für Luft- und Raumfahrt (DLR)
Bunsenstraße 10, 37073 Göttingen, Germany
H. Zimmermann
O. Sensburg*
J. Becker*
Deutsche Aerospace (DASA), Hünefeldstraße 1-5, 28199 Bremen, Germany
*Deutsche Aerospace (DASA), 81663 Munich, Germany

Abstract

A survey on the structural relevant applications of Active Control Technology is presented. The benefits and disadvantages of various active control systems for transport and fighter aircraft are discussed. The problem of adverse structural coupling is addressed and possible solutions are outlined.

The Smart Structure Technology offers new applications for active control technology, but to exploit the full potential of this technology multidisciplinary design methods have to be improved.

1. Introduction

"**A**ctive **C**ontrol **T**echnology" (ACT) is a term for any feedback control system that operates control surfaces or exciter systems on demand, is measured by sensors, and is prepared by the feedback control laws. The most important functions of this technology are [1]

- Manoeuvre Load Control (MLC)
- Gust Load Alleviation (GLA)
- Fatigue Life Enhancement (FLE)
- Deformation Control and Elastic Mode Control
- Flutter Suppression and Flutter Margin Improvement
- Ride Comfort Improvement

During the sixties and seventies their potential had been studied in theoretical research work, by windtunnel and flight tests on series aircraft and its derivatives. The significant result of this work was that ACT provides a relatively simple concept for improving the performance of an aircraft, in case typical hardware premises are available on the aircraft. During the seventies the term "**C**ontrol **C**onfigured **V**ehicles" (CCV) [2] became popular for aircraft incorporating Active Control functions. This concept already indicated that an integrated ACT system may play a major role in defining the vehicle configuration. With the introduction of fly-by-wire technology into the design of fighter and transport aircraft, real CCV had been created. Its lay-out target, however, was in general the improvement of the **H**andling **Q**uality (HQ) by tailoring the behavior of an aircraft with reduced natural stability through systems.

The introduction of the **E**lectronic **F**light **C**ontrol **S**ystem (EFCS) offers the design engineer a chance to very simply add other Active Control functions, as mentioned above [3], but this requires an interdisciplinary design concept. In order to cover the fly-by-wire system effects on the dynamic stability of aircraft structure, the new discipline "Aeroservoelasticity" [4] was created. To take full advantage of the EFCS, including all possible Active Control functions, a multidisciplinary design approach is the necessary route to cover the structural im plications of ACT already in the design stage. One of the most problematic questions in this context is the influence of ACT on the fatigue life and fatigue damage of an aircraft structure. The process of the application of multidisciplinary analysis and design methods, which are still underdeveloped, leads already to reassessment of some traditional views in aircraft design and the acceptance of ACT in the initial design.

2. Survey on Structural relevant Application of Active Control Technology

2.1 Mechanisms to achieve structural benefits by the use of Active Control Technology

Essential elements of an ACT system are the sensors, the computer with the implemented control laws, and the actuators connected to the control surfaces or other active elements. All the elements used in ACT must be reliable enough that a safe flight and a successful mission of the aircraft is guaranteed. This means that sensors, computers, actuators, etc. have to be multiplied and a failure concept must be elaborated (Quadruplex or Triplex systems). Therefore it is obvious that an Electronic Flight Control System, standard for modern civil and military aircraft, is a premise for an inexpensive way to apply ACT.

Fig. 1 shows the principle of an EFCS. The gains of the different control laws depend on speed, M-number, and configuration features of the aircraft. Integrated into the EFCS are the Pitch Control, Roll Control, Yaw Control, as well as Auto Pilot and Active Control functions.

As already mentioned above, the real lay-out target for an EFCS is in general the improvement of the handling qualities. But an EFCS allows also more extensive use of control surfaces for any manoeuvre, e.g. for better handling in a pull-up manoeuvre, the elevator and symmetrically drooped aileron may be used in addition [6]. A consequence yielded by this more extensive use of control surfaces is a change in the load characteristics of the aircraft. An aircraft equipped with EFCS allows without any additional equipment a "care-free handling" of the aircraft, which means

- the manoeuvres can be automatically limited to a prescribed order
- the pilot can be prevented from operating outside of a desirable envelope.

Paper presented at the Flight Mechanics Panel Symposium held in Turin, Italy, from 9-13 May 1994.

This may lead to lighter structure weights via reduction of safety factors for structure design.

2.1.1 Methods of changing the external forces acting on the structure by ACT to reduce the stresses in the structure

The structure of combat aircraft is usually sized by manoeuvre loads. Gust loads therefore do not play a critical roll, except in the combination of gusts and extreme flight manoeuvres. For the structural dimensioning of transport aircraft, however, gust loads are design criteria. Thus the alleviation of gust loads is one of the most basic ACT applications for transport aircraft. Manoeuvre Load Control can be applied as well in order to reduce manoeuvre-induced bending moments on the wing to the levels induced by gusts. But mainly the GLA application will have remarkable influence on the fatigue life of the airframe.

Without any change in the control surface operation mode, the introduction of the EFCS with its control laws has a tendency to render the reaction of the aircraft motion smoother during manoeuvres which leads to a manoeuvres load reduction compared with the somewhat artificial Design Manoeuvres used for structures design that were formerly required. With the Manoeuvre Load Control, loads on parts of the aircraft structure can be reduced. In order to attain the required acceleration for a flight manoeuvre, the total forces cannot be changed, but the loads can be redistributed as such that part of the airframe experiences lower loads.

On transport aircraft wings, inboard and outboard control surfaces are moved in such a way that during a pull-up manoeuvre the centre of pressure is shifted inboard, reducing bending moments on the inner wing but preserving the same incremental lift. For example, to reach a 2,5 g pull-up manoeuvre with lower bending moments at the inner wing on the Airbus 330 or 340, the ailerons are deflected upwards, and the three outer flight spoilers are extended for g-loads higher than two (Fig. 2). But an elevator deflection is required in addition to compensate the nose-up pitching moment introduced by the deflection of the ailerons and spoilers (Fig. 2).

In the framework of GLA the reduction of severe gust loads on transport aircraft wings plays a major role. The incremental loading produced by a vertical gust has to be counteracted by the lift produced by control surface deflections on the wing. Since the control surfaces area generally is a small fraction of the wing area, the GLA is a high-gain control system. High gains of an ACT system bear the risk of instability problems for higher vibration modes of the aircraft which are not affected by the GLA system. To reduce the loading of the wing due to a severe gust, a very rapid counteraction of the control surfaces is required. The motion of the control surface is, in turn, the inducement of an additional torsion loading on the wing and additional loading on the control surface as well as control surface attachments. Usually the design driver for a transport aircraft wing is the bending load which normally lead to a large margin for torsion load. Therefore only the attachments and possibly the control surfaces themselves must be reinforced when implementing GLA. But very frequent loading on the control surfaces structures may reduce the fatigue life. Therefore GLA operates normally above an acceleration threshold to limit its effects on the control surface fatigue life. Moreover, severe stochastic gust loads are known to retard crack propagation rates, and this beneficial effect is diluted by GLA [7, 8]. This, in turn, may lead to shorter inspection intervals to cover damage tolerance requirements. The combination of all the disadvantages mentioned above gives rise to the idea that GLA will replace on evil with another.
The up gusts are usually more critical for the wing structure because their induced incremental lift force is added to the steady upward forces in level flight. Spoilers can be used to reduce the effect of the up gusts. The spoilers are positioned more inboard of the wing and their efficiency is not aeroelastically degraded as that of outboard ailerons on swept-back wings. Therefore spoilers need lower gains in the controller compared with ailerons and this will attenuate the stability problems. Open-loop (GLA) systems prevent the degradation of H.Q. which closed-loop systems may cause. This was followed halfway by the GLA installed on Airbus A 320 [9]. For the **L**oad **A**lleviation **F**unction (LAF), as the GLA is called on the A 320, the ailerons, the two outboard flight spoilers, and the elevator are used (Fig. 3). The acceleration of the total aircraft caused by a gust is measured by a set of accelerometers positioned at the centre of gravity of the aircraft. The LAF is implemented in the EFCS, and the relevant computers for ailerons and spoilers process the commands. The elevator is deflected proportional to the aileron/spoiler demand. The LAF has two states: active and inactive. The LAF is set to the active state when the 0.3 g threshold of an incremental upward acceleration is exceeded. The system is set into inactive state after the incremental acceleration remains 0,5 sec. below the threshold. Fig. 4 shows the simplified LAF control law for spoilers and ailerons.

The yaw damper installed in the L-1011 [10] reduces the fin loads by up to 27% in continuous turbulence, and this reduction was included in the aircraft strength required to meet design loads. The yaw damper on A 320 and A 330/A 340 fulfills amongst others a similar task. Fig. 5 gives schematically the effect of EFCS and GLA on A 320. Wing and fin loads are reduced, but horizontal tail loads are increased by the system.

This is an example of how AC functions may degrade the fatigue life on the concerned structures as well. On the other hand, the reduction of fatigue loads on a transport aircraft wing due to turbulence is a straight-forward form of **F**atigue **L**ife **E**nhancement (FLE). In contrast to a GLA, such a system for FLE requires the reduction of loads due to small frequent gusts rather than rare severe gusts (Design Gusts). Attention also must be paid to the contributing factors of fatigue damage. Therefore it seems difficult to define the cost function for the application of FLE for an aircraft type. As an example, an "Active Lift Distribution Control" [11, 12] was developed and fitted or to the C-5A transport fleet in order to reduce fatigue load on the wing. The objective of this program was to reduce the wing-root bending moment in manoeuvres and continuous turbulence without increasing the wing root torque by more than 5% and without degradation of aeroservo-elastic stability.

2.1.2 Methods of changing structural system properties by ACT to improve modal damping and dynamic stability.

First of all, a survey shall be presented on several big research programs on flutter suppression and real technical applications which already had been processed in the past. Sometimes this work was performed in combination with GLA.

In the mid 60's a **L**oad **A**lleviation and **M**ode **S**tabilisation (LAMS) system [13, 14] was designed and flight tested on the

B 52. Studies in this framework had been applied to the XB-70 [15] on the basis of the ILAF (**I**dentically **L**ocated **A**ccelerometer and **F**orce) principle. With regard to LAMS the YF-12A [16] was also studied. Structural mode control was incorporated in the B-1 bomber [17] design in order to achieve an acceptable level of ride quality for the crew. This was done using control vanes on the forward fuselage. Comparative design studies showed that passive stiffening of the B-1 fuselage would have required a 4300 kg structural mass to achieve the same ride quality as with the active systems which yielded only a 180 kg weight penalty. For improvement of passenger and crew comfort on the Boeing 747, a yaw damper concept [18, 19] had been applied for controlling not only the Dutch Roll response but also for the damping enhancement of lateral fuselage modes.

Most of the ACT research work in the field of Flutter Suppression had mainly been done in experimental studies in the wind-tunnel. But limited flight demonstrations have been made as well. The main part of the studies done deal with flutter of stores on fighter-aircraft [20] Fig. (6). Apart from mode damping enhancement examples, nearly no practical application of flutter suppression has been done on an aircraft in service. This is due to the fact that the certification requirements can hardly be covered in failure cases and the only possible application of this technology in the near future will be to provide the flutter margin above V_D. In any case, the Garteur Programme [21] for GLA and **F**lutter **S**uppression (FS) shall be mentioned. Garteur stands for **G**roup for **A**eronautical **R**esearch and **T**echnology in Europe. On a common dynamic similar windtunnel model, seven parties of European aircraft industries and aeronautical research establishments carried out tests on FS, GLA, and buffet control in the low-speed tunnel of the DLR in Göttingen (Fig. 7). Each party developed control laws for the disciplines mentioned and tested them. The test results, compared to the theoretical results for the ACT functions, demonstrated the reliability of the methods used for establishing the control laws. This Garteur programme paved the way for the application of ACT functions in European a/c design.

To improve passenger and flight crew comfort, a ride comfort function called **C**omfort **I**n **T**urbulence (CIT) has been developed for the Airbus A 330/A 340 based on the EFCS of the aircraft [22]. The objective of the system is to reduce aircraft response to turbulence in symmetrical and antisymmetrical modes with significant participation of the fuselage by increasing modal damping in the frequency range to 2.0 - 4.0 Hz. Two significant constraints had to be considered in development of CIT: It must not degrade the handling qualities nor the stability of the aircraft even in failure conditions. The accelerations, which have to be controlled, are measured by accelerometers close to the fuselage ends (Fig. 8/9 for the antisymmetrical case).

The signals are fed back in a control loop to the yaw damper actuators, which control the rudder, and to the elevator actuators. A structural bandpass filter incorporated in the control loop limits the frequency range of the system and avoids aeroservo elastic instability. A phase compensation and a phase adjustment filter was developed to optimize improvement of the ride acceleration, taking into account the following points:

- The frequency of the controlled modes vary with payload and fuel loading. The control laws are not adaptive for reasons of simplicity and robustness.
- A phase shift of plus or minus 60 degrees or a doubling of the gain must not decrease modal damping compared to flutter calculations results without CIT.
- CIT failure cases, i.e. a sign switch, may in the worst case lead to a limit cycle oscillation with an uncritical amplitude (proved by calculation).

Aeroservoelastic instabilities induced by the CIT system are covered by the limitation of the CIT command authority, bandpass filter, and an additional monitoring system.

The benefit of the modal damping concept is demonstrated in Fig. 10 by flight test results on A 340. Fig. 11 shows the symmetrical response with and without CIT for slight and strong turbulence. Fig. 12 gives a comparison of calculated and measured Nyquist on A 330 for the light aircraft. The agreement looks excellent.

During the early design process of the A 340, it seemed that the flutter speed requirements could not be covered for the range up to 1,15 V_D. Therefore a flutter margin augmentation system called DAF (**D**amping **A**ugmentation **F**unction) [23, 4] was designed. Due to the shape of the unstable vibration mode, the flutter could optimally be controlled by the rudder. But the linkage of the actuator and its attachments introduced nonlinearities such as dead zones and hysteresis into the control system, as shown in Fig. 13. The effect of the DAF is shown at V_{MO} in Fig. 14 by a simulation in the time domain. A flutter damping augmentation system using a control system with mechanical nonlinearities does not suppress the increase in flutter motion; it only reduces it to a limit cycle amplitude. Since the system provides only the flutter margin, the aircraft will never reach the critical speed. At least such a system did not become necessary because for the final design of the aircraft the flutter speed margins were high enough.

3. Impact of Active Control Technology on aircraft structures design

With the application of ACT on fighter and transport aircraft, a safety and redundancy concept is required for all devices used in ACT, such as sensors, computers, transmission lines, electronic cards and their interactions. The effects of ACT on structural parts of the aircraft with respect to flutter, load, stress, and fatigue have to be considered for:

- the servo control loop of each individual actuator.
- the auto pilot control law with its different modes.
- the EFC laws which improve the actions of the pilot including their degradation in failure states.
- other control laws such as for ride comfort, gust load alleviation, etc. applied on the aircraft.

All control-law states must be considered when handling a fly-by-wire aircraft in failure states. These may be called: normal law, alternate law, and further degraded direct law. These various law states yield not only different handling qualities of the aircraft - they also produce as the consequence of various aircraft motions different and possibly higher loads. This, in turn, leads to a degradation of the stability as well as to the loss of one or the other protections. Keeping in mind that these

systems were installed to improve the relatively low natural stability of the aircraft, a failure state may lead to higher loads. Due to requirements of the **M**inimum **E**quipment **L**ist (MEL), safety-critical systems have to be repaired before a new takeoff of the aircraft is possible in a mission. The consequence is that the benefits of the ACT functions are lost in a failure state of the system. Mainly for long-range transport aircraft a high-failure probability of such a system can cut back the economy of an aircraft. Therefore the integration of safety-critical ACT functions for long-range transport aircraft is still not yet carried out; comfort-relevant ACT functions, which also lead to significant weight savings, are considered desirable for integration.

3.1 Structural Coupling Effects

The sensor unit of an aircraft, the **A**ir **D**ata and **I**nertia **R**eference **U**nit (ADIRU), measures on selected locations of the airframe all neccessary signals for the various integrated control systems. The sensor signals, however, contain not only the rigid body motion but also the aircraft's structural response which is also fed back to the flight computers processing the input commands for the control surface actuators. This means that the control surfaces react not only to pilot commands and low-frequency motions of the aircraft, but also to the aircraft's structural responses. This structural coupling can cause aeroservoelastic instabilities which are as dangerous as flutter instabilities.

Aeroservoelastic instabilities must be avoided by low pass or notch filtering of the measured signals in the control loop. But the closer the frequencies of the structural modes are to the rigid body frequencies, the more difficult the attenuation of the structural responses is in the feedback loop signal. For an aircraft like the A 320, structural modes and rigid body modes are well separated in their frequencies, and the risk of aeroservoelastic instability due to Structural Coupling for the A 320 is negligible on the basis of a reasonable structure filter concept. For an aircraft like the A 340, the fundamental structural frequencies are close to 1 Hz and the risk of adverse structural coupling of the EFCS is high if a similar filter concept as on the A 320 is used. Shown in Fig. 15 is an early development stage of the aircraft. Such a degradation of the damping of certain structural modes by the EFCS due to an insufficient filter concept is not acceptable for any aircraft. This example demonstrates that for aircraft with the structural modes close to the rigid body modes the flight mechanical control laws also have to be established by methods which simultaneously take into account the effects of H.Q., aeroelasticity, and loads.

For fighter aircraft, the structural coupling problems and the methods to cure it are similar. Direct coupling between flight mechanic modes and elastic modes does not occur. High-performance requirements for fighter aircraft, i.e. high roll and pitch rates require a flight-control system of which the transfer functions have a very small phase shift in the low-frequency range. This rejects the application of low-pass filter concepts to avoid structural coupling. The minimization of elastic mode feedback in the control loops of a fighter control system is generally achieved by introduction of notch filters. The elimination of adverse structural mode coupling, i.e. aeroservoelastic instabilities by notch filters, however, can also create significant phase shifts at low frequencies, which in turn will cause unacceptable fighter aircraft handling qualities. This demonstrates that even on fighter aircraft, the H.Q. are pending on the elastic modes stability requirements as well.

The application of active control concepts, combined with the structural notch filters for low frequency elastic modes up to a defined frequency, in order to attain vibration alleviation, can improve the situation on modern fighters.

Previous investigations on fighter aircraft have shown that considerable vibration alleviation of elastic wing / fin modes by using acceleration feedback of measured wing / fin accelerations at optimized sensor locations (24), (25) can be achieved. However, this concept - although often proposed for active flutter suppression - has severe disadvantages with respect to control system redundancy and complexity which must be failsafe in the full-flight envelope for all configurations.

Therefore a combined structure notch filter and active control concept using the existing pitch-roll-yaw rate signals is proposed in order to improve the situation of unacceptable low-frequency phase shifts and resulting handling quality. The elastic mode control - implemented here as vibration damping function - has per se the same redundancy as the flight-control system.

3.2. Proposal of a combined notch filter and active elastic mode control concept to avoid structural coupling

The block diagram in Fig. (16) describes schematically the active control feedback path of a modern fighter flight control system that consists of the measured pitch, roll, and yaw rate signals. The signals are filtered by so-called phase advance filters to reduce the phase shifts at low frequencies which are caused by the „notch" filters. The „notch" filters introduced are designed to provide a sufficient stability margin for the elastic modes and also to act as filters for active elastic mode vibration alleviation. Gain and phase margin requirements to be met by the notch filters and active elastic mode control are described in Fig. (17). When looking at the behaviour of the open-loop frequency response with and without control, the required principles of the concept are self-explanatory:

- Minimization of phase lag from elastic mode control for the rigid aircraft
- Phase shift of the 1st elastic mode to the left with respect to the requirements
- System robustness for all light conditions with respect to aircraft configuration is achieved by using open-loop frequency envelope response functions of all worst-case configurations.

Additional requirements to be met are:

- Minimisation of actuator fatigue life by limiting the additional actuator loads
- No degradation of flutter speeds for the aircraft by elastic mode control.

Benefits of the combined concept are:

- Improvement of aircraft handling quality
- Reduction of elastic aircraft vibration modes through the elastic mode feedback via rate signals
- Possible improvement of flutter margins
- No additional redundancy concept necessary when using the flight-control system feedback paths.

3.3. Structural Coupling Tests

For the design and implementation of structural notch filters, the transfer function of the aircraft without a controller must be known in detail, i.e. the influence of unsteady aerodynamics on the frequencies and amplitudes of the critical vibration modes, changes of the modal behaviour of the aircraft due to under wing stores, etc.

To validate the calculated transfer functions of the aircraft which are used for the filter design, the so called **S**tructural **C**oupling **T**ests (SCT) are performed (Fig. 18). The classical structural coupling tests consist of 3 phases:

1. Measurement of frequency response functions of the aircraft without Flight Control System at zero airspeed

2. Measurement of open-loop transfer functions and loop closure procedures on ground

3. Inflight structural coupling testing to validate the aerodynamic assumptions for notch filter placement and design.

Open-loop testing is not possible on an aerodynamically unstable aircraft in flight. Therefore closed-loop tests and recalculation of the open-loop transfer functions are necessary.

The test procedures applied in structural coupling tests are: The aircraft will be excited by stimulating the control surfaces actuators with sinusoidal inputs (frequency sweep, continuously or stepped) and measurement of the aircraft response at various points, i.e. sensor platform, dedicated points within the Flight Control System. For the test on ground the aircraft is supported on airsprings to simulate the free-free condition at V=0 kts or on wheels, depending on the predicted stability margins. The main problem of the SCT is to generate proper excitation of the aircraft through the control surfaces.

4. Smart Structures Technology

4.1. Integration of Active Control Technoloy with the help of smart materials into passive structures

Historically, the ACT was initiated as a repair solution mainly for solving stability problems and weight reduction measures of existing aircraft structures, as already outlined. This technology used the classical actuator and sensor systems of the aircraft in combination with optimized control laws, as seen in Fig. 19. The new generation of smart materials now offers the potential of a higher grade of integration of the ACT into the structures, because Smart Materials, i.e. Piezo material, can be used simultaneously as a sensor and actuator, and can be integrated directly into the carrying primary structure. These material properties allow the ACT goals, e.g. Gust Load Alleviation, Flutter Suppression, Ride Comfort, etc. to be realized as integrated solutions and offer in addition new potential for solving the current problems and shortcomings of ACT. The combination of sensor and actuator in one material and the possiblity of distributed integration into metallic or composite structures leads to smart structures which are able to actively change the geometry of the structure and modify its stiffness and damping properties.

It must be clearly stated that smart materials will not replace the materials used for primary, i.e. carrying airframe structures and will not replace the optimization of these passive structures in the near future.

4.2. Problems to be solved in the near future

There exist problems in two main areas that need to be solved in the near future. Firstly, the improvement of the materials' performance and properties. Smart materials such as „Piezo materials" are powerful but their elongation or stroke is very small. Thermal stability and aging need to be improved. Also, the necessary voltage level for actuating is still too high but has already been already decreased from 1000 V to 100 V. The second critical area is the integration of the smart material as active members into the passive carrying structure as seen in Fig. 20. This includes the embedding, compatibility, power supply, etc. The redundancy and safety problems in smart structures is anticipated to be of less importance because there is always the passive primary structure which allow a reduced but safe operation of the vehicle. However, the problems addressed in chapter 3 also have to be taken into account.

4.3. Vibration control using smart structures

In the area of smart structures, the concept of active damping has received considerable attention in the past few years. The basic idea of active damping is that piezoelectric materials can be used to induce extra damping in a structure, hence reducing the vibration levels in the various modes of the vibration of a structure. Extra damping can be generated in a structure by a number of methods. The traditional method is to apply forces to the structure which are 90 degrees out of phase to the motion of the structure. The technique described in this paper is to actively enhance the damping of a passive element in the structure. This can be done very effectively when constrained layer damping is used. The constraining layer is bonded to the structure using a viscoelastic material which acts as a passive damping element. The constraining layer effectively induces shear in the damping material, hence improving the damping properties of the structure. One way of inducing even more shear into the damping material is to actively control the motion of the constraining layer. There are two ways of achieving this. One is to use a piezoelectric polymer as the constraining layer and to control its motion by applying the appropriate voltage. The second technique is to use piezoelectric materials in addition to a constraining layer.

As an example of this technology, the following investigation [26] shows that with a countilever beam, the use of piezoceramic and constrained layer damping materials can be effectively combined in a hybrid system to produce considerable levels of vibration reduction.

The choice of sensor/actuator in Feedback Control Systems has always been a major challenge. Piezoelectric materials with their small size and high-strain sensitivity offer a good and practical alternative to traditional magnetic or hydraulic sensors/actuators for active control application. The inverse piezoelectric effect is a property of piezoelectric material that can be fully exploited when one component is to be used both as sensor and actuator.

Fig. 21 shows a piezoceramic pad bonded to the constraining layer of a beam. The viscoelastic material between the beam and the constraining layer is subject to extra shear as a result of the constraining layer. The piezoceramic can be used to control the strain of the constraining layer and hence the

amount of shear in the viscoelastic material. This type of beam was experimentally investigated.

Several experiments were carried out. In the first experiment, acceleration feedback was used to highlight the differences between active control and active damping. Active control is a term used here for a beam with no added damping apart from that provided by the piezoceramic. Active damping, on the other hand, is used to describe the phenomenon of actively controlling the strain of a constraining layer which would enhance the passive damping properties of the beam with **C**onstrained **L**ayer **D**amping (CLD).

The results are shown in Fig. 22. There are four cases shown: a beam with no feedback and no added damping (simple beam), a beam with CLD but no feedback, a beam with feedback but no CLD (active control), and finally a beam with CLD and feedback control (active damping).

The simple beam has the highest peaks in both modes of vibration. Important results are obtained when both modes of vibration are examined closely for each of the four cases mentioned above. Considering the beam with CLD, it can only be seen that the second mode is attenuated significantly more than the first mode. This is not surprising because passive damping elements tend to perform better at high frequencies. On the other hand, the beam with active control has a much lower vibration level in the first mode than in the second mode. Active control increases the damping in the first mode by a factor of 16 and in the second mode by a factor of 3, compared to the simple beam. The beam with active damping produces slightly lower levels of damping in the first mode but is considerably better in the second mode.

Fig. 22 shows that acceleration feedback changes the natural frequencies at both modes of vibration. In order to generate active damping in the beams, it is preferable to maintain the same stiffness because this will ensure that all the energy applied to the feedback system is directed toward controlling the damping.

The same experiment carried out using velocity feedback produces the results shown in Fig. 23. Considering the first mode at 115 Hz, it can be seen that active control and active damping produce similar levels of vibration. It is important to note that the frequency of the first mode does not change when velocity feedback is used. In the second mode, active damping produces better results than active control because the benefits of CLD are combined with that of active control. There is a shift in the frequency of the second mode which can be contributed to small phase shifts introduced into the loop by the amplifiers at high frequencies. The velocity feedback is advantageous in the concept of active damping compared to active control, because in the first mode there are very small differences in the damping levels, and in the second mode active damping provides almost twice the damping of active control.

4.4. Structural health monitoring

Another valuable spin-off technique of smart materials application is structural health monitoring. The use of smart materials as sensors or as an actuator network offers the possibility for structural health monitoring for composites as well as for metallic materials especially in critical areas of primary structures. There is a lot of R&D activity on this subject and different approaches are under investigation. Structural health monitoring is becoming more and more an important aspect for the maintenance of a modern air fleet and therefore effort has to be made on this subject.

5. Conclusions

Active Control Technology started as a repair solution to improve the shortcomings of high performance aircraft due to flutter, gust loads and flight mechanics. It was soon recognised that this technology must be used as a design tool in order to exploit its full potential. In combination with fly-by-wire and high-performance digital control computers, an attempt was made to integrate ACT into the CCV concepts. This concept included improvements of handling qualities, reduction of elastic aircraft vibrations through elastic mode feedback, and possible improvement of flutter margins. Safety-critical Active Control Functions, however, have not yet been implemented into series aircraft because of certification problems. Modern digital flight control concepts seem to facilitate the introduction of AC functions. However, this concept also raises new questions such as: Is it wise to use one central computer or to use decentralized computation?

The combination of ACT with structural optimization, smart materials, and powerful computer techniques opens a new, fascinating field of smart structures applications or adaptronics. Retrospectively analyzing 15 years of experience in this challenging technology, it must be concluded that the full potential of this technology has not been exploited enough. One possible reason may be the strategy of dealing with this technology. ACT is a multidisciplinary technology and it must be developed with the methods of multidisciplinary or concurrent engineering.

References:

[1] Structural Integrity of Aeronautical Vehicles - Impact of Active Control Technology. Subcommitee on Non-Atomic Military Research and Development, Action Group HAG-6, Oct. 1989.

[2] Kujawski, B.T.; Control Configured Vhicles B-52 Program Results, Paper 14 in Agard Cp 157, Impact of Active Control Technology on Airplane Design, Oct. 1974.

[3] Molzow, M. and H. Zimmermann; Influence of Active Control on the Design Process of a Large Transport Aircraft, Agard Report 794 Integrated Airframe Design Technology, Antalya April 1993.

[4] Zimmermann, H.; Aeroservoelasticity. Computer Methods in Appl. Mechanics and Engineering, 1990 (1991) pp. 719-735.

[5] Smart Structures for Aircraft and Spacecraft; Agard Conference Proceedings 531, Papers presented at the 75th Meeting of the Agard S & M Panel, Lindau, Oct. 1992.

[6] Rider, C.K.; An Investigation of the Variability in F/A-18 loading, TTCP HAG-6 Second Workshop on Impact of Active Controls on Structural Integrity, Farnborough, UK, Sept. 1988.

[7] Gray, I.G.; Fatigue Crack Propagation Test Programme for the A 320 Wing, ICAF Montreal, 1987.

[8] Gray, I.G.; Damage Tolerance of Civil Aircraft, the Future of Active Control Technology, TTCP HAG-6, Second workshop on Impact of Active Controls on Structural Integrity, Farnborough, UK, September 1988.

[9] Hockenhull, M.; Gust Load Alleviation on the Airbus A 320, TTCP HAG-6, First workshop on Impact of Active Controls on Structural Integrity. Wright-Patterson AFB, Ohio, USA, September 1987.

[10] Hoblit, F.M.; Effect of Yaw Damper on Lateral Gust Loads in Design of the L-1011 Transport, AGARDograph No. 175 Active Control Systems for Load Alleviation, Flutter Suppression and Ride Control, March 1974.

[11] Disney, T.E.; C-5A Load Alleviation, Paper 10 in Active Controls in Aircraft Design, AGARDograph 234, 1978.

[12] Grosser, W.F., W.W. Hollenbeck and D.C.Eckhold; The C-5A Active Lift Distribution Control System, Paper 24 inAGARD CP 157 Impact of Active Control Technology on Airplane Design, October 1974.

[13] Burris, P.M. and M.A. Bender; Aircraft Load Alleviation and Mode Stabilization, AFFDL-TR-68-158, 1968.

[14] Burris, P.M. and M.A. Bender; Aircraft Load Alleviation and Mode Stabilization, C-5A System Analysis and Synthesis, AFFDL-TR-68-162.

[15] Wykes, J.H., L.U. Nardi and A.S. Mori; XB-70 Structural Mode Control System Design and Performance Analysis, NASA CR-1557, July 1970.

[16] Edinger, L.D., F.L. Schenk and A.R. Curtis; Study of Load Alleviation and Mode Suppression (LAMS) on the YF-12A Airplane, NASA CR 2158, Dec. 1973.

[17] Wykes, J. H. and C.J. Borland; B-1 Ride Control, Paper 9 in Active Controls in Aircraft Design, AGARDograph 234, 1978.

[18] Ho, J.K. et al; Aircraft Modal Suppression System Existing Design Approach and its Shortcomings, Workshop on the Computational Aspects in the Control of Flexible Systems, Williamsburg 1988.

[19] Fuller, J.R.; The Effects of an Airplane Ride Comfort Modal Suppression System on Aircraft Response and Loads, TTCP HAG-6, Second Workshop on Impact of Active Controls on Structural Integrity, Farnborough, UK. September 1988.

[20] Hönlinger; H. Active Flutter Suppression on an Airplane with Wing Mounted External Stores, Paper 3 in AGARD CP 228, Structural Aspects of Active Controls, April 1977.

[21] Försching, H.; Active Control Application for Flutter Suppression and Gust Load Alleviation. Garteur TP-022.

[22] Seyffarth, K., M. Lacabanne, K. König, H. Cassan; Comfort in Turbulence (CIT) for a Large Civil Transport Aircraft. Forum International Aéroélasticité Dynamique De Structure, Strassbourg 1993.

[23] Dehmel, W., K. König; Damping Augmentation Functions of a Civil Aircraft. International Forum on Aeroelasticity and Structural Dynamics, Aachen 1991

[24] Sensburg, O, J. Becker, H. Hönlinger; Active Control of Flutter and Vibration of an Aircraft Proceedings of the International IUTAM; Symposium on Structural Control University of Waterloo, Ontario, Canada, 4th - 7th June 1979

[25] Sensburg, O., H. Hönlinger, M. Kühn; Active Control of Empennage Flutter. Proceedings of the 40th Meeting of Structures and Material Panel of AGARD, Brussels, Belgium 13th - 18th April 1975

[26] Azvine, B., G.R. Tomlinson, R.J. Wynne, O. Sensburg; Vibration Suppression of Flexible Structures Using Active Damping, 4th International Conference on Adaptive Structures.

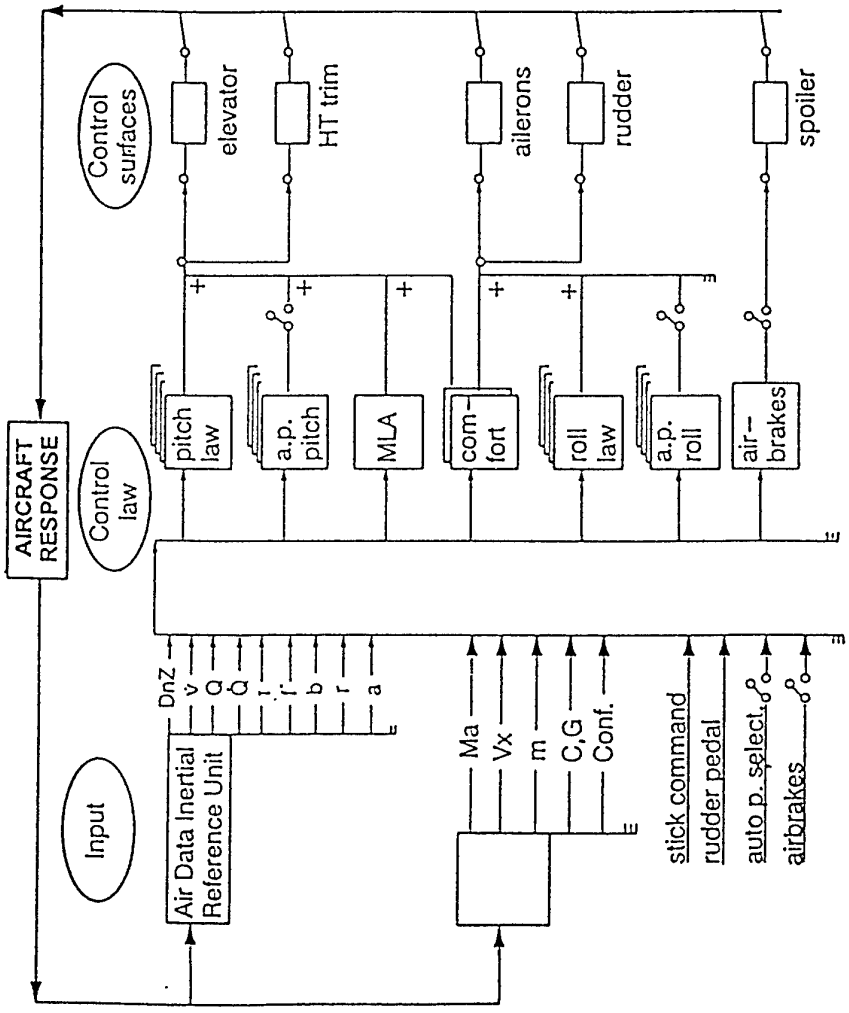

Fig. 1 SIMPLIFIED ELECTRONIC FLIGHT CONTROL CIRCUIT OF AN TRANSPORT AIRCRAFT

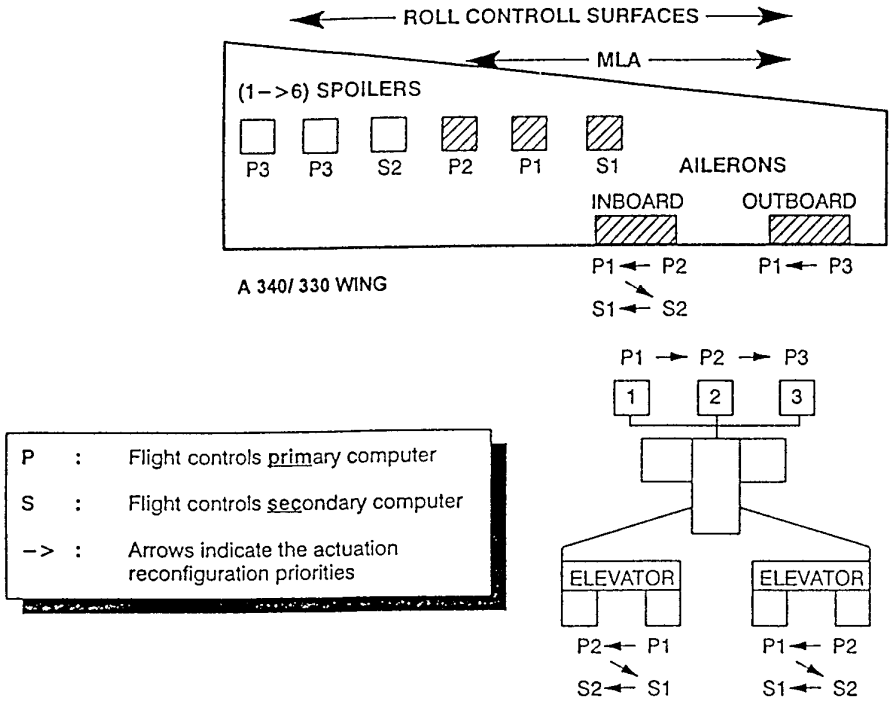

Fig. 2: MANOEUVRE LOAD CONTROL SURFACES A330/340

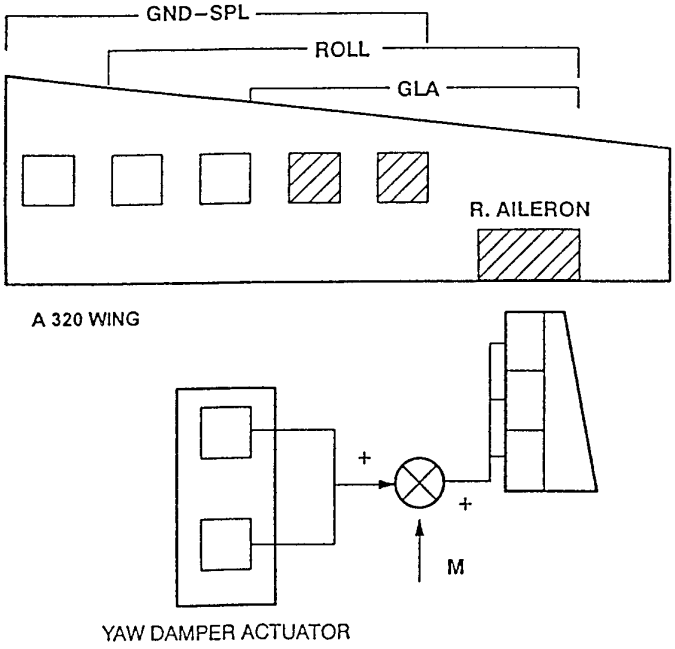

Fig. 3 GUST LOAD CONTROL SURFACES AND YAW DAMPER CONCEPT ON A 320

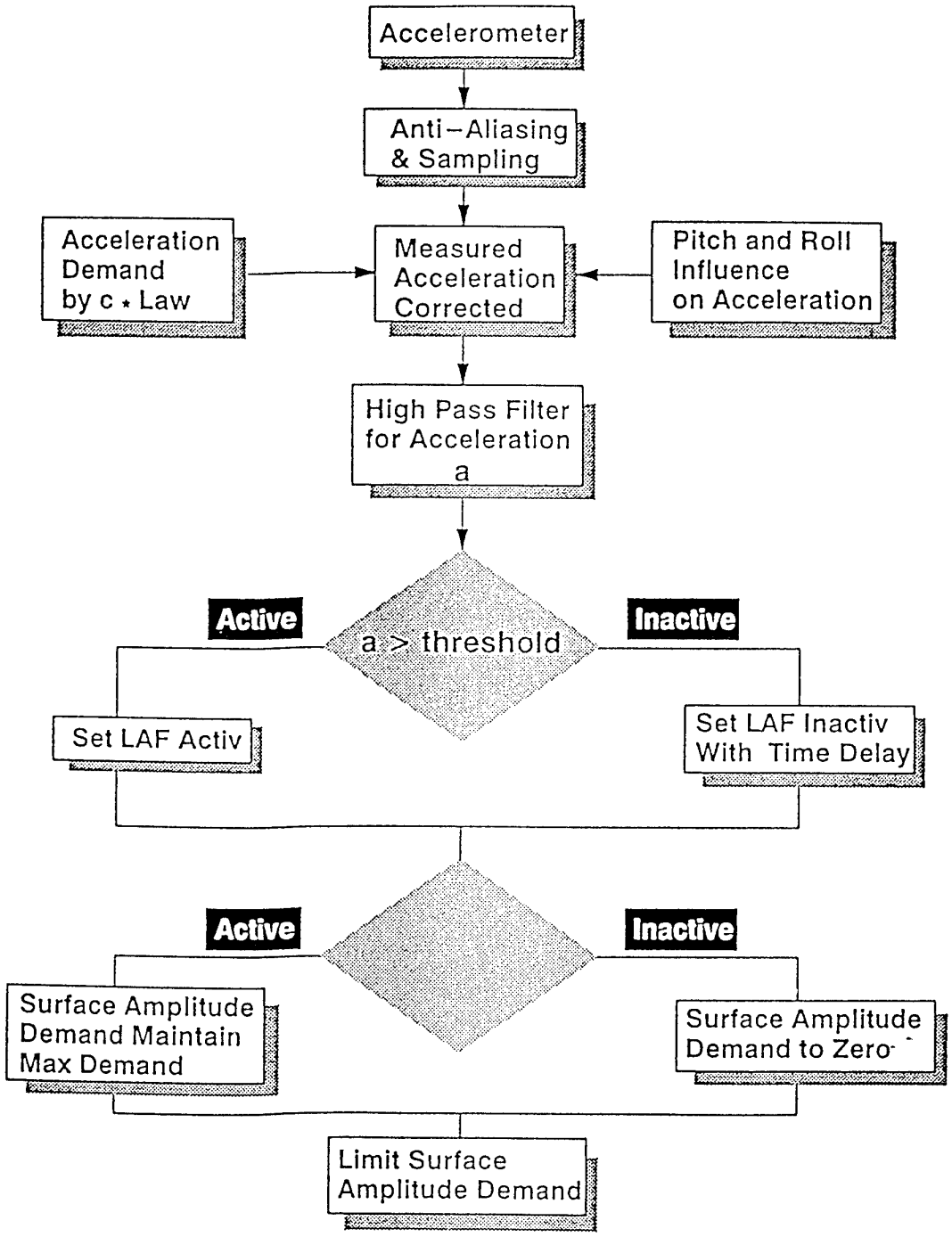

Fig. 4 CONTROL LAW OF LOAD ALLEVIATION FUNCTION

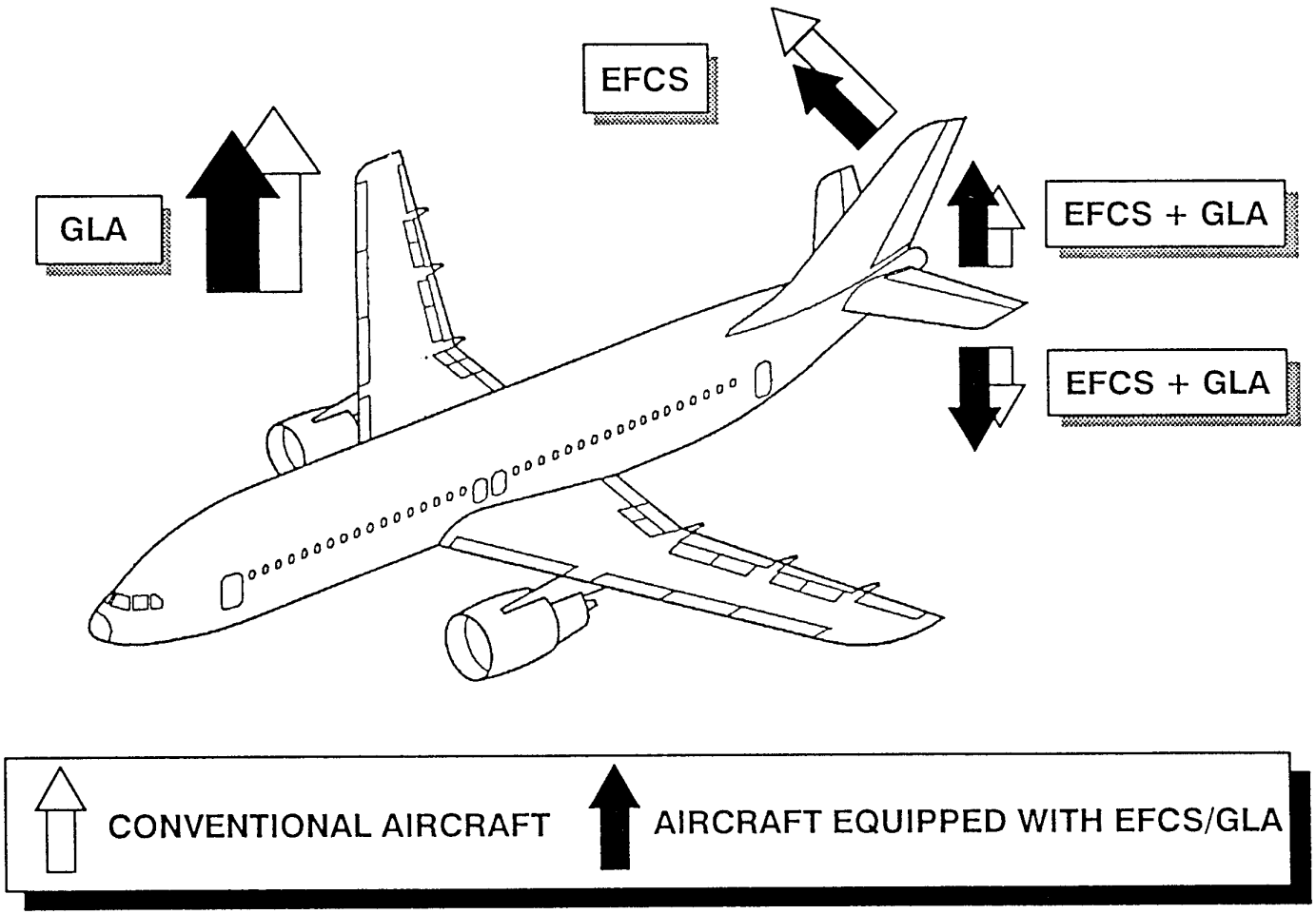

Fig. 5 EFFECTS OF FLY–BY–WIRE SYSTEM TECHNOLOGY ON STRUCTURAL LOADS

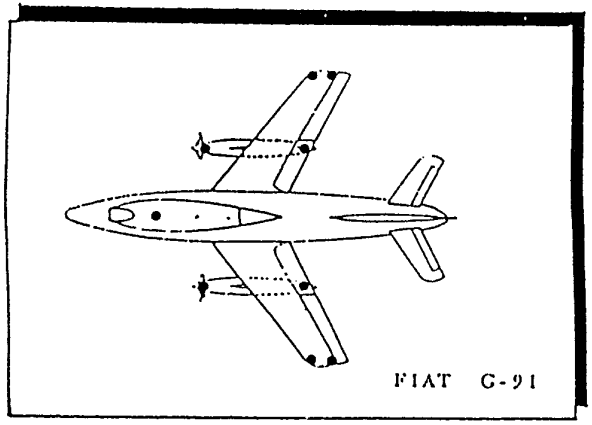

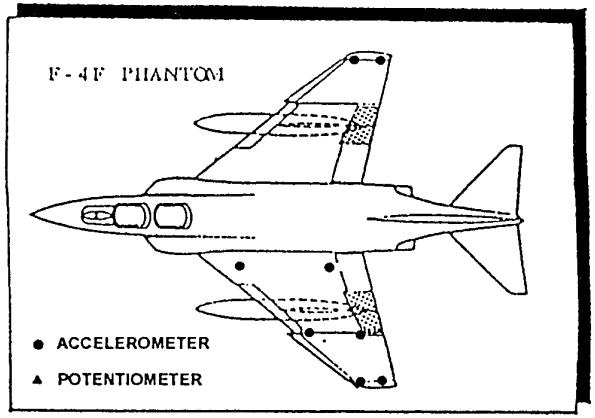

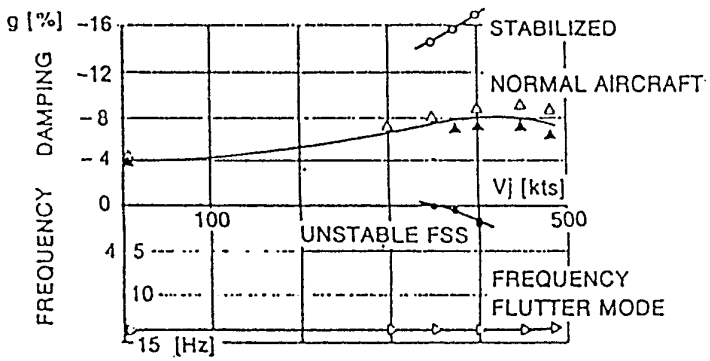

IMPROVEMENT OF FLUTTER STABILITY

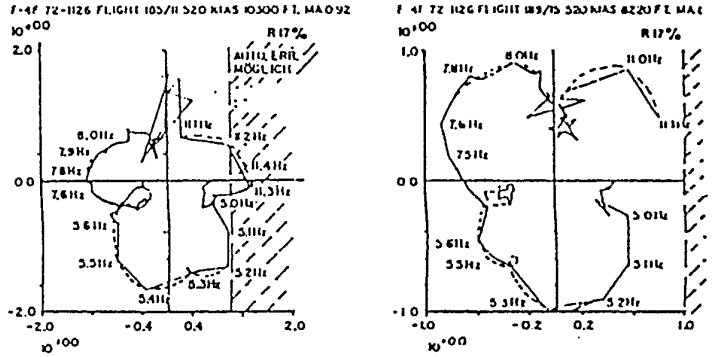

INFLIGHT OPEN LOOP MEASUREMENTS

Fig. 6 FLIGHT TEST PROGRAMS TO INVESTIGATE FLUTTER SUPPRESSION

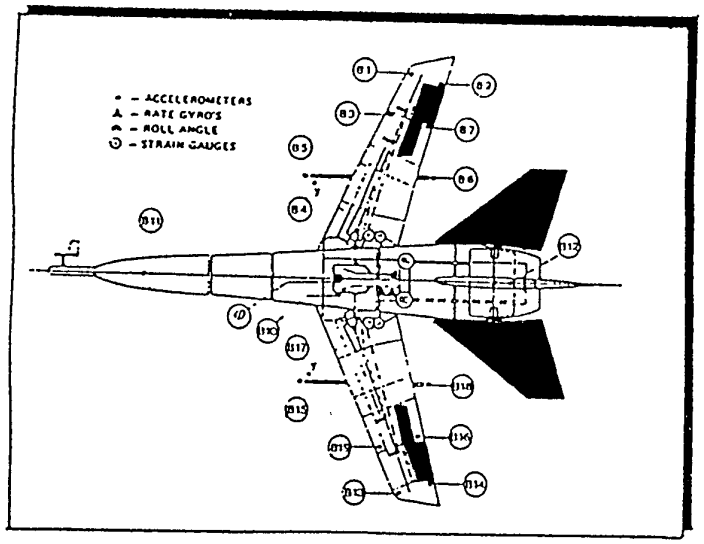

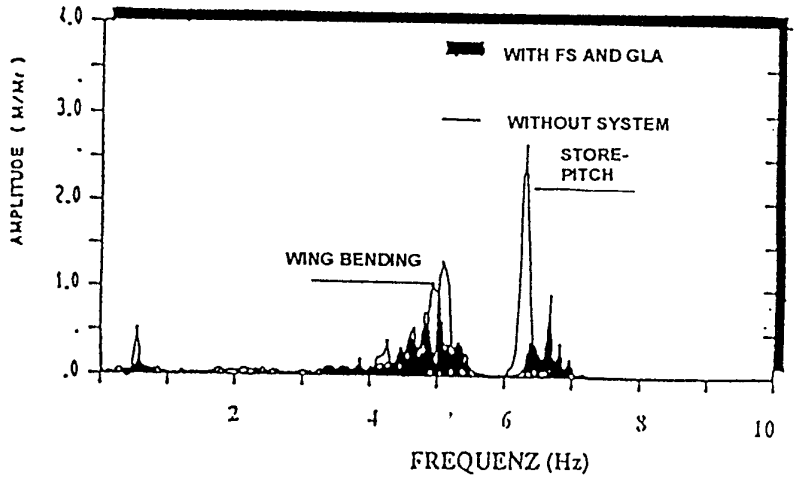

BLOCKDIAGRAM OF AN ADAPTIVE CONTROLLER CONCEPT

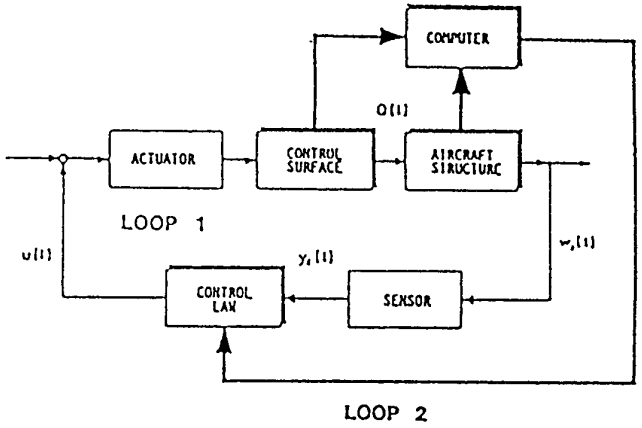

- FLUTTER SUPPRESSION
- GUST LOAD ALLEUIATION
- MULTIFUNCTIONAL CONTROL SURFACES

COMMON PROGRAM OF : BAe/RAE; DA; DLR; NLR
ONERA

Fig. 7 GARTEUR PROGRAM TO INVESTIGATE ACTIVE CONTROL TECHNOLOGIES

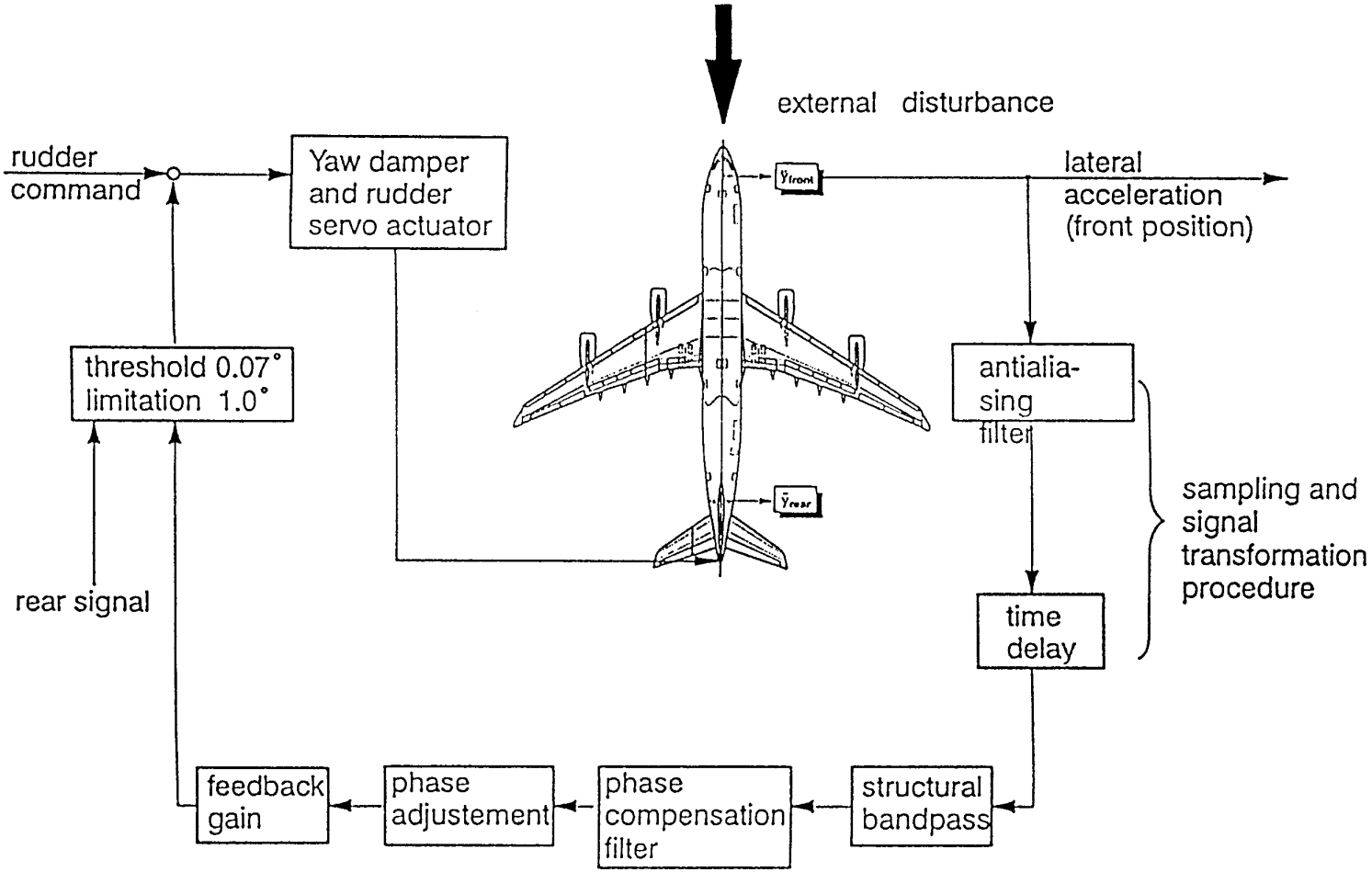

Fig. 8/9 BLOCKDIAGRAM OF COMFORT IN TURBULENCE FUNCTION (CLOSED LOOP CONTROL , FRONT SENSOR)

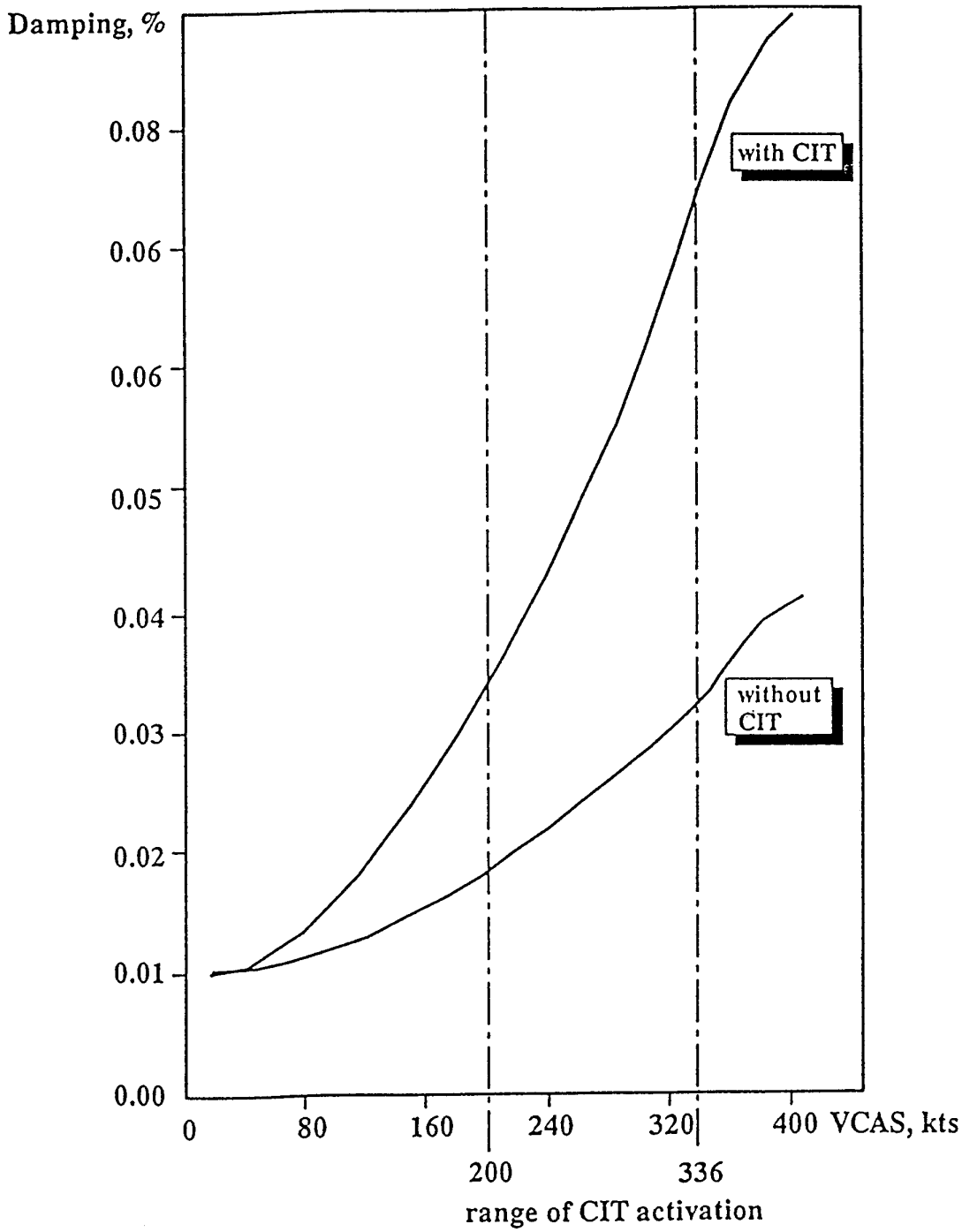

Fig. 10 COMFORT IN TURBULENCE FUNCTION PERFORMANCE; BENEFIT OF MODAL DAMPING; SYMMETRICAL CASE

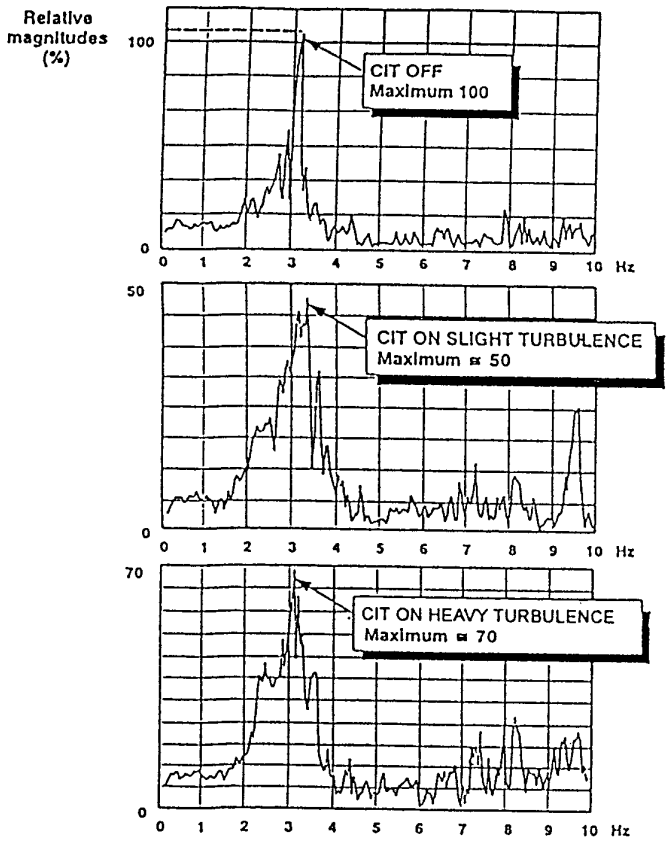

Fig. 11 COMPARISON OF FRONT FUSELAGE TRANSFER FUNCTIONS
CIT OFF - CIT ON IN SLIGHT AND STRONG TURBULENCE

Test : V82 / 19A, light a/c, trim empty, VC = 330 kts / Ma 0.86

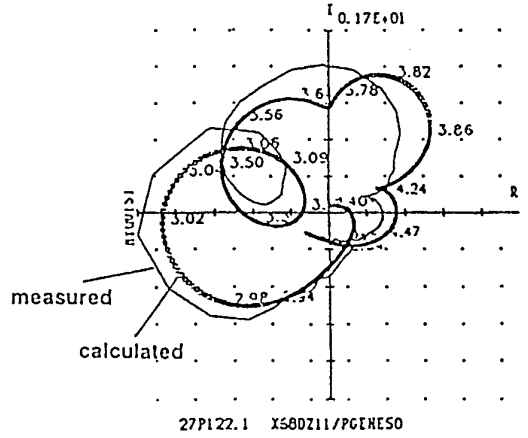

Test : V82 / 07A, light a/c, trim full, VC = 330 kts / Ma 0.86

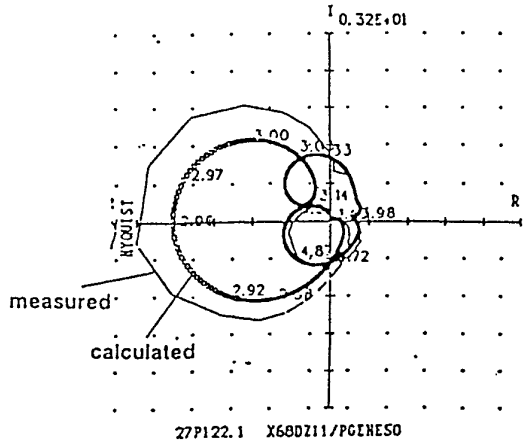

Fig. 12 CIT SYMM:; OPEN LOOP NYQUIST;
CIT COMMAND DUE TO ELEVATOR EXCITATION
COMPARISON OF CALCULATIONS AND MEASUREMENTS

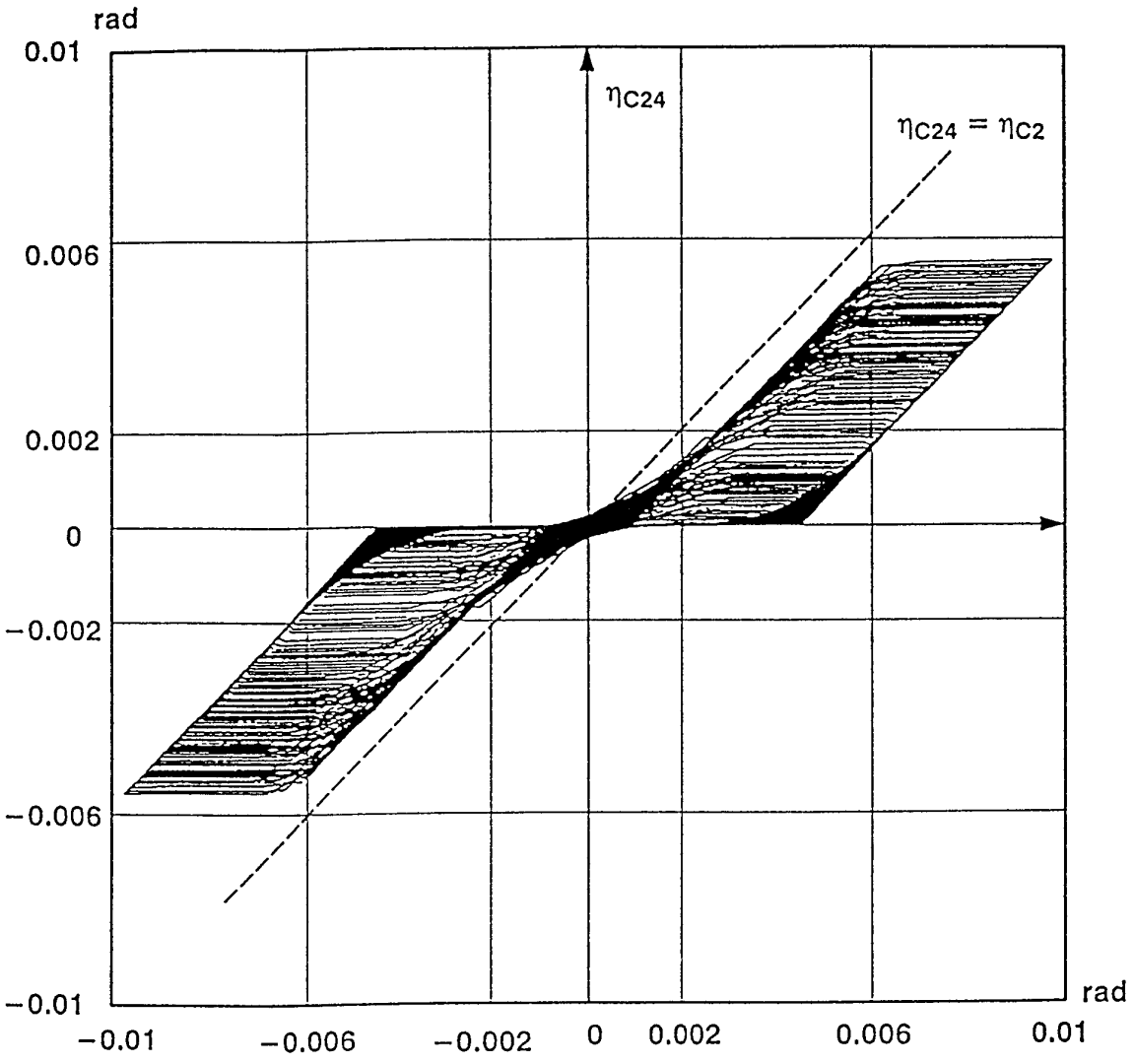

η_{C2} : position of yaw damper servo actuator
η_{C24} : position of valve levers at rudder actuator

Fig. 13 OUTPUT/INPUT DIAGRAM OF THE RUDDER CONTROL

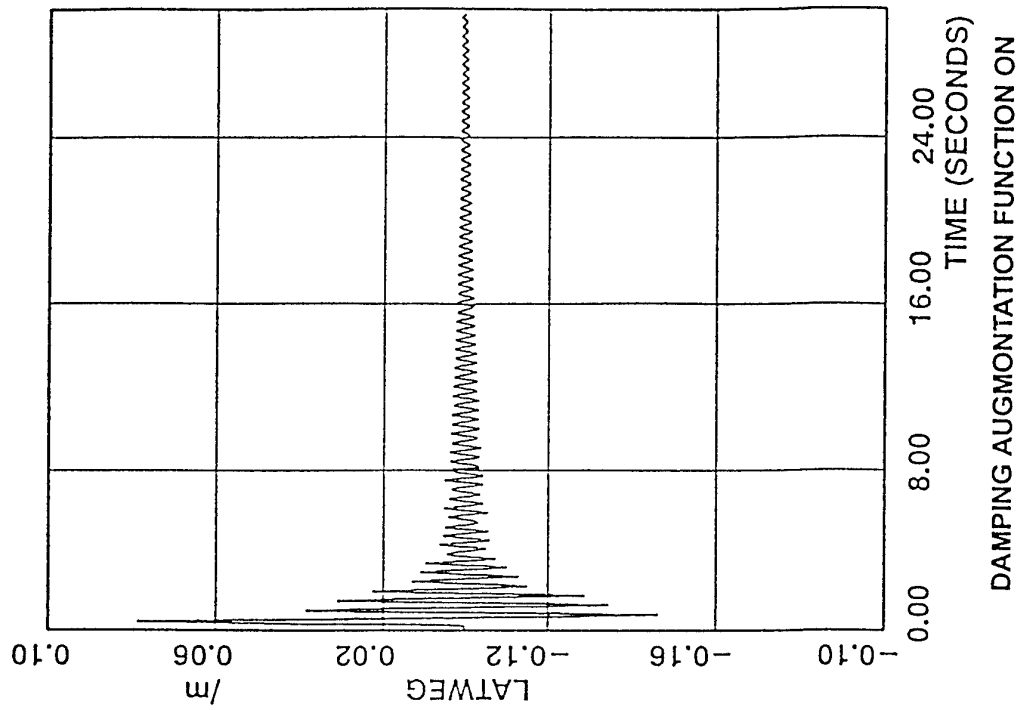

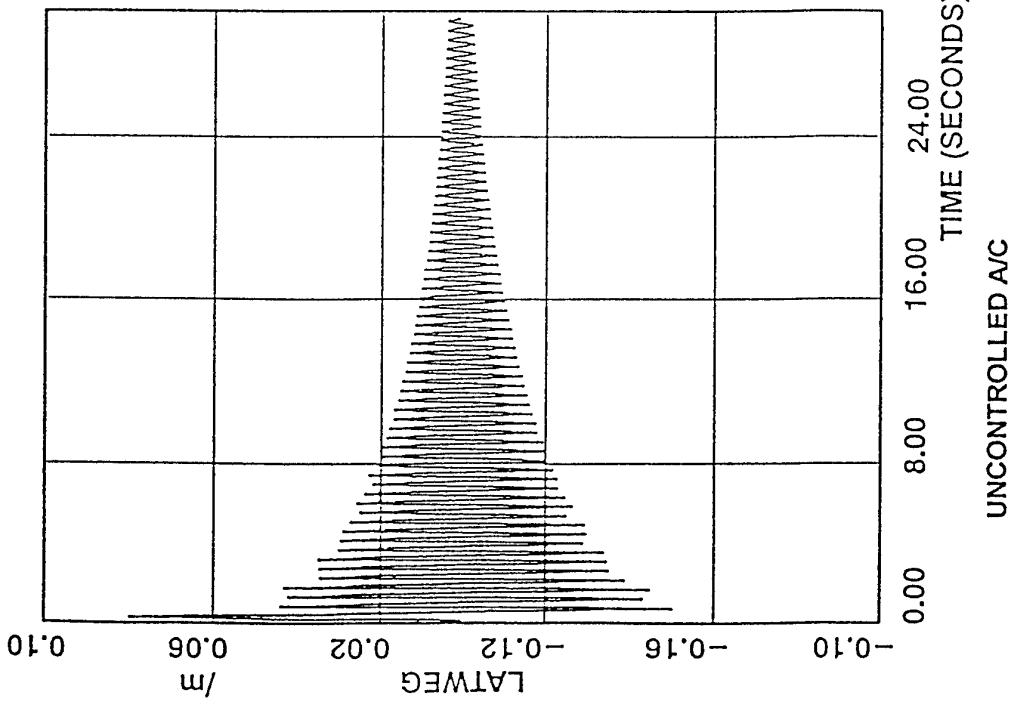

Fig. 14 LATERAL DISPLACEMENT AT V_{MO}

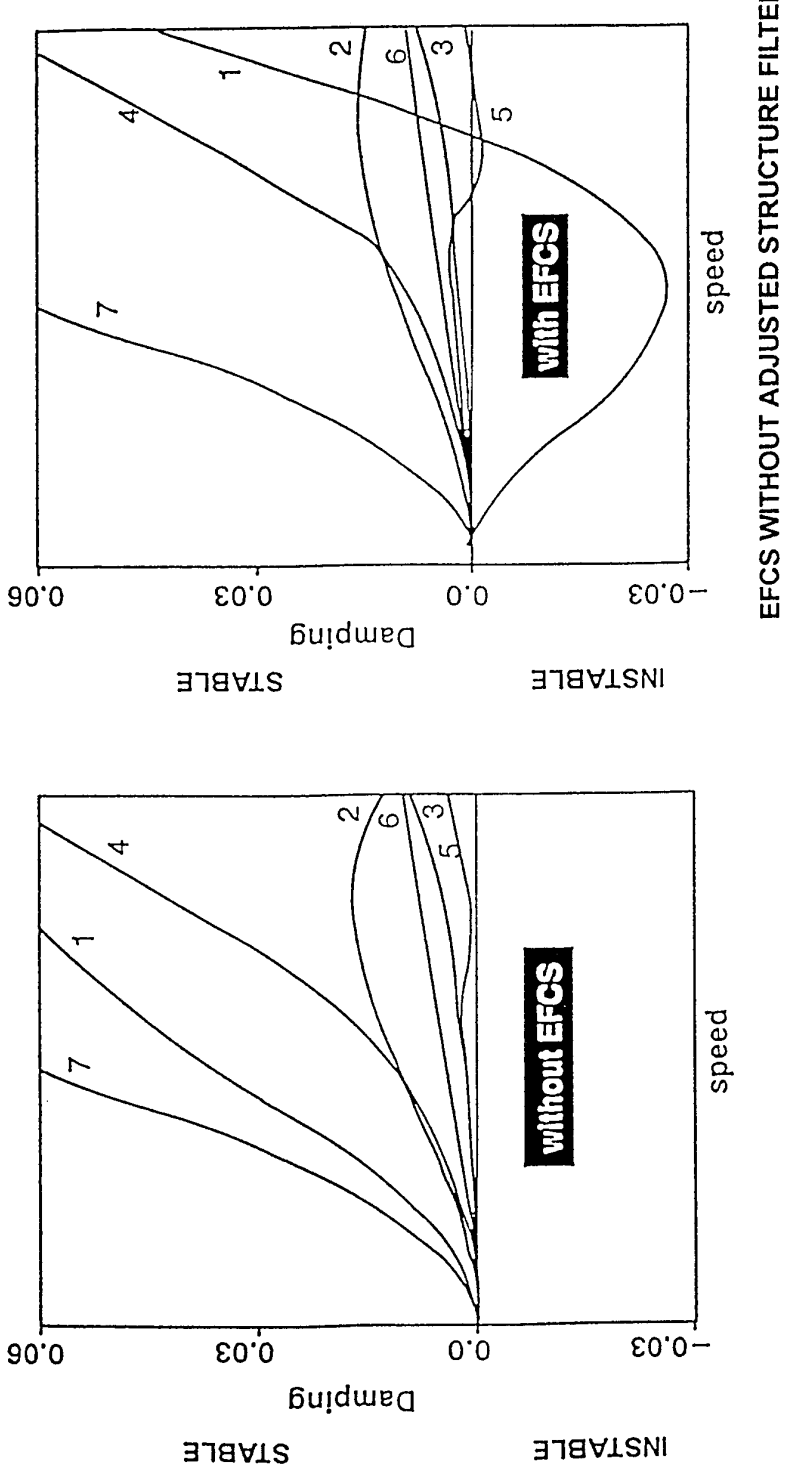

Fig. 15 COMPARISON OF FLUTTER CALCULATION RESULTS WITH AND WITHOUT THE EFFECT OF EFCS

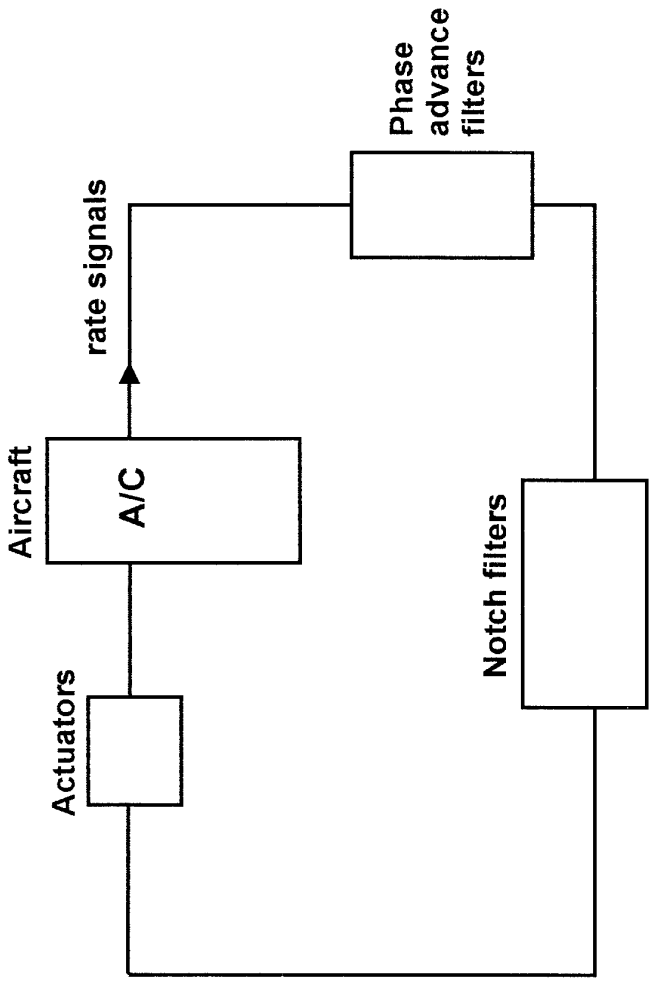

Fig. 16 Schematic Block Diagram of a Fighter Flight Control System

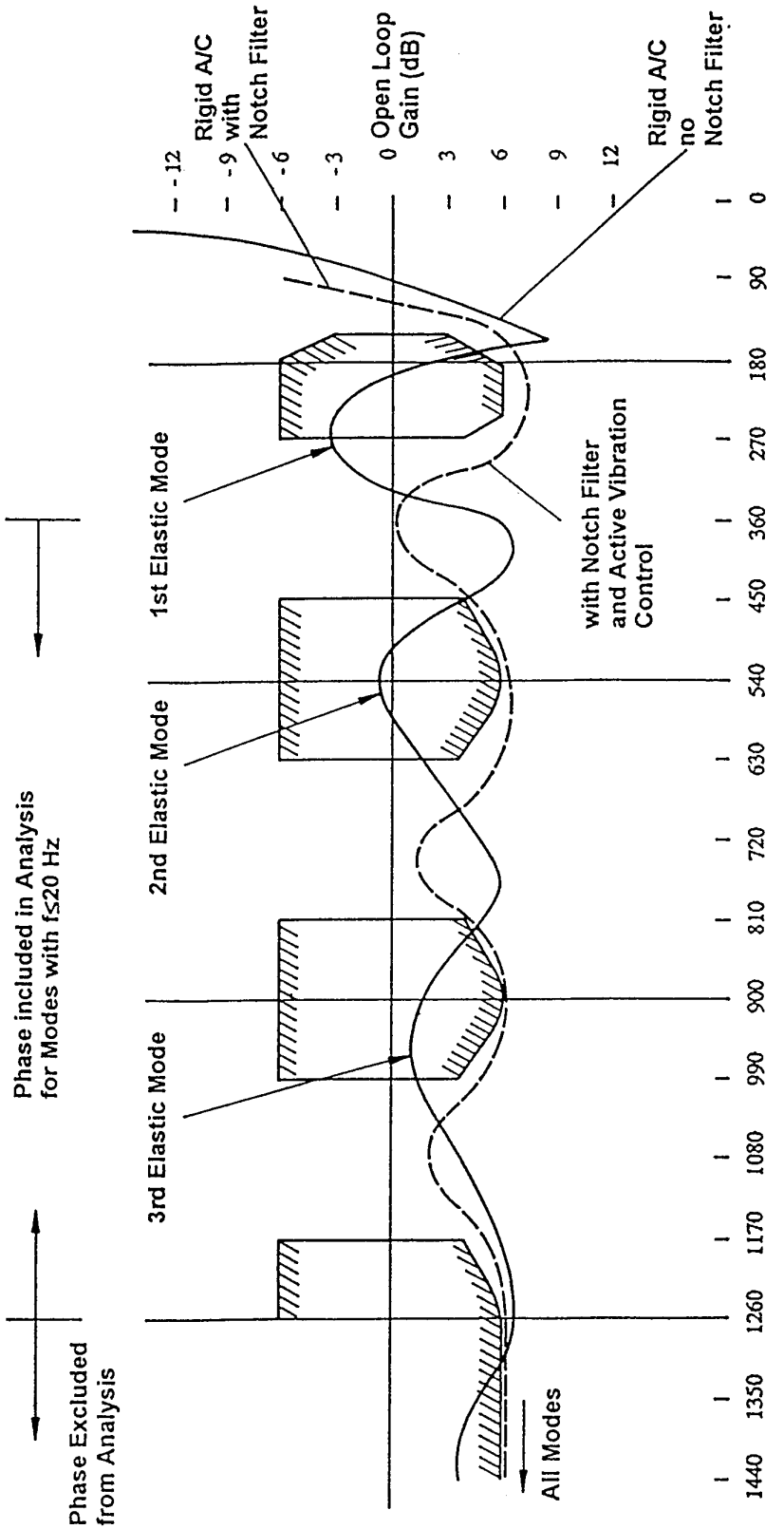

Fig. 17 Structural Coupling Clearance Requirements

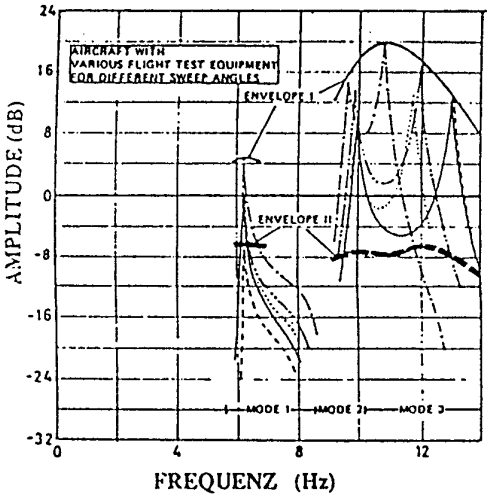

OPEN LOOP TRANSFER FUNCTION

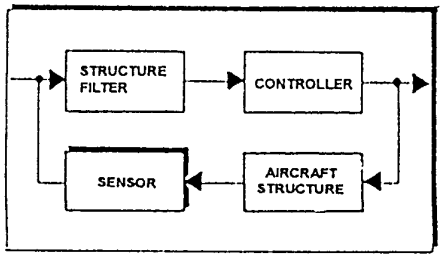

AIRCRAFT WITH CONTROLLER

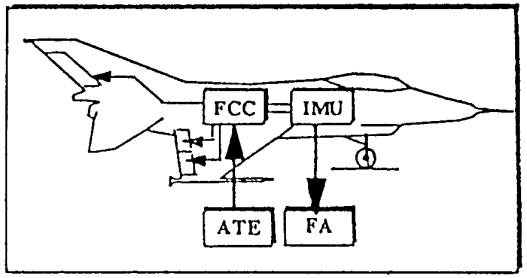

STRUCTURAL COUPLING TEST

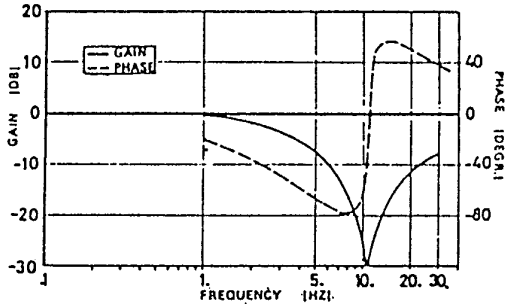

STRUCTURE NOTCH FILTER

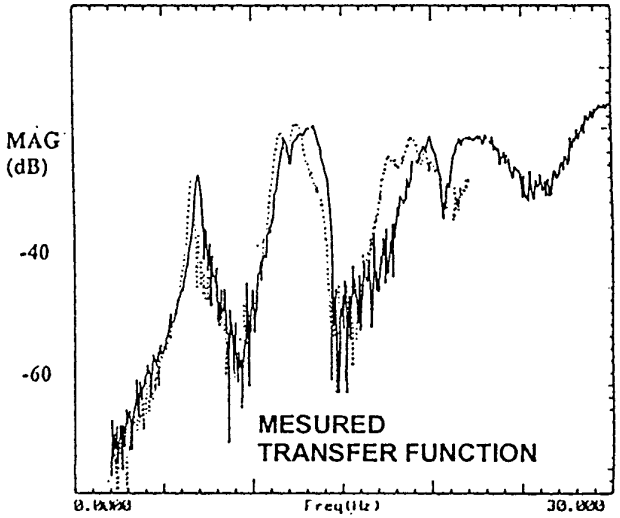

Fig. 18 STRUCTURE FILTER DESIGN AND STRUCTURAL COUPLING TEST

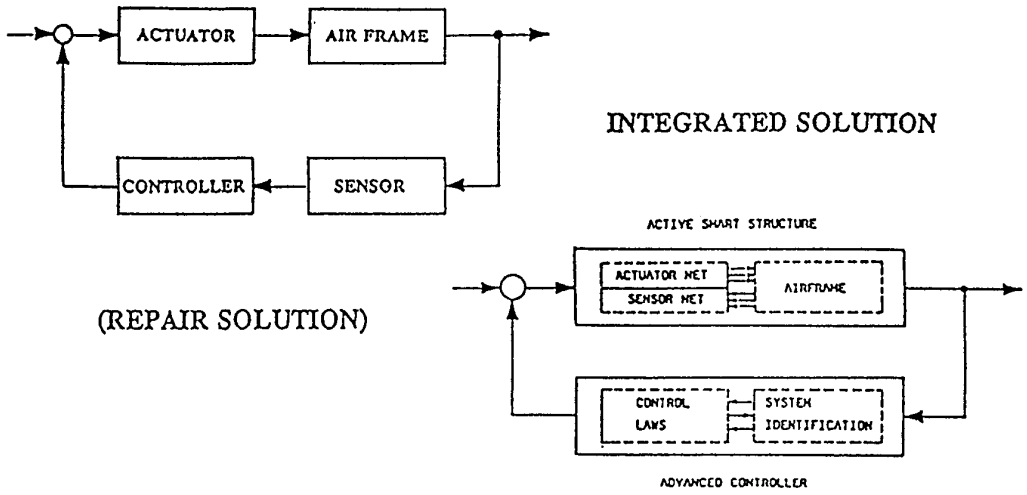

Fig. 19 ACTIVE CONTROL TECHNOLOGY AND SMART STRUCTURES

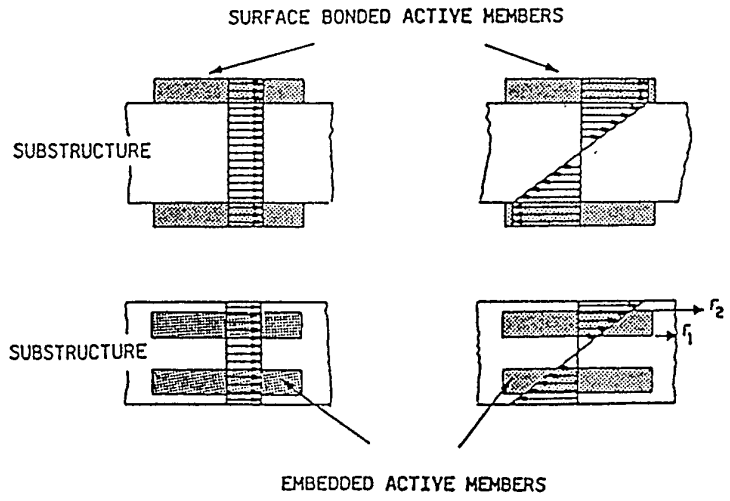

Fig. 20 EXAMPLES OF INTEGRATION OF SMART MATERIAL INTO A PASSIVE STRUCTUR

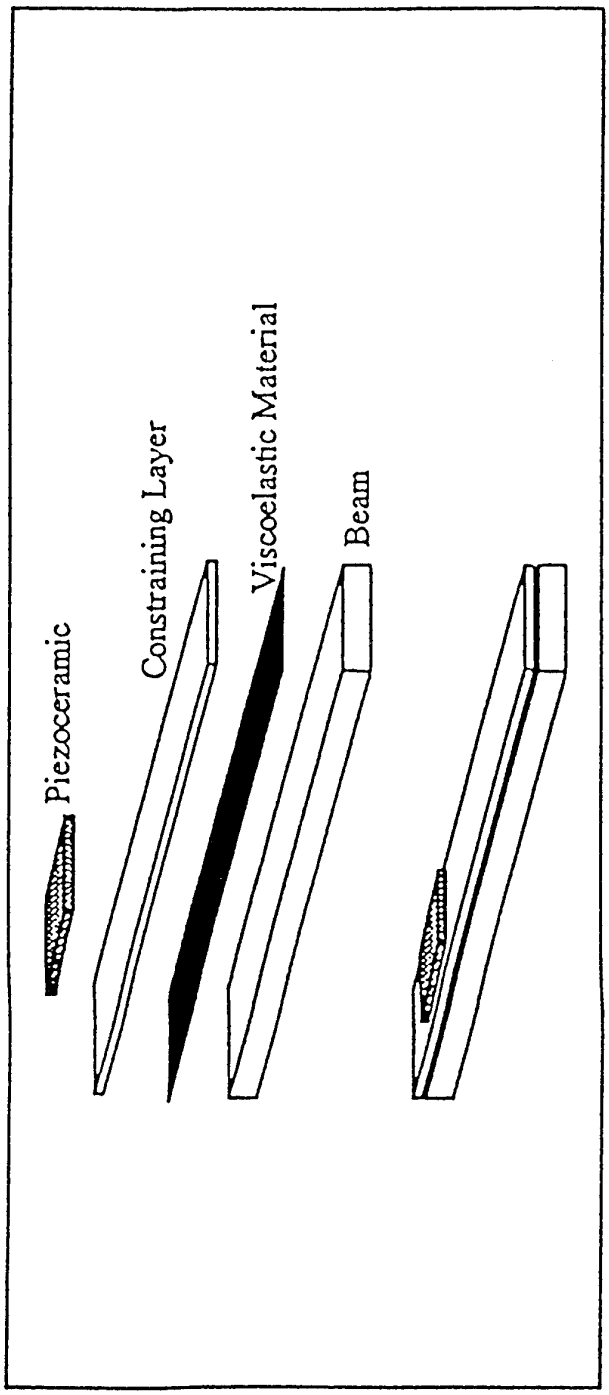

Fig. 21 BEAM CONFIGURATION FOR ACTIVE DAMPING INVESTIGATIONS

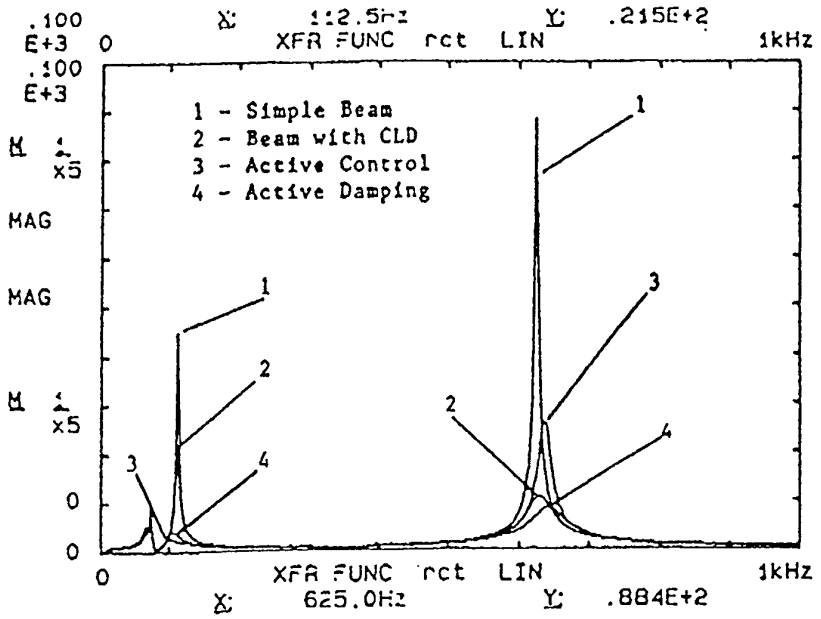

Fig. 22 ACTIVE DAMPING OF THE FIRST TWO MODES OF VIBRATION USING ACCELERATION FEEDBACK

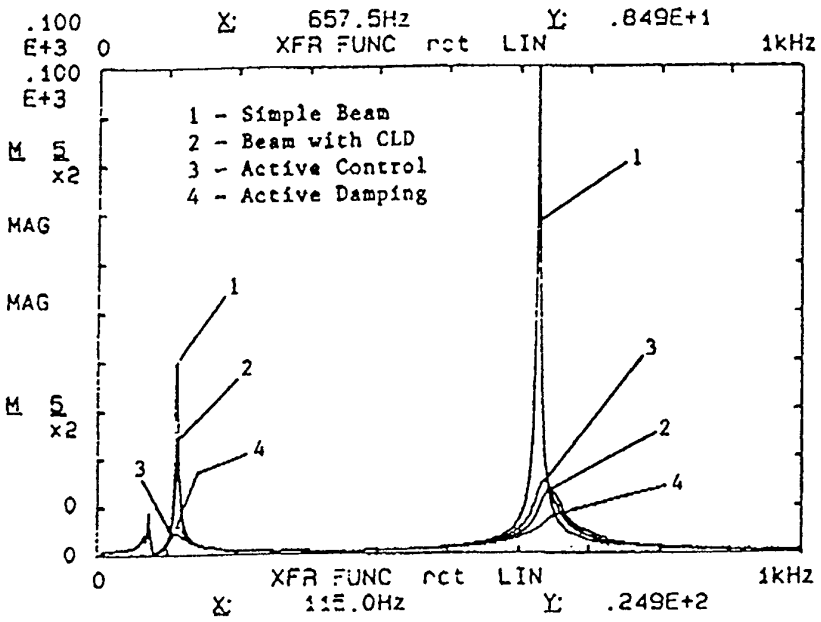

Fig. 23 ACTIVE DAMPING OF THE FIRST TWO MODES OF VIBRATION USING VELOCITY FEEDBACK

FLIGHT TEST RESULTS OF THE F-16 AIRCRAFT MODIFIED WITH THE AXISYMETRIC VECTORING EXHAUST NOZZLE

D. Kidman, D. Vanhoy, Maj Gerzanics, USAF
416th Flight Test Squadron
59 North Flight Line Road
Edwards Air Force Base, California 93524-6150
United States Air Force Flight Test Center
U.S.A.

SUMMARY

This paper presents results from flight testing an F-16 aircraft modified with the Axisymetric Vectoring Exhaust Nozzle (AVEN). This includes an assessment of the AVEN nozzle and the modified F-16 flight control system to provide stability and control power in an expanded maneuvering envelope, an assessment of flying qualities, and an overall assessment of tactical utility. Also included are lessons learned regarding the testing and implementations of active control technology.

INTRODUCTION

Development of thrust vectoring for fighter aircraft has been pursued for many years. Thus far, few actual flight demonstrations of its tactical utility have been accomplished. The technical benefits of thrust vectoring to aircraft stability, control, and handling qualities were analyzed and demonstrated in several other simulations and flight test programs. However, only a few of these programs have actually performed tactical scenarios due to limitations in program scope, and that many of these vectoring systems were designed to only demonstrate the feasibility of vectoring and not the military utility of the overall system. The F-16 Multi-Axis Thrust Vectoring (MATV) program attempted to demonstrate a real, tactical benefit for thrust vectoring with a near-production integrated thrust vectoring system.

TEST ITEM DESCRIPTION

A production F110-GE-100 engine exhaust nozzle was replaced with an Axisymetric Vectoring Exhaust Nozzle (AVEN), Figure 1. The nozzle provided up to 17 degrees of thrust vectoring in every direction. The compression link of the production nozzle was eliminated and was incorporated into a new outer flap that connected to a new divergent flap design. Three unique exit area (A9) actuators positioned the A9 ring to translate the nozzle flaps to desired vector geometry's. The A9 actuators were independently controlled by a Vector Electronic Control (VEC) which was an F110-GE-129 Digital Engine Control (DEC) system modified for this purpose. The VEC also controlled convergent nozzle (A8) control and augmentor operation. The AVEN nozzle also allowed for independent control of the exhaust expansion ratio (A8/A9) for optimum engine performance in both the vectored and non-vectored modes. Engine hydraulic fluid was used to position both the A8 and A9 actuators. In order to handle the increased hydraulic flow demand due to the AVEN nozzle, the capacity of the hydraulic pump was increased from 16 to 24 gallons per minute (gpm).

FLIGHT CONTROL DEVELOPMENT

Baseline Control Laws and Vectoring Capability

The MATV control laws were designed to augment the aerodynamic control surfaces with control moments from nozzle deflections, e.g., the elevator would be augmented with nozzle deflections in the pitch axis, while the rudder would be augmented with nozzle deflections in the yaw axis. The control laws were designed to match the basic F-16 control laws above 350 KCAS, where a g command system was used. As airspeed was decreased and the pilot had selected MATV active and AOA limiter off, the pilot pitch stick was converted from a g command to a pitch rate command system, where normal acceleration feedback was replaced with light AOA feedback to provide a sense of stability with increasing AOA. The normal MATV pitch rate command limit was 30 deg/sec. The pitch axis also included an option for an increased pitch rate command authority, allowing the pilot to command up to 50 deg/sec. The feature was activated via a paddle switch on the side stick controller, and was

Paper presented at the Flight Mechanics Panel Symposium held in Turin, Italy, from 9-13 May 1994.

informally referred to as "MONGO Mode". MONGO Mode allowed more rapid nose pointing and AOA rate capability.

Roll axis control laws were designed to provide maximum controllable roll rates at low angles of attack and blend to stability axis roll response at higher AOAs. Below 25 degrees AOA, the roll axis control laws were identical to a production F-16. Above 25 degrees, yaw nozzle was blended in to augment the rudder in coordinating pure stability axis roll maneuvers when between 35 and 45 degrees. At 45 degrees AOA, the roll axis was again blended to command pure body axis yaw rates when above 60 degrees AOA.

In the yaw axis, control laws were divided into two distinct regions. The first region was below 45 degrees AOA, where sideslip feedback, in conjunction with the nozzle and rudder control power, were used to augment directional stability. The second region was above AOAs of 45 degrees, where the yaw nozzle was commanded by the roll stick and/or rudder pedals to yaw the airplane about the aircraft velocity vector. Yaw accelerations and yaw rates were then fed back to the nozzle to augment directional stability and limit airplane yaw rate.

Revised Control Laws

The MATV program allowed for one DFLCS OFP update to be made during the flight test effort. The test team decided to exercise this option because the MATV mid-AOA (35-50 degrees) lateral-directional flying qualities were less than desirable. This update provided the opportunity to improve flying qualities through several control system changes and various in-flight pilot selectable control law options.

The in-flight pilot selectable gains were the key in optimizing the flight control configuration in the short amount which remained before the tactical utility phase of the program. The range of gains and options were based on experience gained during the initial envelope expansion.

FLIGHT TEST APPROACH

The flight test and demonstration program was performed as a joint effort by the Lockheed Fort Worth Company, General Electric, Wright Labs, and the Air Force Flight Test Center (AFFTC) at Edwards AFB. The flight test program was a three phase effort. Phase I functionally verified the aircraft and systems within the current F-16 Category I AOA limitations, Phase II expanded the envelope utilizing the thrust vectoring system, and Phase III provided a tactical utility assessment and demonstration of the expanded maneuvering envelope. The program attempted to quickly expand the usable F-16 envelope from the current 25 degrees AOA to beyond 80 degrees and attain its final goal of a tactical demonstration of 1 V 1 and 1 V 2 fighter engagement scenarios. Fight testing began in July 1993 and continued through March 1994.

The flight test program was structured as follows:

Phase	I:	Functional Check Flights
	IA:	Fort Worth Flights
	IB:	Edwards Flights
Phase	II:	Envelope Expansion
	IIA:	Open Loop Expansion
	IIB:	Closed Loop Expansion
Phase	III:	Tactical Utility Assessment/ Demonstration
	IIIA:	Functional Agility Maneuver Development
	IIIB:	Operational Assessment
	IIIC:	Flight Demonstrations

PHASE I - Functional Check Flights

The goal of the functional check flight phase was to verify that the F-16 MATV aircraft with its integrated systems demonstrated basic air worthiness and was functionally ready to commence the envelope expansion phase of the flight test program. Phase I consisted of flights at both Fort Worth and Edwards AFB. This phase established the capability of the MATV F-16 to sustain normal operations in KILL and STANDBY modes, provided standard F110 engine operability, and demonstrated standard F-16 departure and deep stall recoveries. No airborne nozzle vectoring was commanded during Phase I.

PHASE II - Envelope Expansion

The primary goal of the Phase II Envelope Expansion was to provide a maneuvering envelope for the F-16 MATV aircraft to be used in the Phase III Tactical Utility Assessment and VIP Demonstrations flights.

Envelope expansion testing therefore proceeded without the precision or demand for tolerances usually inherent in a data intensive flight test program. The envelope expansion used open and closed loop test maneuvers and elevated AOA throttle transients to clear the desired operating envelope. These open and closed loop maneuver definitions were in some cases derived substantially from the evolving Standard Evaluation Maneuver Set (STEMS), developed under contract for Wright Laboratories, and from maneuvers developed for previous and ongoing post-stall maneuvering and thrust vectoring programs (F/A-18 HARV, X-31, and X-29).

Open-loop maneuvers were defined as test maneuvers designed to assess the airframe and flight control system dynamic response to defined pilot input maneuvers. Open-loop maneuvers provided a natural buildup to more aggressive exploration of pilot-in-the-loop handling qualities. The pilot performed the input through the defined combination of stick, pedal, or throttle but did not attempt to control the airplane within task performance criteria. The pilot did attempt to maintain certain specified test parameters (i.e.. AOA throughout a lateral stick input) but only for the purpose of obtaining the desired data. The pilot attempted to control the aircraft if undesired dynamic response arose which threatened aircraft controllability. Open loop maneuvers consisted of stabilized AOA points, pitch/roll/yaw doublets, pushover/pull-ups, lateral stick reversals, yaw pedal reversals, 1-g 360 degree stick and pedal rolls, windup turns, and loaded 360 degree stick and pedal rolls.

Closed-loop maneuvers were defined as test maneuvers designed to assess the F-16 MATV system response to pilot inputs performed as part of a specific mission related task. In this case, the pilot continued to attempt to control the aircraft response to obtain a desired level of task performance. These maneuvers provided the pilot-in-the-loop envelope clearance. Performance criteria were specified to support the task definitions where applicable. Pilot comments were required. Closed loop maneuvers consisted of maximum AOA, maximum pitch rate maneuvers (horizontal plane turns, pull-ups, and split-S maneuvers) limiter disengagements, maximum yaw rate maneuvers, roll and yaw cross control maneuvers, 30 and 60 degree pitch captures and tracking, bank angle captures and tracking, yaw captures and tracking, vertical plane reversals, hammerhead or buttonhook turns, and J-turns.

Elevated AOA throttle transients were designed to help clear the flight envelope used during Phase III. During ACTIVE LIM OFF operation above 25 degrees AOA, the throttle was maintained at MIL or above. Partial power engine operability was not assessed at AOAs above 25 degrees. However, MIL to MAX snap transients and MAX to MIL cancellations were clearance goals for the entire AOA envelope.

Envelope expansion maneuvers were conducted between 20,000 and 35,000 feet MSL. To achieve the goal of providing a cleared tactical maneuvering envelope for Phase III, this testing attempted to verify that the F-16 MATV aircraft was controllable and the F110 engine was operable throughout the achievable flight regime with no restrictions on pilot control or throttle inputs. If pilot input restrictions were required in certain flight regimes, due to undesirable or uncontrollable aircraft or engine response to specific inputs, those input limitations would have been inplace for Phase III of the test effort. AOA limits were not expected to be imposed unless aircraft controllability was questionable even with restricted pure pitch inputs. As stated earlier, all maneuvering above 25 degrees AOA occurred with the throttle at MIL power or above.

Initially, the clearance process involved simple AOA stabilizations, controls release nose-down pitch authority checks, and three axis doublets in MIL power between 30,000 and 35,000 feet. This block was an initial buildup to verify the operability of the basic engine and flight control gain margins at a safe altitude. It was unlikely that any of the tactical utility assessment would actually occur at these altitudes. This buildup was accomplished at 5 degree AOA increments from 25 degrees to 60 degrees and 10 degrees increments above 60 degrees. Doublets were performed 10 degrees below the preceding stabilized AOA point to ensure accompanying dynamics remained below previous stabilized AOA values.

The MAX power open-loop test block at 30,000 to 35,000 feet was the most thorough investigation of the system. The overall control power in this block closely resembled the control power provided in MIL

power at 20,000 to 25,000 feet, which was the key clearance block for a meaningful tactical utility assessment. A complete evaluation of both blocks, however, would have been inefficient. The most prudent approach was to conduct the first full set of maneuvers throughout the detailed AOA envelope at the higher altitude. AOA increments of 5 degrees were examined from 25 degrees to 60 degrees AOA and increments of 10 degrees was used from above 60 degrees to the maximum achievable; stabilized AOA. The 5 degree increment was used in the mid-AOA range since this AOA region exhibited the critical pitching moment and directional stability shortcomings of the basic F-16 airframe. Above 60 degrees AOA, substantial nose down pitching moment was available and the directional stability was strongly positive.

Following completion of the MAX power high altitude block, MIL-MAX-MIL throttle transients were investigated at increasing values of AOA and sideslip. In the case of engine operability, the critical portion of the envelope occurred above 60 degrees, causing the test AOA increment to decrease from 10 degrees to 5 degrees above that value. If afterburner lights were not achieved from MIL at the elevated AOA test runs, MAX was selected at a lower AOA and MAX-MIL-MAX transients were investigated.

Occasional pop stalls were expected during the flight test program. If stalls occurred frequently enough to impact progress of the test program, adjustments to the F110 AVEN control system would have been made or pilot observed limits would have been established. These adjustments to the VEC increased stall margin and were within the range of adjustments tested during the initial, formal, and hot-bench test activity of the MATV program.

The testing at 20,000 to 25,000 feet consisted of the same open-loop maneuvers as performed at 30,000 to 35,000 feet in MAX power. These maneuvers were investigated in both MIL and MAX power at a reduced set of AOA test points, building on the complete set at 30,000 to 35,000 feet. Flying qualities in MIL power at 20,000 to 25,000 feet were similar to that in MAX power at 30,000 to 35,000 feet. Flying qualities in MAX power were improved, due to more available nozzle control power, from the increase in thrust in MAX power at 20,000 to 25,000 feet.

Following completion of the open-loop assessment at the lower altitude, an extensive closed-loop set of maneuvers were performed. These maneuvers were designed to identify where flying qualities difficulties were encountered and if any departure susceptibility to specific pilot input existed.

Envelope Expansion - Revised Control Laws

The evaluation of the revised MATV control laws followed similar procedures for envelope expansion as outlined for the initial envelope expansion. Appropriate build-up procedures were followed. This included building up to the largest system gain, or the lowest gain margin, in anticipation of any system instabilities.

The pilot had the option of de-selecting a specific gain when testing for instabilities but did not have the capability to return all of the gains to their default values without going through several steps. The pilot did, however, retain the option of returning to the baseline F-16 control system at any time through the KILL switch on the side stick controller. Based on initial envelope expansion experience, this evaluation proceeded in an accelerated manner and relied on engineering judgment and pilot comments.

This regression testing was limited to that necessary to satisfy the test team that the changes only affected the planned aircraft response and did not adversely affect other aircraft flight characteristics.

PHASE III: Tactical Utility Assessment and Demonstration Flights

The goal of the Tactical Utility Assessment was to identify the specific tactical advantages gained by the F-16 configured with a multi-axis thrust vectoring exhaust nozzle. Operational test and evaluation pilots were the primary evaluators during this phase. During the initial portion of Phase IIIA, the Lockheed and AFFTC project pilots flew numerous functional agility maneuvers and tactical setups against similar and dissimilar (NASA F/A-18) aircraft. These pilots then acted as rear cockpit safety pilots during the envelope familiarization and functional agility maneuver development flights for the operational pilots. Phase III maneuvers consisted of horizontal plane maximum turn rates, horizontal scissors, split-S capture and tracks, J-turn capture and tracks, and basic fighter maneuvers (similar and dissimilar offensive and defensive perches, and high aspect engagements).

A flight demonstration profile was constructed during Phase IIIB. The demonstration profile emphasized comparisons of the current F-16 maneuvering (STANDBY mode) to F-16 MATV maneuvering (LIM OFF mode) by performing various cleared maneuvers back to back. The demonstration flights were used to highlight the benefits of thrust vectoring on aircraft to key military decision makers.

FLIGHT TEST RESULTS

In the four months that the MATV test program has flown, the test team has conducted 72 sorties, totaling 104 flight hours. During this time, the MATV team was able to expand the usable F-16 envelope from the current 26 degrees AOA limit to beyond 80 degrees. In addition, the MATV aircraft has demonstrated dynamic maneuvering well beyond 125 degrees AOA. Maneuvering was cleared down to 20,000 feet with unrestricted throttle movement between MIL and MAX power. No pilot input restrictions were required to ensure safety of flight.

Functional Check Flights

Initial functional check flights occurred at Lockheed in Fort Worth, and were designed to check out the most basic engine and aircraft operations, and proved to be most valuable. Initial problems with interruptions in MUX communication were causing nuisance engine faults and reversions to the MATV failed mode. By having the MATV system designers and engineers on hand, the team had the ability to respond quickly and efficiently in the troubleshooting and correction of this and other problems inherent in any new program.

More in-depth functional check flights occurred once the plane arrived at the Air Force Flight Test Center at Edwards AFB, California. These checkout flights included determining the departure and recovery characteristics of the MATV aircraft and determining the engine airstart characteristics. These checkout flights were performed to ensure normal F-16 characteristics existed prior to continuing with the elevated risk test flights associated with the envelope expansion effort. During these flights it was determined that the aircraft had predictable and consistent departure characteristics, and always self-recovered with minimum altitude loss. No engine stalls occurred during the IDLE, MIL, and MAX power departures.

The intent of the engine airstarts was to ensure that if engine problems did occur later in the program, an engine restart capability had already been verified at similar flight conditions. During this portion of the functional check flights, it was determined that although the airstart capability was not as good as desired at higher altitudes, 30,000 feet and above, below 25,000 feet the engine started reliably. Time was not spent to analyze why the engine did not restart as expected at the higher altitudes. The intention of this phase of testing was only to verify where predictable and reliable engine restarts could be expected.

Envelope Expansion - Initial Control Laws

During the initial envelope expansion testing at 35,000 feet in military power, it was found that the aircraft could be stabilized, and pitch, roll, and yaw doublets could be performed up to 30 degrees AOA, 5 degrees above the normal F-16 limiter. However, as AOA was increased to 35 degrees in MIL power, the aircraft yawed off to the right, yielding sideslip angles up to -19 degrees. Figure 2 is a time history in MIL power illustrating these lateral-directional flying qualities. This was not considered a classical type of F-16 nose slice because AOA was always controllable.

Two main problems contributed to the undesirable flying qualities. First, was just the lack of thrust at 35,000 feet in MIL power, which resulted in lower than required yawing forces. The second problem was the lack of accurate air data information. Accurate air data sensing or computation is essential when implementing these parameters as feedbacks into the flight control laws. This was the case for our computed sideslip signal from the Inertial Navigation Unit, which deviated from the actual sideslip value by 5-10 degrees in the initial OFP. Figure 2 also illustrates the beta INS drift phenomena.

Military power maneuvers were performed first, as engine buildup due to reduced engine stall margin in MAX power. These maneuvers were however, considered worst case for aircraft controllability. Therefore, it was determined to waive the remainder

of the MIL power envelope expansion in the 35,000 - 30,000 feet altitude block, and that testing would continue in MAX power. As testing proceeded in MAX power, it was again noted that marginal flying qualities still existed between 35 and 50 degrees AOA. In this mid-AOA region, it was still common to see ± 10 degree sideslip angles, with the nozzle and rudder combination working hard to try to compensate. Figure 3 is a time history in MAX power showing both the sideslip oscillations and the yaw nozzle trying to compensate. During this portion of the envelope expansion, AOA and pitch control was solid, with plenty of nose down pitch authority at AOAs ranging from 5 to 75 degrees. Some pilots commented that the light AOA feedback provided to the pilot for a sense of aircraft stability could have been increased.

Although flying qualities of the F-16 MATV aircraft during the initial envelope expansion in the 30,000 - 35,000 feet altitude block were less that desirable, it was determined that testing should continue in the upper altitude block until the team was confident that testing could continue safely in the lower altitude block, 20,000 - 25,000 feet. This continued effort in MAX power included the following open loop maneuvers: Push-over Pull-ups, Stick and Pedal Reversals, and 360 degree Stick and Pedal rolls. These open loop maneuvers were accomplished up to 70 degrees AOA. In addition, wind-up turns from 250 and 150 KCAS to AOA maximum, maximum pitch rate and maximum yaw rate maneuvers, and engine throttle transients were also accomplished.

Open loop pitch response during the push-over pull-ups was excellent showing plenty of pitch authority in both the nose-up and nose-down directions at all angles of attack. Pitch damping was adequate and there was never any concern over pitch axis stability or control. Figures 4 and 5 are time history plots of longitudinal maneuvers designed to demonstrate the pitch axis capability of the MATV aircraft. Figure 4 shows a slow AOA sweep from 20 to 72 degrees AOA, a brief stabilization at maximum AOA, and a full stick nose down recovery input. Figure 5 shows the AOA, pitch attitude, and pitch rate resulting from a pure longitudinal pull-up and push-over maneuver called the "cobra" maneuver. Pitch response was immediate and predictable, with both nose-up and nose-down pitch rates of approximately 45 deg/sec.

Open loop roll and yaw responses in MAX power in the upper altitude block, as eluded to earlier, were marginal at best. Lateral stick and pedal reversals which were intended to reverse bank angle at ± 30 degrees (and/or reverse at heading angle changes of ± 90 degrees) were prone to overshoots. Hesitations and/or initial roll-reversals were commonplace when maneuvering at or above 40 degrees AOA. Similar initial roll-reversals were seen during the 360 degree rolls. Roll response was simply a function of the amount adverse or proverse beta on the aircraft at the time of the roll. Wind-up turn performance also proved to have marginal lateral-directional flying qualities. Although good pitch rates, 30 deg/sec, occurred during the full stick pulls from 150 and 250 KCAS initiation airspeeds, the aircraft exhibited a strong nose right tendency in the 35 to 45 degree AOA region.

To ensure proper engine operation in these extreme flight conditions, prior to proceeding with envelope expansion testing in the lower altitude block, 20,000 to 25,000 feet, numerous MIL to MAX to MIL throttle transients were performed at increasing AOAs, from 5 to 75 degrees, both with and without full pedal inputs. During this portion of the test the aircraft was stabilized in MIL power at 75 degrees AOA, then MAX power was selected simultaneously with a full pedal input to generate maximum aircraft yaw rate acceleration. No compressor stalls or afterburner blowouts were noted, and every attempt to light the afterburner was successful. In addition, during some of the more dynamic maneuvering with AOAs well beyond 125 degrees and yaw rates as high as 45 deg/sec, the engine has only experienced one compressor pop stall. This outstanding performance of the engine was definitely one of the highlights of the MATV program.

Based on the fact that there were no engine problems in MIL or MAX power and that regardless of the marginal lateral-directional flying qualities, there was always sufficient pitch power to prevent an AOA departure it was determined that continued testing in the lower altitude block was prudent. Initial testing at 25,000 feet was in MIL power with results slightly better, but still comparable to the MAX power results at 35,000 feet. The aircraft experienced large sideslip oscillations up to ± 15 degrees and the success of lateral stick or pedal maneuvers was still dependent on initial sideslip conditions. Large sideslip angles could be overcome

to achieve the desired aircraft performance but resulted in long response times. As testing continued with MAX power, flying qualities improved, as predicted primarily due to the increase in thrust. Longitudinal flying qualities in the lower altitude block were similar to longitudinal flying qualities at 35,000 feet. Lateral-directional maneuvers could now be performed with confidence. Although initial roll response might be slow, roll and yaw reversals were non-existent. 360 degree maneuvers could be performed at any AOA with fair precision and good AOA control. Sideslip angles could still be fairly large, especially during roll and yaw reversals. Figure 6 is a time history, illustrating the improved lateral directional flying qualities in MAX power at 25,000 feet.

Closed loop maneuvers consisted of maximum pitch rate maneuvers (horizontal, vertical, Split-S setups), maximum yaw rate maneuvers, 360 degree loaded stick and pedal rolls. Roll and yaw cross control maneuvers were also performed prior to proceeding with the tactical utility evaluation to determine if any flying qualities difficulties would be encountered or if any departure susceptibility to specific pilot inputs existed. These maneuvers gave the team the confidence that the operational pilots could fly the MATV aircraft without input restrictions. Pitch pointing was very good with approximately 90 degrees of pitch angle change with up to 45 deg/sec rate. Maximum yaw rates of 45 deg/sec were obtained from full pedal inputs at 60 degrees AOA. A time history of a maximum yaw rate maneuver can be seen in Figure 7, showing approximately 720 degrees of heading change at approximately 45 deg/sec rate. Roll and yaw cross control maneuvers at 25,000 feet were uneventful, with immediate aircraft recovery upon controls release. Again showing the departure resistance of the MATV aircraft.

Envelope Expansion - Revised Control Laws

The initial flight with the revised flight control laws showed improvement in the lateral-directional axis at 35,000 feet. Sideslip control was better in the 35-50 deg AOA region, and the nozzle was a much more active control force in reducing sideslip oscillations. The nose of the aircraft moved left in yaw as the nozzle tried to reduce the previous nose right sideslip tendency. The aircraft now seemed more sensitive to control system induced roll oscillations above 50 degrees AOA.

Based on the improved flying qualities at 35,000 feet, testing proceeded at 20,000-25,000 feet. Flying qualities again improved with the increase in thrust which comes at the lower altitude. As in the high altitude block, sideslip control in the mid-AOA (35-50 degrees) regime was tighter compared to the baseline control laws, with the sideslip angles of $\pm$ 4 occurring during these maneuvers. A time history illustrating these lateral directional flying qualities is illustrated in Figure 8. As a result of lower initial sideslip conditions, roll response was good. However, large roll/heading angle overshoots of up to 20 degrees occurred when trying to initiate a roll or yaw reversal due to the nozzle opposing the reversal command while trying to reduce sideslip from the initial stick or pedal input. These roll and yaw overshoots appeared to be slightly worse in the 40-55 AOA regime, compared to the previous OFP.

Once again, the closed loop maneuvers were flown to ensure no adverse flying qualities existed prior to beginning the tactical utility assessment and demonstration phases of the MATV program.

During maximum pitch rate maneuvers with the optimized flight control laws, the increased sideslip control freed up the pitch nozzle for greater pitch attitude change. The increase in pitch attitude reserve was on the order of 15-30 degrees more than with the previous OFP. Maximum pitch rate maneuvers initiated from 150 KCAS experienced a slight nose-left sideslip of 5 degrees. At 250 KCAS, the nose movement was moderate, approximately 10 degrees. As airspeed was increased to 325 KCAS, the nose slices became abrupt as AOA increased beyond 25 degrees. The initiation airspeed of 325 KCAS allowed the aircraft to pull above 25 degrees AOA, the normal F-16 limit, while the aircraft had little or no thrust vectoring available due to the 300 knot maximum vector speed. The bottom line was when above 25 degrees AOA and above 250 KCAS expect slightly degraded flying qualities.

Maximum yaw rate maneuvers were generally accomplished with the AOA limiter set to 80 degrees. This eliminated the pitch attitude and AOA oscillations, which were noted during previous attempts of this maneuver with the unlimited AOA option. These oscillations were caused by the pitch

and yaw nozzle competing for authority. As noted before, yaw rates in excess of 45 deg/sec were attained and sustained throughout the maneuvers. Yaw control was precise and the ability to stop on a desired heading could be accomplished without overshoots.

Nine flights after first receiving the revised flight control computer, the pilot selectable gains and options had been tested, optimized, and the flight envelope cleared. As compared to baseline control laws, this revised OFP with the optimized flight control laws generally exhibited better flying qualities during all phases of the evaluation. During the MAX power slow AOA sweep, a stabilized AOA of approximately 85 degrees was sustained, similar to baseline OFP. A time history illustrating the flying qualities during an AOA sweep is shown in Figure 9. Sideslip control was improved throughout the sweep, less than $\pm$ 4 degrees, compared to $\pm$ 7 degrees with the baseline OFP. Wing rock in the 40-55 degree AOA regime was only $\pm$ 10 degrees, compared to $\pm$ 20-30 with the baseline OFP. The aircraft occasionally experienced wing roll-off, however, rudder and nozzle could also be used to raise the low wing. The tightened sideslip control, however, made the roll response somewhat sluggish. Above 55-60 degrees AOA, the rudder and nozzle combination was very effective in commanding responsive bank angle control. While the initial flight control laws required a steady left rudder force of 40-50 lbs to control a steady nose-right yaw tendency, the revised OFP with the optimized flight control laws did not. While both aileron and rudder were required during the slow AOA sweep to maintain a steady heading and wings-level attitude, the forces required were generally small.

Overall, the revised OFP with the optimized flight control laws exhibited improved lateral-directional flying qualities as compared to previous OFP. Pitch axis performance was similar to slightly improved, and the tighter sideslip control, allowed more nozzle available for use in the pitch axis. Lateral directional flying

Generally, control inputs could be made without pilot restrictions and adequate handling qualities were noted throughout the flight envelope. While flying qualities were not ideal it was obvious that the latest configuration of flight control laws would allow a meaningful evaluation of the tactical utility of thrust vectoring.

Although more time and effort could have improved lateral-directional flying qualities somewhat, such was not the intent of this flight test effort. While not perfect it was obvious that the current configuration of flight control laws would allow the tactical utility assessment phase to proceed successfully.

TACTICAL UTILITY ASSESSMENT

The MATV test team flew 16 dedicated tactical utility assessment sorties for a total of 20 flight hours and approximately 170 tactical engagements. These sorties were the culmination of Phase IIIB of the MATV test effort. Prior to this phase, the test team had cleared the MATV flight envelope to provide carefree operations throughout the conventional and post-stall flight regions. The main objective of the MATV program was to determine the tactical utility benefits from operations in the expanded maneuver envelope.

Test Methods

All initial conditions flown were selected by the operational pilots from standard training scenarios. The test team did, however, have two limitations that did impact test point selection. The MATV aircraft was required to be above 17,000 feet AGL for all maneuvering above the normal F-16's AOA limit of 25 degrees. This floor, for test safety, was higher than the normal operational maneuver floor of 5,000 feet AGL. The primary affect of this higher floor was to reduce the thrust and maneuver potential of both the MATV and adversary aircraft and to reduce engagement time. In an effort to better understand the tactical capabilities of the adversary aircraft, F-16C types, at this higher elevation, the operational pilots flew several sorties against each other in like adversary aircraft. These sorties allowed the operational pilots to determine the capabilities of a non-thrust vectored F-16 so that the advantage/disadvantage of thrust vectoring could be determined. Another minor limitation on the MATV aircraft was an airspeed/mach limit of 435 KCAS/0.95 Mach due to the spin chute. The speed limit had little affect on the outcome of the evaluation, as this airspeed was representative of initial engagement conditions for tactical air-to-air training sorties.

Test conditions, as stated above, were derived from standard operational training setups. Offensive, defensive and neutral engagements were flown by the MATV aircraft against a single adversary. In the multi-bogey engagements, MATV versus two

adversaries, only defensive and neutral engagements were flown. Offensive and defensive engagements were flown at tactically representative airspeeds with starting separations varying from 3,000 to 9,000 feet. Neutral engagements were entered from a butterfly set-up maneuver, typical of operational training sorties. Of the 170 engagements, flown by the two operational pilots, approximately 60 were two adversaries versus the MATV aircraft.

The vast majority of engagements were flown against F-16C type aircraft. The F-16C aircraft had fairly comparable conventional, non-post stall performance to the MATV aircraft, but did show a slight turn rate advantage attributed to MATV's higher gross weight. This similarity allowed for an apples to apples comparison, and helped determine the true affect of thrust vectoring. Approximately 15 engagements were flown against an F-18 adversary aircraft in one versus one set-ups only. This limited exposure to dissimilar adversary aircraft ensured that tactics derived would be applicable to adversary aircraft with varied capabilities.

Simulated weapons were employed throughout the various engagements. Weapons available to both MATV and adversary aircraft were generic all-aspect radar missile, generic all-aspect infrared missile, and current generation air-to-air cannon. Shot validity criteria were the same as those employed by operational fighter units for training sorties.

Test Results

The large number of one-versus-one and one-versus-two engagements flown by the MATV team have greatly added to the developing data base of post-stall tactical maneuvering by providing data from an operational fighter aircraft with a near production thrust vectoring system. While specific results are beyond the scope of this paper, a number of observations were made. These observations were consistent with the results from several other high AOA simulation studies and other high AOA flight test programs.

1. An aircraft with post-stall maneuver capability (thrust vectoring in MATV's case) will enjoy a tactical advantage in air-to-air engagements against an otherwise equal
adversary.

2. Post-stall maneuvering provides an evolutionary enhancement in tactical capabilities, not a revolutionary one.

3. Weapons capabilities drive employment tactics. Off-boresight weaponry and helmet mounted displays will significantly enhance the benefits of post-stall maneuvering technologies.

4. Post-stall maneuvering should only be used when it leads to specific advantages, such as to achieve immediate weapons solution or to dictate tactics.

5. Post-stall maneuvering, if properly employed, provided offensive options and reduced impacts of mistakes while also increasing defensive survivability.

6. The operational pilots adapted quickly to post-stall maneuvering and were able to exploit its advantages after minimal practice.

7. Post-stall maneuvering, if not properly employed, resulted in a huge energy deficit. Good BFM was still required.

8. Need to beat down bandits energy prior to exploiting post-stall maneuvering.

LESSONS LEARNED

In-flight pilot selectable gain options allowed the flight control system to be optimized in an efficient manner. The range of gains selected were based on simulation and flight test experiences with the final gain combinations based on actual in-flight aircraft response. Variable control gains allowed the team to solve flying qualities deficiencies in the 35-50 degree AOA flight regime. The ability to eliminate flying quality deficiencies, eliminated pilot observed maneuvering limitations and allowed carefree operation during the operational assessment.

The MATV team performed extensive flight simulations in high fidelity handling qualities simulator. This allowed optimization of the integrated thrust vectoring control laws for the uncharted high AOA flight regime for the F-16 aircraft. These flight simulations also gave insight into the development of effective maneuver definitions and the unique flight test techniques required to evaluate thrust vectoring technology. There by increasing the flight test efficiency immeasurably by practicing maneuvers ahead of time.

The MATV team formed a small integrated team of prime contractor, principal subcontractor, government sponsor, and responsible test organization. With all parties agreeing from the beginning to be a team committed to common goals and objectives. Early team formation and commitment to the program's philosophy guaranteed that program management heard and respected the requirements of the team. Once flight test had begun, this approach ensured that the test plan was understood and followed without interruptions to "study" things. It also ensured that the test points purity was good since both pilots and engineers had already seen the aircraft responses numerous times in the flight simulator.

The MATV team focused the test planning and test conduct on acceptability rather than on stated tolerances from predicted results. More often than not, acceptability was based on the qualitative comments of the pilot and the real-time data analysis of the engineers. For this type of program, this was the only workable approach.

The MATV team maximized the use of airborne refueling capabilities during the flight test program. This is a well known lesson learned, but in a time limited program like ours, it was again highlighted. With four to five tanker hits per flight we were able to accomplish the equivalent of seven to eight unrefueled flights.

Flight research programs with goals of understanding high AOA aerodynamics should be pursued in parallel with the current efforts aimed at the tactical effectiveness. The F-16 has been around for quite some time and yet our understanding of the airplane at high AOA was not complete. In particular, unsteady aerodynamic effects seemed to be very similar to characteristics noted in other high AOA research programs.

Accurate air data sensing or computation is essential when implementing these parameters as feedbacks into the flight control laws. This was the case for our computed sideslip signal from the Inertial Navigation Unit, which deviated from the actual sideslip value by 5-10 degrees in the initial OFP. Initially the winds were held constant when decelerating through 100 KCAS. Sideslip accuracy was improved significantly when the winds were held constant at 145 KCAS, where the differential pressure ports yielded a more accurate starting condition.

Prior to the implementation of thrust vectoring into production aircraft, pilot vehicle interfaces such as AOA cues to the pilot and cockpit switchology should be well thought out. Our pilot vehicle interfaces were considered acceptable for a technology demonstrator program, however, they were also considered cumbersome during the tactical utility portion.

SUMMARY

The F-16 MATV configuration has demonstrated true post stall maneuvering capability with a near production thrust vectoring nozzle. The impressive thrust capability of the F-16 combined with the minimal weight penalty of the AVEN configuration allowed the F-16 MATV to maneuver realistically where previous thrust vectoring technologies were unable. This capability had escaped earlier thrust vectoring programs due to the heavy weight penalties and inefficiencies of early vectoring configurations. Initially clearing a maneuvering envelope for the aircraft and then concentrating on an operational assessment provided the fighter community with its first tangible look at thrust vectoring. In a modern tactical aircraft, the F-16 MATV program has demonstrated the tactical utility of thrust vectoring in an operational representative environment.

REFERENCES

Sweeney J.E., and Gerzanics M. Maj. USAF, "F-16 Multi-Axis Thrust Vectoring Program", in "Presentation to the Thirty Seventh Symposium of the Society of Experimental Test Pilots", September 1993.

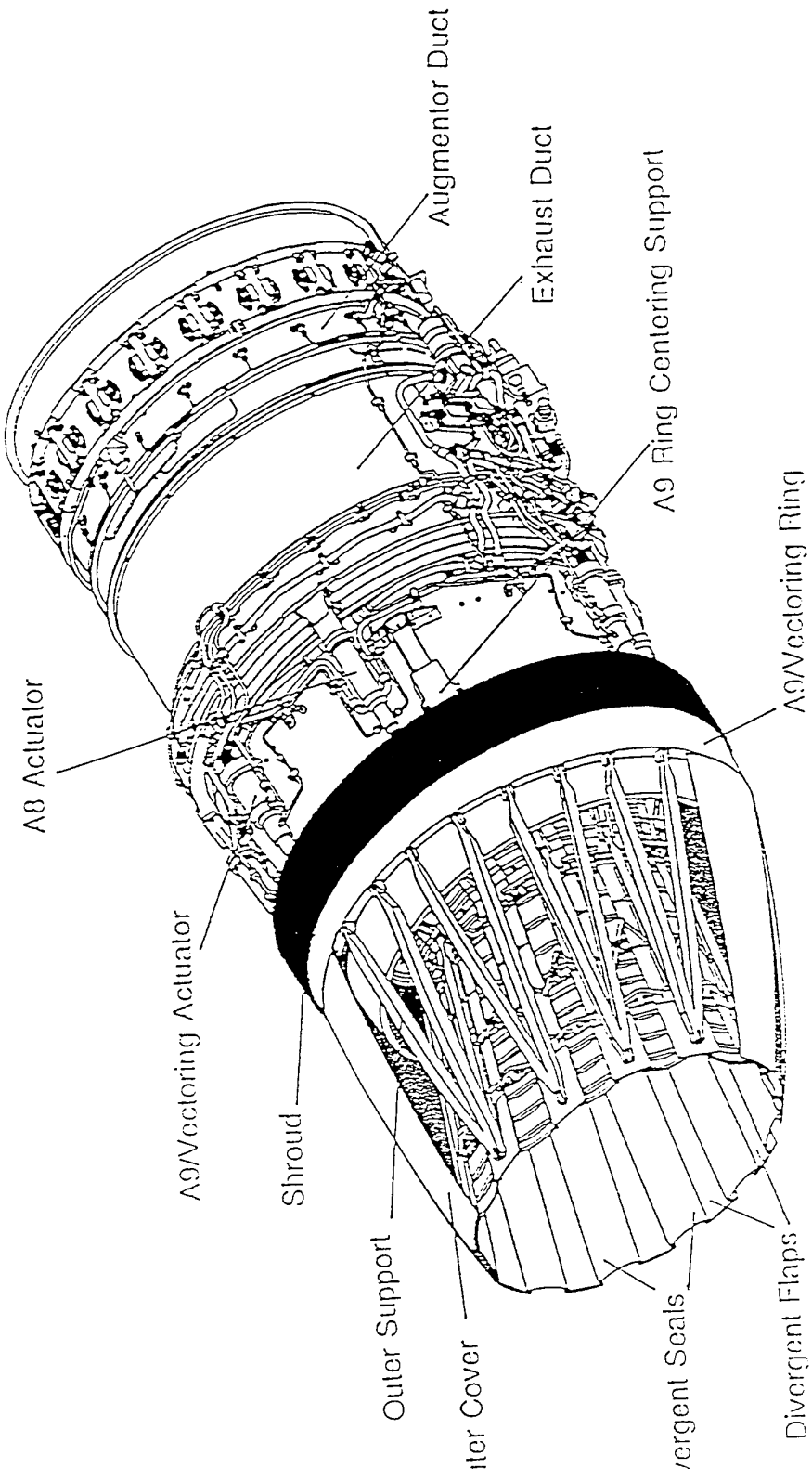

Figure 1: Axisymmetric Vectoring Engine Exhaust Nozzle Design

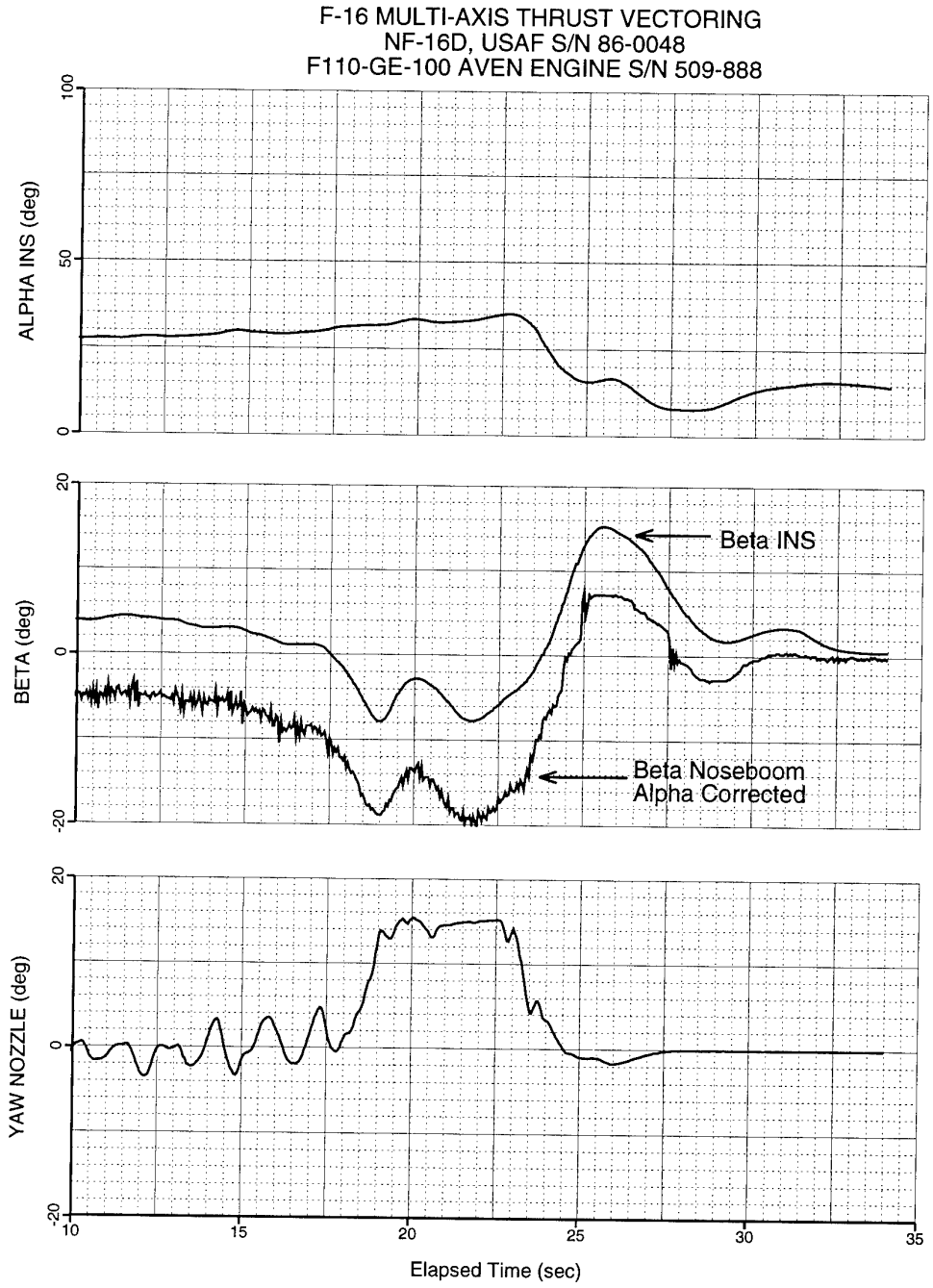

Figure 2: Lateral Directional Flying Qualities, Baseline Flight Control Laws, 35,000 ft MSL, Military Power.

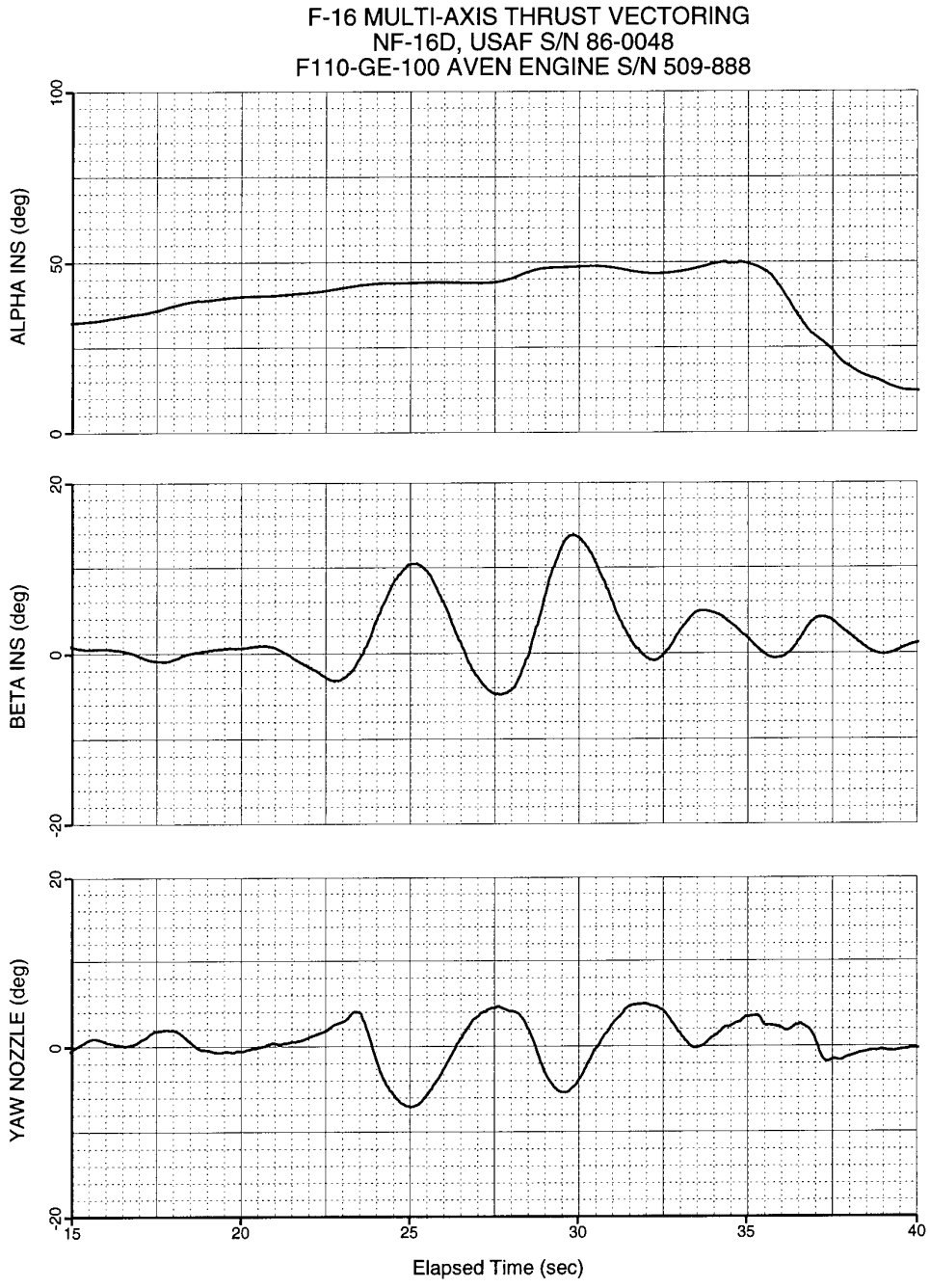

Figure 3: Lateral Directional Flying Qualities, Baseline Flight Control Laws, 35,000 ft MSL, Maximum Power.

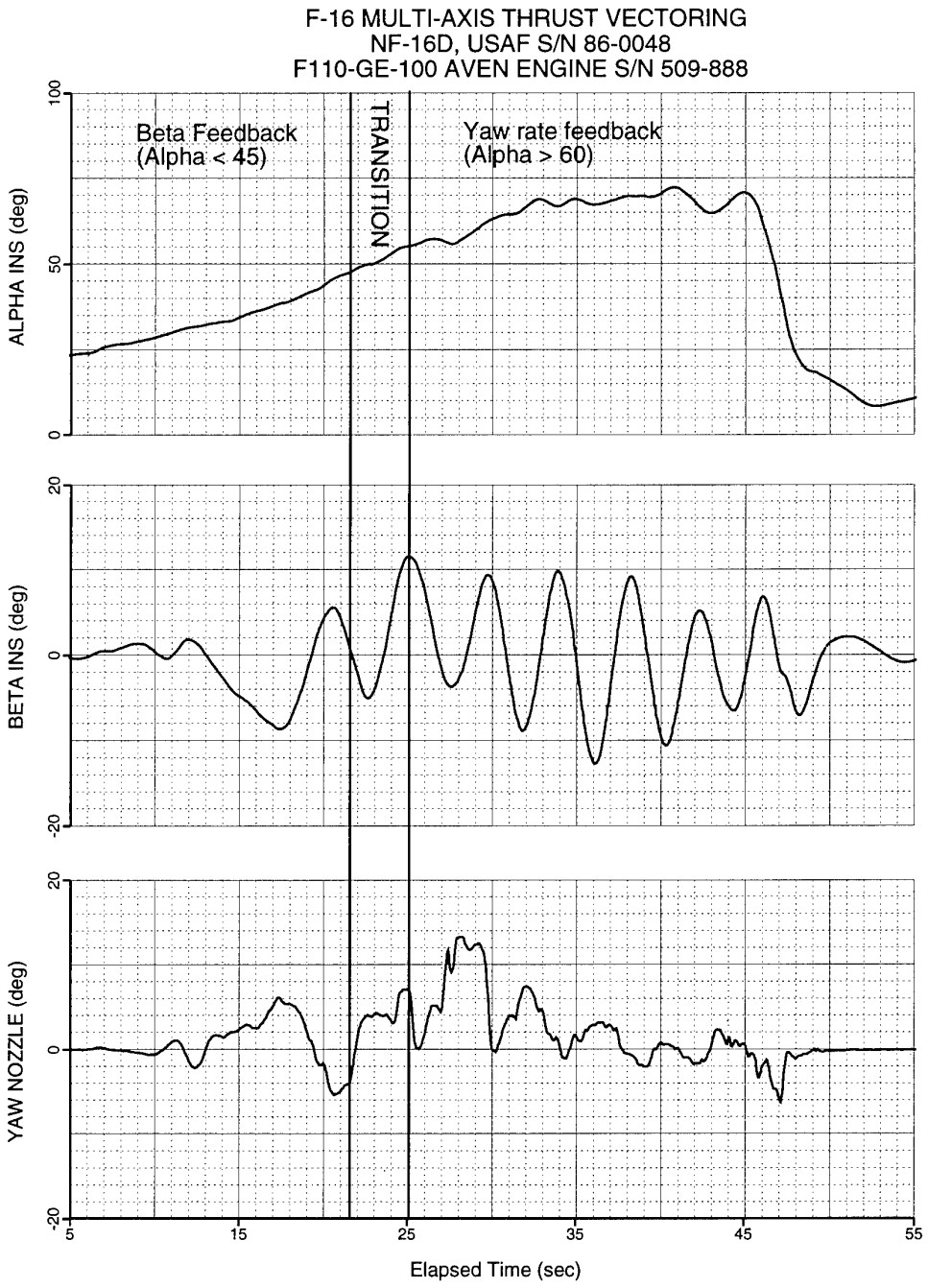

Figure 4: Slow Angle-of-Attack Sweep, Baseline Flight Control Laws, 35,000 ft MSL, Maximum Power.

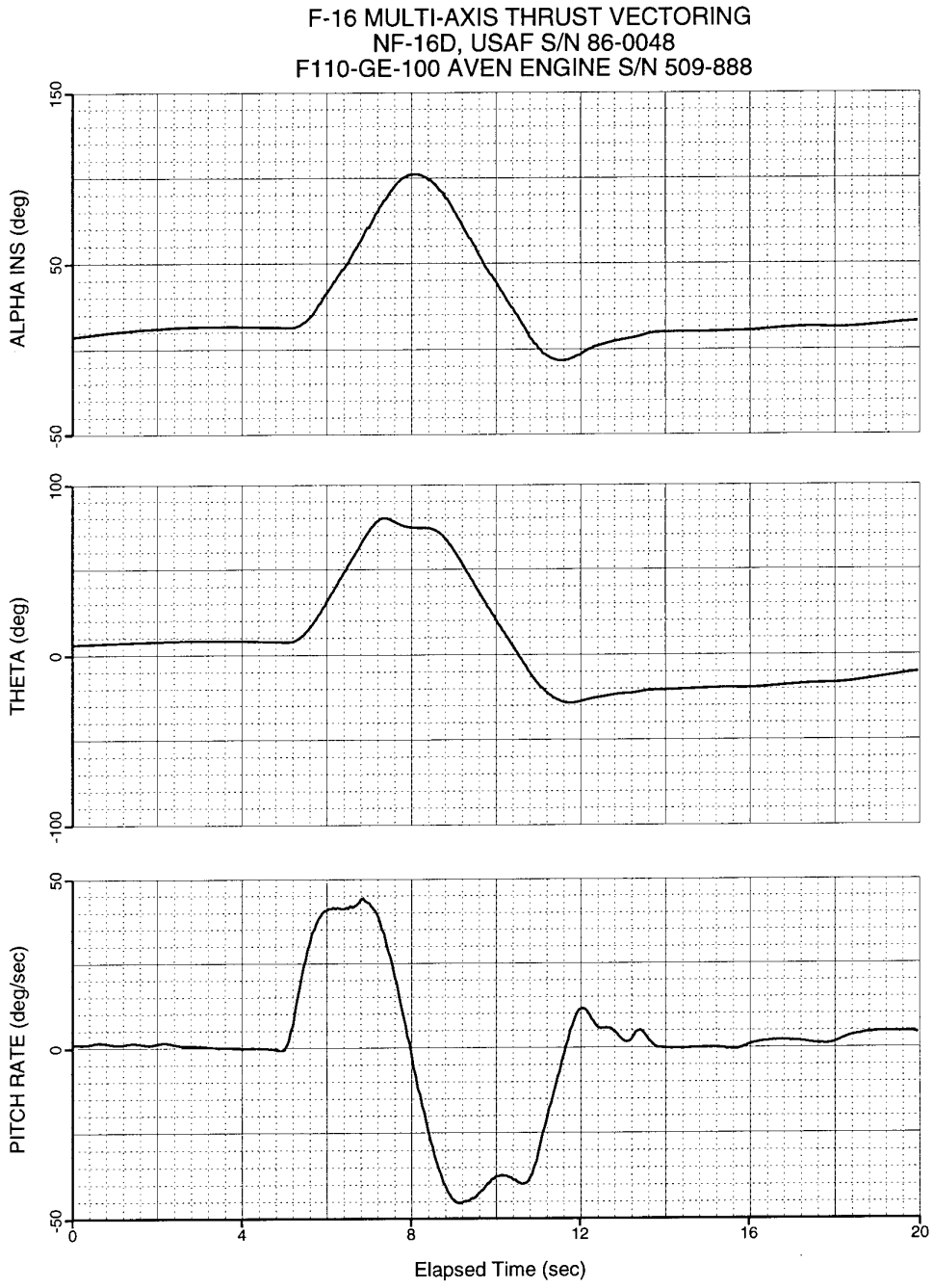

Figure 5: Longitudinal Pull-up and Push-over Maneuver, Baseline Flight Control Laws, 35,000 ft MSL, Maximum Power.

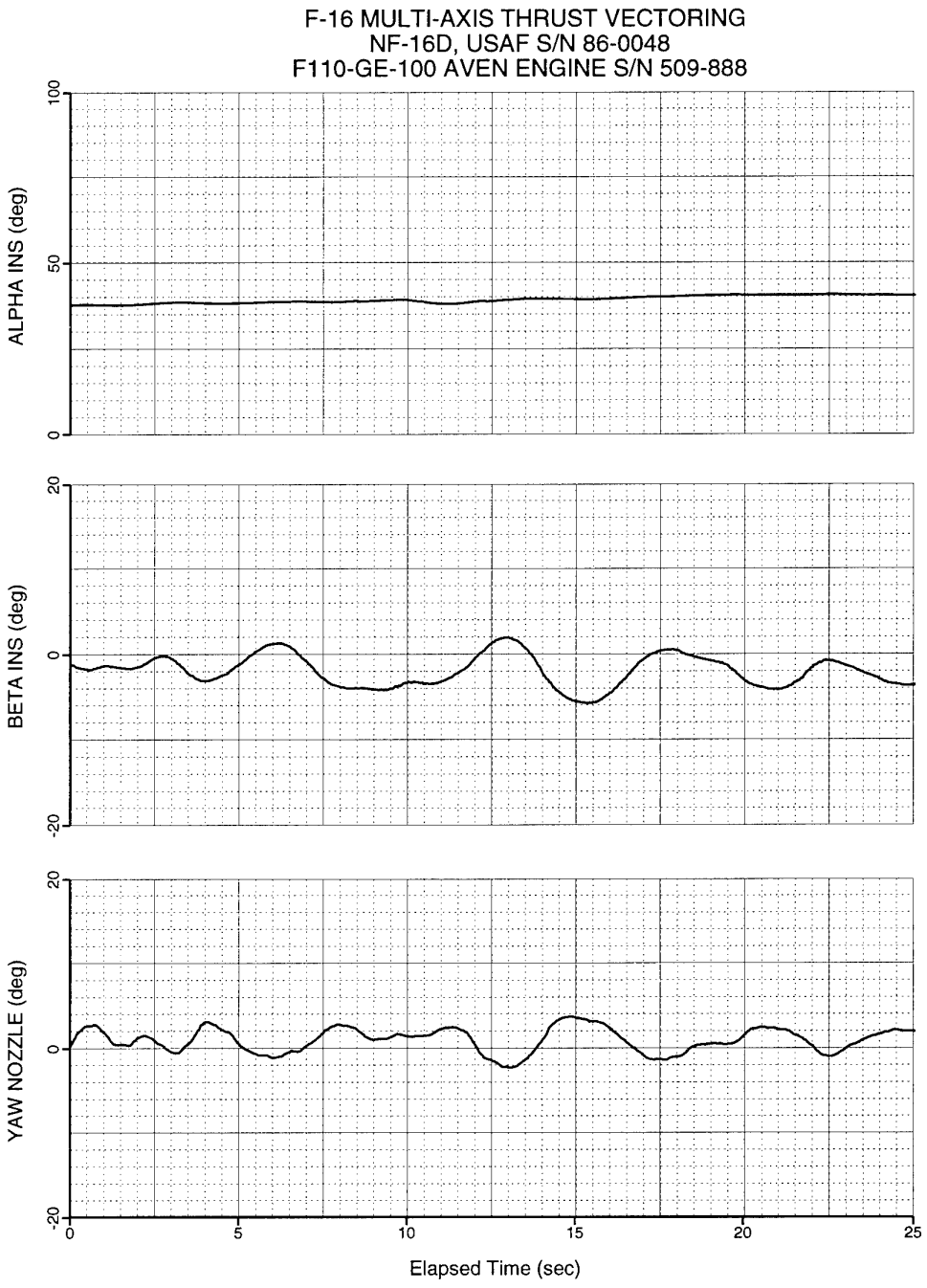

Figure 6: Lateral Directional Flying Qualities, Baseline Flight Control Laws, 25,000 ft MSL, Maximum Power.

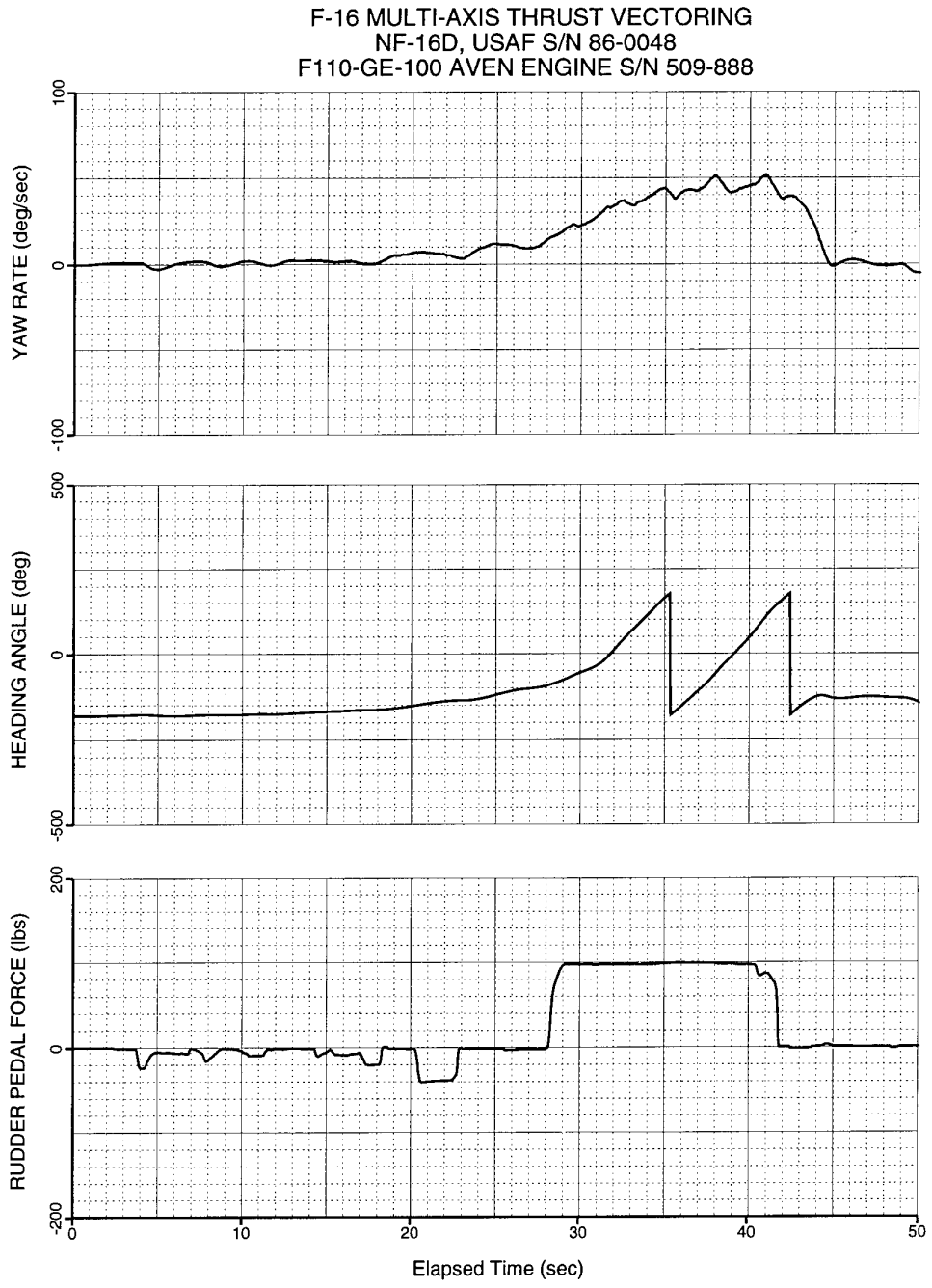

Figure 7: Maximum Yaw Rate Maneuver, Baseline Flight Control Laws, 25,000 ft MSL, Maximum Power.

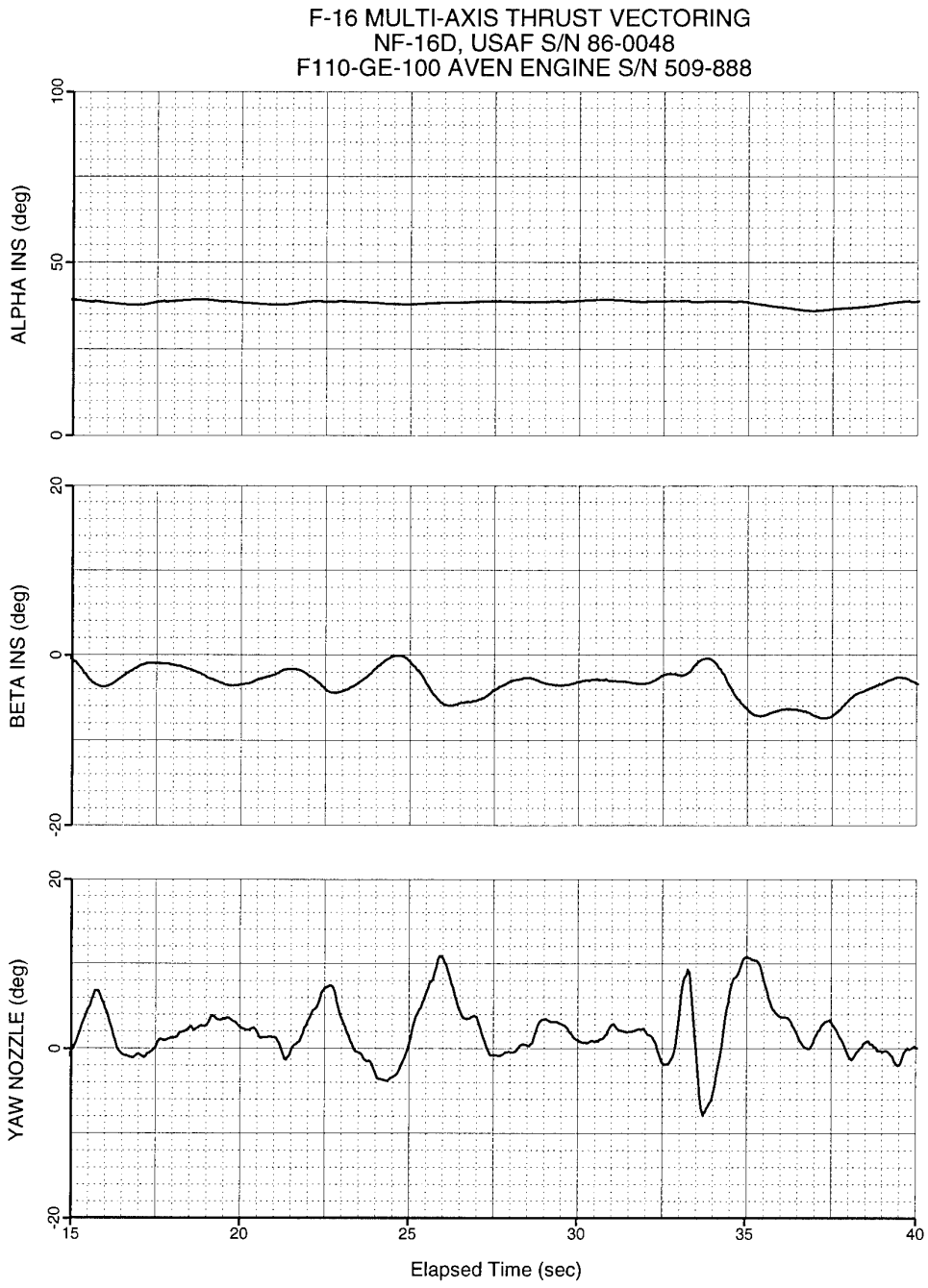

Figure 8: Lateral Directional Flying Qualities, Revised Flight Control Laws, 25,000 ft MSL, Maximum Power.

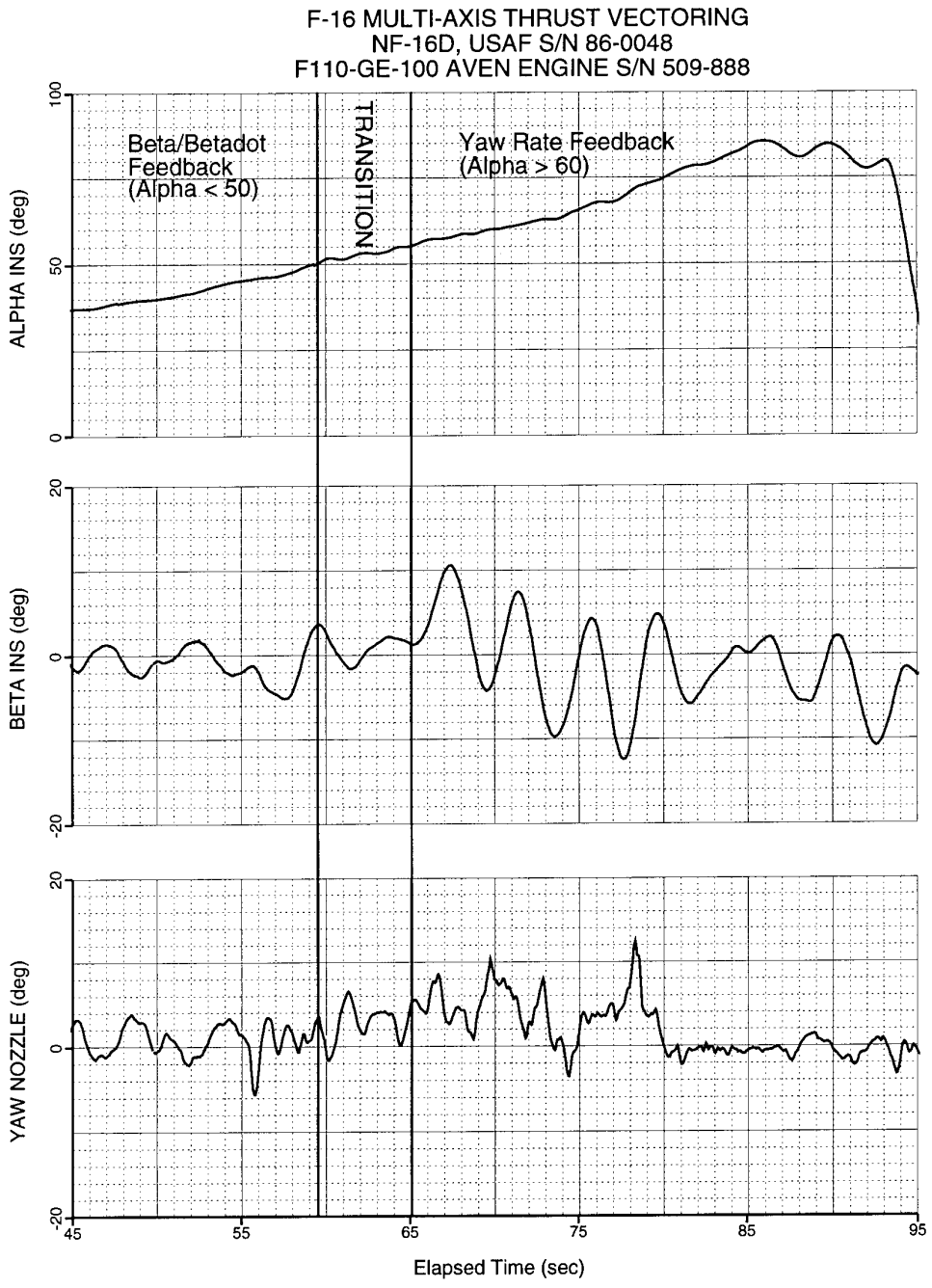

Figure 9: Slow Angle-of-Attack Sweep, Revised Flight Control Laws, 25,000 ft MSL, Maximum Power.

CATAPULTAGE DU RAFALE
CONCEPTION ET EXPERIMENTATION

D. FLEYGNAC
L. LEQUEUX

****

DASSAULT AVIATION - DIRECTION GENERALE TECHNIQUE
CEDEX 300 92552 SAINT-CLOUD
FRANCE

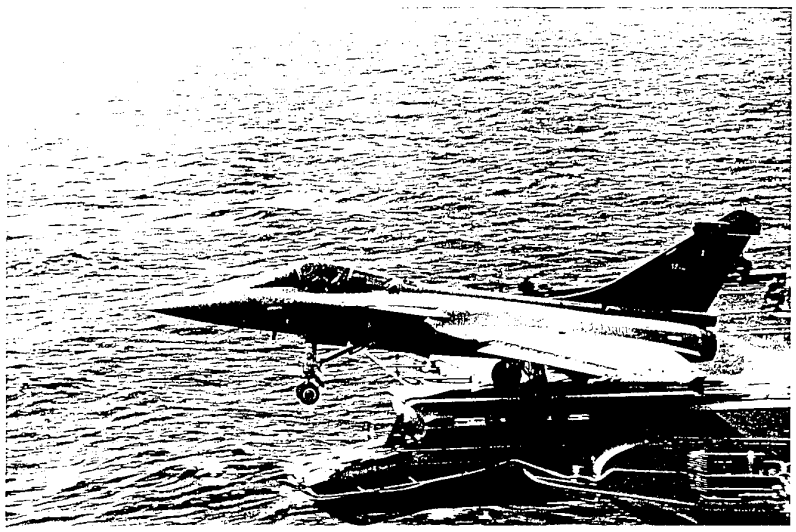

1. INTRODUCTION

Le programme RAFALE a été conçu, dès son origine, pour définir, développer et produire un avion polyvalent répondant aux besoins futurs des Etats-Majors de l'Armée de l'Air et de la Marine. La version Marine est destinée à équiper les forces aéronavales françaises à la fin de la décennie. Elle opèrera à partir du porte-avions à propulsion classique Foch et des porte-avions à propulsion nucléaire du type Charles De Gaulle.

Muni d'un Système de Commandes de Vol (SCV) numérique, le prototype RAFALE M01 est le premier avion à formule delta-canards qui ait été catapulté sur porte-avions (Avril 1993). Il est aussi le premier avion marin à utiliser une formule originale de catapultage assisté par un dièdre d'élancement.

L'étude du catapultage des avions marins recouvre l'ensemble des disciplines techniques usuellement impliquées dans la conception des avions d'armes : aérodynamique, structure, contrôle du vol, systèmes avion... Dans le cadre de ce congrès, la conférence sera plus particulièrement centrée sur la Dynamique du Vol. Elle abordera :

- Les spécificités du catapultage du RAFALE Marine
- Quelques aspects relatifs à la conception du catapultage de l'avion : SCV, dispositifs d'amélioration de performances (dièdre d'élancement, train à haute restitution d'énergie)
- Les campagnes d'expérimentation sur bases à terre
- Les essais en mer

2. SPECIFICITES DU CATAPULTAGE DU RAFALE MARINE

2.1. Considérations générales relatives au catapultage

Le catapultage est une phase particulièrement délicate du point de vue de la sécurité où, sur une piste de quelques dizaines de mètres, on cherche à mettre en vol des avions en configurations lourdes avec emports. Compte-tenu des objectifs opérationnels de l'avion et des configurations qui en résultent, les travaux de conception du catapultage visent essentiellement à permettre la mise en vol de ces configurations dans des conditions de sécurité satisfaisantes.

Pour une configuration avion donnée, la vitesse air en sortie de pont maximale que l'on peut obtenir résulte (Cf. figure 1) :

Paper presented at the Flight Mechanics Panel Symposium held in Turin, Italy, from 9-13 May 1994.

- de la performance de la catapulte caractérisée par la Vitesse de Sortie Catapulte (VSC). Cette vitesse décroit quand la masse augmente
- du Vent Sur Pont lui-même constitué du vent météo et de la Vitesse du Bateau (VB)

Pour cette même configuration avion, on définit une vitesse de référence appelée Vitesse Minimale Sûre (VMS) de catapultage comme étant la vitesse air minimale qui permet le respect de certaines contraintes relatives à la trajectoire en vol de l'avion après sortie de pont (enfoncement, accélération sur trajectoire...).

Cette Vitesse Minimale Sûre augmente avec la masse, et varie avec le centrage.

Au stade de la conception, une configuration sera considérée catapultable si sa VMS est inférieure à la Vitesse air réalisable par vent météo nul soit :

$$VMS \leq VSC + VB$$

En opérations, les conditions de catapultage résultent de la connaissance de la VMS mais tiennent compte aussi des conditions opérationnelles (vent météo, état de la mer ...).

Pour accroître les capacités opérationnelles d'un avion c'est-à-dire, bien souvent, en augmenter le nombre et la masse des emports, deux solutions se présentent :

- Augmenter les capacités des catapultes (VSC) et/ou les performances du porte-avions (VB)
- Réduire les VMS de l'avion

Le premier point peut difficilement être envisagé s'agissant de porte-avions existants. En revanche, il est pris en compte lors de la définition des nouveaux navires dans la limite des efforts acceptables par la structure avion.

Le second point relève très directement de la conception d'un avion marin. Il est même au coeur des travaux de conception du catapultage qui sont présentés plus loin.

2.2. Cas du RAFALE MARINE

La conception générale du RAFALE et notamment de sa formule aérodynamique répond à l'exigence de communalité la plus étroite possible des versions air et mer.

Cette exigence résulte :

- D'une part du constat technique que dans un certain nombre de domaines les spécifications d'emploi des Etats-Majors de la Marine et de l'Armée de l'Air pouvaient se rapprocher. Ainsi la réduction des vitesses d'approche imposée par l'appontage peut correspondre à un besoin terrestre de réduction des longueurs d'atterrissage
- D'autre part de considérations budgétaires ; la conception d'un avion polyvalent réduit sensiblement les coûts unitaires par comparaison avec des réponses spécifiques aux besoins de chaque Etat-Major

La formule aérodynamique retenue est du type delta-canards sans dispositif hyper-sustentateur. La voilure delta résulte d'une longue expérience de DASSAULT AVIATION avec les familles MIRAGE. L'adjonction de plans mobiles canards pilotés permet d'en améliorer encore l'efficacité notamment dans le domaine des basses vitesses par un accroissement significatif de portance. Cette formule ne donne sa pleine efficacité que grâce à un Système de Commandes de Vol à technologie numérique qui gère, à chaque instant, les organes de commande disponibles (y compris les moteurs).

Efficace sur l'ensemble du domaine de vol, la formule retenue impose, toutefois, aux vitesses de catapultage, d'atteindre des incidences relativement élevées assurant un facteur de charge supérieur à 1 et, par ailleurs, d'obtenir cette incidence en sortie de pont le plus rapidement possible afin de limiter la durée de la phase transitoire pendant laquelle la portance n'équilibre pas le poids.

Le RAFALE Marine présente ainsi un comportement dynamique au catapultage relativement différent de ceux des autres avions marins, ainsi que cela sera illustré dans la suite du document. Il convient de souligner que la maîtrise de ce comportement ne peut être assurée que par un Système de Commandes de Vol électriques permettant notamment le contrôle d'un avion naturellement instable dans les conditions de catapultage.

3. QUELQUES ASPECTS DE LA CONCEPTION DU CATAPULTAGE

3.1. Système dynamique considéré - Modélisation

La qualité de la modélisation est, aujourd'hui, un point clé de la conception des systèmes. En effet, la confiance dans les modèles permet de réduire sensiblement les phases de développement et d'essais et notamment les retours importants sur conception qui pourraient résulter d'une mauvaise connaissance, a priori, du comportement de l'avion et des systèmes.

La conception des Systèmes de Commandes de Vol s'appuie usuellement sur une modélisation aérodynamique très détaillée de l'avion résultant d'essais en soufflerie éventuellement recalés du vol. Dans le cas particulier du catapultage, le contrôle automatique porte non seulement sur les conditions de vol stabilisées mais aussi sur la maîtrise du comportement transitoire de

l'avion en sortie de catapulte. Aussi, le système dynamique considéré, et par conséquent la modélisation mise en oeuvre, dépasse-t-il largement le cadre strict de l'avion muni de son SCV. Il est constitué (figure 2) de :

- L'avion, caractérisé par son aérodynamique (tenant compte de l'effet de sol)
- Le Système de Commandes de Vol
- La catapulte, qui via l'interface de pont, transmet à l'avion des efforts de traction dont le profil, fonction du temps, a un effet important sur la dynamique en sortie de pont
- Les atterrisseurs qui sont soumis, au catapultage, à des sollicitations particulièrement fortes de compression et de détente rapides
- Le profil de la piste, plus particulièrement la présence éventuelle d'un dièdre d'élancement sur le fonctionnement duquel nous reviendrons plus loin
- Enfin, les mouvements éventuels de plate-forme

Chaque élément de ce système participe au comportement dynamique de l'avion en sortie de pont dont le SCV doit assurer la maîtrise. Ce constat a conduit à mettre en place des moyens de simulation complets, représentant le comportement dynamique de l'ensemble du système et composés de modèles très détaillés des différents éléments intervenant au catapultage, notamment des atterrisseurs.

La présentation détaillée de ces modèles et d'une première validation obtenue au travers d'une expérimentation originale par franchissement de dièdre avec un MIRAGE 2000 a fait l'objet d'une précédente publication au Congrès AGARD/FMP de Mai 1991 à Séville (Référence 1).

Rappelons simplement que les structures de modélisations utilisées sont du type "modèles de connaissance" (par opposition à un modèle de comportement), c'est à dire des modélisations dont la structure fonctionnelle résulte directement des équations dynamiques du système physique représenté.

3.2. Conception des lois de commandes

Le Système de Commandes de Vol du Rafale comporte une fonction de pilotage spécifiquement destinée à la phase de catapultage appelée "mode catapultage".

3.2.1. Objectifs fonctionnels

La conception du mode catapultage répond à plusieurs objectifs fonctionnels :

- Permettre le catapultage manche libre : le pilote réalise la surveillance du bon déroulement du catapultage par l'observation de quelques paramètres synthétiques de l'Interface Homme Machine, et reprend en mains au bout de quelques secondes
- Optimiser, sur un ensemble de configurations, le comportement dynamique vis à vis des critères de performances évoqués plus haut : comme exprimé au chapitre 2.2, cet objectif fonctionnel se traduit par une recherche de vitesse de rotation importante en sortie de catapulte ainsi que des valeurs d'incidence stabilisée relativement élevées
- Assurer un niveau de sécurité acceptable : robustesse vis à vis de certaines dispersions relatives au fonctionnement des systèmes, indifférence aux pannes de certains équipements

3.2.2. Principes fonctionnels

Le schéma fonctionnel simplifié du mode catapultage et de son intégration dans le SCV est présenté figure 3. Le mode catapultage est une fonction, située en entrée du Système de Commandes de Vol, qui élabore essentiellement :

- les ordres qui permettent de commander une prise d'incidence
- des adaptations des fonctions classiques du SCV pour ajuster l'incidence de vol, manche libre
- des ordres en position des gouvernes de configuration destinés à optimiser la configuration aérodynamique au catapultage
- un certain nombre d'informations destinées à adapter les traitements de modes dégradés ou à assurer l'indifférence à certains de ces modes qui peuvent être particulièrement critiques au catapultage
- enfin, les transitions logiques d'engagement/désengagement du mode

3.2.3 Informations présentées au pilote

En mode catapultage, un certain nombre d'informations spécifiques sont présentées au pilote. Notamment, des réticules du viseur tête haute fournissent des éléments relatifs :

- aux conditions de catapultage
- à la trajectoire en vol et l'énergie de l'avion. Ces paramètres, ainsi que l'ensemble des informations usellement présentées, permettent au pilote d'assurer la surveillance du bon déroulement du catapultage et participent étroitement à la confiance ressentie par celui-ci dans une phase de vol particulièrement dynamique (voir plus loin chapitre 5).

3.3. Dispositifs d'amélioration de performances

La satisfaction des objectifs opérationnels du RAFALE Marine (configuration d'emports, masse au catapultage) a conduit à envisager, dès le stade de la conception de l'avion, l'adjonction de dispositifs destinés à améliorer les performances au catapultage. Cette conception globale de l'avion, de son Système de Commandes de Vol, et des dispositifs d'amélioration de performances a permis de parvenir à une solution cohérente et proche d'un certain optimum. Notamment, les lois de contrôle (mode catapultage) ont été conçues, définies et réglées en tenant compte de ces dispositifs.

Deux dispositifs de nature différente ont été proposés :

- Dièdre d'élancement.
- Train auxiliaire à haute restitution d'énergie.

La suite du chapitre vise à présenter sommairement ces deux dispositifs : caractéristiques et principes de fonctionnement.

3.3.1. Dièdre d'élancement

Des tremplins de taille plus ou moins importante équipent depuis longtemps des porte-avions étrangers. Leur emploi, associé, ou non, à celui d'une catapulte, permet par simple effet géométrique de placer l'avion sur une pente initiale positive en sortie de pont. Le dièdre d'élancement se distingue sensiblement de ces dispositifs tant par ses caractéristiques que par son mode de fonctionnement.

Il consiste en un tremplin de faibles dimensions (Cf. figure 4) :

- longueur 10 mètres
- hauteur 0,25 m

placé à 3 mètres environ de la sortie de catapulte.

Par son implantation, en sortie de catapulte, le dièdre d'élancement a un effet fortement dynamique de recompression des atterrisseurs, comme l'illustrent les historiques présentés figure 4 où, autour d'un cas de catapultage à masse moyenne, sont comparés les résultats obtenus sans dièdre (trait fin) et avec dièdre (trait épais). Le train auxiliaire, déjà partiellement déjaugé au franchissement du dièdre, n'est que faiblement recomprimé (l'effort au franchissement du dièdre reste sensiblement inférieur aux valeurs pratiquées pendant la phase tractée). Cet effort engendre cependant, un surcroît de vitesse de rotation favorable vis-à-vis de la performance au catapultage. Le second effet favorable du dièdre est dû au train principal dont la recompression, à des niveaux d'effort pouvant atteindre 2 x 20 tonnes, puis la détente rapide provoquent une impulsion verticale élevée. La vitesse verticale initiale qui en résulte en sortie de pont permet de limiter l'enfoncement sur trajectoire.

Le gain ainsi obtenu, vis à vis des critères de catapultage, peut être traduit en réduction de la VMS et en accroissement des capacités opérationnelles.

3.3.2. Train à haute restitution d'énergie

Le principe de catapultage par la jambe de train, retenu sur le RAFALE, conduit à comprimer l'atterrisseur auxiliaire pendant la phase tractée. En sortie de catapulte, au lâcher du croc, l'énergie emmagasinée se trouve libérée instantanément et provoque la détente rapide du train auxiliaire. Les efforts de laminage, engendrés par la circulation d'huile dans les amortisseurs et destinés, principalement, à assurer une dissipation d'énergie à l'impact, réduisent toutefois sensiblement le rendement énergétique de cette détente.

Le concept de train à haute restitution d'énergie consiste à disposer d'un réglage des orifices de laminage spécifique pour les phases de catapultage et tel que la détente du train soit la plus rapide possible. A l'inverse, les efforts de laminage en compression sont augmentés pour améliorer l'amortissement des oscillations pendant la phase tractée. Après envol, l'amortisseur revient automatiquement aux réglages nominaux de laminage.

3.3.3. Remarques

Les deux dispositifs qui viennent d'être sommairement décrits sont de nature assez différente :

- d'une part par leurs répercussions sur les conditions d'emploi de l'avion
- d'autre part par le gain de performances qu'ils procurent. L'utilisation du dièdre d'élancement se traduit sur le RAFALE par un gain de performances aux masses élevées (réduction de VMS) de l'ordre de deux fois supérieur à celui du train à haute restitution d'énergie.

En revanche, il convient de noter que, dans les deux cas, les dispositifs utilisés ont la caractéristique commune d'agir par effet essentiellement dynamique où chaque organe constituant le système catapulte/avion/trains/piste est mis à profit pour améliorer la performance de l'avion. L'effet dièdre est principalement fonction de la vitesse de franchissement ; il varie, aussi, avec le niveau de compression des atterrisseurs à l'attaque du tremplin et, à ce titre, est d'autant plus efficace que celui-ci est placé à proximité de la sortie catapulte. L'effet haute restitution d'énergie dépend, quant à lui, du niveau de compression du train auxiliaire lui-même fonction du niveau de l'effort de traction catapulte en fin de course.

Aussi la qualité de la modélisation dynamique du système utilisée durant les phases de conception est-elle essentielle. Sa validation, et le cas échéant son recalage, constituent un des principaux objectifs des campagnes d'essai à terre qui sont présentées au chapitre suivant.

4. EXPERIMENTATION SUR BASE A TERRE

Le schéma général relatif à la méthode de préparation de conduite et d'exploitation des essais est présenté figure 5.

4.1. Objectifs - Contraintes

4.1.1. Objectifs des essais

Les campagnes d'expérimentation sur base à terre visent :

- d'une part à procéder à une première validation des choix de conception : systèmes avion, principes des lois de contrôle, ergonomie de pilotage...
- d'autre part, et surtout, à fournir les éléments d'une identification détaillée des modèles de calcul utilisés.

Par ailleurs, la conduite des essais doit permettre d'assurer une ouverture progressive du domaine d'emploi et notamment des efforts de traction appliqués à l'avion, ainsi que de la tenue des équipements aux forts niveaux d'accélération pratiqués.

4.1.2. Contraintes

Les campagnes d'essais se déroulent sur la base du NAWC à Patuxent River, Maryland et Lakehurst, New Jersey - USA. Les essais de catapultage ont été entièrement réalisés sur cette dernière base. Les moyens disponibles consistent en deux catapultes placées à l'extrémité d'une piste de 2400 m :

- une catapulte au ras du sol d'une longueur de 93 m
- une catapulte surélevée de 1.80 m et d'une longueur de 74 m

L'utilisation de ces catapultes induit des contraintes spécifiques qui doivent être prises en compte pour la définition des essais :

- garde au sol en sortie de catapulte pour les catapultages sur la catapulte au ras du sol
- efforts maximaux dans les atterrisseurs en cas de rebond

D'autre part, un certain nombre de cas de pannes doivent être pris en compte dans la préparation des essais.

4.2. Préparation des essais

4.2.1. Fonction essais du mode catapultage

Afin de permettre la réalisation d'essais à terre, répondant aux objectifs d'identification et aux contraintes de sécurité exprimés plus haut, le mode catapultage des SCV de développement est complété d'un mode d'essais (figure 6).

Ce mode consiste essentiellement en la possibilité d'afficher, pour les paramètres principaux du mode catapultage, des jeux pré-programmés de valeurs numériques. La sélection de ces jeux de valeurs est réalisée par le pilote grâce au boîtier d'essais disposé en cabine.

Les principaux paramètres du mode catapultage pouvant être adaptés sont :

- l'ordre de profondeur, qui permet d'ajuster le braquage des élevons et la vitesse de rotation en sortie de catapulte
- l'adaptation du limiteur d'incidence, qui permet d'ajuster l'incidence de vol, manche libre

4.2.2. Définition des essais

Outre les essais préliminaires destinés à confirmer progressivement la tenue des systèmes aux efforts et aux chocs subis par l'avion au catapultage, les essais réalisés sur base à terre doivent permettre, a posteriori, l'identification détaillée des modèles de calcul. A ce titre, la définition de ces essais s'inscrit dans le processus d'identification.

Notamment afin d'assurer la meilleure identifiabilité possible des caractéristiques de la modélisation, le programme d'essais doit comporter un balayage adapté sur les entrées sensibilisantes du système dynamique telles que :

- l'effort de traction, qui permet de pratiquer différents niveaux de compression des atterrisseurs
- la vitesse de passage sur le dièdre dont dépend la sollicitation en recompression - détente des atterrisseurs
- le braquage des gouvernes qui permet d'améliorer l'identification de leurs efficacités
- les valeurs d'incidence maximale pratiquées qui permettent d'améliorer l'identification de l'aérodynamique de l'avion

4.2.3. Simulation prévisionnelle

La préparation des campagnes d'essais est fondée sur un volume important de simulations réalisées dans les conditions prévues de l'expérimentation et notamment en introduisant dans le calcul les lois exactes de traction catapulte fournies par les responsables américains du NAWC.

Ces simulations permettent d'évaluer l'évolution des grandeurs contraignantes (garde au sol, efforts dans les atterrisseurs...) avec les conditions d'essais et de définir ainsi les restrictions relatives à l'élaboration du programme d'essais.

En outre, un certain nombre d'influences élémentaires sont réalisées autour de ces calculs nominaux, en introduisant, dans le modèle de simulation, des variations réalistes sur quelques paramètres critiques de modélisation. Les résultats de ces calculs sont destinés, au stade de la préparation des campagnes, à évaluer la sensibilité des prévisions aux incertitudes de modélisation et à préciser ainsi les marges qui doivent être prises vis-à-vis des grandeurs contraignantes. Par ailleurs, ils fournissent les éléments nécessaires à une première exploitation, sur place, des résultats obtenus en cours d'expérimentation.

Le rôle essentiel de cette activité de simulation prévisionnelle dans le cadre de la préparation des campagnes doit être souligné. Il permet :

- de parvenir à un programme d'essais adapté à l'activité ultérieure d'identification
- d'acquérir un certain niveau de confiance sur la progressivité et la sécurité des essais tenant compte des incertitudes de modélisation
- de disposer, enfin, de moyens d'analyse, in situ, des résultats d'essai

4.3. Campagnes d'essai

4.3.1. Organisation des essais

La durée de chaque campagne d'essais est de un à deux mois, incluant des essais de catapultage et de prises de brin. La conduite de ces essais est placée sous la responsabilité des équipes du Ministère de la Défense et de la Direction des Essais en Vol de DASSAULT AVIATION, auxquelles quelques ingénieurs spécialistes de la Direction Générale Technique apportent un soutien technique dans leur domaine de compétence.

L'éloignement géographique impose une très grande autonomie des équipes assurant le suivi tant pour l'entretien et la maintenance de l'avion que la surveillance du bon fonctionnement des installations d'essais et le premier dépouillement des résultats.

4.3.2. Déroulement des essais de catapultage

Les travaux de préparation des essais ont permis de bâtir un programme détaillé précisant, pour chaque tir, la configuration avion, le réglage de catapulte, et les réglages des lois de contrôle du SCV. Le vent constitue, naturellement, un paramètre non-maîtrisé ; toutefois son intensité et sa direction doivent se situer à l'intérieur de valeurs imposées par la sécurité des essais.

Chaque catapultage est suivi d'une première exploitation d'une durée de deux heures environ :

- traitement des données et tracés de variables caractéristiques
- surveillance des paramètres critiques relatifs à la sécurité (efforts structuraux notamment)
- analyse du comportement par référence aux simulations ou calculs prévisionnels. Cette analyse vise à obtenir une première validation des modèles de simulation utilisés et confirmer ainsi le programme d'essais. Le cas échéant, des écarts significatifs observés entre les résultats d'essais et ceux de calculs auraient pu conduire à faire évoluer ce programme

Cette première exploitation conditionne l'engagement des essais suivants et permet de les aborder avec un certain niveau de confiance. Elle constitue, par ailleurs, une étape préliminaire de l'opération d'identification. En particulier, la disponibilité, sur place, de résultats d'influences élémentaires sur les paramètres caractéristiques de la modélisation fournit les éléments d'une première interprétation des éventuels écarts observés.

4.3.3. Bilan des trois premières campagnes de catapultage à terre

A ce jour, trois campagnes d'essai ont été réalisées :

- deux campagnes avion lisse qui ont permis de préparer la première campagne sur porte-avions en Avril 1993
- une campagne avec emports destinée à préparer la campagne sur porte-avions de printemps 1994

Le bilan des essais réalisés au cours de ces campagnes et leur répartition par installation à terre sont présentés figure 7. La première campagne a essentiellement été consacrée à la validation des systèmes avion et notamment à l'analyse des efforts et des chocs subis par les différents équipements mécaniques du catapultage. Elle a tout de même permis de réaliser le premier catapultage sur dièdre qui constituait, rappelons-le, une première mondiale ; la seconde campagne, plus complète sur le plan de l'analyse du comportement dynamique au catapultage, a couvert un spectre beaucoup plus large de

conditions d'essais : réglages du SCV, vitesses de catapultage, efforts de traction.

La réalisation de l'ensemble des essais prévus, et principalement des essais sur catapulte surélevée, a permis d'aborder avec confiance la première campagne à la mer d'Avril 1993.

La troisième campagne à terre, qui s'est déroulée fin 93, a permis l'ouverture du catapultage avec emports. Les deux configurations étudiées correspondent aux premières configurations opérationnelles qui équiperont le porte-avions Foch. Cette campagne s'est déroulée de façon tout à fait conforme aux prévisions et a permis de consacrer quelques tirs, sur la catapulte au ras du sol, à l'examen de configurations futures d'emport. Cette campagne a été suivie des essais en mer de Février et Avril 1994 qui viennent de s'achever.

4.4. Exploitation des essais

Outre le recueil d'un premier avis des pilotes sur le comportement avion au catapultage et l'ergonomie de pilotage sur lesquels nous reviendrons plus loin (chapitre 5), les campagnes d'essais à terre fournissent d'une part des enseignements sur les choix fonctionnels des lois de contrôle et, d'autre part, un ensemble de données permettant de conduire, a posteriori, une opération relativement très complète d'identification.

4.4.1. Enseignements fonctionnels

Les premières campagnes à terre ont permis une validation des principes fonctionnels retenus pour le Contrôle du Vol au catapultage et n'ont conduit qu'à des retouches de détail des lois de commandes.

Ce résultat tient essentiellement à la qualité de la modélisation disponible en phase de conception, qualité illustrée par les résultats présentés ci-après.

4.4.2. Identification

Le processus d'identification utilisé est présenté figure 8.

La validation et les éventuels recalages de modélisation sont fondés sur la comparaison :

- des résultats d'essais d'une part
- des résultats de simulations rejouées dans les conditions exactes d'expérimentation, en introduisant dans le calcul : la configuration avion, les mesures atmosphériques, la catapulte utilisée et son réglage...

La comparaison porte essentiellement sur les historiques de paramètres représentatifs du comportement dynamique tels que, pour l'avion, la vitesse sol, l'incidence, l'assiette, la vitesse de tangage, la vitesse verticale ; pour les atterrisseurs, les efforts et enfoncements ; pour le S.C.V., les braquages d'élevons... Compte-tenu de la qualité des résultats obtenus, le critère d'appréciation est d'une part visuel et d'autre part quantitatif. Le bon recoupement observé avec le modèle prévisionnel n'a conduit, à ce jour, qu'à des recalages mineurs de modélisation tels que la prise en compte de la compressibilité d'huile dans les amortisseurs.

La qualité du résultat obtenu peut être appréciée, figure 8, pour un catapultage avec charges sur catapulte au sol avec dièdre. On notera l'excitation structurale provoquée par la sortie du dièdre et particulièrement visible sur le signal mesuré de vitesse de tangage.

Le niveau de recoupement observé sur l'ensemble des essais est jugé satisfaisant pour mener à bien la poursuite des travaux de définition fonctionnelle du SCV ainsi que les estimations de performances de l'avion de série. Les écarts non significatifs qui demeurent, en particulier sur le transitoire de prise d'assiette, sont liés à des effets instationnaires non pris en compte dans la modèlisation.

5. CAMPAGNES EN MER

5.1. Présentation générale

Du point de vue de l'examen du comportement dynamique de l'avion, les campagnes en mer répondent aux mêmes objectifs que les campagnes à terre et notamment aux exigences d'identification des modèles. Toutefois, compte tenu des contraintes fortes de sécurité, le spectre de conditions d'essais est beaucoup plus restreint. En revanche certains phénomènes nouveaux, propres à l'emploi sur porte-avions peuvent être observés (effet de falaise dû à l'étrave du navire par exemple).

Les deux campagnes réalisées à ce jour sur le porte-avions Foch (avion lisse en Avril 93, configurations avec emports au printemps 94) ont confirmé les enseignements des campagnes à terre et la qualité des modèles de prédiction du comportement dynamique disponibles.

Par ailleurs, elles ont été l'occasion de recueillir "en vraie grandeur" l'impression des pilotes sur le catapultage du RAFALE : ergonomie de pilotage, impressions sensorielles... Ce jugement porté en conditions proches de conditions opérationnelles constitue, sur le plan de la dynamique du vol, un des principaux enseignements des essais en mer.

5.2. Jugement des pilotes

Dès leurs premiers catapultages à terre, les pilotes d'essai (Dassault Aviation, CEV, Marine) ont pu apprécier la différence de comportement entre le RAFALE Marine et les autres avions marins : forte vitesse de rotation, incidence et assiette de vol élevées. Cette dynamique rapide, qui fait suite à une accélération longitudinale

pendant la phase tractée pouvant dépasser 5 g, avait, au stade de la conception de l'avion, suscité quelques interrogations liées au risque de perturbation des impressions sensorielles du pilote.

Les campagnes d'essais de catapultage et plus particulièrement les campagnes en mer ont permis de lever ces interrogations :

- d'une part, le catapultage manche libre dispense le pilote de toute action de pilotage pendant plusieurs secondes suivant la sortie de catapulte. La reprise en main s'effectue en vol stabilisé
- d'autre part, les réticules présentés en Viseur Tête Haute fournissent un ensemble d'informations synthétiques relatives au déroulement du catapultage. Ces informations sont jugées utiles et efficaces par l'ensemble des pilotes
- enfin, le comportement dynamique de l'avion est jugé particulièrement sain. Notamment la prise d'assiette, bien que rapide, ne suscite aucune impression défavorable car elle est franche et régulière. De manière générale, la qualité des lois de commandes de vol fait l'unanimité des pilotes qui ont été catapultés sur RAFALE. Elle contribue très largement à la confiance ressentie par ceux-ci durant une phase de vol au demeurant très dynamique et qui engage la sécurité de l'avion.

Cet ensemble de commentaires devra être confirmé par les différents évaluateurs qui, au cours des prochaines campagnes d'essais, seront catapultés sur RAFALE.

Il conviendra, aussi, d'étendre les conditions d'essais à des situations opérationnelles plus critiques : catapultage de nuit, mauvaises conditions météorologiques.

Toutefois, l'unanimité actuelle des pilotes pour souligner la qualité du comportement dynamique de l'avion et sa parfaite maîtrise par le Système de Commandes de Vol permet d'aborder avec confiance l'emploi de l'avion en conditions opérationnelles.

6. CONCLUSION

Le RAFALE Marine présente un comportement dynamique au catapultage relativement différent de celui des autres avions marins, caractérisé, notamment, par une forte vitesse de rotation en sortie de catapulte.

L'avion, son Système de Commandes de Vol, ses atterrisseurs, ainsi que certains aménagements du pont d'envol ont été conçus globalement dans le but de parvenir à une solution proche d'un certain optimum vis à vis des critères actuels de catapultage. En particulier, le dièdre d'élancement qui équipera le porte-avions Foch, et le train à haute restitution d'énergie qui sera activé sur les porte-avions nucléaires n'ont d'efficacité que par leur utilisation combinée avec la catapulte, et par la définition adaptée des lois de Commandes de Vol.

La conception de l'ensemble du système s'appuie sur une modélisation détaillée et complète dont la pré-validation a fait l'objet, par le passé, de plusieurs expérimentations. La qualité de cette modélisation et la confiance avec laquelle elle a permis d'aborder les campagnes d'essai à terre du RAFALE Marine constituent un point clé du bon déroulement du programme.

A ce jour, trois campagnes à terre et deux campagnes en mer ont permis d'ouvrir le catapultage de l'ensemble des configurations qui équiperont le Foch et le Charles De Gaulle avant la fin de la décennie.

Ces campagnes d'essai ont été définies, préparées, réalisées et exploitées dans le but de fournir les éléments nécessaires à une identification détaillée des modèles de calcul. A ce titre, seuls quelques recalages mineurs ont été apportés et, si l'analyse exhaustive des résultats d'essais est encore en cours, le bon recoupement observé d'ores et déjà entre simulation et expérimentation constitue un gage de la bonne qualité des modèles.

Par ailleurs, les campagnes d'essais, et notamment les essais en mer, fournissent un premier avis des pilotes sur l'ergonomie de pilotage et la réponse dynamique de l'avion. Cet avis est, aujourd'hui, très positif. Le comportement dynamique du RAFALE et sa parfaite maîtrise par un Système de Commandes de Vol qui assure le catapultage manche libre suscitent des réactions favorables de la part des différents pilotes d'essai.

La suite du programme permettra de préparer et d'expérimenter à terre le catapultage des futures configurations de l'avion. Une prochaine campagne en mer comportera, en outre, l'évaluation plus précise des performances de l'avion pour les configurations qui équiperont le Foch.

Les travaux réalisés à ce jour permettent d'affirmer que la conception du catapultage du RAFALE Marine est un succès. Les différentes étapes prévues au lancement du programme en 1988, et notamment le premier rendez-vous avec le porte-avions Foch pour la campagne d'essais en mer d'Avril 1993, ont été fidèlement respectées et ont pleinement rempli leurs objectifs techniques.

Le catapultage d'un avion marin de formule aérodynamique delta-canards, ainsi que l'utilisation de dispositifs d'amélioration de performance originaux constituaient un nouveau défi technologique que la maîtrise de DASSAULT AVIATION dans le domaine de l'intégration de systèmes complexes, de la Dynamique du Vol et des Systèmes de Commandes de Vol a permis de relever. Une première flottille de RAFALE Marine équipera les forces aéronavales françaises à partir de 1999.

REFERENCE

CONGRES AGARD/FMP SEVILLE MAI 1991

Comportement dynamique d'un avion sur ses atterrisseurs : expérimentation et validation par franchissement d'un dièdre.
D. FLEYGNAC - E. BOURDAIS

DESIGN RULES

Fig 1

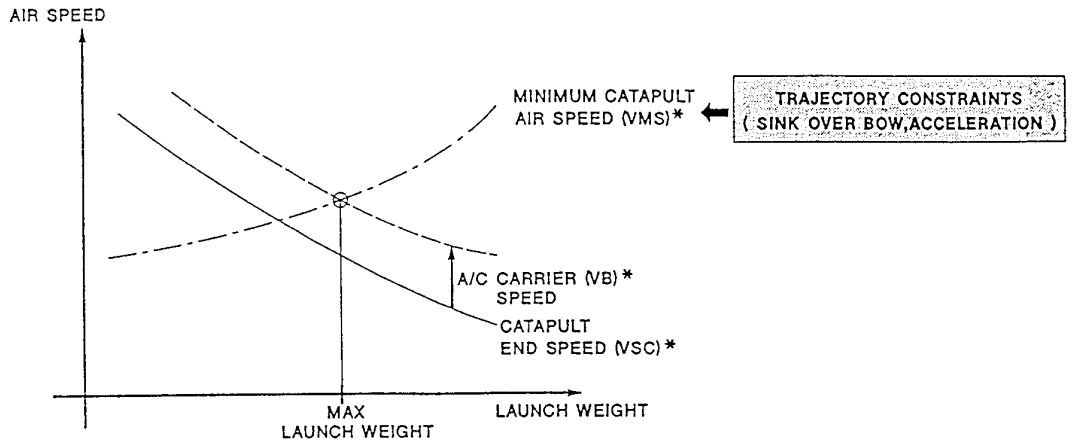

* FRENCH ACRONYMS

MODELING

Fig 2

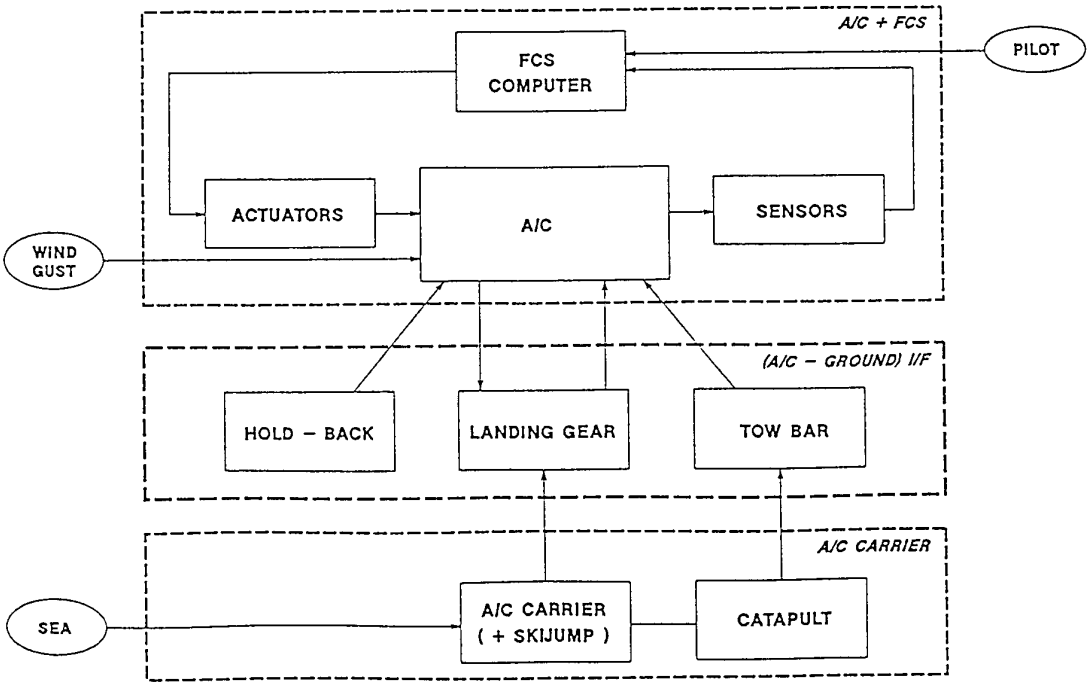

CATAPULTING MODE

Fig 3

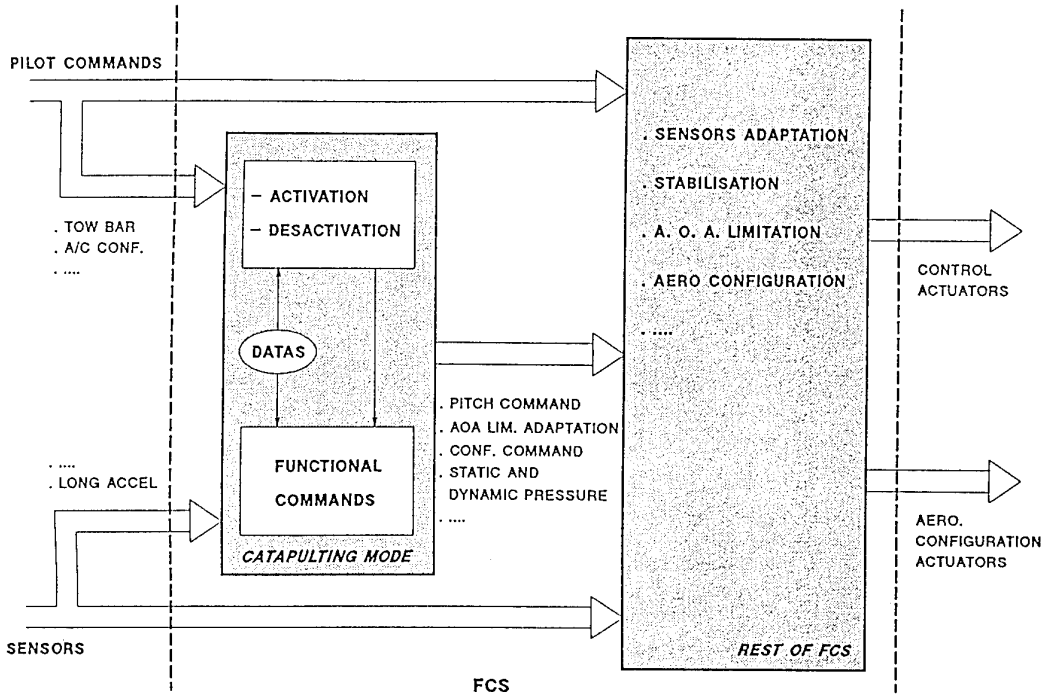

SKIJUMP / FLAT DESK COMPARISON

Fig 4

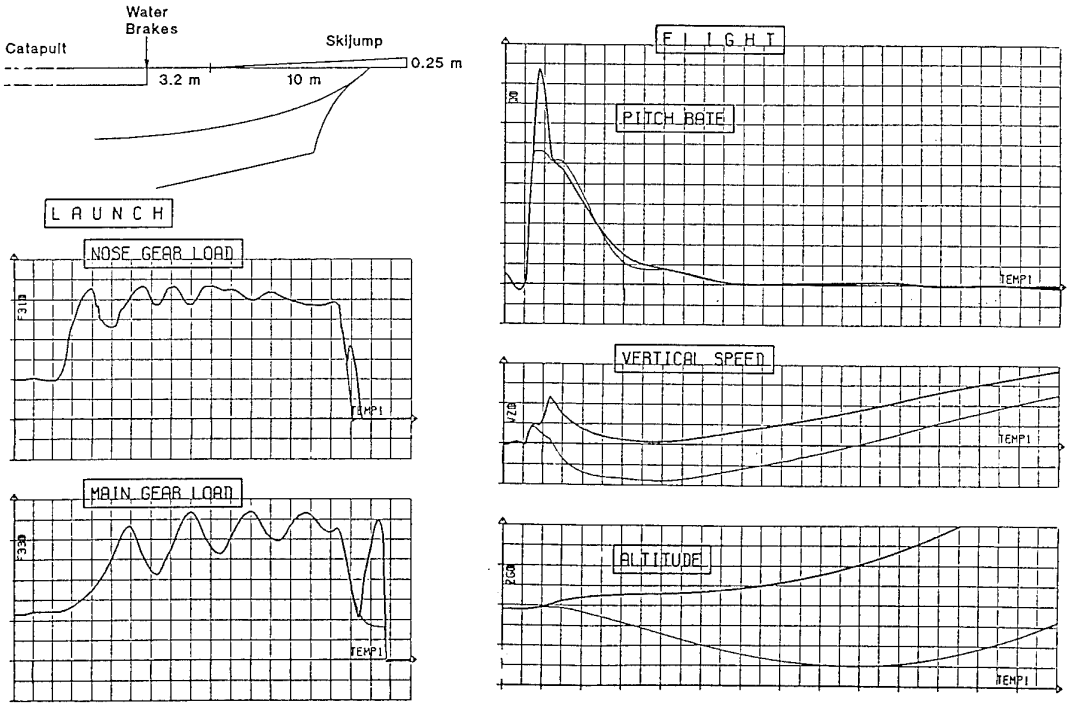

GROUND BASED CAMPAIGNS : GENERAL METHOD

Fig 5

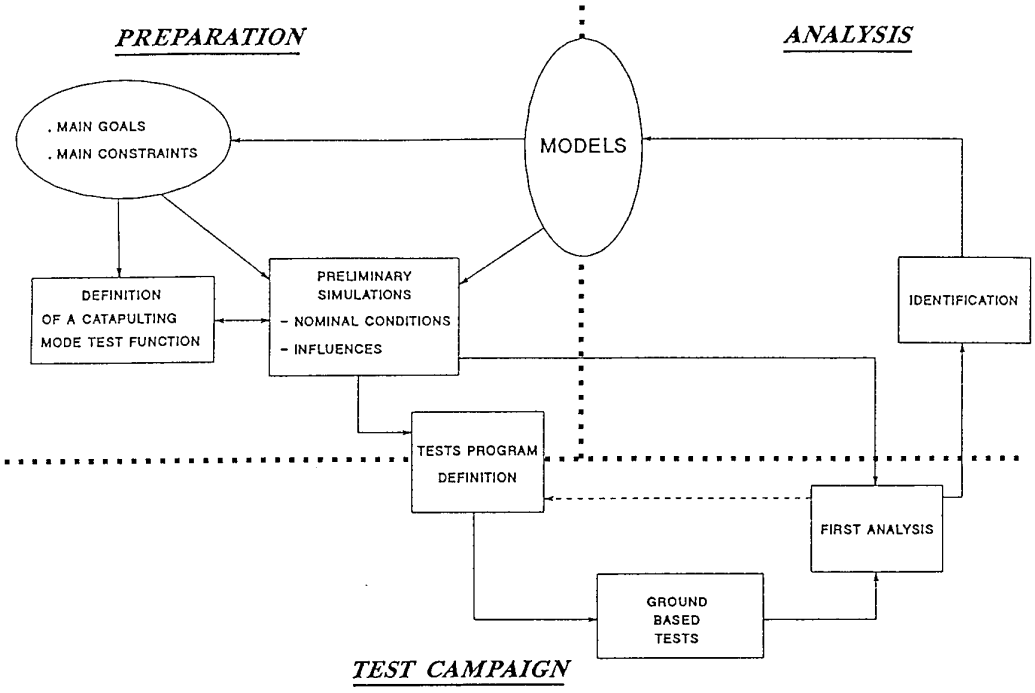

CATAPULTING MODE TEST FUNCTION

Fig 6

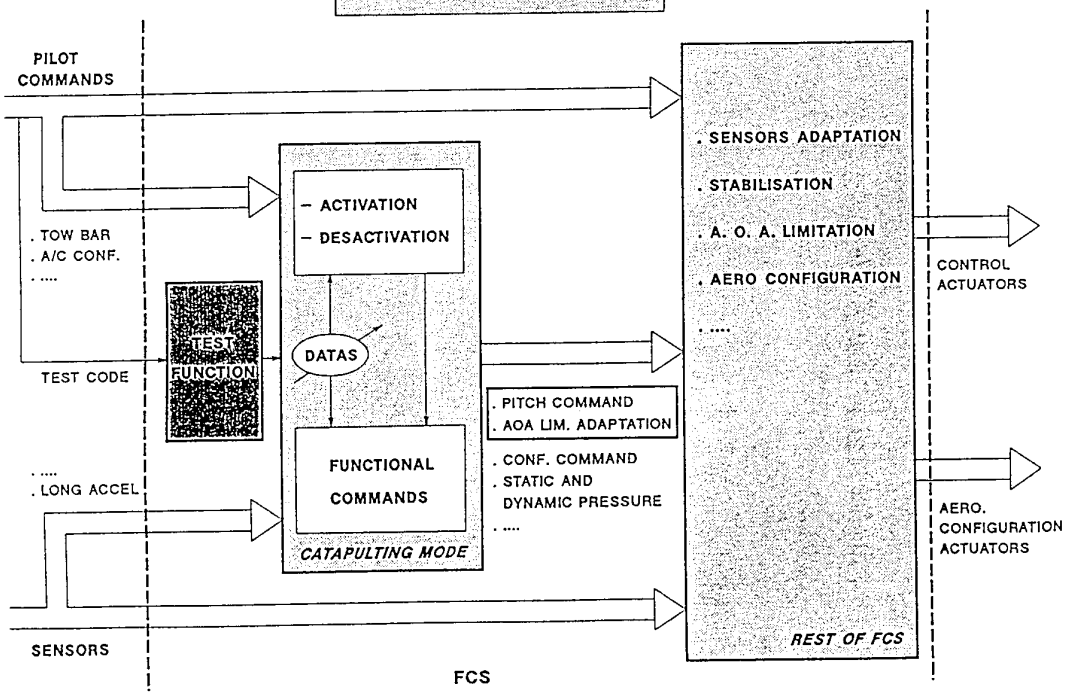

GROUND BASED TEST CAMPAIGNS : NUMBER OF EVENTS

Fig 7

		FLUSH CATAPULT			RAISED CATAPULT		
		NO JUMPSTRUT NO SKIJUMP	JUMPSTRUT	SKIJUMP	NO JUMPSTRUT NO SKIJUMP	JUMPSTRUT	SKIJUMP
1st US CAMPAIGN (JUL–AUG 92)	CLEAN CONF.	22	12	5	–	–	–
2nd US CAMPAIGN (JAN–FEB 93)		5	9	4	4	12	8
FIRST A/C CARRIER FOCH CAMPAIGN : APRIL 1993 (CLEAN CONFIGURATION)							
3rd US CAMPAIGN (NOV–DEC 93)	CLEAN CONF.	–	1	2	1	6	–
	STORE CONF. N° 1	1	8	3	1	3	4
	STORE CONF. N° 2	–	6	8	1	2	4
	OTHER STORE CONF.	1	7	–	–	–	–
SECOND A/C CARRIER FOCH CAMPAIGN : FEB. AND APRIL 1994 (CLEAN CONFIGURATION, STORE CONFIGURATIONS N° 1 AND 2)							

IDENTIFICATION PROCESS

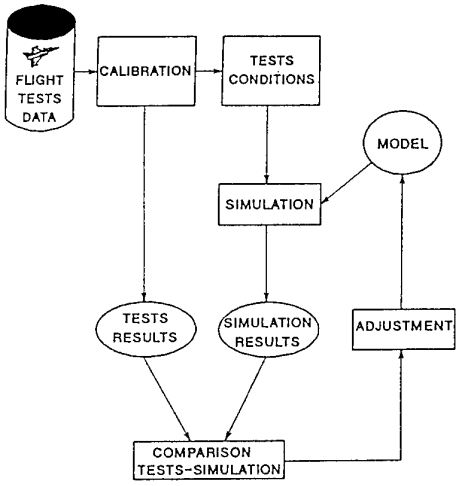

FLUSH CATAPULT + SKI JUMP (STORE CONF. N° 1)

Fig 8

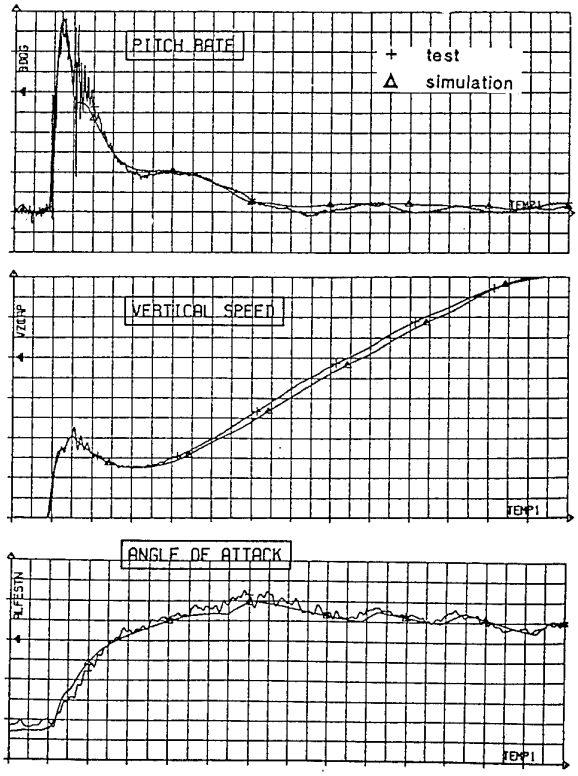

DIGITAL AUTOPILOT DESIGN FOR COMBAT AIRCRAFT IN ALENIA

by

Aldo Tonon
ALENIA Flight Mechanics Group
Corso Marche 41 TURIN
ITALY

Pier Luigi Belluati
ALENIA System Technology Group
Corso Marche 41 TURIN
ITALY

ABSTRACT

ALENIA - Aeronautica has been involved in Digital Autopilot design for the AMX and EF 2000 programmes.
The AMX is a subsonic attack aircraft whose Flight Control System is based on Fly-by-wire technology, incorporating an Hybrid Analog and Digital Flight Control Computer for Control and Stability augmentation in pitch, roll and yaw axes, which guarantees the aircraft capability of full performance; in addition the Flight Control System has also a conventional mechanical back-up in the pitch and roll axes, which guarantees aircraft safe re-entry after failure of both hydraulic and both electrical circuits. The paper deals with the development history of the AMX autopilot through design to flight test. In particular the paper addresses the design to specification relationship, the system development and clearance process and the flight test results.

The EF 2000 programme is an international development for an agile, highly unstable Fly-by-Wire Air Superiority fighter. Within the EF 2000 consortium ALENIA has the responsibility for Basic Autopilot design. This design, currently in the early stages of development, poses peculiar problems due to the interaction of Autopilot (external) feedback loops and the basic stabilization (inner) loops. The paper address these peculiar aspects in conjunction with the specific design methodologies applied.

SYMBOLS

AP	Autopilot
FD	Flight Director
PAH	Pitch Attitude Hold
RAH	Roll Attitude Hold
HH	Heading Hold
ALT	Baro Altitude Acquire
TRK	Track Acquire and Hold
HDG	Heading Acquire and Hold
TH	Attitude Hold
AH	Altitude Hold
BH	Bank Hold
AA	Altitude Acquire
HA	Heading Acquire
AC	Autoclimb
RMS	Root Mean Square
FCC	Flight Control Computer
FCS	Flight Control System

1.0 INTRODUCTION

ALENIA, recently formed by the merge of AERITALIA and SELENIA, has inherited the extensive experience of the AERITALIA - Defense Aircraft Group in the design and development of Combat Aircraft.
In the last twenty years AERITALIA (now ALENIA) has been involved with the development of Autopilot for modern combat aircraft, mainly associated with three major programmes currently in three different stage of development.
For the TORNADO programme, whose development was completed in the mid-eighties, AERITALIA has performed extensive assessment work in support of MBB for the development of the Automatic Terrain Following System.
The AMX program is in the full production phase, but development of some advanced system functions are going. The aircraft was developed with AERMACCHI of ITALY and EMBRAER of Brazil, ALENIA being the prime contractor.
The AMX is a single seat, single engine subsonic aircraft. It was designed to perform close air support to land or naval forces. Therefore the AMX has to operate mainly at low altitude, high subsonic speed and has to carry a large amount of air to ground and air to air weapons. AMX has a high battle damage tolerance due to its configuration.
The Flight Control System is based on a fly-by-wire technology, which incorporates an Hybrid Analog and Digital Flight Control Computer, performs stabilization and control augmentation on pitch, roll

Paper presented at the Flight Mechanics Panel Symposium held in Turin, Italy, from 9-13 May 1994.

and yaw axes. The digital Autopilot integrated in the FCS is provided to reduce the pilot's workload throughout the flight envelope.

EF 2000 is an air superiority fighter. The high instability of the airframe is stabilized by a quad-redundant fly-by-wire full authority FCS.
EF 2000 program recently reached a major milestone having started its flight test activity. Three companies are involved with ALENIA in the EFA development: BAe (Great Britain), CASA (Spain) and DASA (Germany). Concerning the Flight Control System Design ALENIA has the responsibility of the design of the basic autopilot control laws.
EF 2000 autopilot is integrated in the FCS and is designed to alleviate pilot workload and to perform fully automatic procedures during flight, combat and approach phases.

2.0 AMX FLIGHT CONTROL SYSTEM (FCS)

The AMX FCS provides stability augmentation and control in pitch, roll and yaw axes. A general layout is provided in Fig. 1a and Fig. 1b.

Pitch and roll control is provided by a conventional mechanical system with a fly-by-wire electronic augmentation (EFCS) which guarantees full performance capability (Level I Handling Qualities). This allows reversion from powered to manual mode in the case of total loss of hydraulic power, guaranteeing aircraft safe re-entry (Level III Handling Qualities) after failure of both hydraulic and both electrical circuits.

Yaw axis control is provided only by the EFCS with no mechanical back-up.

The primary flight control system is managed by the pilot by means of conventional control stick and rudder pedal.
All controls are powered by two independent hydraulic systems.

The electronic flight control system controls the movements of stabilizers, spoilers and rudder providing pitch, roll and yaw damping and trim capability. They assure adequate responses throughout the flight envelope. Secondary flight controls are flaps and slats while the spoilers are also used as airbrakes and lift dumpers.

Control stick displacements is mechanically transmitted, through conventional rods and cables to four hydraulic actuators that move, respectively, the two aileron surfaces and the elevator surfaces.

With this configuration the Flight Control System is able to operate safely also following a second electrical or hydraulic failure.

2.1 FLIGHT CONTROL COMPUTER (FCC)

The FCC has been designed by ALENIA Avionic Equipment Division and GEC Avionics.
The Flight Control Computer is a dual duplex self-monitoring system to which provides full operation following a first failure.
Each FCC contains one analog lane and two digital lanes.

Analogue Lane : used for the actuators control loops and to compute the primary command functions.

Digital Lane : The digital lanes are arranged to perform different roles. Digital Lane A has a dual role, it generates the digitally implemented control functions and performs a monitor to the analogue command computing, while Lane B computes a complete model of the analogue and digitally implemented functions, and provides an independent monitor function to both Analogue command Lane and Digital command Lane A.

The monitoring is arranged such that each digital lane acts as independent monitor of the analog command computing.
The processors are not synchronized in any way and therefore each processor requires one frame to sample the command computing and make a valid comparison.

The architecture and monitoring have been configured to enable the EFCS to operate safely and minimize failure disconnection transients. This has been achieved with a minimum use of analog components by making full use of digital computing techniques.

2.2 AUTOPILOT FUNCTION

The digital Autopilot function is integrated within the Flight Control Computer (FCC) and provides command signals, via the FCC analogue channels, to the Stabilizer and Spoiler actuators.

2.2.1 Autopilot Modes

The Autopilot modes are divided into the two categories indicated below:

Basic Modes :

- Pitch Attitude Hold (PAH)
- Roll Attitude Hold (RAH) or Heading Hold (HH), depending on the value of the bank angle at the engagement time.

High Level Modes :

- Baro Altitude Hold (ALT)
- Track Acquire and Hold (TRK)
- Heading Acquire and Hold (HDG)

In addition the following functions are available:

Autopilot Override Capability:

This facility provides automatic temporary Autopilot disengagement in both pitch and roll axis by pressing an appropriate switch located on the hand grip. When this switch is released the Autopilot is re-engaged in the Basic modes; in addition in case that the ALT mode was previously engaged the ALT mode is re-engaged if its re-engagement conditions are satisfied.

Autotrim capability on the longitudinal axis:

This function is provided in order to properly trim the aircraft according to the flight condition.

Datum Adjust facility on the longitudinal axis:

This facility is provided in order to update the longitudinal reference parameters. By operating the normal Pitch Trim Switch, it is allowed, with a limited authority, to vary the pitch angle datum reference during the PAH mode operation, or it permits to vary the altitude datum reference during the ALT mode operation.

Instinctive Cut Out (ICO):

This facility provides immediate deselection capability for all the Autopilot and Flight Director functions.

2.2.2 Autopilot Design Criteria

Principal consideration which entered into the design of the Autopilot function were:

- Pilot workload reduction
- Integration with the Flight Director Function
- Autopilot function is not mission critical.

These considerations imply :

- Autopilot disengagement after the first failure of each Flight Control Computer or Avionic Equipment such as Main Computer, Air Data Computer, Inertial Navigation System, Secondary Attitude and Heading System.
- Limited Autopilot demand authority.

2.2.3 System Architecture

A general description of the Autopilot function architecture is shown in Fig. 2, and the Autopilot Pitch and Roll axis block diagram are shown in Fig. 3 and Fig. 4.

Inside the FCC's, both Modes Selection and Control Laws are implemented in the digital lanes.

The Autopilot is integrated with and receives signals from the following sensors: Inertial Navigation system, Secondary Attitude and Heading Reference system, Air Data Computer, from the Heading Situation Indicator, and from the Attitude Direction Indicator, these signals are sent to the Flight Control computer by the Main Computer/Bus Controller via the 1553 Data Bus.

In addition it receives signals to select/deselect either Autopilot or Flight Director functions from the Autopilot/Flight Director Control Panel and the Hand Grip, through an hardwired connection.

Each digital lane of both FCC's is connected to the Autopilot Control Panel and to the Hand Grip switches; each signal is compared between the two lanes, and the consolidated signal is used in order to undertake the relevant actions.

The autopilot demands, both for pitch and roll axis, are cross-fed between the two FCC's; this in order to:

- minimize the mismatch between the actuator demands of the two FCC's.
- monitor the autopilot function performance within each FCC.

All duplicated data, which are available from different sources, are compared prior to being used. In addition the data sources used in the Autopilot function are monitored for validity.

2.2.4 Autopilot Pre-Flight BITE Capability

The Pre-Flight Built-in-Test (BITE) software function, implemented into each FCC, provides on-condition maintenance relative to the whole EFCS, with the failure status being displayed on the Central Maintenance Panel.
Relative to the Autopilot function BITE performs some tests involving :

- Data Bus 1553 Input/Output Data Receive/Transmit
- Input/Output hardwired signal.

2.2.5 AUTOPILOT SOFTWARE DEVELOPMENT

2.2.5.1 Software Requirement Definition

The software requirements are defined by means of:

- Block Diagram relevant to the Control Laws
- Status Diagrams relevant to the Modes Selection Logic

These requirements were implemented first on the Flight Simulator, in order to perform an assessment phase and later an optimization of the Control Laws.

After this assessment phase, they were updated, and with the same form they were sent to the supplier.

2.2.5.2 Software Implementation

Although the Autopilot function is not considered strictly a safety critical function, the flight resident software has been designed by the supplier in accordance with the guide-lines and procedures developed for high integrity fly-by-wire projects.

This because the Autopilot function is integrated with the flight control basic function within the Flight Control computer.

High emphasis has been placed throughout the Software development cycle on visibility, and this is achieved by the use of:

- simple software structures
- clear requirement definition by design audit and detailed documentation
- rigourous production and configuration control

The other aspect to be taken into account was the choice of the software instruction set. The Z8002 microprocessor has a comprehensive ASSEMBLER instruction set and addressing modes, but not all the instruction and the addressing modes are compatible with the guide-lines established, by the supplier (GEC Avionics), for the development the high integrity software, which requires use of a simple instruction set and basic addressing modes. The indirectly addressed instruction, for example, has been prohibited.

2.2.5.3 Software Qualification

The software qualification phase consists of two separate procedures, one performed by the supplier and the other performed by Alenia on the AM-X Flight Control System Rig.

Following completion of these procedures a software Flight Clearance is released.

2.2.5.3.1 Software Supplier Qualification

The Software Integrity Analysis concentrates on identifying potential software defects. This analysis is carried out using a bottom-up approach. The software is subjected to a series of independent design audits on the module design/code. The module design audits consisted of checks on :

- Compatibility of module design specification against software requirements
- Adherence to codes of practice for design and coding
- Overflow protection
- Accuracy and completeness of documentation
- Strict Control of Change incorporation
- Completeness of test

2.2.5.3.2 Software Qualification by ALENIA Rig Test

In addition to the supplier software qualification, Alenia performs system level tests on the Autopilot software on its AM-X Flight Control System Rig.

The Flight Control System Rig is a complete representation of the aircraft in terms of actual aircraft components.

Avionic equipments are not installed into the Flight Control System Rig, but they are simulated by a dedicated host computer; in addition a bus analyzer is provided in order to monitor the data transmission on the 1553 data bus between the Flight Control Computer and the host computer; also a logic analyzer is provided for the microprocessor internal code monitoring in order to verify the correct computation of the received data, and the software module input and output data.

Aim of the Rig Tests is to verify correct implementation of the following:

- Autopilot Control Laws
- Modes Selection Logic
- Failure detection capability
- System behaviour in case of failure
- Confidence Test

Each of these tests involves end to end checks to identify unexpected software behaviour or incorrect software implementation of the requirements.

3.0 Design of Autopilot Control Laws

The design of the AMX autopilot was guided by two conditioning factors:

- The fulfilment of the general design criteria of AMX FCS which established that no safety critical functions shall depend on the FCC.
- The extension of the operational requirements at a mature stage of the design. The autopilot initially included only holding modes conceived to alleviate the pilot workload during navigation. The acquire modes were requested at a later stage.

The above factors resulted in a challenging task for the designers as they had to cope with increased complexity of the control laws against a progressive reduction of the available memory size and throughput capability.

The present activity deals with a tuning of the acquire modes. The basic modes have already been successfully completed and flight tested.

Final design of the autopilot control laws was achieved through several iterations between the following steps:

- Requirement analysis
- Control laws definition
- Stability assessment
- Performance assessment
- Manned simulation
- Flight trials

With each iteration of the process, a configuration that showed good agreement with stability and performances requirements was striven for.

The autopilot control laws design has been carried out according to the traditional design practice. Achievement of appropriate stability margins has been the basic driver in the autopilot control laws synthesis. Extensive use was made of the classical tools, such as Root Locus and Nichols plots.

Once the required stability margins were achieved, the autopilot performances were evaluated through the non-real time and manned simulation. Time response criteria have been expressed in terms of static accuracy for the holding modes and of time-to-acquire and overshoot characteristics for the high level modes. Non compliance with requirements may lead to changes in gains or filters or to the introduction of non linear elements, with the necessity of a new stability checks.

Manned simulation played a significant role for the establishment of the mode logic and the autopilot functions associated with navigation.

During early assessment work, there arose the need for more precise performance assumptions, left initially up to the designer, but to be discussed with pilots to know their point of view.

Later on, during the flight trials, additional tuning of autopilot control laws dealt mainly with aspects such as the aircraft sensitivity to the steering commands.

3.1 Basic Modes

These are the default modes entered at the engagement of the autopilot.

Schematic diagrams of longitudinal and lateral autopilot control laws are shown in Fig. 3 and Fig. 4.

PAH and RAH or HH are the holding modes. They operate to maintain respectively the longitudinal attitude, the lateral attitude and the heading existing at the autopilot engagement. Accuracy and performance requirements are derived from MIL-9490D.

PAH is the pitch attitude hold mode, and is engaged if initial theta is between +/- 30 degrees. The accuracy is of +/- 5 deg. Around the reference. A 5.0 deg attitude error has to be reduced to zero (taking in account the accuracy) in less than 3. seconds with a maximum theta overshoot not to exceed 20% of the disturbance. In presence of turbulence, the error RMS has to be less than 5. deg.
Root locus is used to verify the theta loop stability. An example is presented in Fig. 5 . Proportional-Integral compensation is applied to theta error in order to reduce the residual error in the loop. A lag filter was introduced to attenuate high frequency response. In Fig. 6 we can see a non linear simulation of the aircraft response to a 5.0 deg theta input showing that the disturbance is in fact reduced to the accuracy threshold within the desired time.

RAH mode is the roll attitude hold mode and may be engaged within +/- 60. deg. of bank. Accuracy is of +/- 1. deg around the reference and is required that a 5. deg. bank error has to be reduced to zero (taking in account the accuracy) in less than 3. seconds. In presence of turbulence, the bank error RMS has to be less than 10 deg.
The requirements were satisfied without the necessity of using filters in the bank loop, while the gain value is scheduled with static pressure.

HH mode is selected if at engagement the bank angle is less than +/- 7 degrees. In this case present heading will be held ; requirements are similar to RAH mode. The heading error is converted to a bank error through groundspeed-dependent gain.

3.2 High Level Modes

These are the modes that need a preselection and the presence of a datum to be engaged.

ALT is the barometric altitude hold mode. This mode maintains the altitude existing at the engagement moment.
HDG is the heading acquire and hold mode.
TRK is the track acquire and hold mode. A desired ground track memorised in the main computer is intercepted and followed selecting this mode. Integrated with the navigation system it steers the aircraft into a given course and operates to keep it.

ALT mode accuracy and performances requirements are derived from MIL-9490D requirement.
The altitude error loop is assisted by an altitude rate loop to stabilize the phugoid mode. The altitude rate signal also makes the autopilot response faster against altitude disturbances. The altitude error is converted to a theta error by a gain scheduled with the groundspeed and is processed by the theta loop of the autopilot control laws.

TRK mode performs a manoeuvre to null the distance and the angular error between the desired track and the actual track. The cross error and the heading error produce a bank demand that steers the aircraft on to the desired track.
The mode may acquire only one track (manual/steering and radio/steering modes) or may follow a sequence of tracks that have been memorised in the main computer before the flight or during the mission (auto/steering mode). In manual and radio modes the autopilot, after TRK selection, will engage the HDG mode until an adequate distance from the track is attained, and then track acquire will be performed.
In auto/steering mode, after TRK engagement the nearer track will be selected and the autopilot will turn the aircraft to acquire a heading that intercepts this track at a 45. deg. angle. Then, as with manual/steering and radio/steering modes, the autopilot will start the track acquisition when close to the track.
If at TRK auto/steering mode engagement the angle between heading and track more than 45. deg. the autopilot will drive the aircraft directly to the way point (Fig. 7). The next track will be acquired with the leg change over defined in Fig. 8. The overshoot is due to the limited authority of the autopilot, through which the 3.0 deg/s target turn rate is not always attainable for every condition. This leads to way points which are defined by the minimum turn radius at that phase of mission.

HDG requirements are similar to HH requirements. The heading error is converted to a bank error which is then sent to the bank demand loop. The maximum bank angle is 30. deg. or 45. deg., depending on the dynamic pressure.

3.3 Flight Test Results

Flight test resulted in several modifications to the autopilot control laws. This indicates, to some extent, not always adequate prediction of some aircraft behaviours.

The modifications fall into three basic categories:

- flight conditions in which the build up of the acceleration plays a significant role
- operational aspects
- underestimating some external disturbances.

Examples referring to the above conditions are reported in the following paragraphs.

3.3.1 Acceleration onset at the pilot station

Keeping in mind the MIL requirements, 20. deg/s was chosen as the maximum roll rate for the HDG mode, in order to minimize the acquisition time. Pilots reported that 10. deg/s was a more desiderable value, because the rise in comfort justified the performance reduction. Fig. 9 shows an heading acquisition with the roll rate limit set to the lower value.

During heading acquisition, as heading approaches the target value, the small heading error generates a small bank demand, giving a low turn rate and resulting in a long final phase. For this reason the heading error is forced to a constant value in the initial acquisition phase, faded to the computed error close to the datum. In the first issue of the control law, the reduced time to acquire the desired heading was favoured at the expenses of a quite crisp lateral response. In accordance with the pilots' suggestions a reduced bank/heading ratio sensitivity was introduced.
With this in consideration a study is in progress intended to modify the logic by introducing a bank demand as a function of groundspeed and heading error, giving an open loop signal, that is faded to the heading error by a function of the bank angle and heading rate to reach the datum in the desired time. Fig. 10 shows non linear simulation plots of heading acquisitions, comparing the time response of the two control law versions.

Some more work is necessary to define when, in TRK mode, fast turn in and turn out manoeuvres are desiderable, and when a gentle manoeuvre is better. A slow manoeuvre is necessary when acquisition starts at a low initial cross track error, also if the acquisition time increases.
A compromise between time to acquire and comfort is in study and pilot's experience will be helpful to redefine the requirements.

3.3.2 Operational aspects

In the first release of the autopilot control laws the system was designed to permit engagement of ALT mode only when altitude rate was within +/- 2000 fpm. Beyond this range, the mode was not entered, thus the pilot action produced no effect. Our test pilots found this to be disagreeable, so they asked us to allow the mode selection even with high vertical speeds (up to +/- 10000. fpm) provided an appropriate control of the normal load factor build up and the aircraft motion developed in the expected direction. For this reason the ALT logic was modified introducing a non linear element that reduces the altitude rate input signal at engagement summing a constant opposite signal that is faded to obtain proper g and g-onset levels. Fig. 11 illustrates the ALT flow chart with this modification.

3.3.3 Effect of external disturbances

The radio/steering mode, in which a pilot-selected course to/from a TACAN station is captured and maintained, has led to some problems. The strong noise present in the radio signals used to generate the steering commands was underestimated. The situation is being re-addresssed with a massive filtering technique and lowering the gains close to the course.

4.0 EF 2000 FCS and AUTOPILOT Description

EF 2000 is aerodynamically unstable in pitch and yaw axes. This comes from the necessity to obtain high performances and agile behaviour. A quadruplex full time full authority digital flight control system provides as basic functions stabilization and control. This flight control system has no mechanical back-up. In addition to the basic functions the FCS also provides carefree manoeuvering capability and has integrated autopilot/autothrottle functions.

The aircraft is a twin engined and has a closely coupled delta-canard configuration (Fig. 12). Primary control surfaces are flaperons, canards and rudder; secondary controls are the leading edge slats, air intakes and the airbrake.

ALENIA has the responsibility for the design of the Basic Autopilot Control Laws. The Basic modes are:

- Attitude Hold
- Altitude Acquire
- Heading Acquire
- Autoclimb

Autopilot requirements for stability and performances follows the MIL-F-9490D specifications.

In the current stage of development, the EF 2000 autopilot control law has been extensively verified by linear and non linear simulation, while manned simulation is used to check the moding logic.

Autopilot control laws are divided into two loops: the longitudinal loop, where altitude or theta are controlled sending a pitch rate demand to the FCC and the lateral loop that controls bank angle and heading and outputs a roll rate signal (Fig. 13). Autopilot inputs are introduced into the control law at virtually the same point as pilot inputs. In this way, the carefree functions and the response dynamics of the basic aircraft are maintained. Autopilot signals have an authority limitation before the summing point. The block diagrams of the longitudinal and lateral autopilot control laws are illustrated if Fig. 14 and 15.

4.1 Design of the EF 2000 Autopilot

Experience from the work on the AMX autopilot has been applied to EF 2000 autopilot design, so the lay out of the control laws structure has been made easier, starting with a precise view of the problems that had to be considered.

The addition of new control loops to the basic FCS control laws made it necessary to perform multi-loop analysis (Fig. 16) to verify the stability margins of the outer loop (i.e. altitude loop) and the inner loop (basic FCS).

Autopilot control laws were designed using classical design tools. The control law structure was defined starting with the analysis of the frequency and time response with a linearized model. Nichols and Bode plots were used to verify the stability requirements, while linear model response has been used to assess the system performance in the time domain.

In the second step non-linear simulation was used to evaluate the system response to large manoeuvres and to modify the structure adding non linear elements where needed.

The third step was to verify moding logic through manned simulation. In this phase a large amount of non linear elements were introduced to comply with moding requirements. Simulation model code for batch and manned simulation are essentially the same, so their response is always in good agreement and model updating is easy.

4.2 Hold Modes

The autopilot may be engaged in any of the following sub-modes, depending on the instantaneous aircraft attitude at the moment of engagement :

- Theta Hold (TH)
- Altitude Hold (AH)
- Heading Hold (HH)
- Bank Hold (BH)

If the absolute value of altitude rate is beyond a given threshold, TH mode will be present, otherwise AH mode will enter the aircraft in level flight.

In the same manner, depending on wether or not bank angle is less than +/- 7. degrees, BH mode or HH mode will be engaged.

When engaged, these sub-modes will tend to null error and maintain the datum value according to MIL requirements. Each reference datum may be modified by the pilot applying small corrections with the stick. A large stick deflection will deselect autopilot and return full authority to the pilot.

Altitude hold may also be engaged by pressing the preselection button prior to autopilot engagement or during TH mode. The altitude at the time of engagement will be stored as the altitude datum. In a similar way HH mode may be preselected.

TH mode control laws have a path with a gain and a filter applied to the theta error. Gain is constant, while the filter time constants are scheduled with the altitude to give a smooth response to disturbances.

AH mode needs also altitude rate signal for stabilization. Maximum normal load factor is limited to +/- 0.5 g if altitude rate is within +/- 2000 fpm at the moment of engagement. Outside this threshold, the maximum load factor authority is increased in order to minimize the overshoot of the datum altitude. However, moding and authority details are under study.

BH mode stabilizes the aircraft in a steady turn at the desired bank angle. To compensate for altitude losses during the transient phase, the appropriate command is generated and fed to the pitch axis.

HH mode processes the heading error with a proportional/integral gain (introduced to null heading error in the presence of asymmetric configurations) and creates a bank demand, input to the bank loop.

4.3 Acquire Modes

Acquire modes may be preselected prior to the autopilot engagement. These modes are:

- Altitude Acquire (AA)
- Heading Acquire (HA)
- Autoclimb (AC)

AA mode is engaged when the altitude datum is present and valid, autopilot is engaged and the mode is selected. These inputs may be given in any sequence to activate the mode. The autopilot will initiate acquisition only if altitude rate conforms with the datum to be acquired, otherwise AH mode will be engaged, with AA mode pending an appropriate input to initiate the climb/dive in the proper sense. TH mode will be engaged during the climb (or dive) until the altitude error is small enough to start a blending manoeuvre to reach the datum at a fixed normal load factor. During the TH phase (the initial constant attitude climb/dive phase) the pilot may change the altitude rate modifying the attitude datum with the stick.
The normal load factor during the blending TH-AH phase is scheduled with the initial altitude rate, giving a stronger manoeuvre when the attitude is high, to obtain a reasonably short transition time. Close to the datum AH mode will stabilize the aircraft. Fig. 17 shows an acquisition starting from level flight.

Provision for an autolevel function is under study. This function will cause the aircraft to level off (provided autopilot is engaged) at a certain altitude over the ground. If AH mode is engaged and the altitude rate is negative, the system will alert the pilot when altitude becomes low and will automatically engage AA mode to level off at an adequate pre-defined altitude over the ground.

HA mode may be engaged with the same logic of AA mode. Heading is acquired with a turn where its bank angle is a function of the airspeed. Just before the datum is reached, HH mode is engaged to minimize the transients.

AC mode is designed to perform an economy climb. When preselected, provided that throttle deflection is adequate, the mode will follow a climb profile that will maintain a speed schedule designed to minimize fuel consumption. Attitude control is used to keep the speed at the desired value. If AA mode is also preselected, the autopilot will disengage AC mode and perform the acquire when the altitude approaches the datum.

5.0 CONCLUSIONS

The use of digital techniques applied to the flight control system design, yields the following advantages:

- increase in the computation capability
- greater flexibility and more complex algorithms
- no hardware re-qualification after software updating due to control law modifications
- complete integration between FCS and autopilot functions
- reduction in weight and size of equipment.

In spite of the complexity of the software qualification procedure, the benefits mentioned above justify the choice of digital techniques, as confirmed by our experience on the development of the AMX autopilot. Margins for further improvement in the software implementation process into the FCC have been envisaged in the use of ADA code for Control Laws requirement. A programming technique accounting from the beginning for the specific characteristics of the FCC used is expected to significantly speed up the overall Design/Qualification process.

AMX experience was carried over to the development of the EF 2000 autopilot to a maximum extent, and it is showing very helpful in the prediction of the software complexity and pilots' impression of autopilot response when performances are not extensively defined by the requirements.

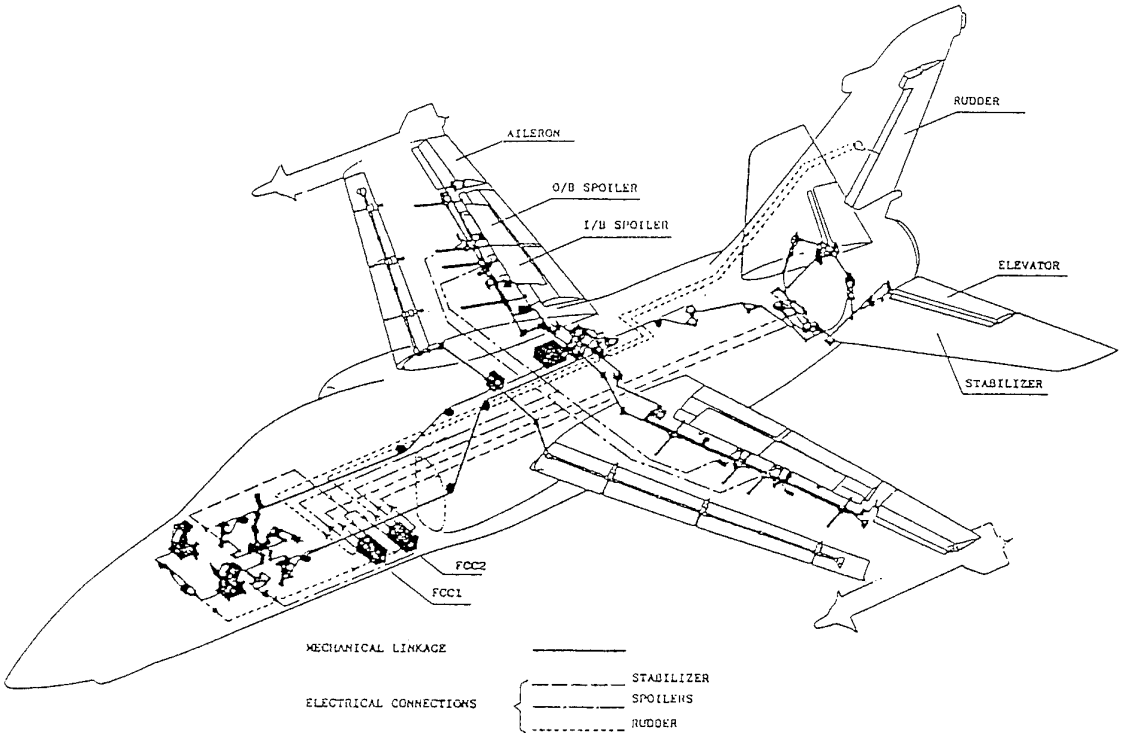

FIG. 1A AMX FCS LAYOUT

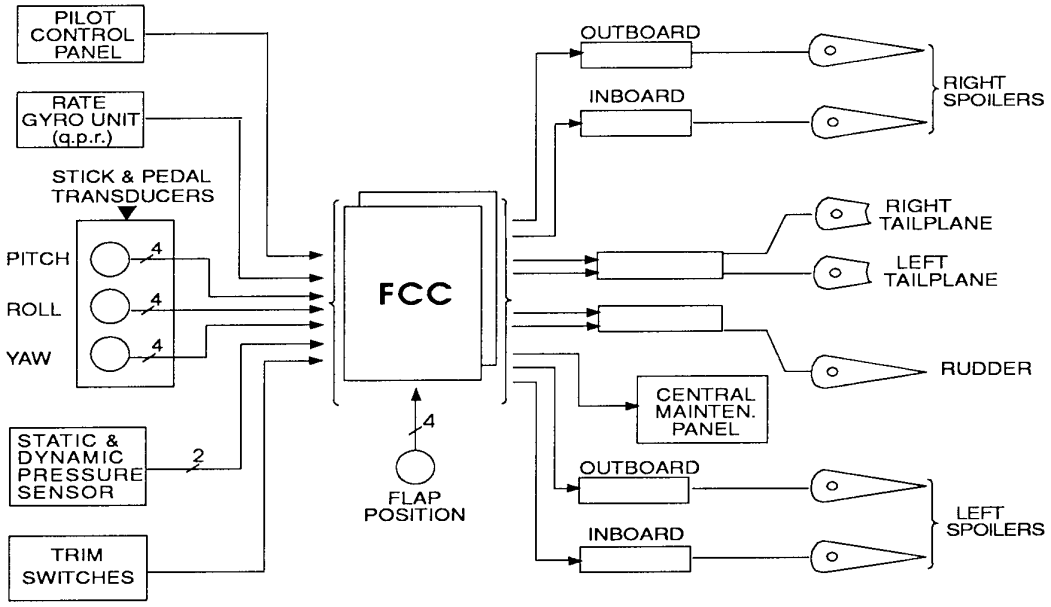

FIG 1B AMX FCS GENERAL SCHEME

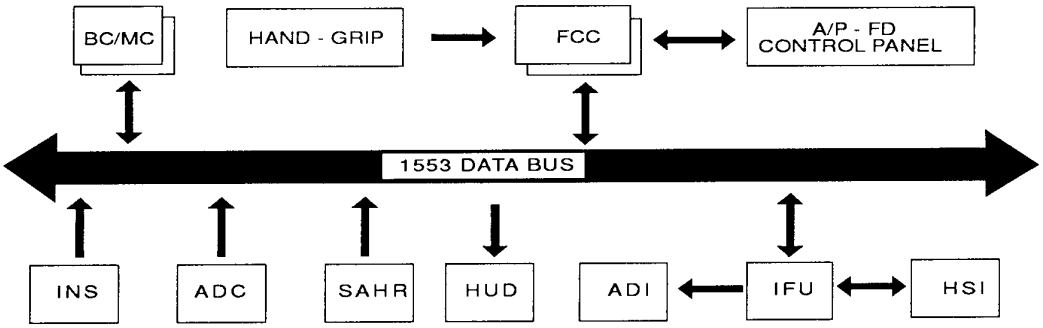

FIG 2 AMX AUTOPILOT FUNCTION ARCHITECTURE

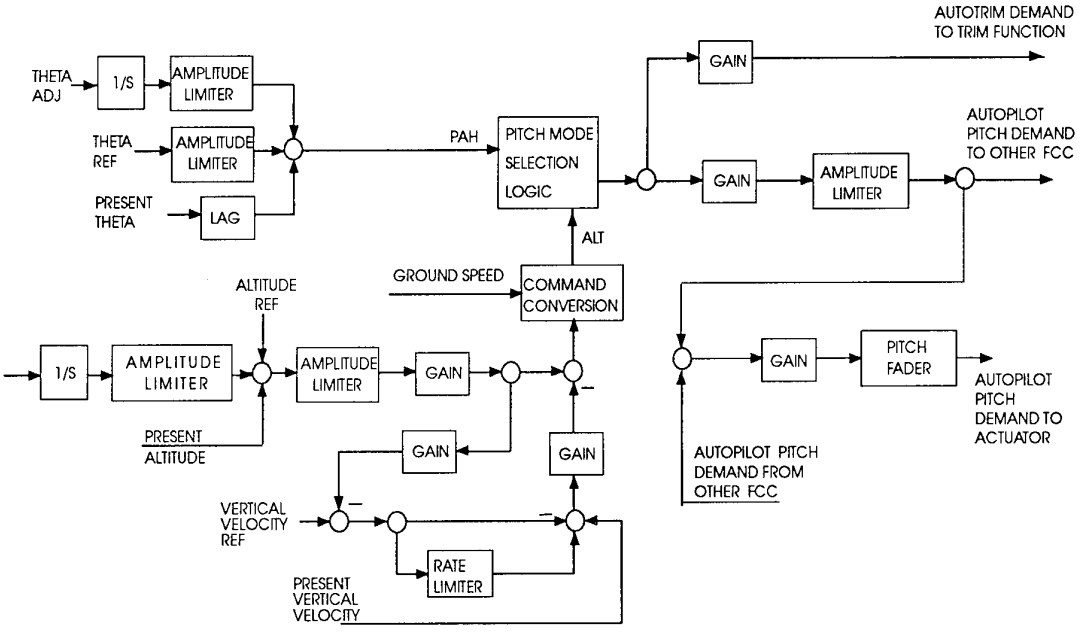

FIG. 3 AMX AUTOPILOT PITCH AXIS BLOCK DIAGRAM

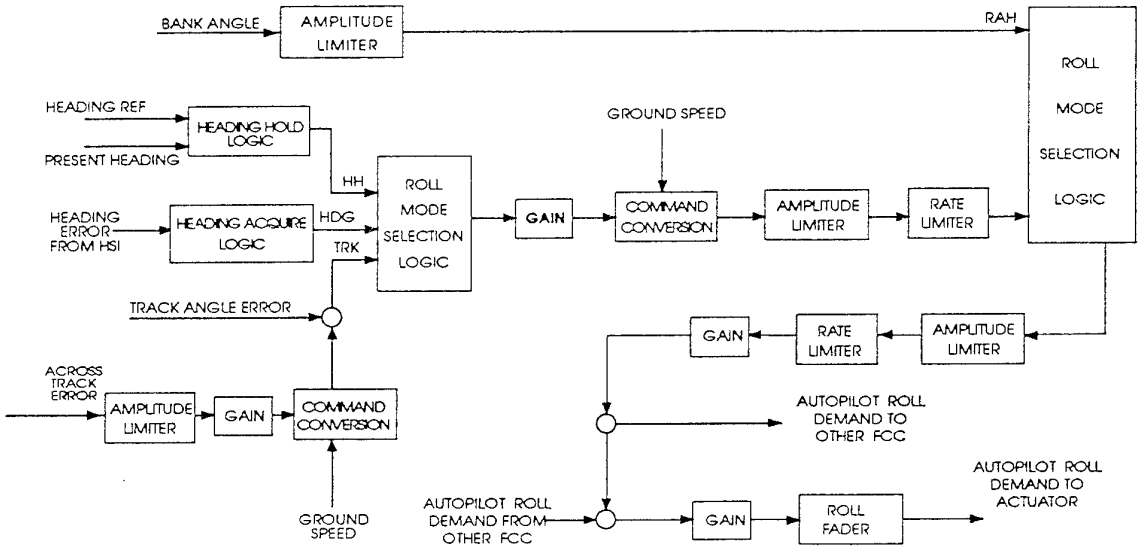

FIG. 4 AMX AUTOPILOT - ROLL AXIS BLOCK DIAGRAM

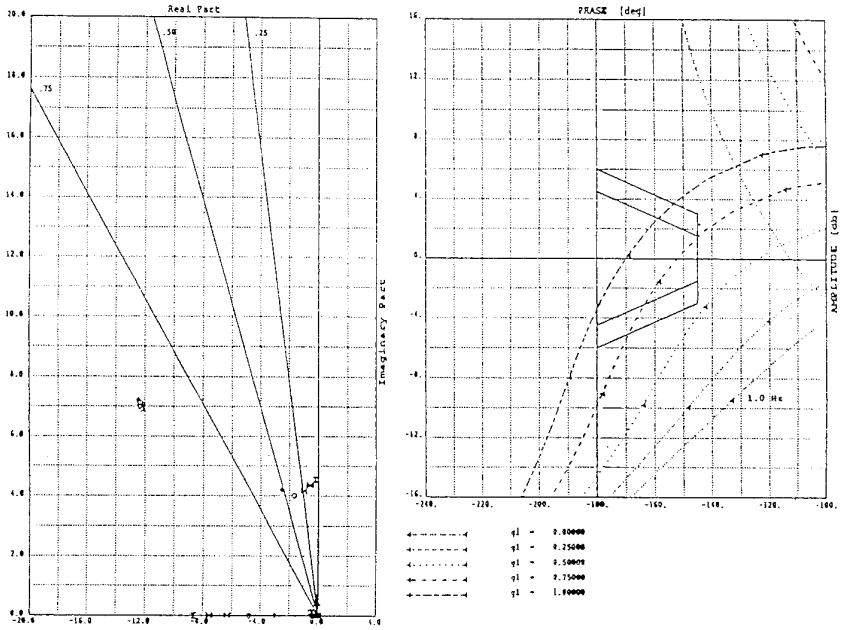

FIG. 5 AMX AUTOPILOT - LINEAR STABILITY ANALYSIS (PAH MODE)

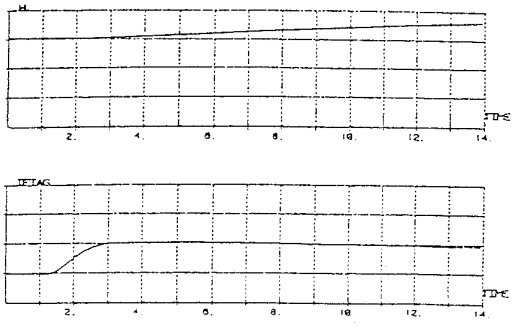

FIG. 6 AMX AUTOPILOT - NON LINEAR SIMULATION (PAH MODE)

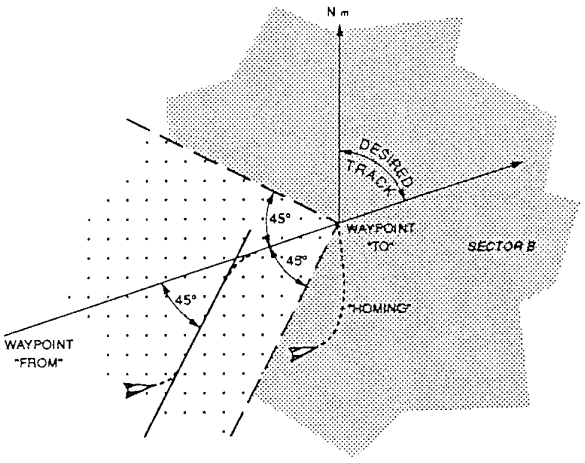

FIG. 7 AMX AUTOPILOT - TRK MODE ENGAGEMENT

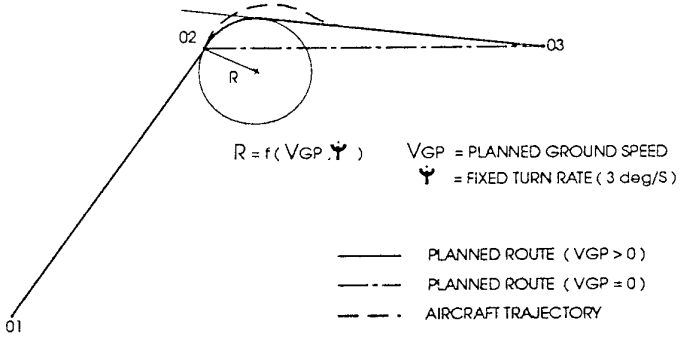

FIG. 8 AMX AUTOPILOT -TRK MODE LEG CHANGE OVER

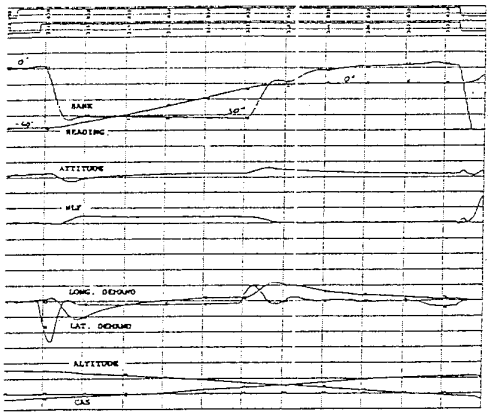

FIG. 9 AMX FLIGHT TRIALS - HDG ACQUISITION

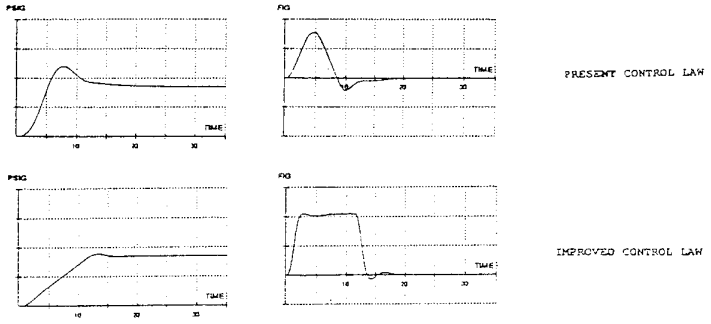

FIG. 10 AMX AUTOPILOT - HDG C/L IMPROVEMENT

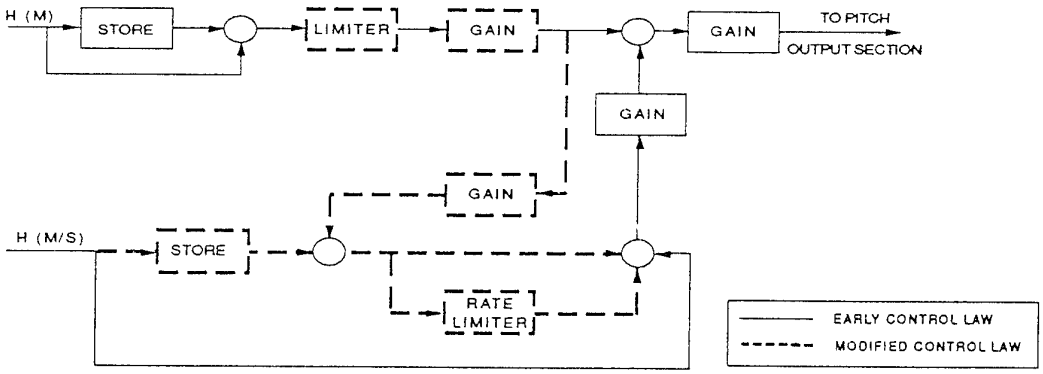

FIG 11 AMX AUTOPILOT - ALT C/L MODIFICATION

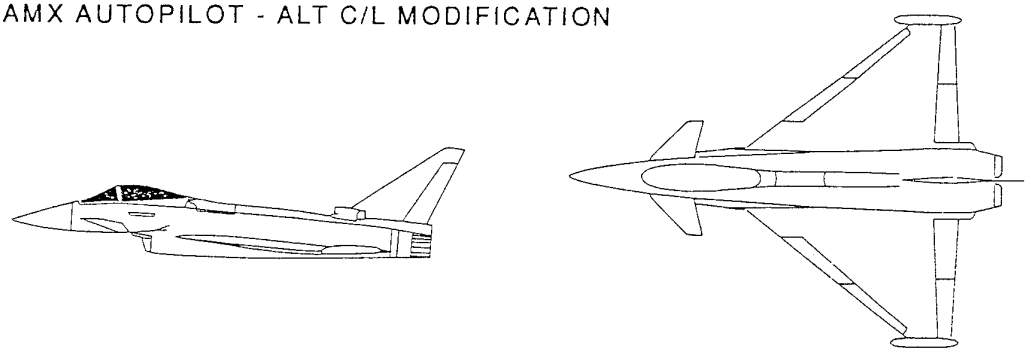

FIG 12 EF 2000

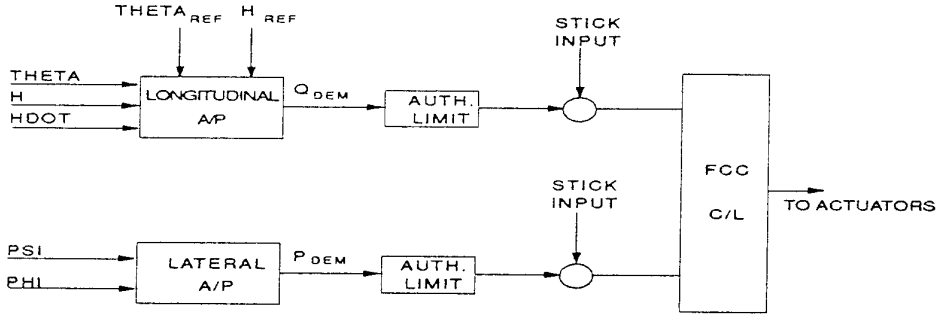

FIG 13 EF 2000 AUTOPILOT C/L INTERFACE WITH FCC

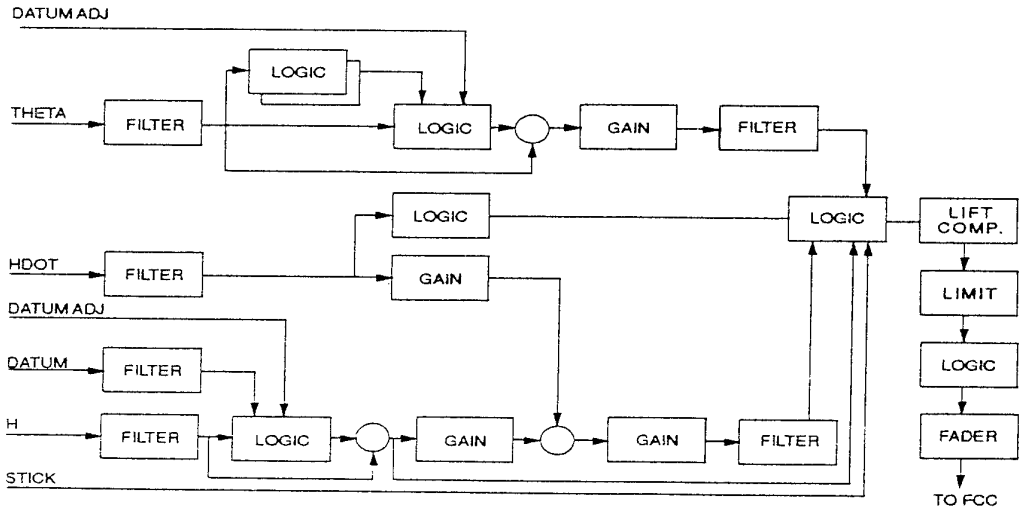

FIG. 14 EF2000 AUTOPILOT LONGITUDINAL C/L

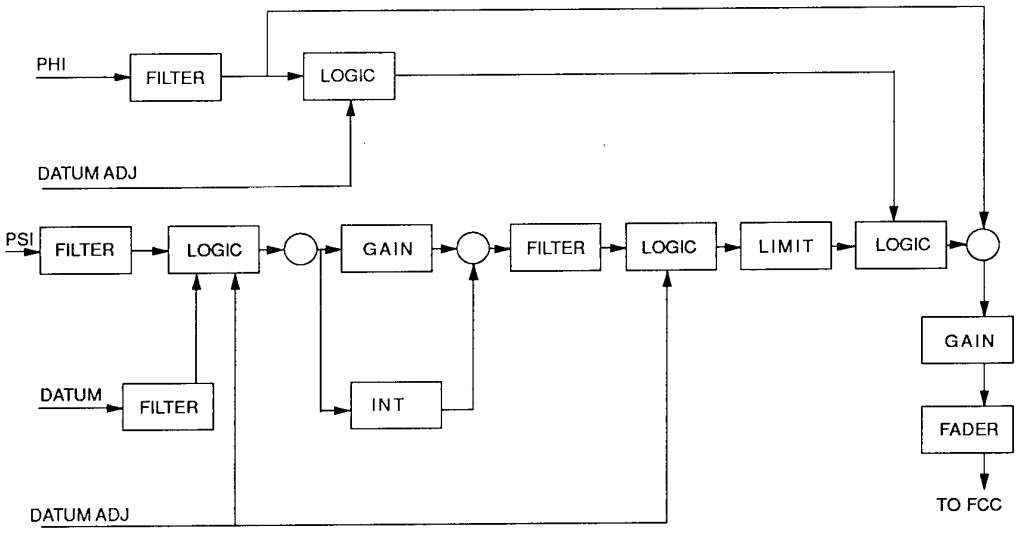

FIG. 15 EF 2000 AUTOPILOT LATERAL C/L

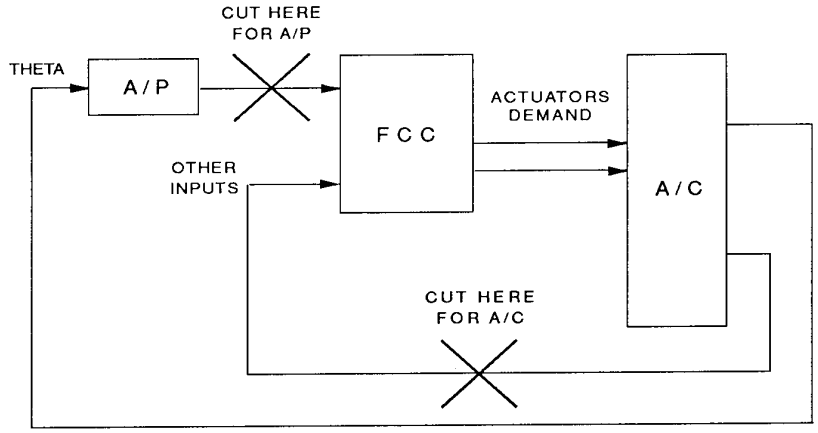

FIG. 16 EF 2000 MULTI LOOP ANALYSIS

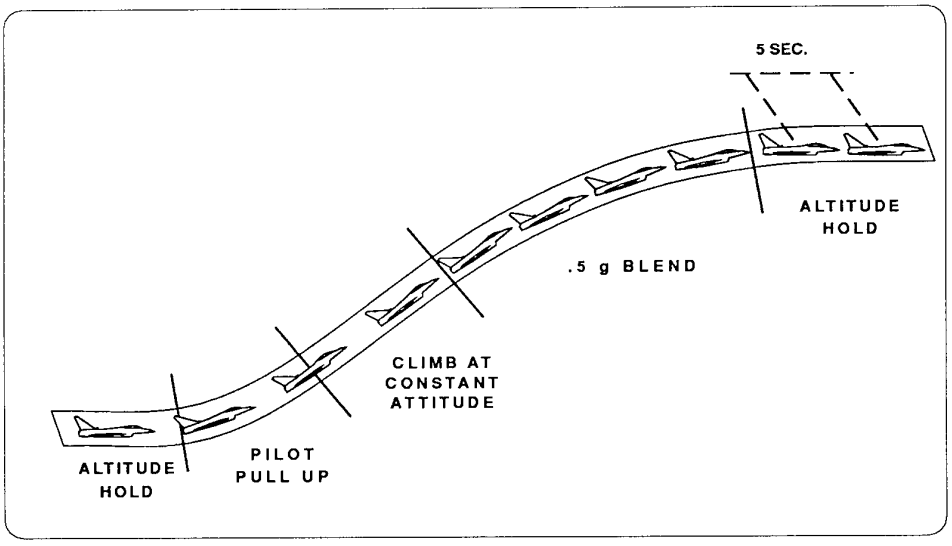

FIG. 17 EF 2000 ALTITUDE AQUIRE AND HOLD MODE

EXPERIMENTAL AIRCRAFT PROGRAMME (EAP) FLIGHT CONTROL SYSTEM DESIGN AND TEST

A.McCuish

Aerodynamics Dept.

BAe Defence Ltd.,

Warton, Lancs. PR4 1AX, UK

1 Summary

The objectives of the Experimental Aircraft Programme were to demonstrate various technologies relevant to a future combat aircraft within the rigours imposed by having to achieve flight clearance and demonstration. Prime areas for demonstration, among others, were modern cockpit displays, avionics systems integration, advanced material construction, advanced aerodynamics and active flight control.

Nearly all future combat aircraft will have an unstable basic airframe due to the advantages that are accrued; smaller, lighter, aerodynamically more efficient etc. Necessary to such an aircraft is a full time active control system. This paper outlines the philosophy and method taken to design the flight control laws and relates their development through the life of the programme. The experience gained from the three phase, 259 flight test programme is summarised. The success of the flight programme has provided a wealth of experience from the operation of the aircraft. In particular, and most impressive to the pilots, was the carefree handling capability; this was considered remarkable. A further success was the complete absence of pilot induced oscillation (PIO) tendency throughout the whole of the flight programme.

2 Introduction

For BAe the flight control system developed under this programme was an evolution of the design used in the Jaguar FBW programme (1977-1984). This FBW programme was aimed at identifying the design methodology and airworthiness criteria necessary for flight certification of a full time digital active control system - with no mechanical back-up. The programme successfully demonstrated, at different stages, a stall departure and spin prevention system and, progressively, the ability to control a highly unstable aircraft; ultimately achieving stability of a basic airframe exhibiting a time to double amplitude of $T_2 = 0.25$ seconds.

The requirements for the EAP were even more demanding than those of Jaguar FBW:-

- - the airframe would be significantly more unstable.
- - it must fly to high angles of attack and load factor.
- - it shall exhibit carefree handling.

Carefree handling was defined as no departure tendency or airframe over-stressing no matter what the pilots inputs are.

To achieve this required an upgrade to the performance of equipments compared to those of the Jaguar FBW and new equipments were manufactured in the areas of;-

- faster computing
- much improved actuator performance
- significantly improved aircraft motion sensor units

Being a flight demonstration programme this equipment had to be manufactured, proven to be up to performance and proven to be flight worthy.

To encompass all the requirements of the flight objectives the control law architecture selected was pitch-rate demand, sometimes known as a rate command attitude hold (RCAH), combined with an alpha demand system. The pitch-rate demand system was a design feature retained from the Jaguar FBW programme where the pilots rated the handling qualities very favourably.

3 The Aeroplane

Being a technology demonstrator, rather than a pre-production or prototype aircraft, existing components were used where this did not compromise the technologies being demonstrated. This included significant airframe sections and equipments resulting in an aircraft that would otherwise be considered overweight thus the absolute performance aspects were somewhat compromised. However extensive use of carbon fibre composites was used to minimise weight eg. wing and foreplanes. Indeed this large component carbon fibre composite constructions was one of the critical technology demonstrations of the programme.

The aircraft, Figure 1, has a layout similar to that of the Eurofighter EF2000 with the aim of achieving the best compromise of supersonic and subsonic performance; delta-canard, twin engine, side-by-side chin intakes, full span trailing edge flaps, leading edge droops and a single fin and rudder.

Paper presented at the Flight Mechanics Panel Symposium held in Turin, Italy, from 9-13 May 1994.

The foreplane and leading edge were scheduled to optimise the lift/drag ratio in the trim state. This scheduling primarily favours trimming on the flaps. Pitch stabilisation utilised all flaps and the foreplanes. The roll control was achieved via anti-symmetric use of the flaps, while the rudder provided directional stability and control; the aircraft being directionally unstable at high Mach numbers and high incidences.

The air-data information system used separate probes for pitot-static pressures and airstream direction data. There were three pitot-static probes located on the nose and tips of each foreplane. The airstream direction data (ADD) consisted of four probes located on the nose section of the fuselage providing a triplex source of incidence and sideslip data.

The control system architecture may be summarised as:-

quadruplex:	computing, angular rates, translational accelerations, pilot inceptors and prime switches.
triplex:	pitot-static and static pressures and air-direction data (incidence and sideslip).

The majority of other functions were duplex.

4 The Pilot Controls

Vital to the handling qualities of any aircraft are the mechanics/ergonomics of the pilot controls. Following on from the good reports and experience with the Jaguar Fly-by-wire centre stick control, the conventional centrally mounted position was retained; as opposed to a side mounted small stick. The EAP stick however utilises movements of around half of a conventional stick. The stick forces were chosen to provide comfortable feel with full deflection loads of approximately 20lb in pitch and 9lb in roll. The stick was sprung to centre and was not encumbered with a q-feel system resulting in a basically low inertia unit. Significant damping was applied sufficient to give a deadbeat response i.e. the stick would not overshoot the centre position if released from full aft. This also ensured a solid feel to the stick characteristics.

The rudder pedal travel was also reduced compared to conventional units and a force of 75lb was required for full deflection. Although there were no complaints about the pedals they were seldom used in flight as the control law performed the necessary co-ordination in dynamic manoeuvres.

The trim system was driven by a rocker button on the stick-top for pitch and roll with a thumb wheel, located on the pilots left-hand panel, for the yaw axis. The trim commands were effected via the flight control computer (FCC) in software. The the rudder and roll surfaces were offset in a conventional manner but the pitch trim introduced a bias to the pitch stick signal. There was no adjustment to the pitch stick position or forces; on a conventional aircraft the stick zero force position would change. Such a system was considered inappropriate here since the control system would automatically trim the aircraft in up-and-away flight. At low airspeeds where some static stability is essential, the stick forces were considered to be low enough as not to be uncomfortable even if they had to be held for a considerable length of time. The omission of this stick force/position adjustment mechanism avoided the complex engineering that would have been required to fit this within what was a very compact stick assembly unit.

The cockpit displays layout included three multi-function displays (MFDs) and a wide angle head-up-display. As well as the usual flashing "attention getters", a voice warning system was developed.

5 Control Laws Design Philosophy and Method

The design philosophy was aimed at ensuring visibility throughout the design and specification of the control law. The linear behaviour of the control laws were derived using classical methods; root locus, nichols plots, linear time and frequency response. This was evolved into a fully engineered controller via a vast amount of non-linear simulation which ensured that integration of the linear control law and the non-linear constraints (e.g. actuator position and rate limits, hydraulic supply limits, design manoeuvring limits, moding between different laws etc.) was appropriate.

Figures 2 and 3 show simplified schematics of the pitch and lateral control law structures. In the pitch axis, figure 2, the basic concept of the control law was "pre-determined" to be a proportional plus integral with pitch rate damper. From experience two first order lead-lag filters in the feedback loops are all that is necessary to give the appropriate stability characteristics. Thus the basic controller is of low order and readily understood. To maintain the visibility, however, an overall structure was imposed which isolated functions and non-linear characteristics e.g. trim distribution, control power normalisation, non-linear variation of stability. Without this structure the variation of the aerodynamics would appear directly in the schedules of the gains masking the function of the gain.

Having isolated these aerodynamic variations across the full envelope, the basic P,I+ q damper mimic the variation of speed and dynamic pressure etc. explicitly i.e. they reflect the basic flight mechanics parameters.

The stability feedbacks being thus defined the next task was to design the handling of the aircraft. This was achieved by using a direct (or forward feed) path summed in down stream of the integrator and utilising command shaping on the pilot demand as shown in figure 4. The use of the direct path has the effect of separating the command response dynamics from the stability feedback dynamics. Thus the feedback dynamics can be designed solely on the stability and gust response requirements and needs no consideration of the aircraft handling requirements. The design freedom this introduces is essential to endow the aircraft with stability and appropriate handling.

In the lateral-directional axes the challenge was to achieve a consistency of behaviour with aerodynamics which varied considerably in all axes and to allow for the variability in the augmented pitch axis. The basic architecture was conventional roll-rate demand with yaw rate damping. Roll co-ordination to rudder was included with the inertial coupling control being via the foreplanes. Here again classical techniques have been used, relying predominantly on root locus and nichols for the linear design. Experience has shown that the non-linear design of the roll co-ordination is dominated by the aerodynamic tolerances that must be considered. (This is not due to the tolerances being large, in fact they are significantly smaller than those considered in previous projects).

The next major design area is the non-linear response where the objective was to provide agile carefree handling (i.e. the ability to rapidly manoeuvre the aircraft without the pilot having to restrict his inputs to respect a loading or incidence limit)

This task required the extensive use of the real time flight simulator to assess the near infinite number of inputs that are possible - though much of the design may be achieved with the non-real time simulation.

The challenge was to retain as much agility as practicable; carefree handling can be "readily" achieved if rates and accelerations are constrained but the aircraft performance is then compromised.

At the lower airspeeds, where a combat aircraft must perform, the limiting factor to agility tends to be the position and rate limiting of the surfaces. The high surface rates required on a basically unstable vehicle requires that hydraulic supply and demand aspects must be considered. On EAP the number of actuators and their high rate would, if used continuously, soon exceed the hydraulic supply.

The integration of the pitch and lateral authorities gave priority to the pitch demand i.e. at full back stick/maximum alpha if roll stick was applied the alpha demand was unchanged and the roll rate was limited to suit. The alternative would have been to reduce the incidence demand by some amount in favour of increased roll rates.

A necessary complexity in the design was to take into account the non-linearities in the aerodynamics particularly pitch breaks in the stability data where these coincide with the stressing limit of the aircraft.

It is also necessary to consider control law design items which, to some extent, do not exits in the design of a classical aircraft as the behaviour is inherent. For example in rapid decelerations from high speed on a classical aircraft the pilot would gradually pull the stick aft to maintain the 'g'. With this controller the full aft stick demands the maximum allowable 'g' but it requires the integrator to achieve the demand. This would result in a significant loss of 'g' in the manoeuvre had there not been a mechanism to assist the integrator in pitching the aircraft up during the rapid slow down. The alternative of increasing the integrator gain is not a solution as this is limited due to linear stability requirements.

The resulting design was specified with individual elements for gains, filters, switches, rate limits, position limits etc. Each of these elements was specified in executable code (Fortran in this case). This coded definition was used throughout the design development and became the formal specification of the control law. It was essential that the specification was executable for the purposes of defining the control law to the implementation specialists, since this defined a unique functional interpretation of the specification. It was also extremely important during development as the design could be exercised in real time non-linear simulation and measured against the requirements.

An essential component of the design was to include the best linear and non-linear models for all the hardware in the control system; actuators, motion sensor units, ADD dynamics, FCC delays, pilot inceptors. It is also necessary to include an allowance for filters required to avoid structural coupling. This allowance was given as a 'budget' of phase delay at low frequencies (rigid body modes) to the structural dynamic engineers within which the total of their filtering must remain.

6 Control Law Development Phases and Associated Flight Testing

Over the life of the EAP programme there were three main control law development phases. The first phase, utilising rate feedbacks only, allowed flight over the majority of the subsonic envelope which verified the majority of the aerodynamics and the calibration of the ADD (incidence and sideslip) gauges. The second phase introduced the alpha and beta feedback signals and the concept of carefree handling. The final phase expanded the carefree handling envelope and was designed around a control law architecture proposed for the Eurofighter EF2000.

6.1 Phase 1 First Flight Standard.

6.1.1 The Reversionary Control Law.

This control law was designed for an aircraft ballasted to constrain the instability to a time to double amplitude of 0.25 seconds. This was the instability ultimately demonstrated on the Jaguar FBW programme. Starting at this instability level with unproven aerodynamics could be done with confidence as the hardware performance on this aircraft was improved over that of the Jaguar FBW and the control law design was similar. The control system was scheduled with air-data (dynamic, static pressure and Mach number) but utilised only the high integrity angular rate information from the motion sensor units; no incidence or side slip data was available. This restricted the incidence to within the more linear region below C_{Lmax} , constrained the ability to co-ordinate rapid rolling and generally limited the performance of the pitch and lateral axes. No carefree handling was available at this control law standard.

A subset of this scheduled controller was also available within the control law which would cater for the remote

possibility of failure of the air-data system. This simply set the air-data parameters in the scheduling if the air-data system was determined to be invalid. In fact two sets of values were used, distinguished by undercarriage selection (up or down). This allowed the largest speed envelope to be cleared without the system becoming over-geared due to the aerodynamic gain effects.

The pitch control law was pitch rate demand using proportional rate damping and a filtered pitch rate integral demand. This rate-command, attitude-hold (RCAH) system results in automatic trimming of the aeroplane for since with the stick at neutral zero pitch rate is demanded. At low speed where it is necessary to give the pilot a tactile sense of the reducing velocity, perceived static stability was introduced by biasing the stick neutral command with the reducing airspeed. This then required the pilot to progressively apply aft stick in the slow down at these flight conditions.

As indicated previously the separation of the feedback design and the pilot command path design was achieved by utilising a feed forward path and command shaping. This allowed a high level of PIO resistance to be designed in to the control laws. The forward feed path allows sufficient pitch acceleration to be generated while the overall command shaping can with only two or three first order filters achieve the correct pitch rate and alpha dynamics while ensuring that the transfer function of pitch attitude to stick displacement is suppressed at the PIO frequency.

The criteria used in this design were standard handling qualities supplemented with the developments gleaned from the Jaguar FBW experience and published literature (Reference 1).

The lateral-directional control law for this phase was roll rate demand plus yaw rate damping. The aim was to perform wind axis rolling. There is no integrator to ensure the roll rate demanded is achieved and the resultant roll rate is a balance of the gains and aerodynamics. For handling purposes the lateral stick to roll rate demand is designed to be near constant around the centre stick position for any flight condition. The demand is increased using a power law to give the appropriate full authority rate at full stick deflection.

The directional control was a scheduled gain of pedal-to-rudder angle. The schedule, a function of airspeed, was such that the demanded sideslip was constrained to permitted levels. Wind axis yaw rate was derived from body axis yaw rate and roll rate and then fed back to the rudder via washout to give the optimum dutch roll damping characteristics.

Within the non-linear design a network was constructed which applied a small transient input to the rudder when the lateral stick was centred. The purpose of this was to remove any residual sideslip on the roll exit. This, combined with the excellent co-ordination provided by the control law, proved very effective in practice, stopping the aircraft roll quickly and cleanly.

6.1.2 Flight Testing

There were 52 flights with this standard of control law which verified the basic pitch rate demand system, aerodynamics and the ADD calibrations. The flight envelope flown covered up to 500 Knots CAS and Mach 1.3. Mach 1.1 was achieved on the first flight. The aircraft was incidence limited to a pilot observed value of 18 degrees. This giving a safe margin from $C_{L,max}$ where the use of pitch-rate demand is no longer feasible due to stall characteristics. The extreme non-linearities of the aerodynamics at these conditions requires a knowledge of alpha to schedule the control system gains.

The early flying was aimed primarily at aerobatic manoeuvres as a work up to the 1986 SBAC airshow at Farnborough. The pilots were impressed by the handling qualities of the aircraft in this phase. The aspect of most concern was in performing loops where, due to the speed variation through the manoeuvre, the incidence required careful monitoring so as not to exceed the limit. The other aspect subject to criticism was a slight over-sensitivity in the roll axis for small amplitude inputs.

Typical pilot comment for this phase of flying were:-

- very natural and easy to fly
- solid and very stable, but still responsive to control
- take off, approach, landing and formation flying was accurate and easy
- steady attitude in turbulence and still easy to fly
- no roll ratcheting or pilot induced oscillation tendency.

6.2 The Second Phase Incidence Limiting and Carefree Flying

6.2.1 The Alpha Limiting Control Law "Paris Laws"

Having proved the basic performance of the FCS, the aerodynamics and the ADD system in the first phase, some the ballast was removed resulting in a time to double amplitude of $T_2 = 0.18$ seconds for the basic airframe. The incidence signal was now used for limiting in the pitch axis and extensive scheduling in the lateral-directional axes. The pitch axis still used a core based on pitch rate demand and this was blended across into the alpha demand system as the demand reached its limit. The limiting incidence was scheduled with flight condition to respect the stress limits of the airframe, thus an Nzw control system was in fact the result; at high mass the normal load was low and at low mass it was high. This maximises the use of the strength available in the airframe.

The roll demand and pilot rudder authorities were reduced as a function of incidence and flight condition in order to respect

the stressing limits and prevent pilot induced departures at high incidences.

The carefree handling of the aircraft is arrived at through the careful integration of the pitch and lateral-directional control laws. This design was only possible with a good deal of effort in pilot-in-the loop simulation as well as off-line simulation in order that the maximum capability and suitable harmony between axes was made available.

As part of the simulation exercises the pilots were requested to try and "beat the system" and cause the aircraft to depart. There were no restrictions to the pilot inputs even if these did not correspond to a "sensible" piloting / combat manoeuvre. The pilots proved very adept at finding the deficiencies in the development control laws and could do so much more quickly than engineers using the off-line facilities.

6.2.2 Phase 2 Flight Testing

EAP was demonstrated with these control laws at the Paris airshow of 1987. This was achieved after a very short flight test programme which proved the effectiveness of the controller at preventing departure. The high incidence high altitude testing, where the aircraft was fitted with an anti-spin gantry, was completed in three weeks with 20 sorties flown. This was followed by a period of testing where the altitude was progressively reduced to prove the carefree handling and the manoeuvre capability. There were no departures and the similarity to the modelling was verified with no changes being required to the control laws or aerodynamic model.

The flight envelope covered here was restricted to 400Knots Mach 0.9. Some 64 flights were flown in this phase with carefree manoeuvres tested throughout this envelope. Incidences of 34 were achieved and speeds down to 100 knots. There were no signs of departure although below 200 knots the pitch handling was rated as ragged and cyclic pitch stick inputs resulted in overshoot of the angle of attack limit. The handling qualities seen in phase 1 flying were repeated here primarily due to the same type of pitch rate demand controller being retained at 1 g flight conditions.

The pilot comments from this phase were very positive:

- exceptional roll acceleration and damping
- excellent handling and control in slow downs to high angles of attack
- flies extremely well
- handling in loops and rolls extremely pleasant
- impressive control of angle of attack, sideslip and roll rate in carefree manoeuvres

The carefree handling was considered remarkable with the pilot able to apply full roll stick and then full aft stick with the roll stick still applied. This feature was seen as particularly useful in combat or low level situations where the pilot need to be looking out of the cockpit.

The aircraft also exhibited good tracking behaviour against ground targets and also in air-to-air tasks although the air combat experience was limited to a few flights. The aircraft also behaved well in turbulent conditions the only criticism being that flight path was unsteady which required attention when flying at low levels. This is a natural response of the pitch rate demand system. A flight path hold or altitude hold auto-pilot function would solve this problem. There was, however, no auto-pilot on EAP as these functions were considered outside the control law demonstration objectives.

In an extension programme to these control laws the rate demand components were developed to allow flight across the full supersonic flight envelope. There was no extension to the carefree capabilities as the purpose was to gather aerodynamic data. During this flight test programme, where there was greater time spent in cruise or cruise climb getting to and from the supersonic test range, a slight lateral/directional miss-trim was detected in the aircraft. There was also a distinct trim change in the transonic range which required re-trimming by the pilot. This detracted from otherwise excellent handling qualities and although considered to be a slight nuisance it was raised at nearly every flight debriefing. In response to this behaviour it was decided to introduce a wings-level hold mode in the next flight phase.

6.3 Phase 3 The "Full System"- AoA/Nz Limiting

A third and final phase was introduced to the EAP programme in order to supply some risk reduction to the EF2000 project. To this end the control laws were to be designed around a structure destined for the EF2000. This in fact was a development of the EAP structure involving the introduction of Nz and attitude feedback signals. This control law aimed to provide Nz and AoA limiting across the complete envelope.

The Nz signal was used at high speed flight conditions where the accuracy of the AoA probes become critical. Low wing loading aircraft such as EAP can easily generate load factors of greater than 1 g per degree of incidence. Thus the accuracy becomes significant at such flight conditions when flying to the stressing limits. In the phase 2 flying which used incidence limiting the aircraft had been flying to higher g than intended. This resulted from the incidence correction term for fuselage bending due to normal g being under estimated. The aircraft achieved the measured incidence but this was less than the true value.

A significant development introduced at this time was the use of inertially derived incidence and sideslip. The inertial incidence was derived from the body rates and accelerations available within the FCC and was mixed with the probe generated signal. The motivation for this was to reduce the sensitivity to probe disturbances when flying at incidence in the low speed envelope. The sensitivity results from the high levels of incidence feedback required for stabilisation. By utilising inertially derived signals the high frequency disturbances (eg. turbulence) are eliminated. An inertial

sideslip signal was used at high speed and here again the motivation was to reduce the effect of disturbances seen on the probes. In this case deriving from shock wave effects seen in the transonic and supersonic envelope.

In the pitch command path an amplitude dependent filter was introduced in order to incorporate particular response characteristics in the air-to-air tracking task. For small amplitude inputs, as required for air-to-air gun tracking, pilots prefer a zero attitude drop-back response. For larger inputs, used during the target acquire phase, then a more aggressive flight path response is required which in turn results in attitude drop-back.

As mentioned earlier a wings-level hold mode was introduced to relieve the pilot of the nuisance re-trimming task as a result of small aircraft asymmetries. This was a "quick-fix" mode with very limited authority but it was included as an inherent component of the control laws; i.e. there was no pilot selection or de-selection, this was fully automatic by the system. This was not an true auto-pilot system, there was no track control or even directional co-ordination. The mode would simply hold the wings at zero roll angle when in cruise conditions. i.e. bank angle within 3 of level and minimal roll rate. The moding was designed such that operation was completely transparent to the pilot.

6.3.1 Phase 3 Flight Testing

The flight testing proved the blending of Nz limiting to alpha limiting was transparent to the pilot. The only time this became noticeable was when flying at the manoeuvring limit in an extremely light mass state the change from Nz limiting to Nzw (AoA) limiting was accompanied by an increase of around 1g. This could be remedied by supplying the Nz control law with the mass state of the aircraft. This will be required for a service aircraft as otherwise performance will be seriously effected at masses below the stressing mass.

Following criticisms of the pitch gross manoeuvring when the aircraft was inverted, attitude scheduling was introduced to the command path in order to boost the manoeuvre. This extra complication results from the architecture of using pitch rate demand as the core, blending to a Nz (or AoA) limiting system. In the inverted state the required change in incidence is larger by 2'g' compared to the upright case. For zero pitch rate, inverted or upright, the stick trim position is neutral hence the pitch stick travel to manoeuvre to the Nz limit will be the same (zero to full aft) in both cases. In the previous flight testing this extra manoeuvring was taken up by the integrator which is a slow acting device.

The assessment of the non-linear amplitude dependent pitch tracking filter was carried out during two flights dedicated to air to air combat manoeuvring with a target aircraft (a Hawk). This provided some interesting results and showed the basic tracking to be very good but spoiled by two faults. The more adverse of these was a result of the non-linear roll damping network described in section 6.1.1. This imparted a kick to the rudder on centring of the lateral stick. This in turn caused the tracking sight to swing off the target in the yaw axis just as the pilot had settled the pipper on the target. This highlights the risks of including highly non-linear effects in a control law; it may work in the case it was designed for but it must produce satisfactory results in all cases. In this particular instance the effect may remedied by introducing an amplitude dependence, possibly similar to the non-linear tracking filter as in the pitch axis. The second effect was the occasional appearance of a 2-3Hz bobble on the pitch tracking. This was surprising as the attitude to stick response is lowly geared at these frequencies and certainly free from PIO tendency. The problem has been identified as neuro-muscular inputs being detected by the stick transducer and suggests that greater attitude attenuation is required for this type of task. The basic pitch gun tracking was rated as Cooper-Harper 2 with the lateral tracking as seen was rated C-H 6 but was estimated to be C-H 2 if the non-linear effect could be removed since it was very easy to bring the pipper onto the target.

This flying also highlighted the need for a C_{Lmax} indicator on this aircraft as it was too easy for the pilot to pull max alpha to bring a solution on the target aircraft. Against a more equal target aircraft the loss of performance incurred for exceeding C_{Lmax} (i.e. a significant increase in drag) would be critical. There are no external clues for the pilot with there being very little buffet or canopy noise to indicate that the aircraft is close to or above C_{Lmax}.

A criticism voiced at this phase of flying was that the normal g onset rate was too low. Throughout the programme this is had been designed to a limit of 8 g/sec and had not been criticised previously. The lack of criticism was probably due to the fact the aircraft was strength limited to 6 g and thus maximum g was achieved within 1.5 second. At low airspeeds the maximum capability was available, this being constrained by actuator rate and position limiting characteristics. Increasing the g onset rate at the higher speeds could be achieved simply by increasing the direct feed gain from the pilot stick to surfaces.

For this standard of control law the roll acceleration performance was increased to a level which the pilots desired based on the previous flying and flight simulation assessments. This lead to a design with a consistently very crisp roll entry and exit across the medium to high speed flight envelope. Initial experience of these characteristics elicited very favourable comments but after a few sorties the acceleration was thought to be slightly too high. In some instances the pilot's head tended to strike the canopy due to the lateral acceleration being generated at this point. From the flight results it is believed that a limit of 0,7 g laterally, at the pilot's head position, would be a sensible limit for roll acceleration. This aspect may require further consideration for a two seat aircraft where the second crew member may not be prepared or braced for the manoeuvre. Also the second crew member, in a tandem cockpit configuration, will be subjected to higher lateral accelerations being positioned higher above the roll axis than the front seat.

The improvement to the pilot workload brought about through the introduction of the wings-leveller was claimed to transform the aircraft. The mode proved completely transparent to the pilot. As a result of the removal of this

nuisance factor from the roll axis, deficiencies in the yaw and pitch axis became more apparent.

The pitch axis, although self-trimming as a result of pitch rate demand, did allow changes in the flight path to occur as a result of Mach accelerations or decelerations particularly across the transonic range. Similarly there is a tendency for the flight path to change as a result of turbulence. This was seen in medium to high turbulence and most notably at low level where flight path is more important. The aircraft does not pitch very much but the g spikes were noticeable. A trade-off can be made here between aircraft attitude and flight path disturbance by adjusting the control law feed backs ie. introducing incidence feedbacks.

The deficiencies in the yaw axes were slight and resulted from the roll damping "rudder kick" and the wings-level hold mode. On rolling out on to a heading the "rudder kick" seen on centring the roll stick had the tendency to backoff the selected heading by around 1 degree. The wings-level mode, which was a "quick-fix" solution to roll miss-trim, was not co-ordinated with the yaw axis. As a result, if the yaw trim was not adjusted by the pilot and the pilot waited long enough, it was possible to detect that the aircraft was performing a flat turn. Neither of these characteristics interfered with the pilot's tasks and were very minor deficiencies.

The pitch trimming characteristics were significantly aggravated by implementation of the pitch trim button mechanisation. As described previously this added a bias into the stick demand requiring the pilot to hold the stick position to maintain trimmed 1g flight. This was designed for the low speed approach conditions and it was not intended for use outside this envelope, however, pilots will 'by instinct' use the trim button if they perceive that the aircraft is out of trim. This perception occurs when achievement of steady state 1g conditions is not acquired quickly enough. The pilots having used the button at these high speeds then found it difficult to reset the trim back to zero; there being no indicator for zero trim. (A function was available to reset the trim to zero but this also reset roll and yaw). A simple solution to this characteristic is to mechanise the trim button input as a transient or as an input to the integrator, thereby the pilot could assist the aircraft to achieve the steady condition in what would appear a natural use of trim control. Unfortunately there was no opportunity to implement this.

The carefree manoeuvring offered by this system was again considered impressive. Examples of the type of input and responses is given Figures 5,6,7. Figure 8 shows approximately two minutes of carefree handling where the pilot uses snatch pulls to the aft stop with and without rolling inputs, roll reversals, four point rolls etc. Also clear in this trace is the effect of loading and unloading the pitch stick while maintaining full roll command; the roll rate is seen to decrease and increase rapidly. The increase in roll rate was at times thought to be too rapid as it was not always possible to select the roll out attitude, however, more conventional use of the controls may be more appropriate for such handling manoeuvres.

Pilot comments from this latter phase of flying:

- carefree handling immensely impressive - copes effortlessly with brutal demands.
- impressive roll acceleration and damping.
- take-off behaviour is excellent.
- air-to-air tracking generally very good.
- wings-level mode is an excellent feature and totally transparent.

7 Conclusions

Overall the programme has been highly successful and has proven the approach taken to design the control laws. The programme also demonstrated the basic control law structure intended for use in EFA verifying the capability of achieving excellent handling qualities and gaining invaluable flight experience of a similar aircraft.

The highlights for the FCS design were the demonstration of an agile carefree handling capability and the level of PIO exhibited by the aircraft. Indeed no PIO tendency was noted in any of the 259 flights by any of the 12 pilots who flew the aircraft. These results supports the philosophy of retaining significant stick travels and the force and damping characteristics designed here. Valuable information on control sensitivity has been gathered particularly in the roll axis where limits to acceptable roll accelerations have been determined.

The success of the transparent automatic wing-level hold mode in transforming the basic long-term trimming / steady state nature of the aircraft is a strong motivator to include such functions in the yaw and pitch axes. The reported reduction in pilot workload suggests that, in the absence of auto-pilot functions, the long-term trim behaviour is a significant contributor to workload.

A major highlight is that throughout the whole programme there have been no great surprises due largely to the quality of the modelling of the aircraft and the control system. The quality of the aerodynamic model is an affirmation of the methods and wind tunnel analysis used, there being remarkably little adjustment to the model as a result of flight testing. There were also very few modifications to the basic control laws resulting in almost uninterrupted flight testing in each phase.

8 References

1) Gibson, J.C.,
" Evaluation of alternate handling qualities criterion in highly augmented unstable aircraft"
Proceedings of the AIAA Atmospheric Flight Conference (90-2844),
Portland, Oregon, USA, pp. 435-444

2) McCuish, A.,
"Development and flight experience of the control laws in the Experimental Aircraft Programme"
International Journal of Control, Vol. 59 No. 1,
January 1994, pp 183-198

Key features of EAP Flight Control System

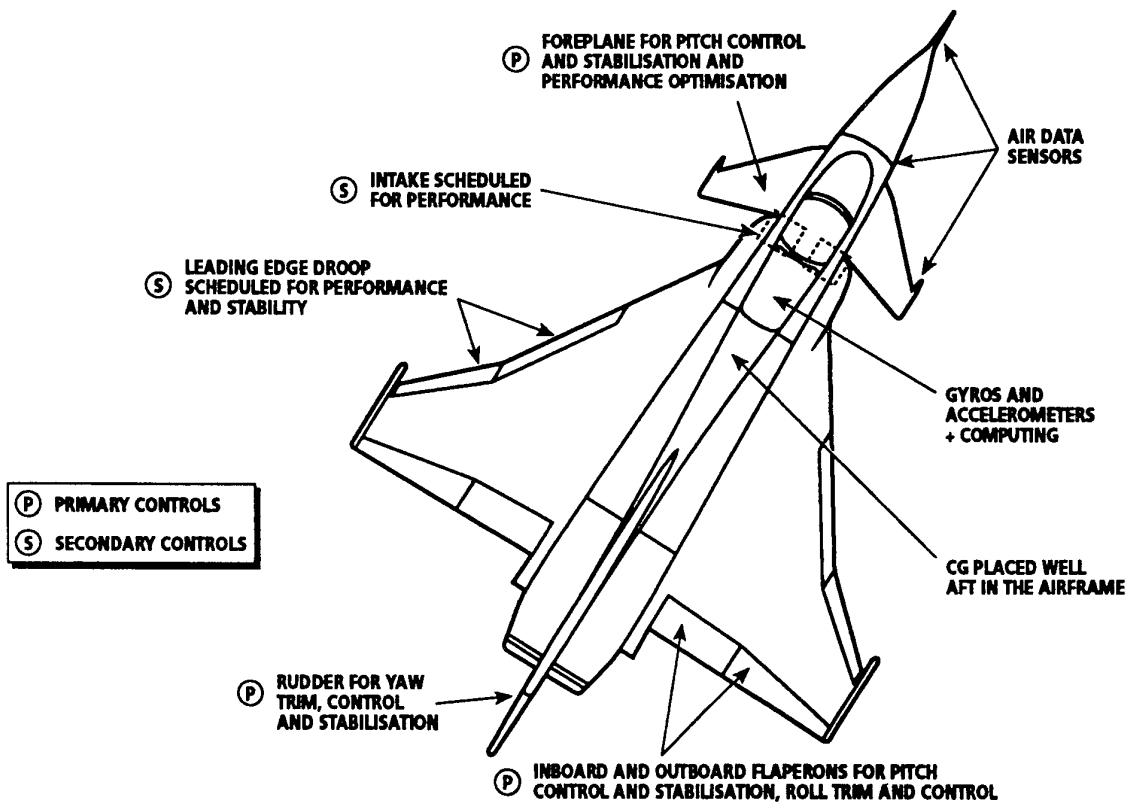

FIGURE 1

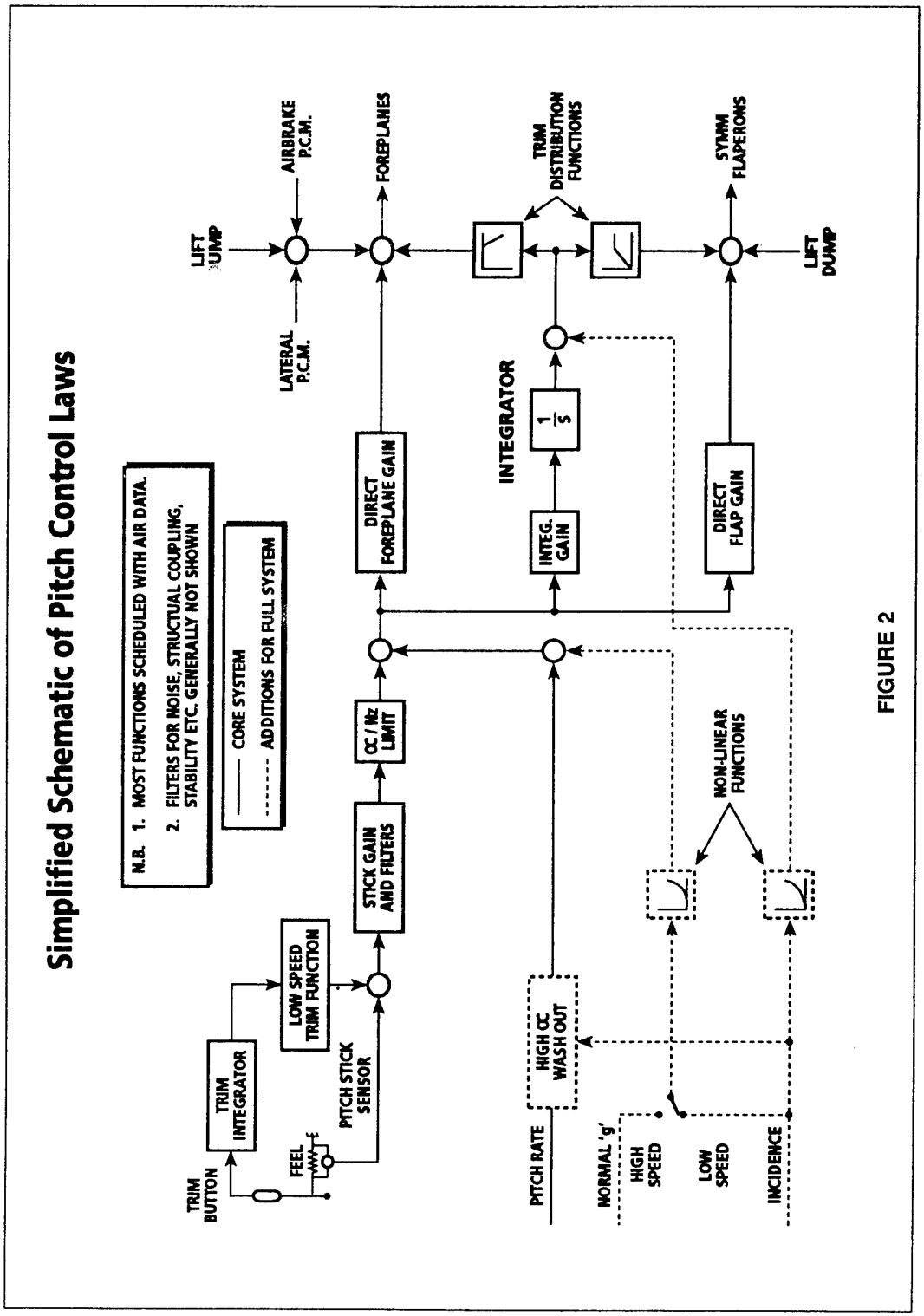
Simplified Schematic of Pitch Control Laws
N.B. 1. MOST FUNCTIONS SCHEDULED WITH AIR DATA.
2. FILTERS FOR NOISE, STRUCTUAL COUPLING, STABILITY ETC. GENERALLY NOT SHOWN
CORE SYSTEM
ADDITIONS FOR FULL SYSTEM
TRIM BUTTON
TRIM INTEGRATOR
FEEL
LOW SPEED TRIM FUNCTION
PITCH STICK SENSOR
STICK GAIN AND FILTERS
α̇C / Nz LIMIT
DIRECT FOREPLANE GAIN
LIFT DUMP
AIRBRAKE P.C.M.
LATERAL P.C.M.
FOREPLANES
INTEGRATOR
1/S
INTEG. GAIN
TRIM DISTRIBUTION FUNCTIONS
DIRECT FLAP GAIN
SYMM FLAPERONS
LIFT DUMP
HIGH α̇C WASH OUT
PITCH RATE
NORMAL 'g'
HIGH SPEED
LOW SPEED
INCIDENCE
NON-LINEAR FUNCTIONS

FIGURE 2

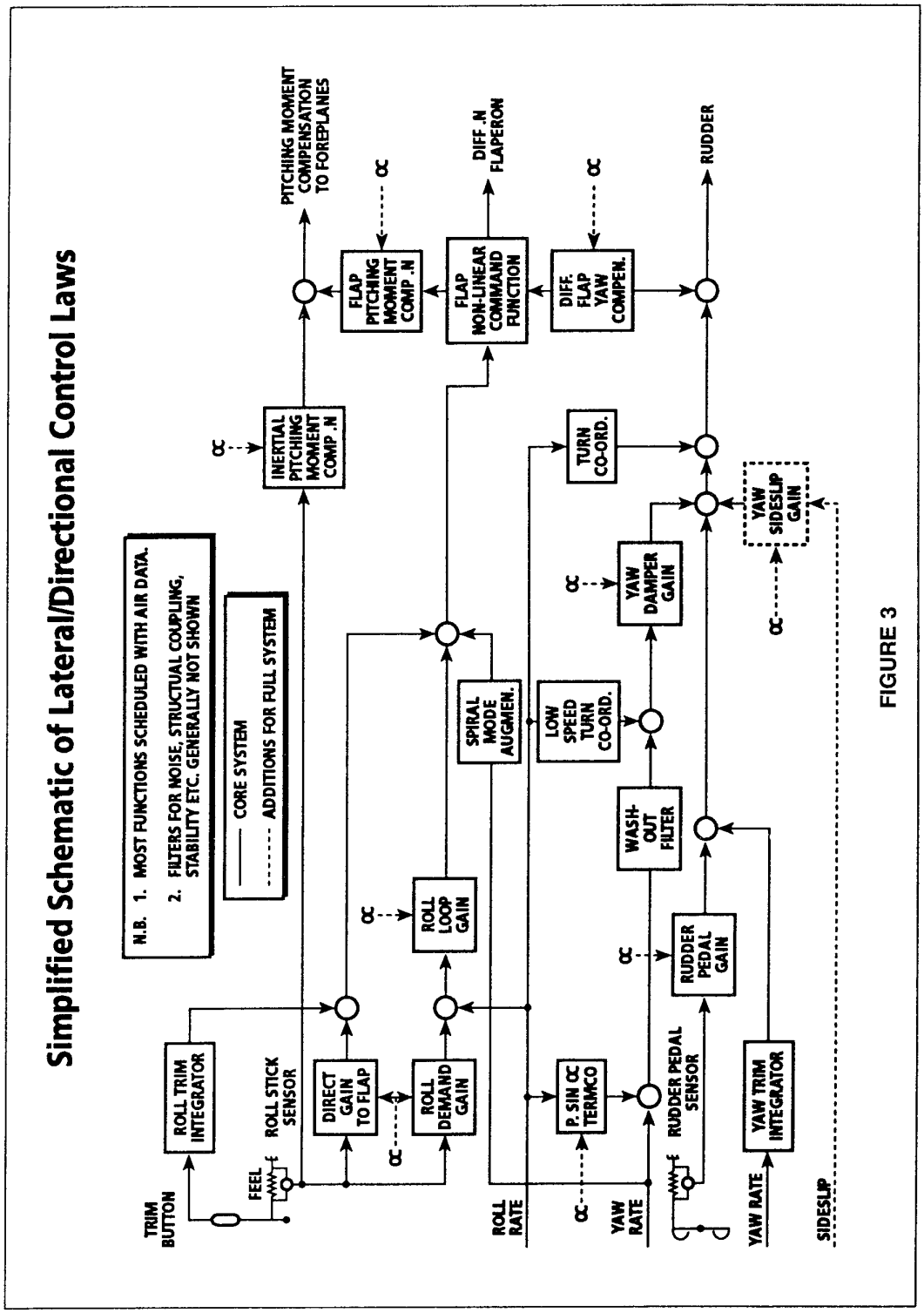
Simplified Schematic of Lateral/Directional Control Laws
N.B. 1. MOST FUNCTIONS SCHEDULED WITH AIR DATA.
2. FILTERS FOR NOISE, STRUCTUAL COUPLING, STABILITY ETC. GENERALLY NOT SHOWN
CORE SYSTEM
ADDITIONS FOR FULL SYSTEM
TRIM BUTTON
ROLL TRIM INTEGRATOR
FEEL
ROLL STICK SENSOR
DIRECT GAIN TO FLAP
ROLL DEMAND GAIN
ROLL LOOP GAIN
ROLL RATE
SPIRAL MODE AUGMEN.
INERTIAL PITCHING MOMENT COMP .N
PITCHING MOMENT COMPENSATION TO FOREPLANES
FLAP PITCHING MOMENT COMP .N
FLAP NON-LINEAR COMMAND FUNCTION
DIFF .N FLAPERON
P. SIN α TERMCO
YAW RATE
LOW SPEED TURN CO-ORD.
WASH-OUT FILTER
RUDDER PEDAL GAIN
RUDDER PEDAL SENSOR
TURN CO-ORD.
DIFF. FLAP YAW COMPEN.
YAW DAMPER GAIN
YAW TRIM INTEGRATOR
YAW RATE
YAW SIDESLIP GAIN
SIDESLIP
RUDDER
α

FIGURE 3

Generic Rate Command/Attitude Hold (RCAH)

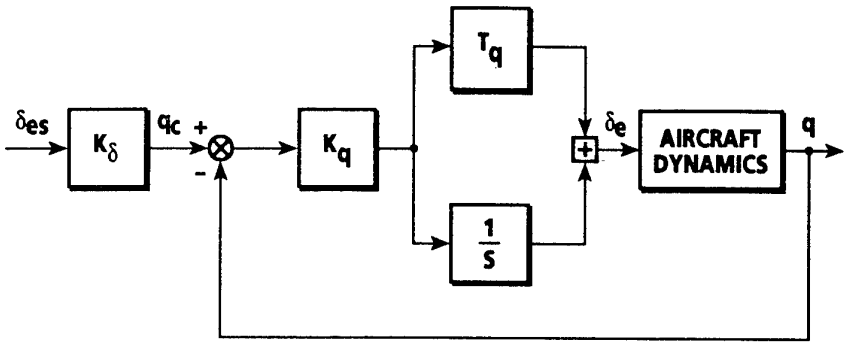

REGULATION AND CONTROL THROUGH COMMON DYNAMICS CAN LEAD TO POOR HANDLING DUE TO SYSTEM STABILITY CONSTRAINTS

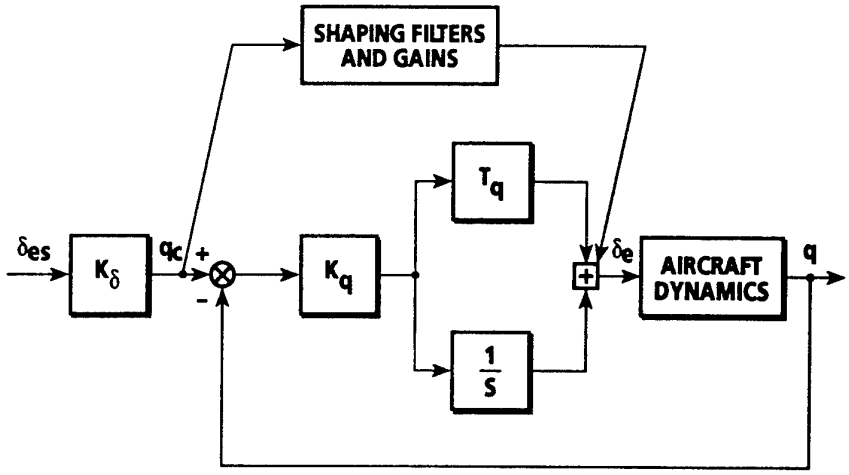

FEEDFORWARD SHAPING OPTIMISES CONTROL WITHOUT ALTERING OR DEPENDENCE ON REGULATION DYNAMICS

FIGURE 4

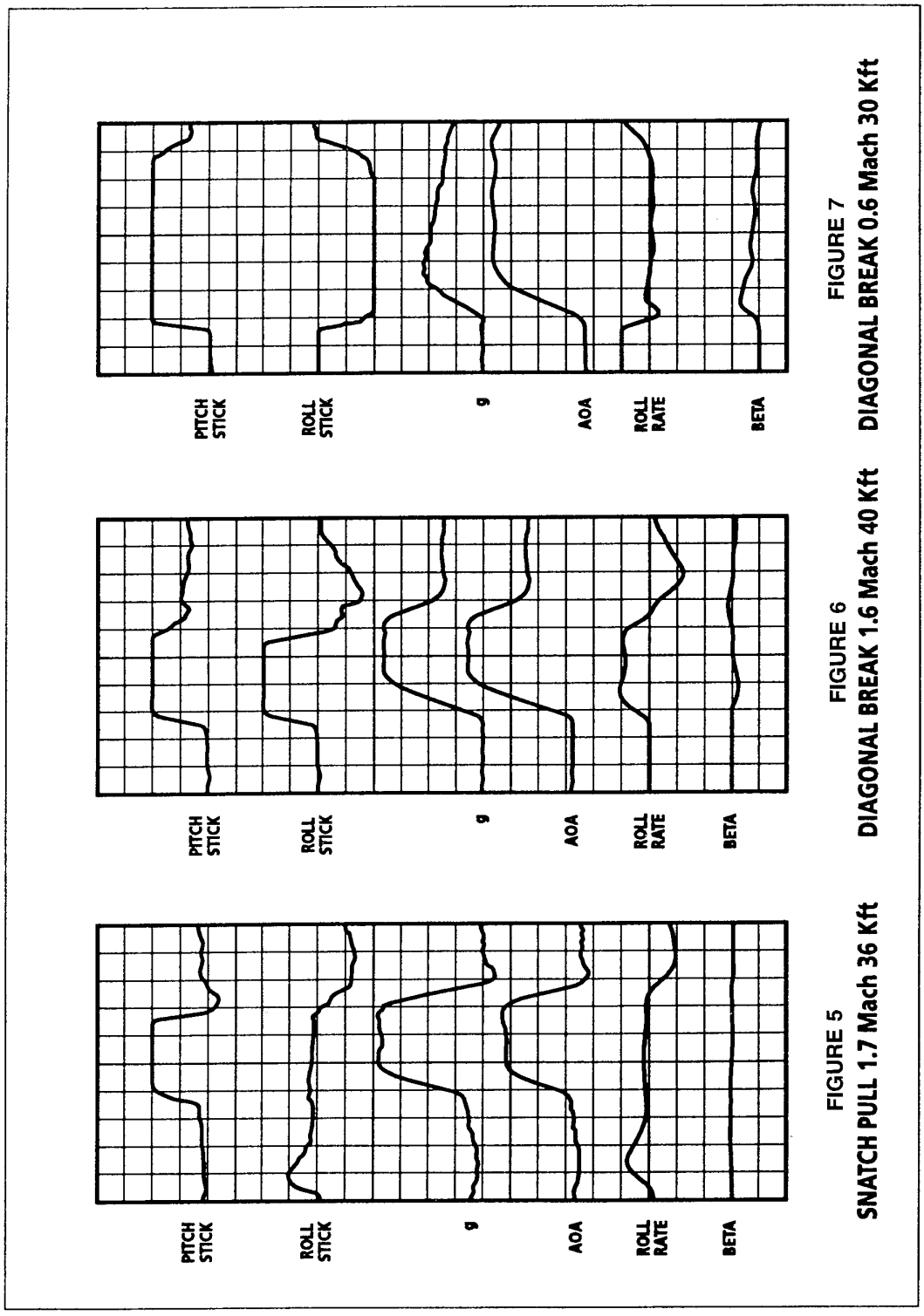

FIGURE 5
SNATCH PULL 1.7 Mach 36 Kft

FIGURE 6
DIAGONAL BREAK 1.6 Mach 40 Kft

FIGURE 7
DIAGONAL BREAK 0.6 Mach 30 Kft

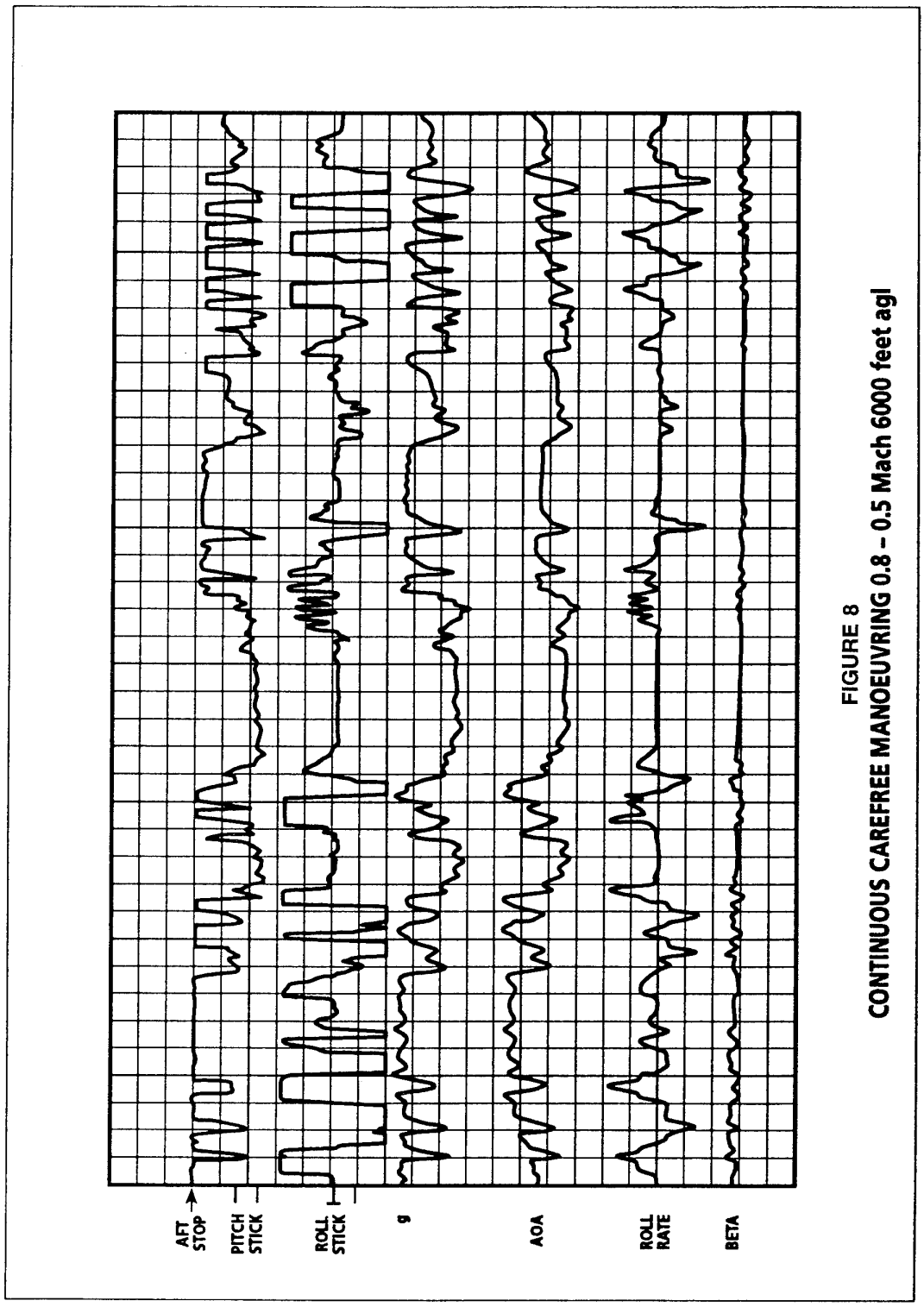

FIGURE 8
CONTINUOUS CAREFREE MANOEUVRING 0.8 – 0.5 Mach 6000 feet agl

AN INVESTIGATION OF PILOT INDUCED OSCILLATION PHENOMENA IN DIGITAL FLIGHT CONTROL SYSTEMS

William A. Flynn, Major, CAF
Robert E. Lee
United States Air Force Flight Test Center
Edwards Air Force Base, California 93524-6150
U.S.A.

SUMMARY

This paper summarizes the results of a technical review of pilot induced oscillations (PIO) in aircraft equipped with digital flight control systems. A review of the causes of PIO, the specific interaction of digital flight control systems, and an evaluation of the flight control development process was conducted. The paper discusses the highlights of the technical review and the recommendations for future development of flight control systems to reduce the occurrences of handling qualities problems in general and PIO in particular.

LIST OF ABBREVIATIONS

PIO	Pilot Induced Oscillation
USAF	United States Air Force
AFB	Air Force Base
AFMC	Air Force Material Command
S/MTD	STOL/ Maneuvering Technology Demonstrator
VISTA	Variable In-flight Simulator Test Aircraft
HQDT	Handling Qualities During Tracking
AFAM	Air Force Acquisition Manual

INTRODUCTION

Following an accident of a United States Air Force (USAF) prototype fighter at Edwards Air Force Base (AFB) in May 1992, a technical review team was formed to investigate pilot induced oscillations in aircraft equipped with digital flight control systems. Senior officers of the Air Force Material Command (AFMC) were concerned that a mature development process for flight control system development was not preventing PIO. The charter was to focus on PIO, examine the current development process and determine why PIO problems continued to occur. Finally, the investigation was to identify the "Best Practices" used in the various programs that contributed to successful flight control system development. The multi-agency, multi-disciplinary team consisted of personnel from management, engineering (from research laboratories, program offices and flight test) and the test pilot community.

The team reviewed all major USAF aircraft programs with digital flight controls, specifically the F-15E, F-16C/D, F-22, F-111, C-17, and B-2. The team interviewed contractor, acquisition program management and flight test team personnel on these programs. In addition, United States Navy personnel were consulted concerning the development of the F/A-18 program. Experimental USAF and National Aeronautics and Space Administration systems with digital flight control systems were investigated including the X-29, X-31, F-15 STOL/Maneuver Technology Demonstrator (S/MTD), and the Variable In-flight Simulator Test Aircraft (VISTA) F-16. Finally, the team discussed the subject with other experts in the field, including personnel from the Calspan Corporation. The team review was conducted in July and August of 1992.

FINDINGS

Digital Mechanization

A review of aircraft that have experienced PIO in the past indicated that PIO is not a result of digital mechanization per se. PIOs have been encountered in a variety of control system mechanizations including mechanical, hydromechanical, electro-mechanical, and analog electronic systems. Some aircraft that have experienced PIO in the past are presented in Table 1.[1]

PAST	RECENT
YB-19	YF-16
F-100C	F-16
F-101B	F-17
F-102A	F/A-18
F-4B	SPACE SHUTTLE
T-37A	JAS 39
T-38A	B-2
F-5A	C-17
KC-135	YF-22

Table 1. PIO Occurrences

The advantages afforded by digital electronic flight control systems have allowed flight control development to break the space, weight, and power

Paper presented at the Flight Mechanics Panel Symposium held in Turin, Italy, from 9-13 May 1994.

barriers that effectively limited the flight control complexity that could be achieved with other control system mechanizations. With digital flight mechanization, designers are able tailor the flight control system for a far wider variety of flight conditions and flight tasks than was previously possible. However, this increased complexity comes at the expense of some additional risk and requires a more disciplined, structured development process.

Developmental Process

The key finding of the investigation lay in the development process and its execution. After reviewing the numerous programs, it was observed that virtually all of the programs used the same development process. A simple schematic of that process is shown in Figure 1. This process is designed to be an iterative effort. Each step is intended to better identify the system and re-evaluate it based on the latest identification. When problems are encountered, the design should be modified, re-identified, and re-evaluated in a closed loop fashion. When problems are overcome, the process moves on to the next step. This process is intended to decrease technical and financial risk by reducing uncertainty. After reviewing the numerous programs, it was concluded that this process had the right steps, however process execution varied greatly among programs.

Problems with the twin constraints of cost and schedule sometimes drove the process to run "open loop" when flying qualities issues (including possible PIO) were encountered. For example, if a simulator evaluation indicated that a design did not meet the quantitative requirements in the specification and the necessary fix significantly impacted cost or schedule, some programs discounted the fidelity of the simulator and decided to proceed with flight test to see if problems really existed. Although the steps were in place to correct the problem, these programs did not adhere to the process guidelines.

Pilot Induced Oscillations

A simplification of the interaction of the pilot with the flight vehicle system is presented in Figure 2. The pilot can be viewed as a feedback system that closes the outer loop around the airframe-sensor-flight control system. The feedback path for the pilot is a multi-channel path that includes the pilot's visual (outside and inside the cockpit), motion, aural, and tactile cues (force and displacement) from his controllers. A PIO occurs when this outer loop becomes dynamically unstable. In the most general sense, a PIO is the result of a disharmony between the pilot's action and the expected aircraft reaction. The disharmony occurs when one or more of these feedback cues provide confusing or conflicting information to the pilot and the pilot's gain is high enough to drive the outer loop system unstable.

An aircraft is susceptible to PIO when it possesses certain characteristics that make it prone to PIO in flight conditions and tasks where it must frequently fly. The typical characteristics which contribute to PIO susceptibility are well known and include: high stick sensitivity, excessive system phase lag, large system nonlinearities, lightly damped response modes, unstable response modes and coupled response modes. Each of these contributors presents a form of disharmony in one or more of the pilot's feedback channels.

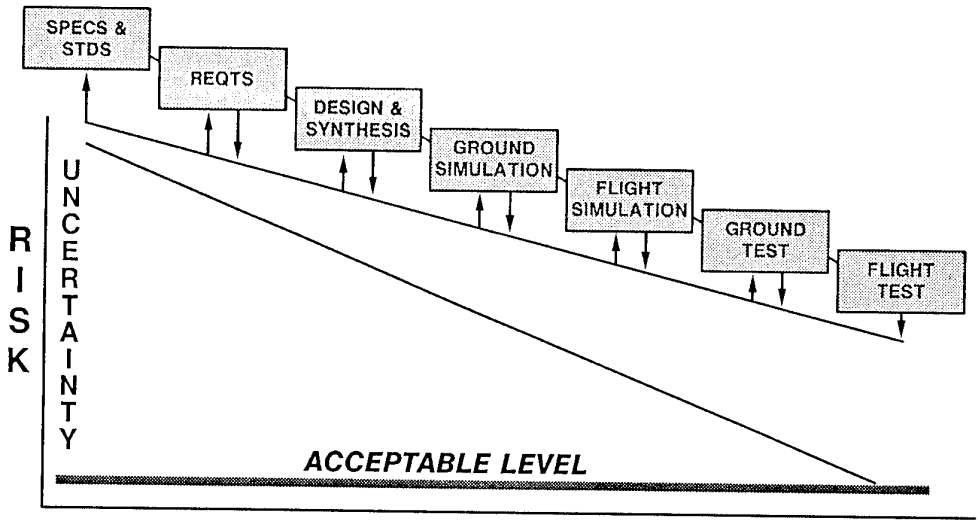

Figure 1. Flight Control Development Process

Although an aircraft exhibits such characteristics, this does not mean that the aircraft will predictably enter a PIO as other factors are involved. An important factor is the unpredictable nature of pilot gain which greatly influences the relative stability of the pilot-vehicle system. Pilot gain is affected by the tolerance required in performing the flying task and the aggressiveness of the pilot in achieving that task. The variances among individual pilots in the level of gain to complete the flying task is significant. Certainly, PIO is more likely to occur when the pilot is performing a "high gain" task such as trying to precisely minimize an error in aircraft attitude or flight path. Representative high gain tasks in a cruise configuration are aerial refueling (particularly probe-and-drogue), close formation flying and target tracking. High gain tasks in the power approach configuration include offset landing tasks and carrier approach and landings.

Although aircraft characteristics and pilot gain increase susceptibility to PIO, the occurrence may still be avoided by pilot compensation. While performing the flying task, and in conditions where an aircraft is PIO prone, the pilot may determine the inputs required to avoid the occurrence. By lowering the input gain, the PIO becomes less likely as the pilot adapts to the particular aircraft in the regimes where it is PIO susceptible. Logically, a pilot is more susceptible to PIO if he is unfamiliar or unaware of the aircraft's PIO tendencies.

The fact that pilot gain is a contributor to PIO should not be interpreted to mean that the pilot is at fault. Susceptibility to PIO is a design flaw as the aircraft is supposed to be designed with a stable outer loop for all reasonable pilot control inputs. An aircraft can and should be designed such that it is not PIO prone in tasks or conditions in which it must commonly operate. The review team struggled with the perception that such a design might be impractical from a cost, weight, or performance perspective. However, the F-15 aircraft was a prime example of a high performance front-line fighter that had never encountered a PIO and was clearly in the *good* handling qualities regime. It was not designed specifically for freedom from PIO but careful attention had been paid during its development to the characteristics that result in good handling qualities.

Initiation of PIO may be a result of a discrete event, commonly called a "trigger event". A trigger event is not necessary for a PIO to occur, nor will the identical event necessarily initiate a PIO every time. A trigger event may be a discontinuity in the control system such as a sudden failure or a large discontinuity in the control gain schedule. Additionally, the trigger mechanism may be an event which perturbs the aircraft such as a large, abrupt atmospheric disturbance or a pilot distraction. If the aircraft is PIO prone, the trigger event may initiate a PIO by driving the pilot to make abrupt corrections. The aircraft's PIO tendencies and the pilot's inability to predictably compensate will provide the sustaining mechanisms for the PIO. If the aircraft is not PIO prone, the trigger event will not likely cause a PIO as the pilot can apply sudden corrections without becoming *confused.* Following the disturbance, the pilot will perceive the corrections required before the motion becomes sustaining.

The pilot factor is not a controllable entity in designing for low susceptibility to PIO. Only the aircraft's susceptibility and certain trigger events are within the control of the designer. Mission requirements may demand that certain high gain tasks be performed.

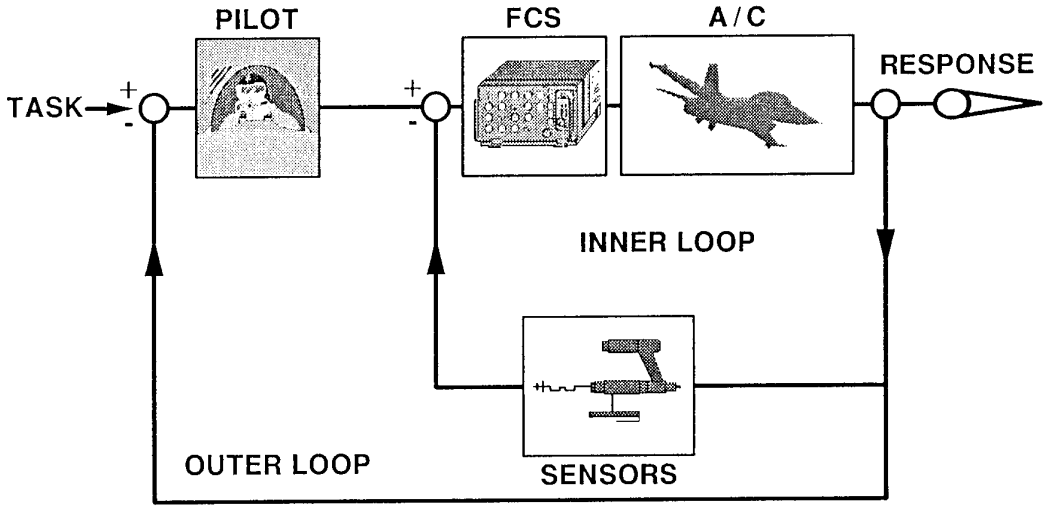

Figure 2. Pilot - Flight Vehicle System Interaction

During its service life, the aircraft will be flown by pilots with a wide range of experience. Some trigger events are random events that have a high probability of occurrence over that extended time span. In order to design an aircraft that is not PIO prone, the designer must minimize those known factors that increase PIO susceptibility. The difficult question for the designer is: "What values of these factors provide the appropriate level of PIO resistance at an acceptable cost and compromise with other affected system characteristics?"

The characteristics of a pilot, as a control element, are not well understood. As a result, flying qualities issues, including PIO susceptibility, have the characteristics of a "soft" science. Since a human's appraisal is the measure of merit, it is subjective in nature, and highly variable depending on which individual is doing the evaluating. This variability exists at all stages of flight control system development. In the research stages, it is difficult to develop quantitative criteria to address the design problem. In the verification stages, difficulties arise in attempting to prove that the delivered product is satisfactory.

Figure 3 illustrates one of the problems in selecting appropriate values for design/validation criteria. Cooper-Harper pilot ratings are the most common quantitative measure used in handling qualities evaluations. For a typical handling qualities experiment, the curve correlating flying qualities criterion with Cooper-Harper ratings would typically be as shown in Figure 3. At the *good* end of the curve, there is a certain point up to which, in a typical experiment, all of the pilots will agree that the aircraft is good, and the diversity of Cooper-Harper ratings will be small. At the *bad* end of the curve, there is a certain point beyond which all of the pilots will agree that the aircraft is bad, and the diversity of Cooper-Harper ratings will be small. Between these two points is an area where it is more difficult to say precisely how bad the aircraft is because the diversity of pilot ratings will be much greater in this region.[2,3] Consequently, quantitative design requirements derived from such correlations in handling qualities research must be considered inferential in nature. That is, meeting the criteria may suggest but will not guarantee that the aircraft will have good handling qualities.

Flying Qualities Specifications

The quantitative PIO criteria available in the current flying qualities specification, MIL-STD-1797, and from other sources, are based largely on data generated in experiments conducted in ground-based and in-flight simulators in the 1960s and 1970s.[4] In the specification, most of the quantitative PIO requirements reside in paragraphs that were intended to assure good overall flying qualities, not specifically to preclude PIO. For example, the requirements on phase lag in the pitch response reside in paragraph 4.2.1.2 Short Term Pitch Response. Paragraphs intended explicitly to preclude PIO problems have been largely qualitative in nature, termed: "there shall be no tendency for PIO". Finally, the requirements in MIL-STD-1797 do not specifically call for verification testing for PIO characteristics. The lack of a strong tie between the requirements and the verification at each stage of the flight control development process has led some programs to defer critical actions which could have precluded significant changes later on.

Flight Test Phase

The final test of the flying qualities and the PIO tendencies of an aircraft is in the flight test phase. Waiting until the flight test phase to determine the degree of PIO susceptibility is generally too late in the development process. By this point, the number of realistic options to resolve problems is reduced, and design changes at this stage have a greater impact on cost and schedule than at earlier stages. Often a cheaper and easier solution at this stage is to train pilots to avoid the PIO if possible. As a result, occasionally, a system with a PIO tendency does not get fixed unless it prevents mission accomplishment or the pilots cannot find a technique to avoid the PIO.

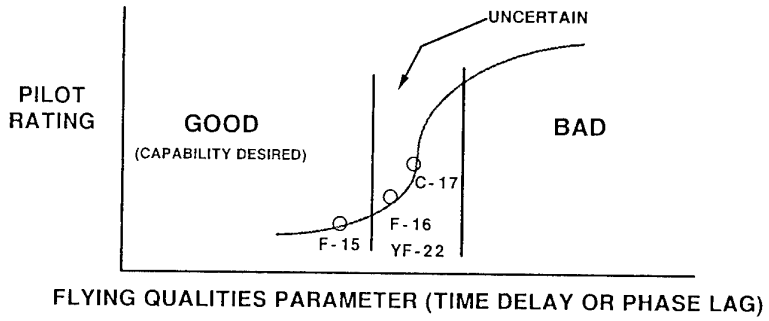

Figure 3. Pilot Rating Versus Handling Qualities Correlation

CONCLUSIONS

As a result of these findings, the Review Team concluded that the flight control development process, as currently implemented, had the following flaws:

1. The available design criteria and analysis methods for PIO are inferential in nature, lack universal acceptance, and the current test requirements are not rigorous.

2. The process lacks firm go/no-go criteria at each stage in the process for the program manager to assess the risk of PIO and to decide whether to proceed or whether further iteration is necessary.

3. The decision of what is good enough is frequently left until the flight test phase, where many options that were available in previous stages of development are now precluded by cost and schedule constraints. Changes to the flight control system are made only if the pilots cannot be trained to avoid the PIO or military utility is unacceptably compromised.

RECOMMENDATIONS

The Review Team made the following recommendations to improve the flight control development process:

1. Establish an Integrity Approach for flight control development similar in nature to those formal AFMC programs established for structures and propulsion. The intent of this program would be to change the paradigm from one of "Proceed unless a PIO problem is proven to exist" to one of "Proceed only when resistance to PIO problem is proven". This was accomplished through establishment of firm go/no-go criteria at each step in the development process. At the design stage, this would consist of improved flying qualities criteria. However, since these would still be inferential in nature, further "gates" would be established at other steps in the process. Rigorous demonstration maneuvers, such as Handling Qualities During Tracking (HQDT) would be required in the ground simulation stage of the development process. In-flight simulation would be recommended, perhaps even required, if results were inconclusive in the earlier stages. Finally, the verification of adequate PIO resistance would require satisfactory handling qualities in specific demonstration maneuvers during flight test. Requirements and verification methods would be agreed to between the USAF and contractor.

2. Establish a Flying Qualities Working Group for each aircraft under development. The purpose of the Flying Qualities Working Group is to monitor the progress of the design through all development stages, help resolve problems, and ensure that potential problems are communicated to all the agencies involved. This group would attempt to achieve an appropriate balance among design, pilot training and military utility. Engineers from the program office, contractor, flying qualities research organizations, and flight test center, and test pilots from the contractor and flight test center would be expected to participate.

3. Enhance the flying qualities research program to improve the criteria and analysis methods available. The primary objectives would be to resolve conflicts between existing criteria, develop a more comprehensive analysis method, and hopefully, reduce the region of uncertainty in the present predictive methodology. A secondary objective would be to develop criteria and analysis methods for new flight regimes (such as high angle of attack) and unconventional response modes (such as direct lift).

4. Incorporate the "Best Practices" into the Air Force Acquisition Model (AFAM), a reference tool for USAF acquisition managers. The Review Team identified 22 "Best Practices", the most important of which are summarized below:

- In the requirements definition stage, use quantitative PIO requirements in the specifications, with specific verification requirements.

- In the design stage, use multiple analysis methods and criteria to assess the flying qualities of the design.

- Keep the needs of flight test in mind during the design. For example, include a means to change flight control system gains during the flight test phase in anticipation of the need to adjust them in order to resolve handling qualities problems.

- Ground test with hardware-in-the-loop to identify system characteristics.

- Use full-up ground simulation and in-flight simulation to assess handling qualities and PIO tendencies and use well-defined "high gain" pilot-in-the-loop tasks (e.g. HQDT).

- In the flight test stage, include the same "high gain" handling qualities testing as part of the envelope expansion process.

On 5 February 1993, the findings and recommendations of the review team were briefed to the commander of AFMC. He has directed that AFMC implement the recommendations.

REFERENCES

1. Ashkenas, Irving L., Henry R. Jex, and Duane T. McRuer, Pilot-Induced Oscillations: Their Cause and Analysis, STI Report TR-239-2, 20 June 1964.

2. Wilson, David J. and David R. Riley, Cooper-Harper Pilot Rating Variability, AIAA Paper 89-3358, 14-16 August 1989.

3. Riley, David R. and David J. Wilson, More on Cooper-Harper Pilot Rating Variability, AIAA Paper 90-2822, 20-22 August 1990.

4. Military Standard, Flying Qualities of Piloted Aircraft, MIL-STD-1797A, 30 January 1990.

FLIGHT DEMONSTRATION OF AN ADVANCED PITCH CONTROL LAW IN THE VAAC HARRIER AIRCRAFT

C.Fielding
Aerodynamics Department
British Aerospace Defence Limited
Warton, Lancashire, PR4 1AX, UK

S.L.Gale and D.V.Griffith
Flight Dynamics & Simulation Department
Defence Research Agency
Bedford, Bedfordshire, MK41 6AE, UK

SUMMARY

'Vectored thrust Aircraft Advanced flight Control' (VAAC) is a UK project, sponsored by the Ministry of Defence and managed by the Defence Research Agency (DRA). The project is investigating, through ground-based simulation and flight test on the VAAC Harrier research aircraft, the low speed flight control, handling and cockpit display concepts applicable to an aircraft replacing the Harrier. As part of the project, British Aerospace Defence Limited have designed a revolutionary two-inceptor pitch plane control law for assessment on the project aircraft. This Control Law has now been flight tested and further developed 'in-flight' by the DRA, culminating in a series of successful flight demonstrations to guest pilots. During the latter stages of flight testing the Control Law was modified to allow single-inceptor operation. Flight testing has shown that both the two- and single-inceptor control strategies result in a large reduction in pilot workload, when compared with the VAAC Harrier's three-inceptor arrangement, during the transition from wing-borne to jet-borne flight and hover.This paper describes the Control Law's evolution from initial concept through to the results obtained from flight testing.

1 INTRODUCTION

The Harrier has, for many years, been the Western World's only operational fixed-wing fighter aircraft with a Vertical/Short Take Off and Landing (VSTOL) capability. From the pilot's perspective, much of its success can be attributed to the airframe/powerplant geometry and the chosen method of thrust vectoring. These have resulted in an aircraft that can be flown manually, ie without a fly-by-wire system, throughout its flight envelope. Notwithstanding this basic capability, the earlier production aircraft were fitted with limited authority autostabilization systems (working in pitch, roll and yaw) to give an acceptable pilot workload during low speed flight. The handling on the latest generation of the Harrier has been further improved by the provision of increased authority stability augmentation and a pilot-selectable pitch and roll attitude hold capability.

Whereas the Harrier exhibits relatively benign and predictable handling characteristics in low speed flight, a future Short Take Off/Vertical Landing (STOVL) aircraft replacing the Harrier will undoubtedly require a significantly more complex airframe/powerplant configuration to satisfy the more demanding operational requirements. Such an aircraft will not be controllable by the pilot without assistance from an integrated flight and powerplant control system using Active Control Technology (ACT). The introduction of ACT will also allow the opportunity to introduce control features (and associated cockpit displays) to further reduce the workload from that currently experienced by Harrier pilots.

Accordingly, the Defence Research Agency's (DRA) Vectored thrust Aircraft Advanced flight Control (VAAC) project (References 1,2), sponsored by the UK Ministry of Defence (MOD), is investigating the low speed flight control, handling and cockpit display concepts applicable to an aircraft replacing the Harrier. Control law studies are taken through off-line simulation to ground-based piloted-simulation, and, ultimately, to flight test and demonstration in the DRA's project aircraft: the 'VAAC Harrier' (Figure 1).

One of the issues being addressed by the VAAC control law studies is the optimum number of pitch plane 'inceptors' (cockpit controls) needed by the pilot to efficiently fly a future STOVL aircraft. Several pitch plane control laws have been developed under VAAC. This paper discusses a two-inceptor pitch control law designed by British Aerospace (BAe), and describes the initial design philosophy, development through piloted-simulation, flight testing in the VAAC Harrier, and identifies some lessons learned in the process.

Paper presented at the Flight Mechanics Panel Symposium held in Turin, Italy, from 9-13 May 1994.

2 VAAC HARRIER AND SUPPORT FACILITIES

2.1 VAAC Harrier

The VAAC Harrier (Reference 1), a highly modified two-seat Harrier T4, has been fitted with an experimental digital flight control system (FCS), which when in operation has full authority, full rate control of the aircraft's tailplane, throttle, nozzle and flap, plus limited authority lateral/directional control (via the existing autostabilizer servos).

The front cockpit is essentially unchanged from the production standard, with the cockpit controls connected to the basic aircraft's mechanical control runs. However, the rear cockpit has been extensively modified for the aircraft's experimental role; its tailplane, throttle and nozzle inceptors have been disconnected from the mechanical control runs and, instead, provide electrical inputs to the VAAC FCS. The FCS then drives special parallel actuators which are connected to the basic aircraft's control runs through clutching mechanisms. This arrangement allows the test pilot in the rear cockpit to fly the aircraft through experimental control laws in the VAAC FCS, which then back-drives the safety pilot's controls, in the front cockpit, through the aircraft's standard mechanical linkages. A major benefit of this arrangement is that, whereas the safety pilot in the front cockpit must be an experienced Harrier pilot, the pilot in the rear cockpit does not need to have any previous Harrier experience.

In addition to the modifications to the primary inceptors, the rear cockpit has a variety of new, FCS software-configurable switches, lights and gauges, and a fully programmable head-up display (HUD). The HUD has a digital interface to the FCS to allow control law-specific symbology to be displayed. Figure 2 shows the HUD format used for control law assessment, which is derived from the VSTOL mode of the DRA's fast-jet format.

Built into the FCS is an array of safety monitoring features which will disengage the experimental system in the event of a system failure or imminent flight envelope exceedence and return control to the safety pilot. The safety pilot may also initiate an FCS disengage at any time by applying an overriding force on his normal cockpit controls (throttle, nozzle lever and centre stick).

The VAAC system was initially cleared for use between the hover (at 100ft) and 250kts indicated airspeed. This clearance has recently been extended to allow vertical landings to be performed onto the 'VSTOL pit' (a facility that significantly reduces the piloting problems associated with the gas recirculation characteristics of the Harrier T4 near the ground) at the DRA's airfield site near Bedford.

2.2 Flight Simulators

Ground-based, piloted flight simulation was employed as an integral part of the control law's development process. Simulator-based assessments were performed at regular intervals during the design. Simulation facilities at BAe Warton's Flight Simulation Department (Figure 3) were used by the control law designers to refine the law's functionality, and the DRA Bedford Advanced Flight Simulator (Figure 4) was used to perform formal assessments using a larger selection of RAF and BAe test pilots.

Both simulators employed the Harrier Wide Envelope Model (see Section 2.3) and were configured with HUD formats and inceptor characteristics representative of the rear cockpit of the VAAC Harrier. No other VAAC cockpit features were represented.

2.3 Harrier Wide Envelope Model

The non-linear Harrier Wide Envelope Model (WEM) was developed by the Royal Aircraft Establishment (now part of the DRA) in the early 1980s and forms the foundation for the off-line control law design, simulation and analysis work. It consists of the full, rigid body, aircraft aerodynamic and Pegasus engine characteristics, including aerodynamic and jet-interaction effects, reaction control systems model, ground effects, hot gas re-ingestion and a full engine hydromechanical control system model.

The WEM has been updated to be more representative of the VAAC Harrier by including transfer function models of the aircraft's sensors, digital computing and actuation systems (as shown in Figure 5). The FCS hardware assumptions were based on VAAC hardware specifications and test data, and BAe's experience with the design of previous fly-by-wire systems.

3 ADVANCED PITCH CONTROL LAW

3.1 Control Philosophy

The advanced pitch plane control law, designed by BAe and subsequently developed through flight test by DRA, is based on a two-inceptor control strategy (which would allow a 'Hands On Throttle And Stick' (HOTAS) implementation). A single-inceptor version was developed during the latter stages of the flight testing (see Section 5). The Control Law provides a unified pitch control strategy by blending in a 'seamless' manner, ie without any discrete mode changes, from a typical pitch rate demand system in wing-borne flight to a height rate demand system at low speed.

The Control Law has been designed primarily for performing decelerating transitions from wing-borne to jet-borne flight and vice-versa. The Control Law, shown in simplified form in Figure 6, provides integrated management of the aircraft's thrust vector and aerodynamic surfaces in response to commands from two cockpit pitch inceptors:

i) The Left Hand Inceptor (LHI) commands aircraft axial thrust in wing-borne flight (like a conventional throttle) and the horizontal thrust component, with closed-loop groundspeed control, in jet-borne flight. The moding change is continuously blended as a function of airspeed.

ii) The Right Hand Inceptor (RHI) commands pitch rate via the tailplane in wingborne flight and height rate via the vertical thrust component in jet-borne flight. The two modes are automatically blended together in the transition region as a function of airspeed. Once the Control Law has fully blended into the height rate mode, the pilot can only control the aircraft's pitch attitude through a stick-top trim button, although this has no effect on flightpath as the Control Law decouples pitch attitude from the thrust vector in this speed regime.

The inceptor functionality is scheduled with airspeed as shown in Figure 7.

3.2 Design Strategy

A visible and logically arranged control law architecture was derived using simple well-proven control law functions (e.g. filters, gain schedules) with a view to readily satisfying the practical issues of implementation, verification and flight clearance. Known physical effects were separated out within the Control Law to simplify the subsequent design of gain schedules; non-linear control functions were introduced into the Control Law, based on studies of the aircraft's physical attributes (for example, thrust vector geometry). The importance of this stage of the design is that significant non-linearities in the basic vehicle characteristics can effectively be 'linearized' by the non-linear part of the Control Law, thus providing a sound basis for gain schedule design and resulting in simple gain schedules. Once the gain schedules have been designed, further non-linear design is necessary to ensure that the system performs satisfactorily when the thrust vector commands exceed the available capability. This involves holding integrators to prevent wind-up and assigning a control hierarchy to ensure that the system achieves the optimum control strategy, despite the system's partially saturated state.

The control laws were designed loop-by-loop, with the most important loop being closed first, followed by the next most important, etc. This approach has significant benefits in that the designer uses a systematic approach to the design, with insight being gained at each stage. The effects of opening a control loop are fully understood and can be used to great advantage as part of the overall design, for example, to satisfy control-hierarchy requirements in the event of thrust vector saturation.

In wing-borne flight, non-linear command filtering was designed using the BAe 'Gibson-criteria' (Reference 3) to provide accurate pitch tracking characteristics for small pilot inputs on the centre stick. The filtering is designed such that a rapid normal acceleration response is achieved for large pilot inputs, as the filter modulates and becomes 'transparent'. In jet-borne and partially jet-borne flight, high-order handling qualities design criteria were not available so a significant degree of engineering judgement had to be used, supported by pilot comments from simulation trials. Parallel piloted simulation research studies have been undertaken at BAe in order to derive criteria suitable for STOVL aircraft handling qualities design. These essentially extend the concepts of the highly successful 'Gibson-criteria' for high-order flight control systems to the low speed regime. It has been shown, by retrospective analysis, that the Control Law conforms to these new criteria.

3.3 Operational Characteristics

As the aircraft decelerates in wing-borne flight the flaps are lowered by an 'open-loop' airspeed schedule. A flap-to-tailplane crossfeed minimizes flap-induced pitch attitude changes. As airspeed decreases, the reduction in aerodynamic lift is compensated for by introducing a vertical thrust component via an airspeed-dependent schedule. This simultaneously rotates the nozzles and increases the thrust. A crossfeed from the nozzle angle to the tailplane minimizes nozzle-induced pitching activity. The aircraft is then flown like a conventional aircraft for the initial part of the transition, using incidence to control the flightpath. A crossfeed from the RHI to the vertical thrust component is used to prevent excessive incidence demands during manoeuvres and to reduce the steady-state angle-of-attack. The vertical thrust component is corrected for bank angle during lateral manoeuvres.

During the later stages of the decelerating transition, the response type blends from pitch rate demand to height rate demand on the RHI, and from open to closed-loop speed control on the LHI. The pitch rate/angle are held by a proportional, integral and derivative (PID) controller in the pitch rate loop down to jet-borne flight. Control of the tailplane and pitch reaction control valves is progressively transferred to the pitch attitude control loop and the aircraft's pitch attitude automatically changes to the datum landing attitude. In jet-borne flight, the LHI demands the 'X-', or fore/aft, component of thrust, in inertial axes, which blends into closed-loop groundspeed control; allowance has been made for the thrust X-component to be negative, to facilitate limited rearwards flight in the hover. The RHI demands the orthogonal 'Z-' component of thrust, also in inertial axes, which translates into height rate demand. The Z-component is governed by a PID controller, the gains of which are scheduled with airspeed, and are sufficiently high to provide aircraft height hold in the absence of external disturbances (to which the system has been shown to be insensitive). Figure 8 shows the 'control-hierarchy' function which ensures that the Z-component of thrust takes priority in the event of the thrust vector demand exceeding the achievable limits. The X- and Z-components of the thrust vector are converted to throttle and nozzle angle demands by a conversion from rectangular to polar co-ordinates, giving 'decoupled control' of the thrust vector components in inertial axes.

3.4 Lateral/Directional Control Laws

Lateral/directional control laws were developed by the DRA for use with the production autostabilizer servos to give limited authority lateral/directional augmentation. These laws are used in conjunction with all experimental pitch control laws.

In roll, the lateral control law gives a roll rate response scheduled with the pilot's lateral stick position, with a bank angle hold term when the undercarriage is down and the stick is centred. In yaw, the directional control law gives automatic sideslip suppression at higher speeds, blending to yaw rate demand, proportional to the pilot's pedal input, at low speed. When commanding yaw rate, the pilot can also invoke a heading hold by centralizing the pedals.

4 SIMULATION RESULTS

Flight response matching, using the off-line simulation facilities, has confirmed that the Harrier WEM (see Section 2.3) is representative of the VAAC Harrier, and that control law operation in flight is as expected; figure 9 shows a rapid deceleration from 200 kts, in which the simulated response is a good match to the flight-recorded data (see Section 5 for a summary of flight test results).

The most significant result from the initial pilot-in-the-loop simulation phase at Warton and Bedford was that although the system was found to be easy to fly by non-VSTOL combat aircraft pilots, difficulty was experienced by Harrier pilots who had to 'unlearn' their training for low speed flying (similar feedback was obtained from assessments of other advanced VAAC control laws). For straight-in approaches with minimal manoeuvring, the system performed well. For more aggressive approaches, such as are sometimes flown in the Harrier, the original system received some adverse pilot comment because the Control Law had reduced the performance capability of the aircraft in terms of maximum deceleration and had not made efficient use of the available aerodynamic lift. These issues were addressed and resolved during subsequent development of the Control Law. In terms of the functionality of the Control Law, the early simulation trials identified two design aspects which needed addressing:

(i) In jet-borne flight, the Control Law needed to provide automatic protection against descent rates which could not be easily reversed by thrust modulation.

(ii) The Control Law used an automatic mode change as the aircraft decelerated through 130 knots, with a significant change in handling qualities.

Both of these aspects were resolved during development, by introducing automatic sink rate limits and continuous airspeed scheduling to achieve the mode change, as described in Section 3.1. The final phase of manned simulation trials have been rated as providing 'Level 1' handling qualities.

The piloted-simulation and off-line system analyses showed that the two-inceptor pitch control strategy had been successfully developed to a standard which was considered to be suitable for in-flight assessment.

5 FLIGHT TESTING AND FURTHER DEVELOPMENT

5.1 Summary of Flight Testing

The Control Law was installed in the VAAC Harrier's FCS without encountering any significant problems. It was first engaged in flight on 23rd February 1993; in the following 13 months, 97 test flights were flown with the Control Law engaged. During these flights the test pilots in the rear cockpit flew the aircraft, through the Control Law, for a total of approximately 39 flight hours of development, assessment and demonstration, including 30 vertical landings on the VSTOL pit.

The Control Law was flown in a wide range of ambient conditions: in temperatures ranging from -2°C to +26°C and in winds from 25kts, gusting 35kts, down to flat calm. The Control Law has performed well in all conditions, and has resulted in a very low pilot workload during the transition and in the hover. Moreover, during their first flight in the VAAC Harrier, pilots with no previous Harrier experience have been able to bring the aircraft to a stable hover, after a well-controlled deceleration from wing-borne flight, and then land vertically on the VSTOL pit.

5.2 In-Flight Control Law Development

During the flight test development, a number of changes were made to the Control Law. These were not only to improve its basic performance, but also to assess changes in its functional design:

(i) The FCS has a 'variable gain', or perhaps more accurately a 'variable scaling factor', facility whereby the test pilot in the rear cockpit can adjust key control law parameters in flight. This facility was used extensively throughout the development process, primarily to optimize changes in the Control Law's functionality, but also to compensate for modelling deficiencies in the Harrier WEM.

(ii) The sink rate demand limiter introduced during the earlier piloted-simulation (see Section 4) was found to be too restrictive; in particular there was a significant reduction in the pilot's ability to achieve acceptable descent rates during the blend from pitch rate to height rate demand. The explicit sink rate limit designed during the piloted simulation was also insensitive to ambient conditions and aircraft's instantaneous weight, which, of course, have a major effect on the aircraft's ability to recover from large rates of descent at low altitudes. Instead, a dynamic throttle and nozzle limiter strategy, using information from the FCS's safety monitoring system, was adopted to ensure that the maximum safe descent rates appropriate to the current situation were not exceeded. This feature worked well; it allowed the pilot to command the descent rate he required, with the knowledge that the Control Law would prevent irrecoverable situations (from the safety pilot's perspective) developing rapidly, without undue restriction of the aircraft's capabilities. The pilot was informed of limiter action by warning lights in the cockpit.

(iii) Pilot workload was found to be relatively high in the early stages of the transition, when compared to the lower end of the transition and hover. This characteristic was particularly apparent in turbulent conditions, where, at higher speeds, the pilot had to actively monitor and control the aircraft's vertical velocity through pitch rate, whereas at lower speeds he was commanding vertical velocity directly. Accordingly, an explicit flightpath hold feature and an automatic pitch rate compensator for turning flight were successfully added to the basic pitch rate demand system to solve the problem.

(iv) As a further workload-reducing measure, with potential applicability to all future fixed-wing combat aircraft, a single inceptor option was implemented and flight tested. This option, which is pilot-selectable, transferred the function of the LHI input to a trim switch on the RHI, which commanded a fixed rate input, scheduled with speed, that was integrated over time to give a signal analogous to that from the LHI. Flight testing has shown that the single-inceptor results in a further workload reduction, particularly for precise positioning around the hover, and leaves the pilot with one hand completely free to perform other system management tasks; indeed, it became the preferred method of flying the aircraft for the majority of pilots.

(v) In order to address concerns from Harrier pilots that a two- or single-inceptor control law reduces the operational flexibility of VSTOL aircraft at low speed, two other low speed modes were added: a pitch attitude trim facility with the two-inceptor option (in the original design, but not implemented initially, see Section 3.1) and a braking nozzle pitch-up for extra deceleration, with the single-inceptor option. Both these modes were successfully tested.

5.3 Flight Test Observations

In addition to the changes described above, a number of observations have arisen from flight experience:

(i) The relatively high reaction control activity commanded by the high performance FCS at low speed in turbulent conditions results in bleed flows that significantly reduce the Harrier's hover capability. This is an important consideration in the design of future STOVL aircraft.

(ii) At low speed, the Control Law's strategy of controlling fore/aft motion by changing the thrust vector angle, without changing pitch attitude, was well received (usual Harrier practice is to adjust pitch attitude with the thrust vector angle fixed relative to the fuselage). This result may have relevance to the design of low speed flight/propulsion control system of future STOVL aircraft.

(iii) For future STOVL aircraft with ACT, traditional carefree handling concepts, such as automatic flight envelope limiting, need to be extended down to the hover, including the landing, by applying an appropriate dynamic limiting strategy to the thrust vector demands.

(iv) Relative to the Harrier's existing arrangement, where the pilot has to control thrust magnitude and direction independently, significant workload reductions and acceleration/deceleration performance improvements can be achieved by integrated control of the thrust vector. Figure 10 shows pilot control activity during two similar decelerating approaches to the hover: the three time histories on the left illustrate the level of pilot control activity required to control the VAAC Harrier in a conventional approach, whereas the two traces on the right show activity during an approach flown with the single-inceptor option of the Control Law.

(v) The control strategy employed by this Control Law could be applied to a possible future derivative of the Harrier aircraft, and would result in further improved handling during low speed flight.

(vi) The consistent response strategy, where the LHI always commands faster/slower and, similarly, the RHI always commands up/down, appears very natural and is easy to fly for non-VSTOL pilots. This potentially raises major savings in the requirements for training the pilots of a future STOVL aircraft, although the experience of pilots familiar with the Harrier's inherent operational flexibilities should not be unwittingly ignored just, for example, to reduce training costs.

6 LESSONS LEARNED

Criteria need to be further developed and validated to provide a guide for the design aims for the integrated systems on future aircraft configurations, to reflect future aircraft operational characteristics. Specifically, work is required to extend and investigate the handling qualities criteria used for fixed wing aircraft, to cover STOVL operation and to define the requirements for carefree handling at low speed and in the hover.

Early standards of the Control Law used an airspeed-triggered switch to transfer from pitch rate to height rate demand modes with associated signal equalization. This proved to be unnecessarily complicated and introduced a discrete, and undesirable, change in handling qualities. The Control Law was developed to include airspeed

blending between the modes leading to a significantly easier implementation and providing continuity of handling characteristics. The resulting unified control strategy has, generally, been very well received by test pilots flying the VAAC Harrier.

The demonstrated reduction in pilot workload is mainly due to the automatic axis transformations inherent in the Control Law. The pilot's thrust vector commands are in inertial axis rectangular co-ordinates (where appropriate) rather than body axis polar coordinates. The former allows the pilot to directly command the flight variables of primary interest and provides decoupled aircraft control. This is the major benefit and can be used in conjunction with either a single-, two- or three-inceptor pilot interface. However, the two-inceptor pilot interface, enables HOTAS throughout transitions between wing-borne and jet-borne flight regimes, thereby further reducing pilot workload.

The flexibility of the VAAC Harrier FCS has also enabled a single-inceptor pilot interface to be developed. The single-inceptor has demonstrated further reductions in workload, particularly at low speed. It has also raised fundamental questions as to how thrust should be controlled in future combat aircraft, for example, it potentially alleviates the need for HOTAS by leaving one hand completely free to operate other aircraft systems.

The control strategy and response type are considered to be appropriate to future STOVL configurations, although research under VAAC is on-going. Similar strategies have already been applied to other BAe STOVL projects (simulation phase only) and are being applied to a RULS (Remote Unaugmented Lift System) aircraft as part of the MOD-sponsored Integrated Flight and Powerplant Control Systems (IFPCS) programme (References 4,5), which is addressing the cost-effective rig demonstration of the key control system technologies required for the next generation of combat aircraft.

7 CONCLUSIONS

This paper has described the design, development and flight testing of an advanced pitch flight Control Law, under the Defence Research Agency's (DRA) Vectored thrust Aircraft Advanced flight Control (VAAC) project. In particular, flight testing, on the VAAC Harrier aircraft has shown that both the single- and two-inceptor versions of the Control Law result in a large reduction in pilot workload, when compared with the basic aircraft's three-inceptor arrangement, during the transition from wing-borne to jet-borne flight, hovering and vertical landings.

The VAAC Harrier's unique safety pilot arrangement has enabled a wide range of pilots, including Harrier pilots, to safely assess the control law. An important result was that the control strategy was easy to fly, irrespective of piloting background; this may fundamentally change the way in which future Short Take Off/Vertical Landing combat aircraft are controlled. Such aircraft will have significantly more complex airframe/engine configurations and more demanding operational requirements; the results from the VAAC programme will form a major contribution to the development of integrated flight and powerplant control systems for these aircraft.

ACKNOWLEDGMENT

The VAAC programme is sponsored by the UK Ministry of Defence.

REFERENCES

1. SHANKS G.T., GRIFFITH D.V. and HAWKINS R.C., 'The Role of the VAAC Harrier Aircraft Programme in the Definition of Future STOVL requirements', International Powered Lift Conference, Santa Clara, AIAA Paper 93-4831-CP, December 1993.

2. SHANKS G.T., FIELDING C., ANDREWS S.J., and HYDE R.A., 'Flight control and handling research with the VAAC Harrier', International Journal of Control, Volume 59, No 1, 1994.

3. GIBSON J.C., 'The Development of Alternate Criteria for FBW Handling Qualities', AGARD Conference Proceedings 508, Paper 9, 1991 .

4. FIELDING C., 'Design of Integrated Flight and Powerplant Control Systems' AGARD Conference Proceedings 548, Paper 4, March 1994.

5. ALLEN D.A., SLEEMAN J.R. and WELLER B.R.C, 'The Integrated Flight and Powerplant Control System Programme', International Powered Lift Conference, Santa Clara, AIAA Paper 93-4830-CP, December 1993.

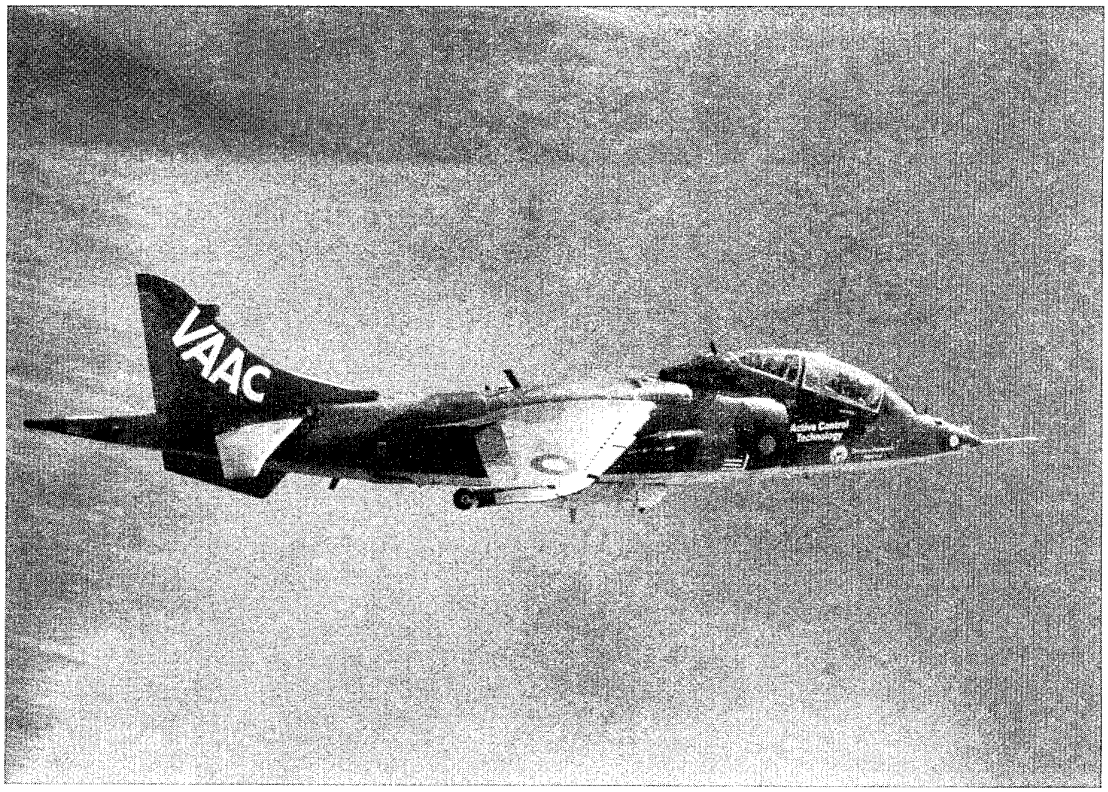

Figure 1. The VAAC Harrier

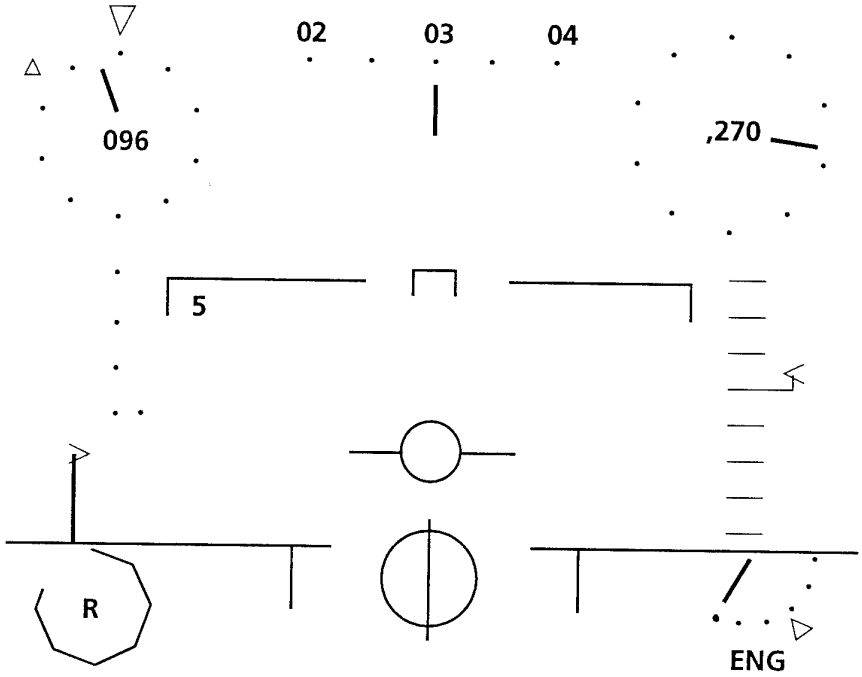

Figure 2: Head-up Display Format

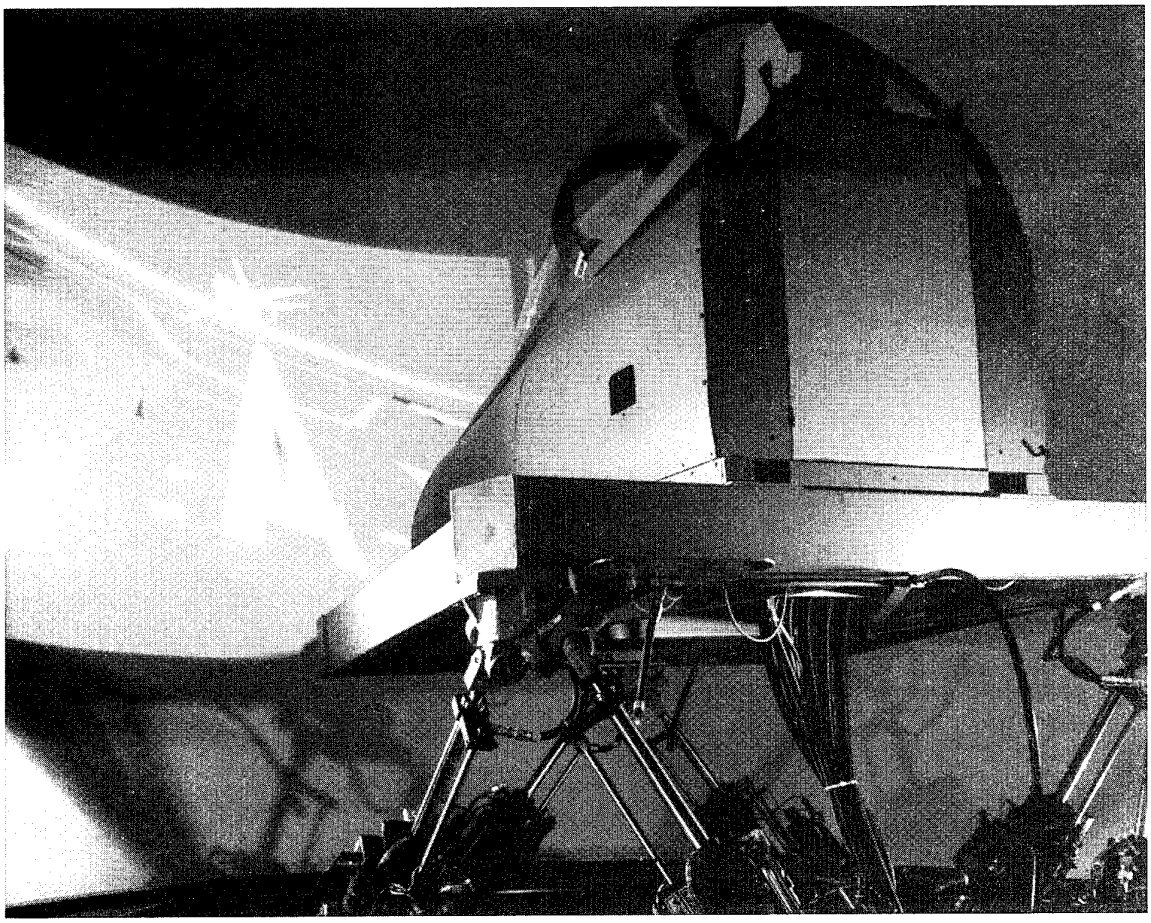

Figure 3: BAe Warton Mission Simulation Dome

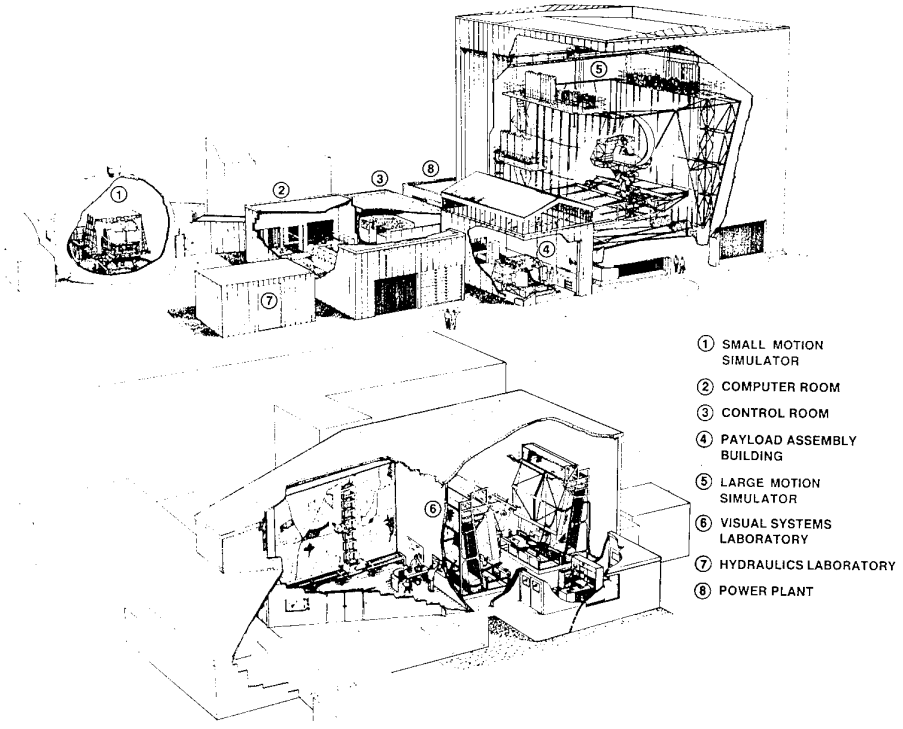

Figure 4: DRA Bedford Advanced Flight Simulator

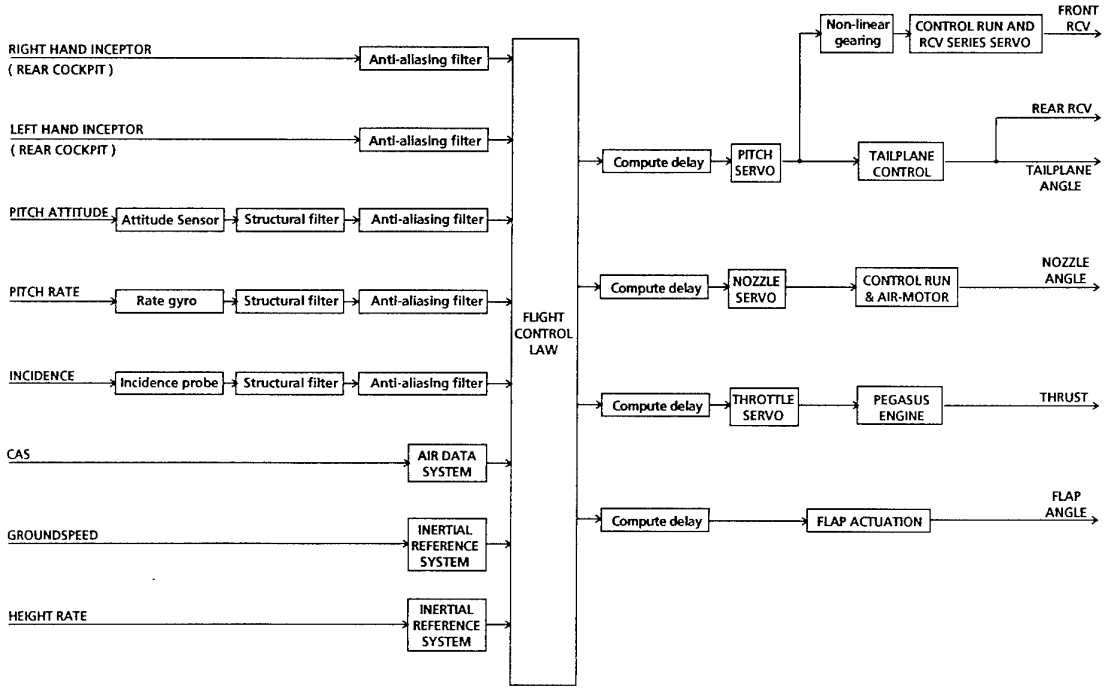

Figure 5: Flight Control System Modelling Arrangement

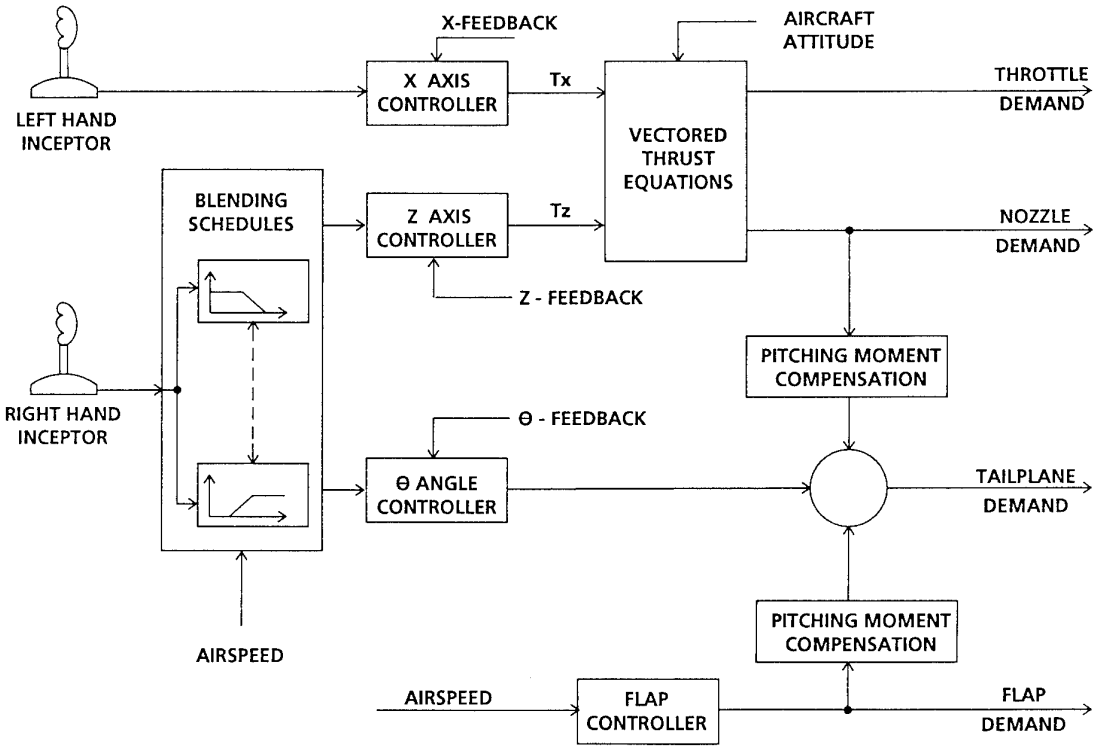

Figure 6: Schematic Arrangement of the Control Law

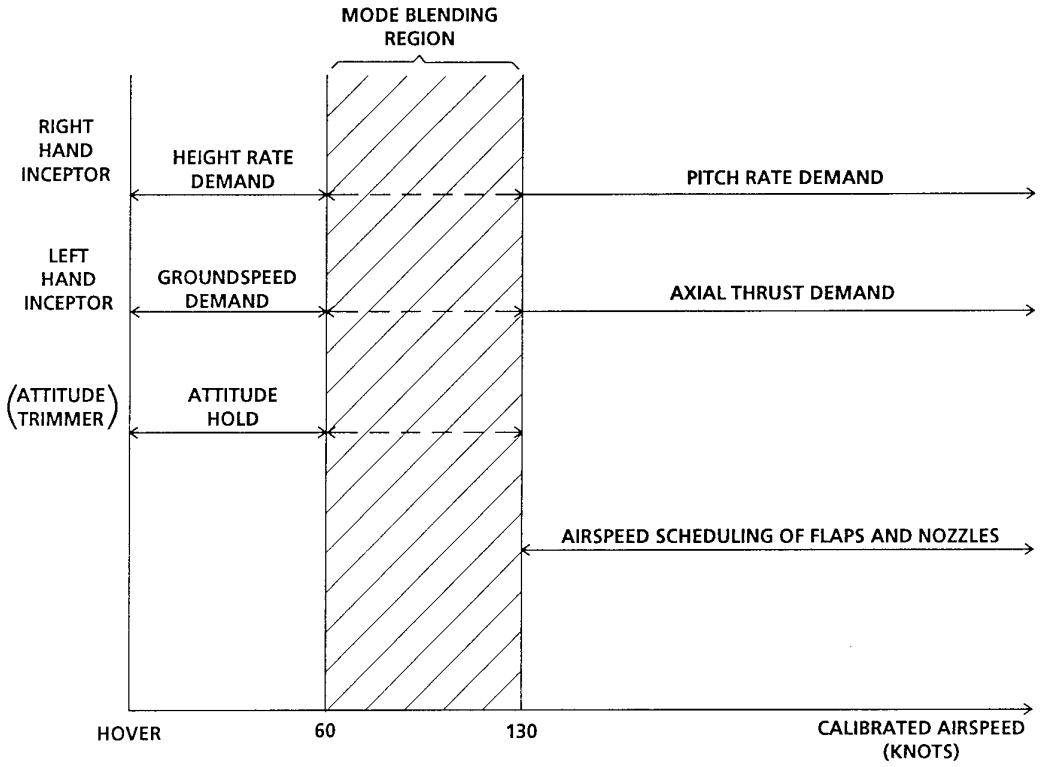

Figure 7: Inceptor Functionality as Scheduled with Airspeed

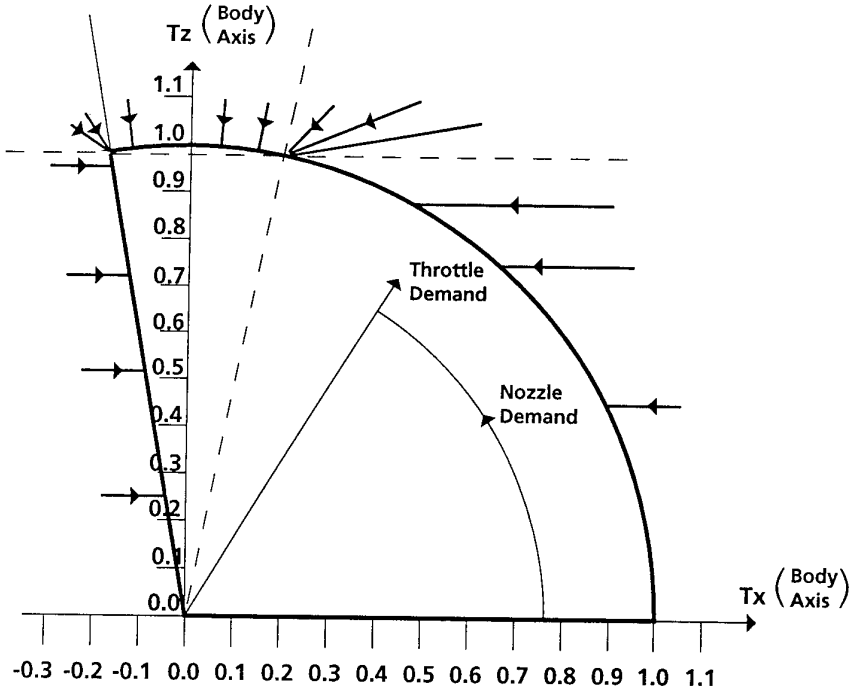

Figure 8: Thrust Vector Transformation Showing Mapping of Excess Demands onto the Achievable Control Boundary

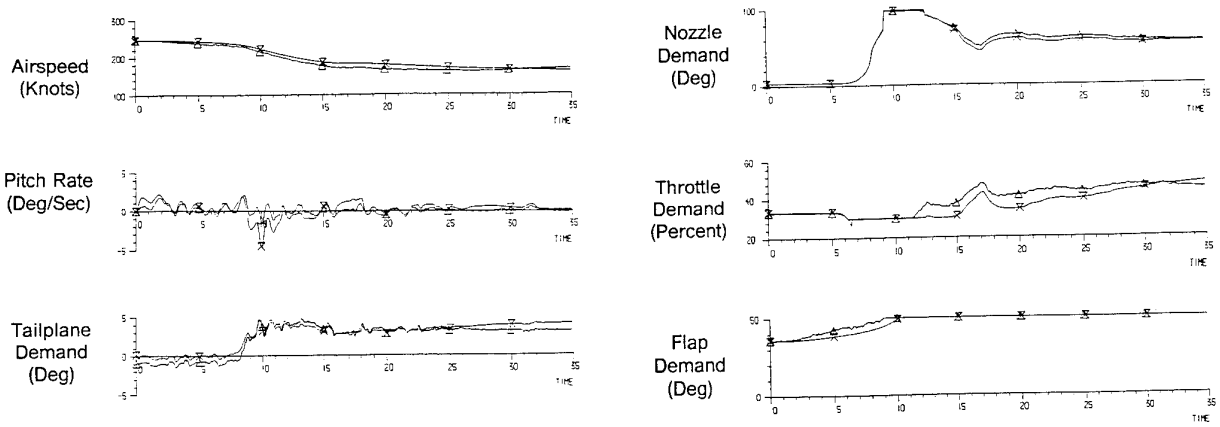

Figure 9: Comparison between Simulated and Flight Data

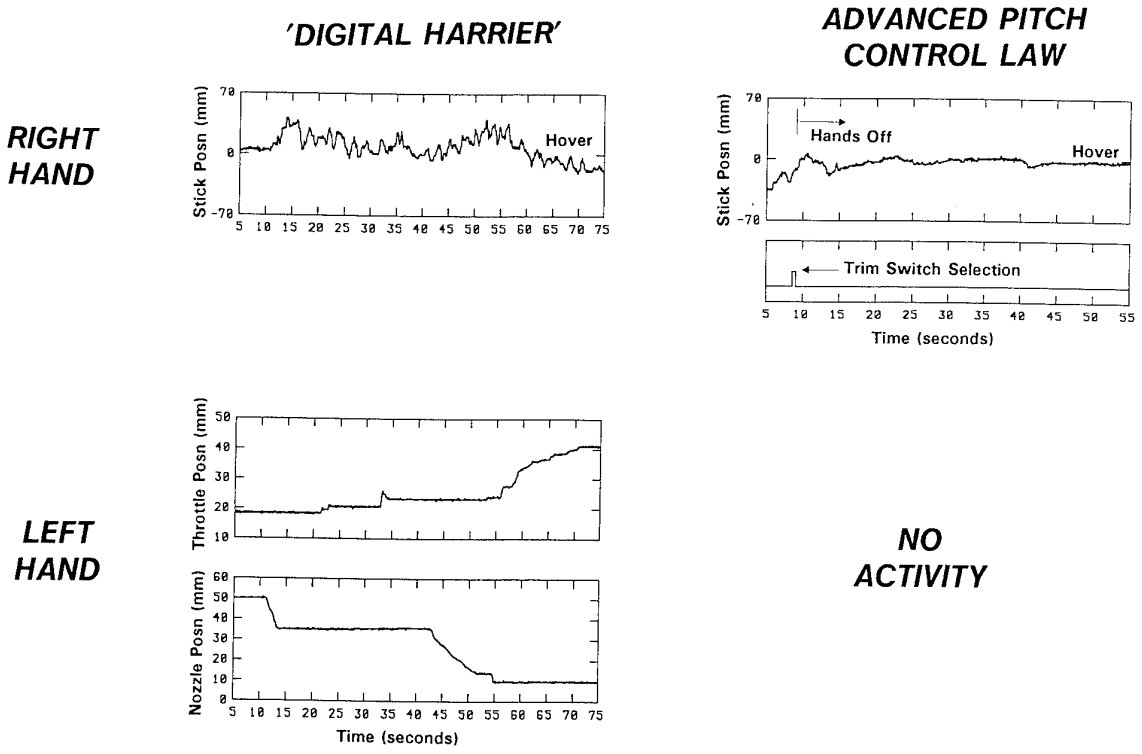

Figure 10: Comparison of Control Strategies During Approaches to the Hover (Showing Reduction in Pilot Workload)

X-31 – A Program Overview and Flight Test Status

H. Ross, U. Neuberger
Deutsche Aerospace AG
Military Aircraft Division
Department LME
81663 Munich
Germany

1. THE CHALLENGE

1.1 Air Combat

As long as manned attack air forces exist, and as long as penetrating aircraft are protected by escort fighters, surface-to-air missiles and air defense fighters are needed to counteract these offensive forces.

Air combat is the inevitable consequence.

Despite the tactical doctrine to engage the attacking forces at large distances under all weather conditions

Close-in combat within visual range cannot be avoided.

Reasons:

- the inevitable closing-in of the aircraft engaged in beyond-visual-range air combat
- delayed aircraft detection due to sensor limitations and/or signature reduction
- electronic/optronic warfare
- identification problems/need for visual identification
- the limited kill probability of guided missiles
- the limited weapon payload
- numerical superiority of the opponent
- the surprise factor

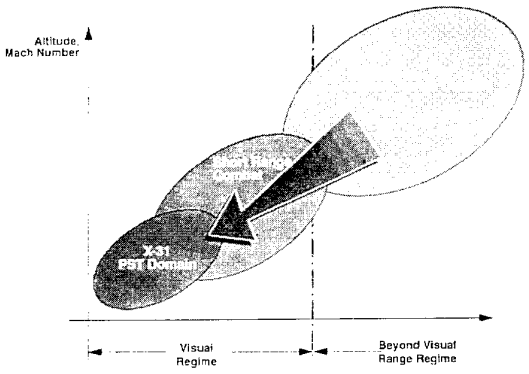

Air Combat Regimes

1.2 Close-in Combat

Due to the relatively small changes in the characteristics of weapons and avionics and the steadily increasing performance of combat aircraft, the basic tactics of close-in combat – turning maneuvers to gain the firing position in the rear hemisphere of the opponent – have remained the same for decades. Only the spatial dimensions have changed and the physical stress of the pilots has increased.

The introduction of modern short-range missiles having the capability to attack the target from all directions has led to a change of the combat tactics and – as a result – to new requirements for fighter aircraft.

After its recognition in the mid 1970s, this problem was investigated in great depth by conducting a large number of digital and manned air combat simulations.

The results showed a strong predominance of firing opportunities in the front aspect and high aircraft losses on both sides. At the same time, the combat profiles showed a strong change from steady to unsteady maneuvers with a decrease in the mean air speed.

The problem identified was the insufficient maneuverability and agility of conventional fighters at low speeds and at high angles of attack as well as the danger of entering uncontrollable flight when approaching the stall boundary. The loss of control in this angle of attack regime resulted in aircraft crashes time and again.

Only an improvement of the aircraft stability and control characteristics in this regime promised a marked increase of one's own survivability and of the opponent's loss rate.

- Weapon launch mainly from the front aspect
- Predominance of unsteady maneuvers
- Shorter flight times under high-g conditions compared to present weapon systems
- Lower mean flight speeds
- Shorter periods of firing opportunity
- Combat in a smaller air space
- Importance of quick pointing
- Small turn radii, high turn rates
- Loss of defensive sanctuary in the front aspect

☞ **Decisive:**
Scoring of kill before adversary gains firing opportunity

Results of Close-in Combat Simulation (1)

Paper presented at the Flight Mechanics Panel Symposium held in Turin, Italy, from 9-13 May 1994.

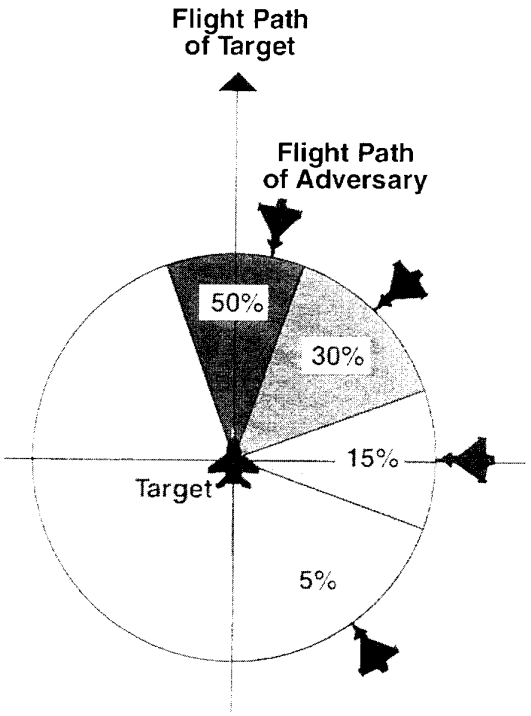

Statistical Distribution of the Attack Aspect Angle

Results of Close-in Combat Simulation (2)

2. THE IDEA

The following solution, developed by Dr. Wolfgang Herbst, was a great technical challenge and was disputed both by engineers and by tactics experts:

A new fighter should be capable of executing tactical maneuvers up to an angle of attack (AOA) of 70 degrees (which is far beyond the stall AOA) without the pilot losing control of the aircraft (poststall capability, PST).

This capability extends aircraft performance with respect to

- deceleration capability
- turn rate and turn radius

and

- pointing capability for weapon firing

considerably and results in a distinctive improvement of the tactical advantages in close-in combat.

The prerequisite for these capabilities is the use of thrust vector control to boost or even replace the aerodynamic controls which lose their effectiveness at low speeds and in the post-stall regime. (A specification for an integrated thrust vectoring nozzle was developed by MBB and was distributed to all western engine manufacturers in the late 1970s.)

The technical development of the PST capability requires the application of new technologies in the areas of aerodynamics (separated vortex flow), propulsion (inlet aerodynamics and jet deflection) and, in particular, flight control (unstable configurations, digital flight control systems, integrated thrust vector control).

With the demonstration of the practicability of the PST concept the last unexploited field of aviation – the safe control of an aircraft in the precarious stall and post-stall regime, that could not be utilized up to now – is conquered.

In a large number of technical studies and tactical simulations the technical feasibility and tactical advantages of this new concept was investigated beginning in 1975. The benefits were found to be unexpectedly high, but this also applied to the technical risk.

The search for German and/or European partners that were prepared to share this risk and to conduct an experimental program on the basis of this promising new idea was without success. Also, the benefits of such a demonstrator program was disputed among the potential users of PST for a long time.

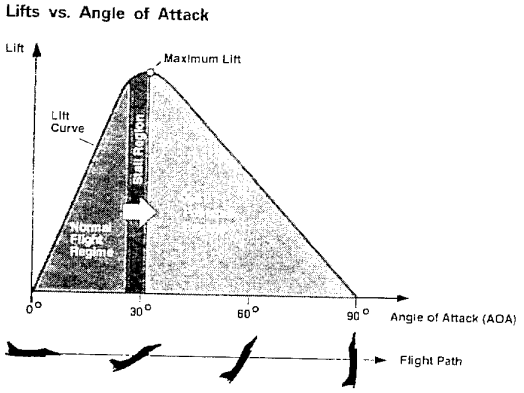

Lifts vs. Angle of Attack

3. THE PROGRAM

3.1 The Partners

Due to a number of technical publications on the subject, the PST concept became well-known throughout the world. However, the US firm Rockwell International (RI) was the only aerospace company that had a strong interest in cooperation. Together with RI the Defense Advanced Research Program Agency (DARPA, a US government agency dedicated to the development of high-payoff, high-risk technologies) could be won for such a cooperative program. In 1985 DARPA commissioned RI with the first study contract which included a subcontract to MBB.

Negotiations between DARPA and the German MOD led to the signing of a "Memorandum of Agreement" in May 1986. Initially, the aim of the agreement was the joint development and testing of two demonstrator aircraft to prove the technical feasibility of the PST concept. Later on, demonstration of the tactical benefits was added.

An exceptional stroke of luck was the "Nunn-Quayle Initiative" for international technology development launched by the US at the time. The kick-off financing made possible by this initiative was decisive for the program.

The main reason for the participation of Germany was not that country's financial contribution but the fact that the conceptual idea had been developed there and a lot of basic technology work had already been performed in the areas of aerodynamic, flight control and thrust vectoring.

The program was given the designation X-31. It was the first international experimental program of the US. The US Navy was commissioned by DARPA to manage the program. On the German side it was the Bundesamt für Wehrtechnik und Beschaffung (BWB). RI and MBB were the corresponding industrial contractors. The Wehrtechnische Dienststelle (WTD-61) and the DLR were engaged in the late 1980s to participate in the program.

In 1992 the US Air Force (USAF) and the National Aerospace Association (NASA) joined the program on the US side. Since April 1992 flight testing is conducted at NASA Dryden (Edwards Air Force Base).

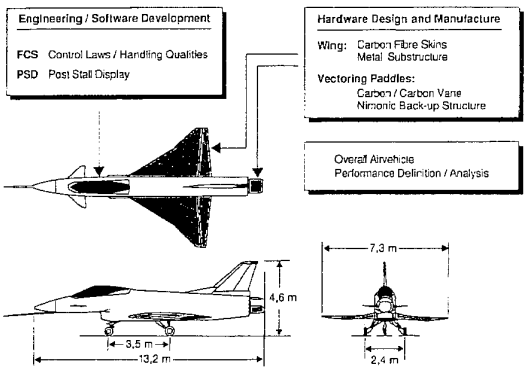

Dasa Workshare

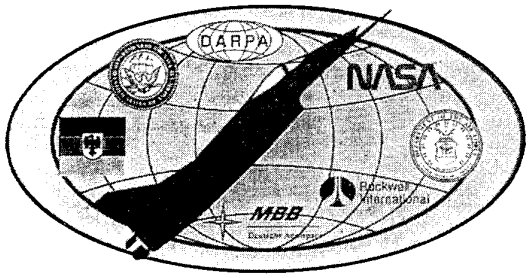

ITO Logo, Partner

3.2 Work Sharing

To keep program costs low, a precise work sharing was defined from the very beginning to avoid work redundancy. Also, clear responsibilities and competences were layed down.

The basic data of the **delta canard configuration** were taken by RI from previous JF90 work by MBB (wing and tail geometry, engine inlet concept). The aircraft was scaled down from a twin-engine to a single-engine design.

The German work share comprised the development and manufacture of

- the wing in carbon fiber composites (preparatory work for EF2000)

and

- the thrust vectoring paddles built from the high-temperature ceramic material carbon/carbon.

MBB/Dasa also was responsible for the implementation of **the heart and brain** of the airplane, the digital flight control system with integrated thrust vector control.

In the development phase of three years the engineering design work was carried out and the individual aircraft components were manufactured in Germany and the US. Aircraft assembly, system integration, and ground testing were carried out in the US. A major effort conducted by RI was the selection, procurement, and integration of the basic aircraft system components, which essentially were "of-the-shelf" equipment.

3.3 Technical Results

From the beginning of flight testing in October 1990 until the end of 1993 more than 300 test flights (approximately 250 flight hours) were conducted with the two demonstrator aircraft. From the beginning, pilots from RI, MBB and the WTD-61 participated. Since 1992 pilots from the USN, USAF, and NASA joined the flight test crew. A Luftwaffe pilot joined the team in 1993.

The four important basic maneuvers of

- safe flight and maneuvering at 70° AOA
- 360° rolls about the velocity vector at 70° AOA
- post-stall maneuvers at high load factors
- the 180° J (or Herbst) turn with extremely small turn radii and high turn rates

have been successfully demonstrated.

In the summer of 1993 the X-31 was cleared for tactical utility testing.

The hopes and expectations that were placed on the demonstrator aircraft have been fully confirmed. The technical performance requirements have been completely fulfilled, and tactical maneuvering in the post-stall regime has been convincingly demonstrated.

In Nov./Dec. 1993 the flight envelope was extended into the supersonic flight regime and flights with a helmet mounted display (HMD) were conducted. The objective of the latter flights is to flight-test special display symbologies developed by Dasa to aid the pilots in the task of spatial orientation in the new PST maneuvers.

Utilization of thrust vectoring also in the supersonic flight regime and HMD testing are two objectives of a possible extension program that could be conducted after the regular X-31 program is terminated in 1994.

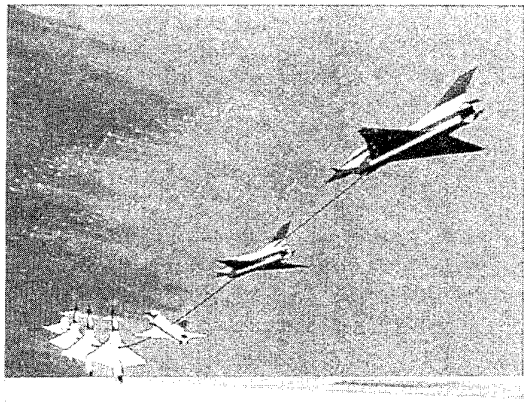

Transition into the Poststall regime (Pitch pointing)

Poststall Maneuvers (1)

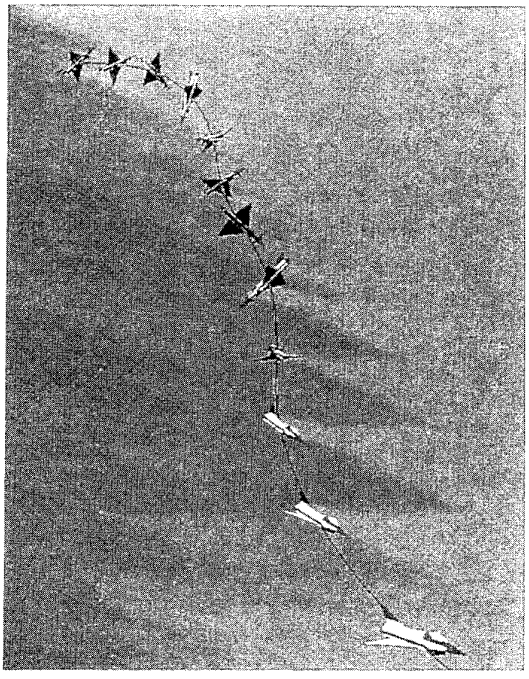

360° Roll at 70° AOA

Poststall Maneuvers (2)

3.4 Tactical Evaluation

After the technical feasibility of PST maneuvering had been demonstrated, it was possible to investigate the tactical benefits of this concept.

In two simulation campaigns at the IABG dual dome facility, in which US and German fighter pilots and test pilots participated, the tactical evaluation flights were prepared and the technical personnel was familiarized with its coming task.

First, the basic tactical maneuvers of the X-31 were practised. This was followed by close-in combat (CIC) engagements against current generation fighters (F-18).

In September 1993, after a six-months training period, the tactical evaluation flights (CIC engagement, X-31 vs F-18) were initiated. Besides the technical aspects, the qualitative and quantitative assessment of the PST concept is primarily based on this tactical evaluation.

As of the end of 1993 more than 60% of the planned CIC engagements have been flown. The results are extremely encouraging:

80% of all engagements were won by X-31
11% were won by F-18
9% were counted neutral

It can be expected that these results will change very little by the end of the complete tactical evaluation program.

With the above air combat results, the tactical benefits of PST maneuvering has been impressively demonstrated. This design concept can, therefore, be included in any future considerations.

However, it has to be pointed out that the dominant superiority as demonstrated in 1 vs 1 close in combat engagements is likely to be reduced in a multibogey situation.

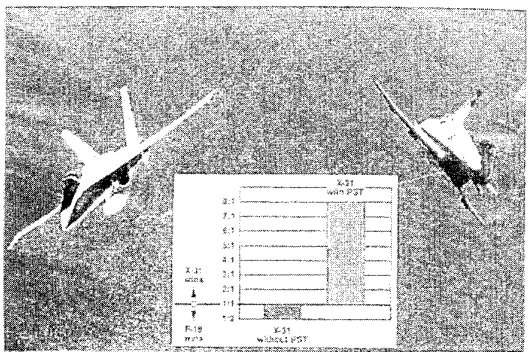

Close-in Combat Effectiveness

3.5 Time Schedule

The X-31 program was planned on the basis of the following premises:

- low-cost approach
- small integrated teams
- no redundant work
- clear responsibilities
- strict program management

Only for years elapsed from the beginning of detailed design until the beginning of flight testing. 3.5 years of flight testing (of which 1.5 years were devoted to the expansion of the conventional flight envelope) for the opening of a fundamentally new flight regime that had previously been inaccessible and unexploited is a remarkable success for experimental programs of this type.

The 160 flights conducted in 1993 also constitute a new record for X-programs.

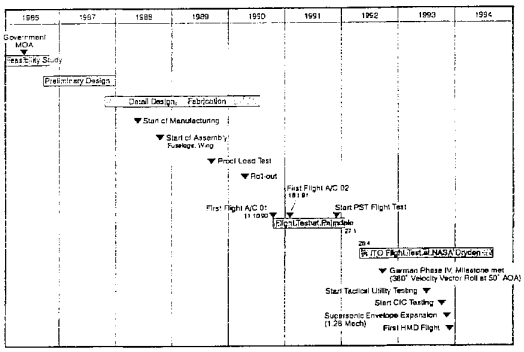

Program Milestones and Schedule

3.6 Cost

It would not have been possible for Germany to conduct such a high technology program without the assistance of a technically and financially powerful partner.

The possibility of procuring existing (off-the-shelf) equipment on the US side was a decisive prerequisite for the success of the program. (These costs are not included in the figure shown on the next page).

Averaged over all phases, the German share of the total program costs (400 million DM) was approximately 25%. Including the expenditures of the DLR and the WTD-61, the German cost share is about 100 million DM. Dasa contributed about 35 million DM in company funding.

It should be stressed that despite its under par financing, the German side has full access to all program results.

Of the total program costs, approximately 75% went into the design and manufacture of the two demonstrator aircraft and "only" 25% into flight testing. Because of this, further use of the demonstrator vehicles for testing other technologies is a very attractive option.

		BWB*	MBB/DASA	BWB + MBB/DASA
Feasibility Study		3.0	0.4	3.4
Detail Design through Technical Flight Test	Part 1	5.5	0.7	6.2
	Part 2	25.0	34.9	59.9
	Part 3	18.4	2.0	20.4
Sum		48.9	37.6	86.5
Tactical Utility Testing		8.0	—	8.0
Total		59.9	38.0	97.9

* without DLR and WTD-61

X-31, German Funding Distribution (Mio. DM)

4. POSSIBLE APPLICATIONS

The original idea – to have the PST capability included in the technical requirements for the new European fighter EF-2000 – could not be realized because of the unforeseeable technical risks and the acceptance problems of the new concept at the time.

In the mean time the PST concept has won recognition. In other programs (X-29, F-18 HARV, YF-22, F-16 MATV, F-15 ACTIVE) and within other antions (SU-27, MIG-29, SU-35) considerable efforts were made to acquire and apply this technology.

The F-16 MATV and the SU-35 programs show that both retrofitting of the PST technology and its integration into new aircraft are possible and aimed at. This also applies to the German/European side, where a later retrofit of the EF-2000 and an integration of thrust vector control into future combat aircraft are being considered.

Although the idea of exploiting the PST regime has its origin in military aviation, the transfer of this technology to civil aviation and its exploitation by transport aircraft is to be expected.

Possible applications of the technologies developed in the X-31program are:

- thrust vector control and trimming for performance improvement and accident avoidance
- partial/complete replacement of stabilisation and control surfaces by thrust vectoring
- reduction of take-off distances
- steep landing approaches
- use of thrust vectoring upon loss of an aerodynamic control surface (due to battle damage, for example).

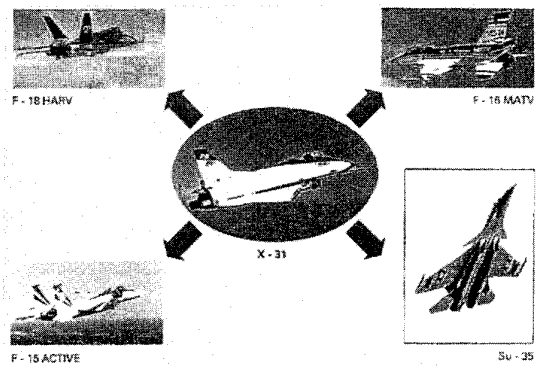

Experimental Programs Poststall-/Thrust Vectoring Technology Development

5. THE X-31 FOLLOW-ON PROGRAM

As the time period between successive aircraft generations is becoming longer and longer and, as a result, the number of weapon system updates is increasing steadily, the timely development and demonstration of new technologies is becoming increasingly important. Also, experimental programs are gaining importance for maintaining a high-technology capability.

Due to the fact that the development costs have been paid for and because of its high potential for further usage, the X-31 is an attractive candidate for a follow-on program with the following key objectives:

- Further research with regard to flying in the high AOA regime (computation, influencing and control of separated vortex flows. High AOA air data systems. Definition of design requirements for future aircraft with PST capability)
- Exploitation of the thrust vectoring technology (performance improvement as a result of the additional trim and control capability, size reduction of the aerodynamic stabilisation and control surfaces)
- Development and integration of systems for increased crew assistance (helmet mounted display, pilot associate, crew assistant) and improved pilot training (in-flight weapon system simulation, coupling of on-board systems with ground-based simulators)

Because of its availability and relatively low operating costs, the X-31 is an attractive candidate for testing these technologies. If the PST flight regime is to be included, the X-31 demonstrator aircraft is a must.

The industry has worked out plans for the above technology programs and these have been submitted to the appropriate government agencies.

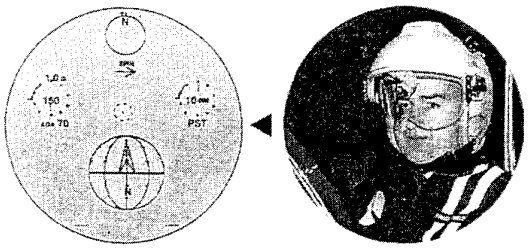

Helmet Mounted Display

6. CONCLUSION

The technical feasibility of PST-maneuvering has been proven.

The tactical utility of PST-maneuvering has been successfully demonstrated.

Application of X-31 technologies

- Control law design
- Thrust vectoring
- High AOA aerodynamics
- HMD utilization

is considered for weapon system improvement and follow-on programs.

The X-31 has used-up only 50% of its design life and is an attractive candidate for a future joint technology development, demonstration and evaluation program.

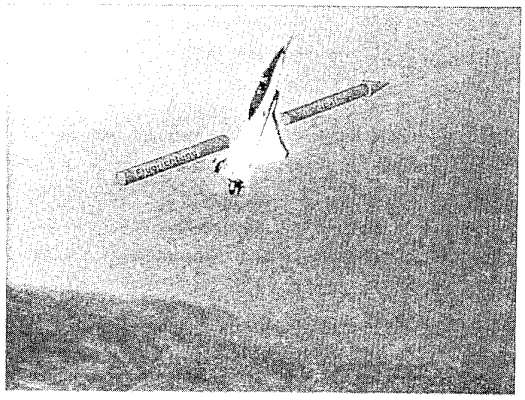

X-31 in a Poststall Maneuver

In Memoriam

Dr. Wolfgang B. Herbst, the inventor, mentor and strong proponent of tactical maneuvering in the Poststall regime initiated the X-31 program together with Michael Robinson and Jim Album (DARPA). The German FMOD, in particular Christian Biener and Helmut Heumann, subsequently supported the feasibility study.

Dr. Herbst was instrumental in keeping the program alive throughout the years and developed and contributed many inspiring ideas which were successfully incorporated into the program. He was convinced about his "dream" despite the many years of heated discussions and lack of support.

The man with the vision of Poststall flying could not live to see his dream come true: He died in his home built subscale Focke-Wulf 190 on the 19th of October 1991, two months before the first X-31 Poststall flight.

The X-31

The First International US/German Experimental Program

Deutsche Aerospace

Aircraft
Military Aircraft

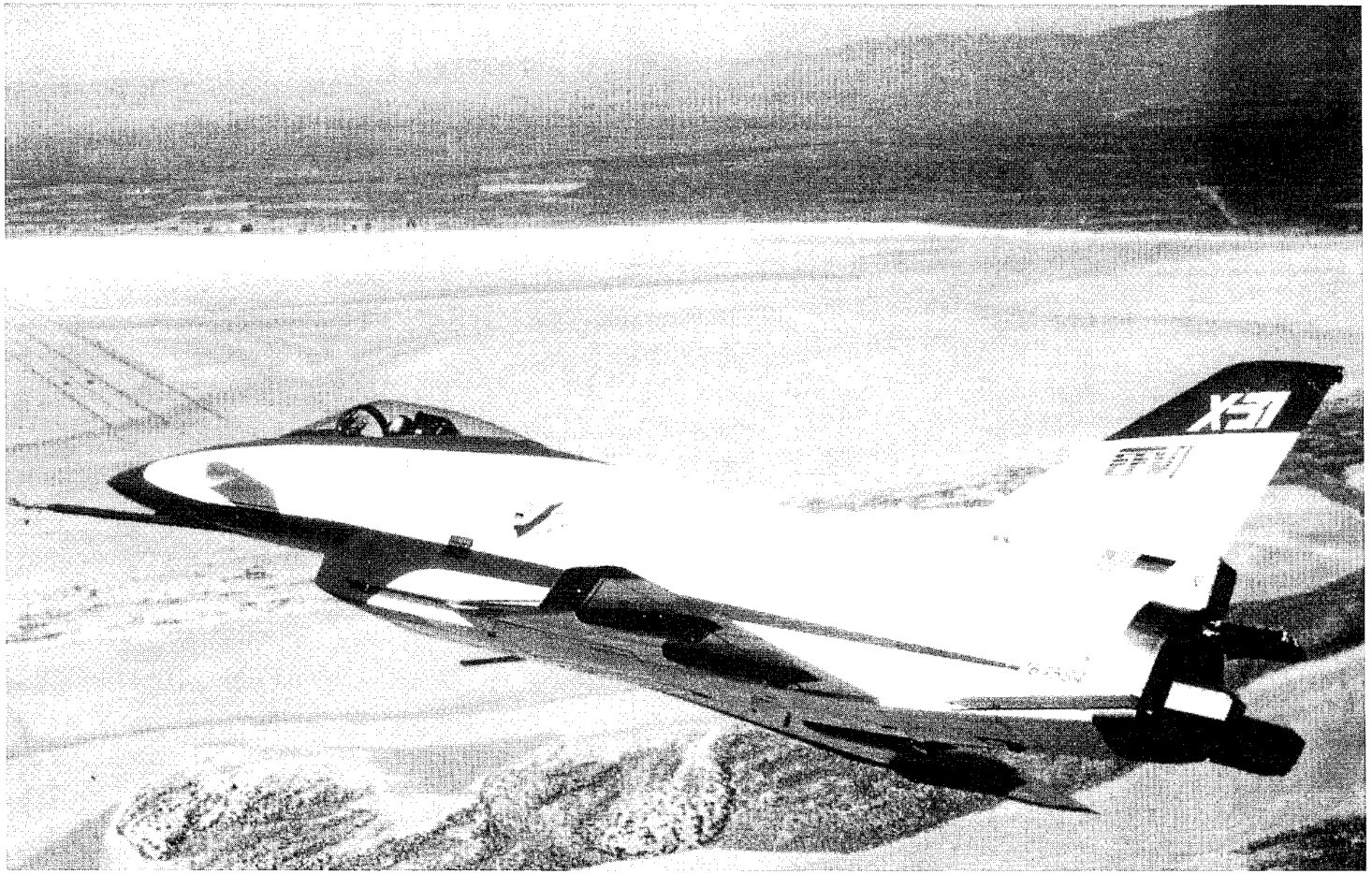

ADVANCED FLIGHT CONTROL TECHNOLOGY ACHIEVEMENTS AT BOEING HELICOPTERS

Kenneth H. Landis
Senior Manager, Flying Qualities

James M. Davis
Chief, Flight Control Design

Charles Dabundo
Manager
Flying Qualities

James F. Keller
Senior Technical Specialist
Flying Qualities

Boeing Defense and Space Group, Helicopters Division,
Mail Stop P32-31, P.O. Box 16858, Philadelphia, PA 19142, USA

SUMMARY

Over the last two decades, flight control system requirements have been in a state of transition. Rotary wing missions have become more demanding, requiring vehicle management systems capable of conducting highly aggressive missions under night / adverse-weather conditions in severe electromagnetic environments. The digital, fly-by-wire / optics control system technologies developed at Boeing Defense and Space Group, Helicopters Division to meet these air vehicle requirements are overviewed. These technologies, which integrate digital multi-mode control laws and sidestick controllers within redundant-reconfigurable architectures, provide the rotorcraft capabilities required for the 21st century. The advances in flight control design, as developed during various technology demonstrator programs and applied in production of the V-22 Osprey tiltrotor and the RAH-66 Comanche scout / attack helicopter , are summarized.

INTRODUCTION

Boeing Helicopter 's role in the technology advancement of full-authority digital fly-by-wire systems was spurred by requirements to improve handling qualities and mission effectiveness, alleviate failure transients, and reduce weight and maintenance activities. The transition of Boeing research programs into production readiness is illustrated in Figure 1. Development efforts on the Tactical Aircraft Guidance System (TAGS), Heavy Lift Helicopter (HLH) and Advanced Digital / Optical Control System (ADOCS) Demonstrator Programs form the basis for design of the V-22 and RAH-66. Currently, the V-22 is progressing through a five-year Engineering Manufacturing Development (EMD) contract for further refinement and demonstration of a production design. The aircraft is being co-developed by Boeing and Bell Helicopter Textron. Lessons learned from the V-22 flight test program are influencing design of the first RAH-66 prototype scheduled for flight in 1995. The Comanche is being co-developed in a teaming arrangement between Boeing Helicopters and Sikorsky Aircraft Division of United Technologies Corporation. Boeing has lead responsibility for the flight control system development and mission equipment integration on both programs.

Safety is the primary objective of flight control system development activities at Boeing. System design concepts are guided by a "safety first" design philosophy, wherein a highly reliable control path is always maintained, thereby minimizing the effects of system failures, and constraining the effects of indeterminate failures. Production type safety requirements are imposed at the outset of the design process, and although backup systems have been available on some programs (e.g. TAGS, ADOCS, and V-22), the design has never relied on them.

Flight control systems integration at Boeing Helicopters covers a wide range of technology disciplines as illustrated in Figure 2 and summarized relative to major programs in Figure 3. With higher levels of integration, advanced flight control systems have taken on a centralized role and have been renamed vehicle management systems. Significant areas of emphasis have been directed toward the following:

- **Improved flight safety and reliability** through the implementation of an architecture which minimizes the effects of system failures through intelligent fault detection algorithms.
- **Advanced control law techniques** using model following control applications for tailoring of the aircraft response to achieve favorable handling qualities and structural loads characteristics.
- **Increased Integration of mission required functions** within the control system including engine, navigation, and fire control systems, along with integration of advanced cockpit controllers.
- **Enhanced mission effectiveness** through selectable control law moding which allows optimization of control characteristics for each task, and automatic modes, such as programmed evasive maneuvers, to counteract known threats.

The purpose of this paper is to highlight advances in flight control design which provide mission capable aircraft for the future. Important developmental programs conducted over the last several decades are discussed. A detailed discussion of vehicle management system design approaches provides insight into the control law architecture / implementation used in Boeing rotorcraft. Integration of subsystems to enhance efficiency, and optimization of control law moding are highlighted as features required for a mission capable aircraft. The control law process employed to design and develop these features is provided for reference. The culmination of this experience as related to the RAH-66 Comanche and the V-22 Osprey Programs is discussed in detail.

Published in the International Journal of Control 1994,vol.59, No. 1,263-290

Paper presented at the Flight Mechanics Panel Symposium held in Turin, Italy, from 9-13 May 1994.

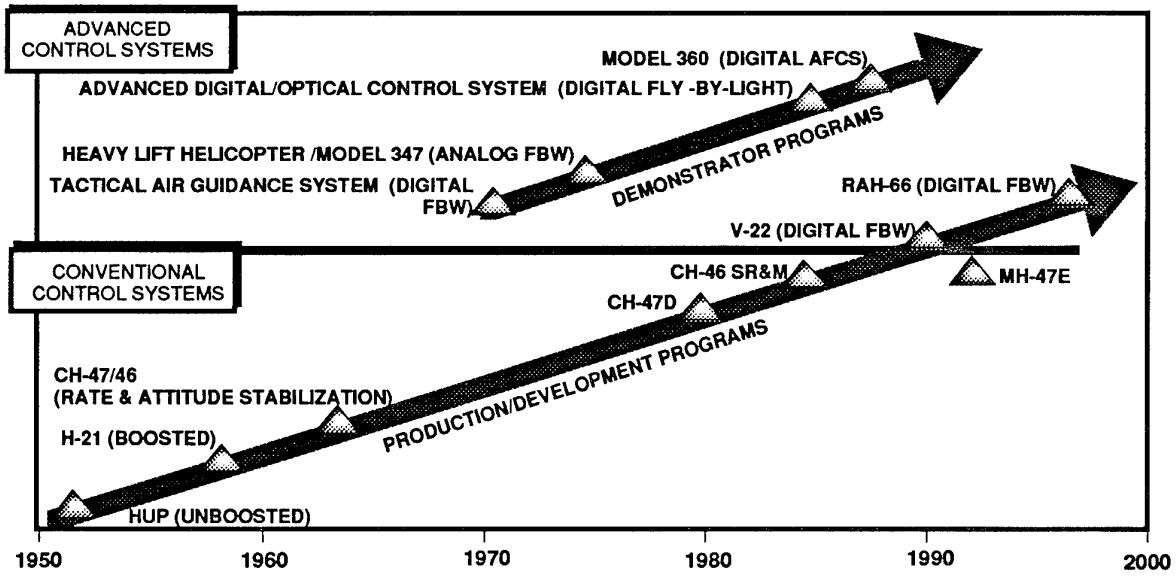

Figure 1 Boeing Helicopters Flight Control Technology Advancement

DEVELOPMENT PROGRAM OVERVIEW

Tactical aircraft guidance system

Fly-by-wire efforts at Boeing began in the late 1960's with the Tactical Aircraft Guidance System (TAGS) research program. TAGS incorporated a triplex full-authority digital system using a sidearm controller. The advanced control concepts developed on TAGS, including ground referenced velocity vector control, command modelling and sensor complementary filtering, are the basis of many features included in the RAH-66 and V-22.

Heavy lift helicopter

Advancements in flight control technology were demonstrated from 1971 to 1974 as part of the U.S. Army Heavy Lift Helicopter Program (Davis 1977). A dual-fail operational full-authority triplex fly-by-wire flight control system was designed and flight tested on the Boeing Model 347 HLH demonstrator helicopter shown in Figure 4. As described in Landis 1975, reconfigurable Automatic Flight Control System (AFCS) modes provided Level 1 handling qualities along with a fully automatic approach to hover capability that enabled the pilot to perform rapid and precise external load operations in all weather conditions. With the Hover Hold mode engaged, the aircraft demonstrated position hold to within 7.0 inches in steady winds of 12 knots, gusting to 24 knots. A load controlling crewman, using a four axis sidearm controller and operating through the Hover Hold Mode, demonstrated impressive capability to precisely control the aircraft for rapid hookup and precision placement of external loads. An automatic load stabilization system provided a significant increase in load damping, both in hover and forward flight, to decrease pilot workload and improve performance during external load operations.

Advanced digital/optical control system (ADOCS) demonstrator

Under a U. S. Army contract, Boeing designed and flight tested the Advanced Digital / Optical Control System (ADOCS) during the 1980's. Over 500 hours of testing with the digital-fly-by-optics control system were accomplished on a modified UH-60A

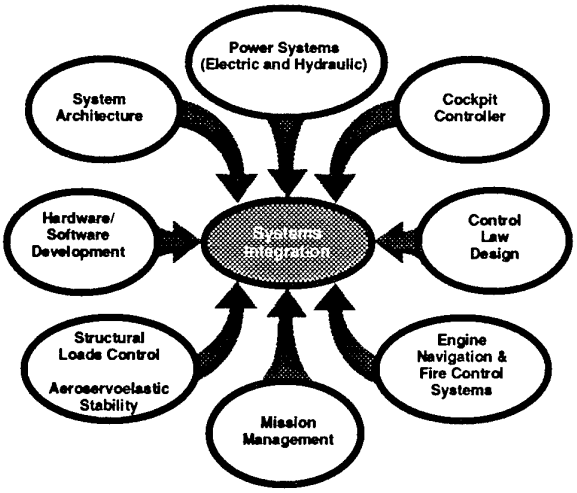

Figure 2 Elements of Flight Control System Integration

Program		TAGS	HLH	ADOCS	V-22	RAH-66
VMS Technology	Flight Hrs.	139	316	551	700+	0
Explicit Model Following		●	●	●	●	●
Multi-mode Control Laws		●	●	●	●	●
Sidestick Controllers		●	●	●		●
Integrated FCS / Navigation				●	●	●
Integrated FCS / Engine					●	●
Integrated Fire & Flight Control						●
Advanced Redundancy Mgmt.		●	●	●	●	●
Integrated Diagnostics					●	●

Figure 3 Boeing Helicopters Vehicle Management System Experience

Black Hawk (Figure 4). The ADOCS program was sponsored by the Army Aviation Applied Technology Directorate (AATD), Fort Eustis, Virginia to demonstrate a battlefield compatible helicopter with a flight control system that would enhance aircraft mission capabilities through decreased pilot workload and improved handling qualities. An increasing hostile ballistic environment, along with consideration of the effects of lightning and electromagnetic interference in the battlefield of the future, led to the selection of fiber optic technology for the ADOCS flight control system. A primary objective of the ADOCS program was to accelerate advancements in rotorcraft control system development, especially in the application of multimode, mission tailored control laws for a scout / attack helicopter. The program also accomplished complementary development of sidestick controller technology.

The early stage of ADOCS development included a comprehensive piloted simulation study (Landis and Glusman 1984) of sidestick controller configurations and levels of system command / stabilization for use under both day and night-time conditions. Various sidestick controller designs, ranging from a right hand 4-axis controller to a more conventional (2+1+1) configuration (pitch and roll control provided through a sidestick, separate pedals for yaw, and a collective controller) were evaluated for numerous attack helicopter flight control tasks. The test matrix also evaluated controller compliance characteristics ranging from rigid force controllers to compliant small displacement controllers. As a result of this simulation study, rigid force controller configurations were eliminated prior to flight test. Throughout the demonstrator program, design improvements were made to the cockpit controllers, culminating with flight demonstration of a small displacement 4-axis sidestick configuration and a (3+1) configuration comprised of a three-axis small displacement sidestick for pitch, roll, and yaw control, and a left-hand medium displacement collective controller with 4.0 inches of total travel. ADOCS flight testing identified the (3+1) controller configuration as the most promising, leading to its application in the RAH-66. In addition, lessons learned about desirable sidestick controller characteristics are being applied in the design of the RAH-66 Comanche.

The ADOCS Demonstrator aircraft provided an excellent testbed for demonstration of major advancements in multimode explicit model following control laws to enhance scout / attack helicopter mission performance. The reconfigurable, digital fly-by-light control system provided the capability to evaluate a wide variety of selectable control laws. Overall success of the ADOCS control law design in providing excellent scout / attack helicopter mission performance and handling qualities was demonstrated in 1987 during nap-of-the-earth (NOE) flight testing conducted by the Army Aviation Engineering Flight Activity (AEFA) at the Army Fort Indiantown Gap test facility. Documentation of the ADOCS Demonstrator design and flight test results is found in Glusman 1987 and Glusman 1990.

RAH-66 Comanche

The ADOCS program preceded two pivotal events in the helicopter handling qualities community, namely, the initiation of the RAH-66 scout / attack helicopter program and the definition of a new handling qualities specification (Aeronauti-

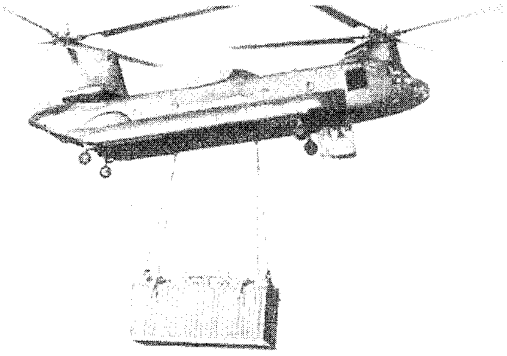

MODEL 347 HLH DEMONSTRATOR

ADOCS DEMONSTRATOR

V-22 OSPREY

RAH-66 COMANACHE

Figure 4

cal Design Standard ADS-33C, August 1989). The RAH-66 Comanche as shown in Figure 4 will be the first helicopter to be procured under the new ADS-33 handling qualities specification. Designed to be the next generation scout / attack helicopter , the Comanche incorporates many advanced technology features, including a FANTAIL antitorque system and a bearingless main rotor with high equivalent flap hinge offset. It will also be the first Army helicopter with a fully digital fly-by-wire control system and a three-axis sidestick controller . The technology base developed during the ADOCS program was well suited for direct extension to the Comanche design.

The Comanche flight control system utilizes a multi-mode control law design that enables the pilot to select flight control system characteristics according to the handling qualities demands of each mission. In satisfying the requirements of ADS-33, the default (normal mode) control laws are designed to achieve Level 1 handling qualities ratings in day / VFR conditions (Useable Cue Environment (UCE) = 1 in the nomenclature of ADS-33). Selectable modes and vision aids allow the Comanche to remain Level 1 under degraded visual conditions (UCE 2 and 3), and provide further handling qualities enhancements for automated navigation and targeting. In addition, adequate (Level 2) handling qualities are provided for safe return-to-base capability in the unlikely event of multiple flight control system (FCS) failures.

The Comanche flight control system capitalizes on many advanced cockpit design technologies. To meet stringent weight and cockpit ergonomic specifications while providing the desired handling qualities, the primary pilot controller for the longitudinal, lateral, and directional axes is a small-displacement sidestick controller, a direct outgrowth of the ADOCS program. Full-time vertical control is provided by a left-hand medium-displacement collective lever having a total travel of 6.0 inches. When the Altitude Hold mode is engaged, a limited small-displacement vertical control axis provided on the right-hand sidestick frees up the pilot's left hand for cockpit management tasks. The Comanche also uses a binocular helmet mounted display (HMD) as its primary instrument display to allow the pilot to keep "eyes out of the cockpit" at critical times. A visual and aural cueing system reduces workload and allows the pilot to access full aircraft capability throughout the flight envelope while not exceeding limits.

V-22 Osprey

The V-22 Osprey (Figure 4) is advanced technology tiltrotor developed for multi-service use in a wide variety of missions. It is capable of airspeeds ranging from 45 knots rearward in VTOL mode to 345 knots forward in airplane mode. The aircraft, described in detail in Rosenstein 1986, is characterized by a high, forward swept wing and H-tail empennage. The tilting nacelle at each wing-tip are comprised of an engine, transmission, and three bladed rotor and rotor swashplate controls. The rotors are mechanically interconnected for continuous power transmission during single engine operation. The V-22 flight control system is a full authority, two-fail operative, triplex digital fly-by-wire system. Control of the V-22 in the hover / lowspeed regime is achieved through cyclic and collective inputs to the swashplate and power demand signals to the Allison T406 engines. Thrust vectoring is achieved by variation of the nacelle incidence between 0 degrees in airplane mode and 97.5 degrees (7.5 degrees aft of vertical) in helicopter mode. Conventional airplane control surfaces (elevator , rudder, flaperons) are active throughout the flight envelope, while helicopter swashplate controls are phased out in forward flight as nacelle incidence is decreased. Figure 5 summarizes the V-22 control mechanisms used in the helicopter and airplane flight modes.

The cockpit controls of the V-22 include a conventional displacement center stick, directional pedals, and a small displacement thrust control lever (TCL) having a total travel of 4 inches. A programmable force-feel system provides airspeed scheduled force-feel characteristics throughout the flight envelope. Early in the full-scale development program, a design study was conducted to evaluate conventional cockpit controls versus a 2+1+1 sidestick controller configuration. In this study, handling qualities were judged to be similar with either control configuration design. Although weight and control system complexity are reduced with a sidestick configuration, conventional controls were selected for the V-22 aircraft to reduce program risk and provide for an easier transition of pilots from other VTOL aircraft.

Development of the V-22 has involved a balance between handling qualities, structural, and aeroservoelastic stability requirements. The stringent V-22 design requirements of Military Specification SD-572 mandate a maneuver envelope to 4.0 g's at speeds up to 345 knots (Figure 6). These requirements, along with the wide range of flight conditions within the operational flight envelope present design challenges not seen in conventional helicopters or fixed-wing airplanes. The aircraft components must provide the performance to hover at 47500 pounds gross weight, the agility to attain Level 1 handling qualities for aggressive operational mission tasks, and the

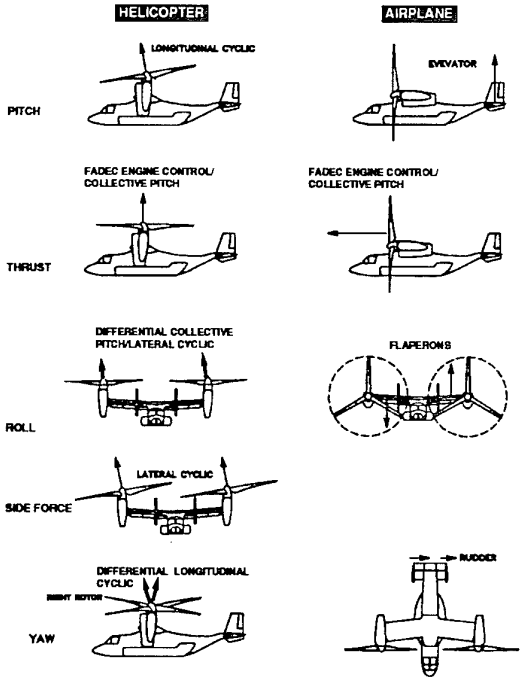

Figure 5 V-22 Helicopter and Airplane Flight Control Configuration

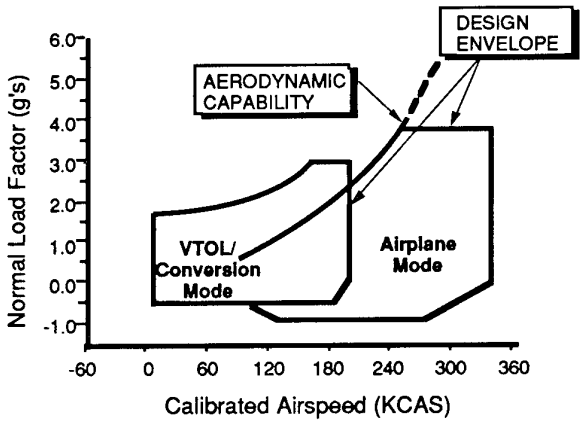

Figure 6 V-22 Maneuver Envelope

strength to withstand maneuvering at maximum aerodynamic capability as limited by the FCS (Figure 6). Further challenges are imposed by aeroservoelastic stability characteristics of the V-22 due to the proximity of structural and rigid body mode frequencies. The flexibility offered by digital flight control systems has enabled the achievement of an effective design for the V-22 which satisfies all requirements.

FLIGHT CONTROL LAW DESIGN

Flight control laws are designed to provide desired mission control functions, along with acceptable handling qualities, flight loads, and aeroservoelastic (ASE) stability characteristics. Specific flight control law features used to meet specification requirements include forward loop control shaping to quicken the aircraft response to pilot inputs, control command filtering to eliminate pilot bio-mechanical feedback for acceptable closed loop structural mode damping, and airspeed / nacelle gain scheduling to tailor aircraft stability and control characteristics throughout the flight envelope. Control law algorithms are also utilized to provide acceptable maneuvering flight loads throughout the operational flight envelope of the aircraft.

General features of the control laws developed at Boeing which have proven successful include: (1) explicit model following control incorporated within an architecture designed to maximize safety, (2) manual / automatic reconfiguration to tailor the handling characteristics to the task at hand, (3) increased integration of subsystems such as engine control, fire and flight control, and (4) structural loads / dynamics regulating elements. Design approaches used to integrate these features and satisfy overall air vehicle design requirements are highlighted below .

Control law architecture

PFCS /AFCS Architecture

The Boeing systems design approach developed over numerous programs incorporates partitioning of control laws. As shown in Figure 7, the control laws are functionally separated into a

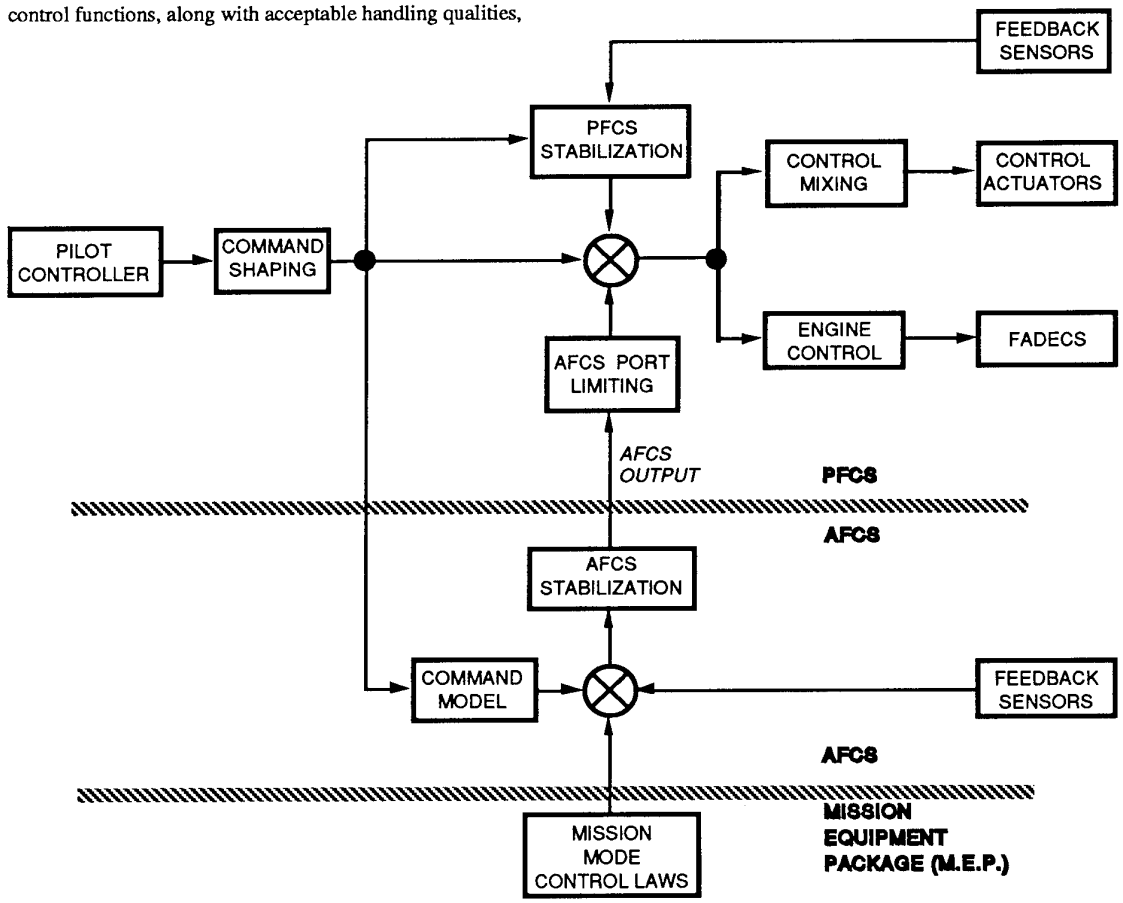

Figure 7 Flight Control Law Architecture Overview

Primary Flight Control System (PFCS) and an Automatic Flight Control System (AFCS). Each level is also physically separated using its own processor. The PFCS contains flight critical control laws and possesses a higher level of reliability than the mission critical AFCS. The PFCS must provide the minimum required flight capability in the event of multiple failures, while the AFCS provides enhanced handling qualities for mission capability under all conditions. The required level of PFCS reliability is achieved through use of a processor -pair hardware / software architecture, minimization of sensor inputs, and reduced control law complexity. The AFCS processor interfaces to the PFCS through a limit and switching function denoted as AFCS Port Limiting, which serves to isolate the AFCS in the event of detected or undetected multiple system faults.

Explicit Model Following

Explicit model following control laws are well suited for implementation in fly-by-wire digital control systems due to flexibility in the tailoring of control law characteristics. The model following design approach has been refined at Boeing to provide a control law implementation within the PFCS / AFCS architecture which is both safe and effective (Figure 7). In design of the model following control law, a cancellation of the inherent aircraft response is accomplished in the PFCS by the control shaping function. The command model function, located within the AFCS, is used to generate the desired state response of the aircraft. The desired response is then compared to the sensed states to form state errors for stability and command response augmentation. The primary attributes of model following control approach are: (1) Aircraft response consistancy over the complete range of ambient conditions and aircraft configurations, (2) Independently designed stability and command response characteristics since sensor feedback is used only to augment the trajectory with respect to the commanded aircraft state, and (3) Robust full-time feedback stabilization by minimizing errors between the desired and actual control response, and increasing stability levels for gust rejection, even while maneuvering. Since the feedback signal in each axis is an error signal based on commanded minus actual response, the sluggish response typical of a conventional SAS with high rate feedback is overcome. Furthermore, synchronization and loss of attitude stabilization while maneuvering is not required, and mode switching transients associated with a conventional synchronized attitude feedback system are eliminated.

As shown in Figure 7, the AFCS error signal is passed through a port limiting / switching algorithm which provides fail-safety in the event of multiple system failures. The port is designed to provide adequate control authority for operation of the model following control laws. The ADOCS design implemented all feedback augmentation within the AFCS, causing the AFCS port limit to saturate for large amplitude maneuvers. To reduce the occurrence of port saturation, the RAH-66 design incorporates the feed-forward angular rate response command models and the associated feedback loops in the PFCS. The rate feedback loops are only active when the AFCS is operational, but by being resident in the PFCS, they are not subject to port limiting. By providing control response fidelity with respect to the rate model in the PFCS, desired levels of control augmentation (i.e. attitude command / hold functions) can be implemented in the AFCS with a minimum port authority. Improved redundancy management algorithms to detect and eliminate failure modes of the PFCS are also implemented to maintain the required degree of system safety.

Attitude Command Model Following

As discussed above, the model following control law approach allows command response characteristics of the vehicle to be tailored based on mission requirements. Figure 8 describes the command / stabilization characteristics implemented on the RAH-66 Comanche. Since the Comanche is designed for aggressive air combat maneuver scenarios, its control laws must operate to extreme aircraft orientations. Although the angular

	COMMAND RESPONSE / STABILIZATION				
	CORE AFCS		SELECTABLE AFCS (VELOCITY STAB / ALT HOLD)		
AXIS	HOVER & LOW-SPEED	HIGH SPEED FORWARD FLIGHT	HOVER	LOW-SPEED	HIGH-SPEED FORWARD FLIGHT
LONGITUDINAL	RATE / ATTITUDE		VELOCITY COMMAND/ POSITION HOLD	ATTITUDE COMMAND/ ATTITUDE HOLD	ATTITUDE COMMAND/ AIRSPEED HOLD
LATERAL	RATE / ATTITUDE		VELOCITY COMMAND/ POSITION HOLD	ATTITUDE COMMAND/ ATTITUDE HOLD	RATE COMMAND/ ATTITUDE HOLD
DIRECTIONAL	RATE / HEADING	RATE / HEADING WITH AUTOMATIC TURN COORDINATION	RATE COMMAND/ HEADING HOLD	RATE COMMAND/ HEADING HOLD WITH AUTO-TURN COORDINATION BASED ON GROUNDSPEED	RATE COMMAND/ HEADING HOLD WITH AUTO-TURN COORDINATION
VERTICAL	RATE OF CLIMB		RATE OF CLIMB	RATE OF CLIMB /ALTITUDE	

Figure 8 RAH-66 Comanche Command Response / Stabilization Characteristics

rate sensors are based in the aircraft body axes, the attitude references need to be inertially based for l arge amplitude maneuvers. Thus, the attitude signals must be accurately transformed for precision attitude control during extreme maneuvers. To address this requirement, the Comanche design performs Euler Angle transformations on the attitude signals within the model following control law structure. The attitude errors are then inversely transformed back into the body axis, where the aircraft control is referenced. Since the Euler Angle reference system inherently possesses singularities at +90 and -90 degrees of pitch attitude, the control laws are synchronized within a narrow cone about these orientations to eliminate divergence of the attitude signal.

Control Mixing / Scheduling

Mixing of the cockpit controllers and the AFCS commands to generate required rotor, control surface, and engine commands is performed in the PFCS. Capability to vary mechanical mixing and rotor control gearing gains of current production helicopters, e.g. CH-47 Chinook and UH-60 Blackhawk, is limited, thereby restricting the total optimization of control response and coupling characteristics throughout the flight envelope. Alternatively, the Comanche features airspeed scheduled control mixing with a fully populated mixing matrix to formulate rotor control commands in the aircraft control axes. In this manner , the highly coupled high hinge of fset rotor is decoupled as a function of airspeed, providing desirable control responses in all axes over a wide range of flight conditions.

V-22 mixing is programmed to provide optimal use of both rotor and control surface commands. The mixing gains are scheduled with both airspeed and nacelle angle to provide consistent handling characteristics throughout the helicopter , conversion, and airplane flight envelope.

Ccokpit Controller Integration

Control law implementation for landing / tak eoff and control trim operation is discussed below for both conventional large-displacement center stick controls and unique-trim sidestick controllers.

Automatic Trim Transfer

Regardless of the type of controller selected for the aircraft, the explicit model following approach may result in the storage of control trim in the AFCS . Therefore, control laws are required to automatically transfer control trim of fsets from the limited authority AFCS to the PFCS.

The conventional displacement controller used on the V-22 has a relatively large range of control motion. Stick positions are sensed electronically by LVDT's and passed to a digital flight computer which processes rotor and control surface commands. Pitching moment variation due to changes in longitudinal center - of-gravity and nacelle position create a wide range of possible trim elevator positions at a given airspeed. As illustrated in Figure 9, parallel backdriving of the longitudinal stick is utilized to avoid storing trim within the limited authority AFCS, thereby reducing the potential for port saturation. The low frequency component of the AFCS port signal is fed to a backdrive actuator which smoothly drives the stick to reduce the AFCS offset to zero. In a trim condition, the AFCS port is centered, and the cockpit stick trim position provides the pilot a tactile cue of the actual aircraft rotor and control surface position.

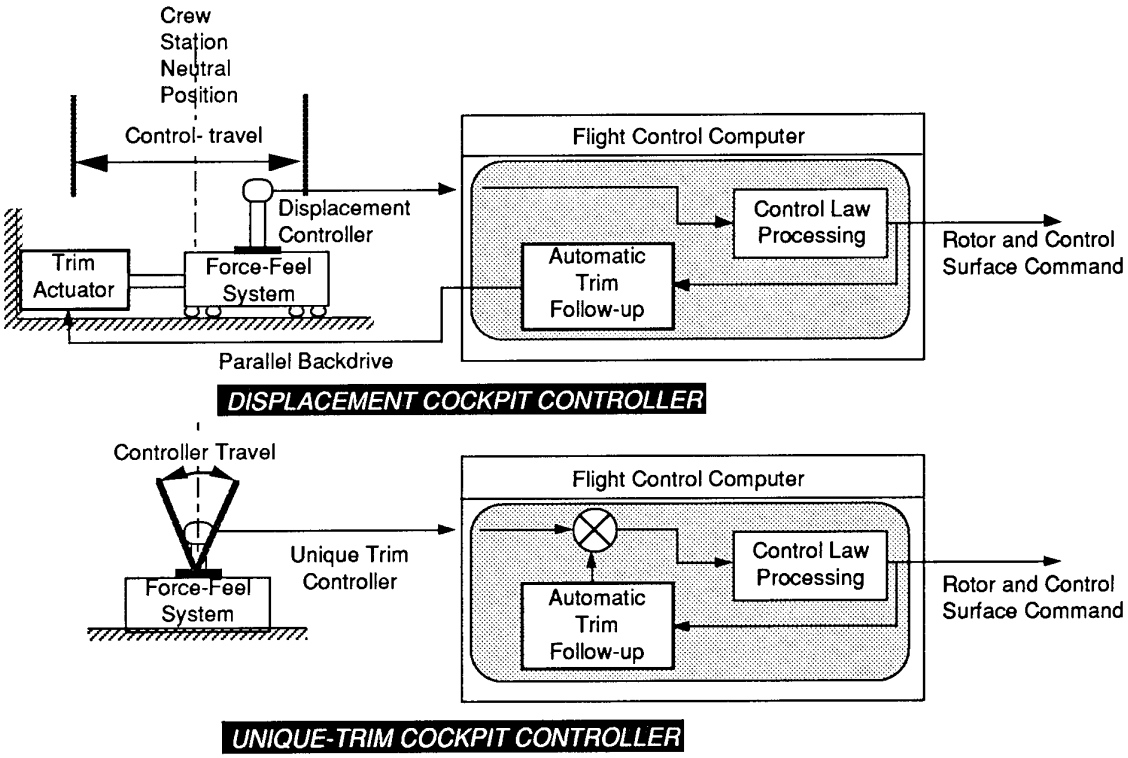

Figure 9 Cockpit Controller Integration - Displacement versus Unique Trim

Aside from the obvious physical differences with respect to conventional displacement controls, sidestick controllers are unique in the manner in which aircraft trim is represented. The unique trim sidestick controller, because of its size and mechanical simplicity, cannot provide sufficient motion to reflect both trim and maneuvering commands. Therefore, the sidestick uses a common, or unique, centered reference position to represent trim for all flight conditions. Relative to the fixed trim position, the aircraft exhibits neutral stick static stability to the pilot. The actual trim control surface position must be stored within the control laws. The low frequency component of trim resident in the AFCS output is continually transferred to the PFCS so all trim resides at a single point in the PFCS regardless of augmentation level. In this manner, the transients associated with deselection or loss of the AFCS are minimized.

Landing and Takeoff / Ground Handling

As shown on Figure 9, displacement cockpit controllers provide a direct relationship between cockpit stick position and the resultant control surface position. Hence, the pilot is provided with cues to establish a control strategy for landing and take- off. Pilots rely on experience to anticipate the magnitude of control displacement required for a smooth transition between a ground and fly state. In contrast, unique trim sidestick controllers do not provide such cues. With a sidestick controller the pilot can no longer judge control surface position based on stick deflection since the trim is stored in the FCS and not at the pilot controller. This sidestick limitation is of no consequence for hover or forward flight operations where the pilot adjusts the control input based purely on aircraft response. In addition, pilot workload with both controller configurations is increased during landing or take-off since the pilot must compensate for a change in control responsiveness which occurs upon transition from a ground to fly state condition.

Sidestick controller handling qualities during landing and takeoff maneuvers was identified as an area of risk during ADOCS Demonstrator flight testing. A detailed design study, including piloted simulation along with flight testing on the SHADOW aircraft, was conducted for the Comanche to resolve key control law issues regarding the landing and take-off task. The study, discussed in Bauer 1993, produced new control law features for the Comanche to improve pilot kinesthetic cues, resulting in reduced workload and improved task performance for landing and takeoff maneuvers. To accomplish this, in-flight control laws are progressively altered to a ground state mode, based on the combinations of landing gear constraint imposed by ground contact. Weight-on-wheel switches are installed in each landing gear strut to sense ground and flight states. The sensed weight-on-wheel state is filtered to prevent rapid toggling between logic states during a light-on-gear condition.

The combinations of gear contact, listed sequentially for a landing maneuver, include:

- initial contact of any landing gear
- individual aircraft axis (pitch,roll or yaw) constrained by the ground
- initial contact of all gear with the ground plane
- aircraft heavy on all gear

These combinations are used to transition control law functions for feedforward shaping, rate stabilization, attitude stabilization, automatic trim follow-up and rotor reference position with respect to cockpit control position. For example, upon contact of any gear with the ground, the feed-forward dynamic shaping functions required to achieve desired fly-mode control response characteristics, are changed to proportional control for ground operations. The transition from frequency shaped to constant forward loop control gains is depicted in Figure 10. Additionally, upon any gear contact, the trim follow-up function in each axis is held so that the constant gain forward path allows the pilot to accurately judge control requirements based on stick position. All AFCS stabilization, i.e. attitude, velocity or position, is also eliminated at this time through transient-free switching to prevent degradation of aircraft controllability resulting from false command model errors which may arise due to ground contact.

To enhance handling qualities during transition between ground and in-flight states, rate stabilization is retained in each control axis if the associated rotational degree of freedom is not fully constrained by gear contact. When an individual axis becomes constrained, the corresponding rate feedback channel is faded to zero. The elimination of rate stabilization when constrained is essential for shipboard operations where deck motions must not be transferred to the rotor while the aircraft is on the deck.

Finally, when the aircraft is fully down on the ground (heavy on all gear), the rotor control rigging position is referenced directly to the sidestick controller neutral position. The reference positioning process is initiated when the collective stick has been lowered 5% below the point at which all gear initiated ground contact. Trim follow-up in all axes is also nulled as the rotor reference position for ground operation is acquired. The setting of all stored trim values to zero restores an attribute inherent with conventional large-displacement controls, i.e. a fixed relationship of cockpit controller position and rotor control position while on the ground.

Control Law Moding

The experience base with multimode control laws accrued from the TAGS, HLH, ADOCS and V-22 programs was transferred to control law moding design requirements for the RAH-66 Comanche scout / attack mission. The PFCS modes are designed to minimize handling qualities degradation when multiple failures result in loss of the AFCS. AFCS control laws are designed to allow the pilot to tailor handling qualities to mission requirements with minimal cognitive effort. AFCS moding enhances handling qualities based on the usable cueing

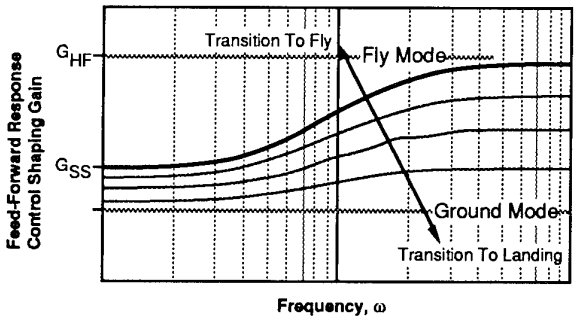

Figure 10 Dynamic Control Response Shaping Function for Landing and Takeoff

environment (UCE) available to the pilot. Thus, a wide range of enhancing control modes are made available with minimum pilot interaction.

The pilot interface to the multimode control laws is through the FCS panel, located in the center of the cockpit console below the twin multi-functional displays. Figure 1 1 illustrates the levels of augmentation available to the pilot ranked from highest to lowest. The system powers-up in the Core AFCS configuration, shown in the center of Figure 1 1. Higher levels of stability augmentation, i. e. Velocity Stabilization / Hover Hold and Altitude Hold, are selected by the pilot. The Flight Director can be selected to provide a maximum level of augmentation and to automate many facets of navigation and weapons delivery to reduce pilot workload and improve mission e ffectiveness.

Core / Mission PFCS

During the definition of design criteria for degraded control mode operation, fully attended nap-of-the-earth (NOE) flight was identified as a primary design driver for the PFCS control laws. Based on simulation studies, yaw rate stabilization, as a minimum, was required to provide Level 2 handling qualities ratings for NOE flight on PFCS (Figure 12). The ***Mission PFCS*** design employs yaw rate feedback layered on top of a minimal set of flight critical control laws and allows the pilot to return to base using an NOE flight profile. The Mission PFCS is engaged manually by pilot deselect of the AFCS, or automatically by loss of the AFCS due to a sensed second failure. The ***Core PFCS*** provides the minimum control laws required for Level 2 handling qualities for up and away flight, and landings on level, sloped, and shipboard sites. Reversion to this mode will occur only in event of failure of two yaw rate sensors in the PFCS. The yaw rate sensor redundancy provides a two-fail operative capability to meet PFCS system level reliability requirements.

Core / Selectable Mode AFCS

The ***Core AFCS*** is the normal flight control mode for the Comanche. It is designed with rate command / attitude hold functions in pitch, roll, and yaw to allow the pilot to maximize

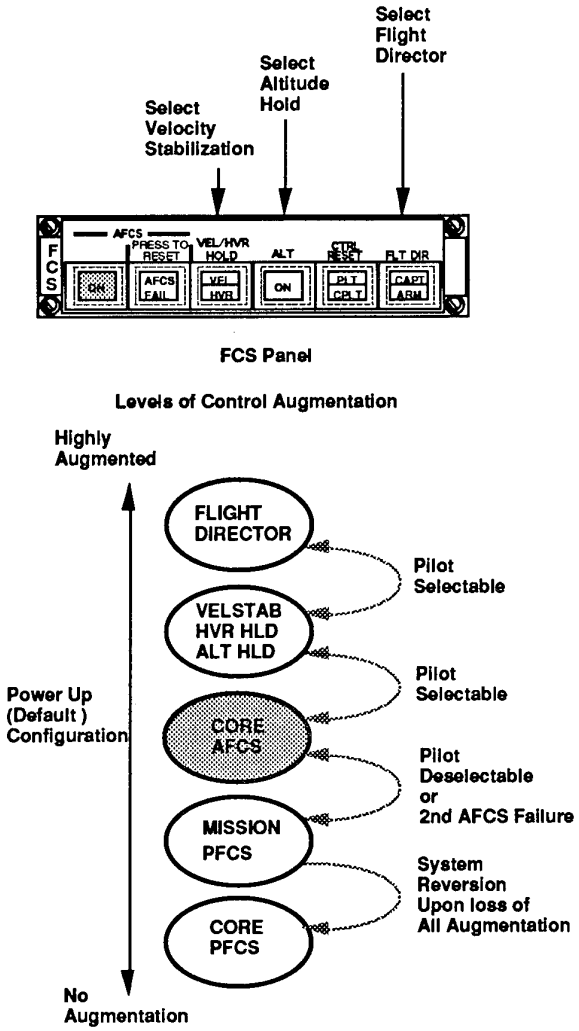

Figure 11 Pilot Interface with RAH-66 Flight Control System

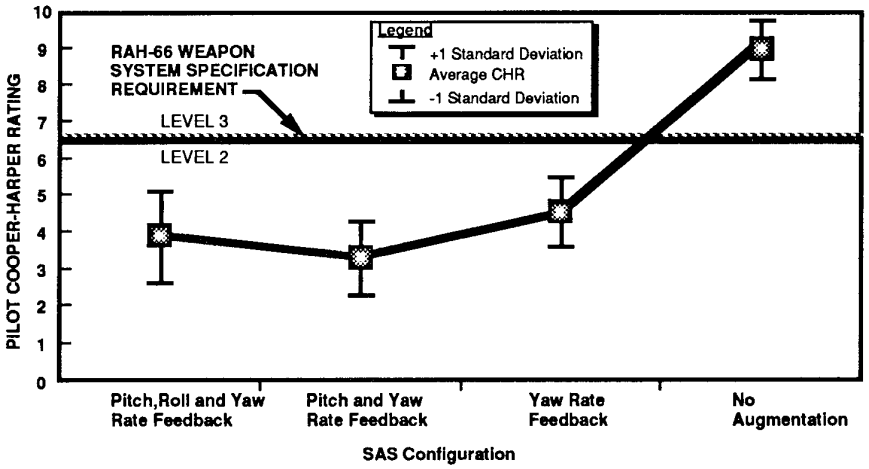

Figure 12 Effect of Stability Augmentation on Handling Qualities for Nap-of-Earth Flight

maneuverability and agility of the Comanche. Automatic turn coordination is provided at airspeeds above 60 knots to improve handling qualities through reduced workload. Figure 8 gives a description of the command response and stabilization characteristics of the Core AFCS as a function of airspeed. Additional details of the design are given in Fogler and Keller 1992.

Two ***Selectable AFCS Mode*** sets (Altitude Hold and Velocity Stabilization) are available to the pilot for mission enhancement. *Altitude Hold* provides a blended sensor hold function that uses a radar sensor reference while the aircraft is at low altitude and a barometric sensor reference for high altitude flight. When the pilot desires operation with a specific sensor reference, the blended altitude reference function may be overridden through the MEP. The *Velocity Stabilization* mode provides the highest level of platform stabilization available to the pilot. Figure 8 depicts the features of these control laws, which vary according to groundspeed and airspeed. Hover Hold is a submode of Velocity Stabilization which automatically engages when the aircraft is brought to hover to provide a hands-off position hold capability. As seen in Figure 11, the Velocity Stabilization button features a split lamp indicator to annunciate when the Hover Hold submode is active. In order to provide three-dimensional hover hold capability, Altitude Hold is automatically enabled when the Hover Hold submode is engaged. Additional information on design of the Comanche selectable modes can be obtained from Dryfoos and Gold 1993.

INTEGRATED FLIGHT CONTROL LAW DESIGN

The increasing demands placed on vehicle management systems have led to the requirement for integration of flight control, engine control, and fire control systems. Furthermore, flight control systems are being utilized to meet structural design and ASE stability requirements. This section summarizes aspects of the integration of system control functions in design of the V-22 and RAH-66 flight control laws.

Flight Control System / Engine Integration

The Comanche is powered by twin LHTEC T800 engines controlled by a full authority digital engine controller (FADEC). Precise regulation of rotor RPM during targeting operations has been shown to be critical during adaptive fuel control flight testing (Sweet 1989). Collective, lateral, and directional control commands typically couple with rotor torque demand to degrade targeting precision. To minimize RPM excursions during targeting maneuvers, Comanche flight control commands are directly coupled to the FADEC RPM governing control laws to provide engine response quickening and compensation. This alleviates undesired coupling and enhances handling qualities.

Integration of the flight and engine controls on the Comanche also includes two selectable modes that allow the pilot to change engine set speed. The ***Quiet Mode*** reduces main rotor RPM to 95% nominal to reduce the Comanche's acoustic signature. The ***Load Factor Enhancement Mode*** automatically increases the main rotor RPM to 107% nominal to enhance the normal load factor envelope and to reduce control loads at high speeds. These additional rotor speed options expand the mission capability of the RAH-66.

Unique engine control requirements for the V-22, as described in Schaeffer 1991, are met through incorporation of the Thrust Power Management System (TPMS), which contains control law provisions to enhance both the helicopter and airplane flight modes. Precise height control for hover operations and shipboard landings is required in helicopter mode, while tight airspeed control and gust rejection are important in airplane mode. Precise power control and rotor speed governing is required in all flight modes.

Figure 13 provides an overview of the integrated V-22 engine / rotor control system, i. e., the TPMS. Pilot commands are input through the engine control levers (ECL) during startup operations, and through the thrust control lever (TCL) during flight operations. The TPMS, which is integrated within the primary flight control system, provides command quickening, rotor governing, and torque command shaping and limiting during all modes of flight. Vertical damping is also provided by the AFCS for VTOL mode operations. Many TPMS parameters are scheduled with nacelle angle and airspeed to provide desired characteristics throughout the flight envelope. The flight control system provides a power demand signal to the FADEC (Full Authority Digital Engine Control), which regulates engine gas generator and power turbine speed. Average rotor RPM is sensed and fed to a proportional plus integral (P + I) controller for regulation of rotor RPM.

The design of a rotor speed governor was an interesting challenge on the V-22. Traditionally, helicopters use engine governing, where the pilot sets blade collective and the control system adjusts engine power to maintain rotor RPM. This control approach provides a predictable pilot control response in hover since thrust response to collective is of relatively high bandwidth. Airplanes on the other hand, generally use "beta" governing where the pilot sets engine power and the governor adjusts propellor angle of attack to maintain rpm. This control approach is generally acceptable for airplanes since the pilot operates the thrust controller at relatively low frequencies.

The throttle governing approach typical of helicopters was not practical for the V-22 due to the large sensitivity of mast torque to collective pitch at high inflow ratios in airplane mode. The V-22 utilizes a collective ("beta") governor in all modes of flight. Acceptable hover characteristics are achieved using TCL quickening in the control laws, with high frequency thrust control response actuated through collective blade pitch and low frequency thrust commands provided through the engine response.

Integrated Fire / Flight Control (IFFC)

Fire control systems typically operate autonomously from other aircraft systems. Wide regard weapons such as seeker guided missiles, e.g. HELLFIRE, do not require significant aircraft maneuvering, since the fire control system automatically compensates for aircraft motion. With unguided limited regard weapons, the success rate is directly affected by the crew's ability to coordinate the aircraft trajectory within target sight constraints. Therefore, handling qualities and hence the aircraft control laws directly influence the successful accomplishment of the targeting task. The launch precision accuracy of unguided limited regard weapons is affected foremost by crew targeting errors, and secondarily by accuracy of the fire control solution.

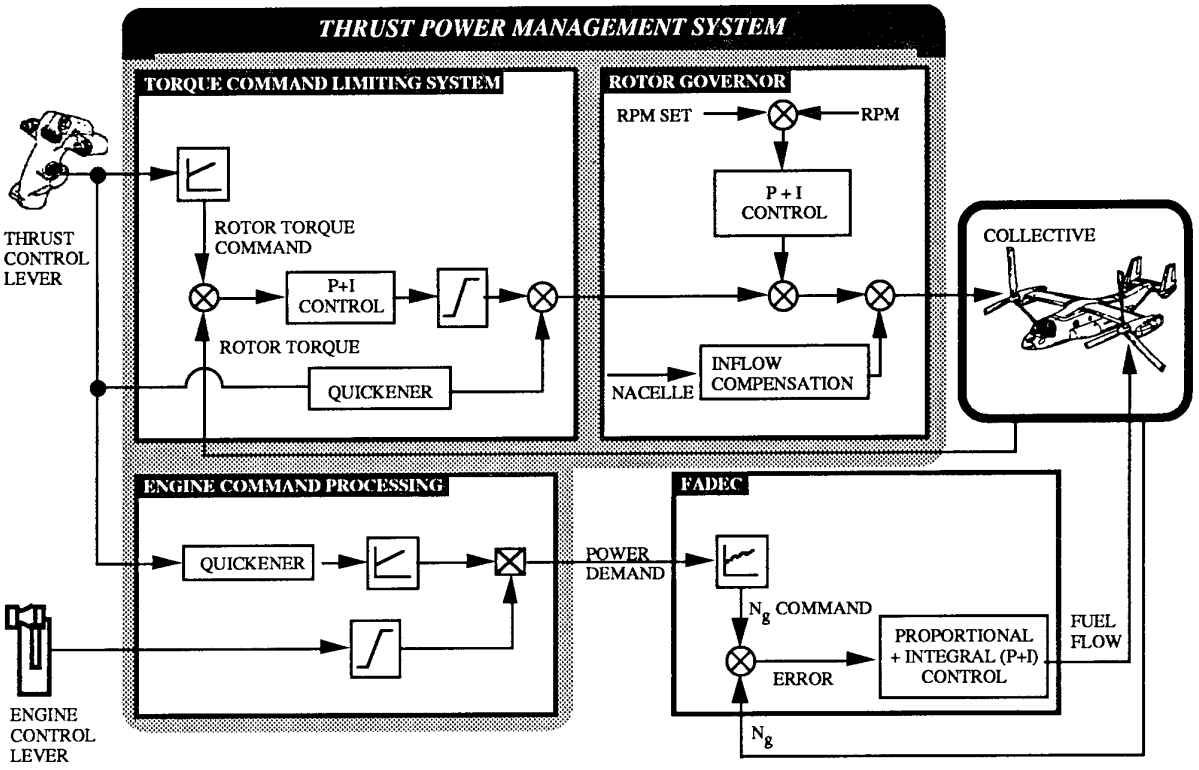

Figure 13 V-22 Thrusr Power Management System

The Comanche fly-by-wire digital system architecture is well suited for integration of the weapons' fire and flight control systems to reduce pilot workload associated with weapons aiming. When the IFFC system is engaged, the fire control solution is presented as a maneuvering command on the Helmet Mounted Display (HMD). The IFFC maneuvering command is also coupled to the flight control system by referencing the rate and attitude state variables of the command model to the fire control solution. The authority of the IFFC control is highest when the aircraft is closely aligned with the ta rget. As the aircraft attitude is moved outside of the engagement window , the IFFC authority is reduced to zero. In this manner , the pilot is provided with a "sticky pipper" to improve basic ta rgeting accuracy. The IFFC system is designed to allow the aircraft to be stabilized within ± 0.1 degrees of the fire control solution. The pilot command path remains active, so that the pilot can override the system at all times. The IFFC system is easily disengaged by release of a grip switch which must be depressed at all times when using IFFC. The design and development of IFFC control laws is discussed in Fowler 1992.

Structural Loads Limiting

The unique requirements of the V-22 mandate flight operations to the maximum aircraft aerodynamic capability . Since the strength of structural components is constrained by weight, size, and cost considerations, control laws were optimized to alleviate trim/maneuver loads as described in King 1993. The V-22 system design ensures that structural component limit and fatigue loads are not exceeded for the full range of aircraft maneuvers, while retaining Level 1 handling qualities. The digital flight control system provides a cost / weight e ffective means of meeting both structural loads and handling qualities requirements throughout the flight envelope. Two examples of structural load limiting control laws are presented, namely (1) the use of roll rate feedback applied in airplane mode, and (2) the implementation of a longitudinal flapping limiter in the VTOL / Conversion flight mode.

Roll Rate Feedback

The V-22 rotor system is comprised of counter -rotating rotors mounted at the wingtip, connected by an interconnect drive shaft which maintains equal rotor rpm at both rotors. During roll maneuvers in airplane mode, aircraft roll rate induces an effective increase in the rate of rotation of the downward rolling rotor, and an effective decrease in the rate of rotation of the upward rolling rotor. This variation in the effective rate of rotation on the left and right rotors causes a torque split which is transmitted through the interconnect drive shaft during maneu-vers. These maneuver induced loads are a design concern with respect to the fatigue and limit loading characteristics of the shaft.

To minimize weight and cost of the drive system, roll rate to differential collective pitch feedback is provided in airplane mode to alleviate cross shaft loads during roll maneuvers. By sensing roll rate and making the appropriate di fferential collective pitch change, the torque split between the rotors, and thus the loads carried through the interconnect shaft during maneuvers can be minimized. Figure 14 presents simulation and flight test data showing the benefit of roll rate feedback in reducing interconnect drive shaft torque for roll maneuvers.

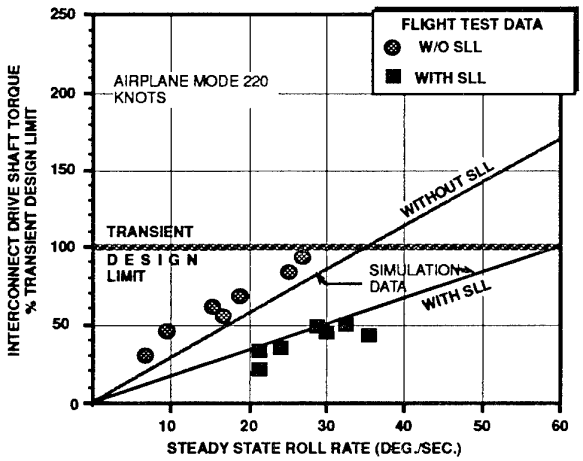

Figure 14 Effect of Structural Load Limiting on Roll Maneuver Capability

With Structural Load Limiting, i. e. roll rate feedback, the maneuvering capability of the V-22 as limited by transient design limit loads is increased from 30 to 60 degrees / second.

Flapping Limiter

The relatively small disk area of the V-22 rotor results in operation at relatively high thrust coefficients in VTOL / conversion mode forward flight. Regions of blade stall can develop at moderate speeds which induce increased blade flapping and rotor yoke chord bending loads. Furthermore, the aircraft operates over a large range of nacelle / airspeed and CG conditions. At the envelope extremes, trim flapping increases, thereby presenting fatigue issues in trim and limit flapping issues during maneuvering flight.

A control law was developed to feed rotor blade flapping to the elevator in order to reduce trim flapping of the rotor in both VTOL and conversion flight modes. A frequency splitter was also implemented in the longitudinal stick command path to alleviate high frequency longitudinal cyclic inputs which can lead to excessive flapping during aggressive pitch maneuvers. The frequency splitter, which modifies the command split between the rotor and elevator, was set to maintain required control power throughout the conversion envelope. This control law was successful in reducing trim and maneuver flapping throughout the V-22 envelope, while maintaining acceptable handling characteristics.

Aeroservoelastic Stability

Aeroservoelastic (ASE) stability characteristics are becoming more important for modern aircraft programs as the requirement to minimize weight and maximize maneuverability becomes more critical. Analysis, design, and testing of ASE stability characteristics are key tasks in the development of air vehicle/ vehicle management system (VMS) characteristics. Both the V-22 and RAH-66 programs have shown that the VMS provides a powerful tool to meet weight and maneuverability design requirements.

The large roll/yaw inertia of the V-22 coupled with the relatively soft wing/fuselage interface (induced by the wing fold mechanism) creates a situation where the frequencies of the aircraft' s structural modes are relatively low, and in proximity of the rigid body modes. As described by Parham, 1991, flight testing of the V-22 identified three conditions where the pilot/control system tended to couple with the aircraft, resulting in a pilot assisted oscillation (PAO). These PAO's involved a de-stabilizing acceleration feedback through the pilot/control stick at a rigid body or structural mode frequency. Initial ASE analyses for the V-22 did not include a model of biodynamic feedback and, therefore, did not predict the pilot assisted oscillations. Subsequently, generalized pilot/control models were established using measured data taken from ground-shake tests and in-flight excitations of the aircraft/pilot. These models were correlated to measured stability data and then used to design system enhancements as described below.

The initial PAO experienced during V-22 testing occurred while light on the gear and is attributed to coupling of lateral pilot motion with a 1.4 hertz rigid body mode. Mass balancing of the cockpit lateral control (a large displacement center stick) eliminated this mode by effectively breaking the look from lateral acceleration to pilot/stick input. Two in-flight occurrences of PAO were encountered which involved a de-stabilizing pilot/control system feedback loop at structural mode frequencies. These pilot assisted oscillations were present in airplane mode and involved: (1) a coupled pilot/control system response to lateral acceleration at the asymmetric wing chord (A WC) mode frequency (3.4 hertz) at speeds greater than 250 knots, and (2) a coupled pilot/control system response to longitudinal acceleration at the symmetric wing chord (SWC) mode frequency (4.2 hertz) at speeds greater than 300 knots. Both in-flight PAO cases were addressed by incorporating digital "notch" filters in the feedforward command path to effectively break the feedback loop at the critical structural mode frequency without inducing unacceptable phase lag in the handling qualities frequency range.

The analysis of the complex interactions between the various sources of aeroelastic forces was performed at an early stage of the Comanche program due, in part, to lessons learned on the Bell-Boeing V-22 Program. Extensive use of composites throughout the Comanche to reduce weight has lead to the lowest fuselage structural modes being in close proximity to the rotor 1/Rev frequency (Figure 15). Figure 16 summarizes elements of the Comanche design which drive the requirement for a comprehensive ASE analysis.

The RAH-66 Comanche is required to meet the stringent specifications of Aeronautical Design Standard ADS-33C and MIL-F-9490D. ADS-33C requires that the handling qualities be tailored to the specific mission task element (MTE) being performed and the usable cue environment (UCE) in which the task will be flown. Different levels of flight control system augmentation and performance are specified depending upon the MTE and UCE. In addition, certain MTE' s place strict simultaneous requirements on the allowable bandwidth, system stability, inter-axis coupling, and maximum achievable rates. To satisfy these diverse requirements, the RAH-66 Comanche uses a high-gain, full-authority, digital fly-by-wire AFCS with several hierarchical levels of augmentation. Pilot inputs into the control system come from a small-displacement sidestick and medium-displacement collective controller. A comprehensive ASE analysis tool was developed and utilized throughout design of

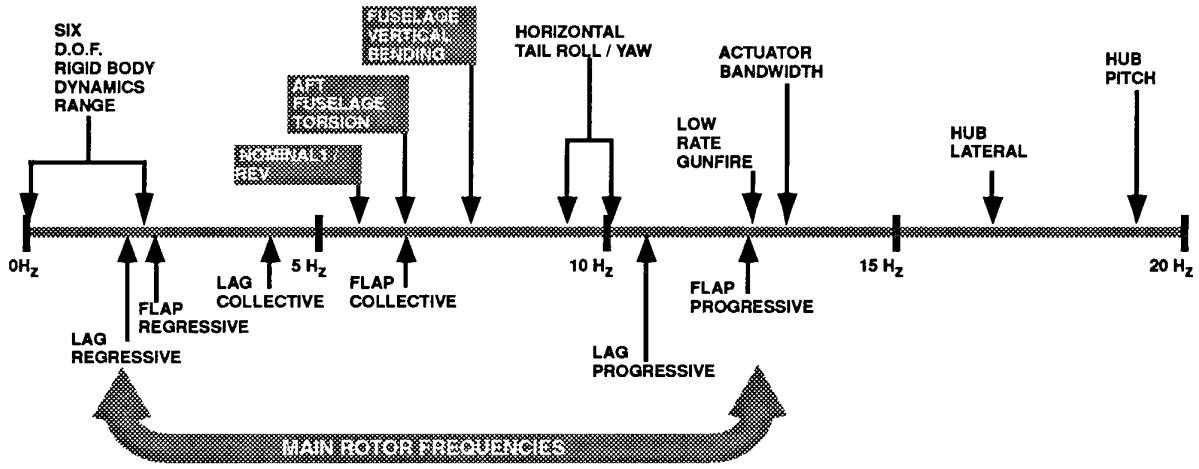

Figure 15 Spectrum of RAH-66 Dynamic Mode Frequencies

the Comanche VMS to meet all design requirements while minimizing cost and weight of the aircraft structure.

CONTROL LAW DESIGN PROCESS

The control law design process employed at Boeing Helicopters has evolved from experience with major flight control research and development programs. Advanced computer analysis, design, and simulation tools have been developed over the course of these programs, thereby increasing overall quality and productivity of the design process. The flight control law design process, highlighted in Figure 17 includes four phases; namely , preliminary design, detailed design, implementation / verification, and acceptance testing.

The ***Preliminary Design*** process begins with the development of design criteria based on air vehicle specification requirements. An iterative process is applied in which the combined vehicle / system characteristics are analyzed, simulated, and assessed against the air vehicle specification requirements for handling qualities, structural loads, and aeroservoelastic stability. This phase of development establishes the control law architecture, sensor requirements, and system component bandwidth requirements. For example, the handling qualities specification may quantify the minimum required level of dutch roll damping. An assessment of the vehicle's inherent stability and control characteristics may indicate that artificial stabilization is required to increase yaw damping to meet the established design criteria. The need for stabilization will then flow down a set of requirements for the system architecture, sensor characteristics, and actuator performance.

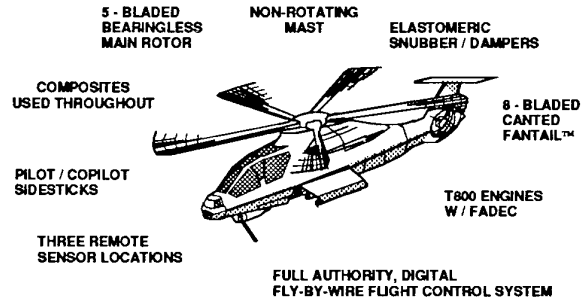

Figure 16 Key Sources of RAH-66 Aeroservoelastic Coupling

Once the preliminary control law design process is complete, a ***Detailed Design*** phase is conducted. Again, an iterative process is applied which utilizes extensive analysis and piloted simulation evaluations to ensure acceptability of the control laws for a wide range of maneuvers. Mission effectiveness of the aircraft is assessed for specific mission task elements based on the handling qualities requirements defined during the preliminary design phase. The detailed control law development process ensures that all handling qualities, system, and structural requirements are simultaneously met.

Comprehensive models are developed during detailed design to assess rigid body and elastic stability characteristics, along with their interaction with the coupled pilot / flight control system (Figure 18). Aeroelastic stability analyses are conducted to ensure that no ground or air resonance conditions occur in the coupled rotor / fuselage / drive / landing gear system. These analyses are considered to be "open loop" in the sense that the control surfaces remain fixed. Aeroservoelastic (ASE) stability analyses, however, examine the stability of the "closed loop" system where the control surfaces respond to control law commands, elastic structural deformations at the hub or sensors, and any undesired pilot inputs created by the biodynamic transmission of pilot seat accelerations to the control sticks (also called "pilot assisted oscillations").

Figure 18 shows the primary components of the rotorcraft linear model used to analyze stability and control, ASE, and structural loads characteristics. Using this model the ASE stability of the closed loop system including pilot dynamics is determined and compared to the gain and phase margin guidelines established in Military Specification MIL-F-9490D. Components of the analytical model are discussed below.

The *air vehicle model* is a linear representation of the vehicle dynamics of interest including fully coupled rigid body dynamics, rotor dynamics, landing gear dynamics, and flexible fuselage and drive systems. This model is based on the same

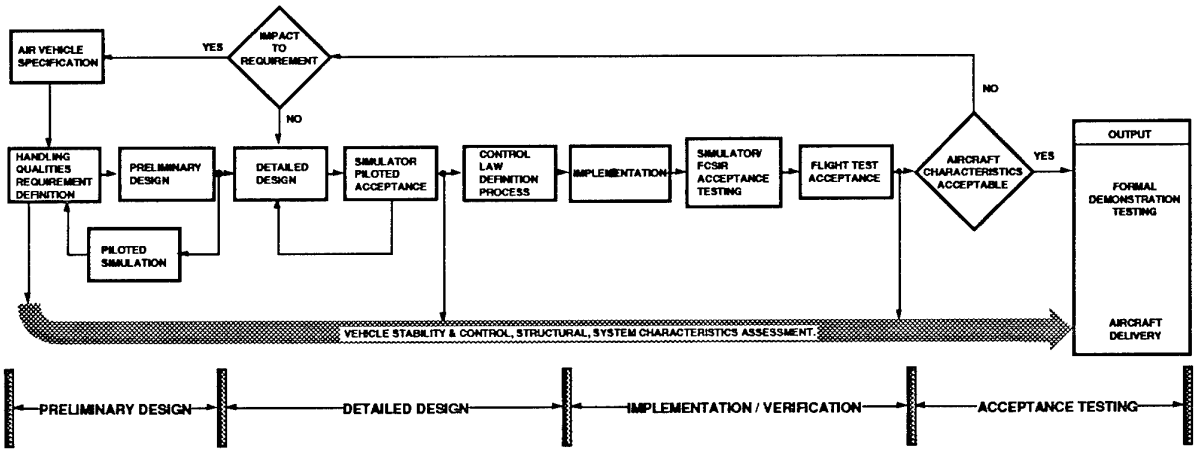

Figure 17 Control Law Design Process

full-force, non-linear aircraft model used for real-time piloted simulation. The air vehicle model provides outputs to represent the linear accelerations felt at the crew stations, and sensor feedback signals referenced to sensor package locations in the flexible fuselage. Structural loads models are also included for real-time assessment of loads during batch and piloted simulation of control response characteristics.

The *sensor models* receive the feedback signals from the air vehicle model and calculate the dynamic response characteristics of each individual sensor package. Location of the sensor packages or the design of their mounting structures are important variables that influence the ASE stability characteristics.

The *pilot models* are linear transfer functions representing the pilot and copilot biodynamic transmission of seat accelerations through his body to the control sticks. Ideally this model should account for accelerations in all three orthogonal axes and produce control motions in all axes simultaneously, but single axis models have proven adequate. These models are developed empirically from flight or ground based shake test data. Although defined as "pilot" models, this element of the model represents the dynamics of the combined pilot / seat / controller system.

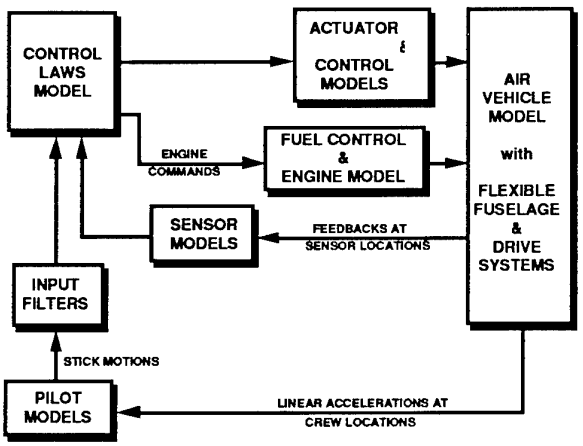

Figure 18 Rotorcraft Analytical Model Overview

The *control law model* provides a detailed representation of the the flight control system. In addition to the feedback stabilization loops, all feedforward control paths are included since the biodynamically closed acceleration feedback paths are of primary importance. Since total loop computational delay has a significant effect on levels of stability, all input, processing and output delays must be represented accurately.

The *fuel control and engine model* couples the flight control laws with the flexible drive system and rotor dynamics. Accurate modelling of fuel control and engine dynamics is essential to insure a high fidelity model.

The end product of this phase of the detailed design process is the definition of a complete set of integrated control laws. A formal control law definition process ensures that a rigorous and disciplined review of the system is accomplished, and that a valid control law definition results prior to coding flight critical control system software. Over the past 20 years Boeing Helicopters has developed numerous computer design tools to streamline and shorten the time required for detailed design. These tools are packaged in a workstation environment to maximize efficiency of the process.

Verification and Validation of the total flight control system including the control laws is performed to ensure that system integrity is maintained. Verification of the control laws ensures proper coding to the requirements by testing at the unit, module and package levels. Implementation errors are ef fectively eliminated by using the exact flight control element algorithms in the design phase. Validation of the flight control software involves an assessment at the system level. Non-piloted, open loop test conditions are run in the Flight Control System Integration Rig (FCSIR) to evaluate the overall system response. These runs are compared to expected results generated by the FCS simulation. After successful open-loop testing is accomplished, the simulator is interfaced with the FCSIR (Figure 19)

(a) (b) (c)

Figure 19. V-22 and RAH-66 flight simulators and flight control integration rig
(a) V-22 on motion system (b) RAH-66 simulator with dome visual display (c) FCSIR laboratory

to conduct a formal final pilot acceptance test of the total system as described for the V-22 in Robinson 1989. A wide range of maneuvers and flight conditions are evaluated. System failures are introduced to evaluate failure mode effects and degraded mode handling qualities with hardware-in-the-loop. The validated software is then installed on the aircraft, and a flight assessment of the aircraft is made to demonstrate that handling qualities, system, and structural requirements are met prior to delivery of the aircraft to the customer for acceptance testing.

SUMMARY

Advanced flight control system technology at Boeing Helicopters has matured over two decades of developmental programs, culminating with integration of advanced technologies in the RAH-66 Comanche and V-22 Osprey. An integrated design solution is achieved by applying a balanced approach using state of the art analysis tools and real-time piloted hardware-in-the-loop simulation.

The PFCS / AFCS system architecture provides a safe approach to control partitioning for explicit model following control laws. This approach has proven to be adaptable to a wide range of aircraft configurations, providing the flexibility to address new directions in handling qualities requirements. Enhanced mission effectiveness is achieved through integration of stability and control augmentation and structural load control law functions. Integration of these control law functions, along with advanced cockpit displays and controls, engine control, and fire control systems have proven to be key in providing a total vehicle management system capable of meeting future military requirements.

FUTURE DEVELOPMENT TRENDS

Research into advanced flight control techniques continues at Boeing Helicopters. Future control system designs will be optimized for multiple missions and configurations, and provide increased levels of stability and command augmentation throughout the flight regime, with intelligent system reconfiguration to compensate for failures. System bandwidth will be increased through control system algorithms that provide active stabilization of fundamental airframe and rotor modes. Control algorithms based on rotor state feedback and individual blade sensing will provide means of extending usable bandwidth and improving gust rejection and stability characteristics. Integrated design approaches will simultaneously optimize handling qualities, maneuver control, elastic stability, and airframe and rotor structural loads limiting characteristics.

Advances in computing speed are enabling adaptive compensation for changing aircraft configuration, flight condition, and level of aggressiveness through the application of real-time system identification techniques. Increasingly sophisticated analytical redundancy techniques (including real-time system identification methods) will be used for failure prognosis detection and isolation. These analytical redundancy techniques will also provide improved failure tolerance with less physical hardware. Computer speed advances will also make digital control algorithms feasible for active vibration suppression, higher harmonic and individual blade control, and active modal damping enhancement. Parallel on-line computing will allow the implementation of high order controller structures using finite impulse or neural controller structures.

Integration of cockpit displays, sensors, stability augmentation, and flight director functions will allow the pilots of the future to survive an increasing array of threats while improving mission effectiveness. Automatic control system technologies will be applied to on-line mission planning and flight director functions based on more accurate navigational, threat, and obstacle avoidance information provided from phased array radars, Forward Looking Infrared (FLIR), video, and Global Positioning Sensor (GPS) technologies.

LIST OF REFERENCES

Aeronautical Design Standard ADS-33C, August 1989, Handling Qualities Requirements For Military Rotorcraft, *United States Army Aviation Systems Command, St. Louis, Missouri.*

King, D. W., Dabundo, C., Kisor, R. L., and Agnihotri, A., May 1993, V-22 Load Limiting Control Law Development, *Presented at the 49th Annual National Forum of the American Helicopter Society, St. Louis, Missouri.*

Bauer, C. J., May 1993, A Landing and Takeoff Control Law for Unique-Trim, Fly-By-Wire Rotorcraft Flight Control Systems, *Presented at the 49th Annual National Forum of the American Helicopter Society, St. Louis, Missouri.*

Dabundo, C., White, J., and Joglekar, M., May 1991, Flying Qualities Evaluation for the V-22 Tiltrotor, *Presented at the 47th Annual National Forum of the American Helicopter Society.*

Davis, J., Garnett, T., and Gaul, J., September 1977, Heavy Lift Helicopter
Flight Control System, Volume III - Automatic Flight Control System Development and Feasibility Demonstration, *USAAMRDL TR-77-40C .*

Fowler, D. W., Lappos, N. D., Dryfoos, J. B., and Keller, J. F., June 1992, RAH-66 Comanche Integrated Fire and Flight Control Development and Tests, *Presented at the 48th Annual National Forum of the American Helicopter Society, Washington D. C.*

Dryfoos, J. B., and Gold, P. J., January 1993, Design and Pilot Evaluation of the RAH-66 Comanche Selectable Control Modes, *Presented at the AHS Specialist Meeting, Monterey, California.*

Fogler, D. L., and Keller, J. F., June 1992, Design and Pilot Evaluation of the RAH-66 Comanche Core AFCS, *Presented at the 48th Annual National Forum of the American Helicopter Society, St. Louis, Missouri.*

Glusman, S. I., Dabundo, C., and Landis, K. H., October 1987, Advanced Flight Control System for Nap-of-the Earth Flight, *NATO-AGARD Symposium Paper No.28, Stuttgart, West Germany.*

Glusman, S. I., Conover, H. W., and Black, T. M., November 1990, Advanced Digital Optical Control System (ADOCS), Volume III - Handling Qualities, *U. S. Army Aviation Systems Command TR 90-D-11C.*

Landis, K. H., Davis, J. M., and Leet, J. R., May 1975, Development of Heavy Lift Helicopter Handling Qualities for Precision Cargo Operations, *Presented at the 31st Annual National Forum of the American Helicopter Society.*

Landis, K. H., and Glusman, S. I., July 1984, Development of ADOCS Controllers and Control Laws, Volume 3 - Simulation Results and Recommendations, *NASA Technical Report NAS2-10880.*

Military Specification MIL-F-9490D, June 1975, Flight Control Systems - General Specification For Design, Installation, and Test Of Piloted Aircraft, *United States Air Force.*

Military Specification SD-572, January 1993, Detailed Design Specification
for V-22 Engineering Manufacturing Development (EMD), *Naval Air Systems Command, Washington, D. C.*

Parham, T., Popelka, D., Miller, D. G., and Froebel, A. T., May 1991, V-22 Pilot-In-The-Loop Aeroelastic Stability Analysis, *Presented at the 47th Annual National Forum of the American Helicopter Society, Phoenix, Arizona.*

Robinson, C., Dabundo, C., and White, J., August 1989, Hardware-in-the-Loop Testing of the V-22 Flight Control System Using Piloted Simulation, *AIAA Flight Simulation Technologies Conference, Boston, MA.*

Rosenstein, H., and Clark, R., October 1986, Aerodynamic Development of the V-22 Tiltrotor, *AIAA / AHS / ASEE Aircraft Systems Design and Technology Conference, Dayton, Ohio.*

Schaeffer, J. M., Alwang, J. R., Joglekar, M. M., May 1991, Thrust /Power Management Control Law Development, *Presented at the 47th Annual National Forum of the American Helicopter Society.*

Sweet, D., August 1989, S-76 Adaptive Fuel Control Ground and Flight Tests, *USAAVSCOM TR-89-D-8.*

Practical Experiences in Control Systems Design Using the NCR Bell 205 Airborne Simulator

Stewart W. Baillie, J. Murray Morgan
Flight Research Laboratory, IAR/NRC
Institute for Aerospace Research
National Research Council, Montreal Road
OTTAWA, Ontario K1A 0R6 CANADA

Dr Kevin R. Goheen
Carleton University, Ottawa

Introduction

Since 1961, the Flight Research Laboratory of the Institute for Aerospace Research, National Research Council of Canada, has been involved in research using airborne simulation. This program has, since 1969, been conducted using a full authority, digital fly-by-wire Bell 205A helicopter, modified for the airborne simulation role by the laboratory. As an airborne simulator, this aircraft enables the in-flight, piloted evaluation of aircraft with dynamic characteristics which may or may not resemble the dynamics of a Bell 205A. The alteration of the dynamics of the airborne simulator from its own characteristics to that which is desired for evaluation is accomplished by the use of fly-by-wire actuation and the development of model following or feedforward/feedback control systems.

Over the course of the 25 years that the Bell 205 aircraft has been used in a research role, the NRC Airborne Simulator has been programmed and reprogrammed for a wide variety of control response and effective "open-loop" characteristics. In most cases the objective of this activity has been the piloted evaluation of the aircraft to discern information regarding the tradeoff between aircraft dynamics and handling qualities. These research programs include a large number of experiments conducted to develop a handling qualities data base to support the development of the US Army Aeronautical Design Standard for Rotorcraft Handling Qualities (ADS-33C), Reference 1, and activities associated with improving the rules for civil rotorcraft flight in instrument meteorological conditions (IMC), Reference 2.

While the results of the handling qualities research performed using the Bell 205 may be of limited interest to a control systems design community, the techniques, successes and failures associated with modifying the dynamics of an old, low bandwidth, moderately cross-coupled helicopter to obtain dynamics relevant to the design of the next generation rotorcraft are more pertinent.

In general, the majority of control system design performed for the Bell 205 is based on classical methodology. With the continual development of new or revised control systems in the Bell 205, however, there is an opportunity to apply and practically evaluate the wide variety of "modern" control law design techniques. While the evaluation of modern techniques has only recently become a major priority at the laboratory, a discussion of this activity is also appropriate in a control law designer forum.

The objective of this paper is to describe a variety of examples of control system design and application on the NRC Bell 205 Airborne Simulator. For background, this paper will first examine the physical characteristics of the Bell 205 and the mathematical models which have been developed to describe them. The paper then reviews the classical control design techniques which have been used to develop high bandwidth rate and attitude response type systems on the aircraft, and describes the empirically determined fixes which have become standard elements of these types of systems. To complete the paper, two sections will deal with application of modern control theories; the first describes a limited effort to develop a translational rate command system using a six degree of freedom model of the Bell 205 and a publicly available software package, MATLAB/Simulink. The second modern control theory section deals with a more detailed study performed in collaboration with Carleton University and supported by DND/CRAD to devise modern control theory controllers for the Bell 205.

All discussions of the paper are substantiated with actual, in-flight validation data to clearly demonstrate design successes and failures.

The Bell 205 Airborne Simulator

Physical Description - The NRC Bell 205 Airborne Simulator is an extensively modified Bell 205A-1 with special fly-by-wire capabilities that have evolved considerably over the last twenty-five years (Figure 1). The standard hydraulically boosted mechanical control actuators on this aircraft incorporate servo-valves that can be positioned either mechanically from the left

Paper presented at the Flight Mechanics Panel Symposium held in Turin, Italy, from 9-13 May 1994.

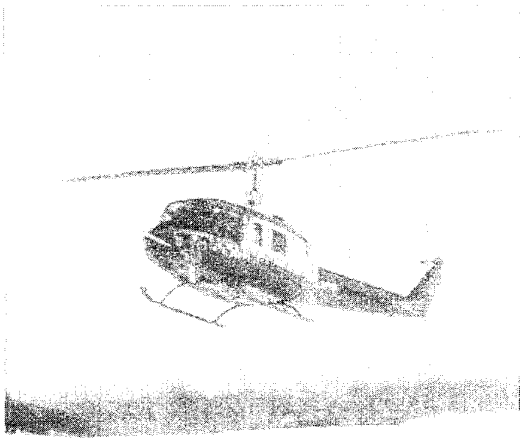

Figure 1 The NRC Bell 205 Airborne Simulator

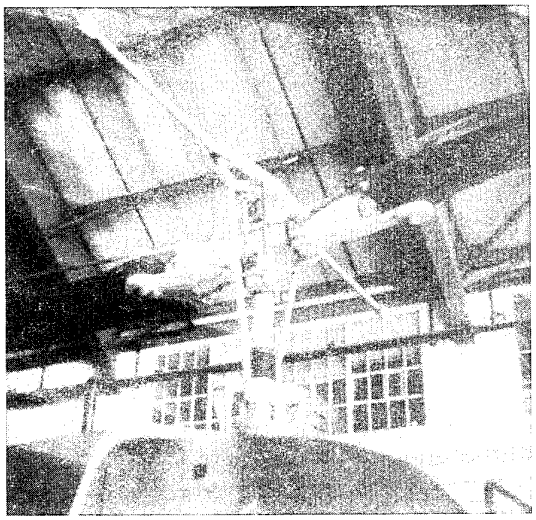

Figure 2 A Bell 205 Stabiliser Bar

(safety pilot) seat or electrically by the aircraft computing system. Evaluation pilot (right seat) control inputs from either conventional cyclic, collective and pedals or integrated side arm controllers are measured and fed into a computing system consisting of two LSI 11/73 microprocessors and a wide variety of project dedicated hardware. Full authority fly-by-wire actuator commands are generated by software which manipulates inputs made by the evaluation pilot and data from a full suite of aircraft state sensors.

Additional modifications to the Airborne Simulator have been incorporated to increase the simulation envelope of the facility. A standard Bell 205A has a device known as a stabiliser bar on the teetering rotor (Figure 2). As analysed by Heffley et al (Reference 3), this device provides pitch and roll rate feedback to the rotor system after an approximate 3 second lag. Since this stabilisation effectively reduces the aircraft control authority, the system was removed to enhance the available control response of the teetering rotor system.

A second modification of the Bell 205 was the removal of the fixed cyclic-to-elevator surface gearing which provides an improved attitude trim curve for the basic aircraft. In the NRC aircraft this cyclic-to-elevator link has been replaced with an electro-hydraulic actuator, so that the elevator surface can be used as an additional, programmable pitch control. In general, however, the elevator is usually kept in a fixed neutral position for most programs. As with all commercial Bell 205's, the NRC Bell 205 was also modified to possess the wide chord, right-side mounted, tail rotor of the standard Bell 212. This modification was a result of a worldwide Airworthiness directive for the aircraft and results in improved yaw axis control and maintenance schedules. For further information on the NRC Bell 205 Airborne Simulator, the reader is directed to Reference 4.

Aircraft Mathematical Modelling - Heffley et al (Reference 3) provides a six degree of freedom, stability derivative model of the Bell 205 with stabiliser bar on for a wide variety of trim conditions. This model was derived from the calculated response of the aircraft using a helicopter simulation program known as C-81. It is this model that is generally used in most control law design activities for the NRC Bell 205 Airborne Simulator.

The Heffley model fidelity can best be judged by reference to measured versus modelled frequency domain plots of the aircraft primary control response characteristics. These plots are found as Figures 3-6. Figures 3 and 4 display bode plots of model and actual aircraft rate response due to cyclic input in pitch and roll axes. The discrepancies between the model and aircraft response can be summarized in three points:

1- The model includes the dynamics of the stabiliser bar, causing the features of the model response bode plot to be shifted to a slightly lower frequency than that of the aircraft.

2- The model does not include higher order rotor dynamics. In general the dynamics of the Bell 205 teetering rotor can be satisfactorily modelled by a

simple time delay in angular rate response. While the bode plots do not show a significant phase rolloff at the frequencies plotted, the phase rolloff caused by the rotor dynamics is important at frequencies of 10 rad/sec and above.

3- The aircraft has a structural mode involving movement of the rotor transmission at approximately 14 rad/sec. This mode involves significant pitch and roll motion of the entire rotor system with respect to the fuselage and is generally the primary mode of concern for control system stability considerations.

Unlike pitch and roll axes, the heave and yaw axes have significantly larger discrepancies in model versus aircraft control response transfer functions. The agreement in vertical reponse of the Bell 205 and the model, Figure 5, is relatively poor and can be attributed to the lack of rotor in-flow and engine governor characteristics in the simple six-degree of freedom model. The accuracy of the model yaw rate response can be judged by examination of Figure 6. In general this figure demonstrates that the behaviour of the aircraft is adequately represented at frequencies above 1.5 rad/sec. The cause of the discrepancy between model and aircraft response at low frequencies is undetermined.

While the above discussion shows that the Bell 205 model response contains some significant errors when compared to the actual aircraft response, this situation is not unlike the situation faced by designers of control systems for aircraft which are still in design phases: the model is simple and only moderately representative. In practice, the Heffley model is used in all control law developments for the NRC Bell 205.

" Mixed " Angular Rate Signals- As described above, the Bell 205 possesses relatively low control power and

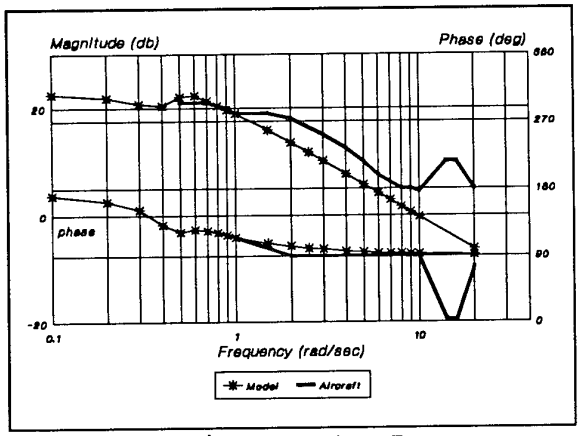

Figure 3 Pitch Rate Response - Aircraft vs. Model

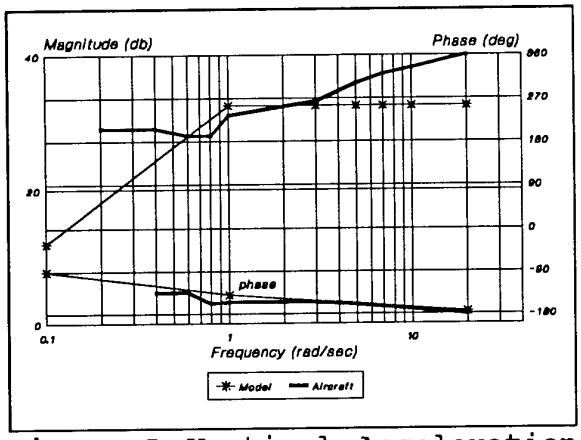

Figure 5 Vertical Acceleration Response - Aircraft vs. Model

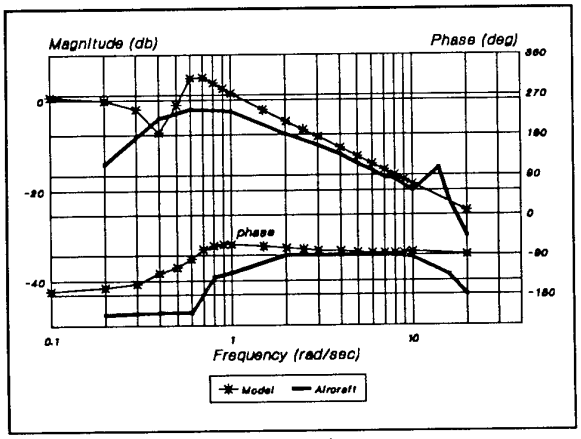

Figure 4 Roll Rate Response - Aircraft vs. Model

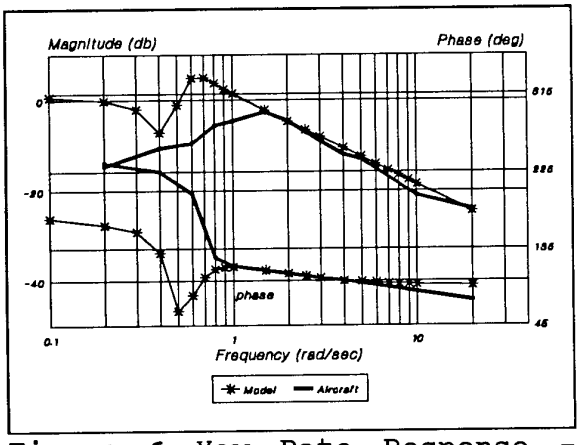

Figure 6 Yaw Rate Response - Aircraft vs. Model

considerable control response lag. The lag, which appears as a pure time delay between control input and fuselage response, is caused by the dynamics of the teetering rotor system and the fact that the fuselage is pendulously suspended below the rotor head. For closed loop control, the effective control response time lag is significant; approximately 150 msec in pitch and roll axes, 180 msec in the yaw axis and 120 msec in heave axis. If angular rates are used for high gain feedback, this effective time delay puts very strict limits on the achievable bandwidth of control systems. In addition, the angular rate sensor output includes measures of the aircraft motion due to aircraft transmission and other structural modes which are not described in the simple, linear model of the aircraft used in control system design work. Use of the measured angular rates at high gain would serve to feedback these structural modes with a significant time delay, the perfect recipe for a closed loop instability to develop. To overcome this fundamental difficulty, it has become customary to develop a "mixed" rate signal for use in feedback loops.

To the best of the author's knowledge, the idea of "mixed rates" stems from work done at NASA Langley some time ago. In essence, the mixed rate signal is manufactured by feeding the measured aircraft angular rate signal through the low pass section of a complementary filter and summing it with the output of the high passed section of the filter, as shown below.

$$p_{mix} = p_{measured}\left(\frac{\alpha_{filter}}{(s+\alpha_{filter})}\right) + p_{model}\left(\frac{s}{(s+\alpha_{filter})}\right)$$

The high passed section of the p_{mix} equation is driven by a simple, lag free, first order, on-axis control response model of the Bell 205, ie:

$$p_{model} = \frac{\delta_{actuator}\, L_{\delta_{a\ model}}}{s+L_{p\ model}}$$

Where:

$\delta_{actuator}$ is the command to the aircraft and,
$L_{p\ model}$ and $L_{\delta a\ model}$ are the model damping and control power derivatives, available as second order functions of airspeed.

The result of the process is a lag and noise free angular rate signal which, when used as a feedback quantity, develops an essentially open loop "predictor-type" of control system at frequencies above approximately 11.5 rad/sec. The use of mixed rates has significantly increased the potential bandwidth of control response of the Bell 205.

Designs for Rate and Attitude Respone Types

Rate Response Design - At the FRL, rate response types, based on state feedback designs have been employed for several decades. As design experience has increased, so has the quality of these designs, in terms of both achieved bandwidth and off axis coupling. The current 'best' rate response system, has an architecture as shown in Figure 7.

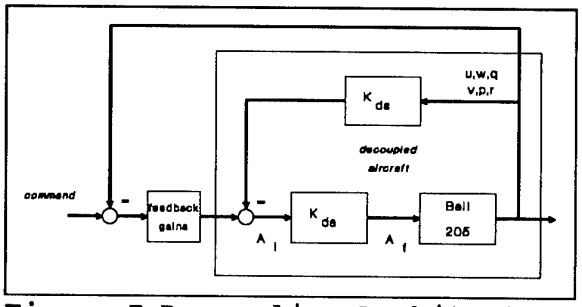

Figure 7 Decoupling Architecture

This system currently produces bandwidths of approximately 4.9 rad/sec in roll and 2.4 rad/sec in pitch, a great improvement over the limiting values of some 3.0 and 1.8 achievable only four years ago. The difference has been realised by the implementation of two decoupling matrices K_{ds} and K_{da} to decouple the aircraft to a large extent.

The limiting factor on feedback gains used in the Bell 205 (when using the mixed feedback quantities described earlier) is the excitation of a disturbing and possibly damaging fuselage/transmission mode at 14.6 rad/sec. This manifests itself as a 'galloping' motion throughout the entire airframe and, once excited, proves to be very lightly damped. Full decoupling of the aircraft via the state feedback matrix has proved effective in reducing the excitation of this mode.

The decoupling takes place in two stages, initially the state vector (u,w,q,v,p,r) is used to multiply the feedback matrix K_{ds} which contains as its elements the ratios between the negative values of the stability derivatives of the aircraft and the control power applicable to the specific row of K_{ds} .

$$K_{ds} = \begin{bmatrix} -\frac{Z_u}{Z_{\delta_c}} & -\frac{Z_w}{Z_{\delta_c}} & \cdots & -\frac{Z_r}{Z_{\delta_c}} \\ -\frac{M_u}{M_{\delta_a}} & -\frac{M_w}{M_{\delta_a}} & \cdots & -\frac{M_r}{M_{\delta_a}} \\ -\frac{L_u}{L_{\delta_b}} & -\frac{L_w}{L_{\delta_b}} & \cdots & -\frac{L_p}{L_{\delta_b}} \\ -\frac{N_u}{N_{\delta_p}} & -\frac{N_w}{N_{\delta_c}} & \cdots & -\frac{N_r}{N_{\delta_p}} \end{bmatrix}$$

$$K_{da} = \begin{bmatrix} 1.0 & -\frac{Z_{\delta_a}}{Z_{\delta_c}} & -\frac{Z_{\delta_b}}{Z_{\delta_c}} & -\frac{Z_p}{Z_{\delta_c}} \\ -\frac{M_{\delta_c}}{M_{\delta_a}} & 1.0 & -\frac{M_{\delta_b}}{M_{\delta_a}} & -\frac{M_{\delta_p}}{M_{\delta_a}} \\ -\frac{L_{\delta_c}}{L_{\delta_b}} & -\frac{L_{\delta_a}}{L_{\delta_b}} & 1.0 & -\frac{L_{\delta_p}}{L_{\delta_b}} \\ -\frac{N_{\delta_c}}{N_{\delta_p}} & -\frac{N_{\delta_a}}{N_{\delta_p}} & -\frac{N_{\delta_b}}{N_{\delta_p}} & 1.0 \end{bmatrix}$$

The four element product (A_i) contains intermediate actuator drive signals. These are processed to further improve the aircraft decoupling by multiplication with the 4 by 4 matrix K_{da} to remove the control cross axis effects inherent in the aircraft. K_{da} is composed of the major cross coupling terms, as shown above. With this, the full decoupling process is described by the equation for A_f, the final actuator signals.

$$A_f = K_{da} \times K_{ds} \cdot \begin{bmatrix} u \\ w \\ q \\ v \\ p \\ r \end{bmatrix}$$

Note that the decoupling process is applied to all six states, even those that are to be controlled. This is a convenience in the research environment since it yields a consistent starting point for the design of any control system required for the experiment at hand.

In the above discussion, it is clear that the success of decoupling the aircraft is related to how well the various stability derivatives describe the actual Bell 205 in flight. While the Heffley model of the aircraft has been shown to possess deficiencies in describing the Bell 205, the use of these model derivatives has been successful in improving the aircraft tolerance for high gain control systems. The decoupling process overall should be considered as 'taking the stress off the control system feedback loops' rather than an exercise in perfect decoupling.

With the decoupling in place, the aircraft can be assumed to behave in a K/S - like manner in angular rate response to control input in the rotational axes and a simple first order response of vertical velocity to collective input. As such, the gains on the state error can be derived theoretically using very simple models to achieve the desired control response bandwidth. Since the transmission mode is not modelled in this entire process, and since it is this mode which is primarily responsible for limiting system stability, the stability of any final system design using this process is not predicted.

The theoretical determination of state error gains is done for each control axis separately. For example, the initial calculation for pitch rate feedback gain, G_q, to produce a 2 rad/sec bandwidth rate command system in pitch can be developed from the block diagram of Figure 8.

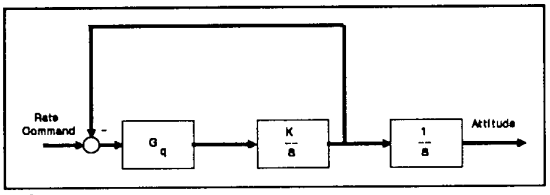

Figure 8 Rate Response Type

The system in this figure can be described by:

$$\frac{\theta(s)}{q(s)_{command}} = \frac{G_q M_\delta}{s\ (\ s+G_q M_\delta\ )}$$

Clearly, the value of G_qM_δ represents the characteristic frequency of the system. For the decoupled Bell 205 the

control power in pitch, M_δ, is approximately 0.16 rad/sec^2/in, so for a 2.0 rad/sec rate command system, G_q must be 12.5 in/rad/sec. In practice, the value of 16.0 in/rad/sec must be used to result in a 2.0 rad/sec characteristic frequency. This difference in value is due, at least in part, to modelling imperfections.

A typical attitude command system can be designed on the same principles, except that now the state error gain G_θ is augmented by a gain G_q in the feedback path, Figure 9.

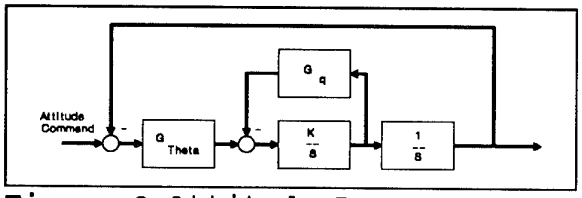

Figure 9 Attitude Response Type

$$\frac{\theta}{\theta_{command}} = \frac{M_\delta G_\theta}{(s^2 + G_q M_\delta s + M_\delta G_\theta)}$$

The system in Figure 9 develops into the equation for $\theta/\theta_{command}$. This equation describes a typical second order response, with the gain on rate being used to set the system damping. The gains thus are derived from a selected natural frequency and damping ratio, as:

$$G_\theta = \frac{\omega^2}{M_\delta}$$

and

$$G_q = \frac{2\zeta\omega}{M_\delta}$$

In practice, the value of ζ is usually chosen as 0.8. Again, some empirical adjustment of the attitude gain is usually necessary to obtain precisely the bandwidth desired, though it has rarely been necessary to adjust the damping (rate) gain.

For completeness, bode plots of rate and attitude controllers in pitch and roll for the Bell 205 are included as Figures 10 and 11.

Design of an LQR based TRC System

Analytical Design - In response to the request to present this backup paper at the Spring 1994 AGARD symposium on Active Control, it was decided to try a pure "cookbook" approach to design a translational rate command system for the Bell 205 using a modern control theory and to analyse the success and/or failure of the attempt. This process started with the installation of the MATLAB\Simulink software package, including the controls system toolbox, on to a 486 computer. After a short time of inspecting the manuals, a full-state

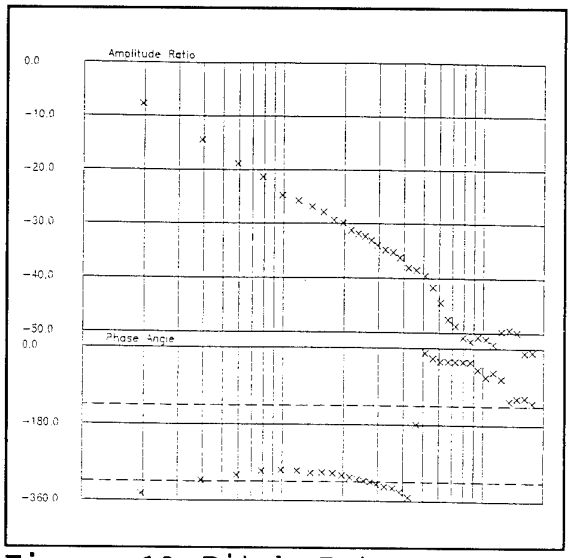

Figure 10 Pitch Rate Response Type derived from Classical Methods

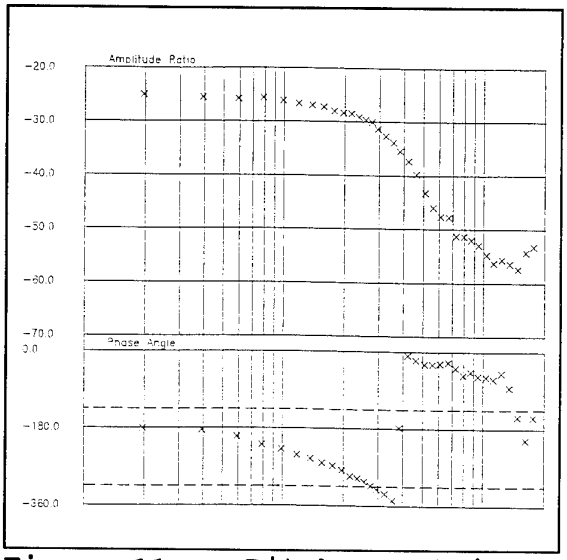

Figure 11 Pitch Attitude Response Type derived from Classical Methods

feedback, LQR design methodology was chosen and the example of a Boiler System Controller found in the User's Guide for the Control System Toolbox (page 1-44 - 58, Reference 5) was chosen as a role model to be followed to the extent possible.

The plant model chosen as a basis for the design was an eight state version of the Heffley-Bell 205 model which included the aircraft pitch and roll attitudes as states and assumed small angles so the sine of an angle could be represented as the angle itself.

Input and output weighting matrices for the LQR design, **Q** and **R**, were chosen by picking values of state error which could be assumed as equally desirable (ie. a 1 knot of speed error was equated to 1 degree of attitude error and 4 deg/sec of angular rate error.) From analysis of the final controller response to controller input, the relationships of these weighting values become clear. The ratio of rate to attitude error is associated with the system attitude damping while the ratio of speed to attitude error defines the speed command damping and effective bandwidth of the system. **Q** matrix values were set as the reciprocal squared of these assumed state errors for each diagonal element and zeros for off-diagonal elements. The values of the **R** matrix determine how much control activity is desired for a given state error. In the case of this design, the value of 1/2 inch of control per unit error was chosen, resulting in an **R** matix of the identity matrix times 4.0 .

The MATLAB " lqry " command developed a matrix of state feedback gains. It should be pointed out that the process to this stage, from opening the software package to having state feedback gains in hand, took approximately 2 hours. Bode plots of the designed system response took a little while to generate due to the author's unfamiliarity with the software package but overall a reasonably documented system was developed in well less than 1 man-day. The effectiveness of that man-day effort must be judged by measuring how well the system performed in the actual aircraft.

System Flight Test - Since the LQR methodology resulted in a full state feedback control system, and since all required feedback states are routinely measured on the Bell 205, the programming of the system was relatively easy. Comparison of the TRC gain values to the values used in empirically derived control systems suggested that the gain matrix for the LQR system was "in the right ball park". Following some in-the-hangar testing of the aircraft to ensure that the closed loop system was statically stable (engine not running, hydraulics on) and that feedback of state errors resulted in reasonable control inputs, the aircraft was rolled out for flight trials.

The initial engagement of the LQR derived TRC system occured with the author at the evaluator controls and the aircraft in a 15 foot skid-height hover. As the time histories in Figure 12 suggest, the aircraft was initially stable in position and attitude. After about 20 seconds of a slowly drifitng hover with no control input, a small input in both pitch and roll axes was made. The resulting aircraft response initiated pitch, roll and yaw oscillations in resonance with the aircraft transmission mode at a frequency of approximately 2 Hz. The LQR designed TRC system was disengaged after 40 seconds. A second trial engagement confirmed that the LQR

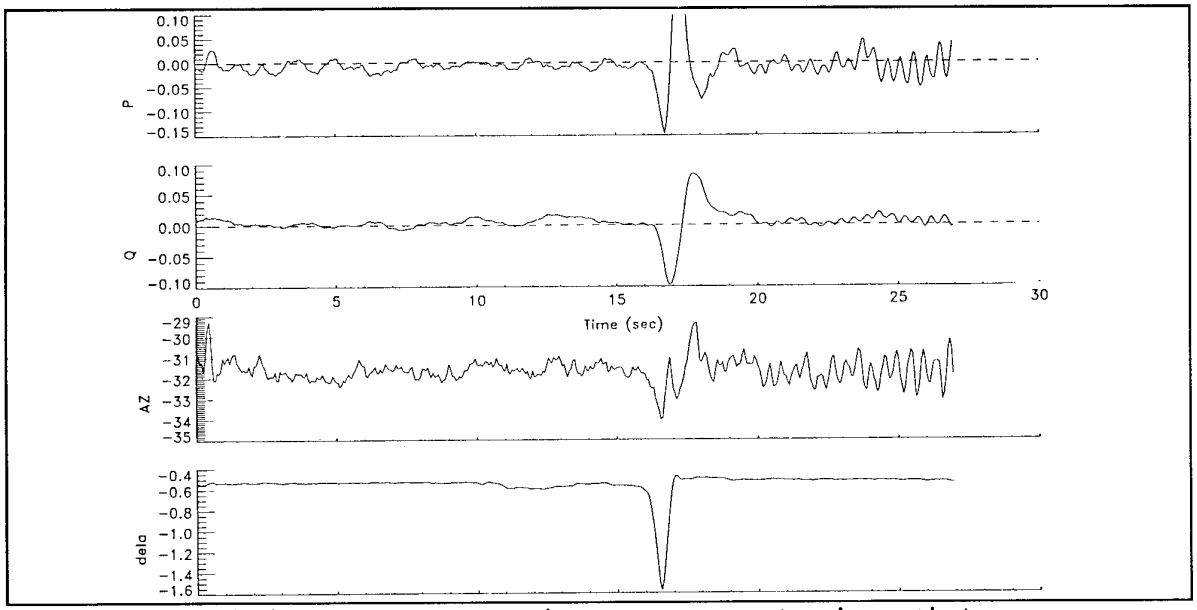

Figure 12 Initial LQR TRC Design Engagement Time History

feedback gains caused an excitation of the transmission mode at a frequency of approximately 2 Hz. The LQR designed TRC system was disengaged after 40 seconds. A second trial engagement confirmed that the LQR feedback gains caused an excitation of the transmission mode of the aircraft and in general the gains were unsuitable for flight.

The excitation of the transmission mode was not unexpected based on prior experience and the knowledge that the plant model did not represent this aircraft mode. Provisions in the Bell 205 programming had been made, prior to the first flight, to make available the aircraft "mixed" angular rates for rate feedback instead of the actual angular rate sensor signals. The switches to enable this conversion were set and subsequent engagements of the TRC system yielded a stable and moderately well behaved TRC system. Following a considerable amount of hover manoeuvring to try to initiate further instabilities to appear, the aircraft was subjected to frequency sweeps in all control axes to document the system. The general performance of the system and a discussion of the model versus aircraft match of transfer functions will now be discussed.

Overall system performance - From a limited evaluation of the handling qualities of the TRC system, it was clear that the system performance was quite good. The on-axis response of the TRC system was quite crisp in attitude response and the resulting horizontal velocity characteristics were quite acceptable. It was clear that the control of earth axis vertical velocity would have been preferable over control of body axis vertical velocity (w) but given that design choice, the control of the vertical axis of the aircraft was acceptable. The system also appeared to have exceptionally good decoupling between control axes.

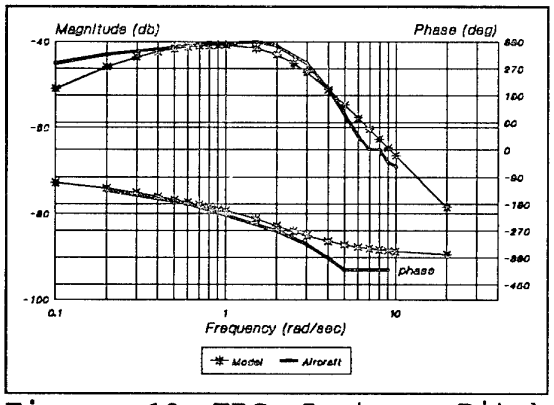

Figure 13 TRC System, Pitch Attitude Transfer Function

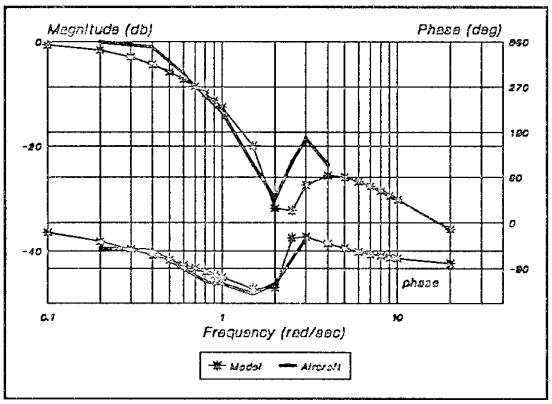

Figure 14 TRC System, Forward Velocity Transfer Function

Figures 13-15 demonstrate the predicted versus actual control response dynamics of the Bell 205 for the TRC control system. The match between the two sets of curves is quite good, with the exception of the phase curve in the yaw axis response plot.

In general, the success of the TRC system, with such a limited expenditure of time in the design process, suggests that the LQR technique is appropriate for the design of simple control systems. The success of this design in decoupling of the aircraft will be studied further and the technique will also be used for future control sytem designs.

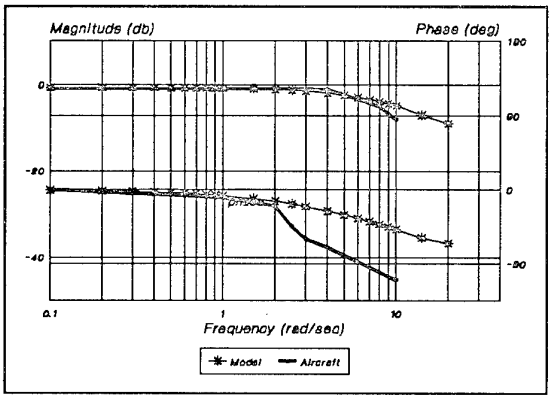

Figure 15 TRC System, Yaw Rate Transfer Function

Design of an H_2 based ACAH System

This section describes selected results of a two-year study into the modelling and control of rotary-wing aircraft. The work was carried out by researchers in the

Department of Mechanical and Aerospace Engineering at Carleton University, Ottawa, on contract to NRC and funded by CRAD/DND. In this contract a number of different attitude command/attitude hold control systems, each designed using a different modern control design technique, were developed for use on the Bell 205. Here, the results of one such design using Robust H_2 are described.

Theory -The robust control problem is essentially that of designing and analyzing accurate controllers for plant models which contain some degree of uncertainty. The term "robust" was first used in this context in 1972. Prior to that time, such control problems were generally described as "sensitivity design problems," or problems of "control system design with uncertain plants" (Reference 6).

The general robust control problem is set up by defining the plant as being one of a bounded set rather than a known model. The bounded set is considered to include all plant models which fall within the range of uncertainty of the model. This means that if the range of uncertainty has been correctly evaluated, the true plant is a member of the set. Thus, if a controller can be designed such that it provides reasonable control for all of the plants within the set, it will be acceptable for use with the real plant.

In the last 20 years or so, design methods have been developed which can aid in solving the robust control problem. These include both time and frequency domain models. Many are in fact adaptations or expansions of classical feedback control design methods. The proposed methods include the so-called H_2 methods, H_∞ methods, Inverse Nyquist Arrays, Loop Shaping, Robust LQG and Robust root-locus. In this section, we demonstrate the H_2 method, based upon the successful application of H_∞ design to the helicopter controller problem by Yue and Postlethwaite (Reference 7).

Analytical H2 Design for the Bell 205 - As in previous examples described in this report, the eight state, four input linearized (about hover) model of the Bell 205 (described earlier as the "Heffley model") was used as the baseline system. The robustness of the resultant closed-loop system was tested by substituting the linearized model trimmed at 130 knots in place of the model for hover conditions. This test simulation also included position and rate limits on the four control actuators present on the aircraft.

The H_2 controller was designed to develop attitude command for longitudinal and lateral stick inputs, body axis vertical rate command for collective lever input and yaw rate command for pedal input. The chosen state and input vectors, x and u, were:

$$x = [\theta\ ,\ p\ ,\ q\ ,\ r\ ,\ u\ ,\ v\ ,\ w]^T$$
$$u = [\delta_a\ ,\ \delta_b\ ,\ \delta_c\ ,\ \delta_r]^T$$

while the assumed measured outputs were:

$$y = [\theta\ ,\ \phi\ ,\ w\ ,\ r\ ,\ p\ ,\ q]^T$$

The outputs were scaled such that a 10 cm step input on each of the pilot controls would result in the following peak responses: θ, 0.4 radians; Φ, 0.4 radians; w, 2.0 m/s; r, 0.5 radians/s; p, 0.2 radians/s; q, 0.1 radians/s. These scalings signify the relative tracking accuracy desired in each output channel.

Analysis of the open-loop model of the Bell 205 shows that two of the output channels have small singular values at low frequency, indicating that closed-loop tracking of these outputs will be difficult. In addition, the ratio of the largest and smallest singular value (the so-called condition number) is 710, indicating that the plant is nearly singular at low frequencies and hence, attempts to employ a simple feed forward approach to aircraft control will likely fail.

The performance criteria used in the H_2 controller determination procedure is:

$$\left\| \begin{bmatrix} W_1 (I+GK)^{-1} W_3 \\ W_2 K (I+GK)^{-1} W_3 \end{bmatrix} \right\|_2$$

where W_1, W_2 and W_3 are stable, minimum-phase weighting functions. These three functions, which provide a frequency domain weighting on output errors and actuator inputs, are shown in Figure 16. The sensitivity term $(I+GK)^{-1}$ in the performance criteria is used to reduce the tracking deviations and to reduce the effect of system disturbances. The term $K(I+GK)^{-1}$ is used to reduce the effect of modelling errors and the signals to the actuators.

Yue and Postlethwaite chose the weighting functions as follows. $W_1(s)$ was chosen to have a 1/s shape, thus ensuring good tracking performance for w, r, θ and ϕ. This gain was levelled off at low frequencies as tracking cannot be achieved at resolutions less than those achieved by the sensors. W_1 (s) was also chosen to be dominant only up to 10 rad/s since unmodelled rotor dynamics makes it impractical to widen the range

beyond this. Pitch and roll rates were not controlled, but second-order bandpass filters were used to reject disturbances and cross-coupling effects in the 4 to 7 rad/s range.

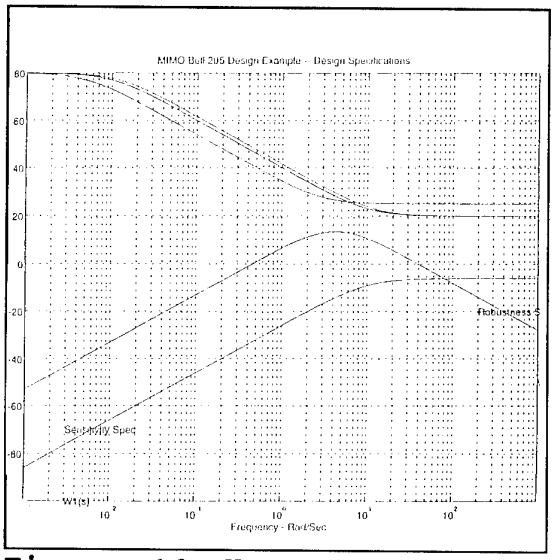

Figure 16 H_2 ACAH System Weighting Functions

$W_2(s)$ was defined to be a set of first-order highpass filters with a cut-off frequency of 10 rad/s to limit the system bandwidth and inhibit fast actuator movement. A small low frequency gain was used to allow W_1 to dominate at low frequencies. $W_3(s)$ was defined as a diagonal weighting function with a weight of 1 on the θ, ϕ, w and r channels and 0.1 of pitch and roll rates, in order to force good tracking on the output channels while having some disturbance rejection on the rate channels.

MATLAB's Robust Control Toolbox was used to carry out the minimization of the Robust H_2 performance criteria. The resultant H_2 controller has 20 states and was implemented in the forward path as a state-space (AF,BF,CF,DF) configuration (Figure 17), where the input to the controller are the six error signals and the outputs are the four commands to the actuators.

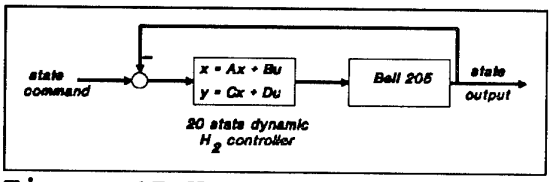

Figure 17 H_2 ACAH System

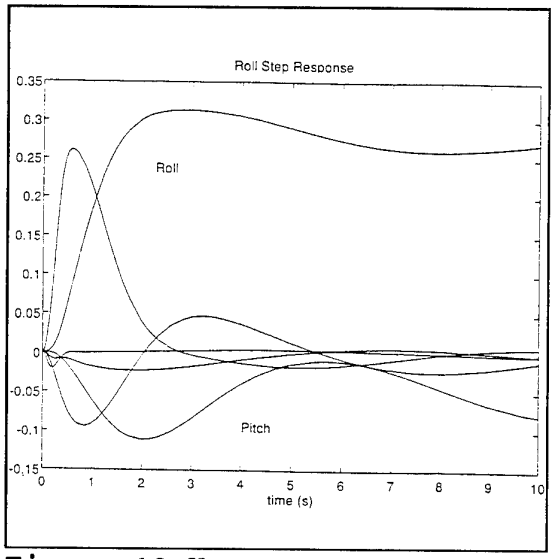

Figure 18 Hover - H_2 ACAH Roll Step Response

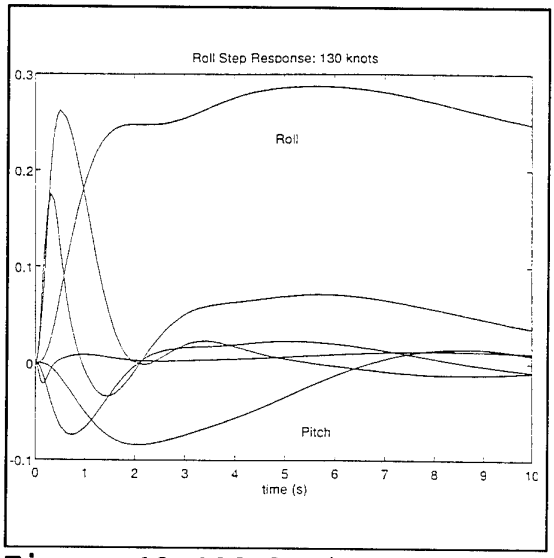

Figure 19 130 Knots - H_2 ACAH Roll Step Response

The controller was tested in the time domain through a Simulink nonlinear simulation (the linear model supplemented by control actuator magnitude and rate limits). Step responses in roll attitude command are shown in Figure 18. The speed of response and amount of cross-coupling on all four step responses is consistent with Level 1 handling qualities specifications. The frequency response of each output channel was evaluated for this nonlinear system by applying sinusoidal reference commands to each channel, in turn. The control response bandwidths were calculated to be 1.5 rad/s in pitch, 2.3 rad/s in roll, 1.86 rad/s in yaw

rate and 4.3 rad/s in heave. Robustness of the controller design was evaluated by substituting a state-space description of the Bell 205 linearized about 130 knots forward velocity for the original plan (linearized about the hover). The simulated response of the aircraft to a step in roll attitude command at the hover and at 130 knots is shown in Figure 19.

Experimental results of the H_2 ACAH Controller - Unlike the simple full state feedback LQR designed TRC system, the programming of the H_2 ACAH system entailed a number of problems. The requirement to calculate and maintain the 20 dynamic states and yet remain within the time slice allowed for the aircraft computational system was not trivial to meet. Since quite a number of the elements in the H_2 matrices were 0.0, a technique of using special indices to control the evaluation of non-zero terms of all of the matrix equations was finally used to make the controller execution time fit into the 1/64th of a second time slice requirement. As with other programmed controllers, the H_2 controller was subjected to on-ground, engine - off, hydraulics - on testing as well as thorough analytical program debugging to ensure that the system was essentially as designed. Unfortunately, with the aircraft not able to respond to control during this test, it became unclear as to whether the dynamics of the controller states would be the same as in flight. To circumvent this concern, the Heffley - Bell 205 hover model was programmed on the aircraft computer so that the controller software could be checked closed loop with the aircraft model on the ground. This simulation provided a reasonable assurance that the airborne software was free from error.

Another problem with the H_2 controller was highlighted during this testing phase. While with a simple state feedback controller, an analyst can directly assess the effect of each element in the feedback matrix, ie. element (4,2) results in so much of control x for so much y state error, the elements of the matrices in the H_2 controller cannot be similarly assessed. The H_2 design involved significantly larger numbers than used in more conventional designs (eg 150-200 vs 30) and thus the concern over "what the controller was doing" was strong.

The flight test of the H_2 derived controller was relatively short. As Figure 20 demonstrates, the aircraft diverged in a pitch/roll oscillation and the controller was disengaged after 6-8 seconds. Numerous trials, both with and without the use of "mixed" rate feedback, ended in similar fashion. Unfortunately the flight trials have yet to be rigorously analysed however the following can summarize our knowledge to date:

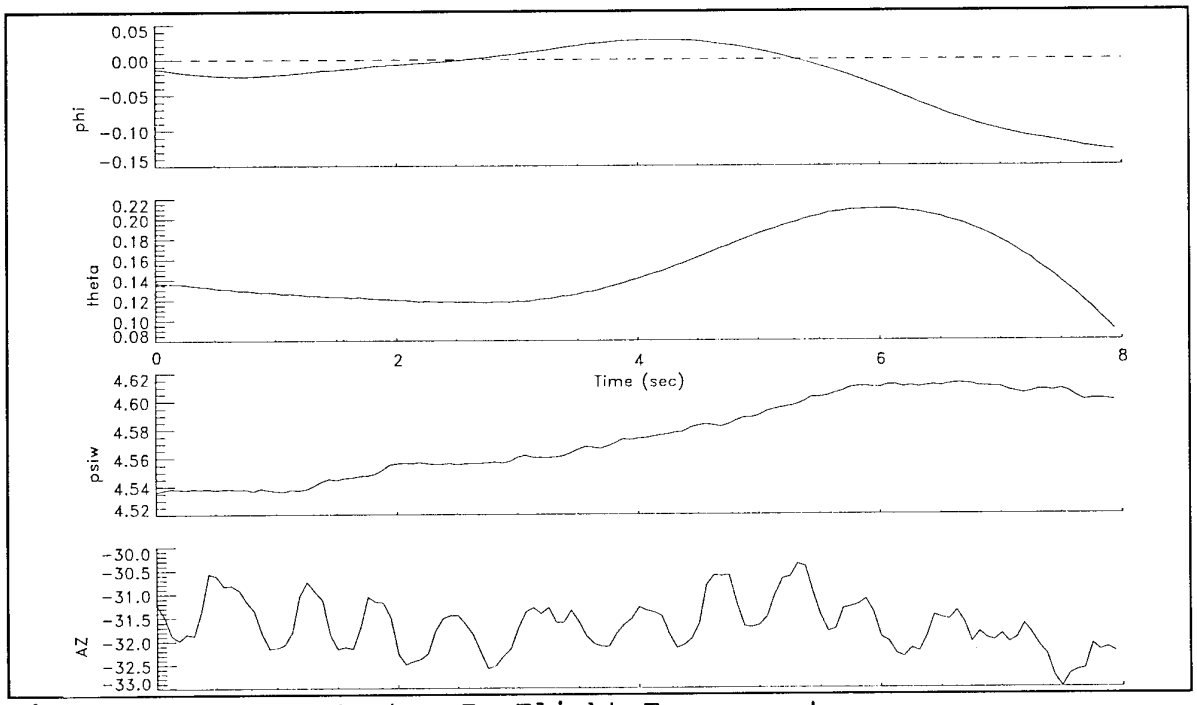

Figure 20 H_2 ACAH System In-Flight Engagement

1) the model upon which the design was based does have inaccuracies,

2) the H_2 controller and model combination performance is satisfactory,

3) other, more conventional, controllers have shown that the simulation of the controller response results in charactersitics which compare favourably to the actual aircraft measured characteristics,

4) the H_2 controller was unstable in flight, and

5) the reasons behind this instability are unknown at this time.

Further research in this area is being conducted.

Summary

The control systems described in this paper stem from 25 years of operational experience with the NRC Bell 205 Airborne Simulator. With such a well-known platform, the development of empirical techniques and fixes over such a time period has resulted in aircraft control systems which are well understood and provide the dynamic characteristics that are required. The use of the NRC Bell 205 to evaluate modern control design techniques is a new avenue of research. The results of initial testing with an LQR based design shows promise while further investigation of the H_2 based controller is required to understand its current shortcomings.

References

1. J. Murray Morgan, Stewart W.Baillie, "*ADS-33C Related Handling Qualities Research Performed Using the NRC Bell 205 Airborne Simulator*", Piloting Vertical Flight Aircraft: A Conference on Flying Qualities and Human Factors, Sponsored by the Anerican Helicopter Society, San Francisco, California, January 1993

2. S.W. Baillie, S. Kereliuk, J.M. Morgan, "*The Effects of Tailwinds and Control Cross Coupling on Rotorcraft Handling Qualities for Steep, Decelerating Instrument Approaches and Missed Approaches*" , Aeronautical Note IAR-AN-77, Institute for Aersopace Research, Natinal Research Council of Canada, Ottawa, September 1993

3. Heffley R.K., W.F. Jewell, J.M. Lehman and R.A. Van Winkle, *A Compilation and Analysis of Helicopter Handling Qualities Data.* NASA Contractor Report 3144, 1979.

4. Sattler, D.E. ,*The National Aeronautical Establishment Airborne Simulation Facility,* NRC, NAE Misc 58, May 1984.

5. Grace, Andrew, et al, *Matlab - Control System Toolbox - User's Guide* ,July 1992

6. Dorato, P., 1987, *Robust Control*, IEEE Press, New York.

7. Yue, A. and I. Postlethwaite, 1990, I*mprovement of Helicopter Handling Qualities Using H∞ Optimization,* IEE Proc., vol.137, Pt.D, no.3, pp.115-129.

LES QUALITES DE VOL DES AVIONS DE TRANSPORT CIVIL A COMMANDES DE VOL ELECTRIQUES

by D. Chatrenet
Head of Handling Qualities Dept.
AEROSPATIALE – M0131-1, 316, Route de Bayonne
31060 Toulouse Cedex 03 FRANCE

1. INTRODUCTION - RAPPEL HISTORIQUE

L'A320 a effectué son premier vol en 1987 et fut certifié et mis en service en 1988. La presse a longuement commenté ces événements comme marquant le début d'une nouvelle ère technologique, notamment en raison des commandes de vol électriques qui équipent cet avion.

Pour les spécialistes concernés, cette appréciation a été jugée largement exagérée, car elle semblait faire fi de tout un passé riche en développements technologiques significatifs, dont l'A320 apparaît finalement comme une étape. Il est bon de les rappeler ici brièvement :

- Depuis 1969, Concorde vole avec un système de commandes de vol électriques, avec pleine autorité sur les trois axes, à base de calculateurs analogiques avec voies Commande et Surveillance ; un secours mécanique est disponible sur les trois axes, mais est normalement débrayé. A ce titre, Concorde est le premier avion de transport civil à avoir été équipé de commandes de vol électriques.
- En 1978, le premier Concorde de présérie a servi de plate-forme à une intéressante expérimentation du pilotage à travers un manche latéral et avec une loi de pilotage longitudinale du type C*. (Loi en facteur de charge commandé).
- En 1981, la version FFCC (Forward Facing Crew Cockpit) de l'Airbus A300B4 fut développée pour la compagnie Garuda. A cette occasion, les calculateurs analogiques du pilote automatique furent remplacés par des calculateurs digitaux, qui marquèrent ainsi l'avènement de la technologie digitale doublée surveillée (dual/dual : deux calculateurs identiques, chacun avec une voie commande et une voie surveillance), y compris pour une fonction de guidage critique qui est celle de l'Atterrissage automatique Tout Temps.
- En 1982, le programme A310 a étendu l'usage de cette technologie à une partie des commandes de vol primaires, les spoilers, dont la fonction est critique d'un point de vue sécurité et aux commandes de vol secondaires.
- En 1983 et 1985, l'avion de série n° 3 de la famille A300 a servi de support à une série d'expérimentations en vol préparant le programme A320 ; au cours de ces campagnes, furent essayés et évalués par un large éventail de pilotes des compagnies :
  - le manche latéral, d'abord en place gauche seulement, puis des deux côtés avec les logiques de priorité associées,
  - les lois de pilotage longitudinales et latérales,
  - les protections du domaine de vol.
- 1987/1988, certification et mise en service de l'A320, avec un système de commandes de vol électriques digitales à pleine autorité sur les trois axes, à base d'architecture doublée surveillée et dissimilaire (calculateurs ELAC/SEC) et un secours mécanique permanent disponible sur deux axes.
- 1992/1993, certification et mise en service des A340 et A330 avec un système de commandes de vol pratiquement identique à celui de l'A320.

Ce rappel historique montre bien combien le développement du système de commandes de vol électriques des avions européens a été progressif, chaque étape s'appuyant sur l'expérience et les enseignements tirés de l'étape précédente. Il s'agit bel et bien d'une évolution et non pas d'une révolution, délibérément choisie afin de minimiser les risques pour l'utilisateur client et pour l'avionneur concepteur.

Ce qui vient d'être rappelé concernant le **système** s'applique de la même façon en ce qui concerne les **Qualités de Vol**.

L'objet de cette présentation est de décrire et commenter les étapes qui ont marqué l'évolution des qualités de vol de Concorde à l'A340.

2. QUALITES DE VOL ET LOIS DE PILOTAGE

Pour un avion non équipé de commandes de vol électriques, dit "conventionnel", il existe une relation bi-univoque entre la position des organes de pilotage et la position des gouvernes, résultant du mode de transmission mécanique des ordres de pilotage. Pendant des décennies, les qualités de vol des avions conventionnels (la façon dont le pilote perçoit la réponse de l'avion à ses actions sur les organes de pilotage) ont été évaluées dans ce contexte ; elles dépendent en grande partie des caractéristiques aérodynamiques et massiques de la cellule.

Sur un avion à commandes de vol électriques, la transmission mécanique est remplacée par un signal électrique avec un calculateur au milieu. Il est alors très facile d'altérer la relation position organe de pilotage/position gouverne (en fonction du point du domaine de vol, du centrage etc...) et même d'introduire des asservissements en fonction de la mesure des mouvements de l'avion.

La relation plus complexe entre organe de pilotage et gouvernes s'appelle alors Loi de Pilotage et l'on conçoit que cette dernière vienne elle aussi jouer un rôle prépondérant dans l'analyse des Qualités de Vol.

Nota : Cette vision est simplifiée, car les dernières générations d'avions "conventionnels" utilisent partiellement la notion de lois de pilotage afin de moduler la liaison mécanique organe de pilotage/gouverne (exemples : stabilisateur de lacet, mach trim, etc...).

3. QUALITES DE VOL DU CONCORDE

Ce texte ne prétend pas décrire l'ensemble des qualités de vol de ce magnifique appareil, mais de se limiter aux aspects qui ont été impactés par le système de commandes de vol électriques ou qui ont fortement pesé sur sa définition.

Paper presented at the Flight Mechanics Panel Symposium held in Turin, Italy, from 9-13 May 1994.

3.1 . Pourquoi un système de commandes de vol électriques ?

La décision d'adopter pour Concorde un tel système de commandes de vol a été fortement influencée par la contrainte d'obtenir un contrôle très précis de la position des gouvernes : en effet, la traversée du régime transsonique est caractérisée par une variation importante du foyer et du point de manœuvre ; lors de cette phase, le contrôle actif de la position du centre de gravité est assuré par le transfert du carburant, avec pour objectif de maintenir marge de manœuvre et stabilité statique. Malgré cela, des caractéristiques d'effort/g ou de déplacement/g très faibles étaient prédits. Dans ce contexte, les défauts de qualité inhérents à un système mécanique (jeu, hystérésis, friction) risquaient de conduire à de mauvaises Qualités de Vol.

3.2 . L'introduction des fonctions de stabilisation

L'adoption de commandes de vol électriques, même avec une simple relation linéaire entre organes de pilotage et gouvernes, permettait donc de satisfaire à l'objectif précédent. Un avantage supplémentaire de cette décision fut vite exploité : la possibilité d'introduire des retours gyrométriques.

L'objectif poursuivi était alors la réduction des charges de travail de l'équipage et l'amélioration classique du confort passager pour l'axe latéral.

L'adoption d'un stab de tangage sur l'axe longitudinal a permis d'augmenter la marge de manœuvre et de compenser la diminution de l'amortissement de l'oscillation d'incidence à grand mach.

L'amortissement du roulis hollandais a bien sûr été considérablement amélioré par l'adoption d'un stab de lacet, qui fut aussi complété par un stab de roulis afin de diminuer l'excitation du roulis hollandais par la commande de gauchissement (critère $\omega\phi/\omega d$).

L'ensemble ainsi obtenu se caractérise par de bonnes qualités de vol, bien homogènes dans tout le domaine de vitesses tant subsoniques que supersoniques. On peut alors se demander ce qu'il en est en cas de réversion en secours mécanique. A ce jour, aucune réversion totale n'a été rapportée ; dans un tel cas de panne, le vol supersonique doit être abandonné. Ce scénario a été testé en développement et certification et les qualités de vol, bien que sensiblement détériorées, permettent encore un retour dans le domaine subsonique et la fin du vol à la portée d'un pilote normalement adroit et entraîné.

3.3 . Les "super stabs"

Des objectifs supplémentaires de qualités de vol ont été fixés aux limites du domaine de vol, afin de tenir compte du comportement naturel de la voilure delta à grande incidence, de la qualité recherchée de l'écoulement aérodynamique au niveau des entrées d'air, et de la dégradation constatée des caractéristiques longitudinales en fonction du dérapage. Un domaine incidence/dérapage a été déterminé et des "super stabs" ont été introduits pour empêcher les excursions en dehors de ce domaine. A l'inverse des stabs dont l'action est permanente et procure un amortissement artificiel, ces super stabs ne sont introduits que de façon conditionnelle, en fonction de seuils sur l'incidence et le dérapage et constituent des fonctions de rappel.

4 . QUALITES DE VOL DE L'A320

4.1 . Qualités de vol de l'avion naturel

La conception initiale et le dimensionnement général de l'avion ont été effectués avant de prendre la décision d'utiliser des commandes de vol électriques.

La taille des empennages, le diagramme de centrage en font un avion stable sur tous les axes. En vol, l'avion a révélé d'excellentes qualités de vol en loi directe, un décrochage "comme dans les livres" et des efficacités de gouvernes plus importantes que nécessaires. Paradoxalement, de telles qualités de vol de l'avion naturel réduisent le potentiel d'améliorations que l'on peut attendre des commandes de vol électriques.

Pour tempérer les propos ci-dessus, il faut signaler que l'usage des aérofreins internes (le panneau situé entre la cassure du bord de fuite et le fuselage) a dû être abandonné en raison de l'inconfort et du niveau vibratoire engendré par l'interférence avec l'empennage horizontal. L'efficacité résiduelle de l'aérofreinage ainsi amputé est encore amplement suffisante, mais la configuration d'aérofreinage ainsi obtenue ne peut plus être optimisée en couple de tangage (couple cabreur résultant).

4.2 . Les lois de pilotage "normales"

Il n'y a pas grand chose à dire sur ces lois qui sont des types classiques :

- C* en longitudinal, (commande en facteur de charge, avec mélange de vitesse de tangage à basse vitesse),
- commande en vitesse de roulis/maintien d'assiette en latéral.

Grâce à l'exercice de conception et d'adaptation de ces lois à l'Airbus n° 3 en 1983 et 1985, la mise au point de ces lois sur l'A320 n'a soulevé aucun problème particulier.

Les qualités de vol qui en résultent sont bien connues :

- fonction autotrim en longitudinal,
- stabilité de plate-forme et stabilité statique neutre,
- stabilité spirale neutre commandée, stabilité spirale positive vis-à-vis des perturbations,
- amélioration de l'amortissement du roulis hollandais,
- coordination de virage sans action au pied,
- effet de la panne moteur contenu tout en restant suffisamment alertant et du sens conventionnel.

4.3 . La protection d'incidence

Il est intéressant de rappeler les considérations qui ont conduit à adopter une protection insurpassable de l'incidence. Tout d'abord, les qualités en manœuvre et en stabilité d'assiette offertes par la loi C* sont associées avec la perte de stabilité statique ; cette perte n'est pas gênante dans le domaine de vol mais demande à être restaurée aux limites de celui-ci et notamment vers les basses vitesses/grandes incidences. Ensuite, le décrochage demeure statistiquement un écueil à la sécurité, même sur les avions où celui-ci est réputé sain et reconnaissable ; les gradients de vent en donnent une illustration. Enfin, un avantage industriel était pressenti par la possibilité de s'affranchir de la mise au point et de l'utilisation des dispositifs généralement nécessaires sur les avions à voilure subsonique optimisée, pour obtenir un décrochage

sain et reconnaissable (tels que générateurs de tourbillons, fences, alpha trim, pousseur de manche...).

Paradoxalement, ce dernier point s'est révélé non applicable à l'A320, en raison de l'exceptionnelle qualité de la voilure et de ses caractéristiques de décrochage. Dans le même temps, la non résolution des aspects de certification relatifs à la définition de la vitesse de décrochage sur un avion protégé faisaient craindre à l'A320 d'être gratifié de vitesses de décrochage plus élevées que celles d'un avion non protégé (avec donc des pénalités de performances). L'utilité de la protection pouvait être remise en question...

Heureusement, de longues discussions avec les Services Officiels aboutirent à un texte réglementaire ni favorable, ni pénalisant, basé sur la démonstration d'une vitesse conventionnelle de décrochage ramenée à facteur de charge unitaire, assortie de la démonstration d'efficacité de la protection et d'une manœuvrabilité minimale.

Autant les discussions précédentes furent animées par l'esprit de la détermination d'un niveau minimum acceptable de sécurité (et de manœuvrabilité), autant la conception de la protection elle-même fut animée par le principe d'offrir toujours le maximum de manœuvrabilité et donc de fixer l'incidence maximale limitée par la protection à la valeur la plus élevée possible. Pour ce faire, ce calage de l'incidence max fut augmenté pas à pas et essayé en vol jusqu'à obtention d'un comportement à la limite de l'acceptable.

Sur le plan de la mécanique du vol, s'il n'y a pas de difficulté particulière à réaliser une commande en incidence, il faut signaler que le maintien strict d'une incidence (max) pour une position de l'organe de pilotage (butée) favorise le développement de la phugoïde dont les variations d'altitude ne sont pas idéales près du sol. Un compromis trajectoire/incidence a été préféré, conduisant à des variations acceptées de l'incidence autour de l'incidence de consigne.

Il faut également rappeler que si l'avion est effectivement protégé contre le décrochage (protection du mouvement de l'avion autour de son centre de gravité), la seule protection d'incidence ne peut éviter une trajectoire à long terme descendante si la poussée est inférieure à la traînée. Une remise des gaz automatique a été adjointe à la protection d'incidence (déclenchée sur un seuil en incidence) pour adapter le niveau d'énergie à la manœuvrabilité recherchée. Cette fonction, appelée "alpha floor", a malheureusement été assimilée à un avertisseur de décrochage, vis-à-vis duquel les vitesses opérationnelles doivent donc réglementairement posséder des marges minimales. On aboutit alors au paradoxe selon lequel un système destiné à accroître la sécurité et auquel on applique un règlement inadapté conduit soit à des pénalités de performances, soit à l'exploitation incomplète du potentiel de la protection.

Enfin, la mise au point de la protection d'incidence a été compliquée par la nécessité de la rendre compatible avec des manœuvres latérales ; il a fallu pour cela tenir compte de l'effet du dérapage sur la mesure de l'incidence. Quoiqu'il en soit, la protection d'incidence a ses limites et il n'entre pas dans ses objectifs de protéger l'avion en cas d'action excessive au palonnier à haute incidence (action pas plus recommandée sur les avions conventionnels !).

Le résultat global de cette protection, telle que réglée et mise au point est d'offrir au pilote qui en aurait besoin le maximum de manœuvrabilité qui soit sûr et facilement accessible.

4.4 . La loi d'atterrissage

Les premières études sur les lois de pilotage, notamment l'expérimentation Concorde de 1978, ont permis de tirer entre autres deux enseignements :

- des lois de pilotage élaborées ne doivent pas conduire à une modification radicale de la façon de piloter (le pilotage doit rester instinctif),
- la loi C* n'est pas bien adaptée pour l'atterrissage : elle masque l'effet de sol, conduit à des arrondis "à facettes", voire nécessite une action à piquer pour poser l'avion.

Il fallait donc sur A320, pour l'atterrissage, abandonner la loi C* et faire la transition vers une loi spécifique. Les objectifs fixés à cette loi furent :

- ne pas cacher ou restaurer pour le pilote la sensation d'un avion pénétrant dans l'effet de sol,
- posséder de bonnes marges vis-à-vis du PIO,
- être cependant capable d'arrêter un taux de descente excessif,
- offrir une homogénéité de réponse quel que soit le centrage,
- cependant utiliser si nécessaire toute la plage de gouverne disponible,
- assurer une transition facile pour la dérotation ou la remise des gaz.

La mise au point ne fut pas facile et de nombreuses lois furent essayées, tant au simulateur qu'en vol. Certaines ne furent pas de francs succès et ont laissé des souvenirs impérissables aux équipes d'essais en vol. La meilleure loi fut retenue relativement tard dans le programme d'essais et consiste en l'adjonction à la C*, en dessous de 50 ft, d'un fort retour en assiette. La commande en facteur de charge est alors remplacée en pratique par une commande en assiette ; l'assiette de consigne manche au neutre est constante de 50 ft à 30 ft et égale à celle mémorisée à 50 ft ; en dessous de 30 ft, elle est progressivement dégonflée jusqu'à atteindre - 2°, ce qui incite le pilote à tirer sur le manche pour compenser et restitue ainsi un effet de sol conventionnel.

Une anecdote vaut la peine d'être mentionnée, car elle illustre bien les difficultés rencontrées par le spécialiste de Qualités de Vol pour interpréter des appréciations subjectives des pilotes : dans les débuts de la mise en service, les équipages se sont plaints de la loi d'atterrissage : il leur semblait difficile de maîtriser la vitesse verticale à l'impact et l'adresse développée pour tenter d'effectuer un "kiss landing" était souvent payée de retour par un atterrissage bien ferme. Les opérateurs indiens, avec la même loi, mais un train d'atterrissage différent (à bogies) ne souffraient pas du même phénomène. Ultérieurement, le train principal d'origine à été amélioré par l'introduction d'un amortisseur double chambre et les plaintes ont cessé aussitôt.

4.5 . Ergonomie du manche latéral et logique de priorité

Les caractéristiques ergonomiques du manche latéral ont été finalisées longtemps avant les vols de l'A320, à la suite d'un parcours intensif de recherche et de développement impliquant les milieux médicaux et l'usage de modèles anthropométriques ; c'est ainsi que furent déterminés :

- la taille de la poignée,

- son inclinaison à braquage neutre,
- la position des axes de rotation,
- les déplacements angulaires maximaux,
- les gradients d'effort par déplacement,
- les seuils d'effort.

Le manche retenu à l'issu de ces études est un manche à déplacement significatif (± 20° en gauchissement, ± 16° en profondeur), à efforts maxi adaptés sur chaque axe (10 daN en profondeur, environ 3 daN en gauchissement), avec sur l'axe de gauchissement une différentiation des efforts entre mouvement vers l'extérieur et vers l'intérieur, et des seuils d'effort minimisés (0,5 daN). Dès 1978, lors de l'expérimentation Concorde, ces caractéristiques étaient sélectionnées. Cette expérimentation a permis de démontrer, ce qui était nouveau pour nous à l'époque et est devenu universellement reconnu depuis, qu'il n'y avait aucun problème particulier de pilotage avec ce type de manipulateur.

La non-conjugaison mécanique de deux manches latéraux a nécessité de définir une logique de prise en compte des ordres de chaque manche et de priorité en cas de blocage ou d'action intempestive sur un manche. Ces logiques ont été essayées et finalisées avant les vols de l'A320, grâce à des essais au simulateur et à la campagne d'essai en vol de l'Airbus n° 3 en 1985. Le principe de symétrie entre les deux manches a été préféré à celui de l'identification a priori du seul manche pris en compte, voire d'un manche prioritaire ou principal vis-à-vis de l'autre. En conséquence, l'ordre qui entre dans les lois de pilotage est en permanence la somme algébrique des ordres droite et gauche, ce qui donne à chaque pilote la possibilité d'avoir à tout instant et sans action préalable la pleine autorité. Les cas de blocage d'un manche défléchi ou d'incapacitation d'un des pilotes ont conduit à l'adjonction d'un bouton de prise de priorité qui permet d'annuler le cas échéant la prise en compte des ordres venant de l'autre manche ; selon le principe de symétrie, c'est le dernier bouton enfoncé qui a la priorité (suprématie du pilote le plus intelligent sur le plus fort). D'autres solutions ont été considérées et certaines essayées en vol, puis abandonnées en raison de leur caractère confusant.

La phase d'essais en vol de l'A320 n'a remis en cause aucune des caractéristiques précédemment énumérées. Seul l'angle de calage (pincement) des boîtiers de manche a été ajusté de façon à éviter, lors de mouvements très rapides, la pollution d'un axe par l'autre.

C'est aussi lors de la phase d'essais en vol que furent déterminées les synchronisations optimales entre le pilotage automatique et le pilotage manuel afin bien sûr d'éviter les à-coups lors de la reprise en main mais aussi de permettre la prise en compte sans délai des ordres de pilotage manuel lorsque cela est nécessaire.

On obtient ainsi par logiciel une synchronisation en effort et déplacement sans avoir besoin de recourir à un système de motorisation des organes de pilotage complexe et potentiellement source de problèmes.

5. LES QUALITES DE VOL DE L'A340

5.1. Objectifs

Pour des raisons évidentes de minimisation des risques de développement et pour faciliter la qualification commune des équipages sur la nouvelle génération des Airbus, il a été décidé d'adopter pour l'A340 (et l'A330) les mêmes lois de pilotage que celles de l'A320, en les adaptant au contexte du nouveau programme :

- avion souple de grande taille,
- avion long courrier,
- performances plus critiques.

5.2. Impact sur les qualités de vol de l'avion souple

Plus la taille de l'avion souple est importante, et plus la fréquence des modes structuraux est faible. Sur l'A320, cette fréquence est telle que la bande passante du système de commandes de vol atténue suffisamment pour ne pas craindre de rebouclage entre la structure et les commandes de vol à travers les retours. Sur l'A340, ce n'est plus le cas ; le pilote automatique et les lois de pilotage doivent être conçus en prenant les précautions nécessaires pour éviter de déstabiliser la structure.

Parmi ces précautions, les plus simples consistent à filtrer et à limiter les gains de retour. Lorsque les fréquences des premiers modes se rapprochent de celles du pilotage, le filtrage ne peut se faire que aux dépens des qualités de vol, tout comme la limitation des gains.

Ces contraintes ont donc rendu plus difficile la tâche de réglage des gains des lois de pilotage, car la marge entre la satisfaction des objectifs de qualités de vol et le respect des contraintes de stabilité structurale était ténue. Par ailleurs, le maintien de la sécurité des vols d'essais a nécessité le respect de procédures rigoureuses de validation des lois de pilotage par les experts de structure et de vérification de la présence des filtres. Il faut signaler aussi que l'architecture du filtrage retenue a été déterminée afin de conserver le maximum de marges vis-à-vis du PIO.

5.3. Impact sur les Qualités de Vol de l'avion long courrier

Sur un avion long courrier, l'optimisation des performances de croisière (rayon d'action spécifique V/C) est amplifiée par l'effet boule de neige dû à la distance et joue un rôle fondamental sur l'économie et la charge marchande transportable de la machine. Il n'est donc pas étonnant que l'A340 ait été optimisé dans ce contexte, en tolérant volontairement des qualités de vol de l'avion naturel d'un niveau inférieur à celles de l'A320. C'est ainsi que les empennages sont de taille minimale (mais l'avion reste naturellement stable) et que la voilure présente des non-linéarités plus marquées à grande incidence.

Le système de commandes de vol électriques a permis de compenser cette moindre optimisation des qualités de vol de l'avion naturel :

- Le roulis hollandais, naturellement très peu amorti dans certaines parties du domaine de vol, est artificiellement amorti par les lois de pilotage dont l'architecture est renforcée pour rendre la perte de la fonction amortissement du roulis hollandais Extrêmement Improbable (utilisation si nécessaire des ailerons). Néanmoins, pour couvrir le recours momentané au secours mécanique, c'est-à-dire le scénario forfaitaire et hors règlement de

perte totale électrique, le BYDU (Back-up Yaw Damper Unit) a été développé. Il s'agit d'un ensemble autonome, tirant son énergie de la pression hydraulique, capable de se substituer aux vérins normaux de stab de lacet et comportant micro-générations locales, un gyromètre, un circuit analogique et un servo-moteur électrique.

- La protection d'incidence a été renforcée et pour cela comporte deux régimes ; à incidence modérée et comme sur l'A320, un compromis est obtenu entre maintien de trajectoire et maintien d'incidence, à incidence proche de l'incidence maxi, un contrôle plus fort de l'incidence est privilégié.

5.4 . Optimisation des performances : VMCG

Les capacités de charge marchande/rayon d'action de l'A340, comme tout long courrier quadri-réacteur, sont souvent limitées par les performances au décollage. L'utilisation de cet avion sur des routes à faible densité peut le conduire à opérer sur des pistes relativement courtes ; sur ces pistes, les performances sont limitées par la VMCG (Vitesse Minimale de Contrôle au sol), en raison du bras de levier du moteur externe et de l'inertie importante de la machine (cette dernière peut retarder la reconnaissance de la panne moteur lors de roulage au décollage).

Les commandes de vol électriques ont permis par leur souplesse d'améliorer les VMCG de l'A340 : il a été tiré parti du couple de lacet induit par les surfaces de gauchissement pour augmenter artificiellement l'efficacité de la direction et aider au contre du couple dû à la panne moteur. Les lois de pilotage sont telles que, même sans ordre de gauchissement, et au-delà d'un certain braquage du palonnier, un spoiler et deux ailerons sont braqués "à contre" sur la même demi-voilure, générant ainsi un couple de lacet à moment de roulis quasi inchangé.

5.5 . Optimisation des performances : VMU

Les mêmes remarques que celles du paragraphe précédent sont valables et sont complétées par le fait que sur pistes longues, l'A340 est limité VMU (vitesse minimale à laquelle l'avion peut quitter le sol). La VMU est directement liée à l'assiette maxi que l'avion peut développer pour quitter le sol sans toucher la piste avec la partie arrière du fuselage.

Pour optimiser la VMU, l'A340 est équipé d'un train à bogie dont la rotation est cinématiquement liée à la détente de l'amortisseur en fin de course. Contrairement au bogie classique (dont la rotation est quasi-libre), ce train est encore capable au décollage de générer des forces de contact avec le sol considérables jusqu'à la fin de la rotation du bogie. Cela donne simultanément, lorsque l'avion est au sol à assiette nul, un train court (léger) et un seuil de portes pas trop haut, et lors de la démonstration de la VMU une assiette importante car obtenue avec le bogie complètement pivoté et l'avion "debout" sur les roues arrière.

Ce principe élégant sur le papier s'est heurté à un écueil pratique en essais en vol : lors de manœuvres de décollage très dynamiques, le bogie n'avait pas le temps de terminer sa rotation avant que l'arrière du fuselage n'impacte le sol et le gain sur la VMU prenait un caractère quelque peu artificiel car le but recherché par le règlement relatif à la VMU, qui est d'éviter entre autre un contact de l'arrière du fuselage avec la piste, n'était pas complètement atteint.

Pour restaurer les bénéfices potentiels associés au train à bogie basculant, une loi de pilotage a été développée spécifiquement pour la phase de rotation ou décollage, avec pour objectif d'éviter les taux de rotation excessifs.

La loi retenue est en fait un simple stab de tangage, mais son réglage (gain, seuil, autorité) et la transition qui suit avec la loi vol ont été déterminés après plusieurs essais en vol, à la fois pour satisfaire l'objectif fixé, mais aussi et surtout pour s'intégrer harmonieusement avec les actions naturelles du pilote dans cette phase.

6 . CONCLUSION

Ce rappel historique montre bien les étapes successives et progressives qui ont marqué l'évolution des Qualités de Vol des avions de transport à commandes de vol électriques :

- incorporation de stabs et super stabs pour Concorde,
- lois de pilotage C* et commande en vitesse de roulis, protection du domaine de vol, loi d'atterrissage et manches latéraux non conjugués mécaniquement pour l'A320,
- optimisation des performances et prise en compte des contraintes de l'avion souple pour l'A340.

Compte tenu du ralentissement du rythme des nouveaux programmes de la famille Airbus et pour des raisons évidentes de communalité, il n'est pas envisagé d'évolution majeure des Qualités de Vol dans le proche avenir.

Le programme FLA, bien que militaire, sera cependant une étape intéressante à suivre. Il sera certainement à commandes de vol électriques et ses exigences opérationnelles seront assez différentes de celles d'un avion civil. En conséquences, certaines des caractéristiques de qualités de vol et de lois de pilotages énoncées dans cette présentation pourront être reconduites, d'autres devront être adaptées ou modifiées. Dans tous les cas, l'expérience accumulée sur les programmes ici cités sera d'une incontestable valeur.

Pour préparer ces avions de demain, notre effort de recherche est déjà engagé et on peut citer quelques uns de nos axes :

- couplage poussée/tangage (contrôle du plan vertical par une commande globale double profondeur/moteur),
- lois de pilotage pour le ravitaillement en vol,
- lois de pilotage optimisées pour un avion très flexible,
- méthodologie de robustesse des lois de pilotage,
- ...

Copyright © Aerospatiale 1994.
Published by Agard with permission

Pilot Induced Oscillation - A Report on the AGARD Workshop on PIO, 13th May, 1994

K.McKay*

British Aerospace Defence (Military Aircraft Division)

Warton Aerodrome, Preston PR4 1AX

United Kingdom

Abstract

Instability of the pilot/airframe combination has been a problem from the beginning of manned flight. The rapid advances made in aviation following the Second World War greatly increased the incidence of PIO problems and led to a large amount of research and development work aimed at understanding and mitigating these difficulties. Criteria and requirements were developed which could be used in design to obtain satisfactory PIO qualities. Nevertheless, in spite of all this work, and even with the great flexibility in modern control technologies available to the designer, PIO problems still often occur with new aircraft; in fact it is the power and responsiveness of modern control systems which makes them susceptible to various "non-linear" effects such as time delays, rate limits, actuator saturation, etc., leading to unexpected PIO difficulties. With current experience, it is clear that a universal solution of the PIO problem still evades the engineering community. The cost of these problems in programme delay and financial terms is significant. The gathering together of specialists to discuss this problem, from their various points of view, has led to positive gains in the state of knowledge regarding PIOs; it has provided a significant step toward their elimination and contributed to the avoidance of PIO associated programme costs and penalties. This paper provides an overview of the results from the Workshop. Fuller details are to be published by AGARD in the proceedings of the Conference and Workshop in the near future and in a separate Advisory Report.

The Workshop Proposal

It was thought that an Advisory Group for Aeronautical Research & Development (AGARD) Flight Mechanics Panel (FMP), (since reorganised by AGARD as the Flight Vehicle Integration Panel or FVP) initiative on this topic would be timely and relevant.

A Workshop, involving presentations from appropriate specialists in the Handling Qualities, Control System Design and Testing fields, was proposed, to be coincident with the Active Control Technology Symposium , with the objectives of:

- Re-examining the latest PIO research.
- Defining factors which may contribute to the development of PIO problems in an aircraft.
- Illuminating new methods which are being used to analyse and avoid or overcome these problems.

This Workshop was integrated with the AGARD Flight Mechanics Panel Symposium on the subject of Active Control Technology, Applications and Lessons Learned, held in Turin between May 9th and 12th, 1994. A large number of specialists with the relevant experience were expected to be gathered for this meeting. The Workshop, itself, took place on the Friday 13th May, following the symposium.

The AGARD Flight Mechanics Panel symposium on "Active Control Technology, Applications and Lessons Learned" provided an excellent introduction to the workshop, with a number of significant and relevant presentations during the preceding days, culminating in the final round table discussion which set the scene for the Workshop..

Workshop Presenters

A number of experts in the fields of Flying Qualities, Flight Testing, and Pilot Modelling were invited to attend the workshop and give their views and experience before an audience made up of those pilots and ACT engineering specialists, with an interest in the PIO problem, who cared to stay on in Turin for the extra day.

The major invited contributors to the Workshop were:

1. Duane McRuer, STI
2. Rogers E. Smith, NASA Dryden
3. Ralph A'Harrah, NASA HQ
4. Ralph H. Smith, H.P.E.
5. Roger Hoh, Hoh Aeronautics
6. John C. Gibson, Consultant
7. David J. Moorhouse, Wright Labs
8. John Hodgkinson, McDonnell Douglas Aerospace
9. Jennifer Martin, DLR
10. Per-Olov Elgcrona & Erik Kullberg, SAAB - Military Aircraft AB
11. Dr. Dietrich Hanke, DLR

* *Fellow of the Royal Aeronautical Society and former U.K. member of the AGARD Flight Mechanics Panel.*

Paper presented at the Flight Mechanics Panel Symposium held in Turin, Italy, from 9-13 May 1994.

12. Charles R. Chalk, Consultant
13. Capt. William Norton, USAF

All of the contributors created an open and frank discussion of the problems which exist and with which the flight controls and flying qualities communities are still struggling to overcome. There were a number of significant inputs from the floor , ,either in response to questions or as comments regarding the individuals experience.

A Historical Perspective

Duane McRuer set the scene for the Workshop by providing a valuable background history to the subject of PIO. In this he was ably supported by Rogers Smith. The records, on both video and as time histories, of the PIOs which have occurred provided very graphic and sobering evidence of the problems and consequences with which pilots can be confronted.

These problems have manifested themselves since the earliest days of manned flight. The earliest recorded examples of Pilot Induced Oscillation date back to the Wright Brothers first aircraft. The earliest video record dates from just before World War II, with the XB-19 aircraft which suffered a pitch PIO on touchdown.

The effects of modern control systems have tended to exacerbate the situation, at least in some cases, as shown in the examples.

The examples on video covered aircraft from the XB-19, through to aircraft such as the Space Shuttle, the YF-22 and, most recently, the JAS-39 Grippen. The video included the F-4 incident, when the aircraft was destroyed as the PIO diverged. It was noted that often in the past the blame had been apportioned to the pilot, who might be referred to as "ham handed", and in one case, the XF-89, the problem was solved by a change of pilot.

Figure 1

PIO Historical Resume

- Essentially Single Axis, Extended Rigid Body Effective Vehicle Dynamics
- Essentially Single Axis, Extended Rigid Body with Significant Feel-System/Manipulator Mechanical Control Elements
- Multiple Axis, Extended Rigid Body Effective Vehicle Dynamics
- PIOs Involving Higher Frequency Modes

The influence of variable pilot gain in the problem is significant, and easily shown by the various types of task for which PIO is notorious, e.g. precision landing in turbulent conditions, air to air tracking, flight refuelling, etc. Most of the videos related to landing, although in the case of the YF-22, the aircraft was performing a low fly by for publicity purposes and the second JAS-39 incident occurred during an airshow.

Figure 2a

Examples of Famous PIOs

- Longitudinal PIOs - Extended Rigid Body

XS-1	Approach & Landing, 24.10.47 Pilot: Herbert Hoover, NACA
XF-89A	Dive Recovery, 1949. Pilot: Fred Bretcher
F-86D	PIO in formation flying under G
F-100	PIO in tight manoeuvring
F-101	Aft c.g.
X-15	Glide approach & landing, 8.6.59 Pilot: Scott Crossfield
Sea Dart	Post take-off destructive PIO
YF-12	Interaction with aircraft flexible dynamics.
MRCA	Short T/O, 1975; Heavy landing, 1976
Shuttle	Approach Glide, 26.10.77 Pilot: Fred Haise
FBW F-8	PIO in Touch & Go, 18.4.78 Pilot: John Manke
YF-22	PIO in low overshoot, 25.4.92 Pilot: Tom Morgenfield
JAS 39	Approach, 1990; Display, 1993

Duane McRuer categorised the PIO into 4 types, as indicated in Figure 1, and has also broken down those PIOs which have been publicly reported in any detail, Figures 2a and 2b, into these categories.

Certainly one of the major problems that was highlighted in this session related to the recognition and reporting of PIO incidents. There is a tendency for pilots not to recognise the event which has occurred as a PIO or to admit or discuss the event, having struggled with the problem and survived. In at least the case of the YF-22, the pilot was unaware that he was in a PIO, although he was aware of a control problem. This is a usual and typical reaction, and is characterised by the pilot feeling totally disconnected from the response of the aircraft.

The presenters have concluded that the occurrence of PIO must be regarded as a failure of the design process. In some cases, such as the YF-16 or the JAS-39, the potential for a problem was identified before flight trials commenced, by various means. However, for one reason or another, the message was not reacted to in time and the consequence was the occurrence of and incident or accident.

There is an apparent strong feeling that to admit to a PIO is to invite blame, which is incorrectly apportioned to the pilot and

Figure 2b

Famous PIOs
Lateral-Directional PIOs - Extended Rigid Body

KC-135A	Associated with omega phi/omega d
B-52	Refuelling
F-101B	Lateral PIO at high q, subsonic
X-15	Lateral PIO, 1961
Parasev	Lateral rocking PIO during ground tow, 1962
B-58	Lateral-directional control associated crash, 14.9.62 Pilot: Ray Tenhoff
M2-F2	Lateral-Directional PIO, 10.5.67 Pilot: Bruce Peterson

Longitudinal PIOs - Extended Body + Mechanical Elaborations

A4D-2	High Speed PIO, Bobweight + Primary Control System involved.
T-38	High Speed PIO, 26.1.60
F-4	Low altitude record run, 18.5.61 Destructive PIO

Lateral-Directional PIO

A-6	Lateral Effective Bobweight effects

PIO Associated with High Frequency Aeroelastic Effects

CH-53E	Coupling with Flexible Modes whilst hovering with underslung loads.

3-D, Multi-Axis PIOs

X-5	31.3.52; Pilot: Joe Walker
YF-16	"First Flight"; Pilot: Phil Oestricher
ALT-5	Lateral PIO just prior to Longitudinal PIO, 26.10.67
F-14	High AoA; Pilot: Don Evans
AD-1	Oblique Wing

this aspect was addressed later and in more detail during the Workshop.

It was noted that all the catastrophic PIO occurrences included the adverse effects of actuator rate limiting. This was to dealt with in some detail in later presentations to the meeting, as were the possible methods of alleviating the problems which arise from the excessive phase delays which actuator rate limiting bring about.

A good initial reference for the understanding of the PIO and its subsequent development is provided by reference 2, published recently by AGARD. This report, which deals with the handling qualities of highly augmented aircraft, and the Working Group that produced it, have provided much needed discussion of the problem and allowed a sharing of the understanding from all interested parties within NATO.

Design Objectives and the PIO Process

The Design Objectives

The objective of the design, as described by Ralph A'Harrah, should be the provision of an aircraft and control system which has Level 1 handling qualities and is free from PIO, or as Ralph preferred, **Aircraft-Pilot Coupling**. This proposed name takes the emphasis away from the contribution of the pilot, although it is recognised that the problem cannot occur in the absence of the pilot. The essence is that Aircraft-Pilot Coupling is a design failure in the flight control system, which the pilot will unwittingly contribute to by performing his task, i.e. that of controlling the aircraft to meet his particular performance requirements.

It was suggested that a good starting point for the design process would be the design requirements set out in Mil-F-8785C, supplemented by the guidelines of Mil-STD-1797, or any other criteria with which the design organisation in question has experience and which can be demonstrated to have merit.

Ralph A'Harrah recommended that the Total Quality message was appropriate for this application, i.e. right first time, and that to achieve this required the building of a design team which sees the design through from concept to implementation and test. The team should consist of control system designers, handling quality experts, pilots, simulation engineers and, most significantly, must include managers for it to be successful and ensure that all buy into the problems and their solutions.

The PIO Process

As described by Duane McRuer and Ralph Smith, the PIO process involves elements of aircraft dynamics, closed loop control and a "trigger". This latter is the item which can suddenly cause the pilot to increase his gain to the point that the total loop is driven unstable. There was considerable debate as to what might constitute a trigger and whether or not it had to be the pilot or the control system which would constitute it.

But the view was also expressed that maybe it does not matter what it is, there will always be one waiting to catch the unwary under some circumstances which will be found under the right conditions one day. The mere fact that there is a possibility of coupling should be enough to say that a change is needed as the problem will occur sometime, under the right stimulus. The design objective should then include ensuring

that there is no possibility of the pilot coupling with the aircraft in a way which could lead to significant oscillation with a large amplitude.

Figure 3

Understanding PIO - Three Necessary Condtions for PIO

PIO = Dynamics (eg Smith-Geddes Criteria)

\+

Trigger (The unexpected response - the catalyst for closed loop control)

\+

Closed Loop Control (Hard to create)

Ralph Smith presented the concept shown in Figure 3, which eloquently summarises the conditions which are necessary for the PIO to occur. In his presentation, Ralph Smith expressed a number of concerns which found accord with members of the audience, especially when he suggested that all FBW aircraft should be designed to be proof against PIO, whether for military or civil application.

It was noted that it is possible to have aircraft with adequate "performance" whilst having deficient handling qualities, and that this then placed heavy demands on pilot training and costs of operation in service, when such a combination occurred. A specific comment related to the behaviour of trainee pilots, which could be very different with respect to their gains employed, until they were familiar with their tasks.

The Space Shuttle was cited as an excellent example of an aircraft for which this was the case. It fails to meet all the available design criteria with regard to resistance to PIO and does have a tendency for PIO unless handled very carefully by experienced, trained pilots. The tables in figure 2 do illustrate this, as did the introductory video sequence, which featured the Shuttle PIO events.

The difficulty arises because the PIO susceptibility is difficult to assess. The essential element of the process which needs to be followed up is to ensure that the control system is adequately stressed during its design and development, using whatever facilities can be thrown at the problem, even if this means flying tight control manoeuvres and in a way which may or may not be realistic of normal pilot activities in flight.

Design Criteria

A common theme which emerged from a number of the presentations is that, as yet, there is no common, unified view with regard to the design criteria which should be used to design and evaluate systems to be free of PIO tendencies.

Design criteria based upon service experience are not available as, it is suspected, most occurrences are not reported or perhaps even recognised. Within experience in Europe, however, those occurrences which are known about, at least to the author, do not show any marked difference in character from those which have occurred in flight test, although the range of configurations may be extended.

The meeting received a verbal blast from Ralph Smith; his feelings are that the problem has been skirted around for a number of years and no real progress has been made. This is an area where there are significant arguments over the effectiveness of the existing criteria at prediction of PIO and even the database upon which the criteria have been based. This latter view is not generally shared , and the consensus of the workshop rather pointed in a different direction.

Existing Design Criteria

During the discussion around his presentation, it became clear that there are considerable arguments over the effectiveness of the various criteria which have been proposed in the past. Rogers Smith, Roger Hoh and Dave Moorhouse all pointed out that all the current criteria have some merit; they are effective in some cases, some more than others perhaps, although no single criteria has yet been identified as "correct" for all applications.

There were considerable arguments as to which was best, but perhaps the message should really be that there is no one criterion, as yet, which fully describes all of the problems which may be encountered and can be applied without significant "limitation as to applicability" and engineering interpretation.

This clash of results from the different criteria currently in use is probably one of the main problems associated with getting management backing for the necessary design changes at an early enough stage. Often the technical arguments are clouded by arguments about whether or not the criteria used really apply. What should be considered is what is actually happening, which is the starting point that Ralph Smith came from.

To an extent, in this argument, the criteria can be either irrelevant or misleading, as they can detract from the presentation of the real problem, serving only to confuse and irritate. This is possibly one reason that managers do not always listen, as there is no cut and dried "yes-no" method of determining if there is a problem. The assessments that are performed are indicative, usually, but may be clouded by pilot opinion.

Theory and empiricism may still be the best way to judge the problem in a consistent fashion, despite the possible drawbacks. The key is to have it applied with the full background of engineering experience, using a team of engineers with an established track record to adequately

"stress" the control system and ensure that the possibilities are addressed adequately.

Handling Qualities Analysis Status

There appears to have been little development in the handling qualities field for some years, at least as far as official minds are concerned, and Low Order Equivalent Systems (LOES) are still standard method. The problem of LOES is understanding when you can use it safely and the limitations which apply to its use. Roger Hoh pointed out that it should not be used with aircraft which do not feature a classical command strategy, such as Command Attitude Hold, as these control systems cannot be approximated by a linear k/s transfer function.

But there is significance in Ralph Smith's comments and in his methods. His ideas from the 1970s do encourage examination of the actual response characteristics as the source of what the pilot actually likes or dislikes about a response.

This is probably a most important contribution which has been overlooked by many researchers until recent times, possibly because of the criteria arguments. This concept had caused John Gibson to develop a set of handling quality criteria and propose his current methodology for PIO prevention by design. Unfortunately, the original Smith-Geddes criterion, as defined in reference 3, would appear to have the similar drawbacks to most of the others, in that it works for some examples, but not for all cases. This does not mean that it cannot and has not been applied without success. It is not general.

To date, the application of the different existing criteria did not give a consistent picture across a range of different cases and none could account for the T-38 PIO.

Development of New Design Criteria

Roger Hoh indicated that the USAF is pursuing the PIO issue actively and is encouraging R&D on a joint basis with a number of researchers. He stated that the phase lag at the crossover frequency was a key. His presentation showed how new criteria based upon phase lag were developing following the debates which had been held by AGARD Working Group 17, which are reported in reference 2. He was at pains to point out the benefits which had accrued by extending the discussion into an international forum; all involved had benefited from sharing of experience and ideas.

Most of the more recent developments with regard to design criteria stem from the activities of Working Group 17, noted in reference 2. This document also provides a good background for anyone new to the Handling Qualities arena and who wishes to quickly acquire a level of understanding of the overall problems which are present, especially with a modern highly augmented aircraft flight control system.

Both Ralph Smith and Chic Chalk proposed pilot models which operated on a simple "bang-bang" basis, with the "decision" being related to the response parameter under consideration. Chic Chalk based his observations on numerous experiments which have been carried out over the years on the Calspan NT-33 and Lear Jet aircraft, combined with the analysis of PIO incidents, such as the F-8.

Figure 4
Example of Synchronous Pilot Behaviour

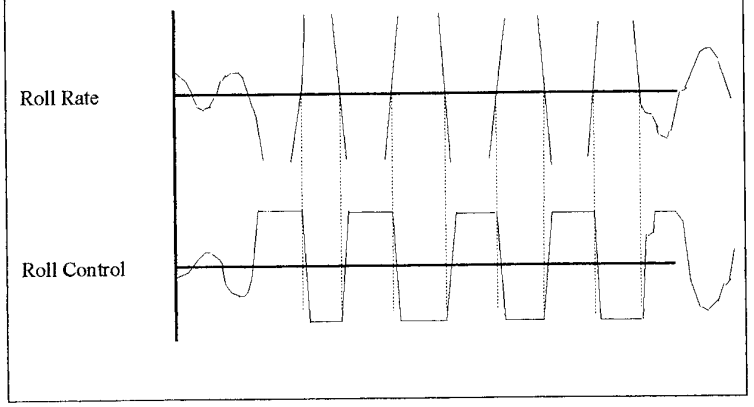

Chic Chalk proposed that the pilot input would be synchronous with the crossover of the rate response through the zero, which corresponds to the attitude starting to move in the opposite direction. Such concepts were supported by John Gibson and others, and are illustrated in figure 4.

Figure 5
High Order Attitude PIO Conditions

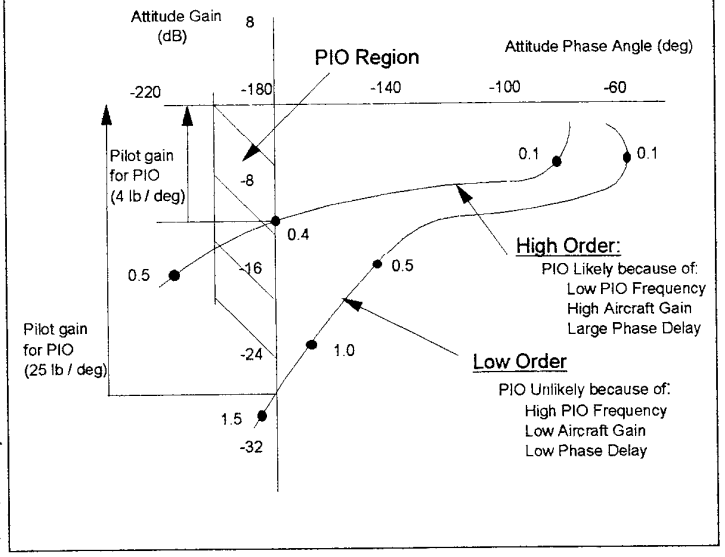

Ralph Smith showed that such a simple model could be used to predict PIO likelihood. If the model resulted in a limit cycle behaviour, then the aircraft had a possibility of PIO.

The view was expressed that whatever criteria was developed, it would have to account for the shape of the frequency response curve, and that how the gain and phase varied around the crossover point is as important as the actual gain at 180° phase, see figure 5. The "Phase Delay" concept captured this nicely, and could even account for rate limiting by its effects on the shape of the frequency response curve. When combined with the "Dropback" criterion proposed by John Gibson, the results were very encouraging.

The Effect of the Feel System on Handling and PIO

The subject of the feel system drew some debate. The tactile cues received by the pilot do include both force and motion and there is a suspicion that sticks which rely only on force detract from the handling. This is again an area of major debate, and it is not clear whether the problem is really one of having pilots learn to cope with a new philosophy, whether there are undesirable tactile effects or whether a combination of the two applies.

Dave Moorhouse expressed the view that the feel system, if well designed, should be transparent to the pilot. If not well designed, then it could be a major source of problem. Certainly, poorly designed feel systems have been major contributors to handling problems in general and PIOs in particular.

John Gibson highlighted that one problem was the gap which occurs between aircraft projects and the influence that this has on keeping expertise current and on the ability to learn the lessons from the past without repeating the same mistakes. Perhaps this further highlights the need to keep design teams current.

Phase Rate or Phase Delay Criteria

John Gibson described the development of criteria based upon the phase rate/phase delay concepts. His comments on the F-8 PIO trace, which he had not seen until the meeting, indicate that the trace developed as he would have anticipated, with a clear decrease in frequency as the amplitude of the oscillation increased, due to the effects of actuator rate limiting. The trace supported his ideas regarding the development and symptoms of PIO, confirming the synchronous behaviour of the pilot with the aircraft attitude.

The YF-22 traces show the same effects, although the initial trigger for the response might not have been the pilot, but was somewhere in the aircraft itself. The pilot commented that he felt "disconnected from the stick".

In developing his approach to designing out the high order rigid body PIO, the LAHOS data base had been used, although this does not include non-linear effects. This had resulted in examination of the Phase Delay (or Average Phase Rate) around the crossover point, coupled with the frequency at the crossover. The gain at this point is important. Clear boundaries were identified, gradeable as Level 1, 2 or 3, which had been subjected to vigorous simulation exercises over the last three years. These are shown in figure 6 and 7.

Figure 6
High Order PIO Boundaries

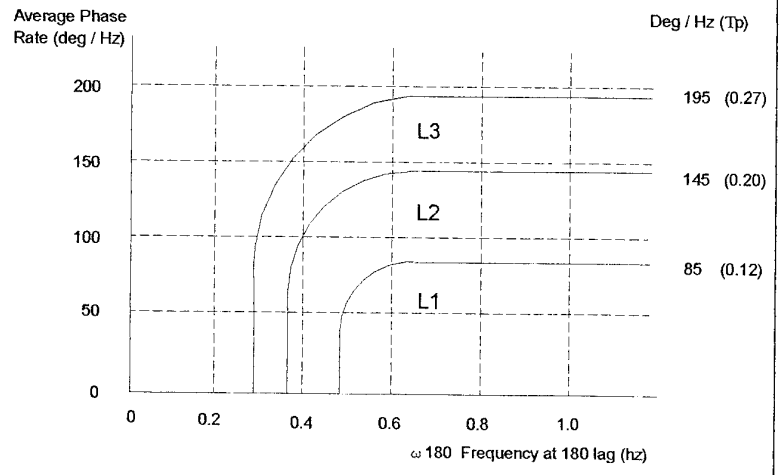

Figure 7
Maximum PIO Frequency Gain

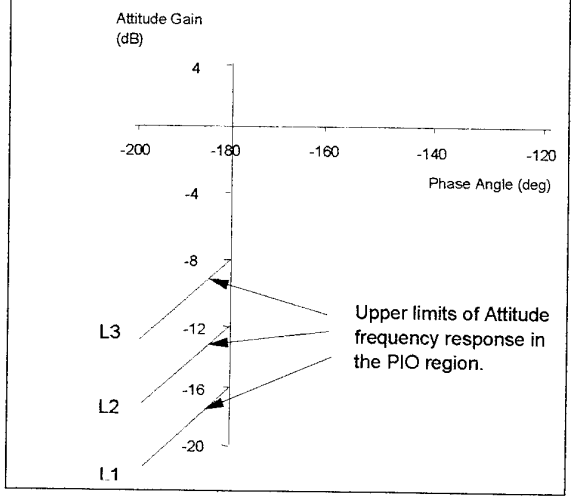

A brief experiment performed on the Calspan Lear Jet had enabled confirmation, in part, of the concepts in flight, as the experiments yielded the predicted answers.

The clear message from this work is that the process must be to design for Level 1 handling qualities and then stress the flight control system to examine its behaviour under high pilot gain conditions, for a range of input amplitudes.

PIO Susceptibility and Relation to Aircraft Safety

John Hodgkinson showed the work which he is undertaking to relate the handling qualities rating to aircraft safety. Another clear message is that the managers must be made aware that the presence of Aircraft-Pilot Coupling is a safety related issue, and is at least as important as structural integrity. (There is a suspicion that more accidents occur due to APC or PIO than due to structural failure!).

It could be shown that the Cooper-Harper ratings could be correlated with probability of aircraft losses, with CHR 6 corresponding to a probability of loss of 1 in 10^{-3} and CHR 3.5 corresponding to a probability of loss of 1 in 10^{-9}, or effectively not within the fleet life of the aircraft. Figure 8 illustrates these findings, as presented by John Hodgkinson at the Workshop.

Figure 8
Relationship Between Mean CHR and P(LOC)

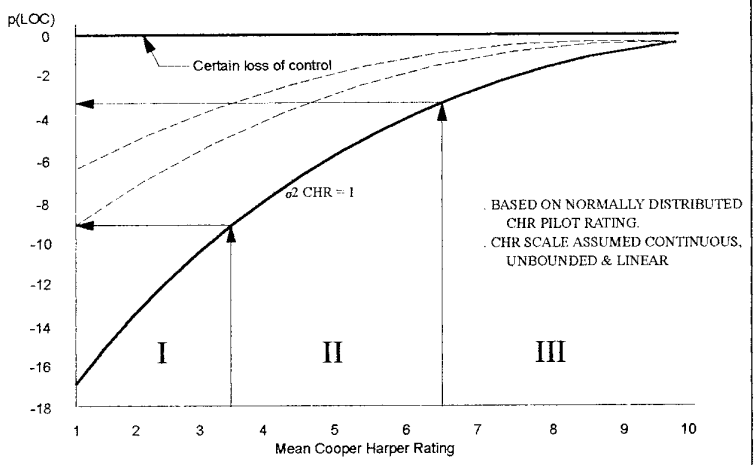

The Adverse Influence of Actuator Rate Limits

One of the major contributions to catastrophic PIO events is that due to actuator rate limiting, as noted in the opening presentation by Duane McRuer and Rogers Smith.

The effect of rate limiting is to add further phase lag between the pilot command and the aircraft response and to reduce the frequency of the crossover point. Figure 9 illustrates the effects of rate limiting with regard to production of a time delay.

A number of the events in the introductory video featured rate limiting, most notable recent examples being the JAS-39 and

Figure 9

Actuator Rate Limiting - Problem Statement

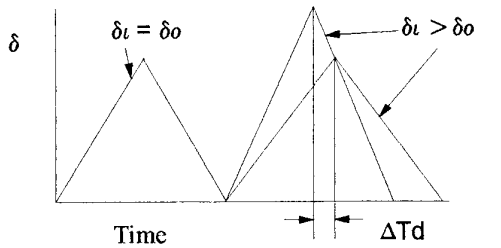

the YF-22 accidents. Rate limiting also featured in the Shuttle, YF-16, Tornado and many other major occurrences of PIO.

The modelling undertaken by BAe arose from the incidents with Tornado (MRCA), where, as noted in reference 4, rate limiting and acceleration limiting in the actuator played a major part in the incidents. Subsequent work lead to very detailed investigation of the actuation system, as there continued to be surprises from this piece of equipment, which eventually led to some modifications in the flight control system of the aircraft. The work identified the extra phase lags which can result very abruptly once the actuator rate limits.

The presentation by Per-Olov Elgcrona and Erik Kullberg is very significant in this respect. They reviewed the past experience in Sweden with PIO, and indicated that the JAS-39 system originated from demonstration work performed on a FBW Viggen aircraft. Although this was reported to have experienced Level 2 or 3 handling, due to excessive time delays, it never experienced rate limiting or PIO.

Rate limiting played a very significant part in both accidents to the JAS-39 Grippen. The first accident was described as a design error, in that the design was known to be sensitive prior to flight. However, the process did not catch up with the evidence and require modification before flight.

The first accident started as a response to lateral turbulence with a control system which augmented the dihedral effect, making the aircraft very sensitive in roll. More than one presenter, who had been involved with Saab in the subsequent work, commented that the JAS-39 "mini-stick" probably had a very significant effect, as it requires only very small movements to demand full control and had a skewed axis. Once the rate limits were reached, the PIO developed initially in roll, then in pitch. Modifications to reduce the gain, which also reduced the manoeuvrability, were introduced and the aircraft was assessed using a HQDT test. Using results of this

a criterion was developed which allowed the margins from rate limit to be established.

However, as development progressed, there was a desire to boost agility at lower speeds and modifications were introduced. Assessment showed that under extreme conditions, using full roll and pitch stick, rate saturation and departure from stabilised flight could be reached. However, the decision was taken to continue.

The second accident featured a roll PIO as the pilot aggressively rolled wings level to accelerate in front of the crowd watching the aircraft at the Stockholm water festival. The subsequent response and pitch up to high AoA caused the pilot to eject after 5.9 seconds, fortunately without causing any harm to those on the ground or the pilot.

A comment was also passed regarding the C-17, where, during the development of the aircraft, a rate limit had been applied to the tailplane, and a pitch PIO had been forecast and occurred.

Figure 10
An Alternative Control Strategy for Alleviation of the effects of Rate Limiting Time Delays

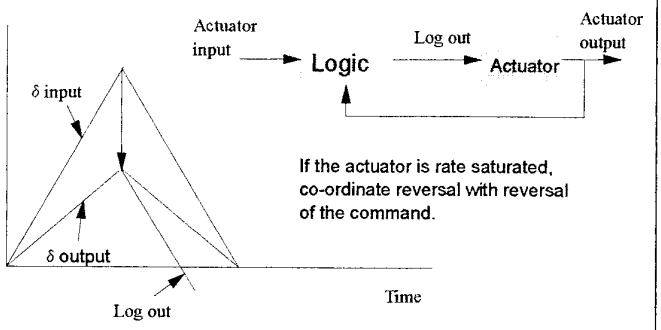

Rate Limiting - Proposals for Alleviation of the Adverse Effects

A number of presenters reported work upon a strategy whereby the effects of rate limiting could be mitigated or even removed. The basic strategy concept was developed by Ralph A'Harrah, but experiments have been carried out at Calspan, at DLR Braunschweig and other centres to examine the benefits which might accrue. The object is to eliminate the undesirable effects of the additional time delays which rate limits add to the control system.

An Alternative Actuation Control Loop Strategy

Ralph A'Harrah recommended that the actuator rate capability should be allocated by the function to be fulfilled, not by the displacement that has to be achieved. Use of this latter can lead to the effect of freezing the pilot out of the control loop.

The first presentation on this subject to the Workshop was made by Jennifer Martin, who is currently working at DLR Braunschweig. The presentation described the testing performed on an actuator alternative control strategy which causes the actuator to reverse immediately the input demand reverses, rather than waiting for the actuator to reach the demanded position before reversing.

This effect of this additional logic block is illustrated in figure 10.

The main benefit of the strategy, tested as the Project Scarlet on the ATTAS in-flight simulator during 1992, is the removal of the adverse phase lag effects due to rate limiting. The testing performed showed that even with the actuator in rate limit, the control movement followed the demanded input much better than with that in the case without this modification to the actuator loop. PIO was successfully prevented, whereas without the modification, a PIO did occur. The experiments progressed to examine the effects with a Rate Command, Attitude Hold control system, again showing the benefit of having the actuator follow the command. These flight experiments are continuing.

The alternative approach to rate limiting, as proposed by Ralph A'Harrah, whereby the actuator control loop incorporates additional logic to command the reversal as soon as the command reverses is clearly very beneficial, but does require some care in its implementation, in order to correctly match input and output, once the high rate demands cease.

The solution being implemented on the JAS-39 is similar to that proposed by Ralph A'Harrah and tested in the Scarlet experiment at DLR and also on the Calspan Lear Jet. This works well to reduce the phase loss due to the actuator, but needs careful blending of the signals to avoid further problems due to the actuator not being at the demanded position.

Development of Handling Qualities Criteria Including Rate Limiting

Dietrich Hanke, of DLR, had assessed the impact of rate limiting and the alternative control strategy on the aircraft handling qualities, with a view to defining possible new criteria for use in design and assessment of such systems. A Model was developed allowing the effects of actuator rate limiting to be described in the frequency domain, from which appropriate handling qualities criteria can be derived. Using describing functions, he had arrived at a margin between the bandwidth of the system and the onset of rate limit, which he titled the "Amplitude Margin".

His work clearly showed the effects of rate limiting, with the cliff-edged behaviour apparent as the frequency reaches that for onset of rate limiting, for a given amplitude of input. Clearly, amplitude and frequency effects will need to be accounted for in any new handling qualities criteria.

Coupling with Aircraft Aeroelastic Modes

In one of the final presentations, we were brought back to the possibility of the pilot coupling with the elastic modes of the aircraft. Duane McRuer had already indicated that this coupling with higher dynamic modes had been responsible for the loss of several CH-53 helicopters, particularly with underslung loads.

The presentation centred around the coupling of the pilot with the structural modes of the airframe. A number of examples were quoted, the most notable being the F-111 when carrying heavy external store loads under wing. When the pilot made an abrupt roll input, this excited the wing bending and torsion, which due to its low frequency and the effect on the response, he tried to oppose. He recognised the coupling, so clamped the stick, whereupon the aircraft shook both him and the stick.

This was referred to as a "Pilot Assisted Oscillation" or perhaps a "Pilot Augmented Oscillation". He let go, and due to the out of balance, the stick travelled stop to stop!

A further example was that of a large transport aircraft, in this case the C-17. Excitation of the wing frequencies, in a somewhat similar manner to the F-111, had coupled with the pilot's stick inputs, causing a "ratcheting" effect on the response of the aircraft. A brief paper describing these effects was made available prior to the workshop and is contained in reference 5, which will be included in the full report of the Workshop which will be prepared for AGARD over the next few months.

During the week of the ACT Symposium, of which the Workshop was the final part, a number of persons expressed their concerns with this problem in connection with the large transport aircraft, where the sheer size of the aircraft will place the structural primary modes within the frequency range of both the pilot and FCS.

This is clearly an area where there could be increasing concern and activity, if safety records are to maintained in line with current expectations, particularly of the travelling public.

The Design Process

Ralph ATHarrah described his view of the process which should be followed to ensure that the design is free from PIO.

Essentially, the objective is to ensure that the aircraft and flight control system achieve Level 1 handling qualities and that there are no adverse Aircraft Pilot Coupling tendencies present. This goal was supported by a significant number of the speakers, and is clearly seen as a universal goal for control system designers.

It is not sufficient to rely on A-PC avoidance on the basis that the pilot will never fly the aircraft that way, as experience has shown that if it is possible, then following the appropriate "trigger", **the inevitable will happen**.

It is essential that the process is set out to look for the problem in the design phase. To achieve this requires all involved to understand the objectives, the tools and techniques to be used, an adequate set of design criteria and that the project management provides the necessary support to the design team.

In assessment of the design, it is essential that the system be stressed by the exercises which are set out in the design and assessment task. The assessment must cover those tasks which result in high pilot gains, using whatever simulation facilities are available, but preferably including some in-flight simulation to ensure the correct cues are present. Those responsible for testing and assessing must even be prepared to examine inputs which might be considered unrealistic.

One method which was suggested for this, and which received support from more than one of the presenters, was to excite the aircraft with a cyclic input, varying the frequency and the amplitude, and then looking at the response for the tell tale signs of rate limiting, excessive phase lags and the ability to couple with the attitude or path response.

The key to designing out the problem lies with establishing the correct design team, covering the obvious specialities of FCS, handling qualities and test pilots, but also the simulation experts, both ground and flight based, and project team management. The latter are essential to provide any support to the implementation of changes to the design.

It was even suggested that, where possible, the managers should be exposed to the demonstration of the problem in the case where there is any doubt as to the effects on the aircraft performance or safety.

Conclusions

There are a number of conclusions which can be drawn from the data presented and the discussions which occurred at the Workshop:

1. **The term PIO places an unwarranted emphasis on the pilot**, when the problem is actually due to the flight control system design.
2. The phenomenon is better named **Aircraft Pilot Coupling**, thus avoiding the stigma which might be attached to the pilot by the unknowing and uninitiated.
3. **Aircraft Pilot Coupling is a result of the design process failing**
4. **The "design process" objective should be the achievement of Level 1 handling qualities and freedom from undesirable APC.**
5. The design team who will implement the process should **include FCS designers, handling qualities experts, simulation engineers, pilots and project management**, to ensure communication and ownership regarding possible development events.
6. In the design process, every effort should be made, using whatever criteria are decided upon, to **search**

for the problem and to **"stress" the flight control system design adequately** to ensure the problem has been designed out.

7. **Adverse APC should be designed out** not avoided by requiring the pilot to fly the aircraft in a very controlled manner. This can never be relied upon under all circumstances and will almost inevitably catch the design out some day.
8. **Large transport aircraft should be designed to meet the same handling requirements** as military fighter aircraft, whether for military or civil application.
9. **Care is required before passing to a flight test stage in the event that there are aspects of the aircraft response that are not understood.** It is necessary to completely understand any unexpected happenings which might occur during analysis, simulation - both manned and non-real time, rig test, etc.
10. **Remember that Murphy's Law applies, i.e. "If it can happen, it will happen".** The design process should recognise this, not only as a technical problem, but also as a management problem. The management obligation is to **listen, understand and act** accordingly.
11. Aircraft-Pilot Coupling probably accounts for more aircraft incidents and accidents than does structural failure. **Never rely on the adage, *"the pilot never will fly that way"*! He probably will, given the "right" circumstances.**
12. Control System design and development will remain a **"Discovery Process"**. This should be recognised and the whole design team should recognise this and plan to be flexible in their approach.

Recommendations

The first recommendation is that the term **"Pilot Induced Oscillation" should be avoided and replaced by "Aircraft Pilot Coupling".**

It is accepted that the pilot is involved in closing the loop that causes the instability, but the phenomenon is essentially a control system design failure. The current naming attaches blame, even if inadvertently, where there should be none.

The second recommendation is that **the processes involved in the design, qualification and certification should be re-examined.**

Aircraft Pilot Coupling obeys Murphy's Law, i.e. if it can happen, it will happen. It is no defence to say "the pilot will never fly that way". It may be improbable, but not impossible. The design process should set out to positively search for signs of Aircraft Pilot Coupling problems in the design process and act accordingly if they manifest themselves.

Finally, the Flying Qualities community should seek to arrive at one set of universally accepted criteria to describe and evaluate the sensitivity of a design to Aircraft Pilot Coupling.

At present, there are a number of criteria which may be partially successful, with some of the latest ideas looking very promising. It would be productive to seek the common ground rather than concentrate on the differences all the time. From the discussions which took place at the Workshop, it is clear that there are a number of possible approaches to the problem. It is important to share ideas, and the AGARD meeting has once again facilitated this, as it did for Handling Qualities with Working Group 17.

Reporting of the Workshop

As the presentations and discussions placed much information on the table, some of which was new to many at the Workshop, it has been decided in conjunction with the Flight Vehicle Integration Panel and the Technical Programme Committee for the Turin meeting, that the Workshop will be fully written up as a separate report, to provide a detail record. This report will be published as AGARD Advisory Report AR.335.

Acknowledgements

To Mr. Peter Sully, Department of National Defence, Canada, for proposing the original idea for the Workshop and Mr. Stewart Baillie, Flight Research Laboratory, N.R.C., Canada, for his assistance in finalising the proposal.

To Mr Franco Sella and Prof. Fulvia Quagliotti for providing the opportunity and facilities to hold the Workshop and to the Students of the Politecnico of Turin for their assistance.

To all the contributors to the Workshop, but especially Per-Olov Elgcrona and Erik Kullberg for sharing their experiences with the JAS-39 so readily and openly, that all workers in this field may benefit from their unfortunate experiences.

References

1. Duane McRuer; "Human Dynamics and Pilot Induced Oscillations." 22nd Minta Martin Lecture, Dec 2, 1992, M.I.T.
2. Wunnenberg. H. et al; "Handling Qualities of Unstable Highly Augmented Aircraft". AGARD Advisory Report AR279.
3. Smith R.H. & Geddes; "Handling Quality Requirements for Advanced Aircraft Design: Longitudinal Mode". AFFDL-TR-78-154
4. Gibson J.C.; "Flying Qualities and the Fly-by-Wire Airplane". AGARD CP-260.
5. Norton Capt. W.J.; "Aeroelastic Pilot-in-the-Loop Oscillations"

REPORT DOCUMENTATION PAGE

1. Recipient's Reference	2. Originator's Reference	3. Further Reference	4. Security Classification of Document
	AGARD-CP-560	ISBN 92-836-0007-X	UNCLASSIFIED

5. Originator Advisory Group for Aerospace Research and Development
North Atlantic Treaty Organization
7 rue Ancelle, 92200 Neuilly-sur-Seine, France

6. Title

Active Control Technology:
Applications and Lessons Learned

7. Presented at

The Flight Mechanics Panel Symposium
held in Turin, Italy, from 9-13 May 1994.

8. Author(s)/Editor(s)	9. Date
Multiple	January 1995
10. Author's/Editor's Address	**11. Pages**
Multiple	420

12. Distribution Statement There are no restrictions on the distribution of this document. Information about the availability of this and other AGARD unclassified publications is given on the back cover.

13. Keywords/Descriptors

Active control
Flight control
Flying qualities
Flight maneuvers
Control equipment
Maneuverability
Design
Vortices
Aeroelasticity
Fuzzy control
Fighter aircraft

14. Abstract

In the last decade, Active Control Technology (ACT) has emerged from the realm of theory and modest experimental applications to full-scale use on production aircraft, while more elaborate forms of ACT are under test for the future production of aircraft. New technologies have been applied in military fighters to maximize maneuverability and agility, and in civil transports to reduce trim drag, lower pilot workload and improve riding qualities.

During this symposium the status of Active Control Technology was assessed in light of the experience gained over the last decade.

The symposium was organised around four sessions comprising 28 technical papers in all. These sessions focused on: Specifications for flight control design, Design and analysis methods, System integration and implementation of experience.

Two keynote speakers introduced the forum with balanced operational and research viewpoints.

A Technical Evaluation Report on the Symposium is also included in this Conference Proceedings Document.

Copies of papers presented at the Flight Mechanics Panel Symposium held in Turin, Italy, 9-13 May 1994.

<table>
<tr>
<td>AGARD Conference Proceedings 560
Advisory Group for Aerospace Research and Development, NATO
ACTIVE CONTROL TECHNOLOGY: APPLICATIONS AND LESSONS LEARNED
Published January 1995
420 pages

In the last decade, Active Control Technology (ACT) has emerged from the realm of theory and modest experimental applications to full-scale use on production aircraft, while more elaborate forms of ACT are under test for the future production of aircraft. New technologies have been applied in military fighters to maximize maneuverability and agility, and in civil transports to reduce trim drag, lower pilot workload and improve riding qualities.</td>
<td>AGARD-CP-560

Active control
Flight control
Flying qualities
Flight maneuvers
Control equipment
Maneuverability
Design
Vortices
Aeroelasticity
Fuzzy control
Fighter aircraft</td>
<td>AGARD Conference Proceedings 560
Advisory Group for Aerospace Research and Development, NATO
ACTIVE CONTROL TECHNOLOGY: APPLICATIONS AND LESSONS LEARNED
Published January 1995
420 pages

In the last decade, Active Control Technology (ACT) has emerged from the realm of theory and modest experimental applications to full-scale use on production aircraft, while more elaborate forms of ACT are under test for the future production of aircraft. New technologies have been applied in military fighters to maximize maneuverability and agility, and in civil transports to reduce trim drag, lower pilot workload and improve riding qualities.</td>
<td>AGARD-CP-560

Active control
Flight control
Flying qualities
Flight maneuvers
Control equipment
Maneuverability
Design
Vortices
Aeroelasticity
Fuzzy control
Fighter aircraft</td>
</tr>
<tr>
<td>AGARD Conference Proceedings 560
Advisory Group for Aerospace Research and Development, NATO
ACTIVE CONTROL TECHNOLOGY: APPLICATIONS AND LESSONS LEARNED
Published January 1995
420 pages

In the last decade, Active Control Technology (ACT) has emerged from the realm of theory and modest experimental applications to full-scale use on production aircraft, while more elaborate forms of ACT are under test for the future production of aircraft. New technologies have been applied in military fighters to maximize maneuverability and agility, and in civil transports to reduce trim drag, lower pilot workload and improve riding qualities.</td>
<td>AGARD-CP-560

Active control
Flight control
Flying qualities
Flight maneuvers
Control equipment
Maneuverability
Design
Vortices
Aeroelasticity
Fuzzy control
Fighter aircraft</td>
<td>AGARD Conference Proceedings 560
Advisory Group for Aerospace Research and Development, NATO
ACTIVE CONTROL TECHNOLOGY: APPLICATIONS AND LESSONS LEARNED
Published January 1995
420 pages

In the last decade, Active Control Technology (ACT) has emerged from the realm of theory and modest experimental applications to full-scale use on production aircraft, while more elaborate forms of ACT are under test for the future production of aircraft. New technologies have been applied in military fighters to maximize maneuverability and agility, and in civil transports to reduce trim drag, lower pilot workload and improve riding qualities.</td>
<td>AGARD-CP-560

Active control
Flight control
Flying qualities
Flight maneuvers
Control equipment
Maneuverability
Design
Vortices
Aeroelasticity
Fuzzy control
Fighter aircraft</td>
</tr>
</table>

During this symposium the status of Active Control Technology was assessed in light of the experience gained over the last decade.

The symposium was organised around four sessions comprising 28 technical papers in all. These sessions focused on: Specifications for flight control design, Design and analysis methods, System integration and implementation of experience.

Two keynote speakers introduced the forum with balanced operational and research viewpoints.

A Technical Evaluation Report on the Symposium is also included in this Conference Proceedings Document.

Copies of papers presented at the Flight Mechanics Panel Symposium held in Turin, Italy, 9-13 May 1994.

ISBN 92-836-0007-X

During this symposium the status of Active Control Technology was assessed in light of the experience gained over the last decade.

The symposium was organised around four sessions comprising 28 technical papers in all. These sessions focused on: Specifications for flight control design, Design and analysis methods, System integration and implementation of experience.

Two keynote speakers introduced the forum with balanced operational and research viewpoints.

A Technical Evaluation Report on the Symposium is also included in this Conference Proceedings Document.

Copies of papers presented at the Flight Mechanics Panel Symposium held in Turin, Italy, 9-13 May 1994.

ISBN 92-836-0007-X

During this symposium the status of Active Control Technology was assessed in light of the experience gained over the last decade.

The symposium was organised around four sessions comprising 28 technical papers in all. These sessions focused on: Specifications for flight control design, Design and analysis methods, System integration and implementation of experience.

Two keynote speakers introduced the forum with balanced operational and research viewpoints.

A Technical Evaluation Report on the Symposium is also included in this Conference Proceedings Document.

Copies of papers presented at the Flight Mechanics Panel Symposium held in Turin, Italy, 9-13 May 1994.

ISBN 92-836-0007-X

During this symposium the status of Active Control Technology was assessed in light of the experience gained over the last decade.

The symposium was organised around four sessions comprising 28 technical papers in all. These sessions focused on: Specifications for flight control design, Design and analysis methods, System integration and implementation of experience.

Two keynote speakers introduced the forum with balanced operational and research viewpoints.

A Technical Evaluation Report on the Symposium is also included in this Conference Proceedings Document.

Copies of papers presented at the Flight Mechanics Panel Symposium held in Turin, Italy, 9-13 May 1994.

ISBN 92-836-0007-X

AGARD

NATO OTAN

7 RUE ANCELLE • 92200 NEUILLY-SUR-SEINE

FRANCE

Télécopie (1)47.38.57.99 • Télex 610 176

DIFFUSION DES PUBLICATIONS

AGARD NON CLASSIFIEES

Aucun stock de publications n'a existé à AGARD. A partir de 1993, AGARD détiendra un stock limité des publications associées aux cycles de conférences et cours spéciaux ainsi que les AGARDographies et les rapports des groupes de travail, organisés et publiés à partir de 1993 inclus. Les demandes de renseignements doivent être adressées à AGARD par lettre ou par fax à l'adresse indiquée ci-dessus. *Veuillez ne pas téléphoner.* La diffusion initiale de toutes les publications de l'AGARD est effectuée auprès des pays membres de l'OTAN par l'intermédiaire des centres de distribution nationaux indiqués ci-dessous. Des exemplaires supplémentaires peuvent parfois être obtenus auprès de ces centres (à l'exception des Etats-Unis). Si vous souhaitez recevoir toutes les publications de l'AGARD, ou simplement celles qui concernent certains Panels, vous pouvez demander à être inclu sur la liste d'envoi de l'un de ces centres. Les publications de l'AGARD sont en vente auprès des agences indiquées ci-dessous, sous forme de photocopie ou de microfiche.

CENTRES DE DIFFUSION NATIONAUX

ALLEMAGNE
Fachinformationszentrum,
Karlsruhe
D-76344 Eggenstein-Leopoldshafen 2

BELGIQUE
Coordonnateur AGARD-VSL
Etat-major de la Force aérienne
Quartier Reine Elisabeth
Rue d'Evere, 1140 Bruxelles

CANADA
Directeur, Services d'information scientifique
Ministère de la Défense nationale
Ottawa, Ontario K1A 0K2

DANEMARK
Danish Defence Research Establishment
Ryvangs Allé 1
P.O. Box 2715
DK-2100 Copenhagen Ø

ESPAGNE
INTA (AGARD Publications)
Pintor Rosales 34
28008 Madrid

ETATS-UNIS
NASA Headquarters
Code JOB-1
Washington, D.C. 20546

FRANCE
O.N.E.R.A. (Direction)
29, Avenue de la Division Leclerc
92322 Châtillon Cedex

GRECE
Hellenic Air Force
Air War College
Scientific and Technical Library
Dekelia Air Force Base
Dekelia, Athens TGA 1010

ISLANDE
Director of Aviation
c/o Flugrad
Reykjavik

ITALIE
Aeronautica Militare
Ufficio del Delegato Nazionale all'AGARD
Aeroporto Pratica di Mare
00040 Pomezia (Roma)

LUXEMBOURG
Voir Belgique

NORVEGE
Norwegian Defence Research Establishment
Attn: Biblioteket
P.O. Box 25
N-2007 Kjeller

PAYS-BAS
Netherlands Delegation to AGARD
National Aerospace Laboratory NLR
P.O. Box 90502
1006 BM Amsterdam

PORTUGAL
Força Aérea Portuguesa
Centro de Documentação e Informação
Alfragide
2700 Amadora

ROYAUME-UNI
Defence Research Information Centre
Kentigern House
65 Brown Street
Glasgow G2 8EX

TURQUIE
Millî Savunma Başkanliği (MSB)
ARGE Dairesi Başkanliği (MSB)
06650 Bakanliklar-Ankara

Le centre de distribution national des Etats-Unis ne détient PAS de stocks des publications de l'AGARD.

D'éventuelles demandes de photocopies doivent être formulées directement auprès du NASA Center for AeroSpace Information (CASI) à l'adresse ci-dessous. Toute notification de changement d'adresse doit être fait également auprès de CASI.

AGENCES DE VENTE

NASA Center for
AeroSpace Information (CASI)
800 Elkridge Landing Road
Linthicum Heights, MD 21090-2934
Etats-Unis

ESA/Information Retrieval Service
European Space Agency
10, rue Mario Nikis
75015 Paris
France

The British Library
Document Supply Division
Boston Spa, Wetherby
West Yorkshire LS23 7BQ
Royaume-Uni

Les demandes de microfiches ou de photocopies de documents AGARD (y compris les demandes faites auprès du CASI) doivent comporter la dénomination AGARD, ainsi que le numéro de série d'AGARD (par exemple AGARD-AG-315). Des informations analogues, telles que le titre et la date de publication sont souhaitables. Veuiller noter qu'il y a lieu de spécifier AGARD-R-nnn et AGARD-AR-nnn lors de la commande des rapports AGARD et des rapports consultatifs AGARD respectivement. Des références bibliographiques complètes ainsi que des résumés des publications AGARD figurent dans les journaux suivants:

Scientific and Technical Aerospace Reports (STAR)
publié par la NASA Scientific and Technical
Information Division
NASA Headquarters (JTT)
Washington D.C. 20546
Etats-Unis

Government Reports Announcements and Index (GRA&I)
publié par le National Technical Information Service
Springfield
Virginia 22161
Etats-Unis
(accessible également en mode interactif dans la base de
données bibliographiques en ligne du NTIS, et sur CD-ROM)

Imprimé par le Groupe Communication Canada
45, boul. Sacré-Cœur, Hull (Québec), Canada K1A 0S7

AGARD

NATO OTAN

7 RUE ANCELLE • 92200 NEUILLY-SUR-SEINE

FRANCE

Telefax (1)47.38.57.99 • Telex 610 176

DISTRIBUTION OF UNCLASSIFIED

AGARD PUBLICATIONS

AGARD holds limited quantities of the publications that accompanied Lecture Series and Special Courses held in 1993 or later, and of AGARDographs and Working Group reports published from 1993 onward. For details, write or send a telefax to the address given above. *Please do not telephone.*

AGARD does not hold stocks of publications that accompanied earlier Lecture Series or Courses or of any other publications. Initial distribution of all AGARD publications is made to NATO nations through the National Distribution Centres listed below. Further copies are sometimes available from these centres (except in the United States). If you have a need to receive all AGARD publications, or just those relating to one or more specific AGARD Panels, they may be willing to include you (or your organisation) on their distribution list. AGARD publications may be purchased from the Sales Agencies listed below, in photocopy or microfiche form.

NATIONAL DISTRIBUTION CENTRES

BELGIUM
Coordonnateur AGARD — VSL
Etat-major de la Force aérienne
Quartier Reine Elisabeth
Rue d'Evere, 1140 Bruxelles

CANADA
Director Scientific Information Services
Dept of National Defence
Ottawa, Ontario K1A 0K2

DENMARK
Danish Defence Research Establishment
Ryvangs Allé 1
P.O. Box 2715
DK-2100 Copenhagen Ø

FRANCE
O.N.E.R.A. (Direction)
29 Avenue de la Division Leclerc
92322 Châtillon Cedex

GERMANY
Fachinformationszentrum
Karlsruhe
D-76344 Eggenstein-Leopoldshafen 2

GREECE
Hellenic Air Force
Air War College
Scientific and Technical Library
Dekelia Air Force Base
Dekelia, Athens TGA 1010

ICELAND
Director of Aviation
c/o Flugrad
Reykjavik

ITALY
Aeronautica Militare
Ufficio del Delegato Nazionale all'AGARD
Aeroporto Pratica di Mare
00040 Pomezia (Roma)

LUXEMBOURG
See Belgium

NETHERLANDS
Netherlands Delegation to AGARD
National Aerospace Laboratory, NLR
P.O. Box 90502
1006 BM Amsterdam

NORWAY
Norwegian Defence Research Establishment
Attn: Biblioteket
P.O. Box 25
N-2007 Kjeller

PORTUGAL
Força Aérea Portuguesa
Centro de Documentação e Informação
Alfragide
2700 Amadora

SPAIN
INTA (AGARD Publications)
Pintor Rosales 34
28008 Madrid

TURKEY
Millî Savunma Başkanliği (MSB)
ARGE Dairesi Başkanliği (MSB)
06650 Bakanliklar-Ankara

UNITED KINGDOM
Defence Research Information Centre
Kentigern House
65 Brown Street
Glasgow G2 8EX

UNITED STATES
NASA Headquarters
Code JOB-1
Washington, D.C. 20546

The United States National Distribution Centre does NOT hold stocks of AGARD publications.
Applications for copies should be made direct to the NASA Center for AeroSpace Information (CASI) at the address below. Change of address requests should also go to CASI.

SALES AGENCIES

NASA Center for
AeroSpace Information (CASI)
800 Elkridge Landing Road
Linthicum Heights, MD 21090-2934
United States

ESA/Information Retrieval Service
European Space Agency
10, rue Mario Nikis
75015 Paris
France

The British Library
Document Supply Centre
Boston Spa, Wetherby
West Yorkshire LS23 7BQ
United Kingdom

Requests for microfiches or photocopies of AGARD documents (including requests to CASI) should include the word 'AGARD' and the AGARD serial number (for example AGARD-AG-315). Collateral information such as title and publication date is desirable. Note that AGARD Reports and Advisory Reports should be specified as AGARD-R-nnn and AGARD-AR-nnn, respectively. Full bibliographical references and abstracts of AGARD publications are given in the following journals:

Scientific and Technical Aerospace Reports (STAR)
published by NASA Scientific and Technical
Information Division
NASA Headquarters (JTT)
Washington D.C. 20546
United States

Government Reports Announcements and Index (GRA&I)
published by the National Technical Information Service
Springfield
Virginia 22161
United States
(also available online in the NTIS Bibliographic
Database or on CD-ROM)

Printed by Canada Communication Group
45 Sacré-Cœur Blvd., Hull (Québec), Canada K1A 0S7

ISBN 92-836-0007-X